# A GIS approach to palaeovegetation modelling in the Mediterranean: the case study of southwest Turkey

**By**

**Anneley McMillan**

A thesis submitted to the University of Birmingham for the degree of

DOCTOR OF PHILOSOPHY

School of Geographical, Earth and Environmental Sciences
University of Birmingham
September, 2012

UNIVERSITY OF
BIRMINGHAM

## University of Birmingham Research Archive

### e-theses repository

This unpublished thesis/dissertation is copyright of the author and/or third parties. The intellectual property rights of the author or third parties in respect of this work are as defined by The Copyright Designs and Patents Act 1988 or as modified by any successor legislation.

Any use made of information contained in this thesis/dissertation must be in accordance with that legislation and must be properly acknowledged. Further distribution or reproduction in any format is prohibited without the permission of the copyright holder.

# ABSTRACT

Vegetation is a critical component of Mediterranean palaeolandscape studies, however variable data quality and quantity, a lack of understanding of Mediterranean vegetation processes, and complex environments may preclude important palaeolandscape debates from being answered adequately. Issues of representation and uncertainty, and difficulties comparing palaeoecological data against archaeological records often tend to confound clear conclusions from being drawn. Modelling and simulation studies can alleviate some of these difficulties, however, palaeovegetation models have not been utilized to a great extent in the Mediterranean.

To help redress the balance, this thesis established a vegetation modelling framework set in Mediterranean southwest Turkey. In order to overcome some of the above challenges, a new hybrid suite of modelling techniques were developed. The first modelling section developed a bioclimatic model based recent high resolution data of key species and their environmental distribution. The second modelling section undertook Bayesian modelling of radiocarbon dates and pollen zone boundaries from cores across southwest Turkey, to understand the uncertainty of palaeoecological data from pollen cores. The final modelling section converted vegetation modelling output to pollen simulations to compare model output with actual analytical pollen data. To demonstrate the implementation of the framework, it was employed on three important research questions based on disputed points of Mediterranean palaeoecological history.

Following a discussion of palaeoclimatological and palynological evidence from the last glacial period in southwest Turkey and the wider Mediterranean (23-19 Cal ka yr BP), the modelling framework was first employed to investigate whether climatic change could account for evidence of high lake stands and evidence of steppic vegetation signatures concurrently. Utilising a GIS modelling approach, different aspects of this scenario could be explored, including the investigation of steppic areas, and potential refugia locations for cold and drought intolerant species, and the balance of humidity and aridity across the region that may have allowed glacial advance and high lake levels.

The model was secondly employed to analyse the potential for a lag in tree expansion in southwest Turkey at the beginning of the Holocene (~11 Cal ka yr BP to 8 Cal ka yr BP). By incorporating potential uncertainty surrounding pollen zone chronology, Bayesian modelling provided support for the case that a lag in tree species expansion existed in the southwest, and evidence for high precipitation and temperature was modelled.

The model was finally employed to examine the beginning, expansion and end of the Beyşehir Occupation Phase. This is a phase of intensive arboriculture, grazing and arable activity interpreted from pollen evidence and archaeological analysis. Modelling here investigates the early beginnings of the phase, the expansion into higher elevations during the Hellenistic and Roman period, and the decline of the phase between ~AD 200 and AD 900. Modelling suggests that average temperatures were likely to have been warmer, with higher precipitation than modern times. The modelling study has important implications not just for the palaeoecologists, but also for the archaeological and historian community.

# ACKNOWLEDGEMENTS

I would first and foremost like to thank my supervisors Warren Eastwood and Henry Chapman at Birmingham University, and Hakan Yigitbasioglu at Ankara University for keeping me on track, taking the time to provide very useful and detailed comments, facilitating data collection in Turkey and for providing useful reading materials.

I would like to acknowledge the British Institute at Ankara (BIAA) for their generous grant and the use of their facilities, in particular Lut Vanderput for her help making logistical arrangements. I would also like to acknowledge the Turkish Directorate (Orman Genel Müdürlüğü), which is a division of the Ministry of the Environment and Forestry (Çevre ve Orman Bakanlığı) for their helpful comments and data. Special thanks to Hannelore Vanhaverbeke for giving me a very interesting and thought provoking guided tour of the Sagalassos and providing accommodation for me when I visited. Thank you also to Marleen Vermoere for providing me with a copy of her thesis; it has been a valuable source of inspiration and thought. Thanks to Stephen Mitchell for being involved at the inception of the project. Thank you also to Cetin Senkul for his collection of modern moss polster data that has been a useful addition to this study.

In terms of data analysis, I would like to thank Gary King for his technical assistance with the use of the R package 'Zelig' and his comments on the rare events regression model. I would also like to thank the palynology community in particular Jane Bunting and Richard Middleton for the use of their HUMPOL package, the useful discussions on modelling and the invaluable workshop that I attended in Riga. Thank you to Sinya Sugita for his useful discussions in the same workshop. Thanks also to Günther Seufert and Renate Köble for the use of their data and their useful correspondence.

Finally, I would like to give a heartfelt thank you to all my family and friends that have supported me during these past years, and my workplace for being flexible and understanding.

*'Plants are not just the Environment, part of the scenery of the theatre of historical ecology, the passive recipients of whatever destiny mankind's whims inflict upon them. They are actors in the play.' (Grove and Rackham 2003 p. 45)*

# Table of Contents

**Abstract** ..... 2

**Acknowledgements** ..... 3

1 Research aim, introduction and research scope ..... 22

1.1 Research Aim ..... 22

1.2 Introduction ..... 23

1.3 Overview of the Vegetation Modelling Framework ..... 30

2 The geographical setting and research question context ..... 34

2.1 Study area - Southwest Turkey ..... 34

2.2 Research question context and model hypotheses ..... 36

2.3 Identified barriers to progress with key research questions ..... 42

2.4 Where alternative methodologies can help ..... 45

3 Vegetation modelling: methodological considerations and previous approaches ..... 47

3.1 the importance of modelling ..... 47

3.2 Previous vegetation modelling methodologies ..... 57

3.3 What vegetation to model? ..... 57

3.4 Summary ..... 76

4 Model methodological development ..... 80

4.1 Modelling requirements ..... 80

4.2 Modelling roadmap ..... 81

4.3 identification of key species in southwest Turkish palaeoecology ..... 84

4.4 Model input data ..... 88

4.5 characterisation of individual species climatic and edaphic envelopes ..... 92
4.6 Species bioclimatic ranges ..... 92
4.7 Multivariate regression and species probability ..... 96
4.8 Rare events Logistic Regression model results ..... 104
4.9 Methodological development 2: Developing and validating a multiple species bioclimatic model. ..... 107
4.10 Methodological assumptions and review ..... 114
4.11 Summary ..... 120
5 Vegetation modelling Analysis ..... 122
5.1 Model Runs ..... 123
5.2 Simulating pollen assemblages from model output ..... 154
5.3 Summary ..... 158
6 Chronological refinement of pollen data and validation methodology ..... 160
6.1 The importance of a consistent pollen zone chronology ..... 160
6.2 Approaches to age-depth modelling ..... 162
6.3 The Bayesian approach to deposition models. ..... 164
6.4 Model Set Up 1: Likelihood and Prior information ..... 166
6.5 Model set up 2: Age depth modelling ..... 171
6.6 Model set up 3: Model diagnostics and visual output ..... 175
6.7 Results ..... 177
6.8 Revised pollen zone chronology ..... 188
6.9 Calculation of pollen percentages to compare with model output ..... 190
6.10 Validating model-data comparison using modern pollen data ..... 196

6.11 Summary ..... 199

7 Research Question 1: Vegetation modelling framework results and discussion ..... 200

7.1 Research Question ..... 200

7.2 Research question 1 hypothesis ..... 200

7.3 Chronological modelling ..... 202

7.4 Vegetation model output under a variety of climate conditions: Dissimilarity with analytical pollen evidence ..... 205

7.5 Climatic implications for key species ..... 210

7.6 Restriction in precipitation: implications for steppe ..... 214

7.7 Aridity and humidity distribution ..... 216

7.8 Potential vegetation distribution; a regional perspective ..... 219

7.9 Elevation limits under reduced temperature and precipitation ..... 224

7.10 Discussion ..... 227

7.11 Summary of findings for Research Question 1 ..... 233

8 Research Question 2: Vegetation Modelling Framework results and discussion ..... 234

8.1 Research question ..... 234

8.2 Research Question 2 hypotheses ..... 234

8.3 Chronological modelling ..... 235

8.4 Vegetation model output under a variety of climate conditions: Dissimilarity with analytical pollen evidence ..... 239

8.5 Potential vegetation distribution; a local perspective ..... 249

8.6 Discussion ..... 259

8.7 Summary of findings for Research Question 2 ..... 269

9 Research Question 3: Vegetation modelling framework results and discussion ..... 270

9.1 Research Question ..... 270

9.2 Research Question hypotheses ..... 270

9.3 Chronological modelling ..... 272

9.4 Multiple species probability under a variety of climate conditions: Dissimilarity with analytical pollen evidence ..... 287

9.5 Significant climate-species relationships ..... 293

9.6 Summary of Research Question 3 ..... 302

10 Evaluative Discussion and Conclusions ..... 303

10.1 Success of thesis against overall research aim ..... 303

10.2 Evaluative discussion ..... 306

10.3 Improvements to the model and future work ..... 309

10.4 Conclusions ..... 312

Bibliography ..... 318

# Table of Figures

Figure 2-1 A map showing the modelling extent and study area of southwest Turkey, including provincial boundaries and perennial water bodies. ..... 35

Figure 2-2 Model hypothesis for Research Question 1. ..... 38

Figure 2-3 Hypotheses for Research Question 3 ..... 40

Figure 2-4 Hypotheses for Research Question 3 ..... 42

Figure 3-1 Overview diagram of approaches to vegetation modelling ..... 48

Figure 3-2 Conceptual model to show a deductive reasoning process, with the incorporation of data and models ..... 50

Figure 3-3 Conceptual model to show a deductive reasoning process, with the incorporation of data and models ..... 51

Figure 3-4 Technical considerations in model development ..... 56

Figure 3-5 Temporal framework of the ETEMA modelling system (Sykes, Prentice et al. 2001) 62

Figure 3-6 Method used by Spikins to selecting dominant vegetation types (Redrawn from Spikins 2000) ..... 67

Figure 3-7 (a) Conceptual diagram showing the simplification of input vegetation distribution and composition for the POLLSCAPE model (Redrawn from Sugita, Gaillard et al. 1999). (b) Schematic of POLLSCAPE approach, where *v* is the vegetation abundance parameter calculated for each ring source distance Z from the point of deposition, and ω is the background term. (redrawn from Bunting and Middleton 2005) (c) Schematic of HUMPOL approach showing cellular calculation of vegetation abundance *v* at each distance (*z*) and angle (*θ)* from the point of deposition (Redrawn from Bunting and Middleton 2005) ..... 72

Figure 4-1 Overview flow diagram of Methodology, Results and Discussion chapters ..... 83

Figure 4-2 Overview flow diagram of Chapter 5 ..... 84

Figure 4-3 Processing steps to model bioclimatic range ..... 92

Figure 4-4 Multivariate regression and species probability methodological steps ..... 96

Figure 4-5 Overall model accuracy by species ..... 105
Figure 4-6 Species probability of (a) *Castanea sativa,* and (b) *Olea europaea* across Europe. Overlaid is actual species distribution. ..... 106
Figure 4-7 Average species probability across southwest Turkey based on modern data ..... 109
Figure 4-8 *Pinus nigra* point spread weighted by the continuous probability surface beneath 111
Figure 4-9 All species points after probability distribution ..... 112
Figure 4-10 Vegetation model surface converted to raster map ready to load into HUMPOL suite ..... 113
Figure 4-11 Main species percentage in southwest Turkey, comparing model output and actual data. ..... 114
Figure 5-1 Overview of Chapter 5 methodology ..... 122
Figure 5-2 Recap of methodology ..... 125
Figure 5-3(a) Forest species potential relative percentage under modern conditions (b) Arboriculture species potential relative percentage under modern conditions (c) Relative percentage of coniferous, deciduous, steppic and grassland species potential under modern conditions ..... 129
Figure 5-4(a) Forest species potential relative percentage with varying winter minimum temperature (b) Arboriculture species potential relative percentage with decreasing winter minimum temperature (c) Relative percentage of coniferous, deciduous, steppic and grassland species potential with decreasing winter absolute temperature. ..... 130
Figure 5-5(a) Forest species potential relative percentage with varying average temperature (b) Arboriculture species potential relative percentage with decreasing winter minimum temperature (c) Relative percentage of coniferous, deciduous, steppic and grassland species potential with decreasing winter absolute temperature. ..... 131
Figure 5-6 Relative percentage with decrease in winter precipitation (a) Forest species (b) Arboriculture (c) Broad vegetation classes ..... 132

Figure 5-7 Relative percentage with increase in winter precipitation (a) Forest species (b) Arboriculture (c) Broad vegetation classes ..... 133
Figure 5-8 Relative percentage with decrease in winter precipitation and low average temperatures (a) Forest species (b) Arboriculture (c) Broad vegetation classes ..... 134
Figure 5-9 relative percentage of forest species under changes in radiation, summer precipitation and summer temperature ..... 135
Figure 5-10 relative percentage of arboriculture species under changes in radiation, summer precipitation and summer temperature ..... 135
Figure 5-11 Area map and modeled species overview under modern conditions ..... 140
Figure 5-12 Modelled species potential and relative percentages by province across southwest Turkey under modern conditions ..... 141
Figure 5-13 Modelled species percentage by species across southwest Turkey under modern conditions ..... 141
Figure 5-14 Area map and modeled species overview under -8°C ..... 142
Figure 5-15 Modelled species potential and relative percentages by province across southwest Turkey under modern conditions ..... 143
Figure 5-16 Modelled relative species concentration across southwest Turkey under -8°C ..... 143
Figure 5-17 Area map and modeled species overview -8°C and -200 mm precipitation ..... 144
Figure 5-18 Modelled species potential and relative percentages by province across southwest Turkey -8°C and -200 mm precipitation ..... 145
Figure 5-19 Modelled relative species concentration across southwest Turkey under -8°C and -200 mm precipitation ..... 145
Figure 5-20 Area map and modeled species overview +2°C ..... 146
Figure 5-21 Modelled species potential and relative percentages by province across southwest Turkey under +2°C ..... 147
Figure 5-22 Modelled relative species concentration across southwest Turkey under +2°C ..... 147
Figure 5-23 Area map and modeled species overview +100 mm precipitation ..... 148

Figure 5-24 Modelled species potential and relative percentages by province across southwest Turkey under +100mm ..... 149
Figure 5-25 Modelled relative species concentration across southwest Turkey under +100 mm precipitation ..... 149
Figure 5-26 Area map and modeled species overview +300 mm ..... 150
Figure 5-27 Modelled species potential and relative percentages by province across southwest Turkey under +300mm ..... 151
Figure 5-28 Modelled relative species concentration across southwest Turkey under +300 mm precipitation ..... 151
Figure 5-29 Area map and modeled species overview with +2°C and +50 mm summer precipitation ..... 152
Figure 5-30 Modelled relative species concentration across southwest Turkey under +2°C +50 mm summer precipitation ..... 153
Figure 5-31 Modelled relative species concentration across southwest Turkey under +2°C +50 mm summer precipitation ..... 153
Figure 5-32 Windrose based on modern values ..... 156
Figure 6-1 Flow diagram showing the overall process undertaken as described in this chapter to calibrate and identify analytical pollen zones for each key period of interest. Red boxes show work done by previous researchers. ..... 162
Figure 6-2 The position of likelihood distributions for two calibrated radiocarbon ages on the radiocarbon curve IntCal09 (Reimer, Baillie et al. 2009) ..... 178
Figure 6-3 Calibrated and modelled radiocarbon dates (a) GrN-6880 and (b) GrN-6881 under a Poisson sequence model and a K value of 0.01. The model agreement with data is 99.7%, and brackets show the 68.2% age probability. ..... 181
Figure 6-4 Karamik age-depth model using a Poisson deposition model (K=0.01). The chart shows the highest posterior density (hpd) distributions for the top and bottom boundaries of the core, 2 radiocarbon dates, and key pollen zone boundaries (i.e. zone 1/2 is the hpd for the

boundary between pollen zone 1 and 2). Convergence integrals (C) are shown for each age. The brackets and the blue boundary shows the 95.4% probability range.....186
Figure 6-5 Prior distributions for Karamik pollen boundaries, showing 68.2% brackets and crosses for median age. Pollen zones with colour gradients show the most likely pollen zone positions, whilst representing uncertainty.....187
Figure 6-6 Overview diagram of pollen sequence synchronicity across southwest Turkey. Each pollen zone is shaded to represent the chronological uncertainty attached to the zone. The core is split into two columns to allow the representation of uncertainty of conjoining pollen zones, so that zone 1 is on the left, 2 on the right, 3 on the left and so on. Brown shading represents a generally steppic pollen signature. Dark green represents predominantly coniferous, light green represents predominantly deciduous. Purple represents zones where there is a high percentage of pollen from potentially cultivated species. Double black lines indicate the position of the Santorini tephra layer, showing independent synchronisation across the cores, and helping to validate the approach .....189
Figure 6-7 Overview of comparison procedure.....194
Figure 6-8 Validation of model and data fit using modern moss polster data (Eastwood 2011, Unpublished data) and modern model output, Avlan and Elmali. .....197
Figure 6-9 Validation of model and data fit using modern moss polster data and modern model output, (Eastwood, Fyfe et al. 2011) at Ağlasun and Bereket. .....198
Figure 7-1 Highest Probability Density plots for key pollen zone boundaries potentially covering the Last Glacial Maximum. The top distribution is the beginning of the zone and the bottom is the end of the zone for each zone. Also highlighted in blue is the temporal extent of the Last Glacial Maximum period. Brackets are the 68.2% highest probability density range.....203
Figure 7-2 Radar diagram showing the similarity between simulated pollen under a variety of climate scenarios and actual pollen from Karamik pollen zones 1 and 2. A high average rank suggests relatively high similarity between model runs and data under this category. The most

similar climate scenario for these two zones is under conditions of low average temperatures and low precipitation. 206
Figure 7-3 Karamik (zones 1 and 2) dissimilarity for each model run. 206
Figure 7-4 Karamik (zones 1 and 2) model ranks for each model run. The highest rank is found under model runs with -200 mm winter precipitation, and low average temperatures (-8°C). 207
Figure 7-5 Modern Olea potential, and actual olive grove positions. 212
Figure 7-6 Olea potential under a scenario of -8°C 213
Figure 7-7 (a) Expansion of montane steppe with decreasing precipitation (b) Expansion of true steppe with decreasing precipitation 215
Figure 7-8 (a) Aridity index classes under a regime of -8°C and -200 mm. (b) Areas where average winter temperature are likely to be below freezing with a -8°C drop in temperatures. (c) A combination of these two pieces of information. This suggests areas where a combination of humidity and cold winters could lead to snow build up, as well as potential refugia areas where mild winters and humid conditions are more likely. Also shown is the location of Mount Sandıras, where maximum glacial advance is found at ~20.4 ± 1.3 $^{10}$Be ka yr BP. 218
Figure 7-9 Summary map identifying some of the mountainous regions where coniferous species are modelled to cluster under conditions of -8°C and -200 mm precipitation 220
Figure 7-10 Relative species percentages across southwest Turkey under conditions of -8°C and -200 mm precipitation 221
Figure 7-11 Model output over Isparta and Afyon showing steppic conditions. 222
Figure 7-12 Model output over Burdur and Denizli showing the predominance of steppe across this area. 222
Figure 7-13 Model output over Beydağları and Uyluk Tepe showing probable snow and ice cover at these high elevation (~3000 m) sites 223
Figure 7-14 Model output over Manavgat in Antalya showing high *Quercus coccifera* probability 223

Figure 7-15 Boxplot showing the elevation spread of a selection of species under modern conditions, showing the 25th, 50th (dashed median line) and 75th quartile. The step value is 1.5 beyond which are outliers. ..... 224
Figure 7-16 Boxplot showing the elevation spread of a selection of species modelled under a low precipitation and temperature scenario, showing the 25th, 50th (dashed median line) and 75th quartile. The step value is 1.5 beyond which are outliers. ..... 225
Figure 7-17 Boxplot showing the elevation spread of a selection of species modelled under a low precipitation and temperature scenario, where it is assumed that areas likely to be under snow and ice will not allow trees to grow. Showing the 25th, 50th (dashed median line) and 75th quartile. The step value is 1.5 beyond which are outliers. ..... 225
Figure 7-18 Palaeolithic site locations from the Tay GIS database overlaid with climate zones and main vegetation zones, under a scenario of -8°C average temperature and -200 mm precipitation. The figure shows that those Palaeolithic sites currently discovered are located relatively close to the coast, generally in humid or dry sub-humid areas, particularly in Antalya, and at low altitude. ..... 231
Figure 8-1 Pollen zones likely to cover the early Holocene period, and associated highest probability density plots. The top distribution is the beginning of the zone and the bottom distribution is the end of the zone. The blue dashed line represents the estimated beginning of climate amelioration. Pollen zones marked in red represent an open landscape. Pollen zones in green represent a significant increase in tree pollen. Brackets are the 68.2% highest probability density range. Chronological modelling suggests a significant lag between climate amelioration and pollen zones reflecting an increase in tree pollen. ..... 237
Figure 8-2 Radar diagram showing degree of similarity between simulated pollen under different climatic scenarios and analytical pollen data for the early Holocene. The most similar climate scenarios are found with low average temperature and precipitation. ..... 240
Figure 8-3 Radar diagram showing degree of similarity between simulated pollen under different climatic scenarios and analytical pollen data after tree expansion. Some spatial

variation is found between Karamik and other pollen cores. In comparison with previous zones, the most similar climate scenarios are now found with increased precipitation, and in some cases, warmer temperatures. ..... 240
Figure 8-4 Model-data similarity for pollen zones representing an open landscape during the Early Holocene. Graph shows average model ranks for a selection of model runs. The highest rank is found under a model run with -200 mm winter precipitation, and low average temperatures (-8°C). ..... 242
Figure 8-5 Model-data similarity for pollen zones representing tree expansion during the Early Holocene. Graph shows average model ranks for a selection of model runs. The highest rank is found under a model run with +300 mm winter precipitation, and low average temperatures (-8°C). ..... 242
Figure 8-6 Radar diagram showing degree of similarity between simulated pollen under different climatic scenarios and analytical pollen data for Ova pollen zone 1. This pollen zone shows similarity to scenarios of high precipitation and summer temperature ..... 247
Figure 8-7 Model-data similarity for Ova pollen zone 1 during the Early Holocene. Graph shows average model ranks for a selection of model runs. ..... 248
Figure 8-8 Model output around Karamik matching pollen from zone 4. ..... 250
Figure 8-9 Model output around Karamik matching pollen from zone 5. ..... 251
Figure 8-10 Local vegetation model output around Pınarbaşı under S8-MRs ..... 252
Figure 8-11 Local vegetation model output around Pınarbaşı under S9-MR1 ..... 253
Figure 8-12 Local vegetation model output around Gölhisar under a model run S9-MR2 ..... 254
Figure 8-13 Local vegetation model output around Gölhisar under model run S7-MR3 ..... 255
Figure 8-14 Vegetation model output around Sögüt Gölü before tree expansion, under model run S8-MR2 ..... 257
Figure 8-15 Vegetation model output around Sögüt Gölü under model run S10-MR1 ..... 257
Figure 8-16 Vegetation model output around the site of Ova Gölü under S5-MR1 ..... 258

Figure 8-17 Epipalaeolithic and Neolithic archaeological find density (green points) showing area that was modelled as steppe during the Late Glacial period. 264
Figure 8-18 Bayesian modelling of 14C dates showing the stages of occupation at Hacılar during the Neolithic (From Thissen 2010). 268
Figure 9-1 Hypotheses for Research Question 3 270
Figure 9-2 Comparison of duration and depth of the Beyşehir Occupation Phase in some pollen cores from SW Turkey. After Vermoere, Bottema et al. (2002). Data from: [1]van Zeist et al. (1975); [2]Bottema and Woldring (1984); [3]Eastwood (1997); [4, 5]Vermoere et al. (2000); 273
Figure 9-3 This figure shows posterior age estimates for the beginning of pollen zones that first contain a significant percentage of pollen from species that are commonly cultivated. The original temporal extent of the Beyşehir Occupation Phase is shown in green, and the position of the Santorini tephra is the black dashed line. Brackets show the 68.2% highest probability density range. 275
Figure 9-4 Map of southwest Turkey showing the order that potential arboriculture indicators appearing in pollen core records. 276
Figure 9-5 Map of southwest Turkey showing the order that potential arboriculture indicators appearing in pollen core records. 282
Figure 9-6 Highest probability density plots of pollen zone boundaries marking the beginning of the Beyşehir Occupation Phase 283
Figure 9-7 Relationship between the median probability of onset of the Beyşehir Occupation Phase and elevation, showing a moderately strong correlation. 284
Figure 9-8 Highest probability density plots of pollen zones showing a large decrease in cultivation indicators. 286
Figure 9-9 Median probability of pollen zones representing the end of the Beyşehir Occupation Phase, showing a strong relationship with elevation. 286

Figure 9-10 Comparison of simulated pollen with analytical pollen, Beyşehir Occupation Phase. The vertical scale represents relative rank. The higher the rank, the more similar the simulated pollen is to actual pollen values.....288
Figure 9-11 Model run ranks when compared with Gravgaz zones 2a and 2b. .....289
Figure 9-12 Model run ranks when compared with Bereket zones 2g to 2b .....290
Figure 9-13 Comparison of model output for Bereket zone 2b (During the Beyşehir Occupation Phase) and Bereket 2a (Post Beyşehir Occupation Phase) showing a change in correlation with climate scenarios. .....291
Figure 9-14 Position of probable road positions (AWMC 2011) during the Hellenistic and Roman period cross referenced against known olive oil workshops (Aydinoğlu 2008b) and pollen core locations showing the percentage component Olea pollen during the Beyşehir Occupation Phase (Using data from Eastwood, Leng et al. 2007) .....295
Figure 9-15 Modern *Olea* potential cross referenced with known olive workshop positions and the percentage *Olea* component found in pollen cores.....296
Figure 9-16 Modern *Olea* winter temperature risk cross referenced with known olive workshop positions and the percentage *Olea* component found in pollen cores.....297
Figure 9-17 *Olea* potential under a scenario of +2°C cross referenced with known positions of olive press clusters and the percentage *Olea* component found in pollen cores. .....298
Figure 9-18 Press weight locations across the territory of Hierapolis, with a modern climatic scenario. Purple stars are identified olive presses. Blue stars may be olive or grape presses ...299
Figure 9-19 Press weights locations across the territory of Hierapolis, with a scenario of +2°C temperature. Purple stars are identified olive presses. Blue stars may be olive or grape presses .....299
Figure 9-20 Press weight locations across the territory of Sagalassos, with a modern climatic scenario .....300
Figure 9-21 Press weight locations across the territory of Sagalassos, with a modern climatic scenario .....301

Figure 10-1 Difference between model output and empirical pollen evidence for Karamik zone 1, with -8°C average temperature and -200 mm winter precipitation ..... 308

# Table of Tables

Table 4-1 –Key species found in southwest Turkish pollen cores ..... 86

Table 4-2 Final parameters and data source ..... 89

Table 4-3 Identification of uncertainty of data sources ..... 90

Table 4-4 Final species choice ..... 91

Table 4-5 Species bioclimatic ranges based on European data ..... 94

Table 4-6 Species bioclimatic ranges based on European data (contd.) ..... 95

Table 4-7 Calculation of $\tau$ values for Rare Events correction ..... 103

Table 4-8 Amount of points to be distributed for each species ..... 110

Table 4-9 Summary of the robustness and assumptions of the model ..... 116

Table 5-1 Model Runs ..... 124

Table 5-2 Overview of advantaged species under changing radiation and summer climate ..... 136

Table 5-3 Overview of the HUMPOL suite ..... 154

Table 5-4 Pollen core simulation coordinates ..... 155

Table 5-5 Species PPE and Fall Speed parameterisation ..... 157

Table 6-1 Overview of radiocarbon dates and core characteristics, roughly ordered by chronological robustness ..... 168

Table 6-2 Key model parameters used within the Oxcal Bayesian modelling procedure ..... 174

Table 6-3 Bayesian Modelling Output Diagnostics ..... 176

Table 6-4 The calibration of Karamik core radiocarbon dates (IntCal09) ..... 177

Table 6-5 Output Bayesian modelling using different deposition models, Karamik core ..... 180

Table 6-6 Modelled Karamik core radiocarbon dates and vegetation zones ..... 183

Table 6-7 The 68.2% Highest Posterior Density (hpd) for the beginning each pollen zone in the Karamik core, and the estimated archaeological period that the pollen zone covers. ..... 184

Table 6-8 Example pollen zone from Koycegiz, with pollen sum, calculated percentage, and comparison to simulated pollen percentages under a scenario of modern climate. Similarity between model and data in this instance is relatively low. ..... 195

Table 7-1 Model hypothesis for Research Question 1.....201
Table 7-2 Pollen zones correlated to the Last Glacial Maximum (24 to 19 Cal ka yr BP). .....204
Table 7-3 Chord dissimilarity measures for the Glacial period comparing simulated pollen from model runs with actual pollen evidence. .....208
Table 7-4 Elevation limits of species under modern climatic conditions, and under model run S8-MR2.....226
Table 8-1Model hypotheses for Research Question 2.....234
Table 8-2 Most probable pollen zones to cover the period of aridity between 12 000 and 8000 Cal yr BP .....238
Table 8-3 Dissimilarity measures between model output and data for pollen zones reflecting steppic species at the beginning of the Holocene .....244
Table 8-4 Dissimilarity measures between model output and data for pollen zones reflecting tree expansion at the beginning of the Holocene.....245
Table 8-5 A cross reference of Neolithic find sites with modeled climate classes during the Late Glacial period.....265
Table 8-6 Climate key .....266
Table 9-1 Pollen zones correlated with the 2nd millennium BC, and evidence for cultivation....278
Table 9-2 68.2% highest probability density range for the beginning of pollen zones marking the beginning of the Beyşehir Occupation Phase.....284

# 1 RESEARCH AIM, INTRODUCTION AND RESEARCH SCOPE

## 1.1 RESEARCH AIM

**The research aim for this PhD thesis is to develop and implement a vegetation modelling framework tailored to Mediterranean southwest Turkey. To acknowledge the complexity of the problem space, the model will take a multifaceted approach incorporating bioclimatic, spatial, chronological and palynological modelling elements.**

Once the model framework is established, model scenarios, runs and simulations will be implemented that engage with three important research questions:

i) Can the model framework provide a coherent narrative to explain evidence of high lake stands concurrent with steppic vegetation signatures during the Late Glacial period? (~23 to 19 Cal ka yr BP)

ii) Does the model framework provide further evidence to support or reject a lag in tree expansion at the beginning of the Holocene (~11 to 8 Cal ka yr BP), and if so, is there evidence for a climatic reason for this?

iii) To what extent can the model framework inform on the timing, magnitude and reasons for the Beyşehir Occupation Phase (~3.8 to 1.4 Cal ka yr BP)?

The research questions are formulated around key palaeoecological and cultural debates set in southwest Turkey, but all have relevance in the evolution of the wider Mediterranean. These debates will be discussed throughout the thesis.

## 1.2 INTRODUCTION

The impetus for this thesis is borne out of a recognition that traditional approaches to palaeoenvironmental enquiry have had limited success as single disciplines (i.e. archaeology, palaeoecology, palaeoclimatology) in answering large overarching questions of landscape evolution; such as the relative influence of climate and human agency on the flora, fauna and culture of a particular region, the temporal continuity and discontinuity between environmental events, and the spatial continuity and discontinuity of vegetation, environment and culture across a dynamic landscape. The overwhelming reasons for this are firstly the patchy, heterogeneous and potentially biased nature of palaeoenvironmental, archaeological and palaeoclimatological data available, and secondly the complexity of the systems involved, resulting in a limited picture gained from only one discipline. Until adequate data are collected, which may never be forthcoming, modelling affords a route to move beyond the data, and to deal with the nexus of different disciplines. This can be achieved alongside the use of statistical methods which can define uncertainty and test hypotheses and theories. Ultimately a modelling framework can provide a useful approach to clarify and ultimately understand these events.

These four issues; unresolved palaeoenvironmental debates, patchy, heterogeneous palaeodata, complex systems, and a lack of understanding of the mechanisms, causes and appearance of palaeolandscapes are particularly apparent in the Mediterranean, therefore making it a prime candidate and a challenge for modelling studies. To date, there have been few such modelling studies attempted and even less that engage with the complex vegetation history of the region. This is crucial, as vegetation evidence is one form of palaeodata that can have relatively continuous records (through pollen cores), and reflects the multifarious spheres of influence of climate, topography and human agency. As Di Pasquale et al. state:

> " The forest vegetation can be read as an element of the mosaic of cultural landscapes of various ages and therefore it can be studied like an archaeological

> feature (Rackham 1992); but it is curious that this approach, based on different and rich materials (biological, archaeological and historical), is rarely taken up by ecologists and environmental experts."
>
> (Di Pasquale, Di Martino et al. 2004 p. 14)

The 'curious' nature of a lack of vegetation modelling using multidisciplinary datasets in the Mediterranean can be better understood through examining the successes and limitations of previous vegetation modelling studies, and the particular issues that the Mediterranean environment brings. For instance, there has traditionally been a palaeoecological research focus on Northern European contexts due to the geographical clustering of key researchers in this area (e.g. Andersen 1970; Bradshaw 1980; Caseldine, Fyfe et al. 2007; Broström, Neilson et al. 2008). The types of species studied and the processes of succession and mechanisms of plant proliferation are for the most part based on northern European contexts, therefore creating a relative lack of information on Mediterranean species dynamics. Secondly, there are methodological challenges of the Mediterranean environment, in particular a data deficit and bias due to poor preservation in highly desiccating, erosional or depositional environments. There is also often a mismatch between the types of complex questions and issues that arise in archaeological and palaeoenvironmental discourse (Weiss 1982; Issar 1998; Vanhaverbeke, Vionis et al. 2009), and the quality, scale and amount of data available (Betancourt 1987; Athanassopoulos and Wandsnider 2004). If palaeoecological records are considered poorer in the Mediterranean than in northern Europe, archaeological records are arguably richer, setting up a disjunction between the two fields. The current challenge for the future of palaeoenvironmental study is therefore to move beyond these singular disciplines, in order to understand multidisciplinary links between climate, topography, competition, anthropogenic influence and vegetation development through time, and to understand complex variation through space.

Summarising current debates in Mediterranean palaeoecology, the previous understanding of climate and anthropogenic influence on vegetation has generally been split between processes in the early, mid and late Holocene (e.g. Magny, Miramont et al. 2002). In the Late Glacial and early Holocene periods, discourse focuses around two key areas. Firstly, the climatic restriction of plant and tree species due to cold and / or arid conditions across the Mediterranean is theorised from palaeoecological records, which potentially contradicts evidence from independent climate records of high lake and sea levels (Médail and Diadema 2009). Secondly, the role and distribution of areas of refugia for key Mediterranean and temperate species, and the expansion out of these favourable areas at the beginning of the Holocene is still a developing topic (Brewer, Cheddadi et al. 2002; Taberlet and Cheddadi 2002; Krebs, Conedera et al. 2004), and the timing and extent of a lag between climate change and migration of tree species at the beginning of the Holocene is also a key debate (van Zeist and Bottema 1991; Roberts and Wright 1993; Stevens, Wright et al. 2001).

In the mid Holocene, there is traditionally assumed to be a 'golden age' for Mediterranean vegetation, with Mediterranean forest and maquis prevalent across large swaths of the environment (Tomaselli 1977; Thirgood 1981). However, this in the main depends on interpretations of palynological records, which are now known to have a large number of issues, assumptions and provisos in order to interpret them robustly (Prentice 1985; Sugita 1997; Sugita, Gaillard et al. 1999; Neilsen 2005). In the later Holocene, the main unanswered landscape debates revolve around the nature of human exploitation of the environment, and its impact on natural succession cycles. From an ecological perspective there is particular interest in understanding polyclimax succession through a continuous landscape, the extent and longevity of the natural Mediterranean forest stage and what constitutes a natural landscape (Naveh 1982; Christensen 1988). From an archaeological perspective issues cluster around the extent and intensity of anthropogenic influence on the landscape, through agriculture, grazing, settlement, deforestation and fire (Forbes and Koster 1976). The principal dichotomy is therefore between the mainly climatically influenced early Holocene vegetation, and the

predominantly anthropogenically influenced late Holocene vegetation, with around 5000 BP being the dividing line (e.g. Médail and Diadema 2009). The assumption of a modern degraded Mediterranean landscape necessarily accepts the premise of a rich Mediterranean vegetative environment prior to the impact of intensive human agency on the landscape. However, as stated above, this premise has not yet been satisfactorily proven, and it is becoming apparent that the subtleties and nuances of these relative influences through time are not yet developed enough to be confident in this assumption (Grove and Rackham 2003).

With these multidisciplinary debates in mind, this thesis aims to develop a Mediterranean based multidisciplinary model with vegetation modelling as its core, allowing the model to be useful in a range of contexts, which will engage with theories of natural processes, climatic influence and human agency.

To review, the context for this research can be summarized as being based on three key premises defined below:

(a) Late Glacial and Holocene vegetation change in the Mediterranean is a topic of major importance as it reflects periods of significant change in landscape evolution, climate and culture.

(b) More research is required to characterize Late Glacial and Holocene vegetation change and landscape diversity in the Mediterranean than can be provided by the direct interpretation of data from single disciplines, such as palynological, archaeological and climatological data.

(c) Given the uncertainties involved in reconstructing past landscape and vegetation patterns using traditional methods such as palynology, particularly in Mediterranean environments, multidisciplinary modelling is a required approach in order to combine climatological and ecological processes, and move forward.

This thesis demonstrates that modelling can bring together data from disparate disciplines, whilst robustly defining uncertainty, allowing the testing of hypotheses through scenario and simulation. By developing a new multidisciplinary model tailored to the southwest of Turkey, this thesis showcases the potential of vegetation modelling as a promising approach within Mediterranean environments.

### 1.2.1 The case study of southwest Turkey

The significance and strength of southwest Turkey as a particular lens on the Mediterranean, and a basis for the vegetation model lies firstly in its geographical position, being at the margin of Mediterranean and steppic regions today, but previously showing signs of more temperate vegetation (Roberts and Wright 1993). It is secondly significant as it provides a substantial archive of palaeoecological records for such a marginal environment, its lake records, allowing for palynological and climatic assessment (van Zeist, Woldring et al. 1975; Bottema and Woldring 1984; Eastwood, Roberts et al. 1999; Vermoere 2002; Eastwood, Leng et al. 2007; Kaniewski, De Laet et al. 2007). Furthermore, it has an incredibly rich cultural history, and as importantly, a series of rigorous historical, archaeological and geoarchaeological studies to provide a resource for discussion (Broughton 1938; Magie 1950; Roberts 1987; Mitchell 1995; Vermoere, Smets et al. 2000; Vanhaverbeke and Waelkens 2003; Kaniewski, De Laet et al. 2007; Vanhaverbeke, Vionis et al. 2009).

Decades of palynological and palaeoclimatological research throughout Anatolia, and southwest Turkey in particular, have uncovered tantalising evidence of major landscape changes since the end of the last ice age, which echoes the major themes across the Mediterranean. As across the rest of the Mediterranean, palaeoclimate proxies from Turkey show a discrepancy between steppic vegetation interpreted from fossil pollen evidence, and advancing glaciers and high lake levels interpreted from sedimentological and geochemical analysis during the Late Glacial

period (van Zeist, Woldring et al. 1975; van Zeist and Bottema 1982; Eastwood, Roberts et al. 1999; Eastwood, Leng et al. 2007). During the Early Holocene, a potential lag between climate amelioration and vegetation is apparent, apart from a key area surrounding the Black Sea, which is considered to be a potential refugia area (Wick, Lemcke et al. 2003; Eastwood, Leng et al. 2007; Fleitmann, Cheng et al. 2009). As in other areas of the Mediterranean, a coherent narrative of vegetation development alongside climatological records is yet to be forthcoming, due in part to difficulty in providing adequate evidence from any one discipline to deal with complex issues, and secondly to a series of challenging mismatches in data interpretation between different disciplines. However, overcoming these issues by fully utilising the rich available data, and employing a modelling approach to explore and counter these difficulties has the capacity to inform not just on vegetation and climate, but also on key questions of historical and archaeological importance.

Until fairly recently, analysis in Anatolia had focused on the major extant remains of settlement, from the remarkable remains of Neolithic Çatal Höyük (Mellaart 1962; Mellaart 1962), to Bronze Age settlements of Hacılar and Boğazdöy (Mellaart 1958), through Iron Age Gordion, to the magnificent Imperial cities, such as Byzantium, Sagalassos, Termessos and Kibyra (Coulton 1988; Waelkens, Paulissen et al. 1997; Baird 2004). However, archaeologists and historians have become increasingly interested in how the environment and the landscape potentially affects the development of human society. Reaching back to the Neolithic, Anatolia was an incredibly important place for the development of hunter-gatherer communities, as well as the development of agriculture and stable farming communities (Schoop 2005). In particular, it is acknowledged that marginal environments such as the mountainous areas of Turkey may become particularly important in understanding experiments in societal development. Changes in climate at the beginning of the Holocene could have key implications for the adaptation, trade and movement of Neolithic communities.

Furthermore, detailed historical and archaeological analysis has discovered that along with the emergence and expansion of symbols of sophisticated urban society, material wealth and power during the mid to late Holocene, were periods of intense turbulence and contraction (Mitchell 1995; Vermoere, Smets et al. 2000; Vanhaverbeke and Waelkens 2003). Preliminary comparisons with palynological evidence shows that these events are sometimes reflected in pollen records, but at other times can show contradictory evidence of cultivation and a thriving rural economy in periods of supposed societal decline. For example, during the 2nd millenium BC (Mid-Bronze Age) archaeological evidence of settlement is rare (Waelkens 2000; Vermoere 2002), however, pollen evidence suggests cultivation and grazing indicators (van Zeist, Woldring et al. 1975). A further example is the period between the collapse of the Phrygian kingdom at the end of the 7th century BC, to the 4th century BC. This is a known gap in both historical and archaeological evidence (Mitchell 1995). Nonetheless, palynological evidence again reflects a continuing period of cultivation during this phase (van Zeist, Woldring et al. 1975; Bottema and Woldring 1984), suggesting a potential contraction to rural areas.

The later Holocene encapsulates the enigmatic period known as the Beyşehir Occupation Phase (BOP). Palynological evidence suggests a period of deforestation at around 3.7 Cal ka yr BP, followed by cultivation intensification throughout most of the southwest (van Zeist, Woldring et al. 1975; Bottema and Woldring 1984; Eastwood, Roberts et al. 1998; Vermoere, Bottema et al. 2002). The BOP is one of the first expressions of human impact on the natural environment for the east Mediterranean region, and southwest Turkey in particular. However, the agricultural carrying capacities of these environments through the Hellenistic, Persian, Roman and Byzantine periods are not well understood (Mitchell 1995; Mitchell 2005). Complicating matters are the extent to which agricultural intensity in montane regions (such as olive cultivation) finds expression in the pollen data alongside evidence of climate change (Izdebski 2011).

Contraction is also seen in the Roman period, notably during the 3rd Century AD crisis, evidenced from the sharp decline in visible prosperity and urban organisation across the Empire (Mitchell 1995). As stated by Mitchell, the extent of the crisis in Anatolia is a key issue for debate; emphasising the importance and resilience of rural life and the agricultural economy in providing a continuation of culture and economic prosperity through to the 4th Century AD when imperial recovery was underway (Mitchell 1995). This theme of rural resilience further emerges during the Late Roman and early Byzantine era. During this period, Mitchell theorises a distinction between the rising power of the Church throughout urban networks of the region, and the relative autonomy of rural areas. With the eventual decline of civic institutions during the 6th and 7th Centuries and the invasion of the Persians under Chosroes in AD 613, a historical and archaeological 'dark age' had begun. But the actual extent of societal contraction has been questioned by a number of scholars, including Mitchell, and notably Vanhaverbeke (2009) and Haldon (2006)

One of the underlying themes of recent historical and archaeological analysis is therefore the potential contrast between urban volatility, and rural continuation during these times of upheaval. Palaeoecological evidence may provide a unique way of assessing the continuation of rural life during periods of institutional breakdown, however to do so it is key to assess and understand the resolution, chronology and representation of such ecological records so that they can be used in an appropriate manner. The combination of vegetation and palynological as proposed in this thesis may bring to bear new perspectives on this important discourse.

## 1.3 Overview of the Vegetation Modelling Framework

This thesis is set in an area with one of the most interesting, important and complex areas in the world, with a tradition of expert archaeological, historical and palynological analysis, and vibrant multidisciplinary debate. This thesis will demonstrate that a vegetation modelling framework is capable of engaging with these key debates in a multidisciplinary manner.

The framework essentially contains three components. The bioclimatic model first defines a probabilistic basis for modern species distribution, through climate, soils and topography. This section alone can provide important insights into the potential reasons behind species expansion and contraction (although it must be remembered that in order utilise the model for palaeoecological purposes the method requires certain assumptions of Uniformitarianism to be upheld).

As a second component, it was deemed important to compare model output to actual palaeoecological data. However, the most widespread evidence for palaeovegetation distribution across the whole region is considered to be sourced from palynological (fossil pollen) data. This presented two main challenges for the comparison of model output with data. Firstly, vegetation model output was not directly comparable with pollen data, the reasons for which will be elaborated upon in Chapter 4. Secondly, in order to investigate the spatial variability of pollen assemblage across the landscape at particular points in time, a synchronised pollen basis was required, which did not exist due to chronological issues discussed in Chapter 7. Therefore two further modelling components were required. Vegetation model output was converted to simulated pollen assemblages using the HUMPOL model suite, to create comparable datasets. This section raises important questions regarding the representation of vegetation in the pollen record, and assumptions of pollen travel.

Secondly, Bayesian modelling of the analytical pollen core chronology was undertaken to synchronise pollen cores and define the chronological uncertainty through time. This section raises issues concerning the amount of uncertainty attached to key vegetation phases, and requires assumptions of deposition criteria where data is not available.

Once these methodological challenges were achieved, and assumptions identified, the bioclimatic model was run under a number of modelling scenarios. These were then converted to pollen simulations for key points in the landscape using the HUMPOL model. This allowed comparison of simulated pollen with analytical pollen for key periods of time. By comparing the

best fitting climate scenarios with independent climate evidence it was possible to discuss whether climate and vegetation were likely to be telling a coherent narrative. If climate evidence and model output are not coherent, it provides clues as to whether other factors such as human agency have overridden the climate-vegetation signal.

Furthermore, GIS visualisations of climate and individual species relationships will be explored where useful to demonstrate key correlations and mechanisms. The implications of model results will also be briefly discussed against archaeological and historical data where possible.

The thesis details a novel approach to modelling in terms of the species assemblage used, the geographical area studied, and resolution of analysis undertaken. It develops a model framework through which palaeoclimate scenarios can be compared with empirical palaeoenvironmental data which has been chronologically modelled, providing context for discussion against archaeological and historical data. By this combination of approaches, the model will be released from the constraints of empirical data from single disciplines, and will instead use the breadth of data as a comparison and evidential support for a series of scenarios based on actual hypothesis.

In order to contextualise the thesis, the next chapter will begin by introducing the Mediterranean region, and the study area of southwest Turkey.

# Chapter 2

# The Geographical Setting and Research Question Context

The aim of this chapter is to provide context to the three key research questions of this thesis. Because the research questions are interdisciplinary and sit at the nexus of many important debates the chapter summarises a series of in-depth, wide reaching literature searches to contextualise model development. The chapter highlights key literature that provides the basis for the research questions, however, a series of informational appendices are also presented at the end of the thesis for reference, that elaborate on specific aspects of the research. Following a summary of each research question, the issues will be crystallised into a number of hypotheses that will later be testable by the model.

As a result of this research, the chapter assesses the main barriers that have so far precluded the research questions being answered. The chapter ends by highlighting how the modelling approach in this thesis may overcome the identified barriers to provide new insight.

# 2 THE GEOGRAPHICAL SETTING AND RESEARCH QUESTION CONTEXT

## 2.1 STUDY AREA - SOUTHWEST TURKEY

Southwest Turkey has particular significance as a test bed for palaeoecological modelling due to its geographical position and rich palynological archive (van Zeist, Woldring et al. 1975; Bottema and Woldring 1984; Bottema, Woldring et al. 1986; Roberts 1990; Bottema, Woldring et al. 1993; Roberts, Reed et al. 2001; Wick, Lemcke et al. 2003). It also hosts an array of palaeoclimatic studies from lake and speleothem studies to geomorphological and gastropod studies (Roberts, Eastwood et al. 1997; Wick, Lemcke et al. 2003; Eastwood, Leng et al. 2007). Further to this it has an established record of archaeological excavations and field surveys due partly to the work of the British Institute at Ankara, and important historical and cultural works (Broughton 1938; Mellaart 1958; Mellaart 1962; Mellaart 1962; Coulton 1988; Mitchell 1995; Waelkens, Paulissen et al. 1997; Waelkens 1999; Waelkens 2000; Vanhaverbeke, Vionis et al. 2009)

Figure 2-1 shows a map of Turkey, including provincial boundaries and water bodies, and defines the region of southwest Turkey that is the focus for this study. It also defines the area that will be used for modelling. The modelling extent is larger than the study area in order to avoid any edge effects when modelling (Wheatley and Gillings 2002).

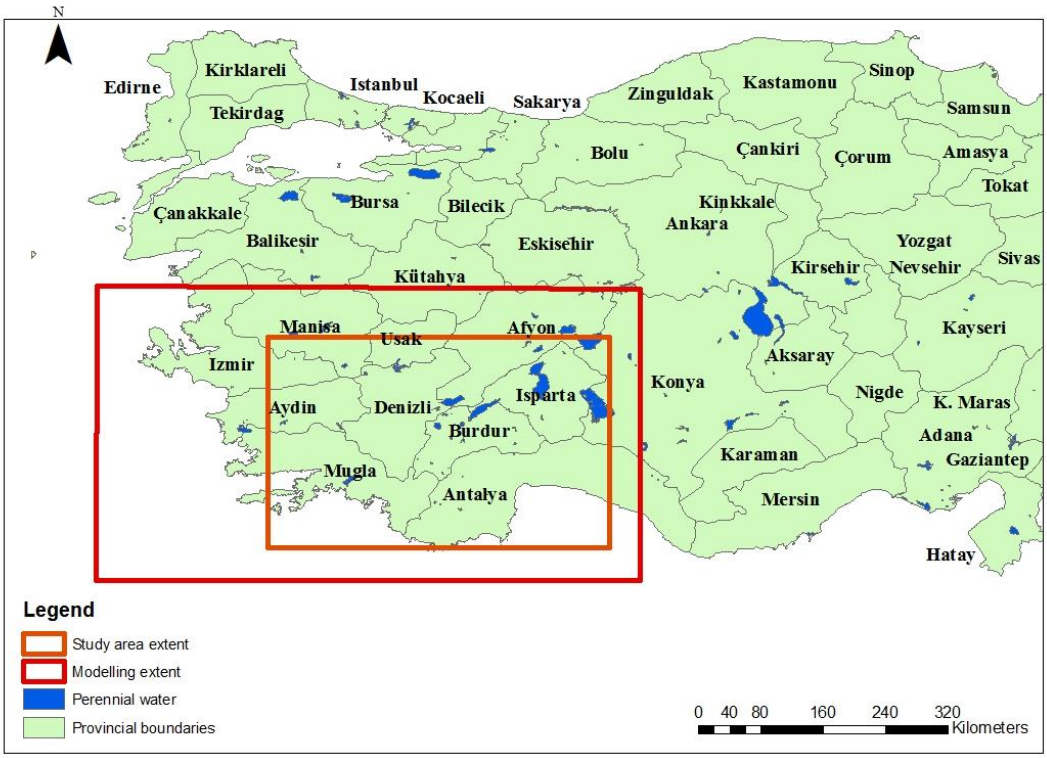


**Figure 2-1 A map showing the modelling extent and study area of southwest Turkey, including provincial boundaries and perennial water bodies.**

Four preliminary research areas were considered important to provide background context to the aim and research quesstions of this thesis. They were to:

1. Understand and define what is meant by the Mediterranean
2. Assess palaeoclimatological and palaeoecological information from the wider Mediterranean relevant to the thesis
3. Understand the physical setting of southwest Turkey
4. Assess palaeoclimatological and palaeoecological information from southwest Turkey

As part of contextualisation of this thesis, all of these aspects were considered and summarised to provide a useful reference to the development of the thesis proper. As each topic is not insignificant in scope and breadth, they were considered to divert from the main focus of the thesis and are therefore not included in the main body, however, as they are likely to provide a useful reference to the reader, these summaries are positioned in appendices 1-5.

## 2.2 RESEARCH QUESTION CONTEXT AND MODEL HYPOTHESES

Drawing from summaries provided in appendices 1-5, this section will provide a concise précis for each research question.

### 2.2.1 Context for Research Question 1

During the Last Glacial Maximum (~24 to 19 Cal ka yr BP) foraminifera proxy data indicates cool SST in the Levantine Basin (Hayes, Kucera et al. 2005), stable isotope analysis indicates low average temperature in Israel (McGarry, Bar-Matthews et al. 2004), and stable isotope analysis suggests climatic aridity in Turkey (Roberts, Jones et al. 2008). A general trend shows high lake levels throughout the period 24 Cal ka yr BP to 19 Cal ka yr BP, after which lake levels drop with a low stand at ~17 Cal ka yr BP (Bartov, Stein et al. 2002; Bartov, Goldstein et al. 2003). Evidence suggests that a marked difference in global climatic conditions was manifest in the Mediterranean during the last glacial period than modern conditions; characterised by cooler temperatures, and relatively high lake levels.

In southwest Turkey in particular, geomorphological data suggest that a 'local' glacial maximum on Mt Sandiras occurred at ~20.4 ± 0.13 $^{10}$Be ka yr BP (Sarıkaya, Zreda et al. 2008). Similarly to Jordan, high lake level stands are apparent (and partially coeval) at Konya basin and Lake Van in Turkey. Fossil shoreline evidence at Beydili and Kılbasan, Konya basin shows high lake levels from approximately 28 to 23 $^{14}$C ka yr BP (Roberts 1983), and evidence from the highest accumulation terrace at Lake Van suggests high lake levels between 20 corr. $^{14}$C ka yr BP to 18 corr. $^{14}$C ka yr BP (Landmann, Reimer et al. 1996). The presence of planktonic diatoms and laminated sediments at Eski Acigöl also points to deep water conditions (Roberts, Reed et al. 2001).

In comparison to climate evidence, pollen data across the Mediterranean and Middle East for this time period is characterised predominantly by a rich steppe community, comprising *Artemisia*, Chenopodiaceae, Gramineae and Cerealia-type pollen (van Zeist and Wright 1963; Niklewski and Van Zeist 1970; van Zeist and Bottema 1977). Where arboreal pollen is found, it

comprises deciduous *Quercus* and *Betula*, along with coniferous taxa comprising *Cedrus*, *Pinus* and *Abies* (van Zeist, Woldring et al. 1975). This presents an apparent dichotomy between cool and humid conditions from palaeoclimatic and sedimentological evidence, and arid conditions from palaeoecology. Although hypotheses have been proposed regarding the impact of low precipitation and temperature together (Prentice, Guiot et al. 1992; Roberts and Wright 1993) modelling studies to fully explore this hypothesis are rare (Robinson, Black et al. 2006). By utilising vegetation modelling and pollen simulation this thesis aims to engage with these hypotheses, linking climate, vegetation and pollen representation.

This period is also important from an archaeological perspective as it provides the context for little understood Epipalaeolithic communities. Climate, topography and vegetation together provide the baseline on which fauna and human society can adapt and evolve. Learning more about the environment that these early communities lived in, and identifying key spatial and temporal variation in their environment provides insight that may lead to future hypotheses regarding key migration patterns, adaptations or evolutionary events.

By examining the probabilistic effects of climate change on vegetation composition, not only through precipitation and temperature modelling but also through the consideration of aridity and humidity, the approach taken provides a unique analysis of possible climate-vegetation linkages at the landscape scale, and species level.

In order to provide a testable basis for the model, a hypothesis is formed that may be supported or rejected by the model output. The working hypothesis is that low evaporation allowed lake levels to remain high, but prevented vegetation from developing particularly in the interior of the region. Whether low precipitation and low temperature combined may have resulted in this scenario can be tested with the model, and forms the basis of a null and alternative hypothesis as shown in Figure 2-2.

**Figure 2-2 Model hypothesis for Research Question 1.**

**H1: Low precipitation and temperature during the Last Glacial Maximum provides a possible climatic basis for steppic species distribution, high lake levels and glacial advance.**

**H0: Low precipitation and temperature during the Last Glacial Maximum does not provide a possible climatic basis for steppic species distribution, high lake levels and glacial advance.**

### 2.2.2 Context for research question 2

A range of climate proxy data including foraminifera (Bar-Matthews, Ayalon et al. 2003), cave speleothem (Bar-Matthews, Ayalon et al. 1999; Bar-Matthews, Ayalon et al. 2000) gastropod characterisation, soil characterisation, (Rossignol-Strick 1999), marine sapropel (Fontugne, Arnold et al. 1994) and climate modelling (Kutzbach and Guetter 1986) suggest a significant increase in precipitation and temperature occurred during the early Holocene period (~11500 to 11000 Cal yr BP). For Turkey in particular, authigenic stable isotopic and mineralogy data from Lake Van suggest that even as early as ~12.4 Cal ka yr BP there was a rapid change to more humid climatic conditions than the preceding late glacial period, and lake levels are high. Geochemical and isotopic indicators from cores taken at Eski Acigöl dry crater lake also reflects deep water conditions and low salinities during this period (Roberts, Reed et al. 2001). As part of the ISOMED synthesis (Roberts, Jones et al. 2008) normalisation of isotopic records across a series of Eastern Mediterranean lakes was carried out, allowing multi-centennial trends to be analysed. This analysis showed that more negative values were found before 7900 $^{14}$C BP, suggesting high moisture availability. In particular analysis of lake shorelines and lake cores

from the Dead Sea provided evidence for high water levels between 10 000 Cal yr BP and 8000 Cal yr BP, and a fall in levels at around 7700 Cal yr (Migowski, Stein et al. 2006).

Analytical pollen data for the early Holocene is found to be significantly different in composition to that of the Late Glacial period. A rapid shift from *Artemisia* steppe to grassland is evident at Eski Acigöl and Lake Van at the beginning of the Holocene, and a rise in *Pistacia*, which seems to reflect climate amelioration (Roberts, Reed et al. 2001). However, a delayed response of Arboreal Pollen is also identified at Lake Van and Lake Zeribar. This lag has been estimated to take in the order of 3000 years or more to reach an AP maximum, which generally occurs between around 7500 – 5500 Cal yr BP (van Zeist and Bottema 1991; Roberts and Wright 1993; Eastwood, Roberts et al. 1999; Roberts, Reed et al. 2001; Roberts, Brayshaw et al. 2011). The precise reasons for this are yet to be established and may include many factors, such as low effective precipitation (Bottema and Woldring 1984) and moisture stress (Roberts, Reed et al. 2001). Evidence from southwest Asia suggests that forest migration lag occurred in interior areas due to a climate drier than present during the early part of the Holocene (Roberts and Wright 1993). However, limnological and pollen evidence from Eski Acigöl (an inland site) suggests a delayed increase in Arboreal Pollen despite deep, dilute lake conditions suggesting greater moisture availability.

Roberts et al. (2001) posit that this evidence together may reflect a significant disequilibrium between woodland density/composition and climate in the semi-arid and sub-humid interior regions of southwest Asia during this period.

To provide further input to this debate, vegetation modelling and pollen simulation will be undertaken to establish the temporal and spatial variability in vegetation change in southwest Turkey at the beginning of the Holocene, and potential links between this distribution and climate will be assessed. Based on previous literature, and reconstructed climate evidence, the modelling process for research question 2 starts out with 2 hypotheses (Figure 2-3), which may be supported or rejected by the model output.

**Figure 2-3 Hypotheses for Research Question 3**

| |
|---|
| **H1: Pollen zones from southwest Turkey suggest a lag in tree expansion at the beginning of the Holocene**<br><br>**H0: Pollen zones from southwest Turkey do not suggest a lag in tree expansion at the beginning of the Holocene** |
| **If H1 is supported, then:** |
| **H2: Model output supports the suggestion of a climatic reason for a lag in tree expansion at the beginning of the Holocene**<br><br>**H0: Model output does not support the suggestion of a climatic reason for a lag in tree expansion at the beginning of the Holocene** |

### 2.2.3 Context for Research Question 3

Palynological investigations from coring activities defined a period of human impact known as the Beyşehir Occupation Phase, named after the place where this anthropogenically influenced period was first discovered (van Zeist, Woldring et al. 1975; Bottema and Woldring 1984; Eastwood, Roberts et al. 1999; Vermoere, Bottema et al. 2002). The traditional chronology of the Beyşehir Occupation Phase is between ~3500 to 1500 $^{14}$C BP, calibrated to ~3800 to 1400 Cal yr BP (~1800 BC to AD 600). The Beyşehir Occupation Phase is most clearly visible in SW Turkey, and definition of the full spatial extent of the Beyşehir Occupation phase is hampered in

that there are only a few sites in central Turkey (such as Nar Gölü) that have yielded palaeoecological records. However a similar phase has been recorded in sporadic sites in NW Turkey and northwestern Greece (England, Eastwood et al. 2008).

The beginning and the end of the phase is defined mainly by arboriculture, with species such as grape (*Vitis vinifera*), walnut (*Juglans regia*), olive (*Olea europaea*) and manna ash (*Fraxinus ornus*), but also the plane tree (*Platanus orientalis*). Secondary Anthropogenic Indicators (SAI) such as *Plantago lanceolata* and *Sanguisorba minor* are also found as part of this phase and are taken as indications of disturbed land, or grazing. Since its discovery at Beyşehir, a number of questions still remain with regards to the timing, intensity and reasons for the phase.

By the Hellenistic and Roman period climate evidence from around the Mediterranean suggests a warmer and wetter phase than present day conditions, particularly between ~1950 and 1600 Cal yr BP, or BC 200 to AD 400 (e.g. Lamb 1977). Speleothem records at Soreq cave provide evidence for a rise in humidity at ~1950 Cal yr BP (Orland, Bar-Matthews et al. 2009) and the Dead Sea shows an increase in levels around this time (Migowski, Stein et al. 2006, Bookman et al. 2004). In addition, an isotopic analysis of trees used to construct a Roman siege ramp at the Fortress of Masada above the Dead Sea also indicates a humid peak at ~ 1950 Cal yr BP (Issar and Yakir 1997). This correlates with an increase in pollen proportion from primary and secondary anthropogenic indicators across southwest Turkey.

Based on reconstructed climate evidence, modelling for this research question is based on 4 hypotheses, which may be supported or rejected by the model output.

**Figure 2-4 Hypotheses for Research Question 3**

| |
|---|
| **H1: The beginning of the BO phase is synchronous across southwest Turkey**<br><br>**H0: The beginning of the BO phase is not synchronous across southwest Turkey** |
| **H2: Chronological modelling suggests the continuation of cultivation throughout the Mid-Bronze Age**<br><br>**H0: Chronological modelling does not suggest the continuation of cultivation throughout the Mid-Bronze Age** |
| **H3: Climate change is implicated in the expansion of the BO phase during the Hellenistic to Late Roman period**<br><br>**H0: Climate change is not implicated in the expansion of the BO phase during the Hellenistic and Late Roman period** |
| **H4: The end of the BO phase is synchronized across southwest Turkey**<br><br>**H0: The end of the BO phase is not synchronized across southwest Turkey** |

## 2.3 IDENTIFIED BARRIERS TO PROGRESS WITH KEY RESEARCH QUESTIONS

As this review was undertaken, a number of issues were encountered with relation to the comparison of evidence from different fields of study, and different scales of analysis, which are likely to hamper multidisciplinary academic investigation.

The first potential issue identified was that chronological differences between dating methods have a profound impact on the potential for comparison of evidence from different fields. Calibrated and un-calibrated radiocarbon dates, laminated lake sediment years, archaeological ages and Beryllium dates were encountered. radiocarbon dates associated with pollen evidence from across Europe were given calibrated ages where possible, however the dates from Turkish pollen core records have traditionally been given in un-calibrated $^{14}C$ years BP. A further

difficulty was being able to compare pollen cores within Turkey, again due to variable chronological control. A subtask for this thesis was therefore to calibrate these dates and to examine how pollen cores could be better compared across the region to facilitate future discussion and analysis.

It is also recognised that palaeodata is in general patchy and heterogeneous. The preservation of palaeoecological data depends on the lithological and climatological conditions under which it has been deposited, palaeoclimate data is often discontinuous, and archaeological data is also notoriously variable in distribution and preservation, making consistent narratives challenging. For this reason it is recommended that a subset of palaeodata is best used as a basis for modelling efforts, which can explore many possibilities, and aid the reconstruction of coherent narratives. These models can then be tested using *independent* palaeodata to compare model output at disparate points throughout the model where evidence exists.

As a further observation, many continuous palaeoenvironmental records from throughout the Holocene have a relatively low temporal resolution. Comparing pollen evidence with archaeological evidence is a case in point, where cores with generally around decadal to centennial resolution are compared with archaeological evidence that has potentially single year precision (the exception being laminated lake sediments, but these are rare). Palaeoclimate data is rarely precise enough to offer exact details of temperature and precipitation change, instead giving estimates of relative climate through time.

The spatial resolution of a climate or vegetation proxy is also a potential issue. Palaeoclimatic evidence tends to be spatially disparate and often does not directly relate to the temporal or spatial granularity of archaeological or palaeoecological data. Archaeological analysis on its own tends to focus on key sites or small areas in great detail, however it is difficult to expand into regional narratives to compare with larger climate models without a great amount of data and excavation, which is timely, costly and falls victim to preservation and excavation bias. Furthermore, pollen productivity differences and pollen dispersal bias between species distorts

a direct interpretation from being made. These issues will be investigated further within this thesis. They are not easily countered, however steps can be taken towards providing high resolution modelling that does not violate the limits of the palaeoenvironmental evidence being used as a basis, whilst providing a mechanism for providing more local realisations of the data than would be possible by pure interpretation.

Finally, divergence was found between interpretations of climate based on independent climate proxies, and the interpretation of vegetation change in southwest Turkey. In the early Holocene, this may be aided by more nuanced modelling efforts to better understand the link between climate and vegetation. It is considered that this level of detail would only be achievable by using modern vegetation-climate relationships as a basis. In the later Holocene, these requirements still hold, but the impact of human agency on vegetation is a parallel contributory factor.

## 2.4 WHERE ALTERNATIVE METHODOLOGIES CAN HELP

This chapter and associated appendices has highlighted the wealth of palaeoenvironmental data available to examine key research questions throughout Holocene Mediterranean, the potential issues of interpreting the past based on only one such proxy, and the challenges of multidisciplinary interpretations.

This thesis proposes a vegetation modelling approach, which aims to counter some of the issues discussed above to deliver useful modelling scenarios of the key research questions discussed above. This will be achieved by following the below recommendations:

1. To refine understanding of the relationship between vegetation and climate, a bioclimatic modelling approach may be useful, using modern vegetation-climate relationships as a basis.
2. Palaeoclimatic data will be used as a grounding to create scenarios for the key research questions, and Palynological and archaeological data will be used as model comparison to move forward from single discipline interpretation, and to aid differentiation of climatic and anthropogenic influence.
3. The chronology of palynological data from southwest Turkey will therefore be reviewed and enhanced to create a better basis for model-data and intra-regional comparisons.
4. To aid usefulness within the archaeological community, the model will be developed using high resolution data to provide local model output.

Having developed a conceptual approach for the modelling framework, the utility of a modelling approach will be elaborated upon in the next chapter, and specific examples of previous vegetation modelling techniques will be critically reviewed, to assess their applicability for this study.

# Chapter 3

# Vegetation modelling: methodological considerations and previous approaches.

This chapter critically assesses the utility of using a variety of vegetation modelling techniques to meet the recommendations of section 2.4, with the aim of creating a bioclimatic vegetation model suited to the Mediterranean environment of southwest Turkey, and engaging with key research questions. The chapter begins by summarizing the importance of modelling, and the philosophical and methodological ways in which a modelling framework can be constructed. It then gives examples of previous vegetation modelling approaches, starting with modern analogue techniques, before examining palaeoclimate-vegetation modelling, and modelling links between vegetation and palynological data. It then discusses the applicability of previous vegetationmodelling approaches to the aim of this thesis.

# 3 VEGETATION MODELLING: METHODOLOGICAL CONSIDERATIONS AND PREVIOUS APPROACHES.

## 3.1 THE IMPORTANCE OF MODELLING

It is rarely feasible to capture data for every facet of a complex system. As such, tractable and constrained representations of reality are necessary in order to understand particular attributes or aspects of a system's behaviour. A model is a purposeful representation of reality (Mooney and Swift 1999), targeted towards a particular research aim. Modelling also has great power to enhance and augment research efforts in areas that are impenetrable to understand by direct measures due to the intermittent and patchy nature of available data. The issues of intermittent data, and hence the potential for modelling is very applicable when dealing with the environmental and cultural systems of the past. Modelling allows researchers to elevate themselves out of pure description and discussion of data into more refined, calibrated and complex reasoning.

The utilization of models to interrogate palaeodata has become beneficial in a number of cases. Within the last thirty years in particular, there have been developments both in the modelling of palaeoecological data to provide evidence for climatic and cultural phases (Bunting and Middleton 2005), and the modelling of environmental and cultural variables to predict and infer vegetation distribution (Cramer, Bondeau et al. 2001; Smith, Prentice et al. 2001). These were largely achieved through the application of statistical and spatial models to source data. The philosophical, methodological and technical attributes of these models are discussed in this section, and an overview diagram is shown in Figure 3-1.

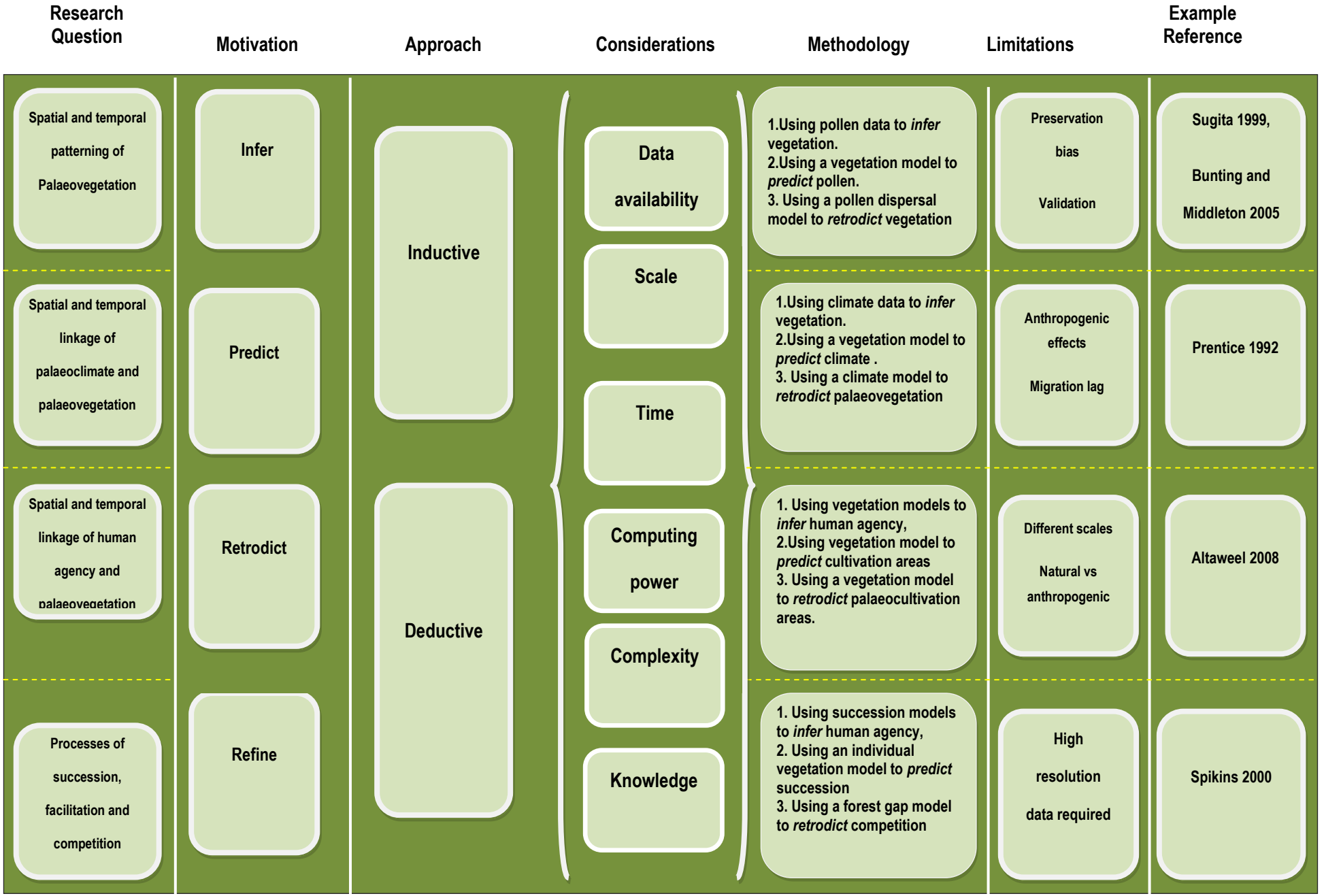


**Figure 3-1 Overview diagram of approaches to vegetation modelling**

### 3.1.1 Philosophical approach to vegetation modelling

After the definition of research aims, objectives and hypotheses, and the recognition of the utility of a modelling approach, a philosophical framework for the study is generally set up. One of the most common divisions in philosophical approach is the distinction of inductive and deductive models (although some may have elements of both). Deductive reasoning starts with a general theory with well defined premises, from which is chosen a more specific hypothesis to test. Modelling of logical processes derives a logically-based conclusion (see Figure 3-2). Where objective, well defined assumptions cease to apply, deductive reasoning becomes weaker (Arthur 1994). In contrast, inductive reasoning starts with individual examples of data, and analyses these data for patterns. From this, a preliminary theory is formed (see Figure 3-3). As the data collected are usually only a sample of all possible data, models can be created which help inform on the wider implications of this preliminary theory. The model can be tested with more data collection, which will either strengthen or weaken the preliminary theory/hypothesis.

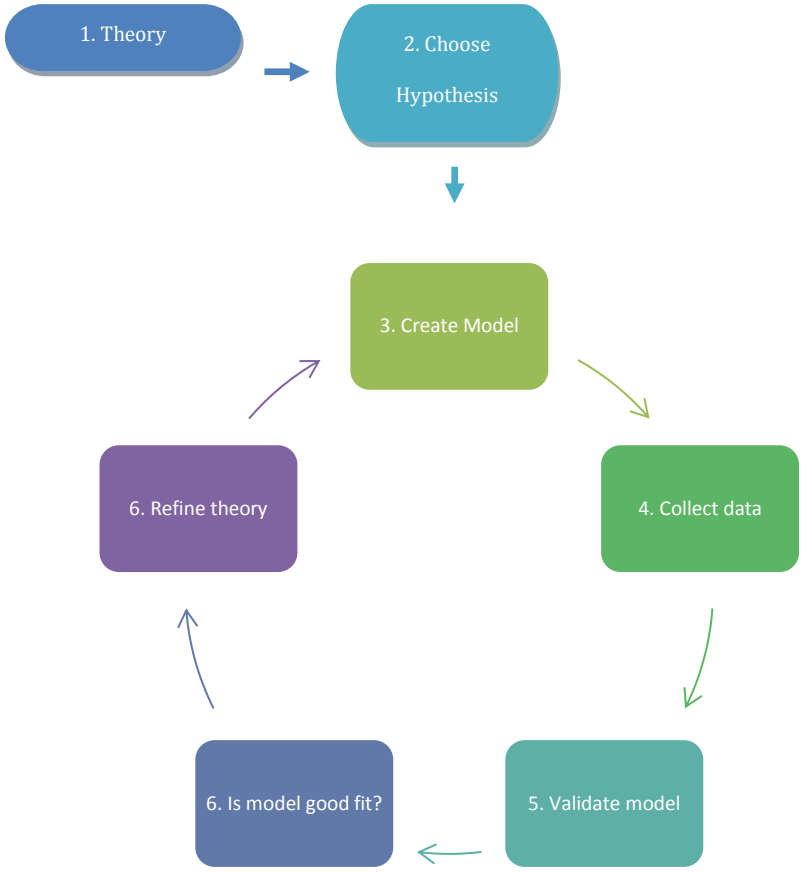


**Figure 3-2 Conceptual model to show a deductive reasoning process, with the incorporation of data and models**

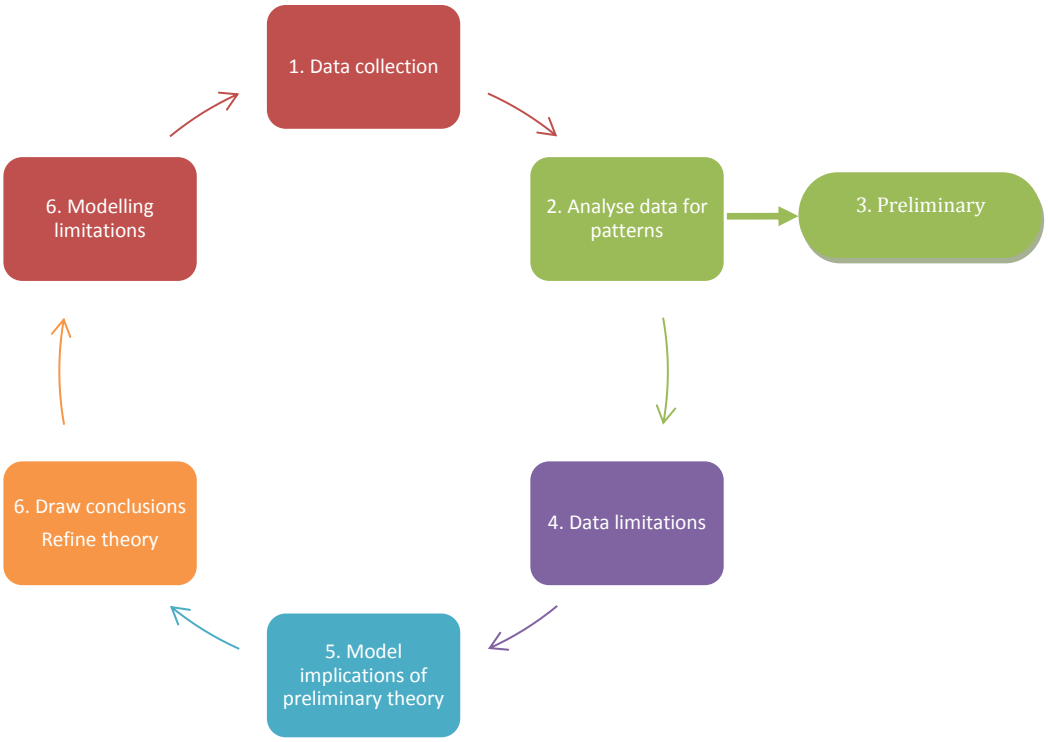


**Figure 3-3 Conceptual model to show a deductive reasoning process, with the incorporation of data and models**

In addition to the inductive and deductive approaches, models may also be classified as using a *top-down*, or *bottom-up* approach (e.g. Hunter 1992).

The top down approach broadly equates with deductive reasoning, and commences with the representation of one main system, before sub-systems are added, and refined, from the top level downwards. The approach affords the possibility of parameterisation of lower subsystems in order to trade mechanistic detail for simpler, generalising models, usually in order to model large and complex systems. In contrast, the bottom up approach would start with sub-systems modelled in great detail. These subsystems would act as modules to be built and connected into larger systems. It allows local optimisation if one process chain is deemed more important than another, but its organic nature needs careful control in order to gain a useful and efficient overall system.

Models can also be classified into simulation (or forward) modelling, which uses physics or biology to predict property distribution, or inverse modelling, which uses observed properties to constrain physical or biological processes (Peng, Guiot et al. 2011). This is another way of describing deductive or inductive approaches. In the vegetation modelling arena, 'Top-down' approaches can be identified within the Digital Global Vegetation Models (Cox 2001), whereas 'Bottom-up' approaches are seen, for example, within individual forest-gap modelling techniques (Friend, Shugart et al. 1993). Distinctions in time are also possible, so models may be described as static or dynamic, as 'snapshot', equilibrium or non-linear. The choice of model approach depends predominantly on the aim of the model, but is also dependent on data availability and knowledge of process and mechanism.

### 3.1.2 **Methodological approaches**

Subsequent to the philosophical approach chosen, modelling is based on one or more methodological approaches. This is an essential section as it defines the nature by which the model reaches beyond the available data.

One of the most widely used methodological approaches used in vegetation modelling is to *predict* relationships and distributions for areas or time periods which are insufficiently populated by data. Predictive vegetation modelling is defined by Franklin (1995) as predicting the vegetation composition across a landscape from mapped environmental variables. This type of modelling was first developed in the 1970s, and expanded with the increase in Geographical Information Systems (GIS), and digital environmental data over subsequent decades.

> "Predictive vegetation models are founded in ecological niche theory and vegetation gradient analysis… and rest on the premise that vegetation distribution can be predicted from the spatial distribution of environmental variables that correlate with or control plant distributions" (Franklin 1995 p.475)

Examples of vegetation predictive modelling that predict for areas of unknown data are found in Vogiatzakis and Griffiths (2006) that examine plant community distribution in Crete.

However, predictive models have also expanded in their remit over time, with predictive modelling not only predicting future events, but also past events such as palaeoclimate and palaeovegetation. A useful study by Peng (2000) reviews the major static and dynamic vegetation models which have been widely used to simulate the potential response of vegetation to past and future climate change. Spikins (2000) uses predictive environmental modelling to examine regional changes in terrestrial vegetation in order to provide a context for archaeological analysis, while Gearey and Chapman (2006) use predictive modelling to examine the potential positioning of alder (*Alnus*) around an Iron Age site using hydrological modelling.

There are however a few issues with the term *predictive* modelling in a palaeoecological sense as prediction implies looking into the future, whereas *retrodiction*[1] may be a more appropriate term. Furthermore, prediction implies a degree of falsification, suggesting a model may in the future be able to be proven true or false. This becomes increasingly more difficult to do in cases where empirical evidence is less frequent spatially or temporally, or where empirical evidence is not available and must be inferred from other data, as often happens when dealing with the past. In this case it rests upon assumptions that the patchy validation, inferred, or comparison evidence is representative, which itself is difficult to prove without knowledge of the statistical population. Predictive models therefore, are often not validated in the true sense, and are seldom compared with data which does exist (cf. Spikins 2000).

One optimal method of validation is the integration of new data as they emerge, such as the integration of new data into climate predictions, which helps to empirically refine future predictions through time. However, although new palaeodata emerge, the potential to collect

[1] Retrodiction is defined as utilizing present information or ideas to infer or explain a past event or state of affairs

the data required to prove a predictive model is slim. It is for this reason that the use of the term predictive is not thought to be advisable in this thesis.

A second commonly utilized methodological approach is to *infer*[2] from one type of data to another. Retrodiction uses inference to gain conclusions about past events. The use of transfer functions (or calibration methods) in palaeoecology are often termed inferential model (Sachs, Webb III et al. 1977; Heiri and André 2010) and are based on modern training sets of species and environmental data, the derivation of a mathematical function such as correlation or regression, which is then applied into the past to infer a conclusion. It is a method that relies on uniformitarian principles. Different types of transfer functions exist, such as the Modern Analogue Technique (MAT) and Analogue matching (AM).

There are however clear disadvantages with these schemes. For a start, the model uses empirical palynological data as input to the model, so there is no way to test it unless independent climate data are available. Secondly, it does not account for pollen source area variability which may influence the result. Thirdly, modern pollen assemblages may not be good match for any previous assemblage due to the influence of human activity or no analogue conditions, relationships between pollen and climate may have changed, or the type of climate during the past may not be represented in modern assemblages.

The further common motivation is to create models that *refine* already available data. These models are used to narrow down plausible possibilities through simulation, in order to tighten precision or define uncertainty through probabilistic modelling, usually for the goal of multidisciplinary data comparison. An example is the multiple-scenario approach of Bunting and Twiddle (2007)

[2] To infer is to deduce or conclude from evidence and reasoning rather than from explicit statements

#### 3.1.2.1 Technical considerations for vegetation modelling

For any given hypothesis, a palaeoecological model is developed by considering a number of practical factors including scale, data availability, computing power, complexity, knowledge, and time, as summarized in Figure 3-4.

A crucial factor is **spatial scale** which is dictated by the hypothesis to be tested, as some processes are very scale dependent, whereas others operate at a variety of scales (for instance investigating the impact of deforestation, which may have different local, landscape and regional processes and effects), potentially ending up with very different results. This has implications for the ways in which data is captured and displayed; for instance:

> 'Polygons and their geometry and topology are themselves artifacts of the modelling process… the real geographic variation is complex and continuous (Goodchild, Guoqing et al. 1992 p. 90; cited in Franklin 1995)

Just as crucial is **temporal scale** as certain phenomena are time dependent and modelling can focus on a particular temporal scale to simplify and drill down to a particular process or set of processes. However, systems and processes usually operate at multiple scales simultaneously, and in this instance modelling can quickly become very complex and potentially intractable.

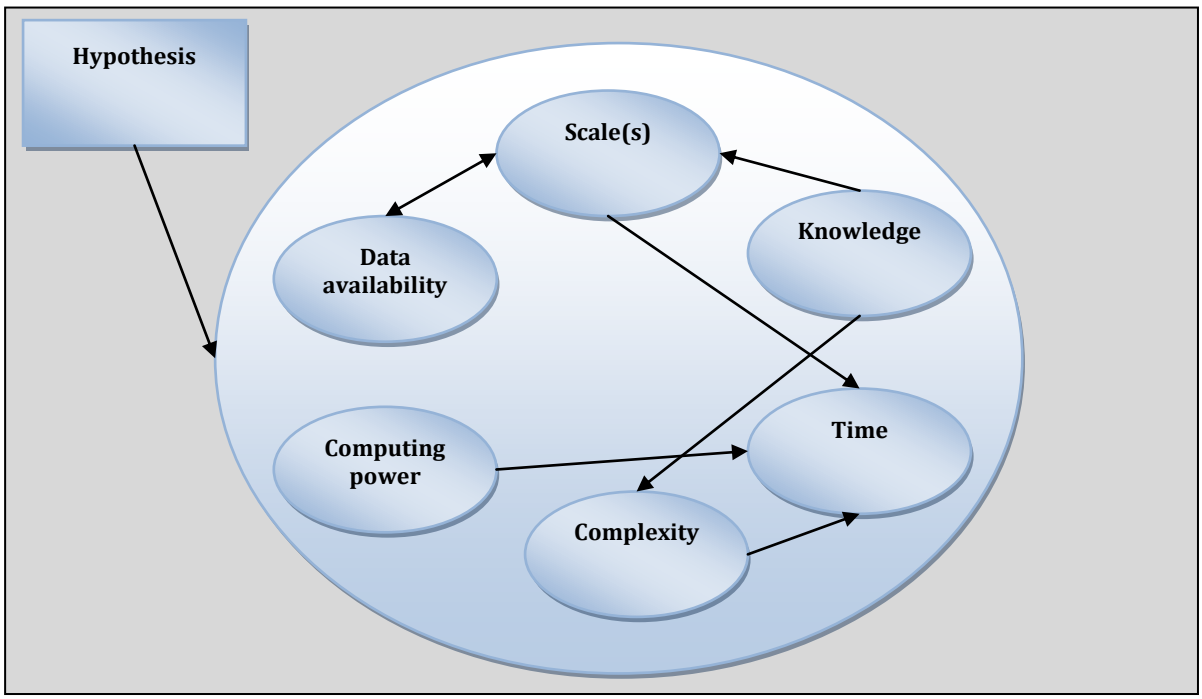


**Figure 3-4 Technical considerations in model development**

In reality, model development and the temporal and spatial scale of analysis is usually restricted by practical considerations such as the **availability of data**. Data availability at any particular scale tends to decrease the further back in time the study aims to look. A lack of palaeodata can be circumvented by using modern analogue data; however, this has its own assumptions, particularly the assumption of Uniformitarianism

As already stated, **validation** is difficult for palaeoecological studies as for example in the case of vegetation modelling, the pollen, phytolith and small amounts of macrofossil evidence are likely to be the only remaining evidence of past vegetation. Instead, validation can be achieved using modern vegetation data, or comparison to other independent palaeoecological proxies (Vermoere 2002).

Other factors such as **computing power** serve to restrict modelling at certain scales (e.g., difficulty in modelling individual plants on a continental scale), and importantly, a lack of theoretical understanding can restrict modelling from occurring until more knowledge is

advanced. Finally, model development should consider the complexity or simplicity required. A model is meant to be a simplified version of reality. However, just how much to simplify, or abstract is an important question. If the process to be modelled is influenced by a multitude of variables, and these variables are all potentially important, then a highly abstracted model may not be the most useful.

## 3.2 PREVIOUS VEGETATION MODELLING METHODOLOGIES

Having discussed typical philosophical and technical considerations of model development, and related it to particular types of vegetation modelling, this section will further outline case studies with similar research aims to those identified in this thesis.

## 3.3 WHAT VEGETATION TO MODEL?

When developing a vegetation model, one of the first decisions to take is the number and type of plant and tree species to model. It is generally unfeasible to model all species that are found in a modern biome or even a fossil pollen assemblage zone. Previous models have had differing methods for modelling species, which will be elaborated below.

The first stage is often dependent on the aim of the research. If agricultural issues are the focus, then sometimes only crop species will be examined, as seen in some of the agent-based agricultural models (e.g. van West 1994; Dean, Gumerman et al. 2000; Altaweel 2008); forgoing a broader investigation of human 'indicative' species such as *Plantago* or *Artemisia*. If the aim is instead to investigate broad scale climate influence on natural vegetation, and link this to cultural change, certain key tree species may be included as a key indicator approach, as in Spikins' (2000) study, which investigated highly abstracted successional sequences.

Although parsimonious, the issue with this very selective choice is that they may miss large effects from species that are not modelled. Conversely, if a great many species are modelled, then any model developed may easily become intractable, and further parameters such as climatic variables may be lacking to populate the model.

In Digital Global Vegetation Models (DGVMs, see below) a Plant Functional Type (PFT) methodology is common, which groups species together and models their global distribution by using key bioclimatic variables. This approach was exemplified by the BIOME model of vegetation as developed by Prentice *et al.* (1992), whose goal was "to find the simplest possible model with the smallest number of plant functional types, constraints and driving variables that could still simulate broad features of present vegetation of the Earth (Prentice, Guiot et al. 1992 p.1) ." The main driving factors for vegetation change were defined as climatic, and so a number of bioclimatic indices were derived addressing vegetation tolerance limits and climatic requirements. This model grouped plant types into broad-leaved evergreen woody plants, boreal evergreen conifers, temperate deciduous trees or C4 grasses (e.g. Woodward 1987; Sykes, Prentice et al. 1996). Biome models can be defined as 'Gleasonian' models (Prentice, Cramer et al. 1992), as biomes emerge through the interaction of constituent plants in a quasi-competitive manner.

Clearly, one issue with this approach is that the broad classes of vegetation are relatively coarse and would not be useful for investigating particular niches of species that have a very specific or unusual climatic or edaphic profile. Although these models are often claimed to be 'Gleasonian', they are only insofar as different combinations of PFT arise, but the subtle differences between species that are within one plant functional type are lost. It is therefore tailored to a more global or regional model than to the landscape or local scale. A second issue is that these models tend only to deal with 'natural' forest and grass species, disregarding the impact of anthropogenic influence and agricultural species.

At the other end of the scale are forest gap models (Friend, Shugart et al. 1993; Bugmann, Yan et al. 1996), which model individual plants and trees, and necessarily model species individually as well in terms of their allometry, climatic preferences, edaphic preferences and restrictions to growth such as shade. However, these models require detailed parameterization, which may not be available for a wide range of species. These models can be used in a number of research questions, both looking at natural and anthropogenically influenced succession, but are often quite restricted in extent due to the individual nature of the model.

Therefore the aim is to achieve a fine balance between selecting enough species that will give a general picture of the dynamics the research is hoping to capture, but without overpopulating the model with poorly parameterized agents or variables.

### 3.3.1 A selection of vegetation modelling examples

Invariably, most palaeoecological models start with components that are developed under modern conditions, a so-called 'Modern Analogue' approach. Although this introduces many assumptions, particularly in terms of Uniformitarianism, it is often the only way to gain enough information on empirical links between vegetation and other variables. Once defined, such models tend to relax modern parameters and variables to encompass different estimations of past situations (which are ideally compared to palaeodata).

It is well established that certain linkages exist between vegetation and climate. For instance, Prentice (1992) considers the transcontinental correspondence between geographic patterns of vegetation and climate as one of the oldest observations in plant ecology (Prentice 1992). Vegetation models that aim to exploit this connection between vegetation and climate often investigate first the influence of modern climate on modern vegetation, before inferring past vegetation assemblages from palaeoclimate records. This is often the first step in disaggregating other influences such as anthropogenic effects.

One of the most longstanding theories of vegetation-climate linkages is proposed by Köppen (1936) which is an empirical classification system based on the link between broad scale vegetation types, temperature and precipitation. The Köppen system traditionally defines climatic classes through vegetation rather than vegetation through climate. Building on this basis, further models were developed that examined the influence of climate on vegetation assemblages (Raunkiaer 1934; Holdridge 1947; Dansereau 1957; Fosberg 1967; Küchler 1967). The Köppen and Holdridge schemes were later improved by Guetter and Kutzbach (1990) and Prentice (1990) respectively while further refinements were made on species cold limits and drought tolerances (Box 1981; Shugart, Antonovsky et al. 1986; Woodward 1987) with the overall aim to 'simulate long-term vegetation dynamics by mimicking physiological mechanisms that express the effect of abiotic and biotic conditions on growth, through simple response functions' (Fyllas, Phillips et al. 2007p. 440).

The culmination of this research has resulted in sophisticated Dynamic Global Vegetation Models (DGVM; low resolution, global extent) and forest dynamics models (high resolution, local extent). One of the more established DGVM methodologies is detailed in Prentice *et al.* (1992). The range limits of tree species were described by using five species-specific bioclimatic constraints. Species are clumped together into groups with similar climate requirements; an approach called a Plant Functional Type approach. These were defined as the amount of growing degree-days on a 5° base ($GDD_5$), the mean temperature of the coldest month ($T_c$) the mean temperature of the warmest month ($T_w$), the Priestley-Taylor coefficient of annual moisture availability ($\alpha$) and the dominance class (D) for each plant type. The advantage of these models is that once biomes have been defined, external forcing of the DGVM can be implemented through changing global $CO_2$, climate and land use. If the relationship is well founded, palaeoclimatic data can then allow retrodictions of past biomes to explore the possible distribution of palaeovegetation.

In order to build up the parameters for Biomization approaches, modern climate data, and palaeoclimate scenarios are required. With DGVM models this has traditionally been rather coarse in resolution due both to the limitations of the data available, and the succinctness of the model desired by Prentice et al. (1992), therefore trading off resolution and complexity for extent. Thus, the vegetation output is global, but consists of broad classes at a fairly coarse resolution (~0.5°), which while ample for certain global change applications, limits its use for other more landscape and local based studies. Another potential issue is that direct validation of DGVMs is impossible due to the long timescales involved (Calamassi, Paoletti et al. 2001).

Moving from the global to the regional scale, further research by Laurent et al. (2004) moves from plant functional types to Bioclimatic Affinity Groups (BAG), correlating the European species ranges of plants and trees with monthly climatic data. Similar species are then clustered into groups using hierarchical clustering. This leads to data that is finer resolution than the BIOME output, but still too coarse for landscape scale analysis. Furthermore only the minimum and maximum thresholds of BAG groups are available, and not the continuous probability of a species to populate a particular area of the landscape.

In order to begin to move beyond these limitations without compromising on model efficiency, more recent models include process-oriented formulations of biogeochemical fluxes as well as vegetation dynamics (e.g. Calamassi, Paoletti et al. 2001) and include time-dependent multi-temporal functions (e.g., 'fast' processes of photosynthesis and respiration, 'medium fast' processes of seasonal and life cycle changes and 'slow' evolutionary processes). The European Terrestrial Network Modelling Activity (ETEMA) Framework shows how bioclimatic models can be utilized within a more complex model structure (Sykes, Prentice et al. 1996; Sykes, Prentice et al. 2001). A model example uses a nested approach with macro (10-50 km) and micro scale cells. The macro scale dictates topographical distributions, whereas the micro-scale represents heterogeneity (e.g. vertical and horizontal fluxes of water). In terms of temporal analysis three tiers of analysis are identified, deemed fast, intermediate and slow processes as shown in Figure

3-5. At the fast scale, daily weather data are used to examine diurnal cycles and soil moisture dynamics. At the intermediate scale phenological processes are modulated by seasonal changes in temp and daylength and nutrient or water availability, and soil organic matter or fire disturbance episodes. At the slow scale vegetation dynamics (changes in vegetation abundance, mortality, migration etc.) are driven by life cycles with natural or human land use modules.

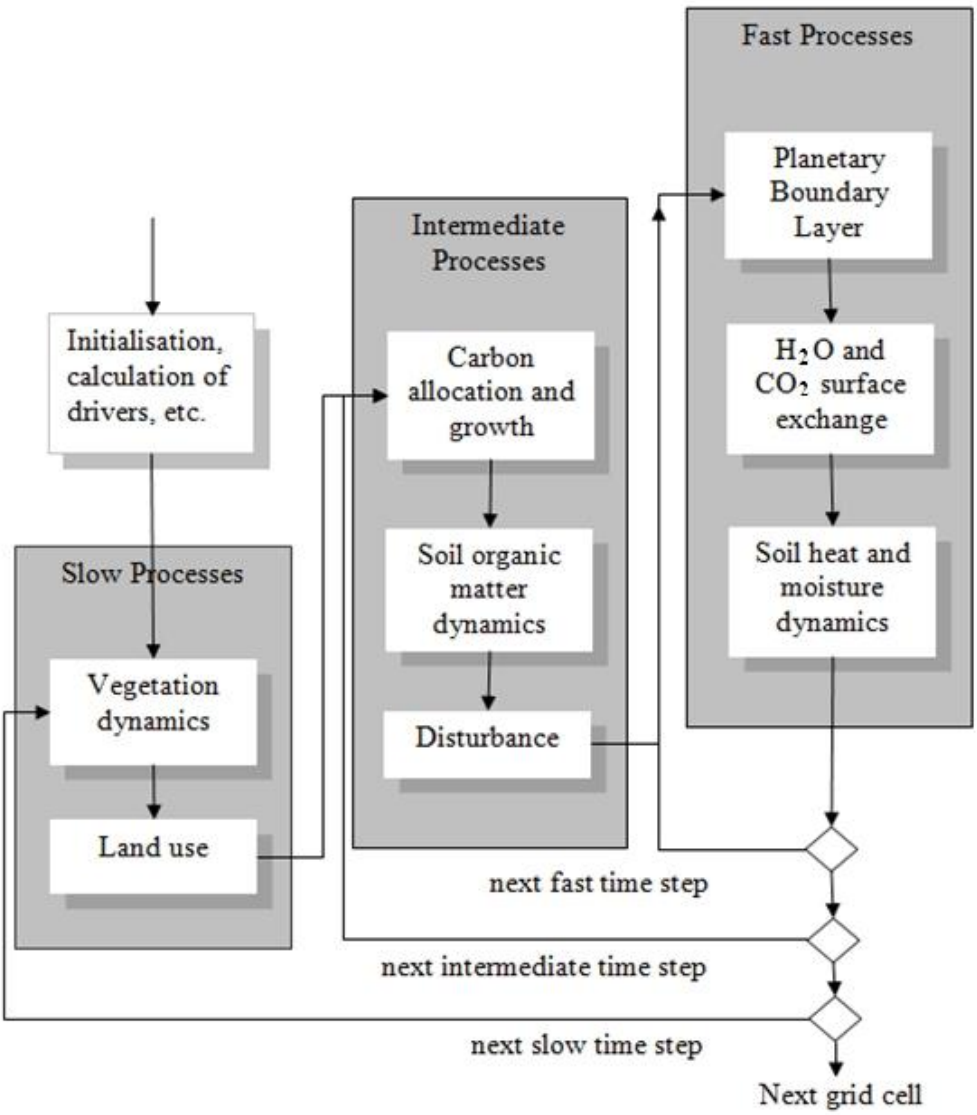


**Figure 3-5 Temporal framework of the ETEMA modelling system (Sykes, Prentice et al. 2001)**

To answer the requirement of Prentice, Cramer et al. (1992) for increasingly mechanistic modelling techniques, forest dynamics models have also developed using a 'Bottom-up'

approach, in order to understand processes of climatic influence and competition at the stand level. As the models turn more mechanistic, they necessarily become more complex than the more straightforward models based on correlation, and as such incorporate a number of sub-models. For instance, FORCLIM (Bugmann 1994), consists of three modular submodels, defining the abiotic environment with a soil water balance model, a soil carbon and nitrogen turnover model and a tree population dynamics model based on gap dynamics.

Forest gap models, in contrast to DGVMs, are high resolution, however require a lot more data to run, in terms of allometry, growth habits, climate and edaphic preferences. However, this is rarely available with northern European vegetation, let alone Mediterranean species. When attempting to use these types of models for palaeoecological applications, the assumptions increase dramatically, as daily weather data are replaced with stochastic weather generators.

One of the first digital computer simulations that attempted to understand complex natural ecosystems was the JABOWA model (Botkin, Janak et al. 1972). This model simulated north American hardwood forest growth, in which general biotic characteristics of tree species such as age height and diameter were included, as were the relations between height and diameter, the total leaf weight and diameter, the rate of photosynthesis, the availability of light, and the relative growth under particular climates. Growth, birth and death submodels were implemented. Since these early models, models of competition have become more complex, to understand phases of succession.

The majority of these succession models have been applied in temperate locations, and therefore follow the traditional succession route with an oak climax community. The Lund-Potsdam-Jena General Ecosystem Generator (LPJ-GUESS) model (Smith, Prentice et al. 2001), is an individual-based model of the type suggested by Sykes et al. (Sykes, Prentice et al. 2001). Plants are modelled individually with attributes such as height, depth, area and leaf area index (LAI), and thus competition between plants can be considered at an individual level. The models' output focuses on carbon and water exchanges, and budgets. Smith *et al.* (2001) were

able to demonstrate that the individual-based models performed particularly well in areas where deciduous and evergreen species meet, and where plants have under pronounced seasonal water deficits, emphasizing that light competition and stress-induced mortality is an important and integral part in plant succession at many scales of analysis.

There are a few examples of very high resolution models employed in the Mediterranean region. For instance, Millington et al. (2009) developed a Landscape Fire-Succession Model (LFSM) to simulate the dynamic interaction of fire, vegetation and climate in a spatially explicit manner. By using a plant functional type approach and incorporating wildfire scenarios, disturbance, succession and resource gradients they can simulate Mediterranean community structures. This type of model is likely to be useful for examining the structure of vegetation in southwest Turkey under various wildfire situations, however it does not directly relate to the research questions set in this thesis. Furthermore, the detail of the model is likely to make it difficult to use over the long timescales required by this study, to compare with empirical palaeoecological evidence. Millington et al. (2009) recognize the difficulties in implementing detailed models of wildfire-vegetation dynamics at the landscape scale over decades, due to the difficulties of scaling process knowledge and information from fine grains to large extents, and the high levels of parameterization required (Keane, Cary et al. 2004).

Zavala *et al.* (2000; 2004) use an analytical mean field approach to study succession within the Mediterranean, specifically the balance between pine and oak presence. In the first study Zavala (2000) examined pine-oak segregation based on precipitation gradients and disturbance, and in the second model, dominance and extinction of species was examined. The detailed models include seed dispersal and likelihood of species establishment. Again, this model is likely to be useful in future work, however both the lack of information on seed dispersal and species establishment for key palaeoecological species in southwest Turkey is likely to be a barrier to the uptake of this model. As well as implementation difficulties over large periods of time, there

are also likely to be computational issues with models of this detail in gaining a region-wide view to compare with empirical data.

As well as regional to global and individual to stand level models, one further scale of analysis is demonstrated, that of the regional to landscape scale models.

The distribution of vegetation across the landscape is not defined by distinct areas, homogenous stands or neat boundaries. However, mapping the continuous distribution of vegetation and species is a challenging area.

As discussed by He et al. (2003), recording the presence / absence of a species or vegetation type is increasingly common due to the proliferation of remote sensing and aerial photogrammetric techniques. Species data are typically presented in the form of an atlas in which species occurrence and other covariates may or may not be fully observed, and are usually at the regional to landscape scale.

The interpretation of presence / absence species distribution in relation to environmental variables has been undertaken by a number of authors, in order to understand which variables determine vegetation distribution and how vegetation shifts due to changes in these variables. One method of doing this is by using a Logistic Regression model, and is often used to predict probabilities of a specific vegetation type or species at each point (Toner and Keddy 1997). A potential issue with these models is one of autocorrelation, however this can be resolved to a certain extent by sampling methodology. This methodology is interesting as it does not require overly mechanistic parameterization, it can be tailored to the resolution of the input data, and the method has been successfully used in Mediterranean environments as shown by Carmel et al. (2001).

A related approach is the use of AutoLogistic Regression models (Besag 1972; Box, Crumpacker et al. 1993; Augustin, Mugglestone et al. 1996; Wu and Huffer 1997) which aims to incorporate autocorrelation by examining the effect of neighbouring cells to assess the influence of

underlying environmental factors (He, Zhou et al. 2003). This may also be done by fitting theoretical variogram models (Albert and McShane 1995).

The linkage of species potential with multivariates is also evidenced by the work of Spikins (2000), Fyfe (2006) and Caseldine et al. (2007). Using a variety of GIS layers, such as topography, pedology, geology or hydrology, and a set of autecological rules, this type of modelling allows the exploration of the spatial distribution of vegetation in the environment. For the purposes of this thesis, this type of modelling will be called a 'natural potential' approach. The attractiveness of the natural potential approach is that it can be used where fossil pollen data are either limited or absent. One of the first modellers to start to incorporate both this spatial aspect of GIS, as well as the temporal aspect of vegetation change at the regional scale came from the field of archaeology. Spikins (2000) drew on the ideas of Box (1981) with respect to the 'natural potential' vegetation of an area based on ecological groupings and rules, which essentially resulted in a set of preferences of vegetation species for certain types of environment, such as particular slope angles, elevations, or soil types (which can also be inferred by geology where soil data is patchy or nonexistent). By classifying and weighting these features a GIS model of preference for each species can be derived (Figure 3-6) Furthermore, rulings on dominance and succession can be employed in order to attempt simple succession while the output can be arranged as timeslices to examine plausible changes in woodland distribution through time (e.g. Spikens, 2000). The incorporation of a temporal aspect to vegetation models allows models to be used with allied disciplines such as archaeology where discourses surrounding possible triggers for population movement, and resource allocation through time can be studied. However, Spikins does not go as far as to compare model output with independent data such as pollen evidence due to differences in scale and representation between the two data sources.

Fyfe (2006) uses a natural potential approach in order to estimate the upland expansion of mixed agriculture in Exmoor during the early Medieval period. Like Spikins (2000), Fyfe (2006)

uses a 50 m DEM to place vegetation in the landscape, but calculated local vegetation assemblages by using a regional analysis within HUMPOL. Four temporal snapshots were created where vegetation position was (arbitrarily) shifted uphill to examine the effect that upward expansion of agriculture had on pollen assemblages. As with Spikins, the simulated pollen assemblages were not however compared to independent data.

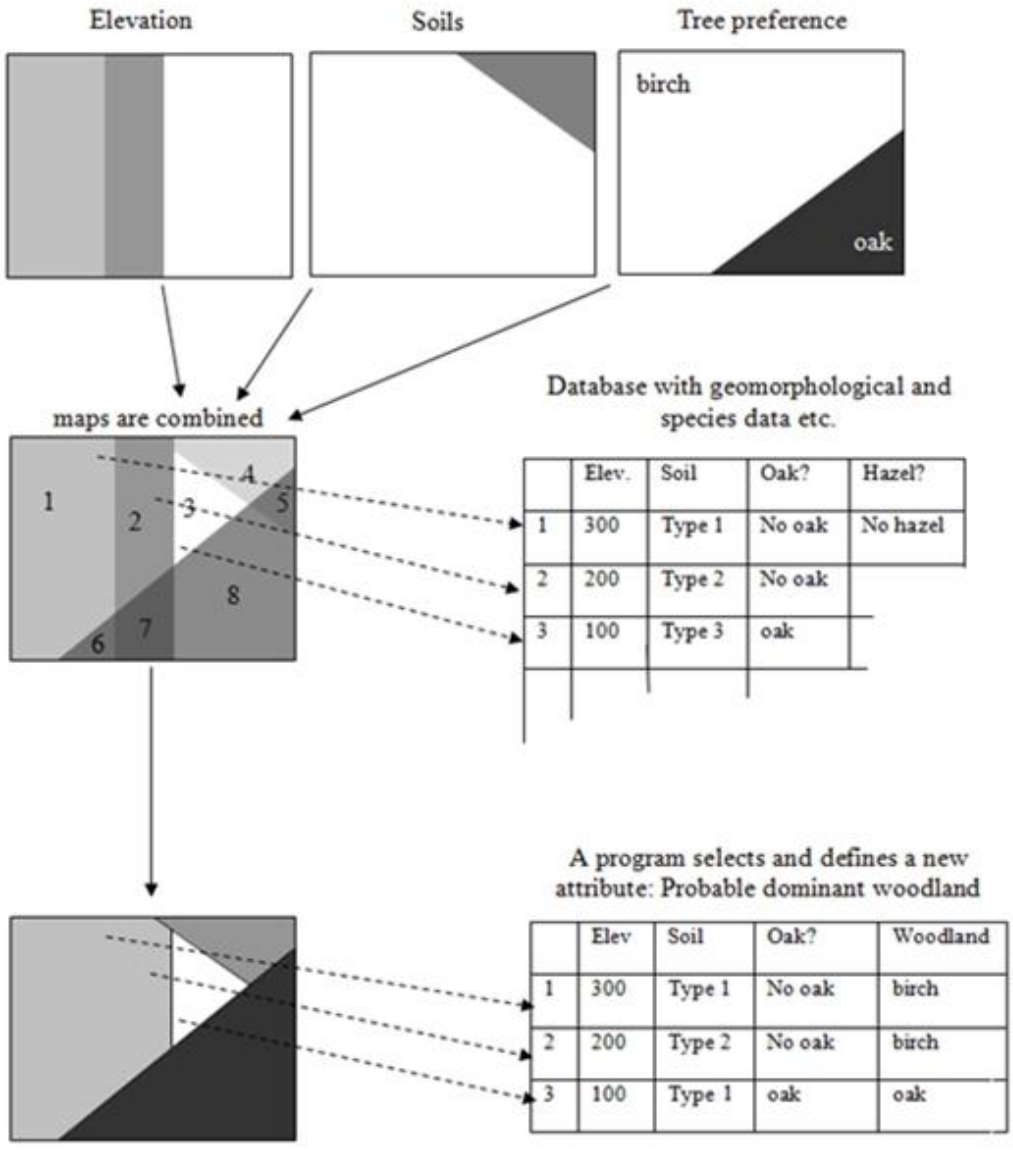


**Figure 3-6** Method used by Spikins to selecting dominant vegetation types (Redrawn from Spikins 2000)

Where fossil pollen data does exist, it enables comparison of model output with another independent source of evidence. Caseldine *et al.* (2007) simulated the nature of vegetation communities at the opening of the Neolithic, on Achill Island, Ireland and suggested that the area is relatively quantifiable as wind regimes are constant through time, and are not thought to have changed significantly throughout the Holocene. The area is also surrounded on three sides by sea, minimising the complicating effects of background pollen. The study is interesting as it uses two versions of vegetation input, one with very simplified blocks of species (with no regard to topography), and another where vegetation is placed depending upon the slope angle, aspect and elevation. Pollen assemblages were simulated with HUMPOL, but then they were compared against the fossil pollen evidence. Even the model with simplified blocks of vegetation actually predicted the empirical fossil pollen data fairly well, and results were most similar to fossil pollen when background pollen was not used. Comparing deviations from the empirical data using the topographically chosen vegetation can show the assumptions of the ecological rules chosen. For example, *Pinus* was assumed to be restricted to steeper and more exposed sites, although this led to its underrepresentation in the pollen assemblage, indicating that pine was more widespread, therefore Caseldine *et al.* (2007) assigned them to smaller pockets where other trees could not flourish. Continuous Digital Elevation Models (DEMs), soil maps, geology and hydrological layers are just some of the inputs which can be combined in a GIS to analyse and model landscape processes across a range of spatial scales, inherently making every input, process, and output spatial in nature.

This methodology is thought to be an increasingly useful one and has therefore been incorporated into the most recent iteration of pollen dispersal modelling software. The Multiple Scenario Approach (MSA) by Bunting et al. (2007) allows the possibility of using cost surfaces such as soil and topography, to assign potential vegetation. From these vegetation models, pollen loading at particular points in the landscape is simulated which can be compared to actual fossil pollen, therefore retrodicting a vegetation model based on modern relationships. The model has a scripting system which aids in the creation of landscape swarms, examining

many possible vegetation distributions that will lead to a particular pollen assemblage and comparing their fit statistically. The use of such a model requires detailed knowledge of vegetation-pollen relationships in order to implement the model well. The next section in this review aims to elaborate on this specific element of vegetation modelling – the translation of fossil pollen data to vegetation distribution and *vice versa* as it is one of the most important sources of data for palaeoecological applications, however it does requires knowledge of particular pollen dispersal mechanisms to interpret well.

### 3.3.2 Approaches to the modelling of vegetation from palynological data

The tradition of reconstructing a quantitative view of past vegetation from fossil pollen data is long standing. Indeed, Lennart von Post (1916) first showed that changes in pollen percentages through the depth of a peat core in Sweden could be consistently measured, concluding that changes in fossil pollen percentage values represented changes in local vegetation assemblages. It was found that changes in pollen percentages did not always represent the same changes in vegetation distribution around a core due to differences in pollen dispersal, as well as the interlinked nature of percentage data (Fagerlind 1952). This discovery, plus a range of other taphonomical factors act to confound reconstructions of past vegetation patterns directly from the data, which prompted the development of models to investigate and better represent the relationship between fossil pollen and the surrounding vegetation which produced it. Many of the early modellers were ecologists and botanists who aimed to understand the proportions and ratios of past vegetation from pollen data. The models were 1-dimensional, and numerical in output, and the spatial component was largely absent.

The R-Value model by Davis (1963) used modern pollen-vegetation relationships to examine the ratio (R-Value) between the amount of pollen deposited at a point, and the relative abundance of vegetation surrounding that point. Once R-values were established for each taxon,

they were used to understand the probable proportion of the same taxa found in post glacial fossil pollen data. This simple measure of differential pollen productivity was to be utilised as the basis for analysis in many models that followed. The main assumption of course was that the modern pollen productivity measure for a taxon was constant over time, allowing fossil pollen to be reconstructed into percentage vegetation in a palaeolandscape.

The models developed throughout the 1970s and 1980s used more complicated statistical correlative methods to describe the relationship between pollen percentage and vegetation composition. In order to define the component of pollen in a (pollen core) sequence that came from long distance travel, a background pollen term was introduced by Andersen (1970), which helped to tighten the pollen productivity parameters for more accurate representation of local pollen (and thus local vegetation distribution). Parsons and Prentice (1981) and Prentice and Parsons (1983) used a maximum likelihood approach to gain general relationships across many sites for specific taxa, and explored various ways to represent background pollen. This was later known as the Extended R-Value (ERV) method, which could be inverted to calculate the vegetation proportion from pollen percentages. As it used a number of sites and a maximum likelihood method for parameter optimisation, it gave a higher confidence level than those models before it. However, it was still spatially limited and only estimated vegetation proportion, not the distribution of vegetation in the landscape.

The next batch of models began to deal with the placement of vegetation in space. Using Tauber's (1965) model of pollen pathways through the environment, Jacobson and Bradshaw (1980) distinguish between extra local, local and regional pollen. forming the basis for further quantitative model development by Prentice (1985; 1988). Borrowing from the field of atmospheric dispersion modelling, Prentice uses a form of Gaussian Plume model, utilising Sutton's equations for atmospheric diffusion (Sutton 1953) and Stokes' law based on the size and weight of individual pollen grains, to approximate the travel of pollen grains through the atmosphere from plant source to the point of deposition. Assuming a forest structure, the model

allows for the prediction of ground-level concentrations of pollen in a 2-dimensional plane away from a point source. An integrated form of the equation predicts the amount of pollen still airborne (or the amount of pollen deposited) for each pollen type at a particular distance from this source. Inverting this model allows for a more defined estimate of vegetation proportion at varying distances away from a point of deposition. A Distance Weighted Plant Abundance (DWPA) parameter meant that an estimation of the pollen source area could then be investigated. Sugita (1993) modified Prentice's model to estimate pollen deposition over the entire surface of a basin (i.e. a closer approximation to a lake scenario than a single point of deposition), and introduced the concept of the Relevant Source Area of Pollen (RSAP) for the point at which the correlation between pollen loading and DWPA does not improve.

From these early inductive models, providing information about the processes between pollen dispersal and pollen deposition, software was developed that turned the methodological process on its head. In order to explore Prentice and Sugita's algorithms under many conditions, the POLLSCAPE software was developed by Sugita (Sugita 1994; Sugita 1997), the main objective of which was to start with scenarios of vegetation cover, to use the model to predict the pollen loading in a lake or bog, and to allow the simulated pollen assemblage to be easily compared with empirical pollen data (Eklöf, Broström et al. 2004). The structure of the vegetation input into the model is simplified, being composed of circular patches of different sizes (Figure **3-7**a). A later version is capable of inputting a vegetation layer directly from a simulated or derived vegetation map from GIS to incorporate more realistic vegetation. The model comprises of a 'ring-source' model used to calculate the cumulative distance-weighted percentages of plant species in a sequence of concentric rings moving outwards from the lake (Figure **3-7**b), assuming this is circular (Eklöf, Broström et al. 2004). The output of the model can then be utilised to calculate pollen productivity estimates or investigate the RSAP.

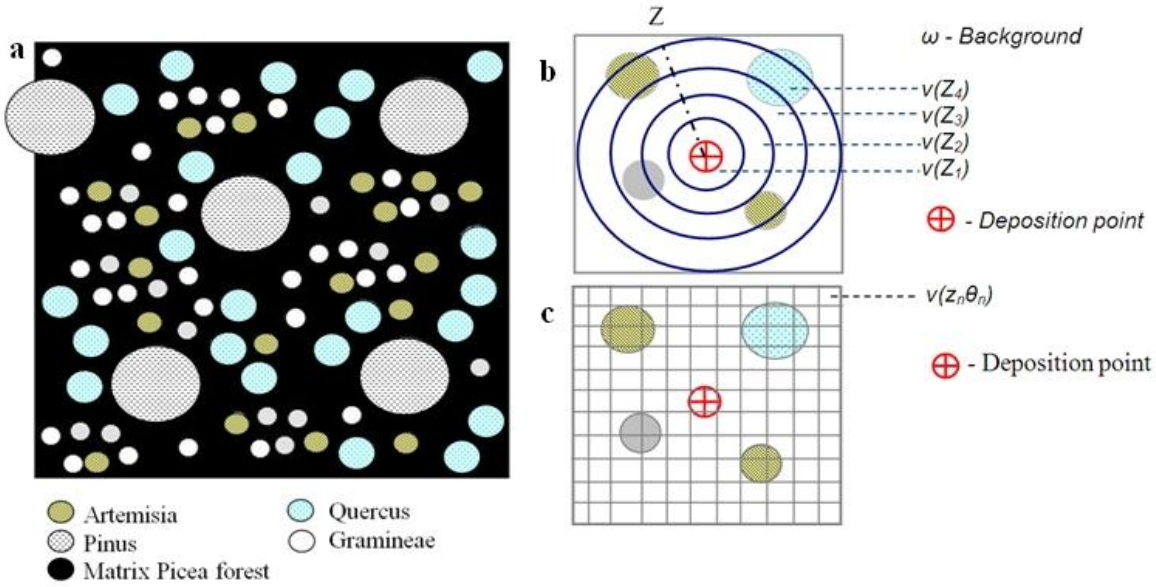


Figure 3-7 (a) Conceptual diagram showing the simplification of input vegetation distribution and composition for the POLLSCAPE model (Redrawn from Sugita, Gaillard et al. 1999). (b) Schematic of POLLSCAPE approach, where *v* is the vegetation abundance parameter calculated for each ring source distance Z from the point of deposition, and ω is the background term. (redrawn from Bunting and Middleton 2005) (c) Schematic of HUMPOL approach showing cellular calculation of vegetation abundance *v* at each distance (z) and angle (*θ)* from the point of deposition (Redrawn from Bunting and Middleton 2005)

POLLSCAPE was deemed successful in predicting the relevant source area of pollen in relatively simple, closed forest systems in the USA and Canada (Sugita 1994; Calcote 1995; Sugita, Andersen et al. 1998), but until Sugita's (1994) study there had been no attempt to understand how vegetation other than continuous forest could be represented by pollen movement, and ultimately in pollen deposition, or at what resolution. The work by Sugita (1994) emphasised the variation in pollen deposition assemblage, depending on the composition of vegetation surrounding the deposition point, making the collection of empirical data in various biomes (as well as a concerted effort to model variations in parameters) necessary to understand the scale and magnitude of this variation. Sugita *et al*. (1999 p.418) identifies that the "degree of landscape openness, the spatial spread of vegetation patches, and regional pollen production and transport" are the main influences on pollen deposition at a site. This has important implications when reconstructing vegetation from pollen cores, particularly when investigating relatively unmanaged 'natural' landscapes, where ecological rules may dominate, versus heavily

managed landscapes where vegetation patch sizes and distributions are controlled or exploited for anthropogenic purposes. Further improvements in the model were developed by modelling a variable background term, thus far assumed a constant. This was part of the 'Landscape Reconstruction Approach' (LRA) outlined by Sugita (2007a; 2007b), noting an important shift in the focus of the literature from reconstructing vegetation as a numerical, empirical exercise, to a wider understanding within the context of a spatial landscape. The Landscape Reconstruction Approach undertakes a tiered methodology, first concentrating on large lake contexts in order to understand the regional pollen component, and then using these data to refine small lake and bog contexts, in order to tease out the local pollen component.

The last major development in vegetation-pollen modelling is due in part to the expansion and development of GIS technology and techniques into the mainstream over the last 20 years, allowing greater investigation into all aspects of landscapes due to its integrative nature.

This paradigm shift allowed the development of a two-dimensional Prentice-Sugita Model, named HUMPOL (Bunting and Middleton 2005). Whereas previous models have emerged from the ecological and botanical fields, the HUMPOL model was developed by those with a geographical background. The theoretical basis was given a new angle by incorporating the spatial domain, utilising the expanding field of GIS. Instead of the one-dimensional ring-source model, HUMPOL was based on the GIS concept of the raster, a cellular grid format (Figure **3-7**c) which allowed a nested multi-resolution approach. In essence this meant that both lower resolution regional and higher resolution local modelling could be undertaken to better characterise vegetation distribution, and the regional pollen signal. The cellular nature of the model meant that independent weightings could also be added to the vegetation map, to begin to model the impact of other parameters; for instance, the effect that wind or topography would have on the pollen deposition assemblage. As previously discussed, more recent additions to this modelling software are being implemented (Bunting, Twiddle et al. 2007)

### 3.3.3 The applicability of previous model approaches to answer thesis aim and key research questions

A selection of previous vegetation modelling approaches have been introduced in this chapter. Their utility in answering the specific requirements of this thesis will now be discussed.

One of the first points raised in this chapter was how vegetation models have previously approached the decision of which plant and tree species to model. Species can be modelled individually as trees or plants, or as Plant Functional Types. They can incorporate anthropogenically introduced species, natural species, or both depending on the aim of the research. The research questions identified in Chapter 1 require engagement with both naturally occurring species, and species that have been taken for cultivation during the later stages of the Holocene. As such, a model that only investigates crop species or a small selection of 'natural' tree species is only of limited use. However, it is acknowledged that attempting to model all possible species occurring in the Mediterranean during these phases is impractical. The answer must therefore lie in the selection of a subset of key species which are instrumental in assessing the climate-vegetation and vegetation-cultural questions investigated. It is considered that previous plant functional type and bioclimatic affinity groupings do not provide the right level of information for the right species set encountered in southwest Turkey, and so the modelling of new bioclimatic relationships between environment and vegetation is recommended. Whether these are modelled as single species, or as representatives of a broader class of vegetation will depend on the availability of species data for the study area and bioclimatic variability between species.

Subsequent to deciding key species, the recommendations developed in Chapter 2 require nuanced relationships to be developed between climate and vegetation using modern data. Exactly how nuanced depends on the practical considerations discussed earlier, in terms of the data availability, resolution and scale of study, and computing power.

Model parameters can range from broad bioclimatic ranges such as relative winter temperature ranges and Growing Degree Day requirement in regional or global models, to detailed biochemical processes in individual models which impact on plant growth, allometry and survival, and probabilistic modelling of seed dispersal with climatic conditions.

Five scales of vegetation model were encountered during the review; global, regional, landscape, nested, or individual stand models. The research questions require a relatively intricate model in order to understand the interplay between species within and between vegetation belts with changes in regional climate at various points in the Holocene. Importantly, it was identified that the model should be comparable with independent evidence such as palynological and archaeological evidence. This is likely to require higher resolution than the 0.5° biome models that characterize continental to global scale vegetation dynamics. Another related issue is that regional models are based on climate-vegetation relationships derived from medium to low resolution species distribution maps. Global BIOME models and regional BAG models are therefore considered to be too coarse to adequately meet the requirements of the research questions set.

However, at the other end of the spectrum, the complexity of Mediterranean landscapes has led some to doubt the feasibility of spatially explicit, physiologically based forest models in a Mediterranean context (Millington, Wainwright et al. 2009). Very detailed information on topography, soils and species distribution may not be available for modern analysis, and detailed microclimatic information will certainly not be available for retrodictions of past environments. Parameterising a model to a level where data does not exist to populate it is not advised, as it would either have such large bounds of uncertainty as to not be useful, or it would give a false sense of precision if parameters were estimated as examples.

The particular complexity of the southwestern Turkish environment warrants a relatively high spatial resolution, as climatic and vegetational changes are apparent with sharp elevation gradients requiring data in the 10s of km resolution. A nested approach could prove fruitful,

however, the available implementations of this approach still require large amounts of parameterization that is not necessarily valid for a palaeoecological model such as this in a Mediterranean environment. The practical considerations of developing a new nested model at a variety of scales are further considered too large for this thesis.

The landscape-scale logistic models and natural potential models of (Carmel, Kadmon et al. 2001) Spikins (2000) Fyfe (2006), and Caseldine (2007) provide the most applicable scale for the modelling of climate-vegetation links to engage with the research questions set. However, it is acknowledged that key enhancements to the models can be made to create a more robust, integrated methodology.

Firstly, it would be advantageous if the climate-vegetation rules behind the model were tailored to Mediterranean species, and were robust in their relationships. This would require the bioclimatic relationships of key species to be defined. Secondly, it was discussed that the model output had clear potential to be ingested into pollen dispersal models, thus creating a model that could be compared to actual pollen evidence. Thirdly, a range of climatic scenarios would need to be developed that engaged with the key research questions.

## 3.4 SUMMARY

This chapter has introduced the key factors that are considered when developing a model including philosophical approach, methodological approach, and the practical considerations of spatial and temporal scale, computing power and data availability. A selection of vegetation modelling case studies were identified and critically assessed for their utility in engaging with the key aim and research questions of this thesis.

Based on this review, none of the previous modelling approaches were immediately 'fit for purpose' for use with the aim of this thesis. Instead, a hybrid modelling process is detailed

below which incorporates ideas from previous models, to create a detailed vegetation model linking climatic, edaphic and vegetation layers to test the hypotheses set out in Chapter 1.

This thesis will take on the form of a deductive model, as research questions have been identified from general theory, and can be rephrased as hypotheses. The thesis will create a modelling framework, and then collate data with which to validate or compare the model to. This process then acts to support or reject the modelling hypotheses, therefore refining the general theory. It is acknowledged that by using this approach, particularly for a palaeoenvironmental situation, assumptions should be well defined to aid robustness.

In terms of species choice for model input, it was decided that a subset of key species would be defined that engaged with the research questions. Which species these were, and whether they were modelled singly or as a plant functional type will be discussed in the methodological chapter of this thesis. Some parameter sets already exist, however it was decided that their previous species range parameters were not wholly appropriate for this study, in that some of the key Mediterranean species were not covered, and that those parameters that were defined were either developed using low resolution climate and vegetation data, or very restricted sample data from one geographical location. It is therefore decided that a new consistent methodology would be developed to define species environmental and climatic limits. This will require that key climatic, edaphic, topographic and vegetative layers will need to be assessed for spatial and temporal resolution and processed to create a consistent input.

In terms of the spatial scale of modelling, it was decided that the landscape scale 'Natural Potential' and Logistic Regression models were most appropriate to the research questions. Regional to Global BIOME models are considered too coarse, and individual forest gap models too detailed. However to use these models will require a revision of the methodology. This new approach could take components of the Modern Analogue and BAG work of researchers such as Laurent et al. (2004), correlating climate and edaphic variables with species limits, but at a finer

scale, also retaining more detailed information to model relative species probability across a continuous landscape.

In order to retrodict the model, climatic scenarios should be defined based on robust climate evidence. This will be done without evidence of climate interpreted from pollen, as the output from the model should be compared to independent evidence such as that from fossil pollen and archaeological evidence. It is acknowledged that to do so may require translation tools such as HUMPOL to create comparable data.

The methodology therefore aims to create a vegetation model partly using components from previous models, and partly developing new processes, as a proof of concept that a vegetation modelling framework can both engage with complex hypotheses at the landscape scale, and be compared to independent evidence such as fossil pollen data. In doing so, the thesis will develop an unprecedented workflow for testing climate-vegetation hypotheses.

# Chapter 4

# Model methodological development

Following the review of modelling approaches and previous methodologies carried out in Chapter 3, a new modelling framework is developed to cater to the particular requirements of the southwest Turkey and research questions of the thesis.

The chapter starts by defining key model requirements based on research from the previous chapters. The overarching roadmap for model development is then introduced. This allows the linkage to be made between key model requirements, and model development.

The second section of the chapter is then involved with modelling preparation, which considers a number of important components of the model that will result in the tailoring of the model to the particular requirements of the southwest. The section starts by identifying key species to include in the model, and environmental parameters that are important in the geographical distribution of these species. Data availability, quality, resolution and appropriateness is considered, in order to construct a robust model investigating the linkages between key species, climatological and edaphic variables. A Logistic Regression approach is developed to model single species variability across the region, and further methodological consideration is given to the modelling of multiple species probability in one vegetation model output.

# 4 MODEL METHODOLOGICAL DEVELOPMENT

## 4.1 MODELLING REQUIREMENTS

Based on the aim and research questions of the thesis, a set of modelling requirements have been developed which have not been fully addressed by the previous vegetation modelling approaches examined in Chapter 4. The requirements are:

a. To incorporate key Mediterranean species, but also provide the flexibility to include other species found in palaeoecological records that are not typically Mediterranean
b. To develop a high resolution approach to engage with the landscape scale
c. To identify the climatological envelopes of key species as a basis for modelling climate-vegetation interactions
d. To incorporate topographical and edaphic preferences to better characterise vegetation potential
e. To model vegetation potential under different climatic conditions, without being intractable or overparameterised.
f. To output probabilistic spatial representations of vegetation change over time as well as statistical metrics of change.
g. To translate model output into a form that is comparable to palaeoecological data
h. To have robust regional palaeoecological evidence to compare with model output
i. To statistically compare model output with palaeoecological evidence

If these requirements are met, it will allow the modelling framework to analyse linkages between climate, vegetation and pollen dispersal. In order to satisfy these requirements within this thesis, a number of key methodological stages will be undertaken. Firstly, to satisfy requirement 'a' key species found in pollen records from southwest Turkey will be identified to create a subset for modelling, To satisfy requirement 'b', a brief review of available vegetation distribution, climatological and edaphic data will be undertaken, to provide the highest quality and resolution dataset to model with. Datasets chosen will be of Europe-wide extent, to provide a wide range of climatic and edaphic conditions, and a statistically robust sample for modelling.

To satisfy requirements 'c' and 'd', the thesis will summarise *a priori* information on key species preferences to provide information on the key parameters required for species envelope

modelling. This will provide the basis for the statistical characterisation of each species in a consistent way.

Using these species characterisations, modelling development will then investigate ways of probabilistically mapping vegetation change over time to engage with requirements 'e' and 'f'. The end product of this development will be a bioclimatic model of vegetation showing different distributions under different climate scenarios. This is the first major output of the thesis, and could represent a standalone model in its own right.

Nonetheless, to fully engage with key research questions this vegetation model output needs to be compared to actual palaeoecological data, as reflected in requirement 'g'.

It is acknowledged that the comparison of vegetation model output to palaeoecological data requires a number of methodological steps. The most comprehensive palaeoecological data is sourced from pollen core sequences. However, as has been discussed in Chapter 3, vegetation distribution cannot be directly compared to pollen distribution. In order for this comparison to be undertaken the vegetation model output can be translated into pollen simulations for key parts of the landscape using HUMPOL.

Furthermore, in order to compare these pollen simulations to palynological data for key time periods requires knowing what analytical pollen data is available for the key time period. This is captured in requirement 'h'. In order to do this, analytical pollen core chronology will be assessed and calibrated in a consistent manner.

Finally, to compare simulated pollen to analytical pollen evidence requires a quantitative measure of comparison (requirement 'i'). In order to address this requirement, a number of statistical tools will be assessed and an optimal tool chosen. Graphical and cartographical displays of model output will also aid discussion.

## 4.2 MODELLING ROADMAP

Figure 4-1 summarises the methodological roadmap that will be undertaken to achieve this comparison, and the process is further elaborated below.

Section 4.3 will discuss the reasoning behind the choice of species to be modelled. Secton 4.4 assesses model data input. Section 4.5 and Appendix 1 summarise *a priori* information on key species preferences. Section 4.7 and Section 4.8 details how to probabilistically map spatial representations of vegetation change over time.

Looking forward, Chapter 5 then displays the results of this modelling effort under different climatic scenarios, and discusses the methodology for translating vegetation into pollen simulations. The chronological modelling of analytical pollen data is then documented in Chapter 6, in preparation for comparison with simulated pollen output. Chapters 7-9 then discuss the result of the modelling and comparison exercises in relation to the three research questions.

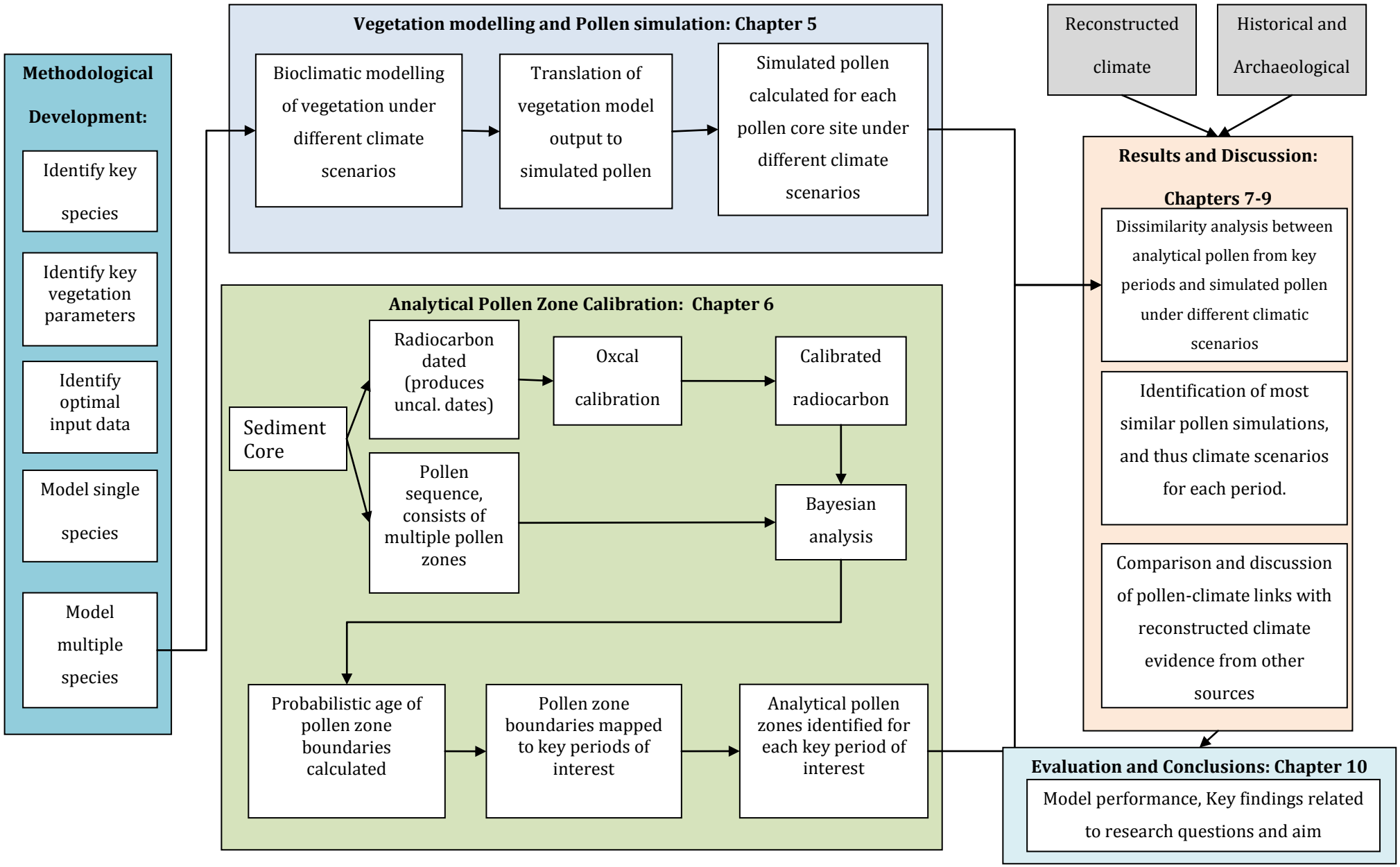


**Figure 4-1 Overview flow diagram of Methodology, Results and Discussion chapters**

This chapter focuses on the first step of the modelling framework; defining the modern bioclimatic limits of key species found in the palaeoenvironmental record of southwest Turkey, and modelling their relative probability across the region. A slightly expanded version of the content of this chapter is shown in Figure 4-2, firstly identifying the key species in the environmental record, secondly assessing the data available to define the bioclimatic limits of key species, and thirdly to develop the modelling methodology to define bioclimatic limits and species probability.

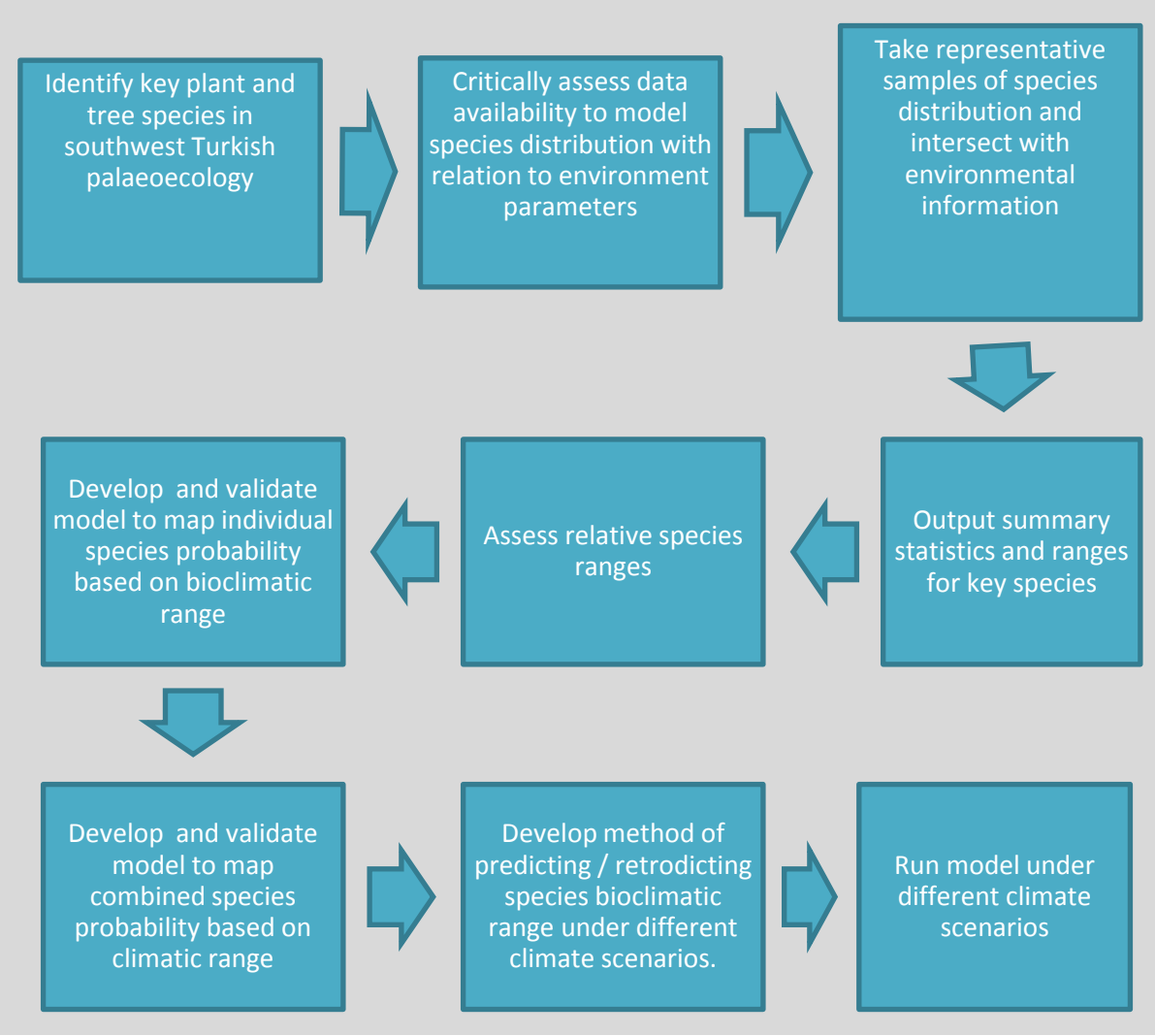


**Figure 4-2 Overview flow diagram of Chapter 5**

## 4.3 IDENTIFICATION OF KEY SPECIES IN SOUTHWEST TURKISH PALAEOECOLOGY

The first methodological task in the development of this vegetation model focused on southwest Turkey is the selection of a suite of plant and tree species. This selection is necessary due to the time and computational effort that would be required to model all the species which could have potentially grown in southwest Turkey during the Holocene.

After an assesment of the key palynological texts from southwest Turkey (van Zeist, Woldring et al. 1975; Bottema and Woldring 1984; Eastwood, Roberts et al. 1999; Vermoere 2002; Kaniewski, De Laet et al. 2007), Table 4-1 shows those species that are present in high numbers in pollen records found across southwest Turkey since the last glacial period, and are identified in the texts as key indicators for a range of climatic and anthropogenic circumstances. The species are classified into forest, herbaceous steppe, cultivation presence and grazing presence indicators. It is important to note that some species, such as *Carpinus betulus* and *Platanus orientalis*, are able to be identified to the species level, whereas others such as *Pinus* are not. This has important implications for further modelling as some species assumptions will need to be made.

**Table 4-1 –Key species found in southwest Turkish pollen cores**

| **Trees / shrubs** | **Herbs, flowers and pteridophyta**[1] | **Cultivation** | **Grazing / disturbance** |
|---|---|---|---|
| *Quercus cerris*-tp *macrolepis* and *trojana* | *Artemisia* | *Olea europaea* | *Centaurea solstitialis* |
| *Quercus coccifera*-tp[2], but also *ilex* or *rotundifolia* | Poaceae / Gramineae | *Juglans regia* | *Plantago lanceolata* |
| *Pinus* (Potentially *nigra* or *brutia*) | Chenopodiaceae | *Pistacia* | *Sanguisorba minor* |
| *Betula* | | Cerealia-tp | |
| *Fagus* | | *Fraxinus ornus* | |
| *Cedrus libani* | | *Vitis vinifera* | |
| *Abies cilicica* | | *Castanea sativa* | |
| *Juniperus* | | *Corylus* | |
| *Alnus* | | | |
| *Picea* | | | |
| *Tilia* | | | |
| *Carpinus betulus* | | | |
| *Platanus orientalis* | | | |
| *Populus* | | | |
| *Ulmus*-tp | | | |

It is also important to note that the selection of species will be impacted by constraints of data availability. The main evidence that exists for vegetation species in the southwest of Turkey come from pollen cores. Macrofossils also exist at archaeological sites for a select group of species, however it is more difficult to determine the provenance of this evidence, as it may

have been transported before being placed in situ. It is assumed that the deposition and preservation of pollen has an inherent spatial component that is related to the surrounding (palaeo)vegetation, thus making it an empirical data source which can be used to compare to model output. However, the pollen species found in palynological records are only a subset of the complex flora that will have grown in any particular environment (Prentice 1988). Those represented in pollen records show pollen from wind pollinated plants only. Furthermore, those pollen grains that are represented in the pollen record are from those plants and trees which have been able to disperse their pollen to a site in the landscape where it falls on, or is carried to a deposition point, that will later be used as a core site (Sugita 1994; Sugita and Scott 2007).

It would be possible to model species that are not represented in pollen cores, where there is other evidence that they were present. However, as pollen cores are analytical data the model will be tested against, other species would not have been able to be validated. For this reason, those species that are present in the pollen record are taken forward as potential model inputs. It is crucial to note that the selection of species to model is the only part of the multivariate modelling process where pollen records are used to inform the model developments to avoid circularity.

Of course, many other species are identified in the pollen record, which potentially play an important part in understanding the connection between climate, culture and vegetation, for instance, aquatic plants, or the wide array of herbs and flowering plants found. However, at the present time not enough information is known regarding their distribution and ecology to adequately understand their climatic preferences, flowering habits, or pollen dispersal mechanism to be able to model them adequately. This will be discussed in the following section as part of data availability considerations.

## 4.4 MODEL INPUT DATA

As identified in Chapter 3, the modelling of high resolution landscape scale processes is significant. Previous modelling approaches that used coarse data are less useful for the archaeological community that tends to work at the finer scale. To this end, the spatial scale and resolution of model input data is considered as a critical part of model development. It is also the case that if the environmental characteristics of individual species are to be discerned, data needs to be collected from a wide area. The third vital data requirement in any modelling exercise is that data needs to be of high quality and consistency. In order to develop this modern analogue model, three attributes are therefore ideally required from the data:

1. High resolution data
2. A large extent to investigate climatic ranges
3. Spatial consistency

In order to capture the main sources of environmental variability in the model, four principal data types will be assessed that form the main components of the model. These are vegetation distribution data, climatic data, topographical data, and edaphic data. A critical review of data sources for these four data types is detailed in Appendix 6.

Considering this review, the final quantitative data layers chosen to build the bioclimatic model are shown in Table 4-2. In order to understand potential sources of error and define the bounds of uncertainty for the model, the potential positional and representational uncertainty connected to each dataset is summarised in Table 4-3. The final species choice is summarised in Table 4-4.

**Table 4-2 Final parameters and data source**

| Final Parameters | Source |
|---|---|
| Species distribution | JRC, CORINE, Turkish forestry directorate |
| Seasonal precipitation | WORLDCLIM |
| Absolute winter minimum temperature | GCHN, WORLDCLIM |
| Average seasonal temperature | WORLDCLIM |
| Average minimum temperature | WORLDCLIM |
| Average maximum temperature | WORLDCLIM |
| Precipitation seasonality | CGIAR |
| Temperature seasonality | CGIAR |
| Aridity, PET | CGIAR |
| Radiation | CGIAR |
| Soil type | Harmonised World Soil Database |
| pH | Harmonised World Soil Database |
| Drainage | Harmonised World Soil Database |
| Available water content | Harmonised World Soil Database |
| Organic carbon | Harmonised World Soil Database |
| Elevation, slope, aspect | SRTM |

**Table 4-3 Identification of uncertainty of data sources**

| Layer | Uncertainty |
|---|---|
| SRTM | 10 m relative vertical height accuracy and <=20 m absolute horizontal accuracy |
| CORINE | 100 m positional accuracy, >85% accurate land cover classification. CORINE data downgraded in resolution to 1km$^2$ to match Pelcom database. |
| Vegetation distribution data | Field data averaged from 16km$^2$ grids. Average of 13% discrepancy between forest area from national forest statistics and Tree Species Distribution map. |
| WorldClim | Generally below 50 m elevation uncertainty, potentially up to 250 m within mountainous areas of Turkey. Cross validation error of precipitation <10 mm/month. Cross validation error of temperature generally <0.3°C. |

**Table 4-4 Final species choice**

| Final species choice | |
|---|---|
| *Pinus brutia, Pinus nigra* | *Populus nigra* |
| *Alnus cordata* | *Tilia cordata* |
| *Quercus cerris* | *Ulmus glabra* |
| *Quercus coccifera* | *Olea europaea* |
| *Betula pendula* | *Juglans regia* |
| *Cedrus deodara* | Dry agriculture |
| *Abies alba* | *Fraxinus ornus* |
| *Juniperus oxycedrus* | *Vitis vinifera* |
| *Carpinus betulus* | *Castanea sativa* |
| *Corylus avellana* | Grassland |
| *Fagus sylvatica* | *Artemisia* Steppe |
| *Platanus orientalis* | |

## 4.5 CHARACTERISATION OF INDIVIDUAL SPECIES CLIMATIC AND EDAPHIC ENVELOPES

This section aims to quantitatively characterise the key species identified in section 4.3 based on the climatic and edaphic data selected in section 4.4. This will provide a basis for probabilistically modelling their distribution both in modern times and retrodictively under different climatic regimes.

A large pool of species distribution and environmental data was available from a wide geographical extent. To be able to define species characteristics and limits does not require assessment of every pixel in every distribution, but instead can be examined using a representative sample (Augustin, Cummins et al. 2001). This section therefore first undertakes a sampling strategy and statistical methodology to investigate species limits.

The analysis then assesses the climatic, edaphic and topographic envelope that each species distribution covers. The outline methodology for this section is summarised in Figure 4-3.

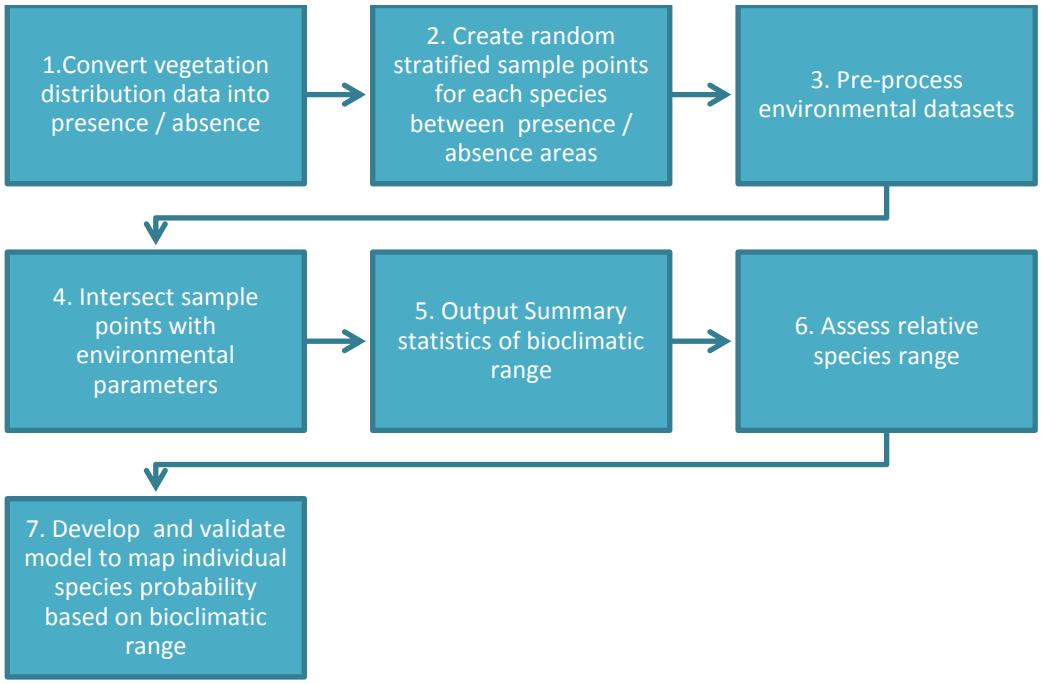


**Figure 4-3 Processing steps to model bioclimatic range**

## 4.6 SPECIES BIOCLIMATIC RANGES

To investigate the climatic and edaphic considerations of each species, a sampling strategy was devised in order to compare the statistical distribution of species presence with the statistical distribution of species absence, and to reduce autocorrelation effects. The details of this methodology are presented in Appendix 7.

Once climatological, topographical and edaphic data had been collected for each sample point for each species, the mean, median, minimum, maximum, 5$^{th}$ and 95$^{th}$ percentiles of each variable for each species was calculated. A summary of these statistics are shown in Table 4-5 and Table 4-6, and the full tabular data for each species is available on request. Although not recorded here, PCA analysis was also used to visualise the relative correlation between species presence and environmental variables.

### 4.6.1 The statistical significance of species bioclimatic ranges

Following the absolute and relative definition of species environmental ranges based on high resolution data, the data was further analysed to discover whether the distribution of environmental variables was significantly different between species presence and absence. This is important as it assesses the potential for each variable to separate between areas that are preferential for species, and those that are not. It is not required for every variable to show significant difference for every species, only that a selection do. This analysis can be done in a number of ways. Certain statistics compare the distribution across groups, while others compare the ranges, or compare the medians. Each statistical test has certain assumptions, one of which is the normality of data. A precheck was undertaken to examine the skewness and kurtosis of the data, before choosing suitable statistical checks to assess the difference in medians, distribution and range between two samples. The statistical tests undertaken and the full results are detailed in Appendix 8. The results show that the median, distribution shape and range of species environmental parameters are significantly different to the European control. The statistics have also shown that all species are distributed on significantly different soil types, pH, aspect, soil texture and soil drainage than the European control. These statistics help to validate the approach of characterising species presence and absence using climatic, topographical and edaphic parameters.

**Table 4-5 Species bioclimatic ranges based on European data**

| Species | Minimum monthly temperature (°C) | Maximum monthly temperature (°C) | Median monthly Spring temperature (°C) | Maximum monthly Summer temperature | Minimum annual precipitation (mm) | Minimum aridity index | Maximum aridity index |
|---|---|---|---|---|---|---|---|
| *Quercus cerris* | -9.9 | 34.6 | 10.1 | 26.2 | 432 | 0.3 | 1.4 |
| *Quercus coccifera* | -9.6 | 34.5 | 11.51 | 26.7 | 432 | 0.4 | 1.4 |
| *Pinus brutia* | -8.2 | 35.1 | 12.3 | 27.0 | 384 | 0.4 | 1.4 |
| *Pinus nigra* | -12.1 | 34.8 | 9.5 | 25.8 | 260 | 0.2 | 2.9 |
| *Betula pendula* | -12.0 | 28.9 | 5.7 | 22.5 | 481 | 0.6 | 3.9 |
| *Olea europaea* | -2.5 | 36.5 | 14.1 | 26.9 | 313 | 0.3 | 1.7 |
| *Cedrus deodara* | -7.4 | 32.5 | 10.7 | 24.7 | 468 | 0.5 | 1.6 |
| *Castanea sativa* | -12 | 30 | 8.9 | 26.0 | 538 | 0.5 | 4.7 |
| *Fraxinus ornus* | -10.4 | 32.1 | 10.6 | 25.1 | 447 | 0.4 | 4.5 |
| *Juglans regia* | -6.5 | 32.5 | 10.73 | 24.7 | 553 | 0.6 | 2.4 |
| *Vitis vinifera* | -9.3 | 39.3 | 12.1 | 29.4 | 276 | 0.2 | 1.5 |
| *Carpinus betulus* | -11.5 | 30.3 | 9.1 | 24.1 | 405 | 0.5 | 2.4 |
| *Platanus orientalis* | -11.5 | 34.6 | 10.7 | 26.7 | 442 | 0.4 | 1.7 |
| *Fagus sylvatica* | -13.1 | 33.8 | 8.0 | 25.8 | 452 | 0.4 | 6.4 |
| *Picea abies* | -13.0 | 31.1 | 5.8 | 23.5 | 454 | 0.4 | 6.4 |
| *Alnus cordata* | -5 | 31.9 | 9.9 | 25.9 | 616 | 0.6 | 1.6 |
| *Abies alba* | -14 | 30.6 | 6.8 | 25.2 | 478 | 0.4 | 7.2 |
| *Ulmus glabra* | -12.7 | 28.6 | 8.6 | 21.8 | 546 | 0.6 | 6.3 |
| *Corylus avellana* | -6.4 | 29.1 | 9.0 | 22.7 | 482 | 0.47 | 2.4 |
| Dry agriculture | -11.7 | 36.1 | 9.2 | 26.9 | 253 | 0 | 2.3 |
| Sclerophyllous | -8.5 | 36.3 | 12.2 | 26.9 | 248 | 0.2 | 2.9 |
| Shrubland | -12.4 | 36.3 | 8.8 | 26.9 | 292 | 0.2 | 6.7 |
| Grassland | -13 | 36.3 | 8.5 | 26.9 | 276 | 0 | 4.9 |

**Table 4-6 Species bioclimatic ranges based on European data (contd.)**

| Species | Maximum elevation | Maximum slope angle | Average pH | Organic carbon | Average drainage | Average texture |
|---|---|---|---|---|---|---|
| *Quercus cerris* | 2510 | 31.0 | 6.5 | 1 | 3 | 2 |
| *Quercus coccifera* | 2278 | 31.9 | 7.2 | 1 | 4 | 2 |
| *Pinus brutia* | 2120 | 30.0 | 7.2 | 1 | 4 | 2 |
| *Pinus nigra* | 2673 | 33.7 | 6.7 | 1 | 4 | 2 |
| *Betula pendula* | 2581 | 36.7 | 5.5 | 3 | 4 | 2 |
| *Olea europaea* | 1524 | 23.3 | 7 | 1 | 4 | 2 |
| *Cedrus deodara* | 2285 | 27.3 | 7.3 | 1 | 3 | 2 |
| *Castanea sativa* | 2791 | 40.8 | 6.2 | 1 | 4 | 2 |
| *Fraxinus ornus* | 2495 | 40.1 | 6.5 | 1 | 3 | 2 |
| *Juglans regia* | 2178 | 23.8 | 8.3 | 1 | 4 | 2 |
| *Vitis vinifera* | 1720 | 39.0 | 7 | 2 | 4 | 2 |
| *Carpinus betulus* | 2355 | 23.4 | 6.2 | 1 | 3 | 2 |
| *Platanus orientalis* | 2653 | 32.1 | 6.6 | 1 | 4 | 2 |
| *Fagus sylvatica* | 3312 | 37.5 | 6.1 | 2 | 4 | 2 |
| *Picea abies* | 2918 | 35.7 | 5.6 | 3 | 4 | 2 |
| *Alnus cordata* | 2163 | 31.2 | 6.2 | 3 | 6 | 3 |
| *Abies alba* | 3310 | 42.8 | 6.1 | 2 | 4 | 2 |
| *Ulmus glabra* | 2957 | 42.8 | 5.9 | 2 | 3 | 2 |
| *Corylus avellana* | 2344 | 33.5 | 6.5 | 2 | 3 | 2 |
| Dry agriculture | 2918 | 35.7 | 5.6 | 3 | 4 | 2 |
| Sclerophyllous | 2681 | 29.8 | 6.9 | 1 | 4 | 2 |
| Shrubland | 3021 | 36.5 | 6.4 | 2 | 4 | 2 |
| Grassland | 2840 | 39.0 | 6.2 | 4 | 3 | 2 |

## 4.7 MULTIVARIATE REGRESSION AND SPECIES PROBABILITY

This chapter has so far identified key model input; choosing species and bioclimatic parameters, before assessing individual species ranges and their statistical significance. The next section will use this information to develop and validate a model to map individual species probability across southwest Turkey, and then develop a method to combine these individual species probabilities together to create a multi-species vegetation model, as shown in Figure 4-4.

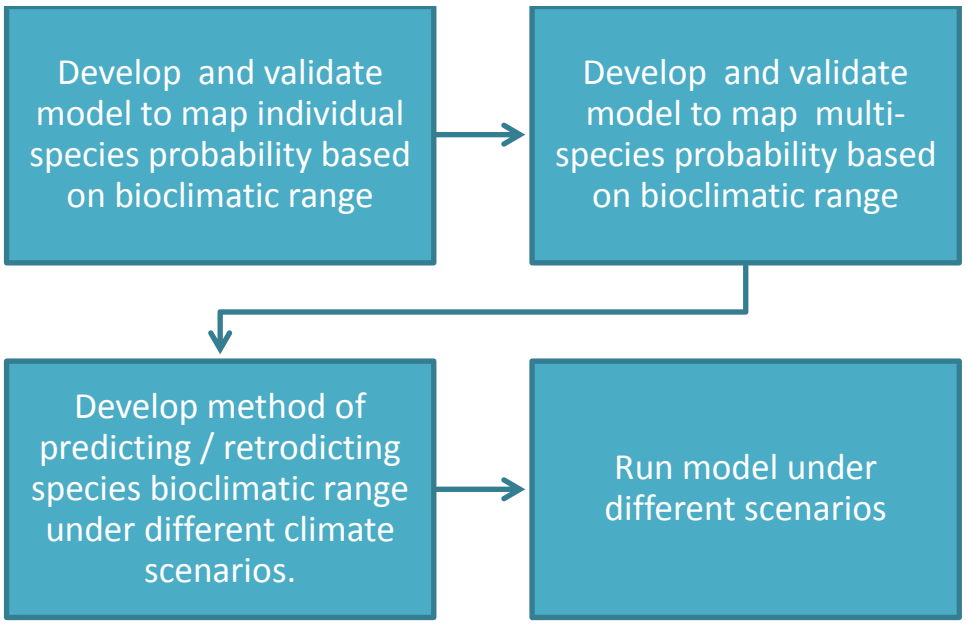


**Figure 4-4 Multivariate regression and species probability methodological steps**

### 4.7.1 Methodological development 1: Developing and validating an individual species bioclimatic model.

As discussed in Chapter 3, the Biome model of Box (1981) identified upper and lower boundaries for plant types, which could be mapped against available climate normals. Section 4.6 tabulated species bioclimatic limits for key Mediterranean palaeoecological species, and this data could be used to undertake a simple ecological modelling exercise. Indeed, this type of model was first created as part of model development of the thesis, however it was found that the threshold method was only useful for simple analyses. One of the main issues was that it did not provide a mechanism to differentiate the relative potential of species at any particular point, and did not allow for more realistic, nuanced spatial analysis of vegetation potential at the landscape scale. Therefore, although these thresholds are a useful component for discussion and single species modelling, they are not adequate to investigate multi-species vegetation modelling.

Chapter 3 also considered more detailed models that included the mechanistic physical processes that control the survival and performance of plants, incorporating water balance models, forest gap model (Cramer, Bondeau et al. 2001) etc. However, as discussed, this tends to involve the grouping of species into Plant Functional Types (PFT), and the population of a number of parameters with information that is not available for palaeoecological investigations. Again, as part of model development a model of this type was created using a software called SIMILE integrated with GIS software, to explore species recruitment, growth and death. These exact issues were faced when trying to consider feasible parameters to put into allometry and hydrology sections of the model, and practical issues were encountered with the size of the model and amount of time required to cover a small area of the region.

This provided the background for the justification of which vegetation model type to employ. A number of statistical tools were investigated alongside GIS analysis, however, considering the source data, a relatively straightforward regression analysis was decided upon as a basis for investigating multivariate relationships of independent variables against a dependent variable.

Considering previous research, it was considered that a regression based analysis would be a potentially appropriate solution to assessing the link between environmental parameters and vegetation distribution (Braak 1987; Carmel, Kadmon et al. 2001). What type of regression analysis to undertake also depended to a certain extent on the type of data available. Here, it takes the form of a dichotomous dependent variable (presence or absence of species), and a number of independent variables in a variety of formats (climate, topography, edaphic). A dichotomous dependent variable restricts the type of regression analysis available. Logistic Regression analysis and Discriminant Analysis are two common methods used to investigate the correlation of independent variables with a binary dependent variable (e.g. Peng et al. 2002, Jain and Jain 2007). Discriminant Analysis assumes normally distributed data, which, from previous analysis, the dataset under consideration is known to violate. Conversely, Logistic Regression does not require normality, linear relations or equal variance, and is therefore considered a suitable statistical tool to predict the event probability of a dichotomous dependent variable. The use of Logistic Regression is a relatively novel choice for modelling vegetation probability at this scale, but has been utilised by a few authors to good effect (Augustin, Cummins et al. 2001; Fangliang, Zhou et al. 2003; Flantua, van Boxel et al. 2007) .

### 4.7.2 Logistic Regression Analysis

#### 4.7.2.1 Model parameter choice: VIF analysis and variable dimension reduction.

Once Logistic Regression analysis was decided upon to assess species potential across the region, a number of practical aspects needed to be considered. If a Logistic Regression analysis is to be successful, it is important to check for multicollinearity amongst variables. Suites of variables were therefore entered into linear regression models in order to calculate Variance Inflationary Factors (VIF). This gives a measure of the severity of multicollinearity, and states how much the variance of the estimated regression coefficients will increase due to collinearity. If variance is too high, it may lead to lack of statistical significance of individual independent variables, and may also result in wrong signs and magnitudes of coefficient estimates leading to incorrect conclusions. VIF values above ~10-12 are a cause for concern. Bivariate correlations were also undertaken to examine the strength of correlations between variables.

If the VIF is too high in the analysis there are a number of options that may be used to reduce it. The first method is to remove those variables with the highest VIF until the overall VIF falls below the threshold value. A second method attempts to merge those variables that have a high VIF into a smaller number of files that contain the majority of variance. This is done via averaging, PCA or some other method of dimension reduction. The difficulty with this method is knowing what these end variables represent once they have been merged. Considering that seasonal climate changes have been recognized as being important to vegetation distribution, the first option is preferred, to maintain the ability to investigate seasonal effects.

### 4.7.3 Logistic Regression methodology

SPSS binary Logistic Regression was first used to calculate a standard Logistic Regression. The linear logistic model is a type of generalized linear model that extends the linear regression model by linking the range of real numbers to the 0-1 range. This is achieved by using a link

function as shown in Equation 1. The addition of a hierarchical scheme adds terms to the regression model in phases, or blocks, in order to examine the influence of particular variables once other variables are accounted for.

$$\pi_i = \frac{e^{Z_i}}{1 + e^{Z_i}} = \frac{1}{1 + e^{-Z_i}}$$

OR

$$Z_i = \log\left(\frac{\pi_i}{1 - \pi_i}\right)$$

**Equation 1 Logistic Regression link function**

Where $Z_i$ is the value of the unobserved continuous variable for the *i*th case, and $\pi_i$ is the probability the *i*th case experiences the event of interest. As with other multiple regression analyses, Z is linearly related to a number of independent variables *x*, as shown in Equation 2.

$$Z_i = b_0 + b_1 x_{i1} + b_1 x_{i2} + \ \ldots + b_p x_{ip}$$

**Equation 2 Logistic Regression equation**

Where $x_{ij}$ is the *j*th predictor for the *i*th case, $b_j$ is the *j*th coefficient and *p* is the number of predictors

The regression coefficients are estimated in SPSS using an iterative maximum likelihood method. The likelihood function *l* for *n* observations $y_{1, \ldots, } y_n$ with probabilities $\pi_{1, \ldots, } \pi_n$ and case weights $w_{1, \ldots, } w_n$, can be written as:

$$l = \prod_{i=1}^{n} \pi_i^{w_i y_i} (1 - \pi_i)^{w_i (1 - y_i)}$$

It follows that the logarithm of l (the logit) is

$$L = \ln(l) = \sum_{i=1}^{n} (w_i y_i \ln(\pi_i) + w_i (1 - y_i) \ln(1 - \pi_i))$$

and the derivative of $L$ with respect to $\beta_j$ is

$$L^*_{X_j} = \frac{\partial L}{\partial \beta_j} = \sum_{i=1}^{n} w_i(y_i - \pi_i)x_{ij}$$

### 4.7.4 **Fitting the model**

The binary regression model may be fitted using one of two main approaches. The first is a simultaneous approach (forced entry), whereby all independent variables are treated simultaneously and equally. This strategy is most appropriate when there is not a logical or theoretical basis for considering any variable prior to another (Foster, Barkus et al. 2006). The second approach uses a stepwise routine, which automates the addition or exclusion procedure of variables. The variables are chosen based on the Wald statistic, a likelihood ratio test or a conditional algorithm. This method is useful for creating parsimonious models, however has been criticized for capitalizing on chance, and may 'throw out' variables that are in fact useful (Foster, Barkus et al. 2006). The third approach is a hierarchical approach, which requires that the point of entry of independent variables into the model is based upon theoretical considerations, thus alleviating those criticisms squared at stepwise regression.

Variables were entered using the forced entry method as opposed to stepwise forward or hierarchical entry. This was because the order of importance of variable entry into the model was not known and presuming this would have potentially created bias.

### 4.7.5 **Rare Events correction**

There is an anticipated issue with the use of standard Logistic Regression given the form of the dataset. Considering the amount of land area under which any one species is cultivated across Europe compared to the amount of area where it is not grown, the amount where it is grown is many times smaller. As such, species presence is considered a rare event (RE). Rare events can cause problems in standard regression models, and an underestimation of the probability of occurrence can commonly occur (King and Zeng 2001). A Logistic Regression that is tailored to

rare events, such as the one developed by Imai et al. (2007) designed to run in the 'R' statistical package is considered to be the most appropriate statistical method for calculation of coefficients.

Rare Events correction was implemented in R, using the Relogit package (Imai et al. 2007, Iami et al. 2008). The approach is composed of three different correction phases. The first requires gaining a representative sample, using choice controlled sampling. This helps to reduce autocorrelation, and is documented in Appendix 7.

The second 'prior' correction is required due to the bias introduced by sampling on the dependent variable. The formula (Equation 3) uses the actual proportion of present to absent values ($\tau$) and the observed proportion of present to absent values ($\bar{y}$) to calibrate the constant of the regression equation ($\alpha$). This value is calculated for each species as shown in Table 4-7

$$\alpha = \hat{\alpha} - ln\left[\left(\frac{1-\tau}{\tau}\right)\left(\frac{\bar{y}}{1-\bar{y}}\right)\right]$$

**Equation 3 Prior correction**

The third correction aims to rectify the underestimation of the probabilities from the substitution of the intercept value.

**Table 4-7 Calculation of $\tau$ values for Rare Events correction**

| Species | Area where present ($Km^2$) | Area where absent ($Km^2$) | $\tau$ |
|---|---|---|---|
| ***Quercus cerris*** | 98578 | 4864853 | 0.020 |
| ***Pinus brutia*** | 15789 | 5054469 | 0.003 |
| ***Pinus nigra*** | 160557 | 4802874 | 0.033 |
| ***Fraxinus ornus*** | 29748 | 4933683 | 0.006 |
| ***Betula Pendula*** | 389574 | 4573857 | 0.085 |
| ***Juglans Regia*** | 2119 | 4961312 | 0.0004 |
| ***Quercus coccifera*** | 20561 | 4942870 | 0.0042 |
| ***Olea europaea*** | 10407 | 4953024 | 0.0021 |
| ***Castanea sativa*** | 125379 | 4838052 | 0.0259 |
| ***Vitis vinifera*** | 66668 | 8236903 | 0.008 |
| ***Abies Alba*** | 167220 | 4796211 | 0.0348 |
| ***Alnus cordata*** | 4214 | 4959217 | 0.000849 |
| ***Carpinus betula*** | 149284 | 4814147 | 0.0310 |
| ***Populus nigra*** | 9319 | 4954112 | 0.00188 |
| ***Corylus avellana*** | 5198 | 4958233 | 0.001 |
| ***Tilia cordata*** | 50053 | 4913378 | 0.010187 |
| ***Juniperus oxycedrus*** | 14052 | 4949379 | 0.0028 |
| ***Sclerophyllous*** | 87614 | 4875753 | 0.017969 |
| ***Shrub*** | 141512 | 4821855 | 0.0293 |
| **Non-irrigated agriculture** | 1200311 | 3763056 | 0.318972 |
| ***Fagus sylvatica*** | 470460 | 4492971 | 0.10471 |
| ***Picea abies*** | 684971 | 3545293 | 0.193 |
| ***Platanus orientalis*** | 10040 | 4216348 | 0.00238 |
| ***Ulmus glabra*** | 15086 | 4213253 | 0.00358 |
| **Grassland** | 37256 | 4926111 | 0.007563 |
| ***Cedrus libani*** | 1364 | 4962067 | 0.000274 |
| ***Populus*** | 9319 | 4954112 | 0.00188 |

### 4.7.6 Model assessment

The output to the Logistic Regression model can be assessed in a number of ways. Some of the statistical values reported in SPSS are not appropriate for the method, for instance, the various $R^2$ values, although calculated, have limited use in Logistic Regressions and are therefore not given consideration. The Hosmer and Lemeshow goodness of fit test is sensitive to sample size (i.e. Kramer and Zimmerman, 2007), and may not be valid for very large or small sample sizes. It has also been criticised for having limited power, as it depends on an arbitrary cut point on predicted probabilities (e.g. Hosmer et al. 1997).

Therefore, classification tables were consulted, as they assess the accuracy of model prediction to observed values. The classification table from each block can be compared to the classification from the baseline (null) model, which only includes the constant. The null model was classified into true and false prediction rates, resulting in an overall accuracy of ~50%, the amount of correct classifications by chance. The addition of variables into the model increases the classification accuracy significantly if the combination of variables are correlated to species presence. A hit ratio of 25% more than chance (i.e. more than the null model) is generally considered acceptable.

## 4.8 RARE EVENTS LOGISTIC REGRESSION MODEL RESULTS

### 4.8.1 Species coefficients

The Logistic Regression coefficients ('b' in Equation 2) from the Rare Events regression analysis of each species are tabulated in Appendix 8. Where variables were removed due to an overly large VIF, this is stated in the table, and where variables are found to have a statistically insignificant relationship to the dependent variable, this is stated with the tern 'INS'.

### 4.8.2 Overall model accuracy

From these coefficients, the user, producer and overall accuracy of the model could be calculated. The results of this analysis are shown in Figure 4-5. Those species with higher accuracy are likely to either be more influenced by the climatic, topographic or edaphic

variables entered, or else are constrained to a specific geographical niche which is easy to differentiate from the rest of Europe. If a species is adaptable and is present over large areas of Europe, it is harder to differentiate by climate or soil type, and therefore the modelling accuracy is lessened. This is why the broader classes of shrubland and grassland are more difficult to predict, compared to the climatically and geographically restricted distributions of *Olea europaea*, or *Quercus coccifera*. However, all species were modelled with accuracy over 70% which still represents a good model fit.

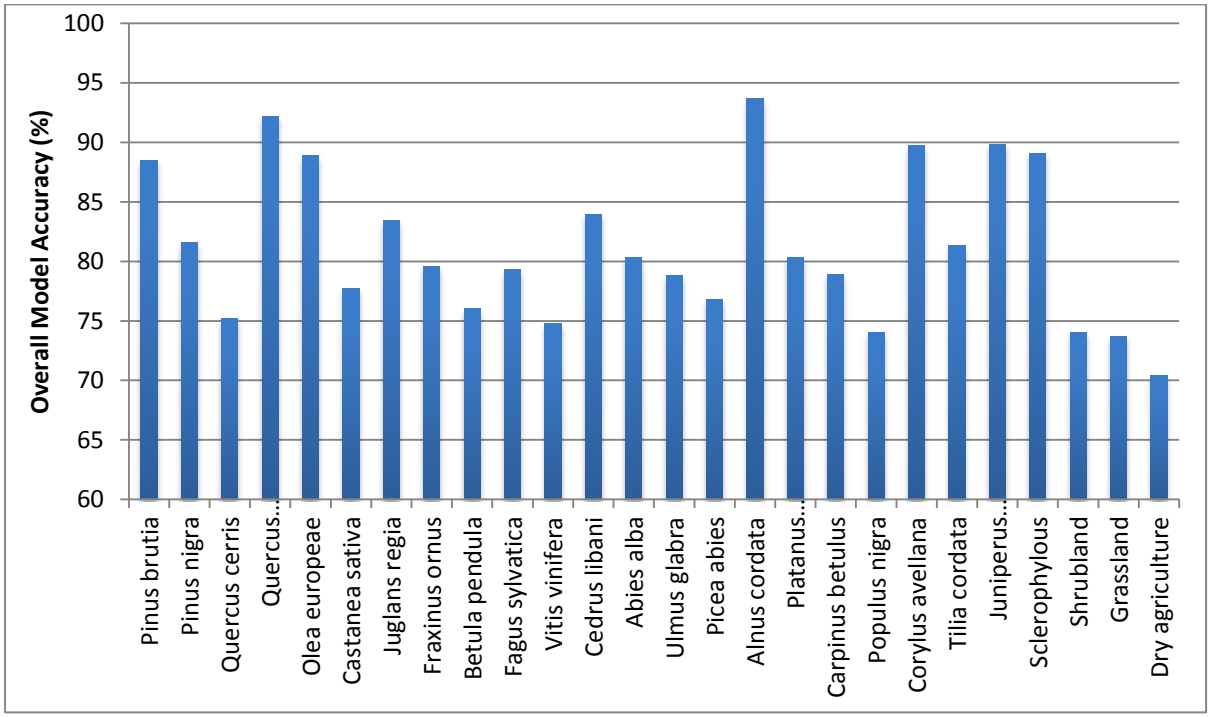


**Figure 4-5 Overall model accuracy by species**

The variables and their associated coefficients were then constructed into equations that would be calculable in ArcGIS. The format of such an equation is shown in Equation 4, the output to which is probability surfaces as detailed in the next section.

Pinus_Brutia = -16.10 + ([ph] * -0.147) + ([slope] * 0.148) + ([SRTM_1km.tif] * -0.001) + ([awc] * 0.290) + ([drainage] * 0.235) + ([texture] * 0.582) + ([prec_sum] * -0.055) + ([prec_aut] * -0.013) + ([ai_cal] * 4.761) + ([tmax] * -0.008) + ([t_seas] * 0.002) + ([p_seas] * -0.028) + ([calcisol] * 1.226) + ([fluvisol] * 0.432) + ([vertisol] * 0.904) + ([east] * 0.267)

**Equation 4 Logistic Regression equation in ArcGIS format**

### 4.8.2.1 Probability maps

Calculating the Logistic Regression equation for each species using significant variables over the whole region allows a probability surface to be built up. For brevity, only two species maps are displayed here. It is important to note that the probability surface represents the relative probability of where a species *could* grow, based on the statistical data collected for the whole of Europe. It does not predict exactly where a species *does* grow, as this is also dictated by many other factors such as urban development, cultural practices and economics. It therefore represents the best estimate of correlation with natural factors given the data available.

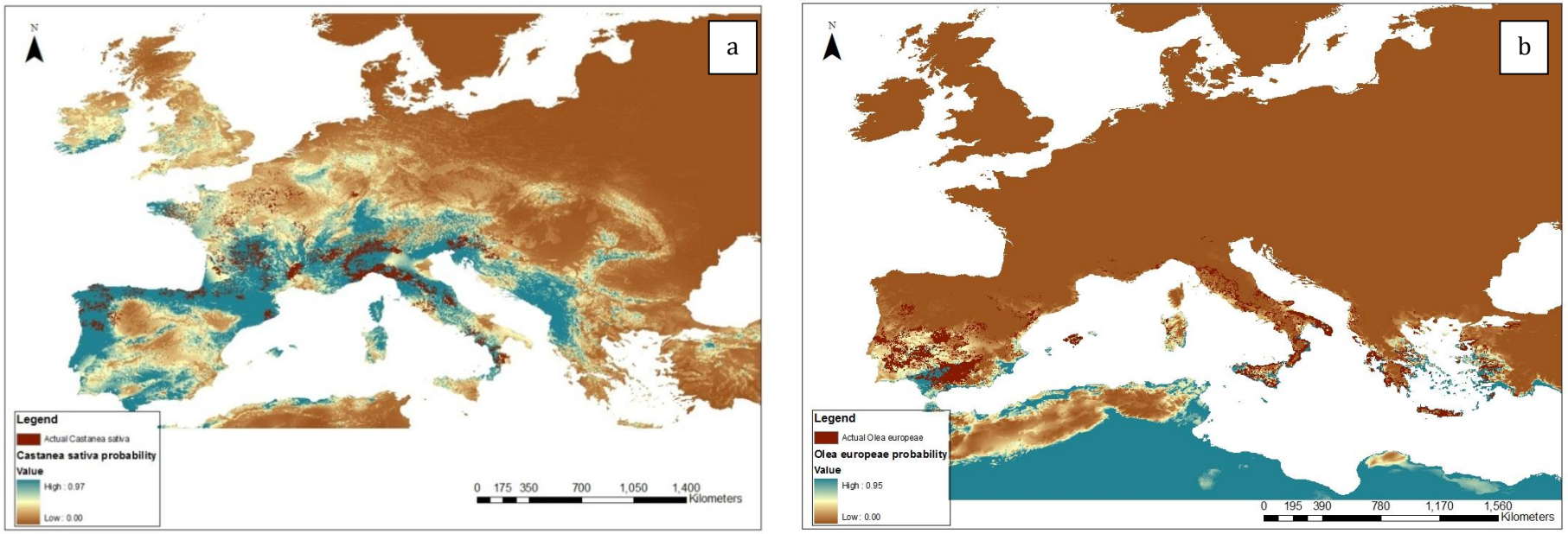


**Figure 4-6 Species probability of (a) *Castanea sativa*, and (b) *Olea europaea* across Europe. Overlaid is actual species distribution.**

## 4.9 METHODOLOGICAL DEVELOPMENT 2: DEVELOPING AND VALIDATING A MULTIPLE SPECIES BIOCLIMATIC MODEL.

The output to the Logistic Regression has been calculated as a continuous probability surface through GIS analysis. In the previous section one probability surface was calculated for each species. In order to create a model of multiple species at once however, requires some combination of this probability, and some decision rules to decide the dominant species at each pixel. A couple of methods were considered. The first used a cutoff of presence / absence of a species, estimated using a Receiver Operator Curve (ROC), followed by logical rules to assign the species with the highest probability at any one pixel to be the present species. However, this created large areas of mono species, due to certain species having an overall higher probability.

It was decided that a more natural process would need to include randomness and heterogeneity. A second method was therefore developed that designated a certain number of points for each species, representing 1km$^2$ stands, to be distributed across the region of interest, weighted towards areas with high potential. As this took a lot of computing power, the analysis from this point onwards focused on southwest Turkey, and therefore subset all the probability surfaces to this extent.

To achieve this, summary statistics were calculated for each species probability surface. The average species probability for the area of southwest Turkey was taken as a measure of relative species probability, and from this, the amount of points were calculated based on a sample size of 30 000, from which the original Logistic Regression was formed, as shown in Equation 5.

$$\left(\frac{1}{n}\sum_{i=1}^{n} a_{ij} = \frac{a_1+a_2\ldots+a_n}{n}\right) c$$

**Equation 5 Species points calculation**

Where a is the probability of the $ij_{th}$ pixel, n is the total number of pixels, and c is the original sample size of 30,000. Figure 4-7 shows the average probability for each species, and Table 4-8 tabulates the amount of points to be distributed for each species given this probability. Points for each species were then distributed randomly, but weighted by the probability surface, using Hawth's Tools 'Generate Random Points' tool. Figure 4-8 shows the distribution of *Pinus nigra* points overlaid on the probability surface, and Figure 4-9 shows all species points when merged into a single shapefile.

To turn this vegetation point file into a final vegetation surface adequate for simulation of pollen dispersal requires 4 more processing steps.

1. The point files for all species are collated and converted to a 1 km resolution raster with metres as the linear unit. Each species is given a unique ID to differentiate them. In certain areas, more than one point is found on a particular pixel. If this is the case then the tool chooses the most frequent species on that point. If there are the same number of points on the pixel from a number of species, then the highest FID is used, essentially a random measure.
2. Steppic areas are mapped based on a threshold of annual precipitation under 400 mm and 300 mm for montane steppe and true steppe respectively. Under 300 to 400 mm tree species are still present, mixed in with steppe. Under 300 mm, the classification is purely steppe.
3. Water bodies are added as a class. HUMPOL requires water bodies are classified as '1'.
4. The final layer is shown in Figure 4-10 with each class as a particular ID value.

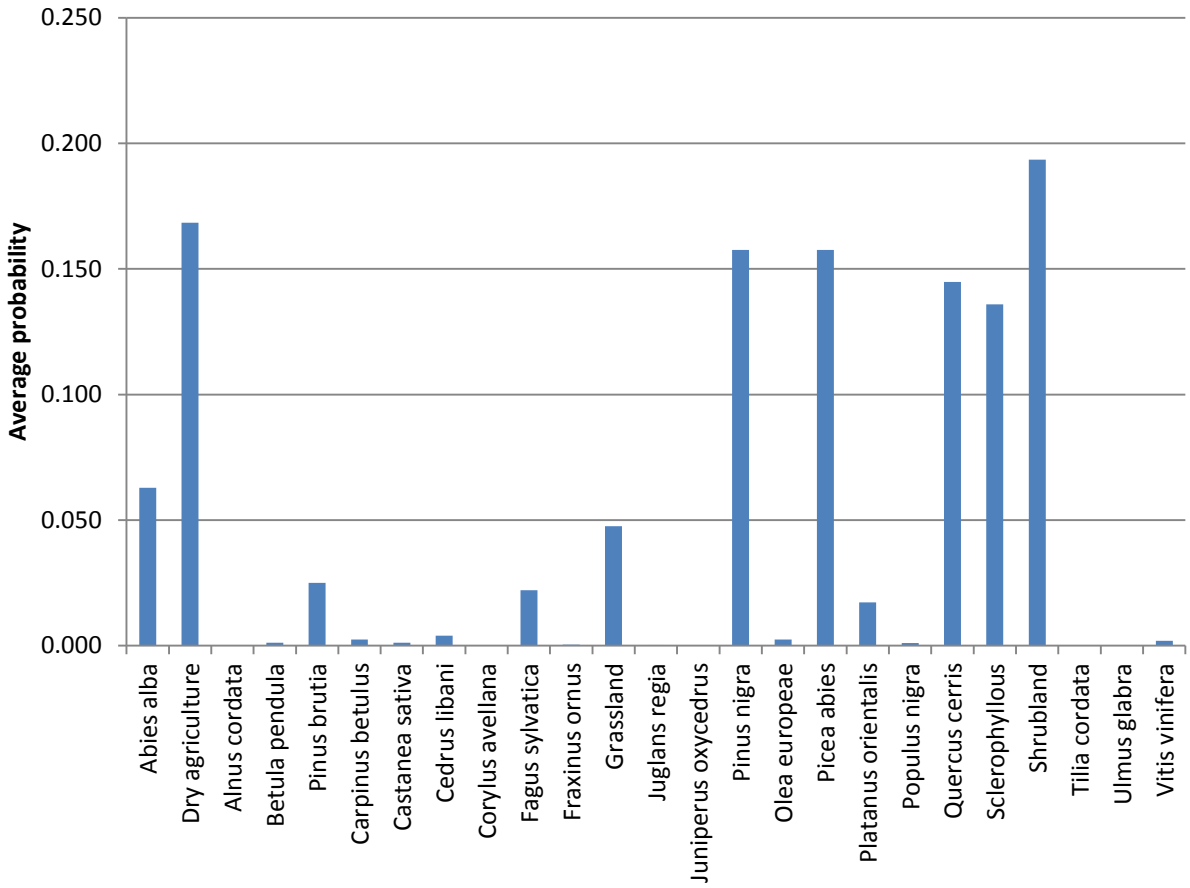


**Figure 4-7 Average species probability across southwest Turkey based on modern data**

**Table 4-8 Amount of points to be distributed for each species**

| Species | Average probability | # of points based on sample size of 30 000 |
|---|---|---|
| *Abies alba* | 0.063 | 1886 |
| Dry agriculture | 0.168 | 5050 |
| *Alnus cordata* | 0.000 | 0 |
| *Betula pendula* | 0.001 | 36 |
| *Pinus brutia* | 0.025 | 750 |
| *Carpinus betulus* | 0.002 | 73 |
| *Castanea sativa* | 0.001 | 38 |
| *Cedrus libani* | 0.004 | 120 |
| *Corylus avellana* | 0.000 | 0 |
| *Fagus sylvatica* | 0.022 | 662 |
| *Fraxinus ornus* | 0.000 | 12 |
| Grassland | 0.048 | 1428 |
| *Juglans regia* | 0.000 | 8 |
| *Juniperus oxycedrus* | 0.000 | 5 |
| *Pinus nigra* | 0.158 | 4727 |
| *Olea europaea* | 0.002 | 72 |
| *Picea abies* | 0.158 | 4727 |
| *Platanus orientalis* | 0.017 | 517 |
| *Populus nigra* | 0.001 | 33 |
| *Quercus cerris* | 0.145 | 783 |
| Sclerophyllous | 0.136 | 3562 |
| Shrubland | 0.193 | 4077 |
| *Tilia cordata* | 0.000 | 5803 |
| *Ulmus glabra* | 0.000 | 5 |
| *Vitis vinifera* | 0.002 | 59 |

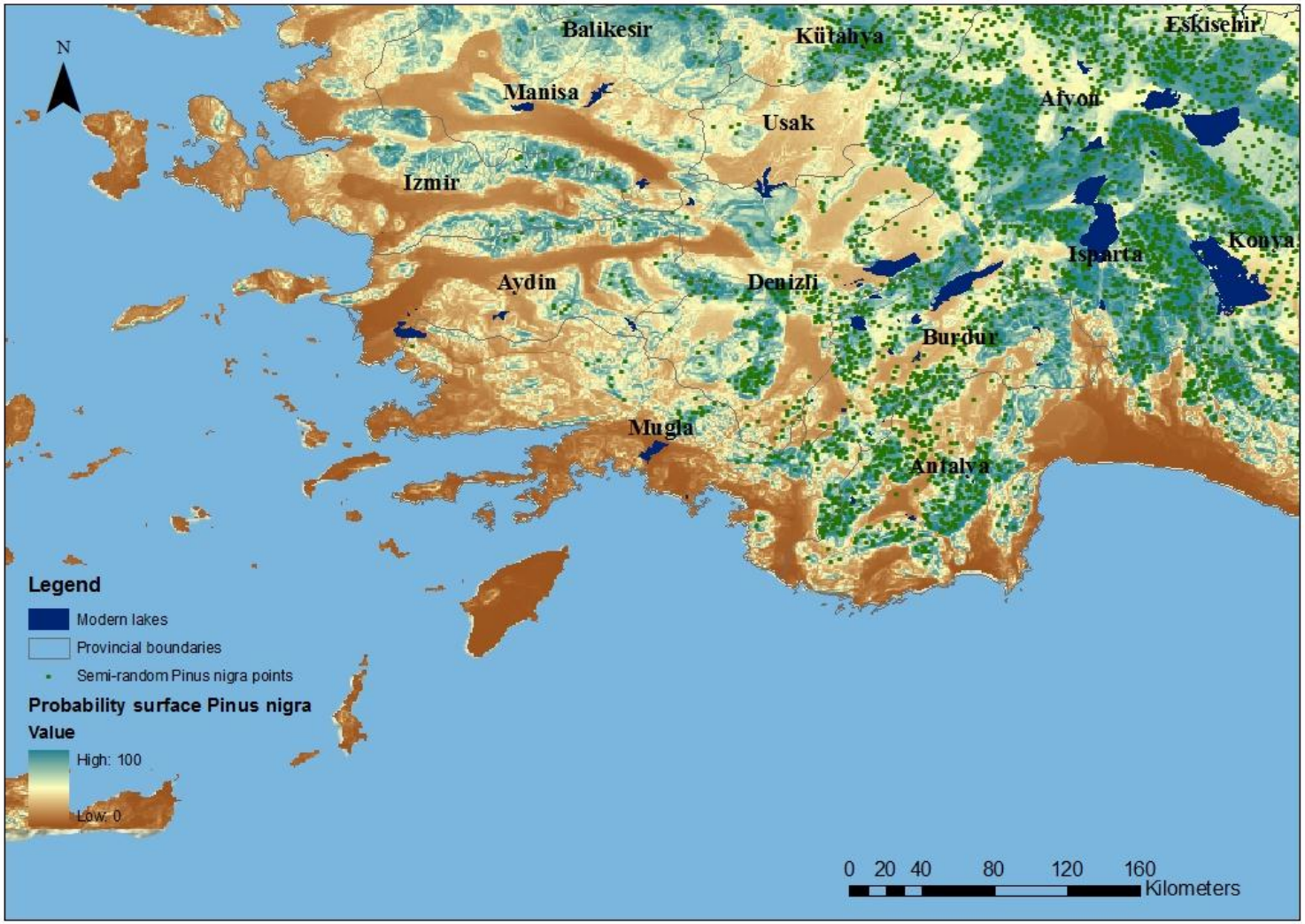


**Figure 4-8 *Pinus nigra* point spread weighted by the continuous probability surface beneath**

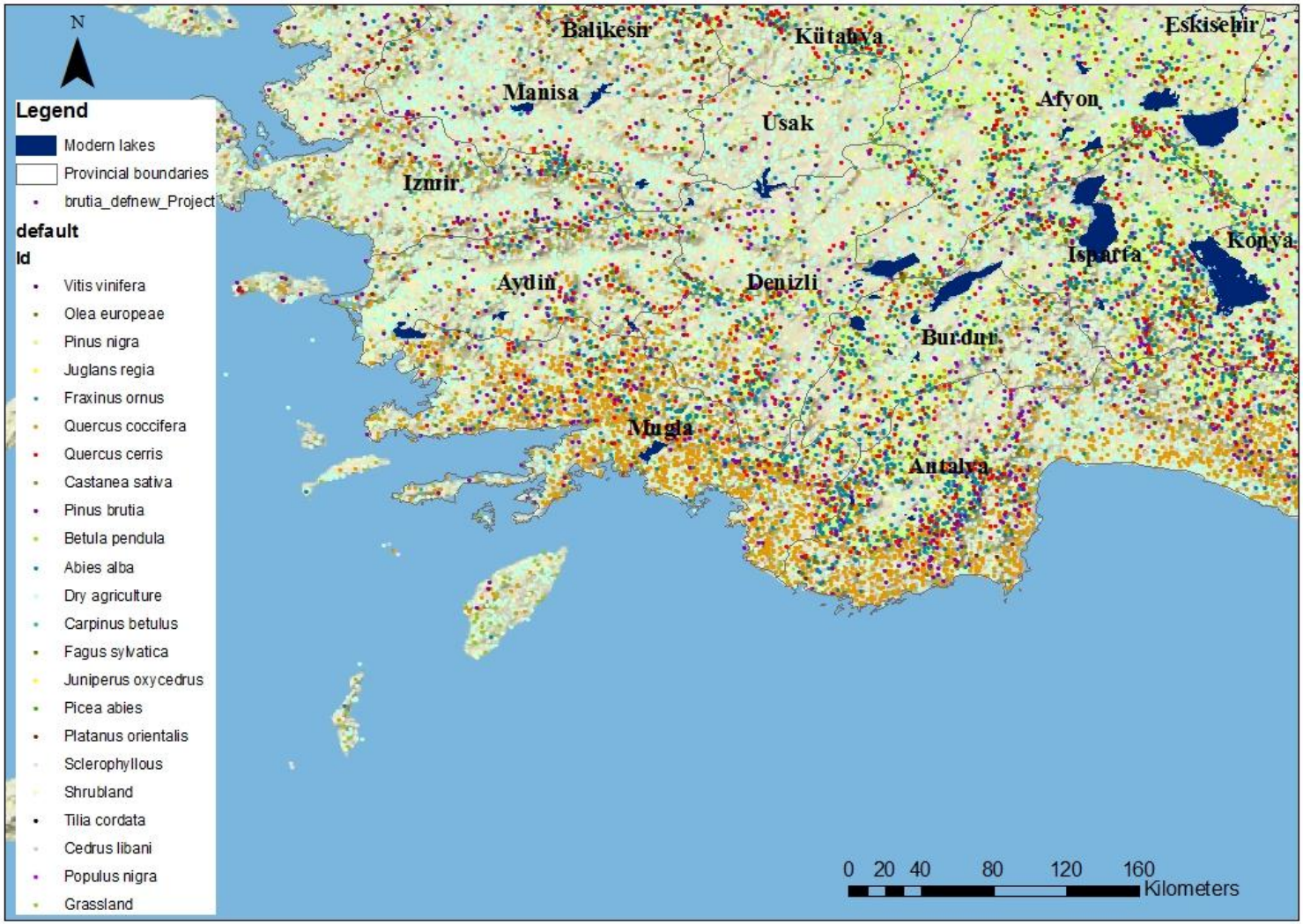


**Figure 4-9 All species points after probability distribution**

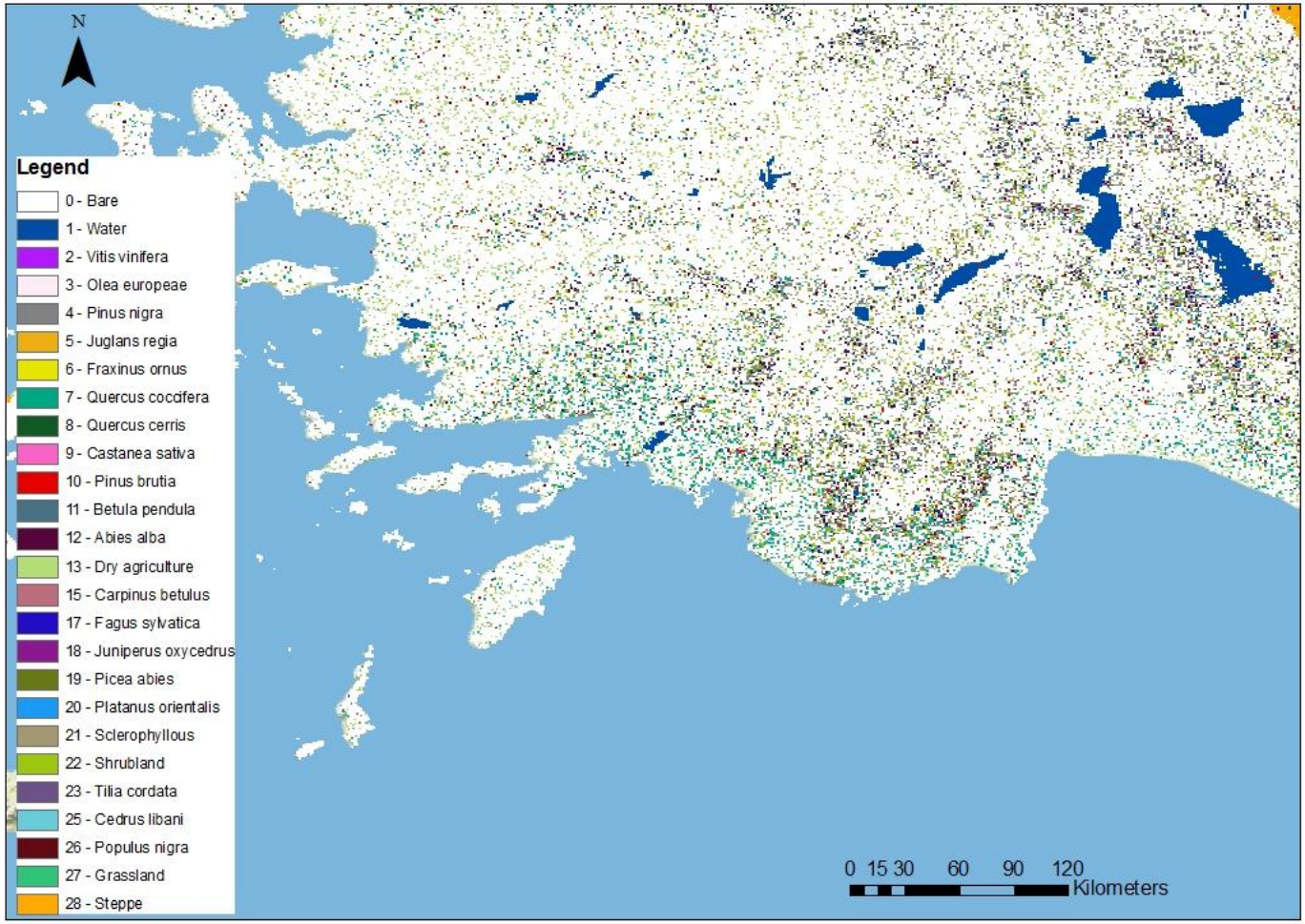


**Figure 4-10 Vegetation model surface converted to raster map ready to load into HUMPOL suite**

A final check was undertaken to compare the percentage of species in the probabilistic model in Figure 4-10 with the percentage of species based on actual species data in Turkey. This essentially assesses whether the probabilistic model developed from data from the whole of Europe predicts species distribution in southwest Turkey. Figure 4-11 displays this comparison, which shows a good agreement between model output and actual data ($R^2$= 0.85).

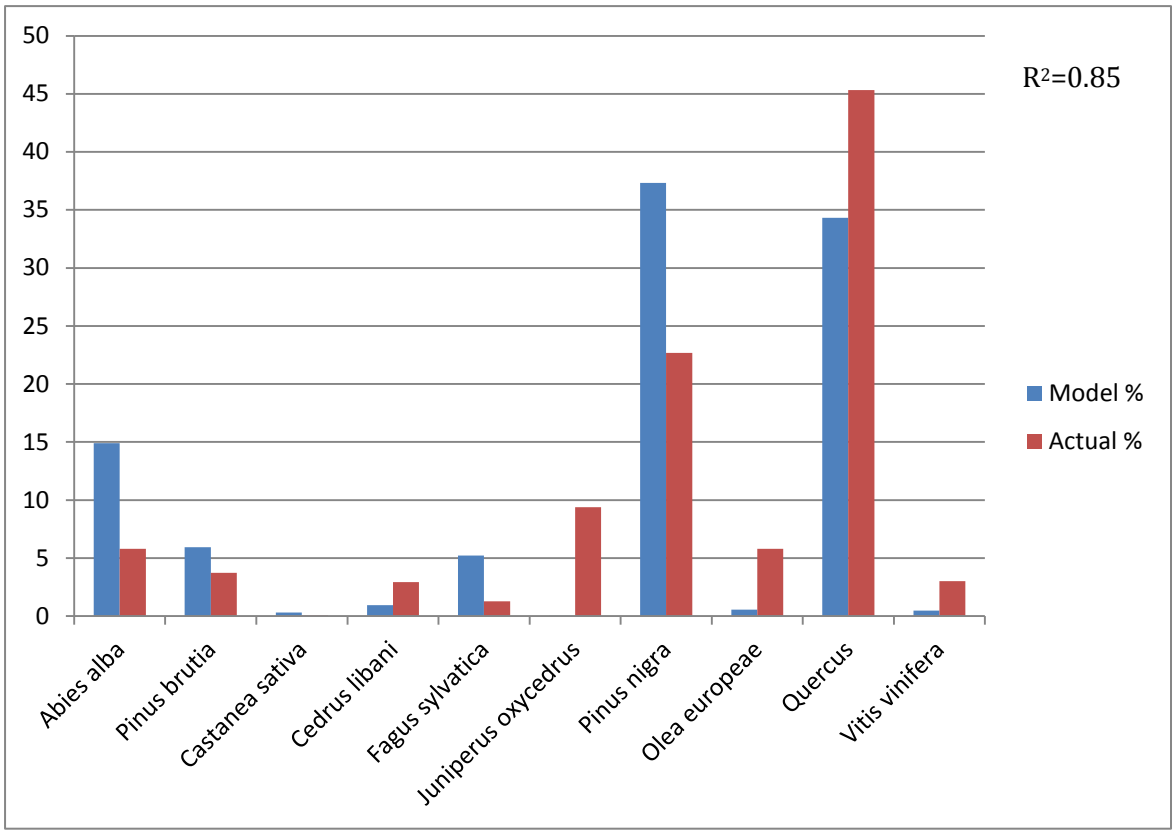


**Figure 4-11 Main species percentage in southwest Turkey, comparing model output and actual data.**

## 4.10 METHODOLOGICAL ASSUMPTIONS AND REVIEW

As this modelling methodology contains data from different sources, a novel approach with many components, and has utilised modern relationships to inform on past events, there are unescapably some assumptions that need to be stated in order to provide a transparent basis for modelling. Once stated, these provide opportunities for future work to accept or reject the assumptions, and to further develop the model and data that feeds into it to provide more

refined and robust model components. Table 4-9 summarises main discussion points on the robustness of the model, and the assumptions that are held to move the model forward.

**Table 4-9 Summary of the robustness and assumptions of the model**

| Area of model | Assumption | Justification | How to improve in future |
|---|---|---|---|
| 1. Is species set representative enough? | Assumes species distribution data adequately represents the distribution of key species | Data is taken from the highest resolution, most coherent dataset currently available. | Requires more comprehensive study of species ranges, and improvement in worldwide plant distribution data. |
| | Assumes broad scale distribution of species adequately represents their climatic envelope | Data was taken from across Europe to examine species distribution under a large range of climate regimes | Requires more laboratory tests on species limits, and increased high quality worldwide data on species distribution. |
| | Assumes that the modern distribution range adequately represents the palaeo-range of species – i.e. that they have not dramatically evolved during the Holocene. | During the last 10 000 years fossil vegetation and genetic data has not yet provided evidence of significant changes in the form of key species modelled, and evidence is also lacking to suggest that their reaction to climate was different to the same modern day species. | Further genetic studies are required to understand whether plant physiology may have undergone subtle changes throughout the Holocene. |

| | | | |
|---|---|---|---|
| 2. Are model inputs valid for the palaeoclimate case? | Assumes summer precipitation was still mainly orographic, autumn and winter precipitation was still frontal. | There is not yet enough evidence to suggest that large scale atmospheric circulation over southwest Turkey was dramatically different during most of the Holocene period. Precipitation during the Late Glacial and early Holocene may have been affected by monsoonal circulation, however this is yet to be proved. | The model will be set up with similar precipitation patterns to the modern situation, but changing their seasonal magnitude. Comparison with pollen records may suggest that this situation is not appropriate for particular periods, which will provide evidence for further work. |
| | Assumes vegetation patterning today is still dictated broadly by climatic, topographic and edaphic factors, despite human interference. | By taking data from across Europe certain local anthropogenic strategies of vegetation placement are likely to have been averaged out. It is also the case that even where vegetation has been planted by humans, the climatic and edaphic scenario still has to be viable for the species to thrive to the extent that is mapped by the species distribution maps. | Requires further study of species distribution under scenarios of low, moderate and high human interference. |

| Area of model | Assumption | Justification | How to improve in future |
|---|---|---|---|
| Are model inputs valid for the palaeoclimate case? (contd.) | Assumes broadly similar topography and soil types | It is acknowledged that soils have developed significantly over the Holocene period, however it is assumed that the broad type of soils that develop on certain bedrock (i.e. calcerous soils over limestone) is likely to be similar to that which was present in the earlier Holocene period. | Requires digitised version of geological data for the whole of southwest Turkey. |
| | Assumes winter minimum temperature from previous studies is assumed realistic | Winter minimum temperatures for species tolerances are generally taken from United States Department of Agriculture plant hardiness zones, a standardised and well known system. | Requires more laboratory tests to understand species hardiness |

| | | | |
|---|---|---|---|
| 3. Are shifts in precipitation and temperature for the whole region valid? | Assumes climate shifts (i.e. -100 mm precipitation) acts across the whole of the southwest, as they generally do today. | Statistical tests were undertaken to examine the pattern of climate across Turkey over the 30 year reference period which suggested that climatic shifts generally occurred similarly at different points across southwest Turkey. This analysis is available on request. | Run further model runs to investigate different precipitation and temperature gradients. |

## 4.11 SUMMARY

This chapter has developed a modelling methodology, which is tailored to the species found in Mediterranean southwest Turkey. It has investigated the climatological and edaphic envelopes of these key species as a basis for modelling climate-vegetation interactions, using high resolution data in order to engage with the landscape scale.

A Rare Events Logistic Regression approach was used to enable the modelling of potential vegetation distribution under different climatic scenarios, in order to engage with the research questions set in this thesis. Model output is displayed as a species specific probability surface across the landscape, on which a semi-random distribution of species instance points is placed. This has allowed heterogenous, multi-species simulations to be created. These simulations can now be driven by particular climatic scenarios of interest. The next chapter defines the climatic scenarios that will be tested and displays the results of those climate scenarios. Model results are displayed in both graphical form to examine relative species probability, and maps of species probability, to understand the potential spatial patterning of vegetation under different climatic scenarios.

# Chapter 5

# Vegetation Modelling Analysis

This chapter first defines the climate scenarios and model runs that the vegetation model will be driven under, before displaying the results from these model runs. The chapter then provides an overview of model output, presenting relative species potential under 27 different model runs.

Results are displayed in the form of relative species potential graphs, to show the impact of variables on species composition, and cartographical representations to investigate the spatial component of vegetation variation. The chapter will finish by describing the methodology used to convert vegetation model output into pollen simulations.

The chapter shows that species composition under modelled scenarios is likely to be dramatically different from modern species distribution. GIS analysis allows the investigation of vegetation across the region, showing the importance of regional variability.

# 5 VEGETATION MODELLING ANALYSIS

An overview of the vegetation modelling analysis undertaken in this chapter is shown in Figure 5-1. The analysis began by identifying key model runs for each research question based on reconstructed climate evidence. The vegetation model was then run using these parameters. An analysis of the relative potential of vegetation cover and the spatial distribution of vegetation was developed, using graphical and cartographical representations. Finally, in order to compare model output with analytical pollen data, the chapter also documents how vegetation model output will be translated into pollen simulations.

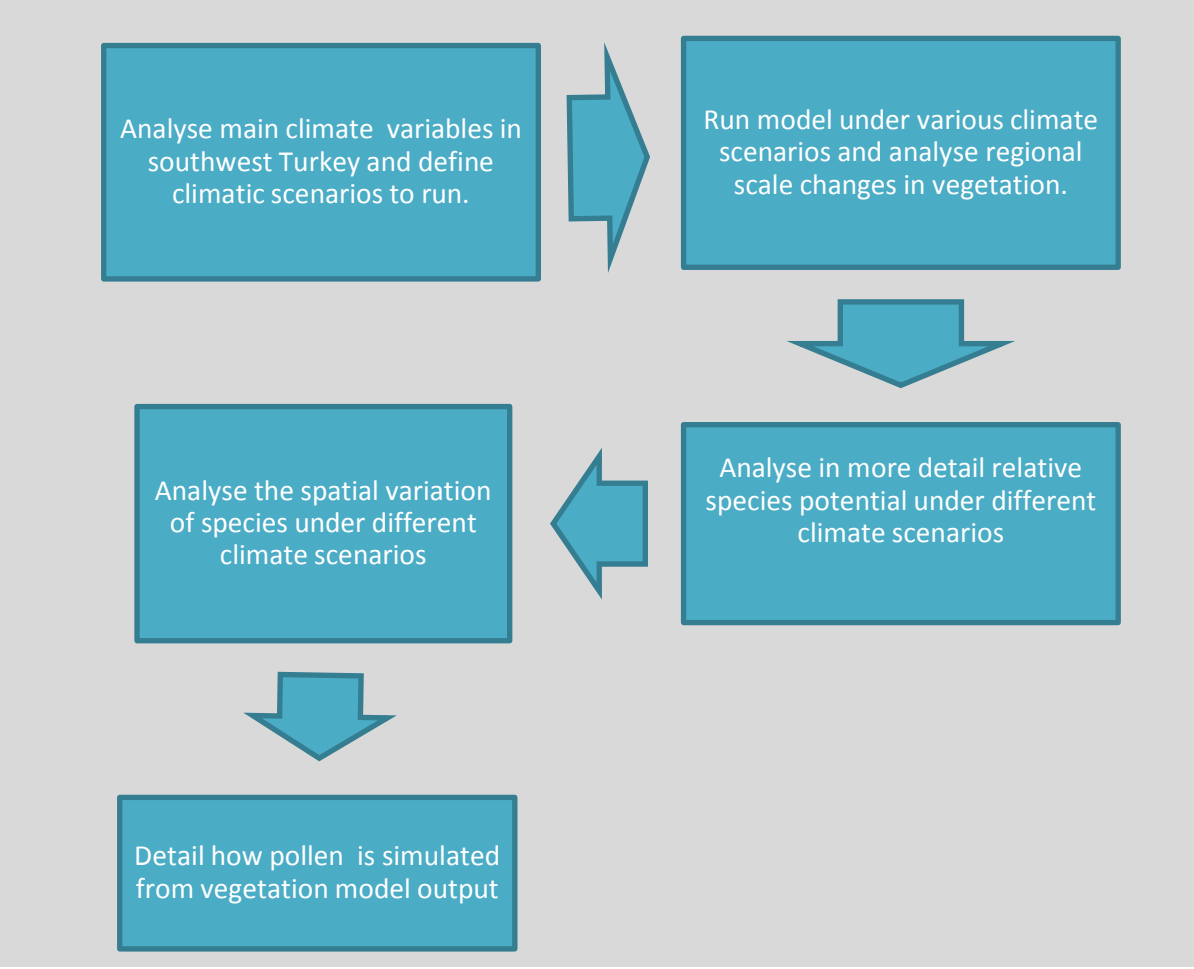


**Figure 5-1 Overview of Chapter 5 methodology**

## 5.1 MODEL RUNS

Table 5-1 summarises the climate anomalies that will be investigated with the bioclimatic vegetation model developed in Chapter 5. The rational for these climate scenarios is discussed in Appendix 10, which introduces the modern spatial distribution of these climate scenarios, and discusses how varying their magnitude may impact the spatial distribution of vegetation in a broad sense. In summary, scenarios are based on key climatic variables known to affect vegetation (based on research from Chapter 3), and Model Runs vary the magnitude of change of these climatic variables (Based on previous palaeoclimatic academic literature discussed in Chapter 2).

Nine different types of scenario were run (for instance change in absolute winter temperature), which each have a scenario identifier. Each scenario also has 1 to 4 model runs associated with it, which examine different climate scenario magnitudes. Model run S1-MR1 for instance would refer to Scenario 1 (absolute winter temperature) and model run 1, in which absolute winter temperature was decreased by -2°C. These identifiers will be referred to in the text for brevity. In all, 27 different model runs were implemented. Which climatic scenarios are likely to impact on the main research questions of the thesis will also be discussed.

**Table 5-1 Model Runs**

| Scenario | Scenario Description | Model Run | | | | | |
|---|---|---|---|---|---|---|---|
| | | MR1 | MR2 | MR3 | MR4 | MR5 | M$6 |
| **S1** | **Modern conditions** | No anomalies | | | | | |
| **S2** | **Decrease in absolute winter temperature** | -2°C | -4°C | -6°C | -8°C | | |
| **S3** | **Increase in absolute winter temperature** | +2°C | - | - | - | | |
| **S4** | **Decrease in average temperature** | -4°C | -8°C | - | - | | |
| **S5** | **Increase in average temperature** | +2°C | +4°C | - | - | | |
| **S6** | **Decrease in winter precipitation** | -100 | -200 | -300 mm | | | |
| **S7** | **Increase in winter precipitation** | +100 | +200 | +300 mm | - | | |
| **S8** | **Decrease in average temperature and winter precipitation** | -8°C -100 mm | -8°C -200 mm | -8°C -300 mm | -4°C -100 mm | -4°C -200 mm | -4°C -300 mm |
| **S9** | **Decrease in average winter temperature and increase in precipitation** | -8°C +100 mm | -8°C, +200 mm | -8°C +300 mm | - | | |
| **S10** | **High summer precipitation and temperature** | +2°C average temperature +50 mm summer precipitation | - | - | - | | |
| **S11** | **7% change in radiation** | 7% change in radiation | 7% change in radiation, +2°C average temperature +50 mm summer precipitation | - | - | | |

The climate scenarios introduced above were converted to regression equations for each species, probability surfaces were calculated, species distributions were modelled, and species distributions were then combined into overall vegetation maps as discussed in Chapter 4. A summary diagram of this process is shown in Figure 5-2.

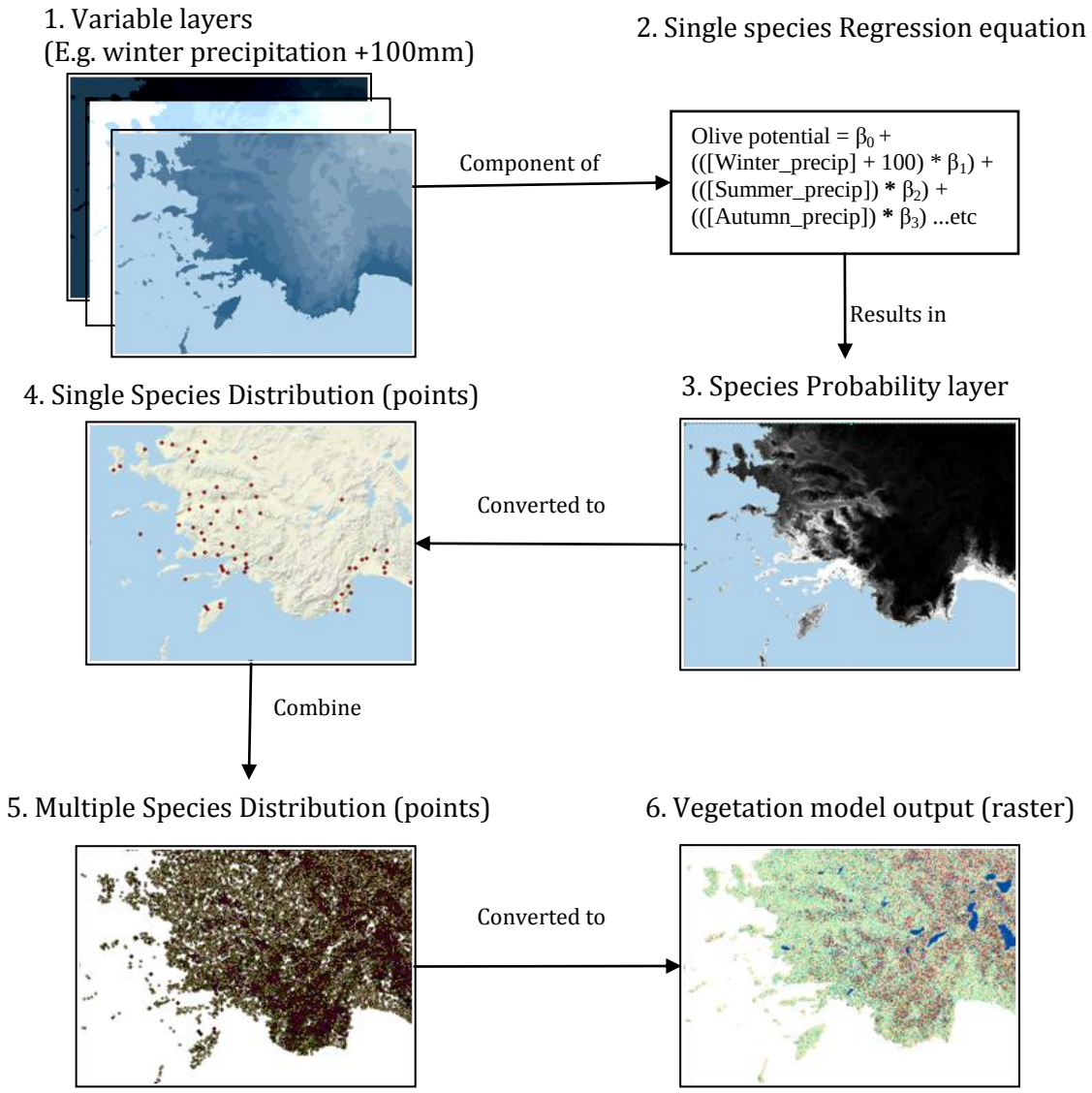


**Figure 5-2 Recap of methodology**

### 5.1.1 Relative species potential – graphical model output

Following model runs, output graphs were calculated that display the relative species potential for the region under different model runs. The graphs are characterized by (a) woodland species, (b) potential arboriculture species, and (c) an overview of broad vegetation classes. Percentage values are calculated within each set of species in order to optimise the visualisation of percentage change, particularly for species with low percentage values.

Figure 5-3 displays the relative potential of species across southwest Turkey based on model results. It shows that of all trees under modern conditions (S1), *Pinus nigra* and *Quercus coccifera* have the highest potential across the region, and of arboriculture species, *Vitis* and *Olea* show highest potential. In general, coniferous and deciduous trees, and cereal and grassland are of equal potential, however true steppe and arboriculture potential is low.

Figure 5-4 shows the relative potential of key vegetation species and classes under the scenario of varying winter absolute minimum temperature (S2 and S3). Figure 5-4a shows that in general, the relative potential for species generally does not change dramatically as winter absolute minimum drops. The main decrease seen is *Pinus brutia*, as this has been documented as having a poor tolerance to cold winter temperatures, although there is also some decrease in *Platanus orientalis*. Figure 5-4b demonstrates that, of the potential arboriculture species, *Olea* in particular is the main species that is restricted by cold winter temperatures. In general, under decreased absolute winter temperatures, the relative potential of deciduous species across the southwest drops (Figure 5-4c) leading to a concurrent rise in the relative potential of coniferous species, grass and cereal. Steppic species and arboriculture species only make up a small fraction of total vegetation potential under these scenarios, but arboriculture potential would also drop due to a lack of *Olea* potential.

Figure 5-5 demonstrates relative vegetation potential under varying average temperatures (S4 and S5). Under low average temperatures *Pinus nigra* and *Abies alba* are found to have the highest potential, and coniferous species in general are preferentially advantaged by low

temperatures. Conversely, under warm conditions, *Quercus coccifera* and *Olea europaea* are found to be particularly advantaged. The proportion of deciduous, arboriculture and grassland vegetation increase under positive temperature anomalies of 2-4°C.

Figure 5-6 demonstrates relative vegetation potential under decreasing winter precipitation (S6). Under this scenario, species potential changes reasonably dramatically. The absolute potential of most species decreases. Figure 5-6a demonstrates that *Quercus coccifera* potential in particular decreases rapidly under a lack of winter precipitation. Also decreasing is *Platanus orientalis* potential, *Pinus nigra* potential and *Quercus cerris* potential. There are a few species (e.g., *Fagus sylvatica*, *Juniperus* and *Picea*) that are seen to increase in potential under decreased winter precipitation. Figure 5-6b shows that *Olea* and *Vitis* are the arboriculture species most affected by a decrease in winter precipitation, although most species are affected to a certain extent. Figure 5-6c emphasizes that as arboriculture, deciduous, coniferous and grassland potential all decrease, steppic areas increase.

Figure 5-7 shows regional vegetation model output with increasing winter precipitation (S7). Under such climatic conditions, most forest and arboriculture species increase in potential. Considering Figure 5-7a, the main forest species to increase under such climatic conditions are *Quercus coccifera*, *Betula pendula*, *Populus nigra*, *Carpinus* and *Fagus*. Species that proportionally decrease are likely to be *Cedrus*, *Pinus nigra*, *Pinus brutia* and *Platanus*. Figure 5-7b shows that *Olea* is particularly advantaged by this increase in winter precipitation, as is *Vitis. Juglans* and *Fraxinus* are less likely. Figure 5-7c shows that under increasing precipitation, deciduous species are likely to increase proportionally compared to coniferous, steppic or grassland areas.

Figure 5-8 demonstrates S8, which modelled both decreasing precipitation and decreasing average temperature. This model run shows relatively similar results to Figure 5-6, although *Pinus brutia* also decreases under lower average temperatures. Other coniferous species however, such as *Abies*, *Cedrus libani* and *Pinus nigra* are more likely to increase in relative importance due to lower temperatures.

Figure 5-9 and Figure 5-10 shows regional vegetation model output with changing solar radiation, increased summer precipitation and temperature, and both effects at once (S10 and S11), and Table 5-2 shows an overview of advantaged species under each model run. All scenarios increase the growing potential of *Abies*, *Carpinus*, *Platanus* and *Olea*. Changing radiation parameters has the effect of increasing *Quercus cerris* and *Pinus brutia* probability. Changing summer temperature advantages *Quercus coccifera*, whereas changing summer precipitation advantages *Vitis vinifera*. Changing all parameters advantages *Quercus cerris*, *Pinus brutia*, *Olea europaea*, *Abies alba* and *Carpinus betulus*.

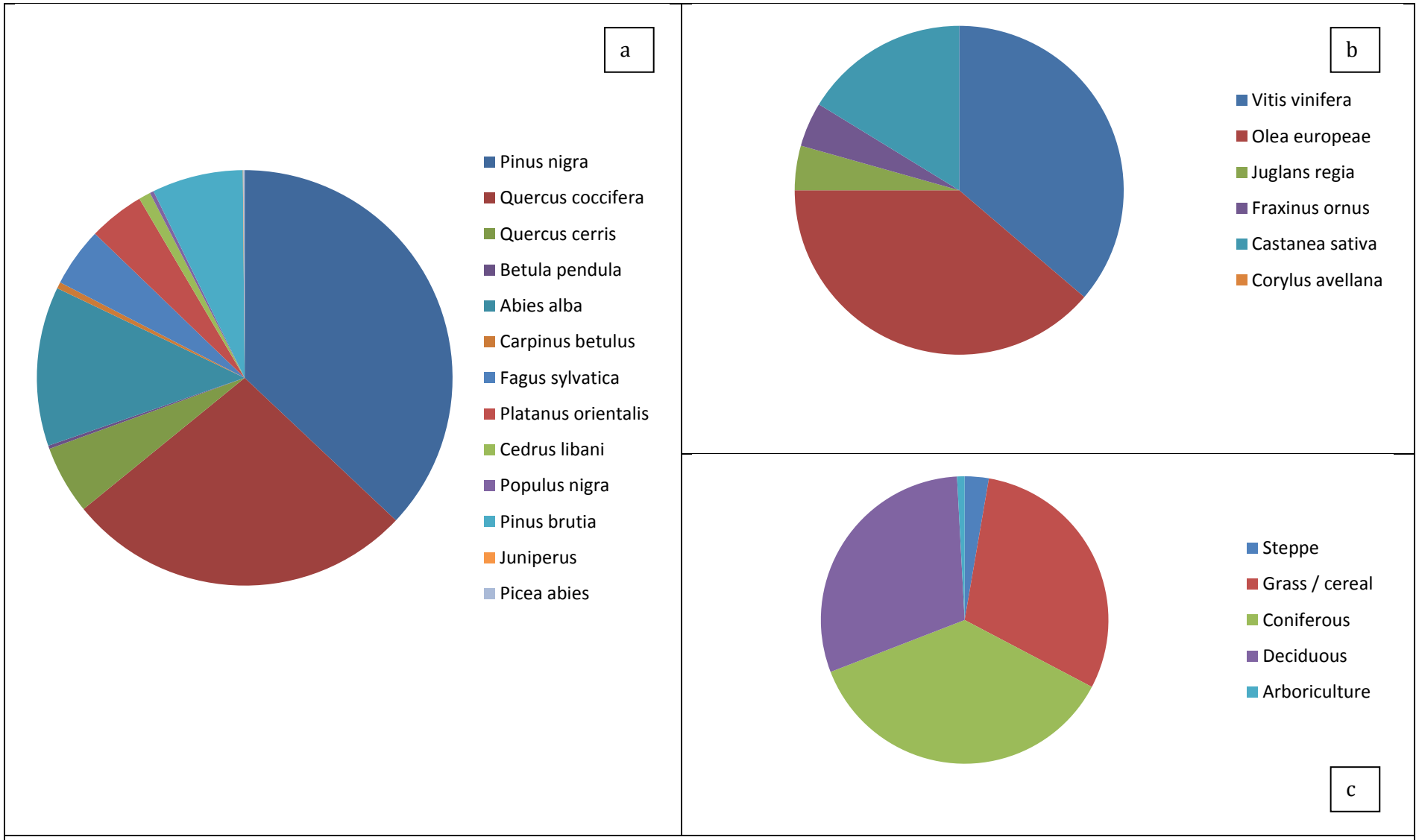


**Figure 5-3(a) Forest species potential relative percentage under modern conditions (b) Arboriculture species potential relative percentage under modern conditions (c) Relative percentage of coniferous, deciduous, steppic and grassland species potential under modern conditions**

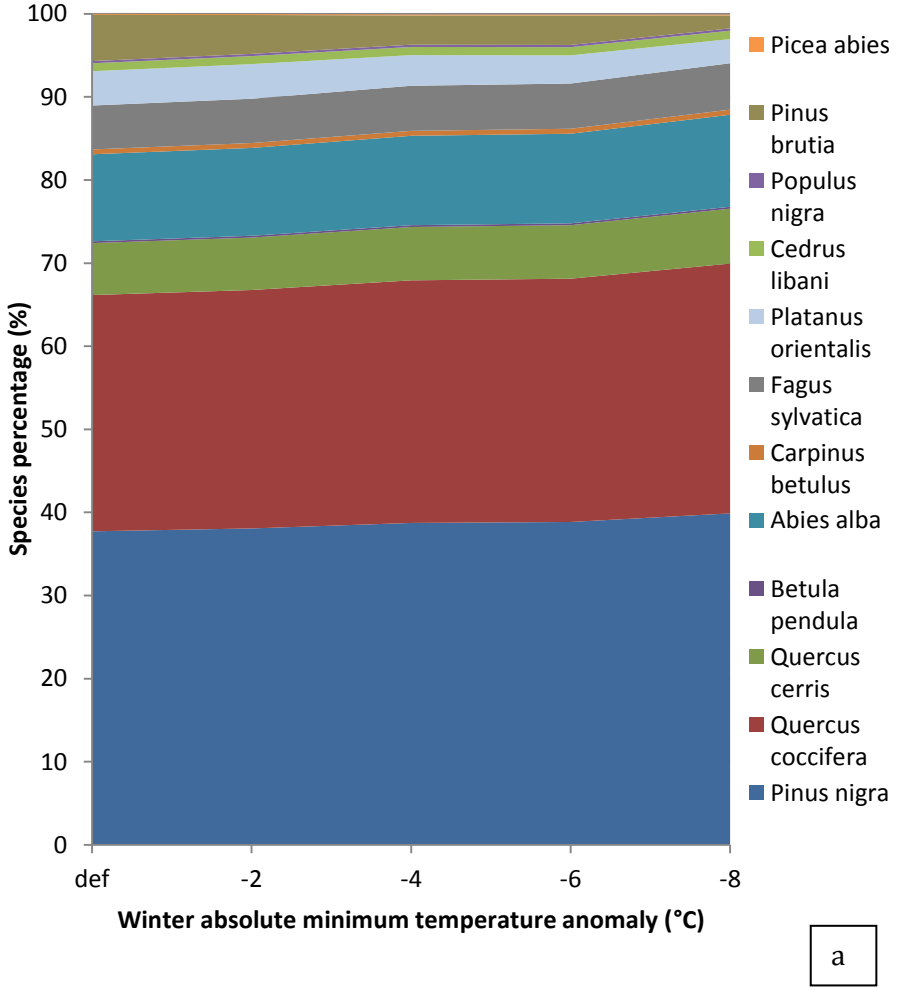


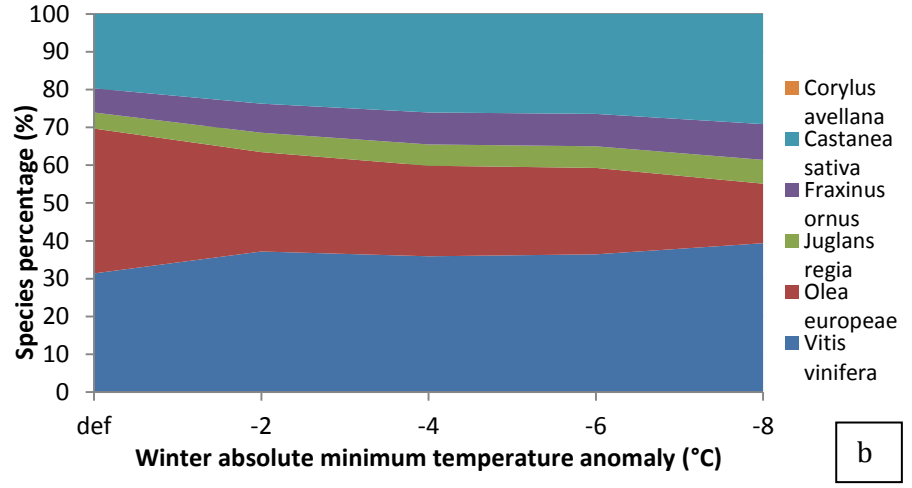


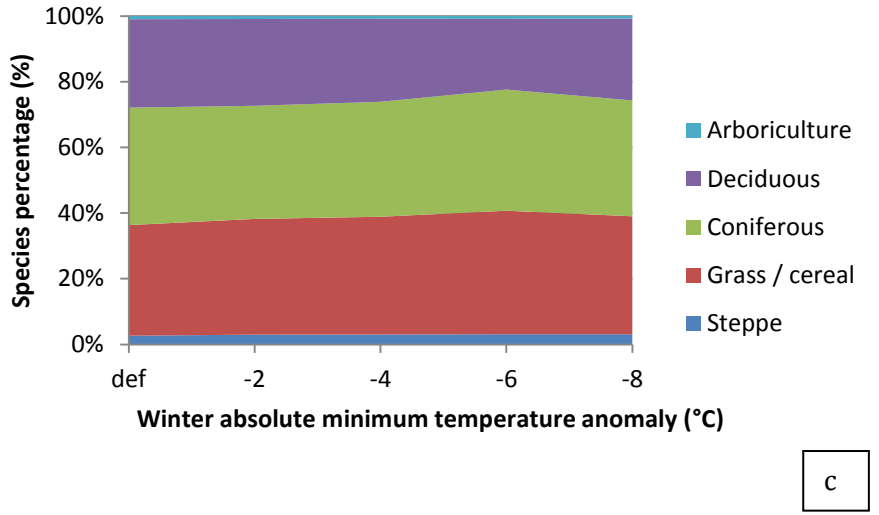


**Figure 5-4(a) Forest species potential relative percentage with varying winter minimum temperature (b) Arboriculture species potential relative percentage with decreasing winter minimum temperature (c) Relative percentage of coniferous, deciduous, steppic and grassland species potential with decreasing winter absolute temperature.**

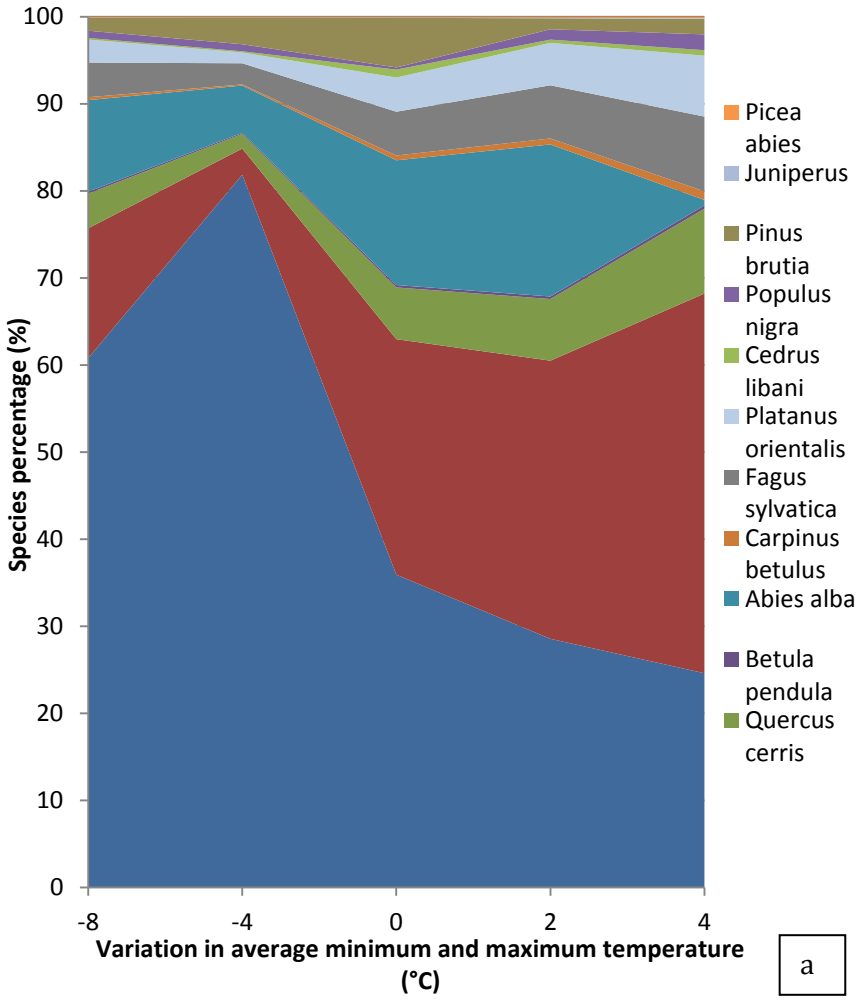


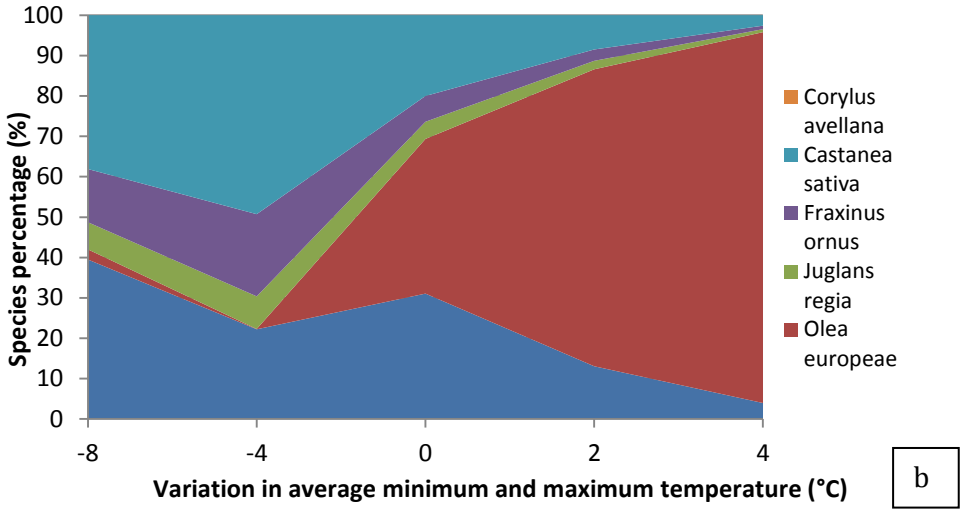


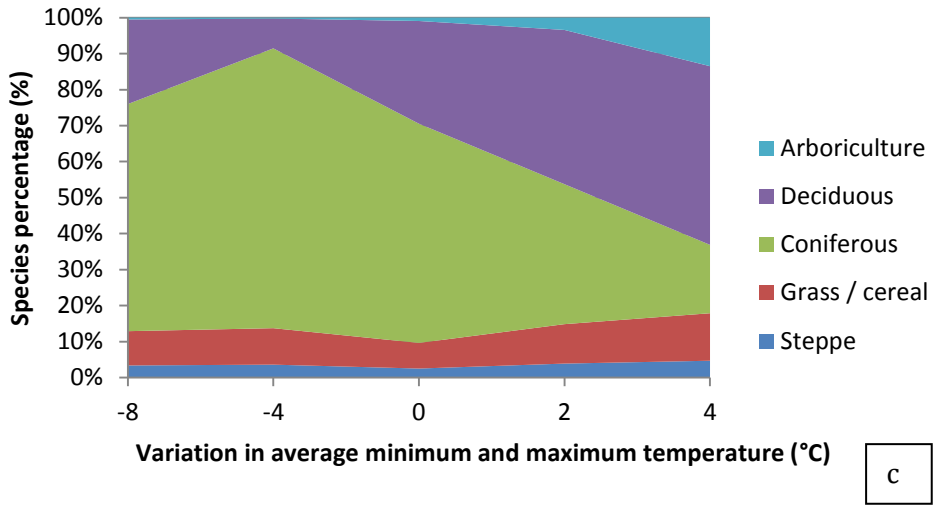


**Figure 5-5(a) Forest species potential relative percentage with varying average temperature (b) Arboriculture species potential relative percentage with decreasing winter minimum temperature (c) Relative percentage of coniferous, deciduous, steppic and grassland species potential with decreasing winter absolute temperature.**

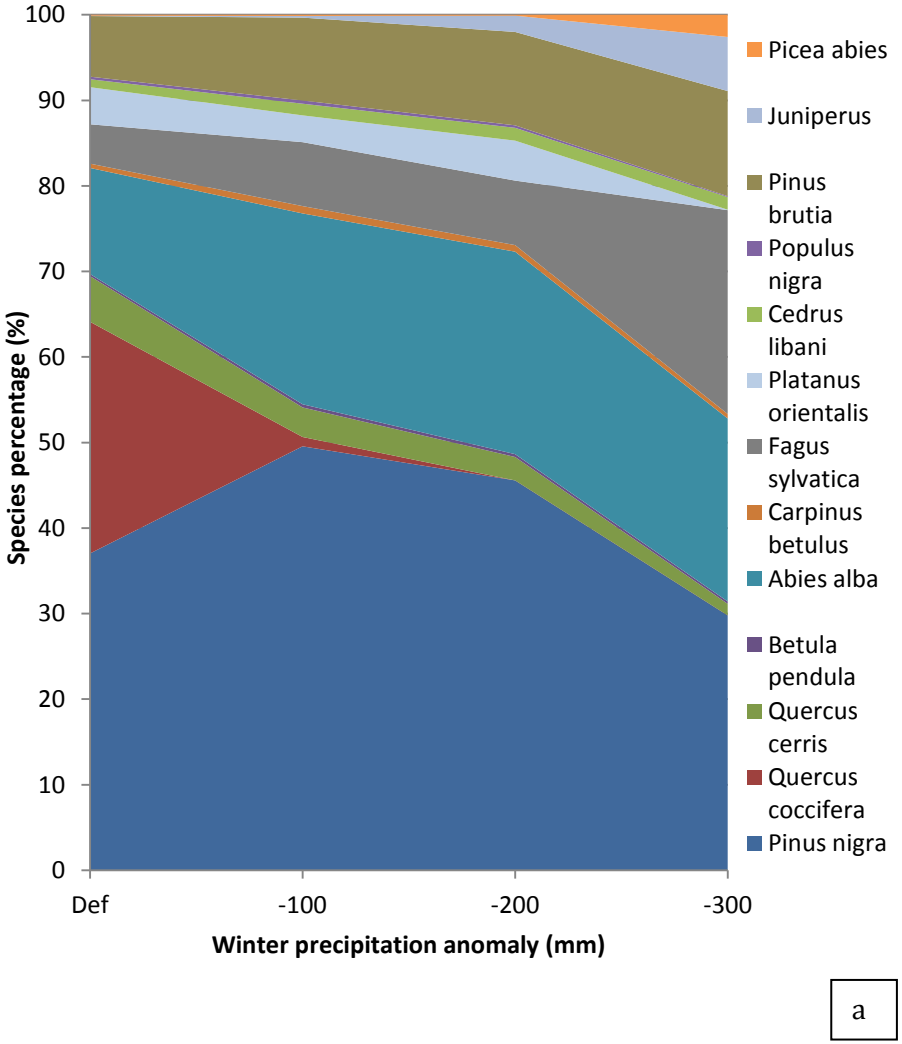


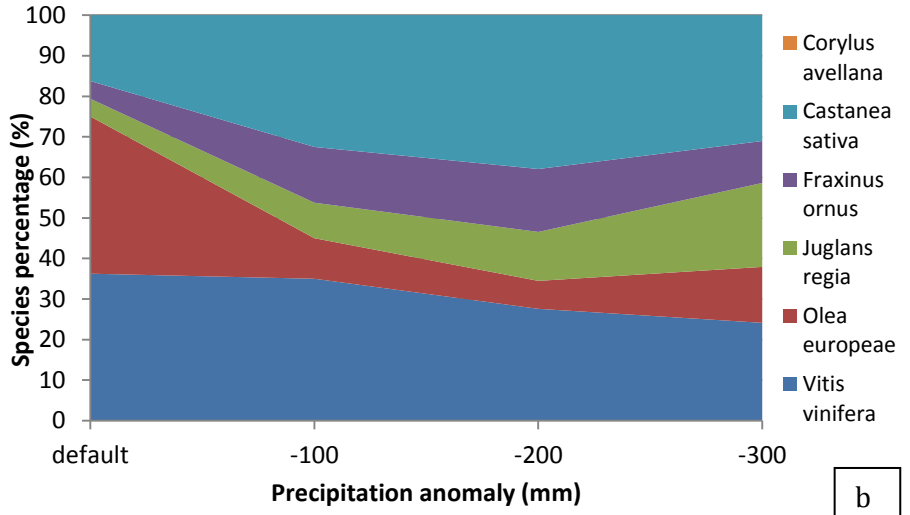


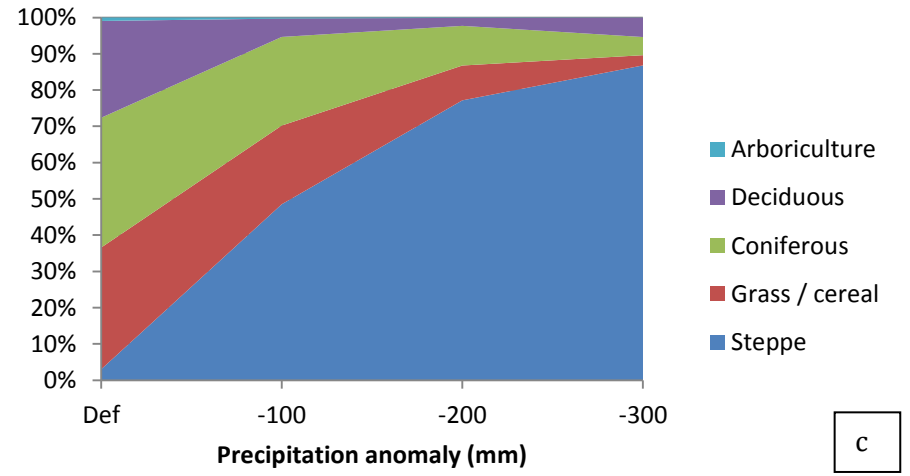


**Figure 5-6 Relative percentage with decrease in winter precipitation (a) Forest species (b) Arboriculture (c) Broad vegetation classes**

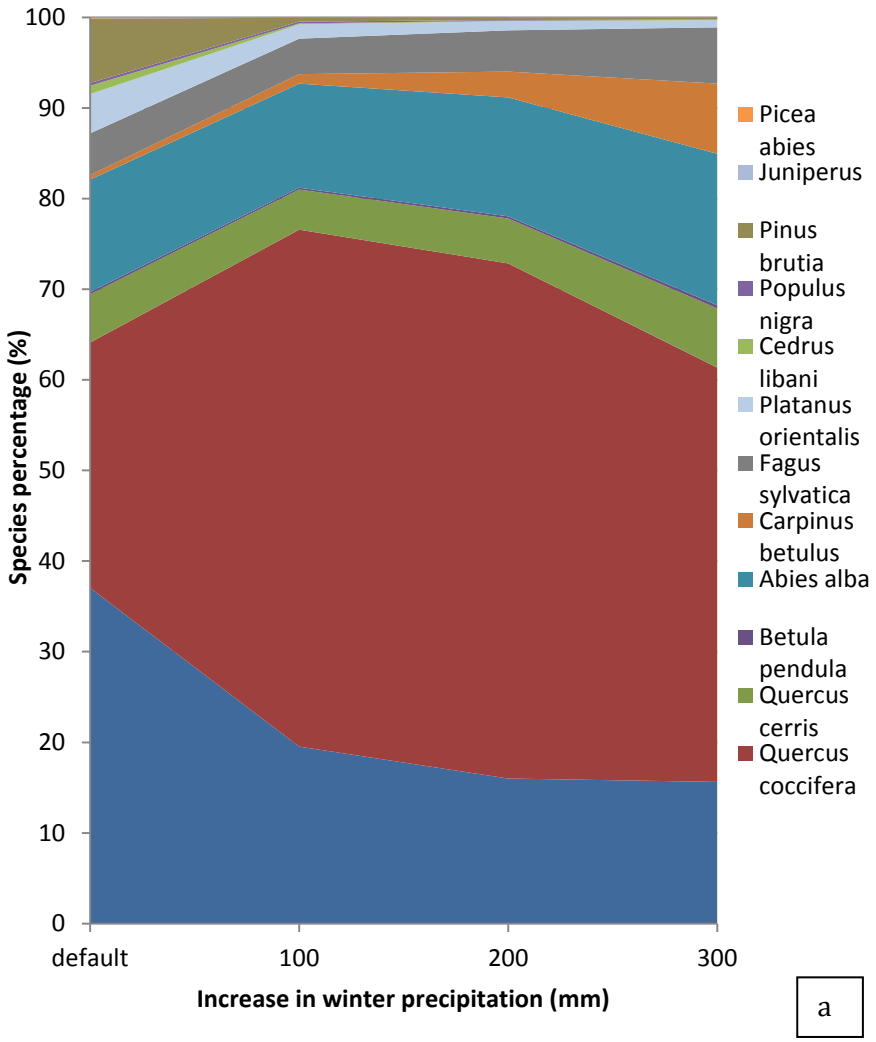


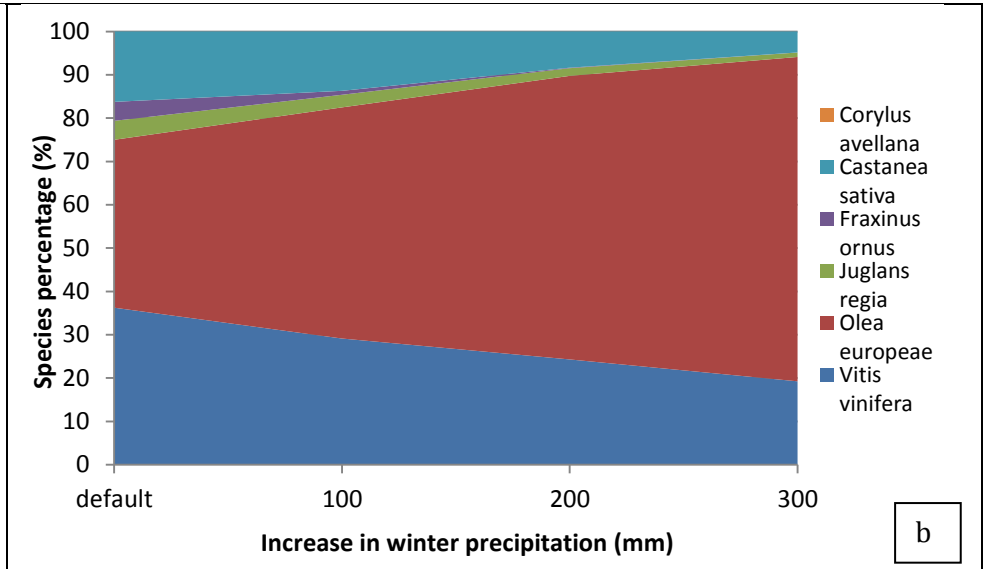


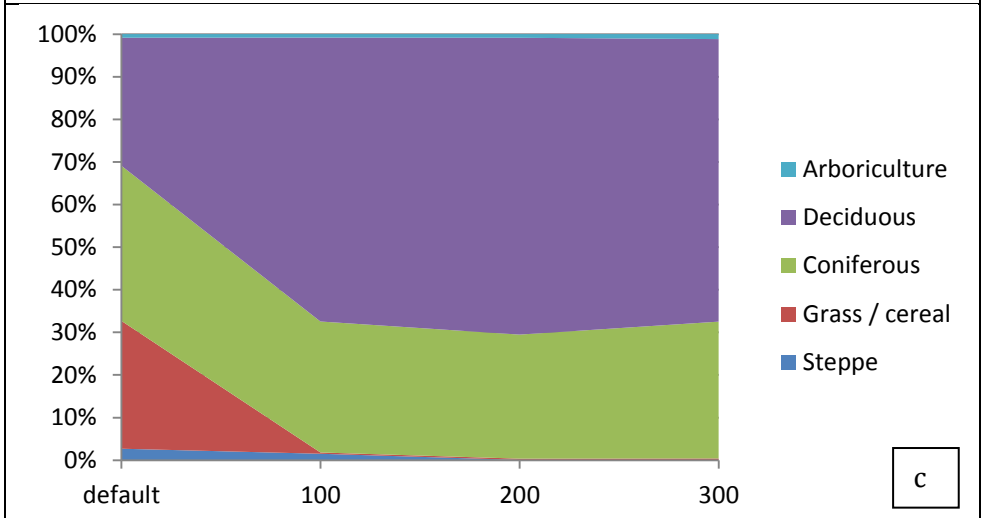


**Figure 5-7 Relative percentage with increase in winter precipitation (a) Forest species (b) Arboriculture (c) Broad vegetation classes**

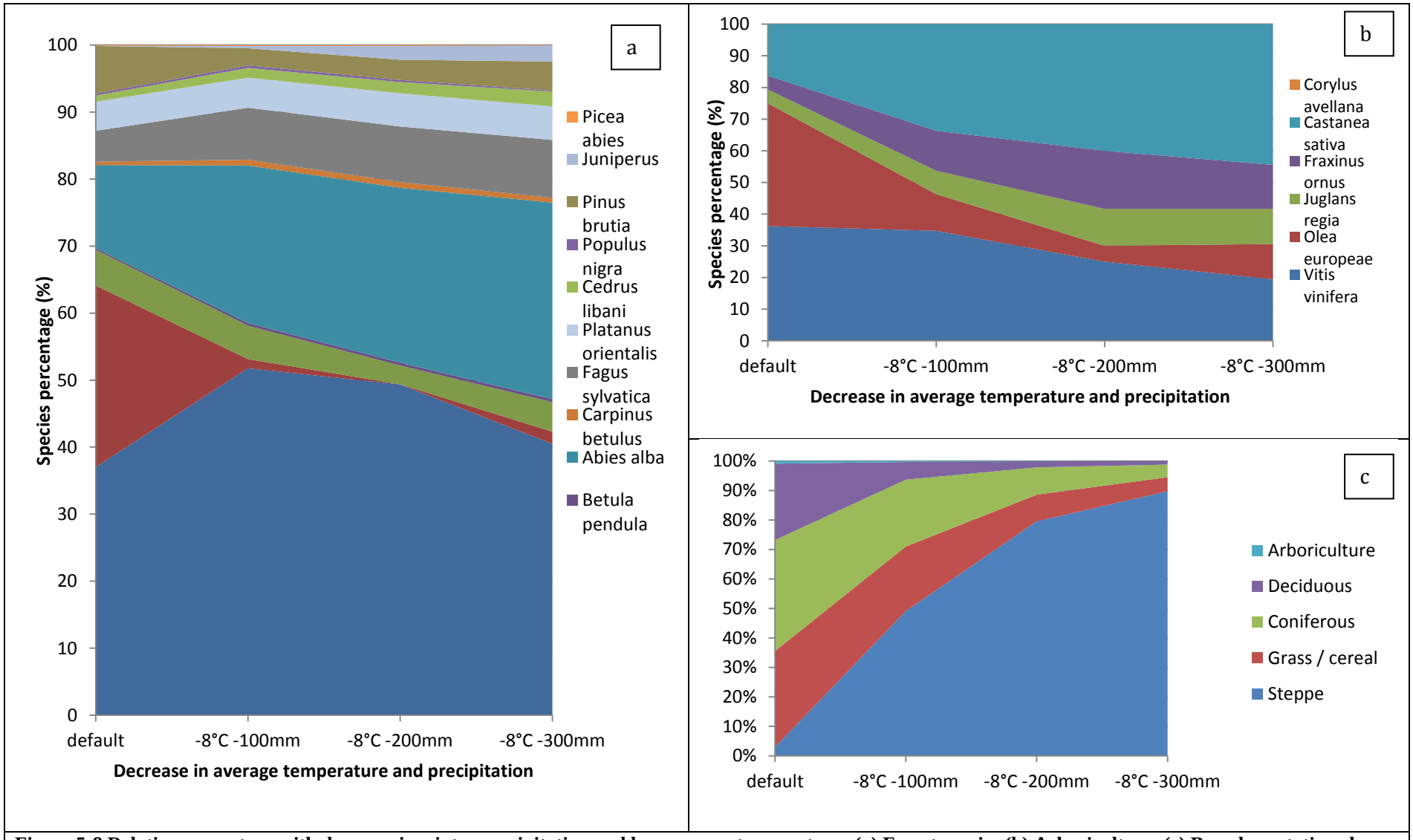


**Figure 5-8 Relative percentage with decrease in winter precipitation and low average temperatures (a) Forest species (b) Arboriculture (c) Broad vegetation classes**

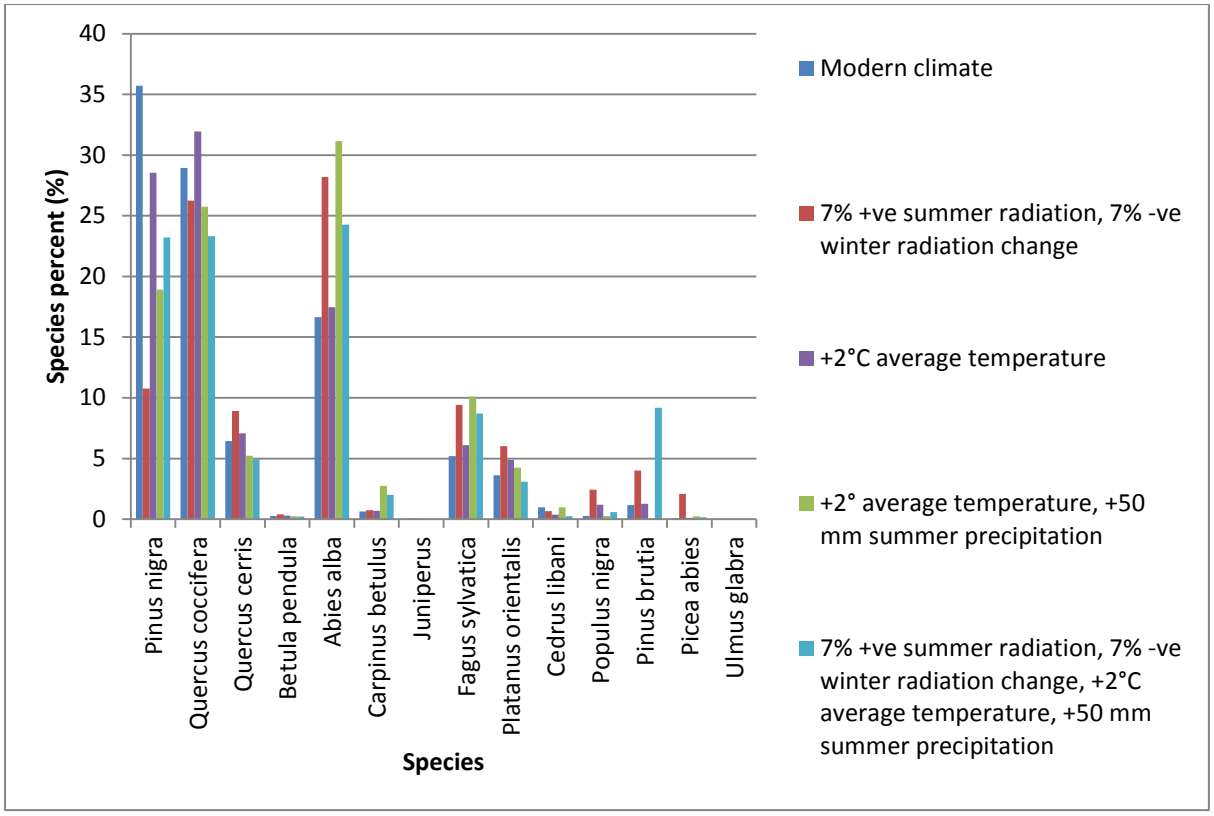


**Figure 5-9 relative percentage of forest species under changes in radiation, summer precipitation and summer temperature**

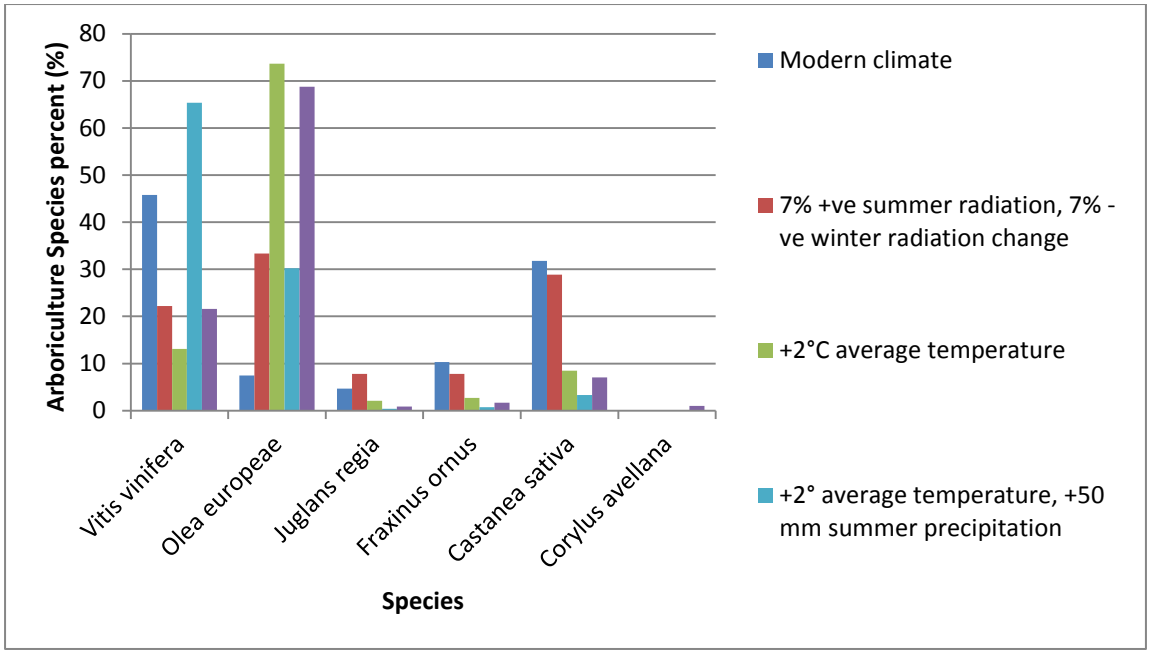


**Figure 5-10 relative percentage of arboriculture species under changes in radiation, summer precipitation and summer temperature**

**Table 5-2 Overview of advantaged species under changing radiation and summer climate**

| Species | Changing radiation | Changing average temperature | Changing summer precipitation and average temperature | Changing radiation, summer precipitation and average temperature |
|---|---|---|---|---|
| *Pinus nigra* | | | | |
| *Quercus coccifera* | | x | | |
| *Quercus cerris* | x | x | | x |
| *Betula pendula* | | | | |
| *Abies alba* | x | x | x | x |
| *Carpinus betulus* | x | x | x | x |
| *Fagus sylvatica* | | x | x | |
| *Platanus orientalis* | x | x | x | x |
| *Cedrus libani* | | | | |
| *Populus nigra* | x | x | | |
| *Pinus brutia* | x | x | | x |
| *Picea abies* | x | | | |
| *Vitis vinifera* | | | x | |
| *Olea europaea* | x | x | x | x |
| *Juglans regia* | x | | | |
| *Fraxinus ornus* | | | | |
| *Castanea sativa* | | | | |
| *Corylus avellana* | | | | |

### 5.1.2 **Spatial variability of model output**

This section examines the spatial distribution of species under modelled climate scenarios. Under modern conditions (S1, Figure 5-11) modelled species concentration is highest in Muğla and Antalya, with shrubland and cereal species potential dominating.

Figure 5-12 shows that a clustering of *Quercus coccifera* probability is shown around the coastal regions of Muğla and Antalya, particularly along the southern coast.

A mixed woodland transition zone was found across the higher elevation areas in Burdur and Denizli, turning into higher probability for *Pinus nigra*, *Quercus cerris* and *Abies alba* among interior parts of the region such as Isparta and Afyon.

Figure 5-13 shows that Afyon is also the region with the highest potential for *Tilia, Populus, Picea, Juniperus* and *Fraxinus ornus.* The potential for cold intolerant species under modern conditions can also be discussed using this figure. Under modern conditions, the environmental potential of *Olea* is seen to reside predominantly in Muğla province, whereas *Vitis* is higher on the lower valley slopes of Izmir and Afyon. The less cold intolerant arboriculture species *Castanea* and *Juglans* also have moderate potential in Afyon, also Denizli, Burdur and Isparta.

This can be compared with Figure 5-14 to Figure 5-16, which maps these species under model run S2-MR4. As previously discussed, woodland species potential does not change significantly for most species. The main species that is affected by the decrease in winter temperatures is *Olea europaea*, which contracts by 52km or 33% of its range. It can be seen on the figure that there is a spatial aspect to this restriction. Its distribution decreases from some of the more interior areas of Muğla. Aydin, Izmir and Muğla now hold olive potential equally, where it clings onto the coastal strip. A  contraction of *Pinus brutia* is also seen, to 28% of its previous range as it has a susceptibility to colder temperatures under ~-12°C. The amount of area potentially covered by *Platanus* decreases by 173km or 1%, and *Juniperus* is also restricted.

Not every model run will be discussed here, however it is interesting to examine some of the more extreme climatic scenarios to assess how vegetation distribution may change under such events. Figure 5-17 to Figure 5-19 displays model output from S8-MR2. Figure 5-17 shows a large shift to steppic conditions. Figure 5-18 shows that the greatest concentration is in the north-east provinces of Afyon and Usak. In comparison to modern conditions, the proportion of *Abies alba* increases, and this was particularly apparent as clusters of modelled coniferous forest at high elevation sites such as Uyluk Tepe and Bey Dağları. Where previously, Quercus *coccifera* had high potential across the Eu-Mediterranean and Oro-Mediterranean zone, now, *Quercus coccifera* is restricted to low elevation sites near the coast in Aydin, Antalya and Muğla. In the western region grassland and shrubland predominates.

When considering only arboriculture species, all modelled species are disadvantaged by decreasing precipitation and temperature, however, *Olea europaea* is the most disadvantaged. Decreasing precipitation and temperature lead to a contraction of all arboriculture to specific valleys and hillsides in the very south and west of the region, in particular Antalya, Isparta, Izmir and Aydin. *Vitis* is more likely in the westernmost provinces of Izmir and Aydin, and *Castanea* is more likely in Antalya and Isparta.

Figure 5-20to Figure 5-22 displays model output from S5-MR1. Under a scenario of increased temperature, mixed shrubland, Cerealia and *Quercus* woodland is found to be advantaged, with *Quercus coccifera* particularly advantaged throughout the humid coastal areas. Another important feature of this model run is the increase in potential for arboriculture species. *Fraxinus ornus* potential is particularly high throughout the region. *Olea* potential around the coast has increased, but *Olea* also increases in range into the interior of Isparta, Uşak and Afyon.

Figure 5-23 to Figure 5-25 displays model output from model run S7-MR1. Under increased precipitation mixed *Quercus* is likely to be advantaged across southwest Turkey, however greater potential is seen in the westernmost provinces of Izmir and Aydin, and the Oro-Mediterranean regions of Denizli and Burdur.

At the furthest extreme (Figure 5-26to Figure 5-28) the effect of increasing winter precipitation (S7-MR1) is predicted to allow the expansion of mixed woodland across most of southwest Turkey. *Quercus coccifera* and *Pinus brutia are l*ikely to be found in valleys at low elevation, whereas *Quercus cerris, Carpinus, Betula* and *Pinus nigra* are found on hillslopes and higher elevation areas. *Olea* and *Vitis* have potential in many provinces, with Olea moving from the coast into Burdur, Isparta, and Izmir, and Vitis having the highest potential in Afyon, Denizli and Burdur.

Finally, Figure 5-29to Figure 5-31 shows vegetation model output with an increase in radiation, average temperature and summer precipitation. Again, an increase in *Quercus coccifera* and *cerris* is expected, and an increase in *Pinus brutia* and *Abies* are also likely in intramontane valley areas. *Pinus nigra* is expected in the interior areas of the region. *Olea* probability is high throughout Muğla and Antalya, but has also increased in other areas such as Aydin, Burdur, Denizli and Izmir. *Vitis* probability is also high throughout the region.

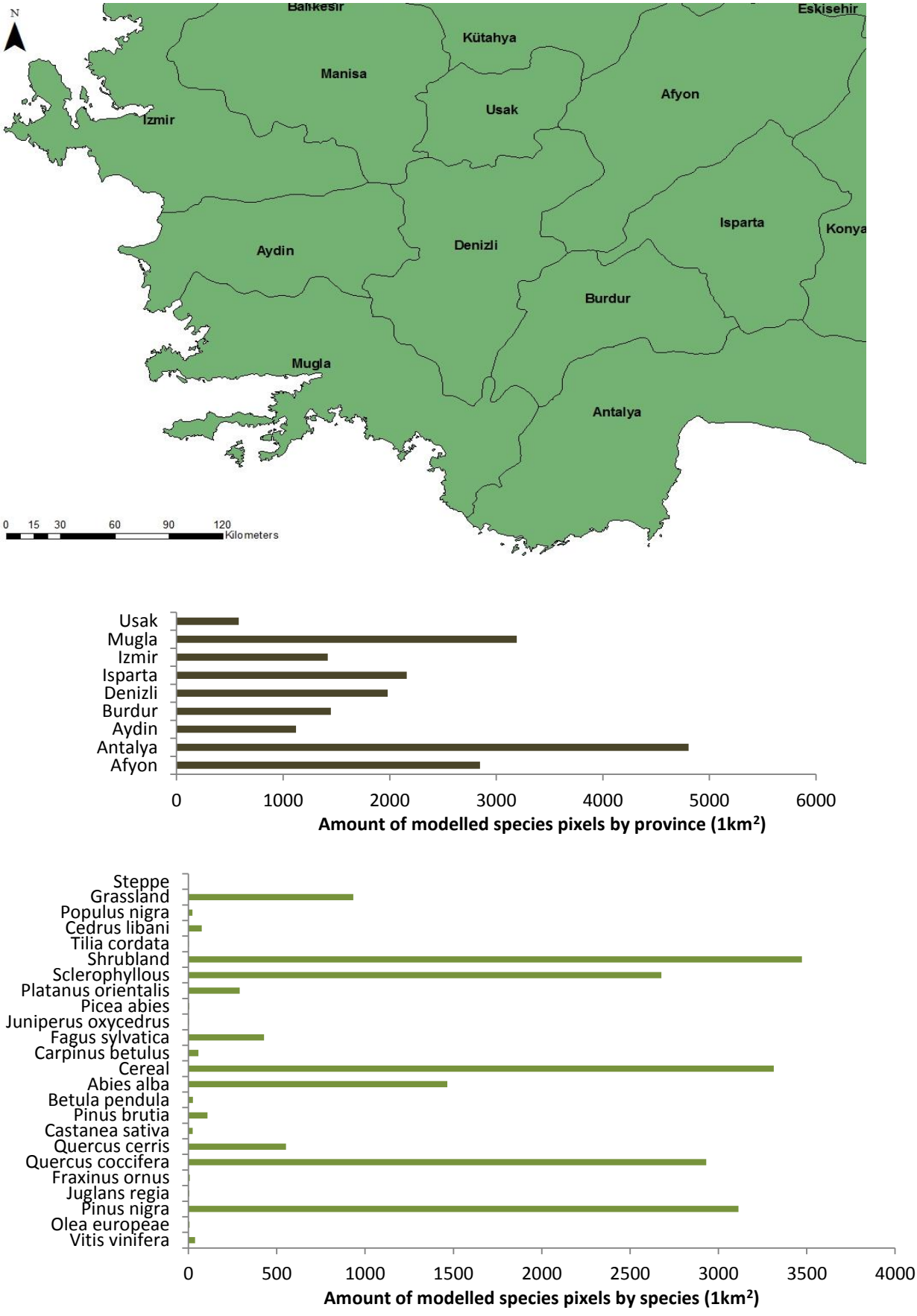


**Figure 5-11 Area map and modeled species overview under modern conditions**

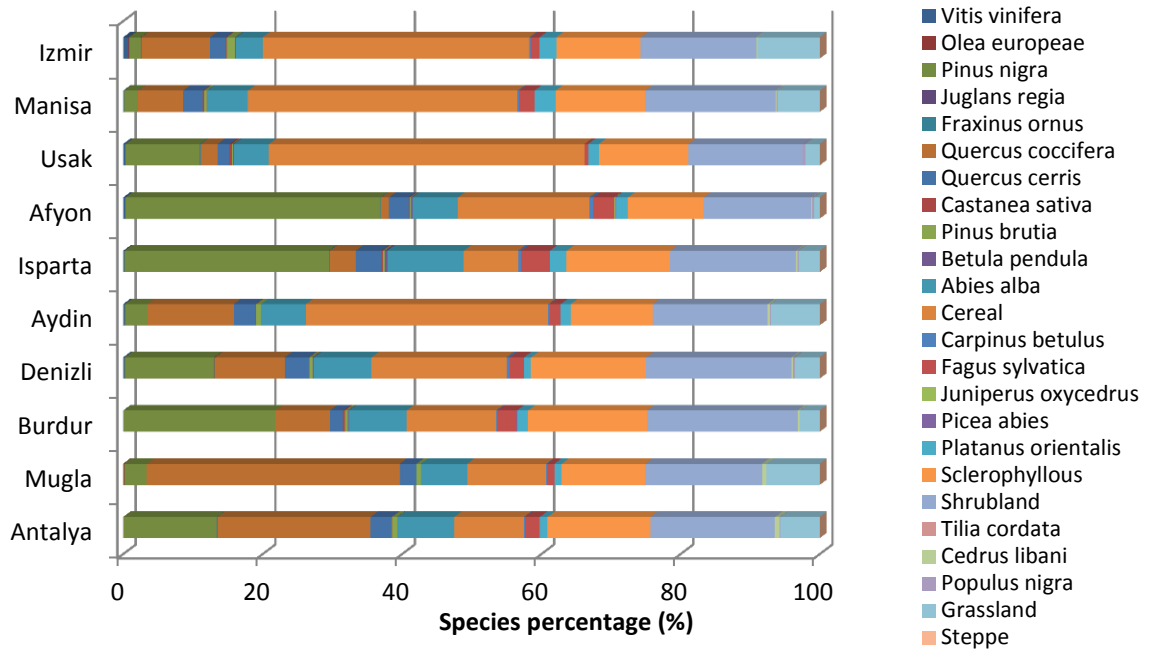


**Figure 5-12 Modelled species potential and relative percentages by province across southwest Turkey under modern conditions**

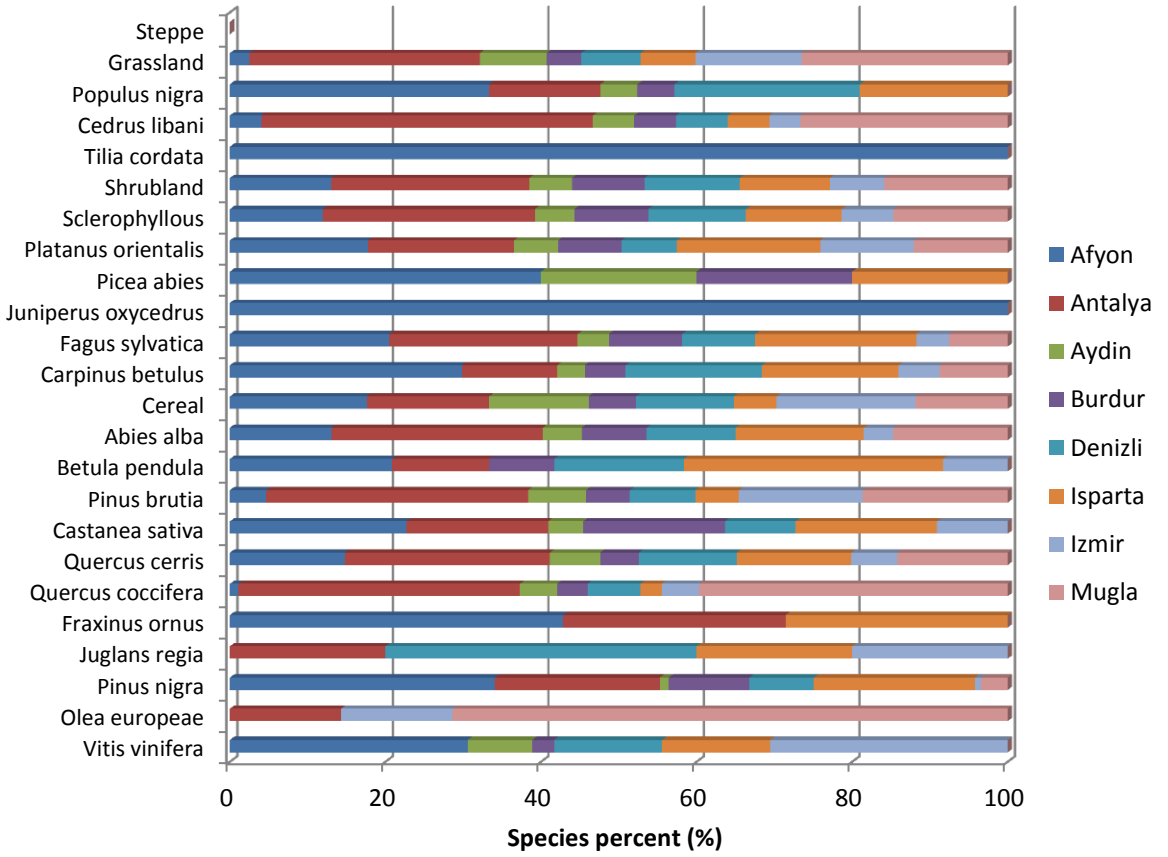


**Figure 5-13 Modelled species percentage by species across southwest Turkey under modern conditions**

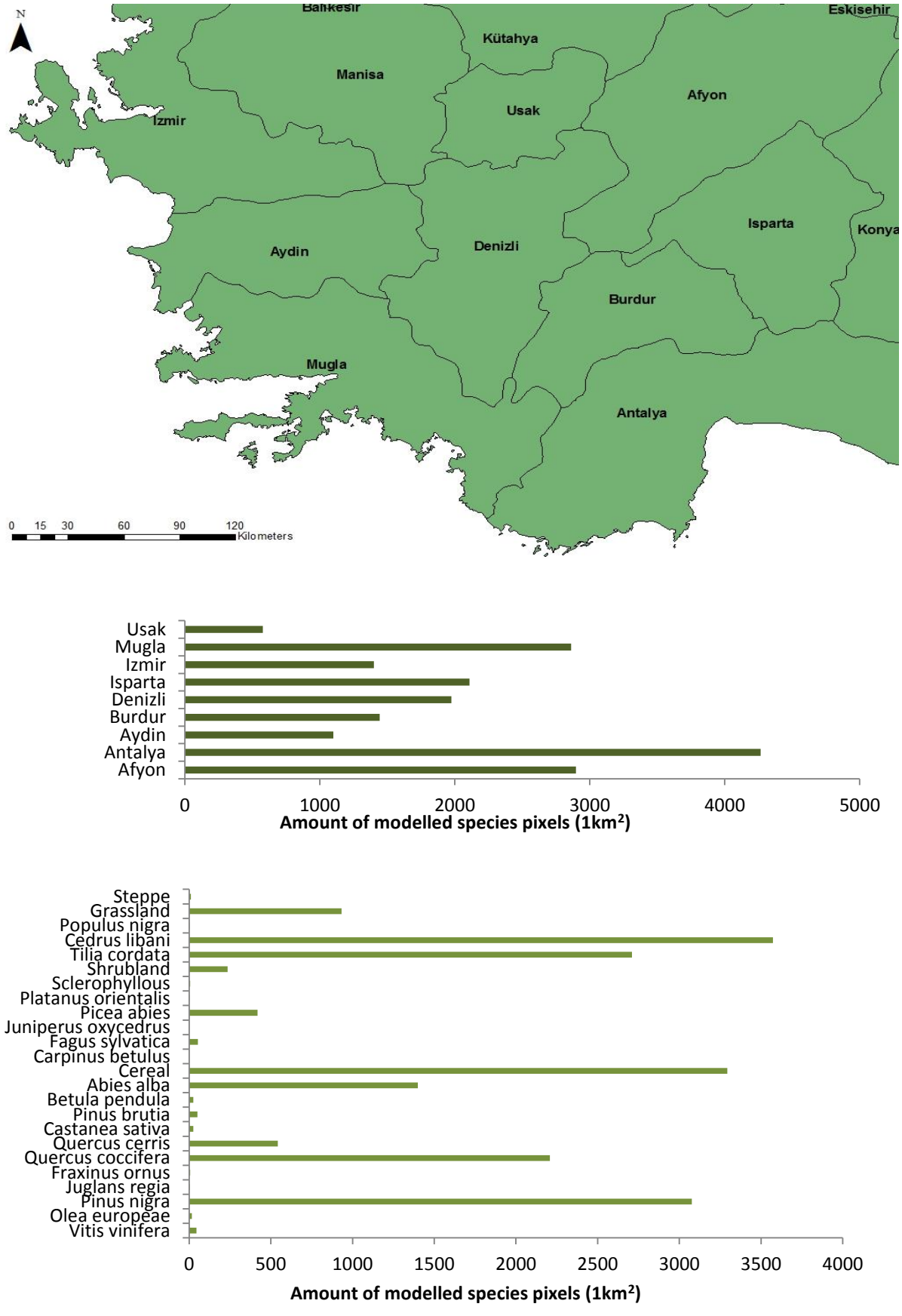


**Figure 5-14 Area map and modeled species overview under -8°C**

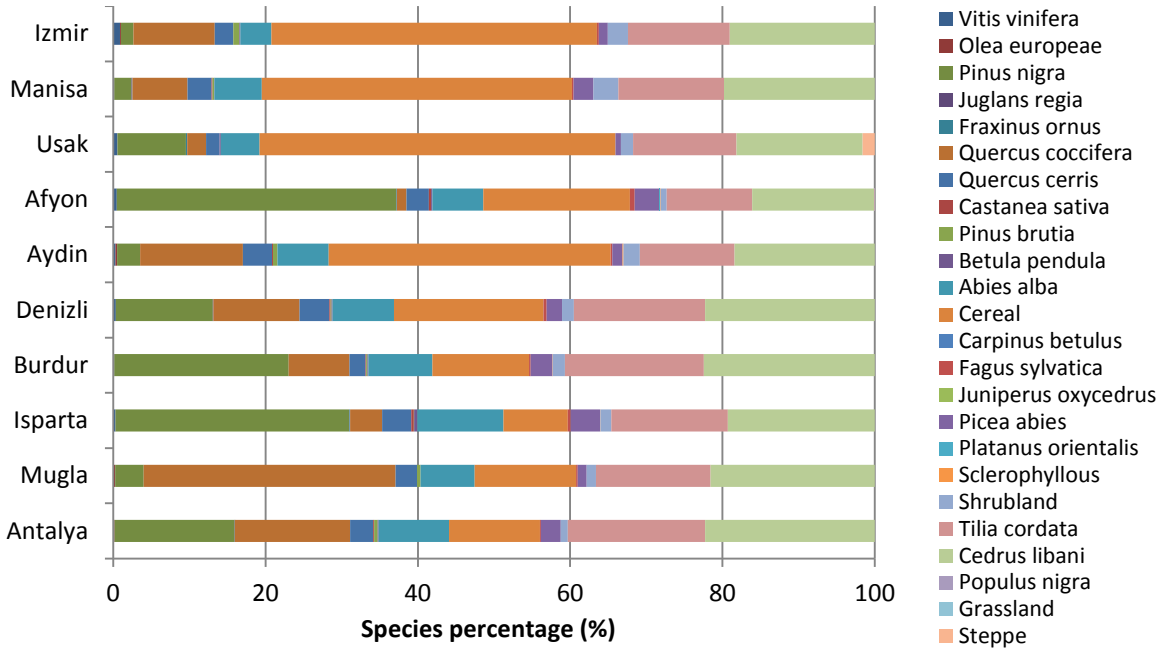


**Figure 5-15 Modelled species potential and relative percentages by province across southwest Turkey under modern conditions**

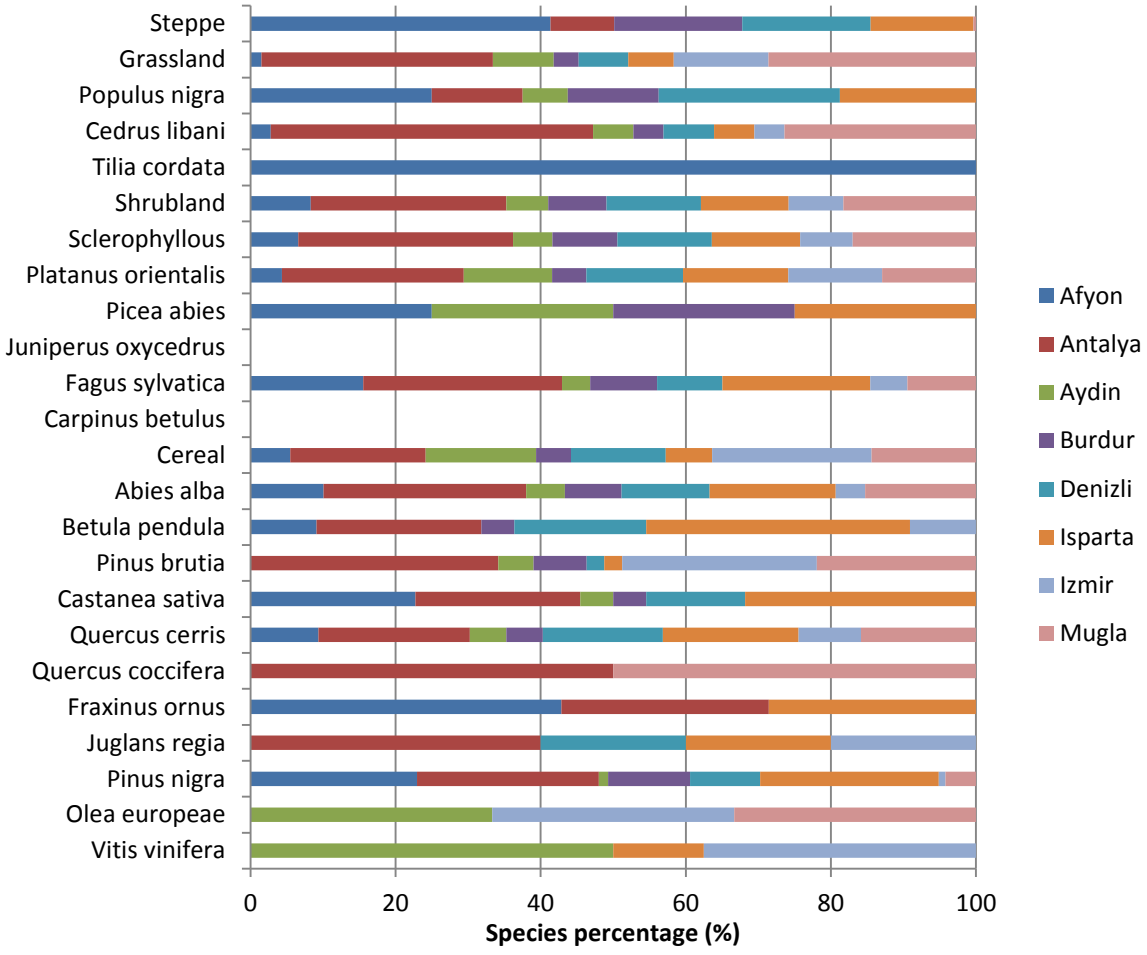


**Figure 5-16 Modelled relative species concentration across southwest Turkey under -8°C**

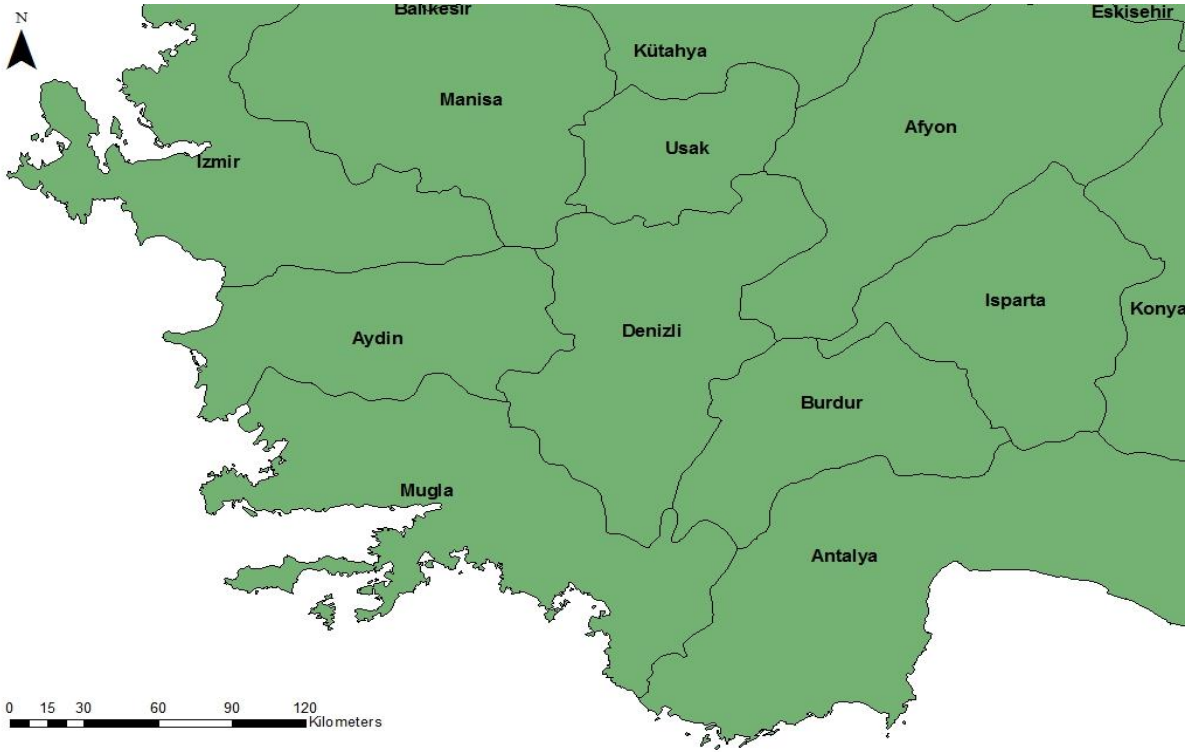


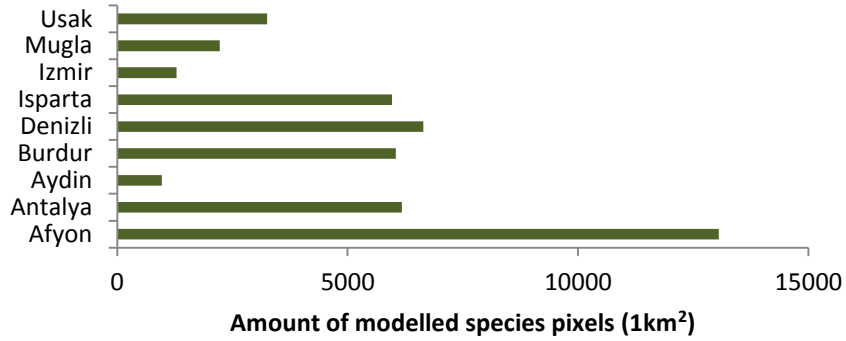


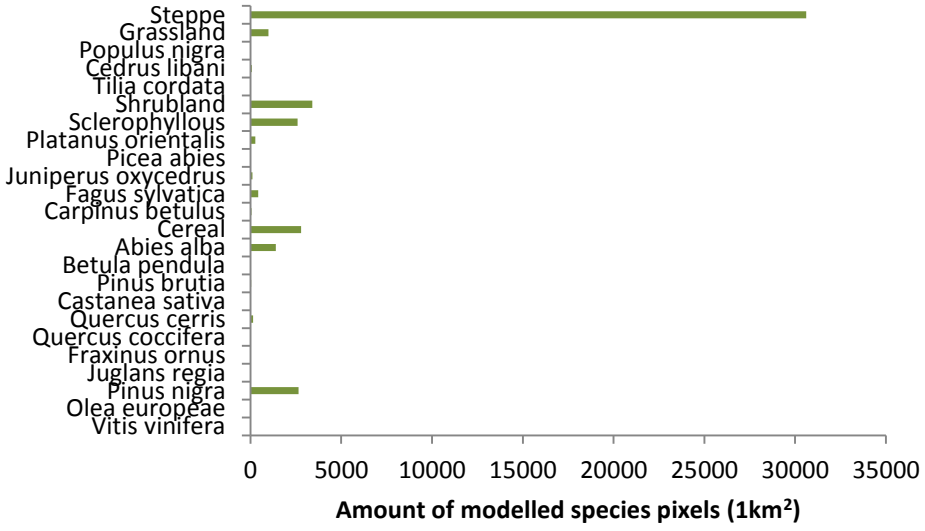


**Figure 5-17 Area map and modeled species overview -8°C and -200 mm precipitation**

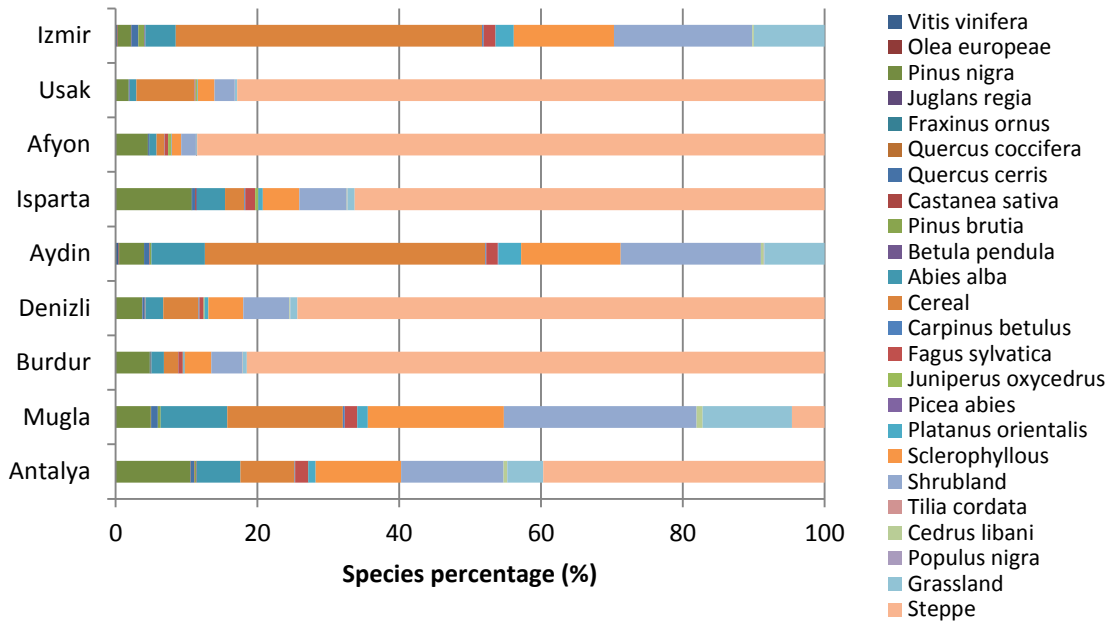


**Figure 5-18 Modelled species potential and relative percentages by province across southwest Turkey - 8°C and -200 mm precipitation**

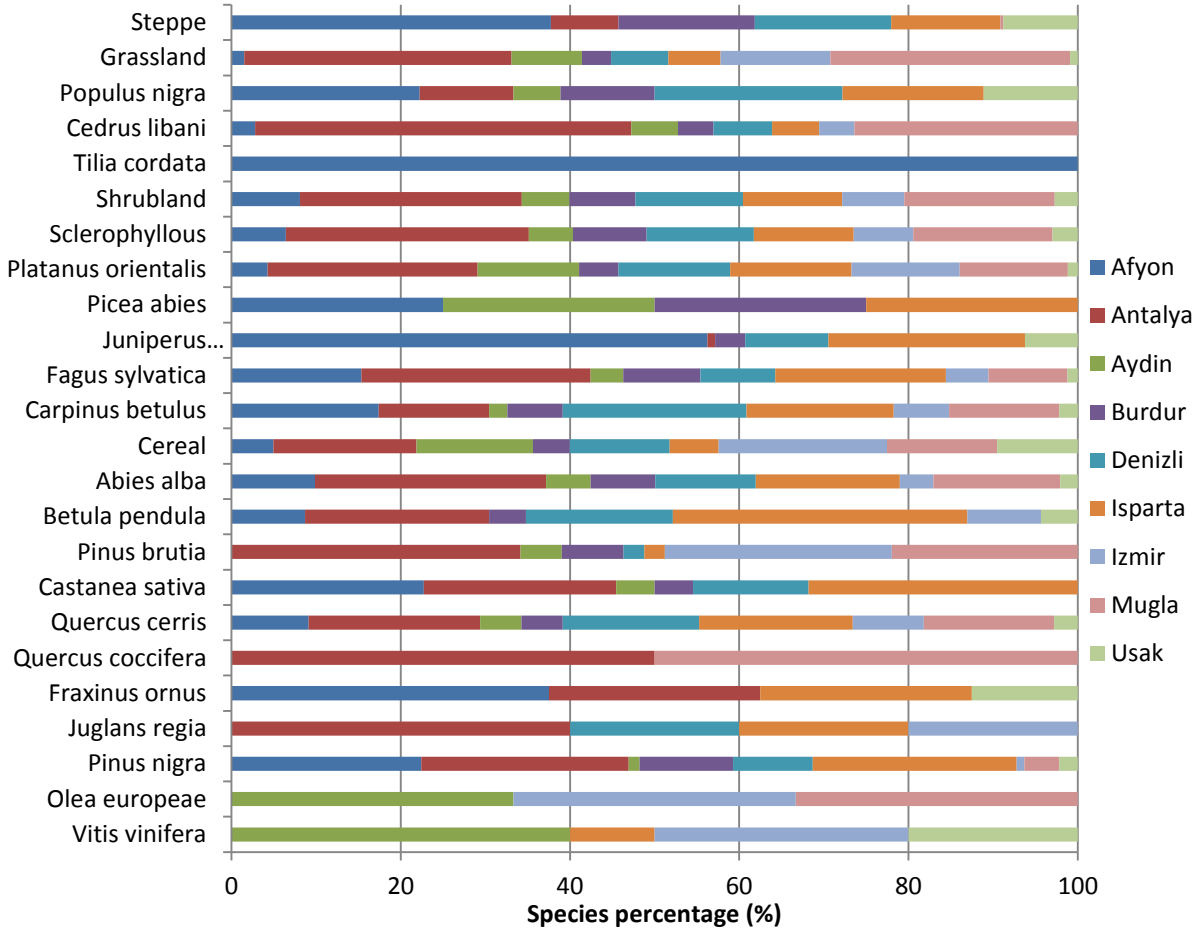


**Figure 5-19 Modelled relative species concentration across southwest Turkey under -8°C and -200 mm precipitation**

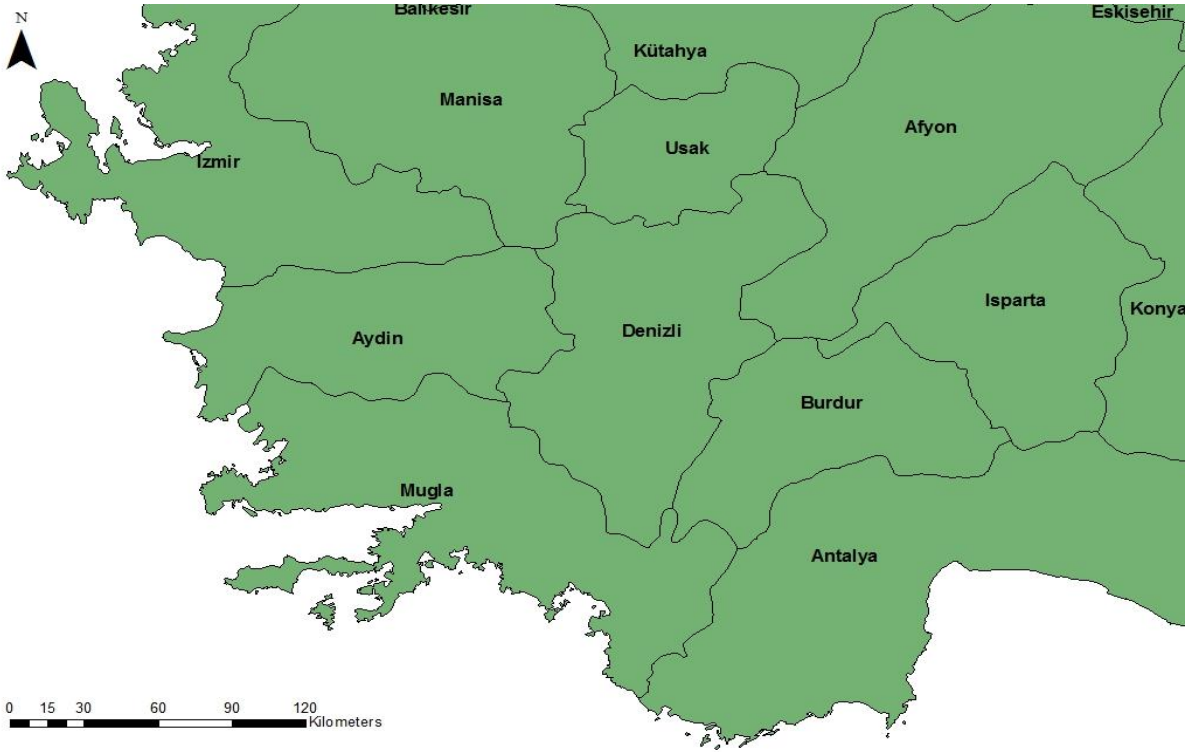


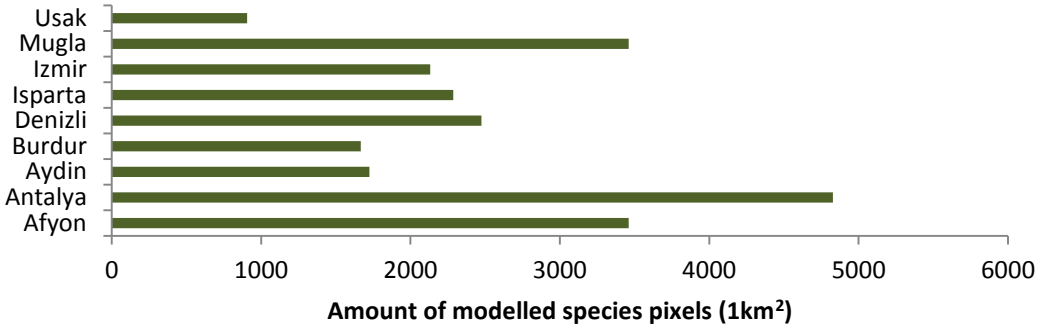


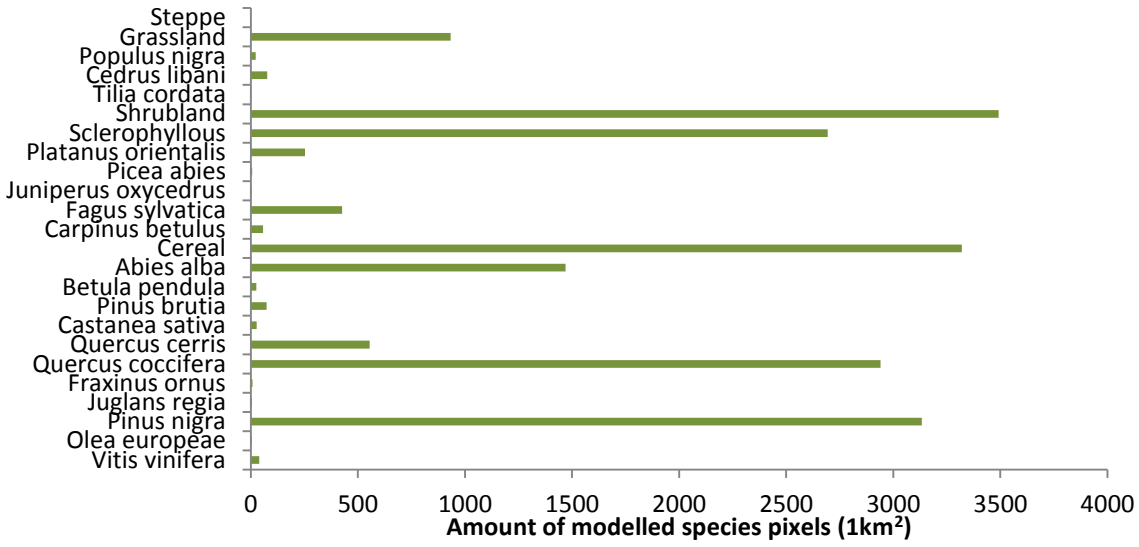


**Figure 5-20 Area map and modeled species overview +2°C**

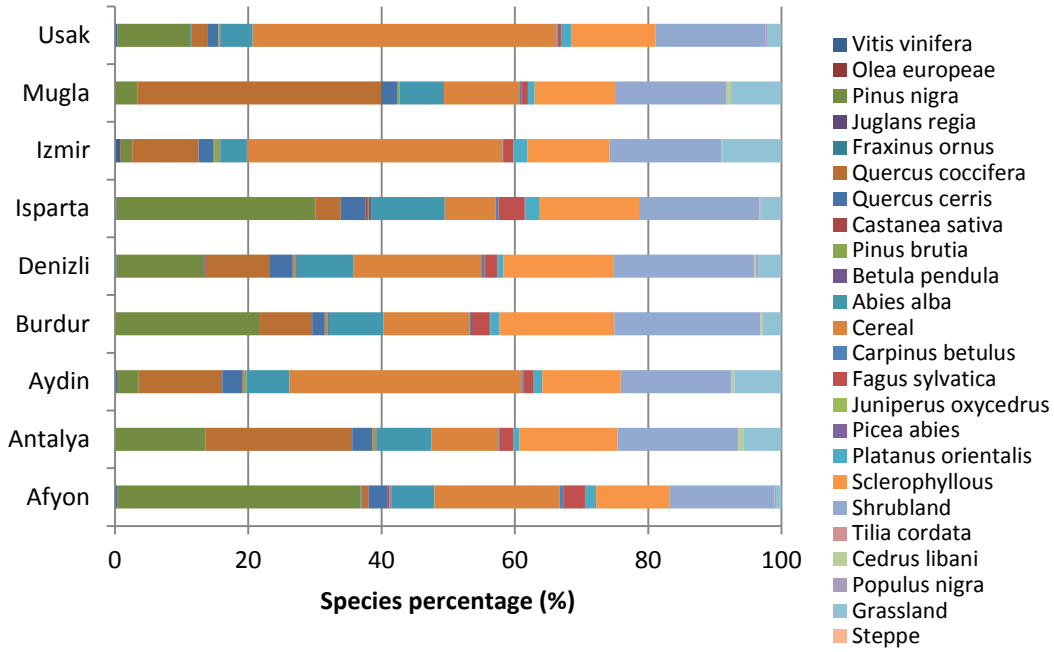


**Figure 5-21 Modelled species potential and relative percentages by province across southwest Turkey under +2°C**

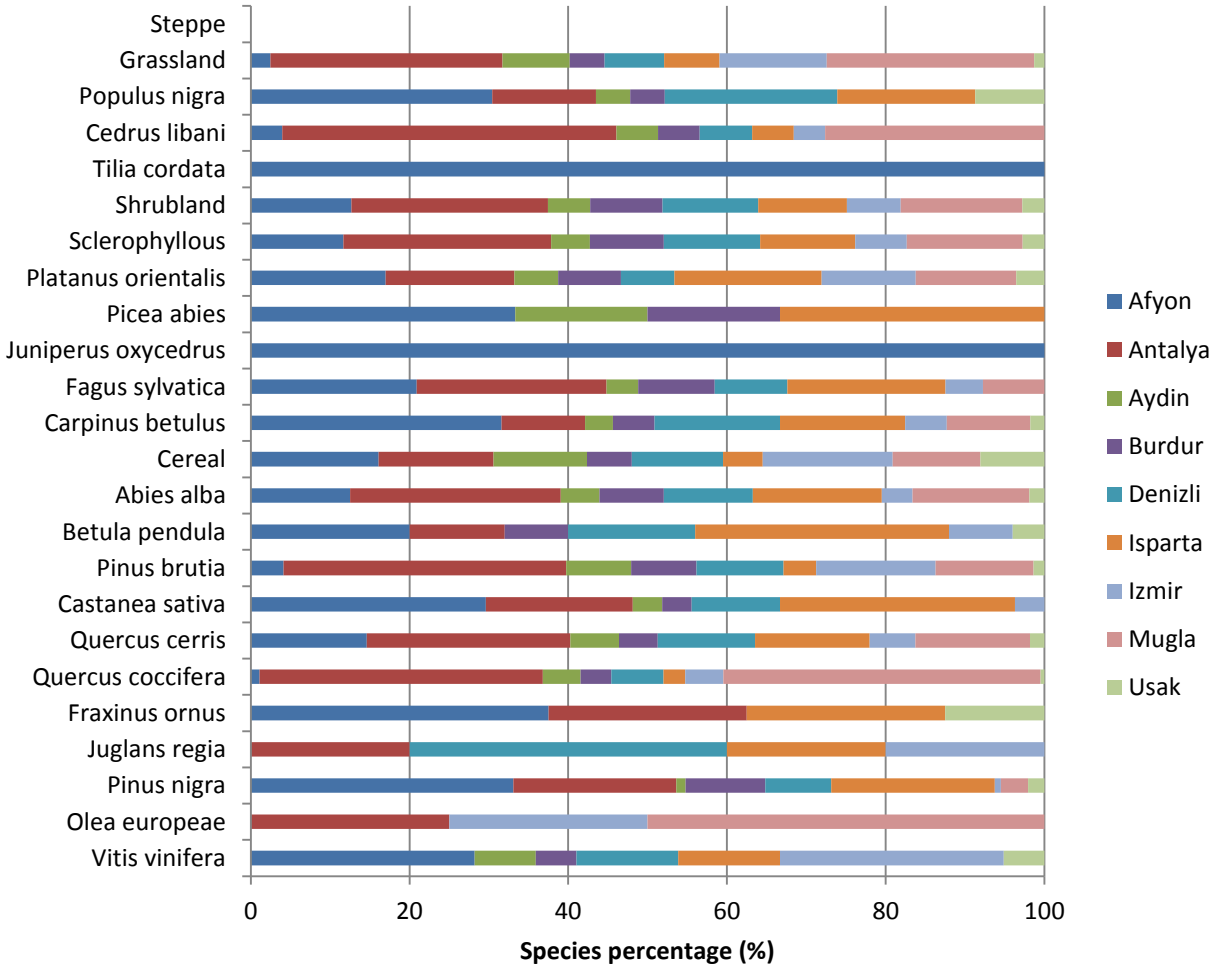


**Figure 5-22 Modelled relative species concentration across southwest Turkey under +2°C**

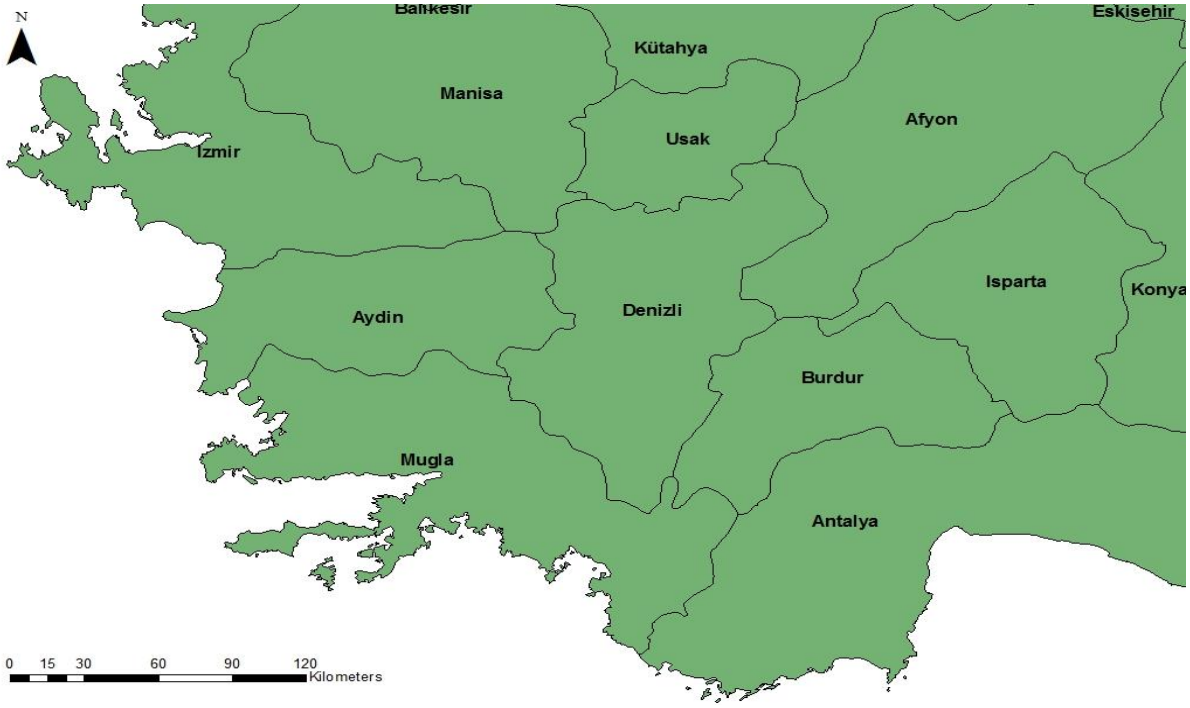


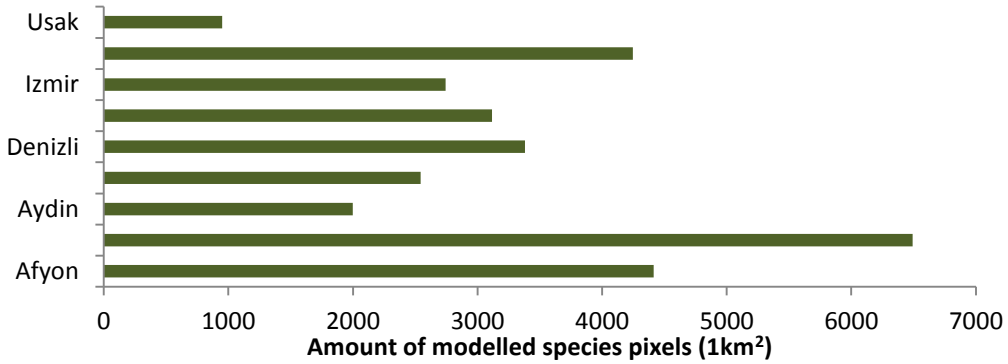


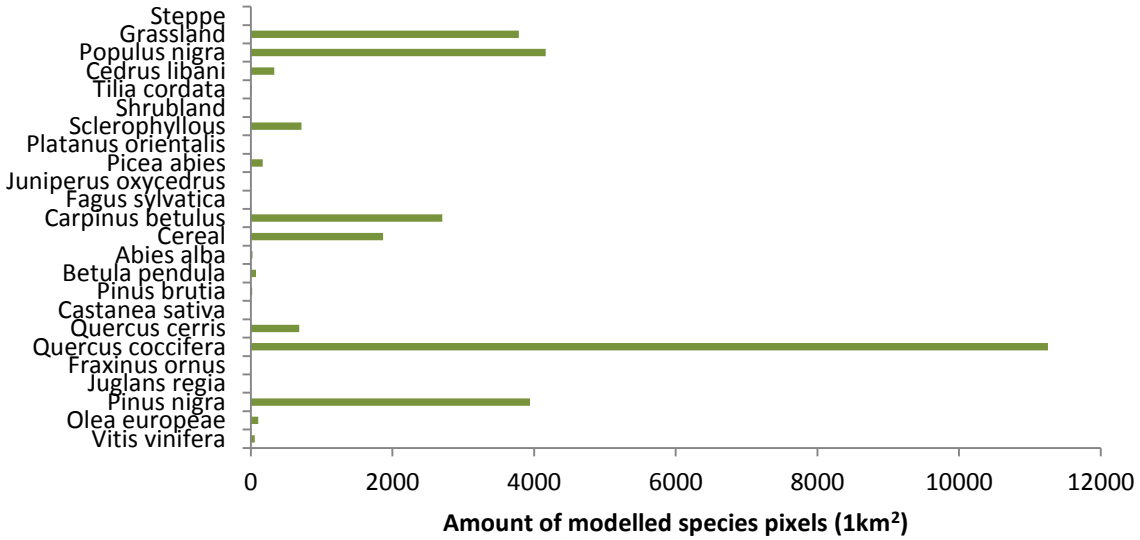


**Figure 5-23 Area map and modeled species overview +100 mm precipitation**

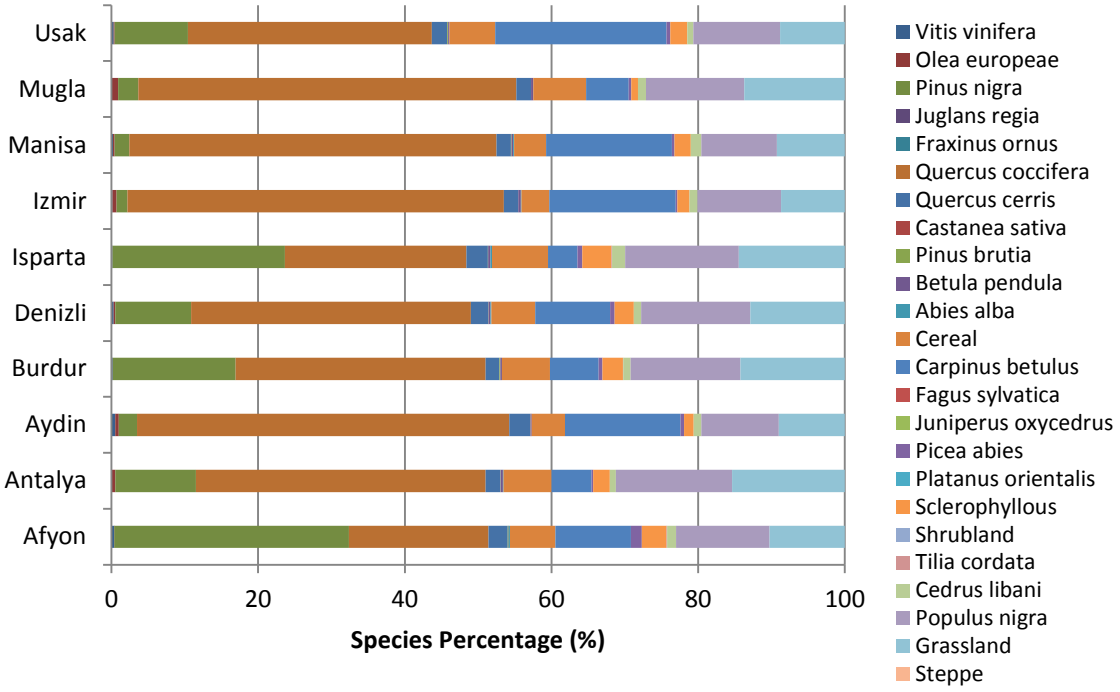


**Figure 5-24 Modelled species potential and relative percentages by province across southwest Turkey under +100mm**

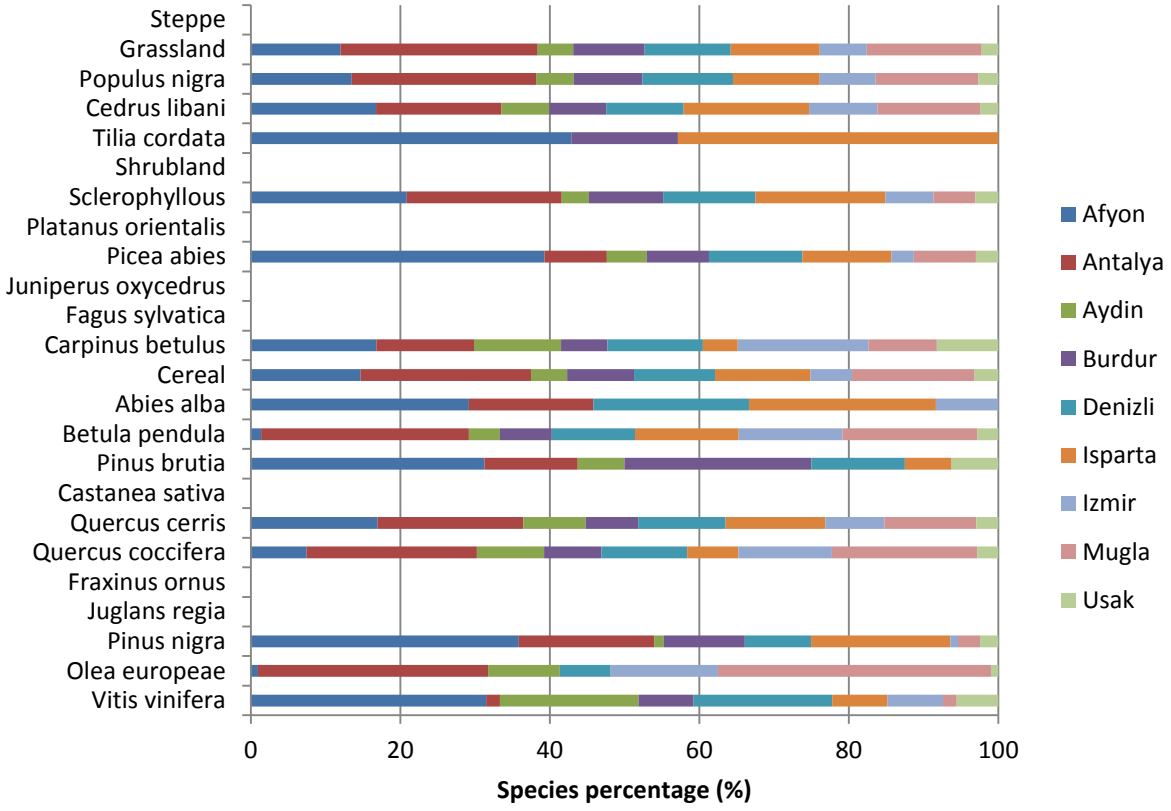


**Figure 5-25 Modelled relative species concentration across southwest Turkey under +100 mm precipitation**

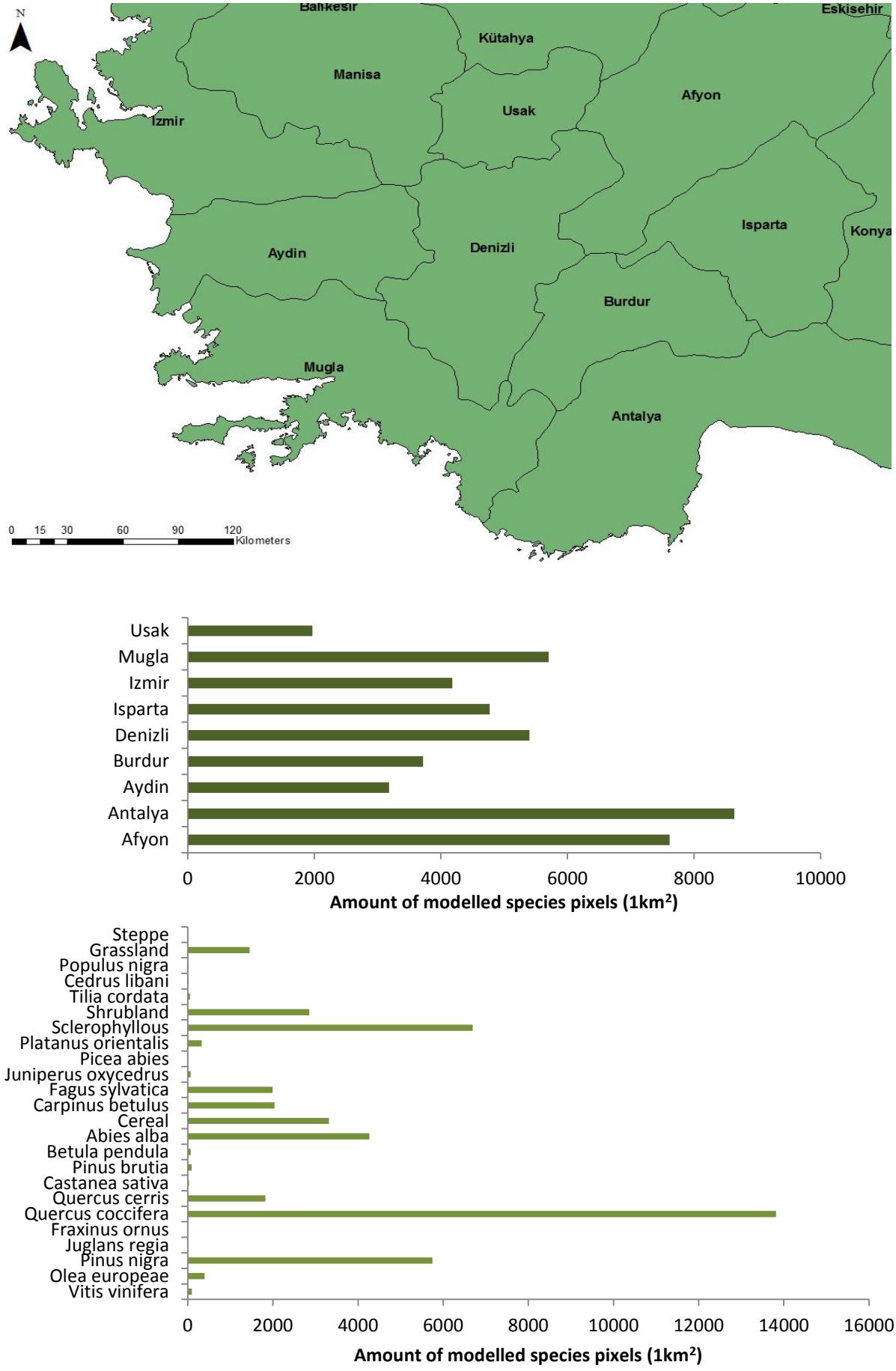


**Figure 5-26 Area map and modeled species overview +300 mm**

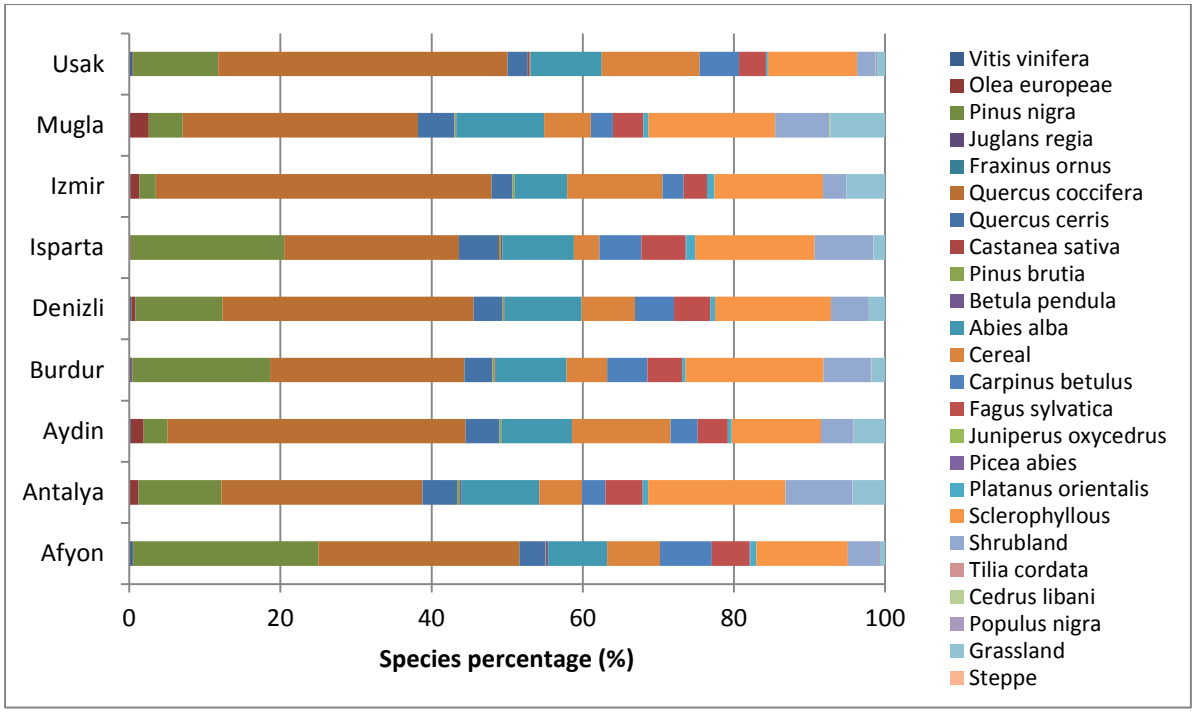


**Figure 5-27 Modelled species potential and relative percentages by province across southwest Turkey under +300mm**

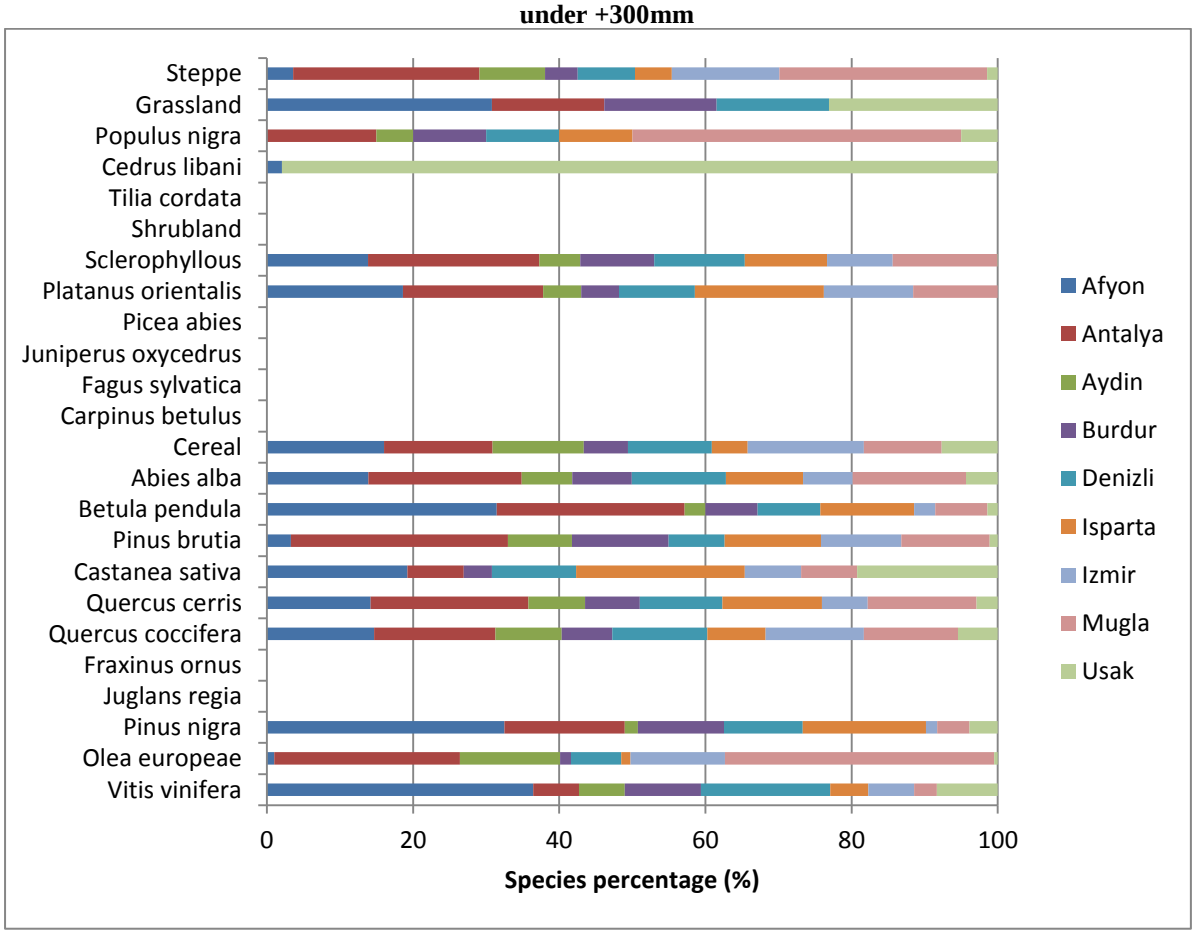


**Figure 5-28 Modelled relative species concentration across southwest Turkey under +300 mm precipitation**

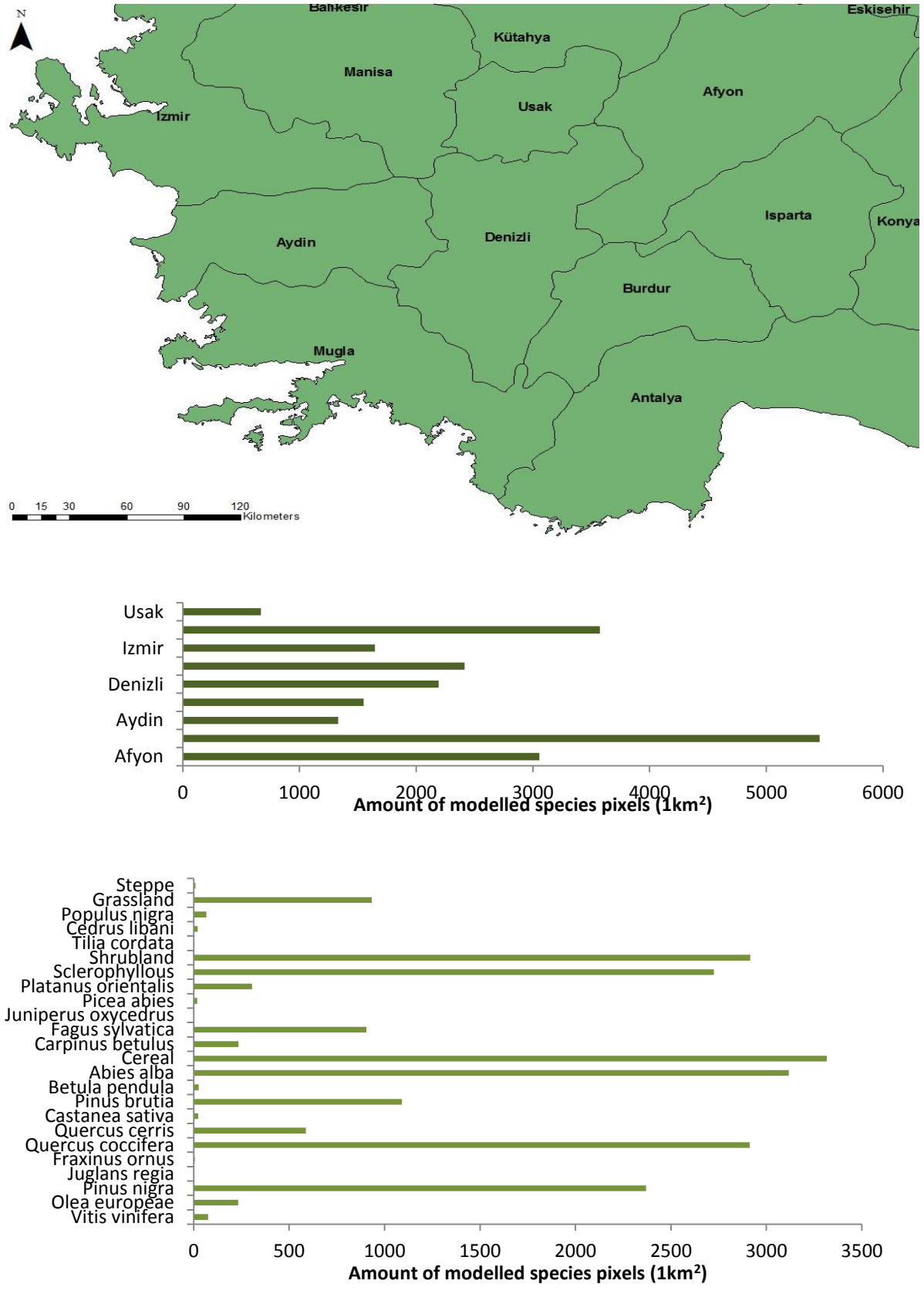


**Figure 5-29 Area map and modeled species overview with +2°C and +50 mm summer precipitation**

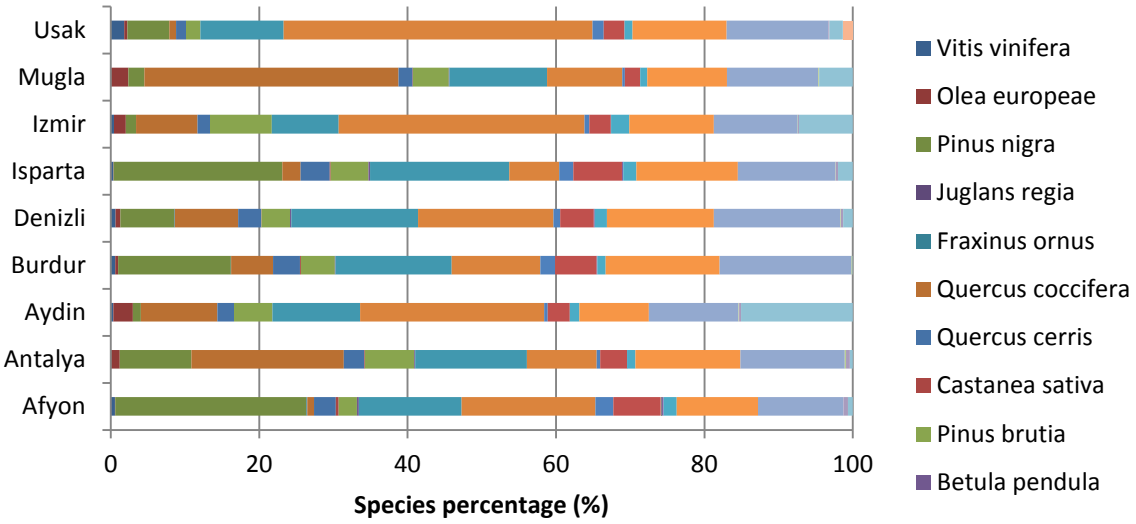


**Figure 5-30 Modelled relative species concentration across southwest Turkey under +2°C +50 mm summer precipitation**

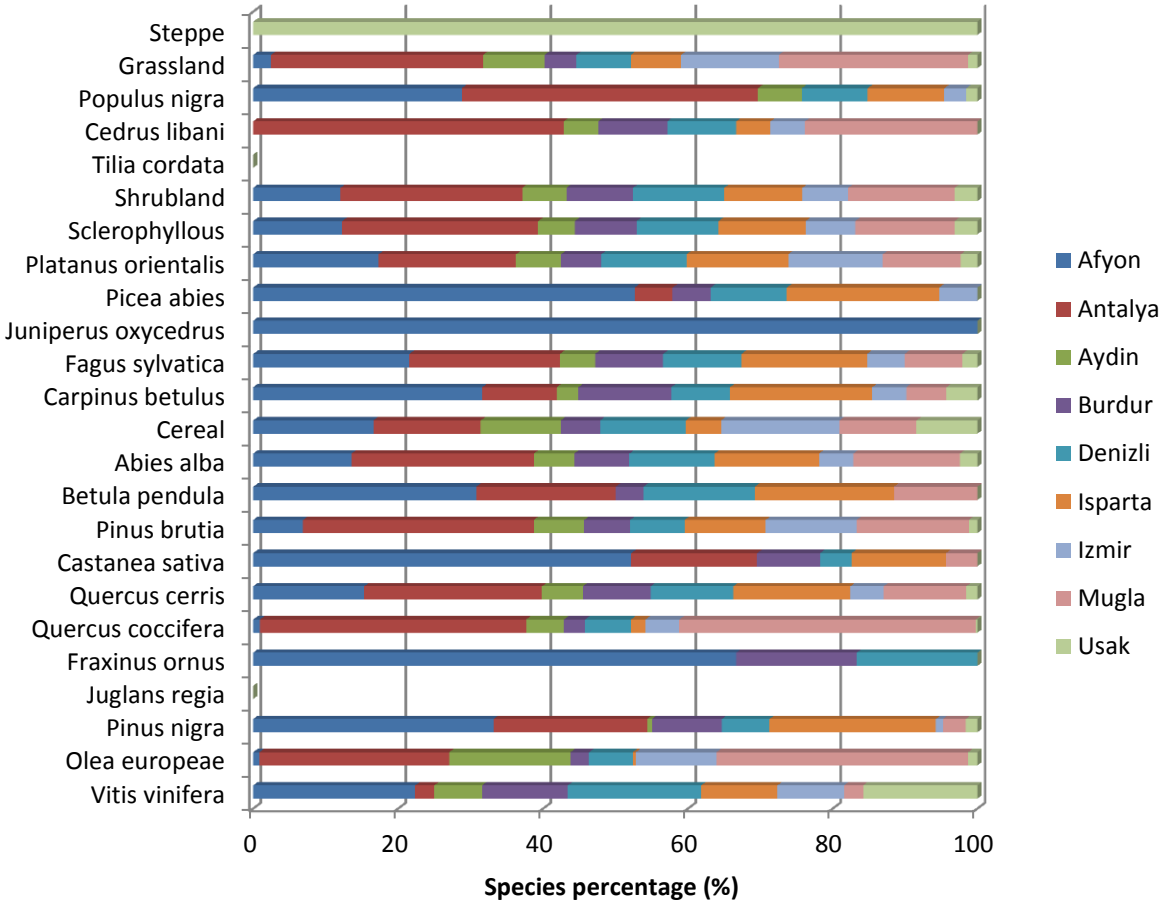


**Figure 5-31 Modelled relative species concentration across southwest Turkey under +2°C +50 mm summer precipitation**

## 5.2 SIMULATING POLLEN ASSEMBLAGES FROM MODEL OUTPUT

In order to compare the model output discussed in this chapter with analytical pollen evidence, the model output from these scenarios needs to be translated into pollen simulations. The process of converting maps of vegetation distribution into simulated pollen has been developed and validated by previous researchers. An implementation of this process is the HUMPOL suite of programs by Bunting and Middleton (2005)

The suite consists of three main programs , the content and order of use of which is shown in Table 5-3.

**Table 5-3 Overview of the HUMPOL suite**

| Program | Function |
|---|---|
| **1. POLGRID** | Image conversion program. Converts ASCII files output by ArcGIS into IDRISSI GRIDs to ingest into POLSACK. |
| **2. POLSACK** | Data collection program. Contains all the taxa to be modelled, with associated Pollen Productivity Estimates (PPE) and Fall Speeds. Also creates communities and dictates the percentage of taxa in each community. Defines sample points for pollen core simulation, and defines a wind rose to adapt pollen dispersal. |
| **3. POLFLOW** | Takes the IDRISSI GRID, and the data collection, to model pollen dispersal using the Prentice-Sugita model. Outputs pollen loading at each sample point for each taxa. |

The first task undertaken to convert vegetation model output into pollen simulations was to export the model output from ArcGIS using an ASCII format, which can then be loaded into POLGRID. This was then converted into IDRISSI GRID format to load into POLSACK. In order for POLSACK to run the pollen simulation task, a number of parameters need to be populated in the program.

The first set of parameters to populate is the pollen core simulation coordinates. These are the locations of the pollen sequences in Eastings and Northings (Table 5-4).

**Table 5-4 Pollen core simulation coordinates**

| Pollen core | Eastings | Northings |
|---|---|---|
| Karamik | 307062 | 4256202 |
| Hoyran | 314005 | 4239712 |
| Beysehir | 366947 | 4156394 |
| Gravgaz | 269742 | 4161601 |
| Bereket | 261064 | 4158998 |
| Pınarbaşı | 238498 | 4148582 |
| Sogut | 222876 | 4104320 |
| Golhisar | 197707 | 4114735 |
| Elmali | 223744 | 4068736 |
| Avlan | 228083 | 4053982 |
| Koycegiz | 111785 | 4092170 |
| Golcuk | 64919 | 4251863 |
| Aglasun | 280157 | 4168545 |
| Ova | 169963 | 4032880 |

The second set of parameters to populate is the Pollen Productivity Estimates (PPE) and Fall Speeds of each species in the model. These are available for most plant species, however empirical data are lacking for some. For the purposes of this model, where Pollen Productivity Estimates were unavailable, values were substituted from other species. This has been an acceptable practice in previous research as long as substitutions are stated as an assumption (Bunting, pers. comms.).

Table 5-5 shows the PPE and Fall Speeds used in this modelling exercise, and their sources. Where PPEs are unknown, values are taken from a species with a middle ranging PPE, such as *Quercus*. This is acknowledged as a limitation of the approach, however PPE data are the subject of a current research initiative in southwest Turkey (Eastwood, Fyfe et al. 2011) so can easily be substituted to update the model as part of future work.

A third parameter allowed a wind rose to be included (Figure 5-32). This was based on modern wind patterns during the spring pollen season, where wind blows predominantly from the west onto the southwest coast (Willemsen 2011). Again, future iterations of the model could investigate this parameter to see how this parameter changes pollen assemblages calculated at each pollen site.

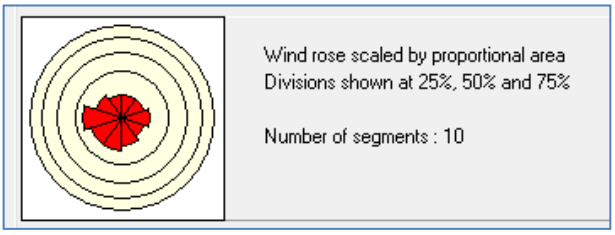


**Figure 5-32 Windrose based on modern values**

**Table 5-5 Species PPE and Fall Speed parameterisation**

| Species | Fall Speed | PPE | Substitution / Clarification | Source |
|---|---|---|---|---|
| Abies alba | 0.12 | 6.88 | | REVEALS - Europe |
| Dry agriculture | 0.06 | 1.85 | Cerealia | REVEALS - Europe |
| *Alnus cordata* | 0.021 | 9.07 | | REVEALS - Europe |
| *Betula pendula* | 0.024 | 3.09 | | REVEALS - Europe |
| *Pinus brutia* | 0.031 | 6.38 | | REVEALS - Europe |
| *Carpinus betulus* | 0.042 | 3.55 | | REVEALS - Europe |
| *Castanea sativa* | 0.015 | 5.38 | *Quercus* for PPE, *Olea* for fall speed | Average PPE |
| *Cedrus libani* | 0.031 | 6.38 | *Pinus* | REVEALS - Europe |
| *Corylus avellana* | 0.025 | 1.99 | | REVEALS - Europe |
| *Fagus sylvatica* | 0.057 | 2.35 | | REVEALS - Europe |
| *Fraxinus ornus* | 0.022 | 1.03 | | REVEALS - Europe |
| Grassland | 0.035 | 1 | Gramineae | REVEALS - Europe |
| *Juglans regia* | 0.037 | 5.38 | *Quercus* | (Filipova, Kvavadze et al. 2010) |
| *Juniperus oxycedrus* | 0.016 | 2.07 | | REVEALS - Europe |
| *Pinus nigra* | 0.031 | 6.38 | | REVEALS - Europe |
| *Olea europaea* | 0.015 | 5.38 | *Quercus* | (Erdtman 1969) |
| *Picea abies* | 0.056 | 2.62 | | REVEALS - Europe |
| *Platanus orientalis* | 0.035 | 5.38 | *Quercus* | REVEALS - Europe |
| *Populus nigra* | 0.035 | 5.38 | *Quercus* | REVEALS - Europe |
| *Quercus cerris* | 0.035 | 5.38 | | REVEALS - Europe |
| *Quercus coccifera* | 0.035 | 5.38 | | REVEALS - Europe |
| Sclerophyllous | NA | NA | *Olea* and *Artemisia* | |
| Shrubland | NA | NA | *Quercus Coccifera* (30%), *Quercus cerris* (30%), *Artemisia* (20%), *Plantago* (20%) | |
| *Tilia cordata* | 0.032 | 0.8 | | REVEALS - Europe |
| *Ulmus glabra* | 0.032 | 1.27 | | REVEALS - Europe |
| *Vitis vinifera* | 0.15 | 5 | *Quercus* for PPE, *Olea* for fall speed | Average PPE |
| Steppe | 0.025 | 1.85 | *Artemisia* | REVEALS - Europe |

Model output is presented in the form of a text file containing pollen yield data (pollen loading) for each sample point specified in the model (i.e. each pollen core location that pollen simulations are calculated for). This represents pollen influx at a specific point, calculated using the Prentice-Sugita algorithm. Pollen loading was calculated for each model run, at each pollen site of interest. This data was then taken forward to compare with analytical pollen data.

## 5.3 SUMMARY

This chapter has provided an overview of model output, presenting relative species potential under 27 different model runs. Uniquely, A GIS approach has allowed an assessment of the spatial aspect of these model runs over a whole region, at the species level.

In summary, under reduced temperature and precipitation, model results indicate that steppe is likely to encroach across southwest Turkey from the north east. Species composition is likely to mainly consist of cold-tolerant species such as *Pinus, Abies* and *Cedrus*, with cold and drought intolerant species being restricted to coastal regions.

Conversely, under increased precipitation and temperature, *Quercus* and arboriculture species are likely to be advantaged, and are shown to increase in density and extent into the Oro-Mediterranean region.

The results of this analysis are likely to have interesting implications when compared to analytical pollen data, as they may provide linkages between climatic theory, vegetation distribution, and pollen assemblage variability across the region of southwest Turkey. To this end, the chapter outlined the methodology for translating vegetation model output into simulated pollen using the HUMPOL suite of software, thus allowing this analysis.

# Chapter 6

# Chronological refinement of pollen data and validation methodology

The vegetation model runs developed in Chapter 5 demonstrated varying species potential under a range of climate change scenarios, based on bioclimatic and edaphic rulings. To compare this model output with analytical pollen data, vegetation model output was converted to simulated pollen assemblages.

In order to compare simulated pollen with analytical pollen data at key stages throughout the Holocene, two further methodological steps are required to create a standardised base of analytical pollen evidence. The first involves analysing the deposition characteristics and chronology of each sediment core and associated analytical pollen sequence in southwest Turkey, to provide a coherent, calibrated chronology. Bayesian modelling will be utilised to allow pollen sequences to be synchronised with one another, and any chronological uncertainties highlighted. The second methodological step requires the calculation of species percentages based on only those species modelled in the vegetation model, to provide a consistent basis for comparison. The details of both of these components are discussed in this chapter.

# 6 CHRONOLOGICAL REFINEMENT OF POLLEN DATA AND VALIDATION METHODOLOGY

## 6.1 THE IMPORTANCE OF A CONSISTENT POLLEN ZONE CHRONOLOGY

Analytical pollen sequences are traditionally divided into pollen assemblage zones that highlight a particular vegetation assemblage, while zone boundaries can be used to distinguish changes in vegetation composition. Pollen assemblage zones can be determined visually (e.g. Bottema and Woldring 1984) or statistically using cluster analysis (Eastwood, Roberts et al. 1999). Once pollen assemblage zones have been determined, chronological ages can be assigned for each zone boundary. Traditionally, this has been achieved using linear interpolation between adjacent radiocarbon ages and extrapolation at depth, which assumes a constant sediment accumulation rate (SAR) between adjacent radiocarbon ages, even though they may be thousands of years apart.

Although some of the more recent pollen sequences do have more reliable chronological frameworks, such as those taken from Gölhisar (Eastwood, Roberts et al. 1999), a generally accepted schema of vegetation change since the Holocene does not exist across the whole region, partly because of variable chronological control on cores, and partly because of a lack of chronological modelling to explore age-depth relationships. In fact, eleven main issues can be identified that have so far complicated and confounded the regional correlation of pollen sequences in the southwest of Turkey:

1. A lack of radiocarbon ages, due to low organic matter content
2. Large error uncertainties with some radiocarbon ages due to low organic matter content
3. Large bulk $^{14}C$ age samples (spread over large segments of core depth) rather than AMS
4. Chronological imprecision introduced upon calibration.

5. Uncertainties (sometimes large) associated with linear interpolation and extrapolation
6. Absence of lithological variability to inform upon sediment accumulation rates (SARs).
7. Notable lack of core sequences with detailed loss-on-ignition and magnetic susceptibility data.
8. Presence of tephra layers in only a few pollen sequences [3]
9. A difference in dating method across sites
10. Assumption that core tops represent the present day
11. $^{14}C$ ages can also be impacted by limestone geology, as ages can be influenced by younger or older carbon, which can lead to a wide margin of error when ages are calibrated to calendrical dates (Eastwood, Roberts et al. 1998).

The combination of variable organic content, radiocarbon age extraction, age uncertainty and tephra identification across different cores makes it difficult to synchronise pollen across the region, or even confidently place pollen zones in historical or pre-historical periods. This in turn makes it difficult to integrate with other records such as archaeological finds.

Whilst not a 'cure-all' for the above issues, recent advances in the application of statistical models to chronological modelling such as the use of Bayesian modelling of $^{14}C$ dates have allowed the impact of different sediment deposition parameters on date calibration to be explored, and the uncertainty associated with variable chronological control to be quantified. Furthermore they allow the extraction of calibrated age probability density functions for any date entered into the model, thus age estimates for pollen zone boundaries can be calculated. This method has not previously been applied to the lake cores of southwest Turkey, but has been employed on other sediment sequences to good effect, providing a more accurate picture of deposition through time (Buck, Kenworthy et al. 1991; Buck, Cavanagh et al. 1996).

The aim of this chapter is therefore to analyse and chronologically model the pollen sequences of southwest Turkey using Bayesian statistical techniques. An assessment will be undertaken of the applicability of Bayesian analysis to multiple sediment cores throughout southwest Turkey,

[3] Tephrochronological studies in the eastern Mediterranean region of Turkey are in their infancy, however there is improvement as more tephra layers are being located in sediment sequences

with a view to provide a more robust base for comparison of model output with analytical pollen evidence. An overview flow diagram is shown in Figure 6-1 that represents the key processes undertaken and described in this chapter.

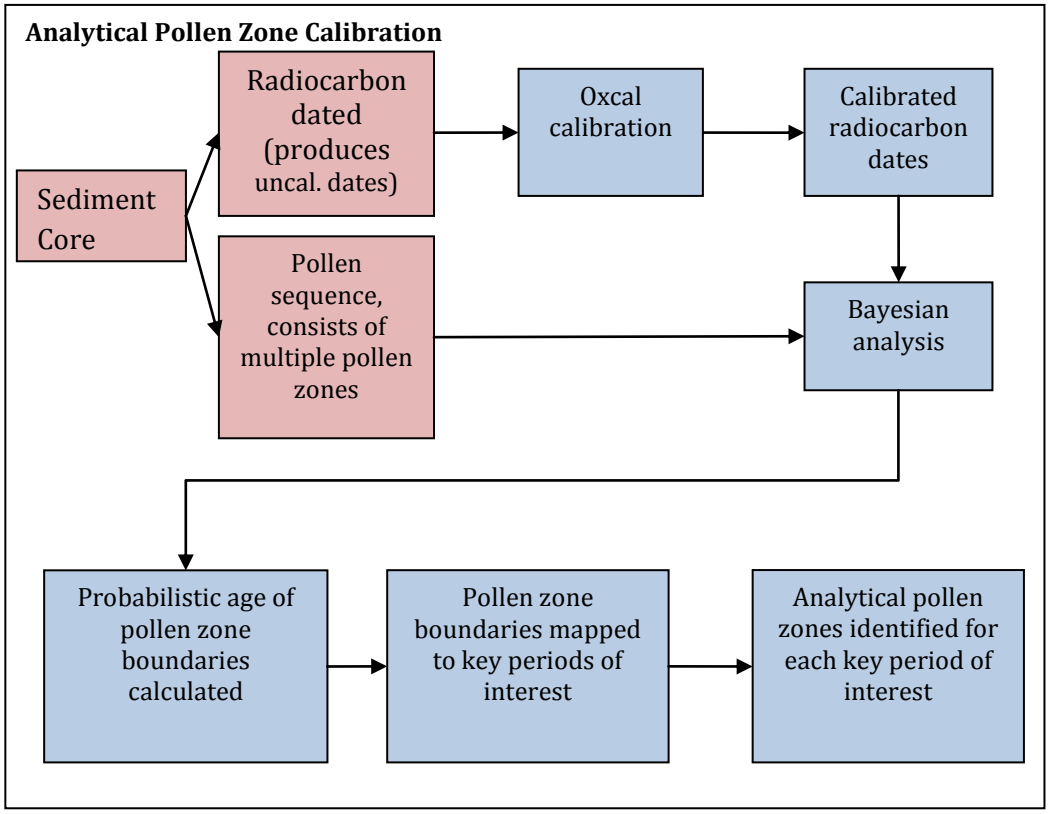


**Figure 6-1 Flow diagram showing the overall process undertaken as described in this chapter to calibrate and identify analytical pollen zones for each key period of interest. Red boxes show work done by previous researchers.**

## 6.2 APPROACHES TO AGE-DEPTH MODELLING

Long term sedimentary core samples with associated pollen sequences provide useful analytical comparison data for the model runs in this thesis. In order to allow comparison with other data, the dating evidence available for these core samples firstly needs to be calibrated in a consistent manner. Furthermore, if such records are to be used to inform on the timing of events, and the relative timing between different sedimentary sequences, age-depth models can be used to estimate the deposition characteristics of a core over time. Undertaking age-depth models are an important step as they allow age estimates of levels of a sediment core that are not dated.

Traditionally, age-depth models are created using a simple linear interpolation model. There are some limitations of this approach. Firstly, most age-modelling routines that calculate linear interpolation tend to reduce the irregular distributions of calibrated $^{14}C$ dates down to single point estimates with symmetric error bars (Blaauw 2010). Furthermore, if a deposit is assumed to accumulate at rates that are relatively constant throughout the whole core (i.e. through multiple aged sediments) then a linear interpolation model may show artificially abrupt SAR changes between each radiocarbon dated pair with depth (Bennett 1994). An alternative is to use spline or polynomial regression, which results in smoother age-depth curves that may not always pass through each individual dated level. Age-depth modelling is therefore a trade off between fitting a curve through most or all dated levels, and obtaining a smooth curve that represents a likely approximation of the true (but unknown) accumulation history of the deposit (Piotrowska, Blaauw et al. 2010 p.7).

When considering complex comparison studies with multiple cores or palaeoecological evidence, further methods may be necessary to provide accurate and precise age-depth models for those sequences (Bronk Ramsey 2008a). One such method is the development of Bayesian modelling, which **can be employed both in the calibration of radiocarbon dates, and the development of age-depth models.** Two packages are currently favoured for comprehensive Bayesian modelling capability; BCAL developed by Sheffield University, and the Oxcal software (currently version 4.1) from the Research Laboratory for Archaeology at Oxford (Bronk Ramsey 2001; Bronk Ramsey 2008b).

Bayesian approaches to age-depth modelling are more advanced than linear interpolation, as they can incorporate chronological ordering and wiggle-match dating. Importantly, it provides better functionality to compare multiple archives than basic interpolation procedures. For these reasons, the Oxcal software package and online capability were used to model sediment cores and associated pollen sequences in southwest Turkey, with the aim of creating a coherent chronology.

## 6.3 THE BAYESIAN APPROACH TO DEPOSITION MODELS.

A useful overview of using Bayesian theory to create deposition models is given by Bronk Ramsey (2008a), and this section includes discussion from that paper. A Bayesian approach is a mathematical framework that allows the combination of information of a probabilistic nature in a formal way. A full discussion of Bayesian theory is outside the scope of this thesis, however the interested reader is directed to Gilks et al. (1996), D'Agostini (2003) and Buck et al. (1996).

Bayes theory details how to quantitatively combine *prior* information with *likelihood* information. *Prior* information is information about a system that we know before measurements are taken. In the context of sediment cores this relates to information such as lithology, the depth of radiocarbon dates and pollen zone boundaries. *Likelihood* information is that which is defined from measurement. In the context of sediment cores this relates to the probability distribution functions which represent the likelihood of any one sample (such as a radiocarbon date) having a particular age.

Bayesian analysis therefore aims to find a representative set of possible ages for each depth point in a sedimentary sequence. In the sediment core case, ages are generally highly correlated by depth, so cannot undertake analytically. Therefore Markov Chain Monte Carlo sampling is used within the Oxcal Bayesian model to build up a distribution of possible solutions (Gilks, Richardson et al. 1996).

Using Bayes theorem the algorithms employed essentially sample over all possible solutions with a probability that is a product of the prior and likelihood probabilities. The resulting distributions are referred to as the posterior probability densities and take account of both the deposition model and the actual age measurements made (Bronk Ramsey 2008a p.3)

Further terminology is used within Bayesian analysis which is also useful to introduce. In a deposition core, deposition is assumed to consist of a discrete series of events. This can equate

to sediment within a sediment core that is dated by radiocarbon dating, or an archaeological artefact for instance. An event is by definition short when compared to the resolution of the measurement techniques employed.

Within a Bayesian depositional model, these events can be grouped into phases or sequences. A phase is a group of events for which there are no fixed relations such as a group of archaeological artefacts with no context. A sequence is a group of elements in a given order such as radiocarbon dated sediment samples from a laminar deposit. Note that it is possible that events can be grouped and groups can be sequenced. The way of grouping events together within Oxcal is to define *boundaries* between which a group of events is placed. These have a particular mathematical formulation based on Buck et al. (Buck, Kenworthy et al. 1991)

## 6.4 MODEL SET UP 1: LIKELIHOOD AND PRIOR INFORMATION

As introduced, the Bayesian models available in Oxcal allow the combination of contextual information from sediment and pollen sequences (such as depth, lithology etc.) with radiocarbon or other direct dating information. This allows the integration of information between different records to provide a coherent chronology on which to base environmental and archaeological research (Bronk Ramsey 2008a).

The modelling of age-depth deposition models across southwest Turkey therefore required the collation of *likelihood* and *prior* information, the input of key events, phases and sequences, and then the appropriate choice of parameters and models from the Oxcal Bayesian analysis suite.

As a first step, an empty model was created for each sediment sequence across southwest Turkey. A summary of likelihood information available for the region is found in Table 6-1. The table details the number, type, quality and uncertainty of radiocarbon ages that are associated with sediment cores across southwest Turkey. Likelihood information could then be entered then into the model as an R_Date function. So for example:

```
R_Date("B-213851", 2230, 40)
```

indicates an event A has a likelihood characterised by a date of 3450 ±28. An R_Date function was added for all radiocarbon dates within a core, and this was repeated for all cores available across southwest Turkey. A parameter to specify which radiocarbon curve to use was set to the IntCal 09 atmospheric curve (Reimer, Baillie et al. 2009). Table 6-1 also summarises core lithology, details on SAR if known, and other relevant information such as the presence of tephra layers, which can be used for *prior* information. The most useful prior information input was the depths at which each radiocarbon date was taken. The depth information from each study was attached to the model as a 'z' parameter under each radiocarbon date as shown below:

```
    R_Date("B-213851", 2230, 40)
{
                    z=783;
};
```

**Table 6-1 Overview of radiocarbon dates and core characteristics, roughly ordered by chronological robustness**

| Core | No. of ages | Type of ages | Tephra | Lithology | Author | SAR | Notes |
|---|---|---|---|---|---|---|---|
| Bereket | 11 | AMS | No | Silt, clay, peat, sand, gravel | Kaniewski 2007 | SAR assumed constant between dates | |
| Gravgaz | 7 | AMS | Not published, but recently discovered | Clay, peat | Vermoere 2002 | High deposition rate between 550-800cm | |
| Gölhisar II GHA and B (spliced) | 7 | Bulk | Yes | Calcareous silt, peat, silt, clay peat | Eastwood et al. 1999 | Changes in SAR with lithology | |
| Ağlasun Core 6 | 5 | Bulk | No | Clay, travertine, marl | Vermoere 2002 | | |
| Gölcük | 4 | Bulk | Yes | | Sullivan 1989 | | |
| Sögüt Gölü | 2 | Bulk | Yes | Clay, clay with shells, marl. | Van Zeist and Wolding 1975 | 10cm per 515 years early part, 10cm per 135 years later part | |
| Köycegiz Gölü | 2 | Bulk | Yes | Peat, clay, gyttia, sand | Van Zeist and Wolding 1975 | | |
| Karamik | 2 | Bulk | No | homogeneous clay | Bottema and Woldring 1984 | 10cm per 680 years | Core top assumed present day |
| Pınarbaşı | 2 | Bulk | No | Clay, sand, gravel | | | |
| Beyşehir Gölü I | 2 | Bulk | No | homogeneous clay, little organic matter | Van Zeist and Wolding 1975 | 10cm per 120 year | Core top assumed present day |
| Ova | 2 | Bulk | No | Clay | Bottema and Woldring 1984 | | Contains 2 haitus, pollen sum is low |
| Hoyran | 1 | Bulk | No | homogeneous clay. | Van Zeist and Wolding 1975 | 10cm per 143 years | |
| Beyşehir Gölü II | 1 | Bulk | No | homogeneous clay | Bottema and Woldring 1984 | | |
| Avlan | 0 | - | No | Clay, peat | Bottema and Woldring 1984 | | |
| Elmalı | 0 | - | No | Clay, sand | Bottema and Woldring 1984 | | |
| Gölhisar I | 0 | - | No | Peat, clay, sand, gravel | Bottema and Woldring 1984 | | |

Four points were considered as part of this stage of the analysis

1. How would depth be notated for bulk as opposed to AMS dates?
2. Should lithological information be included?
3. Should tephra information be included?
4. Could the sediment have been reworked or affected by old carbon?

On point 1, conventional (bulk) radiocarbon dating determines the age of a material by counting decays from $^{14}C$ atoms. The number of decays over a given period allows the $^{14}C$ content of the material to be determined. The departure of the $^{12}C$:$^{14}C$ ratio from the equilibrium value enables calculation of the age of the material (Bennett 1999). This method requires a relatively large sample for dating, usually taking ~5 to 10 cm of sediment from each layer in the core.

In contrast, accelerator (AMS) radiocarbon ages are determined by counting the number of $^{12}C$ to $^{14}C$ atoms directly in a mass spectrometer, and obtaining the age of the material from this (Bennett 1999). AMS dates can be gained from much smaller samples, meaning that the sample taken is smaller, and the depth from which it is taken is more precise.

For bulk samples, the midpoint of the sample depth was taken as the depth parameter. So for instance if a radiocarbon date sample was taken between 340 and 350 cm the depth of sample would be notated as 345 cm. AMS depth parameters were more precise and was taken directly. As the sediment within the cores is not laminar, it is considered that an uncertainty of ~5cm for bulk sample positioning is not likely to dramatically change the age depth model, and so a mean depth is allowable in this instance.

On point 2, although lithological information was available for some cores, it was in the main fairly homogeneous, and so was not included in the model. Except for the Gölhisar cores, SAR information was also not available to investigate whether significant changes to deposition had occurred. This emphasises the importance of measuring SAR for the chronological interpretation of sediment cores and associated pollen sequences.

On point 3, tephra layers can play an important part in synchronising sediment cores from disparate areas. However, to include this as a parameter in the model would have required an agreed calendrical date for the tephra deposition to have occurred. Due to the nature of the calibration curve for this period this is difficult to assign a calendrical date by calibrating using $^{14}C$ dates just below the tephra (Eastwood, Tibby et al. 2002). Instead, as this tephra layer is present in a few cores across southwest Turkey, it was decided that this layer could act as a validation layer to see how well the model synchronised the sediment cores across the region. If the tephra was added at the correct depth after the model was run, and they lined up across the region, this would be an independent test of the validity of the chronology.

On point 4, dating of terrestrial plant macrofossils avoids problems with possible contamination with reworked material in bulk samples and reservoir effects (Hormes, Preusser et al. 2003). AMS dates from Bereket and Gravgaz (using uncharred plant remains) are therefore considered to be reliable and show increasing age with depth (Kaniewski, De Laet et al. 2007). Of the bulk radiocarbon samples taken from other cores, no marine or volcanic margin cores were utilised for modelling, reducing potential reservoir effects.

## 6.5 MODEL SET UP 2: AGE DEPTH MODELLING

In order to choose an appropriate Bayesian age-depth model and associate parameters, it is important to recognise three main factors that can impact on model accuracy and precision. These are considered by Ramsey (2008a) to be:

1. The complexity in the underlying deposition mechanisms,
2. Random elements to the process.
3. Abrupt changes to different modes of deposition

In terms of points 1 and 2, it is often the case that despite the complexity of the underlying processes, the sedimentation rate stays approximately constant. This is often assumed to be the case in peatland deposition for instance (Piotrowska, Blaauw et al. 2010). In this circumstance random processes are of a sufficiently fine scale that they become averaged out over the low resolution of the overall sediment core. This only holds as long as a large slump or flood event does not dramatically change the deposition rate on a large scale of course (Ramsey 2007). Abrupt changes to different modes of deposition can be incorporated through examination of the lithology and sedimentology of the cores, and incorporating any significant changes which may reflect a key change in Sediment Accumulation Rate.

In this instance, lithology in most cores has been assessed as fairly homogenous. The bottom of a couple of cores show coarse gravel changing into clay suggesting a change in deposition rate, however this is generally at the bottom of the core, as it prevents the core from being taken further. Considering one study that did incorporate sediment accumulation rate data (Eastwood 2007) there are potentially two time periods at Gölhisar where mean SAR decreases from ~1.5 mm $yr^{-1}$ to ~0.5 mm $yr^{-1}$ (at ~8200 $^{14}$C yr BP and ~5100 $^{14}$C yr BP) and one period where SAR increases to ~2.5 mm $yr^{-1}$ (at ~ 2900 $^{14}$C yr BP). Whether these constitute 'dramatic'

changes is unclear, but as they tend to last for thousands of years they suggest a long phase of erosion or deposition as opposed to an extreme event slump or flood.

Due to the mixture of circumstances for different cores, a number of deposition models were employed within the Oxcal Bayesian analysis package to investigate the likelihood and prior information that was available (namely the age probability distribution of radiocarbon dated samples, the order of these samples, and the depth at which these were found) to provide an improved estimate of age-depth chronology.

If actual deposition rates were known for all cores, the 'D_Sequence' or 'V_Sequence' model could have been used. A more general model discussed by Bronk Ramsey (2007) is the 'Uniform Deposition' model, where the accumulation rate is unknown, but is assumed to be approximately constant between events (although what constitutes approximately constant is not defined). This model was the first to be taken forward to examine the agreement between it and the actual sediment core evidence.

At the other end of the scale is the 'Simple Sequence' model, which assumes a particular order between radiocarbon dates, but no assumption of a constant accumulation rate. This is an appropriate model when large changes in deposition rates are considered to exist between ages. This was the second model to be taken forward to examine agreement between it and sediment core evidence.

A further model available is the 'Poisson process' model. This model again utilised the depth of radiocarbon ages as an input parameter, but then also included a 'rigidity' parameter, equivalent to the "events per unit depth". In a sediment core, deposition is assumed to be a discrete series of events (particles). If it is assumed that the way particles are deposited over time is essentially a random process, the process can be considered as delivering a Poisson distribution. The model works under the assumption that with particle size much lower than the unit length of measurement, deposition becomes almost constant and therefore approaches the constant deposition model. Conversely, where particles are large compared to the unit

length of measurement, deposition appears more variable. This is reflected in a model parameter defined as the 'k' value, equal to the amount of increment events per unit length. The sediment accumulation rate depends on the size of the particle and the resolution of time over which the measurement is taken. As the time resolution decreases (from minutes to years to centuries), a particular sediment size does not affect the sediment accumulation rate so much and it averages out towards a constant, or uniform deposition model.

In the Bayesian model setup, the depth of radiocarbon dates is measured in cm. The size of particles tends to fall between fine sand (~1mm or less) and gravel (~1cm). Suitable k values are therefore likely to be between 0.01 to 1. In order to examine how this affected model output, three models were run under a Poisson deposition process, with 0.01, 0.1 and 1 as 'k' values.

In addition to radiocarbon dates, depths, model parameters and boundaries, two more important model parameters were added. Firstly, another piece of *prior* information was added, in that the top of the core was constrained by adding a core top date as the year that the core was taken. Blaauw advises that whenever available, such an anchor point should be included (Blaauw 2010). An example of the syntax of this simple sequence is shown below:

C_Date("Core taken", 2007, 0);

This allowed first estimates of calendar age ranges ($t_i$) to be calculated. Secondly, following calibration of the radiocarbon dates and the calculation of an age depth model, it is possible to interpolate a date for a point that is not directly dated. This procedure is essentially a type conversion function that returns a PDF for an age from an expression. This function allows the quantitative estimation of pollen zone boundaries. These boundaries were therefore included in the model in the form:

Date( pollen_boundary_2to3)

With an associated depth (z) value. As a summary, Table 7-1 contains a summary of key parameters used within the Bayesian modelling process.

**Table 6-2 Key model parameters used within the Oxcal Bayesian modelling procedure.**

| Short description | Label | Description |
|---|---|---|
| Model types | | |
| Simple sequence | Sequence | Assumption of order |
| Uniform sequence | U_Sequence | Uniform deposition rate |
| Poisson process | P_Sequence | Interpolated ages. No assumption of order or deposition rate |
| Model Parameters | | |
| Radiocarbon age | R_date() | Radiocarbon age with lab code, measurement for the sample ($r_m$) and surrounding uncertainty ($s_m$ )arguments |
| Depth | z() | Depth of radiocarbon age in core |
| Top and bottom boundary | Boundary | Boundary of core |
| Events per unit (rigidity of model) | k() | Postulated events per unit. Event scale is typically 0.01 to 1cm in sedimentary sequences. |
| Date | Date() | Interpolates date for point that is not directly dated. It is essentially a type conversion function that returns a date or PDF for a date from an expression |
| Prior | Prior() | defines a PDF either from a file with specific data, or copied from earlier in the calculation |
| Order | Order() | Group function or query which gives the relative order of events. Uses the Marco Chain Monte Carlo (MCMC) method to find probability $t_a<t_b$, $t_a<t_c$ |
| Correlation | Correlation() | Provides a probability density plot of $t_b$ against $t_a$ |

## 6.6 MODEL SET UP 3: MODEL DIAGNOSTICS AND VISUAL OUTPUT

A number of diagnostic statistics were available to compare model output (Table 6-3). The main results from the analysis are marginal posterior densities (the probability distribution). The 99.7% range of this distribution is calculated, which is known as the highest posterior density (hpd) range.

Agreement indices can be calculated which show the measure of agreement between the model (prior) and the observational data (likelihood). These are arranged by individual sample agreement (A), which allow the identification of outliers, combined agreement ($A_{comb}$) which assesses whether distributions can be combined, a model agreement index ($A_{model}$), which is an overall measure of model agreement, and an individual agreement index ($A_{overall}$). Values over 60% are deemed adequate agreement for individual sample agreement, model agreement and individual agreement indices, and $1/\sqrt{(2n)}$ for combined agreement (Oxcal 2010). Statistics are also available for the convergence integral, which is a test of the effectiveness of the MCMC algorithm.

**Table 6-3 Bayesian Modelling Output Diagnostics**

| Type of output | Model diagnostic | Description |
|---|---|---|
| Table | Un-modelled and modelled dates | BP or BC/AD |
| | Model indices | A, $A_{comb,}$ $A_{model}$ and $A_{overall}$ |
| Summary report | Model specification | Parameter definitions<br>Likelihood distributions<br>Constraints<br>Prior factors<br>Groupings |
| Plots | Single plot | Single Radiocarbon calibration plot |
| | Multiple plot | Multiple Radiocarbon sequence plot |
| | Curve plot | Position of Radiocarbon ages on calibration curve |
| | Depth plot | Position of dates with depth |

## 6.7 RESULTS

For brevity, this section will provide results for one sediment core in this section, whilst results from other cores can be found in Appendix 11. The Karamik core was chosen as it is one of the longest pollen sequences within the region, and, although it only has two radiocarbon ages, the result will allow demonstration and discussion of uncertainty within the core.

### 6.7.1 Calibration

The two radiocarbon dates available for Karamik were first calibrated in Oxcal using the IntCal09 reference curve (Reimer, Baillie et al. 2009) Calendar ages were calculated for up to 3 standard deviations as shown in Table 6-4. Their likelihood distribution and position on the radiocarbon curve is shown in Figure 6-2.

**Table 6-4 The calibration of Karamik core radiocarbon dates (IntCal09)**

| Name | Depth (m) | Uncalibrated (BP) | Calibrated ( Cal yr BP) | | | | | |
|---|---|---|---|---|---|---|---|---|
| Karamik | | | 68.2% (1σ) | | 95.4%(2σ) | | 99.7% (3σ) | |
| | | | From | to | From | to | from | to |
| R_Date GrN-6881 | 5.75-6.05 | 20130 ± 290 | 24409 | 23713 | 24837 | 23366 | 25131 | 22683 |
| R_Date GrN-6880 | 3.75-4.05 | 6520 ± 70 | 7504 | 7330 | 7567 | 7307 | 7592 | 7251 |

| Name | Depth (m) | Uncalibrated (BP) | Calibrated ( Cal yr BC/AD) | | | | | |
|---|---|---|---|---|---|---|---|---|
| Karamik | | | 68.2% (1σ) | | 95.4%(2σ) | | 99.7% (3σ) | |
| | | | From | to | From | to | from | to |
| R_Date GrN-6881 | 5.75-6.05 | 20130 ± 290 | -22460 | -21764 | -22888 | -21417 | -23182 | -20734 |
| R_Date GrN-6880 | 3.75-4.05 | 6520 ± 70 | -5555 | -5381 | -5618 | -5358 | -5643 | -5302 |

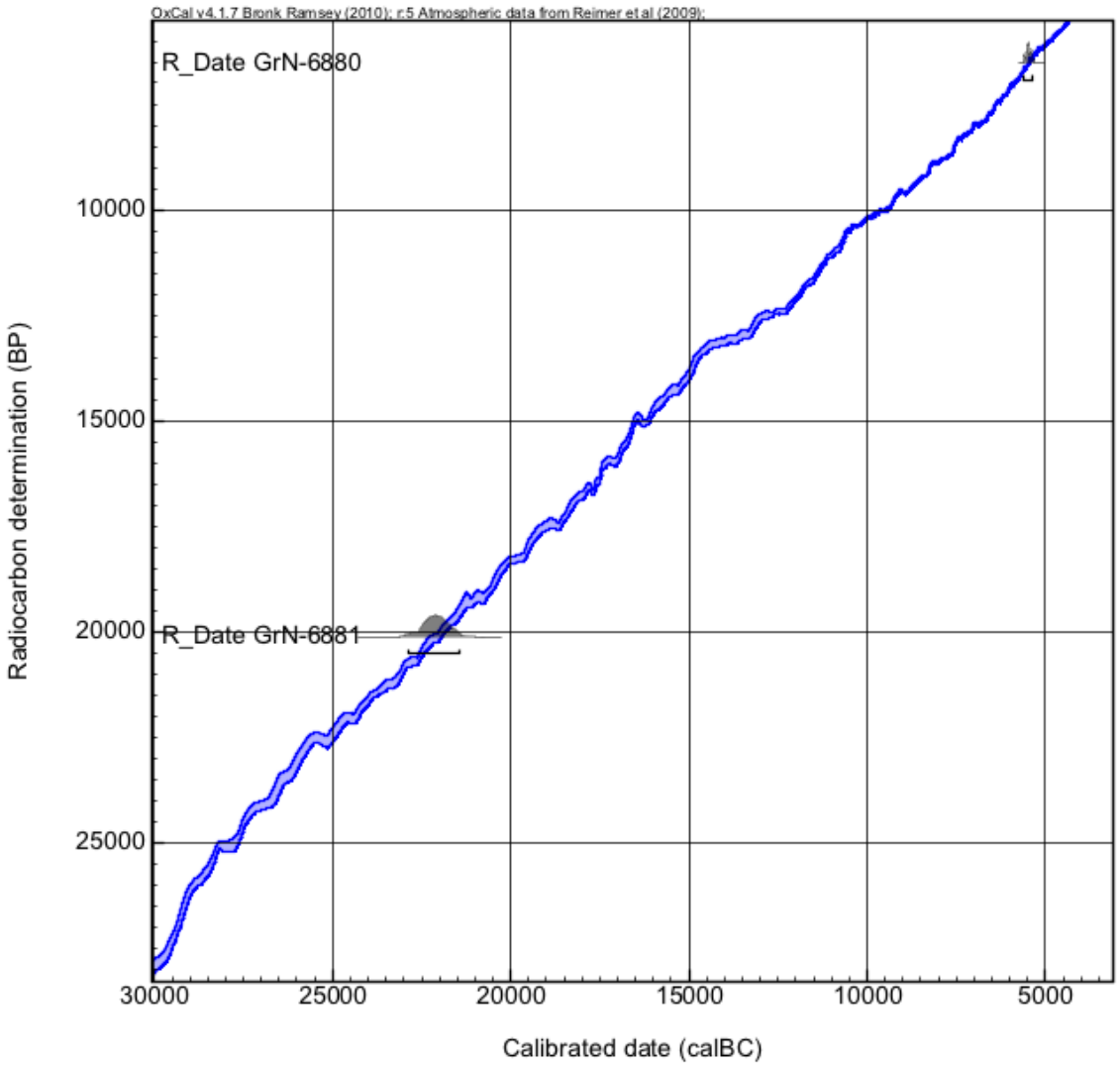


**Figure 6-2 The position of likelihood distributions for two calibrated radiocarbon ages on the radiocarbon curve IntCal09 (Reimer, Baillie et al. 2009)**

These dates were then modelled considering their depth and order, to calculate age likelihood distributions for discrete points in the sediment sequences that are undated (in this case, local pollen assemblage zone boundaries). Lithology was noted throughout the core; this consists largely of clay (suggesting marsh or lake conditions for most of the core); and were not considered distinct enough to enter into Bayesian modelling. A condition was also entered into the model that required all sediment deposition to have occurred before 1975 in order to constrain the top of the core.

Three different types of age-depth model were calculated in order to assess model-data fit under different assumptions. The first model tested was the Uniform Deposition (U_sequence) model. This reflects a known order between events, an unknown deposition rate, but the assumption of the rate being uniform between events. This model leads to poor agreement (A=0%) and an inability to resolve the order of boundaries, suggesting that the assumption of uniform deposition between events is not appropriate.

The second model tested was a simple sequence model (Sequence), which assumes a particular order of events, but does not assume a uniform deposition. This created a model with A=99.8, however the age precision of the top and bottom of the core was seen to be very low.

The third model tested was a Poisson-process deposition model. The k parameter is seen to be a trade off between flexibility of sediment accumulation rate changes (lower k values), and the narrowing date ranges (higher k values). Models with medium to high k values (i.e., above 1) did not resolve (as shown in Table 6-5). As sediment is predominantly clay, it is likely that a small K value of 0.01 or lower is probably most appropriate, and indeed following model runs with different K values, smaller values do lead to better model match with data. As the K value decreased (approaching a Simple Sequence model), the probability density distribution of potential ages also increased. This led to the core top and bottom having increasing uncertainty and decreased precision; in this case in the order of thousands of years. Trading off model fit with precision, and also considering particle size, the Poisson process model with K=0.01 was chosen as the best model to take forward.

**Table 6-5 Output Bayesian modelling using different deposition models, Karamik core.**

| Model | U_seq | K = 4 (4 cm) | K=1 (1 cm) | K=0.1 (1 mm) | K=0.01 (0.1mm) | Sequence (cal BP) |
|---|---|---|---|---|---|---|
| **A_model** | 0 | 0 | 3.8 | 96.3 | 99.8 | 99.9 |
| **A_overall** | 0 | 0 | 3.8 | 96.3 | 99.8 | 99.9 |
| **Age range, Cal yr BP (2σ)** | | | | | | |
| **End of core (top)** | - | - | 95 to -27 | 936 to -27 | 5159 to -27 | 7447 to -23 |
| **GrN-6883** | - | - | 7667 to 7456 | 7570 to 7320 | 7568 to 7307 | 7568 to 7305 |
| **GrN-6881** | - | - | 22858 to 22261 | 24668 to 23018 | 24807 to 23332 | 24817 to 23345 |
| **Start of core (bottom)** | - | - | 23366 to 22560 | 25581 to 23177 | 27677 to 22966 | 52538 to 23550 |

Figure 6-3 shows the probability distribution of calibrated ages in comparison to the modelled ages, including an agreement measure between model and empirical data. Agreement between the model and empirical data is high.

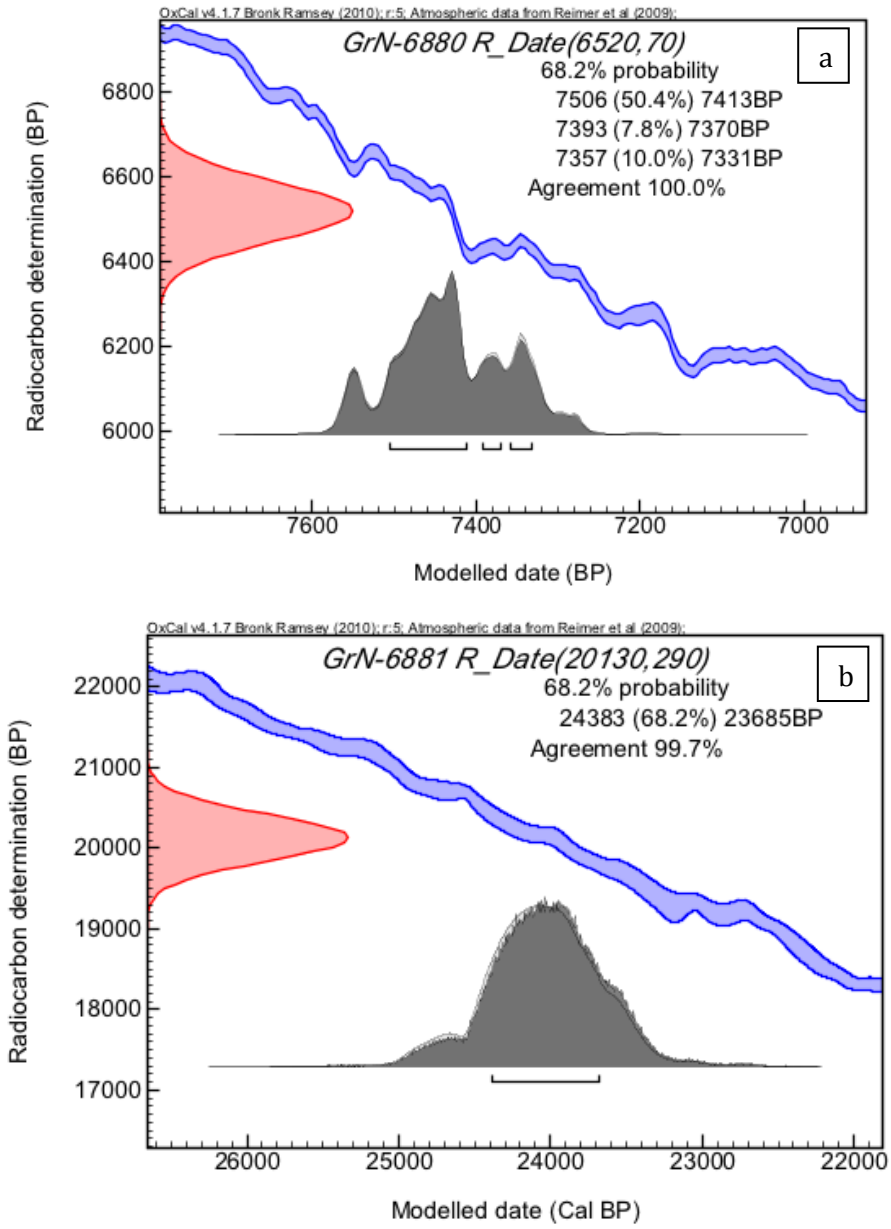


**Figure 6-3 Calibrated and modelled radiocarbon dates (a) GrN-6880 and (b) GrN-6881 under a Poisson sequence model and a K value of 0.01. The model agreement with data is 99.7%, and brackets show the 68.2% age probability.**

Using the chosen Poisson-distribution model, the depths of the local pollen assemblage zone boundaries were incorporated into the model as ages to be calculated. The results (shown in Table 6-6) produce an overall accuracy for this model of 99.9%, with no large outliers.

It is recommended to use at least 2 standard deviations to robustly represent the hpd. The 68.2% hpd for the beginning of each pollen zone was therefore taken forward as shown in Table 6-7, and a concurrent archaeological period was estimated based on periods used by Vermoere

(Vermoere). The uncertainty of pollen zone boundaries was calculated to allow a comparison of the tightness of pollen zone chronology both temporally through the core, and spatially when compared with other cores.

**Table 6-6 Modelled Karamik core radiocarbon dates and vegetation zones**

| Name | Modelled (Cal BP) | | | | | | Modelled (BC/AD) | | | | | | Indices | |
|---|---|---|---|---|---|---|---|---|---|---|---|---|---|---|
| Karamik | 68.2% (1σ) | | 95.4%(2σ) | | 99.7% (3σ) | | 68.2% (1σ) | | 95.4%(2σ) | | 99.7% (3σ) | | Amodel = 99.9 | Aoverall = 99.9 |
| P_sequence (0.1) | from | to | from | to | from | to | from | to | from | to | from | to | A | Convergence |
| Bottom | 24527 | 23552 | 27363 | 22969 | 38487 | 22568 | -22578 | -21603 | -25414 | -21020 | -36538 | -20619 | | 97.1 |
| GrN 6881 | 24383 | 23685 | 24805 | 23333 | 25087 | 22672 | -22434 | -21736 | -22856 | -21384 | -23138 | -20723 | 99.7 | 98.6 |
| Zone 1/2 boundary | 24598 | 21453 | 24944 | 13658 | 25077 | 8797 | -22649 | -19504 | -22995 | -11709 | -23128 | -6848 | | 99.2 |
| Zone 2/3 boundary | 23917 | 13024 | 24028 | 8122 | 24417 | 7408 | -21968 | -11075 | -22079 | -6173 | -22468 | 5459 | | 99.1 |
| Zone 3/4 boundary | 15406 | 7340 | 21763 | 7324 | 23845 | 7286 | -13457 | -5391 | -19814 | -5375 | -21896 | -5337 | | 98.9 |
| Zone 4/5 boundary | 8614 | 7270 | 16062 | 7250 | 21783 | 7175 | -6665 | -5321 | -14113 | -5301 | -19834 | -5226 | | 98.4 |
| GrN 6880 | 7506 | 7331 | 7568 | 7307 | 7592 | 7253 | -5557 | -5382 | -5619 | -5358 | -5643 | -5304 | 100 | 99.9 |
| Zone 5/6 boundary | 7552 | 6779 | 7573 | 5001 | 7607 | 2951 | -5603 | -4830 | -5624 | -3052 | -5658 | -1002 | | 99.8 |
| Zone 6/7 boundary | 4977 | 1449 | 6253 | 412 | 6977 | 53 | -3028 | 501 | -4304 | -1538 | -5028 | 1897 | | 99.8 |
| Top | 2839 | -24 | 5192 | -27 | 6462 | -27 | -890 | 1974 | -3243 | 1978 | -4513 | 1978 | | 99.9 |
| Core taken | -24 | -25 | -24 | -25 | -24 | -25 | 1974 | 1975 | 1974 | 1975 | 1974 | 1975 | 100 | 100 |

**Table 6-7 The 68.2% Highest Posterior Density (hpd) for the beginning each pollen zone in the Karamik core, and the estimated archaeological period that the pollen zone covers.**

| Zone | Highest Posterior Density beginning (68.2%) | | Estimated archaeological period that pollen zone begins | Uncertainty (years) |
|---|---|---|---|---|
| | Cal yr BP | Cal BC / AD | | |
| Zone 1 | 24527 to 23552 | -22578 to -21603 | Palaeolithic | 975 |
| Zone 2 | 24598 to 21453 | -22649 to -19504 | Palaeolithic | 3145 |
| Zone 3 | 23917 to 13024 | -21968 to -11075 | Epipalaeolithic | 10893 |
| Zone 4 | 15406 to 7340 | -13457 to -5391 | Epipalaeolithic or Neolithic | 8066 |
| Zone 5 | 8614 to 7270 | -6665 to -5321 | Aceramic or Ceramic Neolithic | 1344 |
| Zone 6 | 7552 to 6779 | -5603 to -4830 | Ceramic Neolithic or Early Chalcolithic | 773 |
| Zone 7 | 4977 to 1449 | -3028 to 501 | Between Late Chalcolithic and Roman | 3528 |
| Top | 2839 to -24 | -890 to 1974 | Between Phrygian period and Turkish republic | 2863 |

Table 6-7 shows that most pollen boundaries have high chronological uncertainty. However, by examining the final age-depth model as shown in Figure 6-4 it is possible to see that this uncertainty is not equally distributed. As noted by van Zeist et al. (van Zeist, Woldring et al.) deposition on average is slower between the bottom of the core (~24 Cal ka yr BP) and radiocarbon date GrN-6880 (~7 Cal ka yr BP), than between GrN-6880 and the top of the core. By using Bayesian modelling, it is possible to state that between GrN-6881 and GrN-6880 chronological uncertainty is likely to be relatively high, and increases away from chronological control. This suggests that the linear interpolation model implemented by van Zeist et al. (1975) may not have been an appropriate model for this section of the core. Furthermore, although the

hpd around this area is quite wide, the distribution is not normal, and zone boundaries are either negatively or positively skewed.

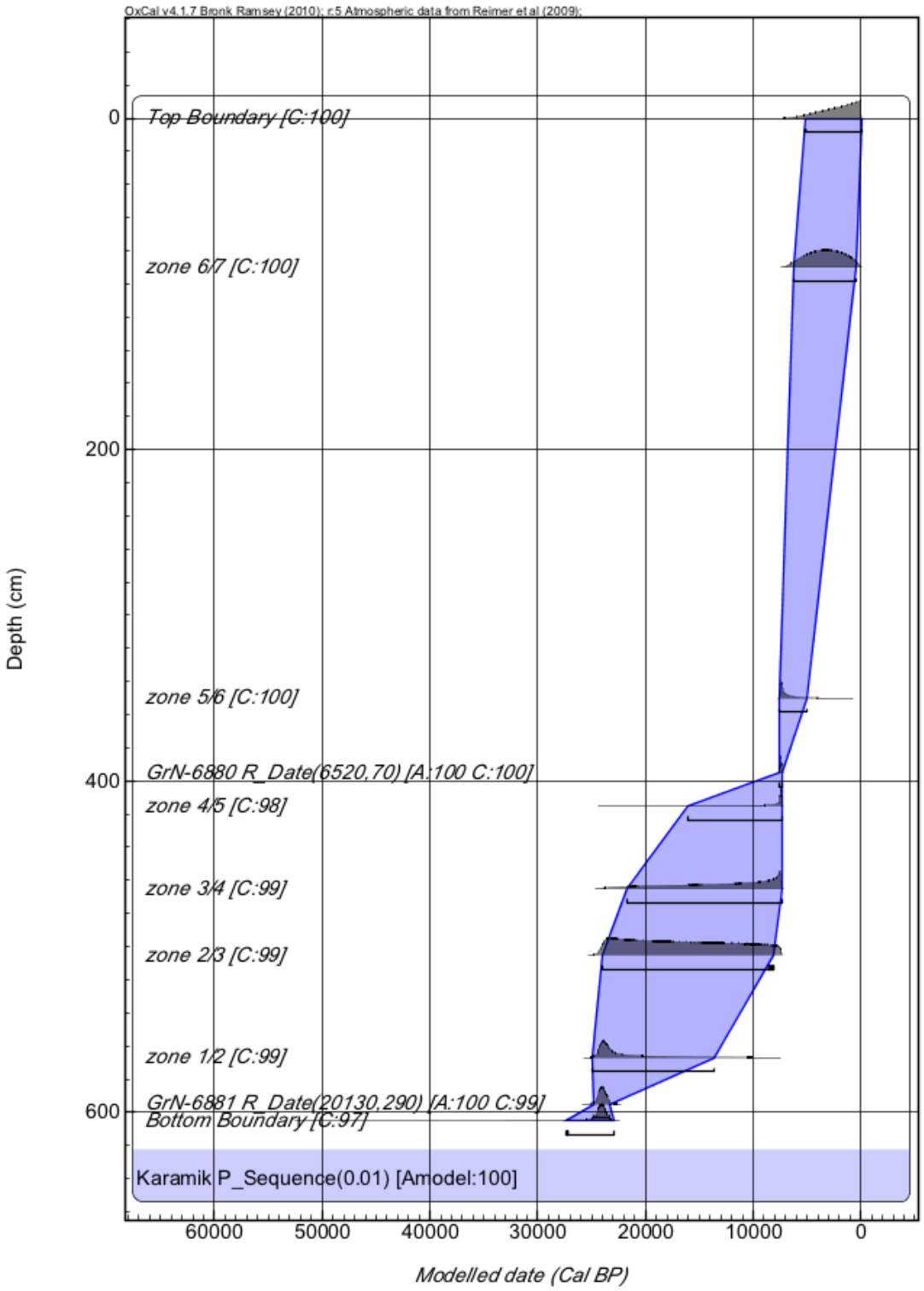


**Figure 6-4 Karamik age-depth model using a Poisson deposition model (K=0.01). The chart shows the highest posterior density (hpd) distributions for the top and bottom boundaries of the core, 2 radiocarbon dates, and key pollen zone boundaries (i.e. zone 1/2 is the hpd for the boundary between pollen zone 1 and 2). Convergence integrals (C) are shown for each age. The brackets and the blue boundary shows the 95.4% probability range.**

Taking into account the shape of the hpd, it is possible to link the peak probability of the beginning and end of each zone, therefore estimating the most likely span for pollen zones through time, whilst still representing uncertainty, as shown in Figure 6-5.

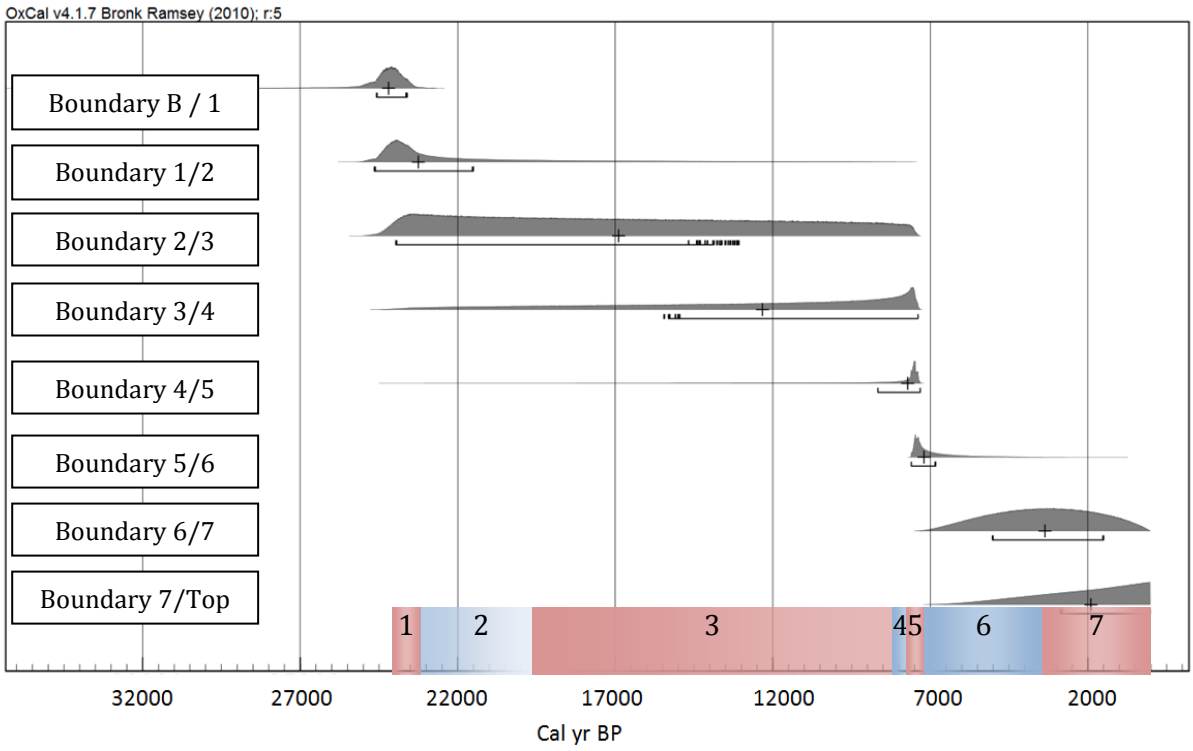


**Figure 6-5 Prior distributions for Karamik pollen boundaries, showing 68.2% brackets and crosses for median age. Pollen zones with colour gradients show the most likely pollen zone positions, whilst representing uncertainty.**

Zones 2 and 3 take up a relatively small amount of depth (62 and 40 cm respectively), but are likely to have been laid down over a long period of time (median likelihood of 6359 and 4566 years respectively) suggesting a low SAR of around 0.1 mm $yr^{-1}$. By zone 5 it is estimated to increase to around 0.3 mm $yr^{-1}$, and by zones 6 and 7, it is estimated at ~0.5 mm $yr^{-1}$. This is in comparison to a SAR of between 0.4 and 1.4 mm $yr^{-1}$ for Golhisar during the late Holocene.

## 6.8 REVISED POLLEN ZONE CHRONOLOGY

Bayesian modelling as described above was carried out for all suitable pollen cores from the southwest of Turkey. Once undertaken, each modelled pollen zone sequence was mapped onto a timeline showing key events as shown in Figure 6-6. Again uncertainty is represented using gradation of colour. This allowed an overview of pollen core synchronisation to be displayed, and the position of the tephra layer is also indicated where found within the core. Following modelling tephra layers are found to be synchronised, which provides an independent check that Bayesian modelling has provided appropriate age-depth models.

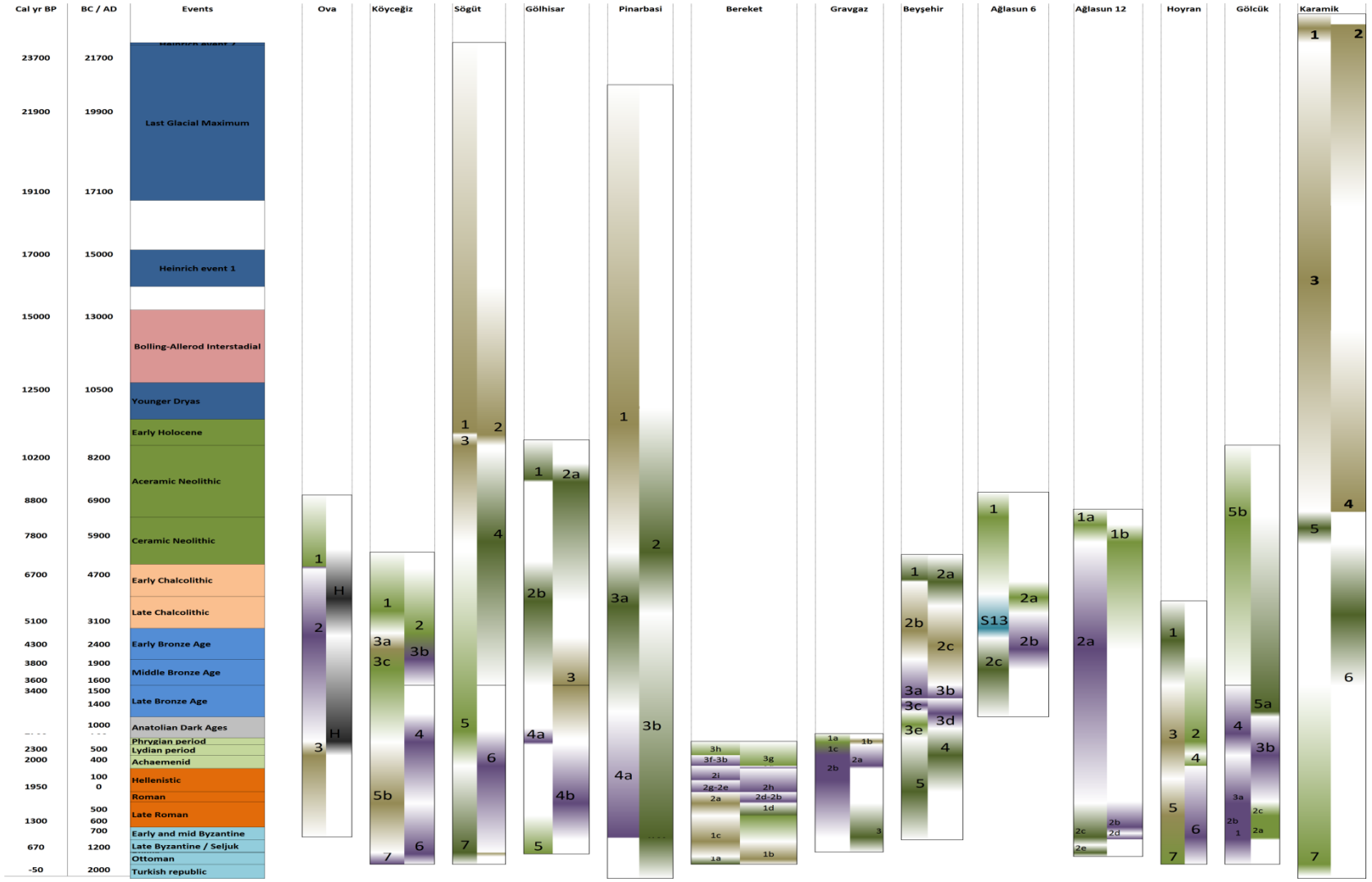


**Figure 6-6 Overview diagram of pollen sequence synchronicity across southwest Turkey. Each pollen zone is shaded to represent the chronological uncertainty attached to the zone. The core is split into two columns to allow the representation of uncertainty of conjoining pollen zones, so that zone 1 is on the left, 2 on the right, 3 on the left and so on. Brown shading represents a generally steppic pollen signature. Dark green represents predominantly coniferous, light green represents predominantly deciduous. Purple represents zones where there is a high percentage of pollen from potentially cultivated species. Double black lines indicate the position of the Santorini tephra layer, showing independent synchronisation across the cores, and helping to validate the approach**

## 6.9 CALCULATION OF POLLEN PERCENTAGES TO COMPARE WITH MODEL OUTPUT

Palynologists use the term *pollen influx* to refer to the amount of pollen grains per year that are deposited in a core sequence from one species. This pollen influx goes towards the pollen sum, which is defined as the basic sum that includes all pollen types on which their percentages can be calculated. It is valid to take a subset of pollen influx to only investigate a forest pollen sum, or only cultivated species (Vermoere 2002) and this technique will be employed below.

In order to quantitatively compare simulated pollen with the analytical pollen zones modelled in the above analysis, the species in the pollen sum of analytical pollen data needs to match the species in the modelled output. Simulated pollen is composed of a subset of species chosen at the beginning of the thesis. To match this, only the pollen influx from those species that are modelled is taken forward for analysis..

Pollen data for most pollen sequences was available from the European Pollen Database (www.europeanpollendatabase.net). Pollen data from Ağlasun and Gravgaz was received from Marleen Vermoere (pers. comms.), and data from Gölhisar was received from Warren Eastwood (pers. comms.). Pollen evidence recorded in pollen diagrams are generally converted from raw pollen counts to relative pollen percentage values. In order to compare simulated pollen with analytical pollen, both datasets were converted to relative pollen percentage.

### 6.9.1 Dissimilarity measures

Once percentages are calculated and compared, an overall quantitative measure of their similarity is required. This is done using a dissimilarity measure. Chord dissimilarity (square chord distance) measures have been used successfully in palaeoecological studies to compare fossil pollen with modern pollen measures (Overpeck, Webb et al. 1985; Baker, Van Nest et al. 1989). They are recommended by Overpeck et al. (1985) in preference to correlation

coefficients or principal components analysis, as correlation coefficients are not appropriate for samples (only variables) and principal components analysis does not examine the 'degree of analogy' between the two sample sets. A range of difference dissimilarity measures exist. Unweighted dissimilarity measures are most heavily influenced by pollen types with large ranges such as *Pinus*, whereas rare pollen types have little influence on the values of these coefficients (Prentice 1980; Overpeck, Webb et al. 1985). Weighted measures such as the Canberra metric and Squared Standardised Euclidean distance give more emphasis to rarer pollen types, but this can lead to noisy results governed by pollen taxa with little magnitude. The signal to noise measures of squared chord distance, the information statistic and squared $X^2$ coefficient are a compromise that aim to identify the signal component of the differences at the expense of the noise component, which is related to random effects (Prentice 1980; Overpeck, Webb et al. 1985). The squared chord distance in particular has been successfully used as the most reliable equation of choice in previous palaeoenvironmental research (Andersen 1970; Overpeck, Webb et al. 1985; Prell 1985). Due to the mixture of common and rare pollen types in the output, and previous research recommendations, this statistic was chosen as the best dissimilarity measure for analysis, and is shown in Equation 6-1.

$$d_{ij} = \sum_k \left( {P_{ik}}^{1/2} - {P_{jk}}^{1/2} \right)^2$$

**Equation 6-1**

The nearer a dissimilarity measure is to zero, the closer the match between two samples. This immediately creates a comparable measure between model runs and between zones. The precise reason for the high or low measure can then be identified by assessing single species correlation with simple difference measures.

In terms of whether the dissimilarity measure is 'good' 'moderate' or 'poor' there are only critical values available based on comparing northern European forest types against each other. For example, Overpeck et al. (1985) used modern northern hemispheric pollen data, and

showed that dissimilarity increased between pollen core sites as latitude and longitude increased, and forest type changed. The critical cutoff value for squared-chord distance here was calculated as 0.12 to 0.15. Oswald et al. (2003) used Receiver Operator Curves (ROC) to identify the critical value using modern analogue data where the dissimilarity measures within and between forest types overlapped slightly, and found the cutoff was 0.075. Maher (2000) suggests 0.2 as the analogue / no analogue cutoff, and 0.7 as the cutoff for very different conditions.

In essence the aim of the measure in this research study is not to compare modern pollen with fossil pollen, but to compare simulated pollen based on a particular climatic scenario, and fossil pollen signatures. This has an impact on potential critical values, primarily because previous critical values are dependent on the similarity of species within and between a particular northern European forest type, which may not be relevant in Mediterranean semi-arid environments.

Furthermore, the vegetation modelled in this thesis is not formed into biome classes, it instead shows dynamic changes across the landscape, which is different from previous studies. Thirdly, previous models are restricted in that they need to compare fossil pollen with a modern analogue. By simulating pollen other combinations of vegetation distribution can be explored that do not have a modern analogue.

It is for these reasons that a constant cutoff value is too premature to be defined for this model. The comparison between model and actual pollen will therefore only be a relative measure, which does not overstate model accuracy. If a relatively low dissimilarity measure is encountered when predicting palaeovegetation, this is taken to mean a closer match between the vegetation output driven by a particular climate scenario, and fossil pollen data. If the dissimilarity measure is relatively large, there are much larger discrepancies between model output and fossil pollen, which means that, accepting the assumptions below, the climate scenario is less probable than those with a lower dissimilarity measure.

It is however very important to note that there is the potential that similarity, instead of being due to a good match with climate, may be due to either equifinality (another climatic scenario that is not modelled giving the same pollen assemblage), or due to inaccurate model parameters such as pollen productivity estimates. There must also be the allowance made for pollen loadings based on pollen counts to be approximations of the true population. Chapter 10 discusses the future work that could be done to further validate the modelling approach. An overview of the process described here is shown in Figure 6-7, and an example of the output is shown in Table 6-8.

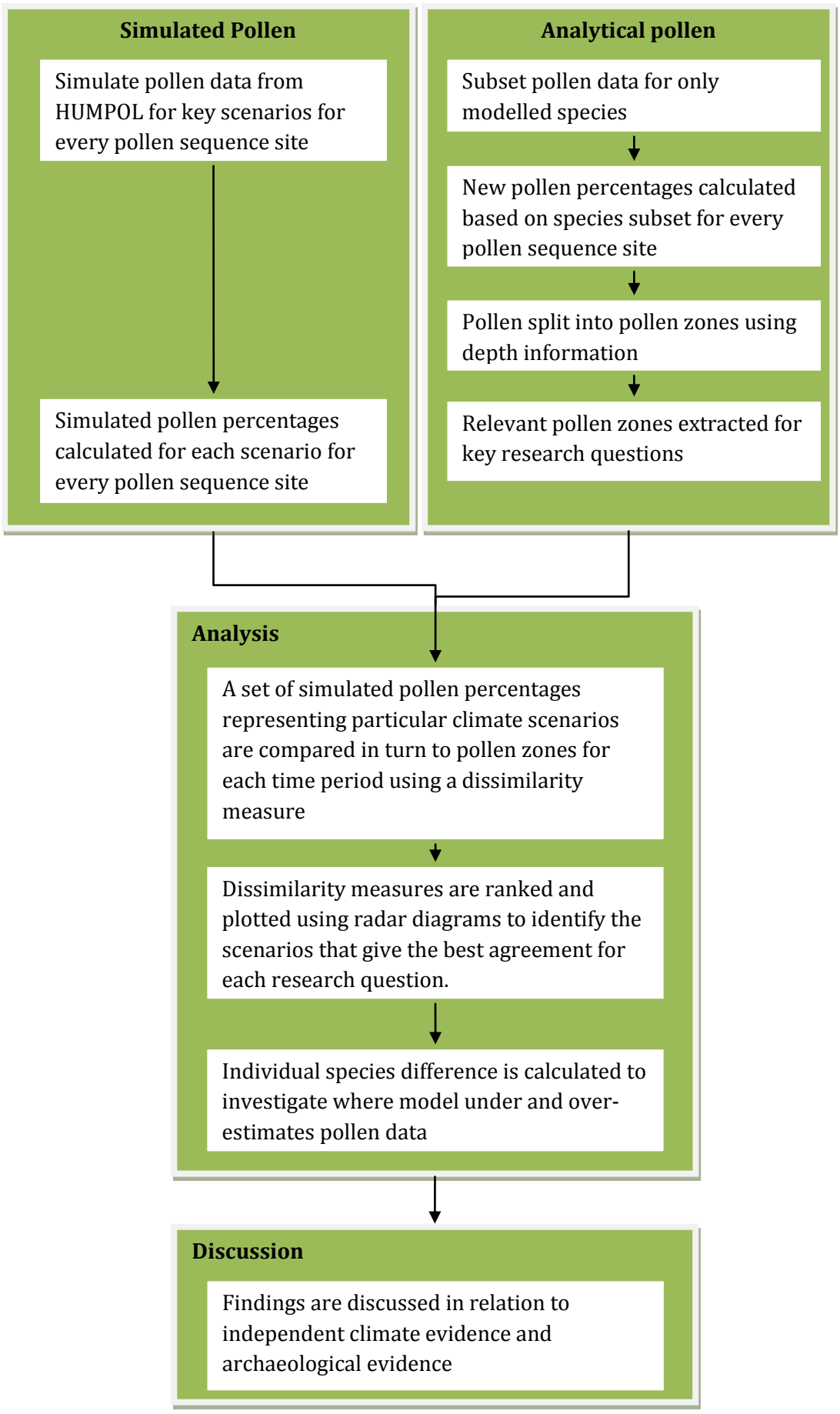


**Figure 6-7 Overview of comparison procedure**

**Table 6-8 Example pollen zone from Koycegiz, with pollen sum, calculated percentage, and comparison to simulated pollen percentages under a scenario of modern climate. Similarity between model and data in this instance is relatively low.**

| Koycegiz zone 3a (555 cm depth) | Pollen sum | % Analytical pollen | % Simulated pollen (modern scenario) | Over/under estimation of model |
|---|---|---|---|---|
| Abies | 12 | 0.14 | 0.01 | -0.14 |
| Alnus | 3 | 0.71 | 0.00 | -0.71 |
| Artemisia | 3 | 13.05 | 4.74 | -8.31 |
| Betula | 0 | 0.00 | 0.01 | 0.01 |
| Carpinus | 0 | 0.28 | 42.32 | 42.04 |
| Castanea | 0 | 0.00 | 0.03 | 0.03 |
| Cedrus | 20 | 2.13 | 0.44 | -1.69 |
| Cerealia | 5 | 1.70 | 1.33 | -0.37 |
| Quercus | 18 | 28.37 | 38.67 | 10.30 |
| Corylus | 0 | 0.00 | 0.00 | 0.00 |
| Fagus | 0 | 0.00 | 0.16 | 0.16 |
| Fraxinus | 0 | 0.00 | 0.00 | 0.00 |
| Juglans | 0 | 0.00 | 0.00 | 0.00 |
| Juniperus | 0 | 0.14 | 0.00 | -0.14 |
| Olea | 0 | 1.84 | 2.46 | 0.62 |
| Pinus | 55 | 39.01 | 2.38 | -36.63 |
| Picea | 0 | 0.00 | 0.00 | 0.00 |
| Plantago | 0 | 0.28 | 5.83 | 5.54 |
| Platanus | 0 | 0.00 | 0.45 | 0.45 |
| Poaceae | 30 | 11.35 | 1.13 | -10.22 |
| Populus | 0 | 0.00 | 0.01 | 0.01 |
| Tilia | 0 | 0.00 | 0.00 | 0.00 |
| Ulmus | 0 | 0.43 | 0.00 | -0.43 |
| Vitus | 0 | 0.57 | 0.03 | -0.54 |
| **Total Sum** | 146 | 100 | 100 | 0.00 |

## 6.10 VALIDATING MODEL-DATA COMPARISON USING MODERN POLLEN DATA

In order to validate the approach, pollen was simulated from the vegetation model under modern conditions. This was then compared to unpublished moss polster data collected as part of a parallel project advancing modern pollen monitoring in southwest Turkey (Eastwood, Fyfe et al. 2011).

In this study, moss polster data were collected in the form of a transect stretching from the Eu-Mediterranean into the Oro-Mediterranean region of southwest Turkey. Six moss polster samples representing the coastal regions to Elmalı (samples MS 10-1 to MS 10-6) were compared with simulated pollen loading for the Elmalı and Avlan pollen sites, while a further six moss polsters from various locations in the mountainous interior (MS 10-45 to MS 10-50) of southwest Turkey (between Keçiborlu-Sandıklı) were compared with simulated pollen loading for the Ağlasun and Bereket pollen sites. Only species within the vegetation model were compared and percentages were calculated based on this subset.

Validation against pollen evidence results show low dissimilarity using the chord dissimilarity measure for Ağlasun and Bereket compared to modern moss polster pollen data, with 0.16 and 0.12 respectively. The sites at Avlan and Elmali show slightly higher dissimilarity with 0.44 for Elmali and 0.40 for Avlan, due mainly to an underestimation in the bioclimatic model of the proportion of *Pinus*. However, both model-data comparisons generally show good fit between simulated pollen and analytical pollen, helping to validate the approach. It is hoped that as more data becomes available, further verification, validation and calibration of the model can occur as part of future work.

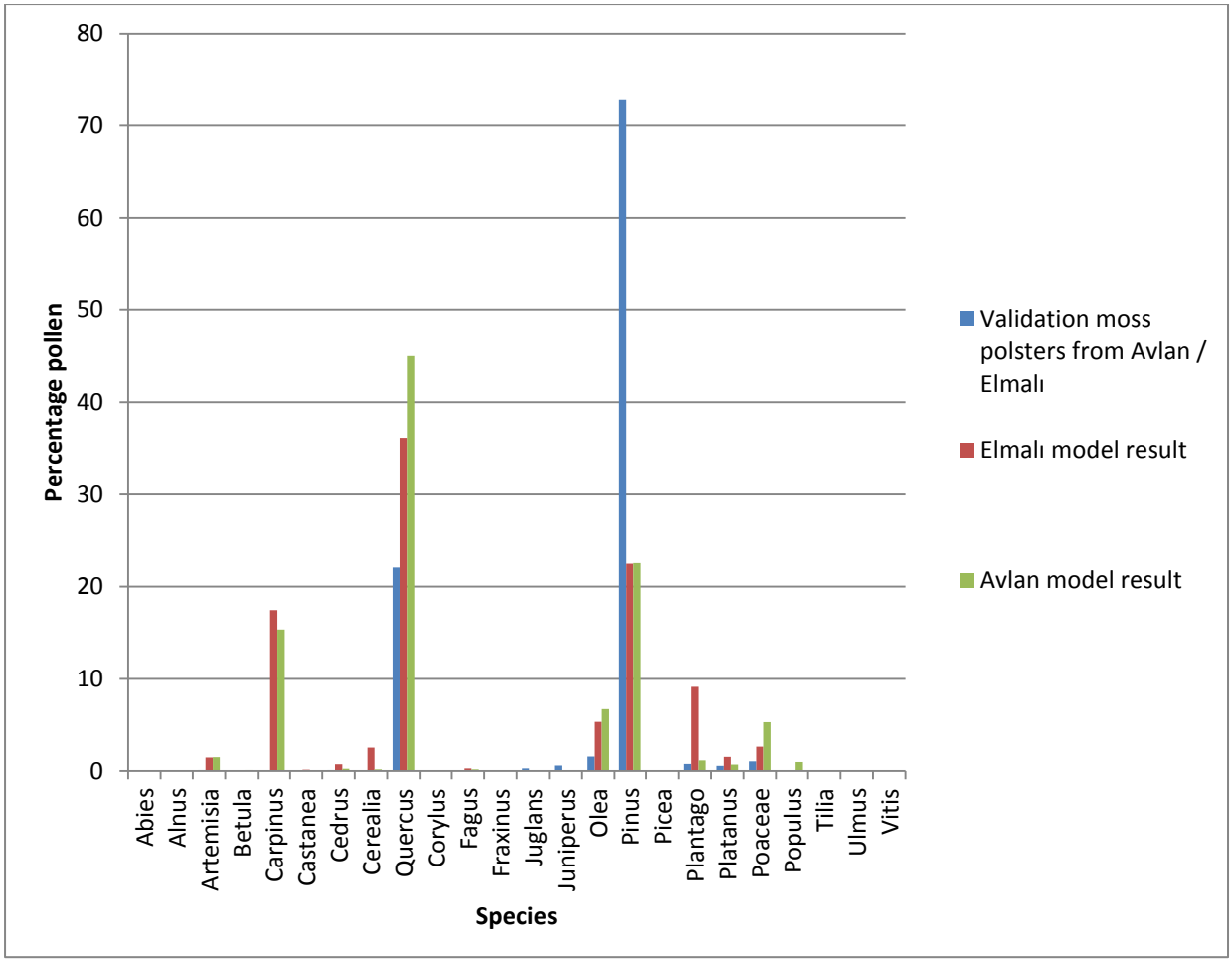


**Figure 6-8 Validation of model and data fit using modern moss polster data (Eastwood 2011, Unpublished data) and modern model output, Avlan and Elmali.**

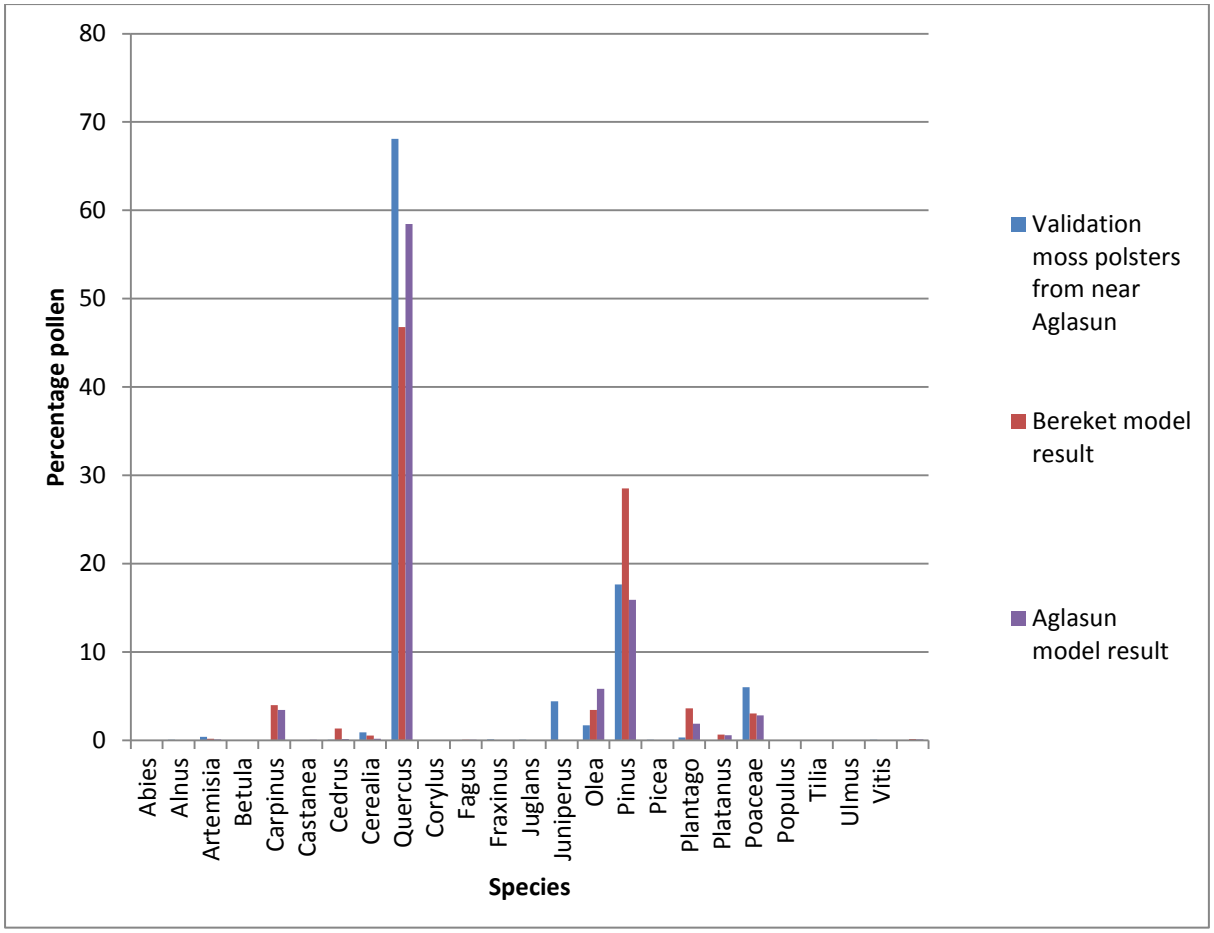


**Figure 6-9 Validation of model and data fit using modern moss polster data and modern model output, (Eastwood, Fyfe et al. 2011) at Ağlasun and Bereket.**

## 6.11 SUMMARY

Age-depth modelling of sediment cores and associated pollen sequences has traditionally involved the assumption of linear interpolation between dated sediments. The age of pollen zone boundaries that fall within two dated sediments are therefore not generally analysed in a quantitative manner for their potential age spread. Traditional age-depth modelling also makes it challenging to quantitatively compare different sediment sequences with each other.

Utilising Bayesian statistics this chapter aimed to provide probabilistic age spreads for pollen zone boundaries, and therefore a more accurate estimate of pollen zone chronologies, aiding the synchronisation of pollen zones across southwest Turkey, and a definition of relative age uncertainties, both spatially and temporally.

The chapter has summarised the methodology used to revise and tighten-up the chronologies of the pollen sequences, before identifying particular pollen zones that were likely to cover the key research questions posed in this thesis.

The chapter has also summarized the process whereby analytical pollen data is pre-processed and then compared with simulated pollen data to investigate correlation between model scenarios and palaeoecological evidence.

# 7 RESEARCH QUESTION 1: VEGETATION MODELLING FRAMEWORK RESULTS AND DISCUSSION

## 7.1 RESEARCH QUESTION

Can the model framework provide a coherent narrative to explain evidence of high lake stands concurrent with steppic vegetation signatures during the Late Glacial period (~24 to 19 Cal ka yr BP)?

## 7.2 RESEARCH QUESTION 1 HYPOTHESIS

In order to provide a testable basis for the model, a hypothesis was formed at the beginning of the thesis that may be supported or rejected by the model output. The working hypothesis is that low evaporation caused by low temperatures allowed lake levels to remain high, and allowed glacial expansion in southwest Turkey, but low precipitation restricted vegetation to steppic assemblages and scattered trees. This scenario can be tested with the vegetation model developed throughout this thesis, and forms the basis of a null and alternative hypothesis as shown in Table 7-1.

**Table 7-1 Model hypothesis for Research Question 1.**

| |
|---|
| **H1: Low precipitation and temperature during the Last Glacial Maximum provides a possible climatic basis for steppic species distribution, high lake levels and glacial advance.** |
| **H0: Low precipitation and temperature during the Last Glacial Maximum does not provide a possible climatic basis for steppic species distribution, high lake levels and glacial advance.** |

In engaging with this hypothesis, a number of modelling results will be discussed, including the chronological matching of pollen core zones to this particular period, the comparison of simulated pollen with analytical pollen under a range of climate scenarios, and GIS modelling of key climate-vegetation relationships. It is intended that the assimilation of these different components provides a rich picture on which to base discussion.

## 7.3 CHRONOLOGICAL MODELLING

This first model results section utilises chronological modelling undertaken in Chapter 6 to identify key pollen zones that cover the period of interest, and the certainty to which they can be assigned to the period.

The LGM covered the period between ~24 and 19 Cal ka yr BP. Bayesian modelling has shown that two sequences of analytical pollen data potentially cover this period; the interior site of Karamik and the high elevation site of Sögüt.

By using Bayesian statistics the estimated likelihood that particular pollen zones began or ended around this period can be assessed. Figure 7-1 highlights in blue the temporal extent of the Last Glacial Maximum period. This is overlain on the posterior estimates of the beginning and end of the pollen zones. Using the Oxcal 'Order' function it is possible to calculate that 60% of the highest probability density (hpd) function (the age distribution) for the beginning of Karamik zone 1 falls within the LGM period. Furthermore, 82% of the hpd for the beginning of Karamik zone 2 also falls within this period. The end of the zone is less well constrained; 65% of the hpd for the end of Karamik zone 2 is outside of the LGM. Considering this analysis, it is likely that most of Karamik zones 1 and 2 were deposited under the conditions of the Last Glacial Maximum.

Assessing now the high elevation site of Sögüt, 80% of the hpd of zone 1 falls outside the LGM, suggesting that the LGM period is likely to have finished before Sögüt zone 1 was deposited.

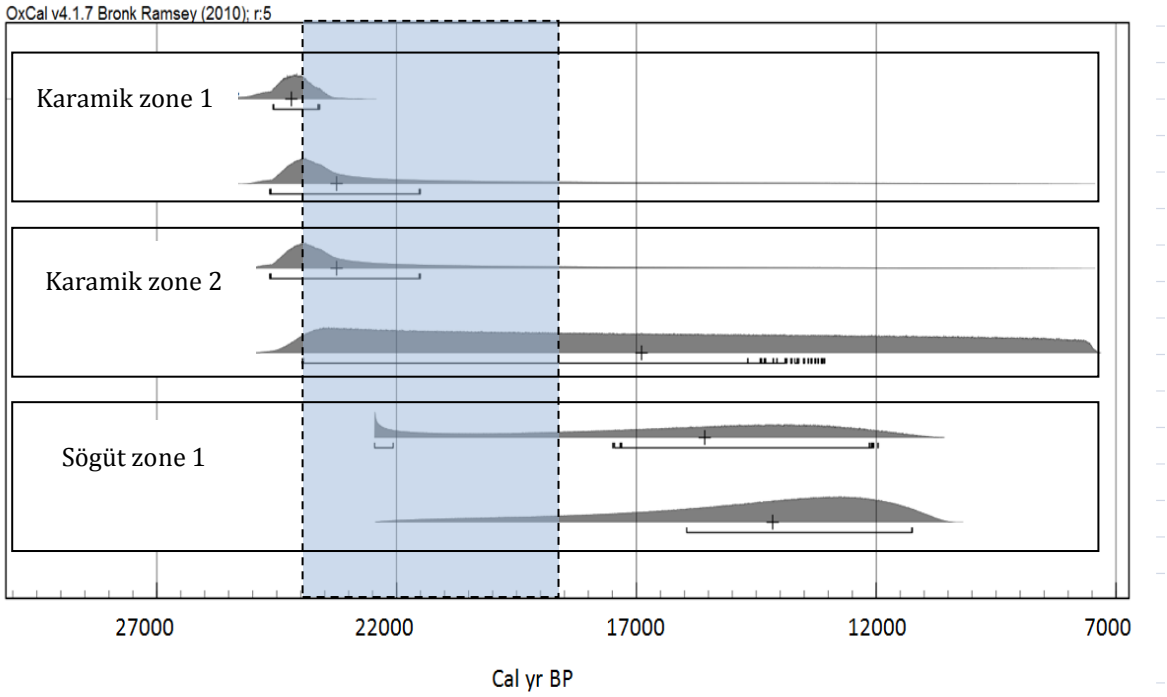


**Figure 7-1 Highest Probability Density plots for key pollen zone boundaries potentially covering the Last Glacial Maximum. The top distribution is the beginning of the zone and the bottom is the end of the zone for each zone. Also highlighted in blue is the temporal extent of the Last Glacial Maximum period. Brackets are the 68.2% highest probability density range.**

Pollen analytical data from Karamik zones 1 and 2 were taken forward for analysis, and their pollen assemblage is summarised in Table 7-2. This shows that pollen reflects a predominantly steppic assemblage during the LGM, comprising *Artemisia*, Chenopodiaceae, Gramineae and Cerealia-type pollen. Arboreal pollen comprised mainly deciduous *Quercus* and *Betula*, with coniferous *Cedrus*, *Pinus* and *Abies*.

Following calibration and analysis, these two pollen zones were compared to pollen simulations under different climatic conditions to assess linkages between climate and vegetation assemblage over this area during the Last Glacial Maximum.

**Table 7-2 Pollen zones correlated to the Last Glacial Maximum (24 to 19 Cal ka yr BP).**

| Site | Zone | Beginning (Cal yr BP 68.2%) | Ending (Cal yr BP 68.2%) | Pollen assemblage |
|---|---|---|---|---|
| Karamik | 1 | 24527 to 23552 | 24598 to 21453 | High NAP, low *Pinus*, high *Artemisia*, Gramineae, Cerealia-type |
| Karamik | 2 | 24598 to 21453 | 23917 to 13024 | High NAP, low *Pinus*, high *Artemisia*, Gramineae, Cerealia-type |

## 7.4 VEGETATION MODEL OUTPUT UNDER A VARIETY OF CLIMATE CONDITIONS: DISSIMILARITY WITH ANALYTICAL POLLEN EVIDENCE

Following the conversion of vegetation model output to simulated pollen, simulated pollen from 27 different model runs (under different climate scenarios) was compared with analytical pollen data for the Last Glacial Maximum period (Karamik zones 1 and 2). Each dissimilarity measure between model and data was given a rank, compared to every other model run. This provided an easily comparable metric of better and worse fitting models.

Figure 7-2 shows the result of this analysis summarised into the 11 main climate scenarios defined in Chapter 5. Scenarios with high ranks represent a better fit between model and data than those with low ranks. The figure shows that the highest similarity between model output and analytical pollen was found under climate scenarios with low winter precipitation and low average temperature. This is found when comparing to both pollen zones (1 and 2). This is an important step in supporting the hypothesis defined in section 7.2, as the modelling exercise demonstrates that pollen from the Karamik core is similar in composition to pollen simulated under a reduced precipitation and temperature regime.

This result can be elaborated by examining individual model runs within each scenario. Figure 7-3 displays the dissimilarity measure for each model run, Figure 7-4 displays rankings for each model run, and Table 7-3 lists the actual dissimilarity values.

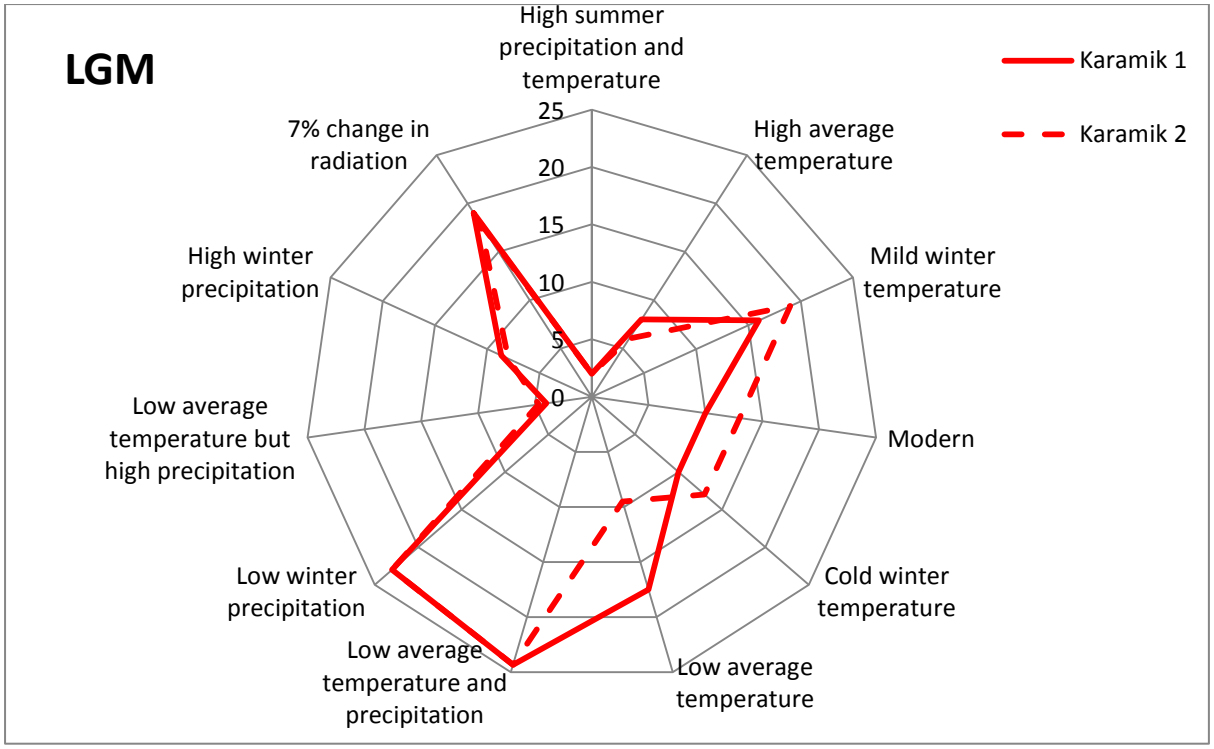


**Figure 7-2 Radar diagram showing the similarity between simulated pollen under a variety of climate scenarios and actual pollen from Karamik pollen zones 1 and 2. A high average rank suggests relatively high similarity between model runs and data under this category. The most similar climate scenario for these two zones is under conditions of low average temperatures and low precipitation.**

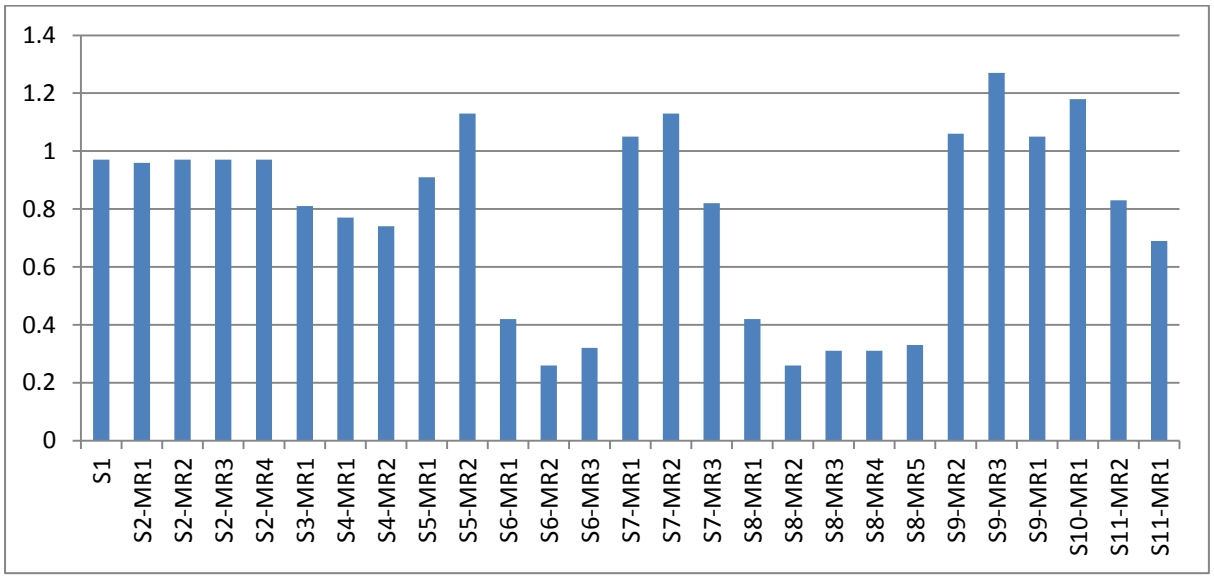


**Figure 7-3 Karamik (zones 1 and 2) dissimilarity for each model run.**

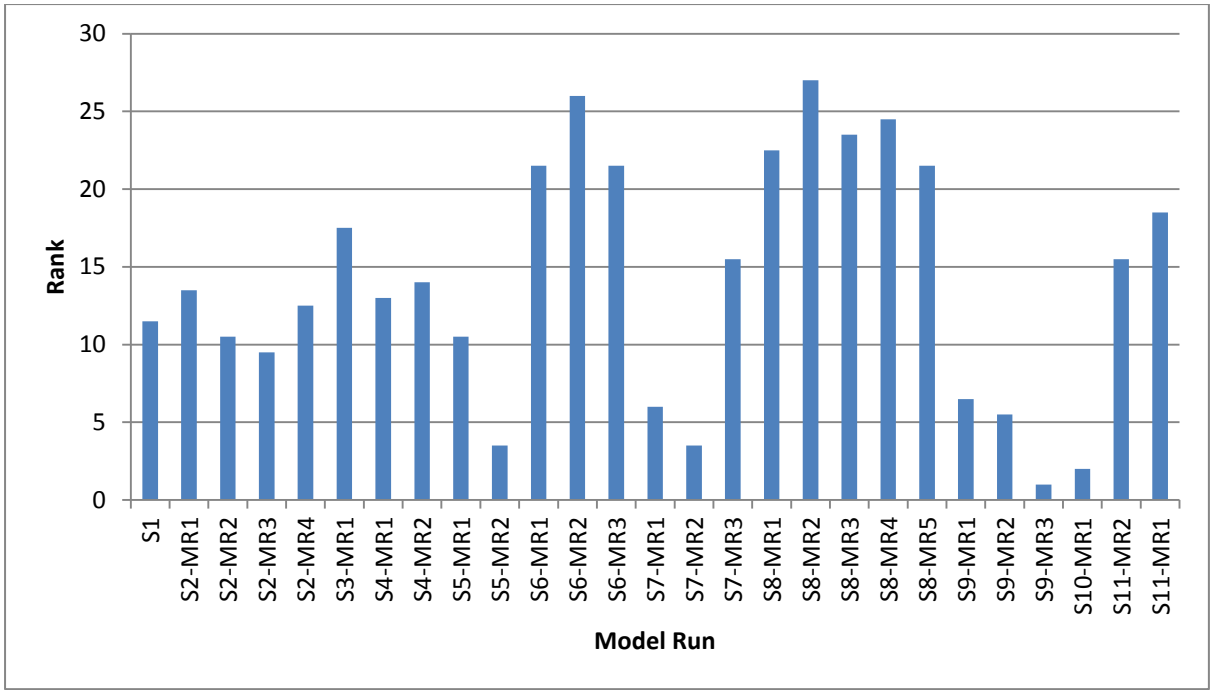


**Figure 7-4 Karamik (zones 1 and 2) model ranks for each model run. The highest rank is found under model runs with -200 mm winter precipitation, and low average temperatures (-8°C).**

Figure 7-3 shows that within certain scenarios (i.e. S2, winter temperature) there is not much variation in dissimilarity between the model runs. They all reflect a relatively poor similarity with pollen data. This leads to the average rank being low as shown in Figure 7-2. For other model runs (i.e. S7, an increase in precipitation) there is more variability in similarity between model runs and data. This leads to a moderate average, which again is reflected in Figure 7-2. Scenario S8 (low temperature and precipitation) shows high similarity under all model runs, hence the average rank for this scenario is high in Figure 7-2.

Figure 7-4 shows that the best similarity between simulated pollen data and pollen analytical data is found under model run S8-MR2, reflecting a winter precipitation departure of -200 mm from modern conditions, and an average temperature departure of -8°C. A relatively low

dissimilarity figure of 0.26 suggests a good fit between model and data, potentially suggesting a strong link between climate and vegetation during this period.

At this point it should however be highlighted that this modelling exercise only explores a small subset of possible climate scenarios. Furthermore, the accuracy and robustness of the model requires further testing before the accuracy of such ranges are given weight. It is therefore strongly advised that the absolute magnitude of climate change should not be taken as the actual situation without a great deal more analysis.

**Table 7-3 Chord dissimilarity measures for the Glacial period comparing simulated pollen from model runs with actual pollen evidence.**

| | **Dissimilarity** | | **Rank** | | |
|---|---|---|---|---|---|
| **Scenario** | KZ-1 | KZ-2 | KZ-1 | KZ-2 | Average Rank |
| S1 | 0.97 | 0.87 | 10 | 13 | 11.5 |
| S2-MR1 | 0.96 | 0.87 | 12 | 15 | 13.5 |
| S2-MR2 | 0.97 | 0.87 | 9 | 12 | 10.5 |
| S2-MR3 | 0.97 | 0.87 | 8 | 11 | 9.5 |
| S2-MR4 | 0.97 | 0.87 | 11 | 14 | 12.5 |
| S3-MR1 | 0.81 | 0.77 | 16 | 19 | 17.5 |
| S4-MR1 | 0.77 | 0.93 | 17 | 9 | 13 |
| S4-MR2 | 0.74 | 0.89 | 18 | 10 | 14 |
| S5-MR1 | 0.91 | 0.95 | 13 | 8 | 10.5 |
| S5-MR2 | 1.13 | 1.14 | 3 | 4 | 3.5 |
| S6-MR1 | 0.42 | 0.51 | 20 | 23 | 21.5 |
| S6-MR2 | 0.26 | 0.48 | 26 | 26 | 26 |
| S6-MR3 | 0.32 | 0.62 | 23 | 20 | 21.5 |
| S7-MR1 | 1.05 | 1.07 | 7 | 5 | 6 |
| S7-MR2 | 1.13 | 1.18 | 4 | 3 | 3.5 |
| S7-MR3 | 0.82 | 0.86 | 15 | 16 | 15.5 |
| S8-MR1 | 0.42 | 0.51 | 21 | 24 | 22.5 |
| S8-MR2 | 0.26 | 0.46 | 27 | 27 | 27 |
| S8-MR3 | 0.31 | 0.60 | 25 | 22 | 23.5 |
| S8-MR4 | 0.31 | 0.49 | 24 | 25 | 24.5 |
| S8-MR5 | 0.33 | 0.61 | 22 | 21 | 21.5 |
| S9-MR2 | 1.06 | 0.97 | 6 | 7 | 6.5 |
| S9-MR3 | 1.27 | 1.26 | 5 | 6 | 5.5 |
| S9-MR1 | 1.05 | 0.96 | 1 | 1 | 1 |
| S10-MR1 | 1.18 | 1.24 | 2 | 2 | 2 |
| S11-MR2 | 0.83 | 0.80 | 14 | 17 | 15.5 |
| S11-MR1 | 0.69 | 0.78 | 19 | 18 | 18.5 |

Nonetheless, comparison of simulated pollen with analytical pollen data has produced a relatively good fit between model and data under a climate scenario of significantly lower precipitation and average temperatures than modern conditions. This scenario was theorised from previous palaeoclimate literature, but has now been quantitatively modelled by comparing bioclimatic modelling output to pollen evidence. This result can be further investigated by examining the particular species characteristics that may have led to the assemblage at Karamik, and theorising what this type of climate scenario would potentially mean for the vegetation of the whole region.

## 7.5 CLIMATIC IMPLICATIONS FOR KEY SPECIES

### 7.5.1 Reduced temperature

A number of the species examined as part of this thesis have been found to be restricted by a decrease in temperature. Some are particulary intolerant of cold winter temperatures, whereas others require a certain level of spring temperatures to germinate and are also potentially frost intolerant. Some species also depend on the cumulative amount of growing degree days across the year to succesfully develop fruit. *Olea, Vitis, Pinus brutia, Platanus* and *Juniperus* are known to be particularly intolerant of low temperatures. Examining now the fossil pollen record of Karamik, *Olea* is not present, and *Vitis* and *Juniperus* pollen are also very low in pollen core records during the last glacial period, suggesting that cold temperatures are restricting vegetation at least around the locality of Karamik.

If reduced temperatures in the region of -8°C were actually experienced, it is interesting to see what effect this may have had on some of the more cold-intolerant species. *Olea* will be taken as a test case here. It is known from the literature that aerial damage to olive tree leaves can occur under a winter absolute minimum of as little as -7°C. Under modern conditions, the distribution of olive is likely to be restricted by this to the 'optimal conditions' zone as shown in Figure 7-5, essentially the lower elevation Eu-Mediterranean and intramontane valley sites of southwest Turkey. This area guarantees little risk of aerial damage or death due to cold winters.

In reality, the actual location of groves do not cover the whole of this optimal zone, as distribution also reflects other factors such as precipitation, soil type, topography and land use. This can be seen on the map as also plotted are actual olive grove locations. Having intersected the position of modern olive grove across the whole of Europe with elevation data, the median height that olive groves are planted under modern conditions is ~310 m, which is generally well into this optimal zone. However, some cultivated olive groves can be found at elevations up to 1500 m suggesting that some higher elevation sites can also prove favourable and have winter conditions warm enough for growth. Beyond this optimal zone are areas where olive

trees may endure significant damage if a bad winter hits. It is unlikely that farmers will choose to grow their cultivated crop here, however it is assumed that wild olives will grow in areas that are more marginal than those that are cultivated (i.e. at least up to the limit where they may be killed by a minimum winter temperature of around -10 to -12°C, or an average winter temperature around 1°C). Under a modern climate these olive trees may potentially grow up to a median height of 700 m (i.e. almost the full range of the Eu-Mediterranean zone), with certain favourable places potentially supporting *Olea* up to a maximum of 2000 m. This zone is also mapped in Figure 7-5 as the class 'may grow wild'. Of course, again this is only one factor, and other factors such as the amount of precipitation and quality of soils also has an important role to play.

If the optimal and sub optimal *Olea* zones are now modelled under a scenario of -8°C as is suggested by model output, then its geographical distribution is likely to be severely restricted. This is plotted in Figure 7-6. The maximum elevation that olive could safely grow under 'optimum conditions' is at a median elevation of ~134 m, up to a maximum of 1146 m at favourable locations. Under sub-optimum conditions, it may still grow to a median of 227 m, and an absolute maximum of 1529 m. Under such a scenario, the geographical distribution of optimal areas is likely to be restricted to very specific areas of the coast; around Manavgat, Antalya and Muğla, and further afield, the islands of Rhodes and Kos.

Of course, other factors such as precipitation also impact on the distribution of olive which the full regression model incorporates, but as a simple thought exercise this delineation is potentially useful for understanding the main restriction on olive during this period.

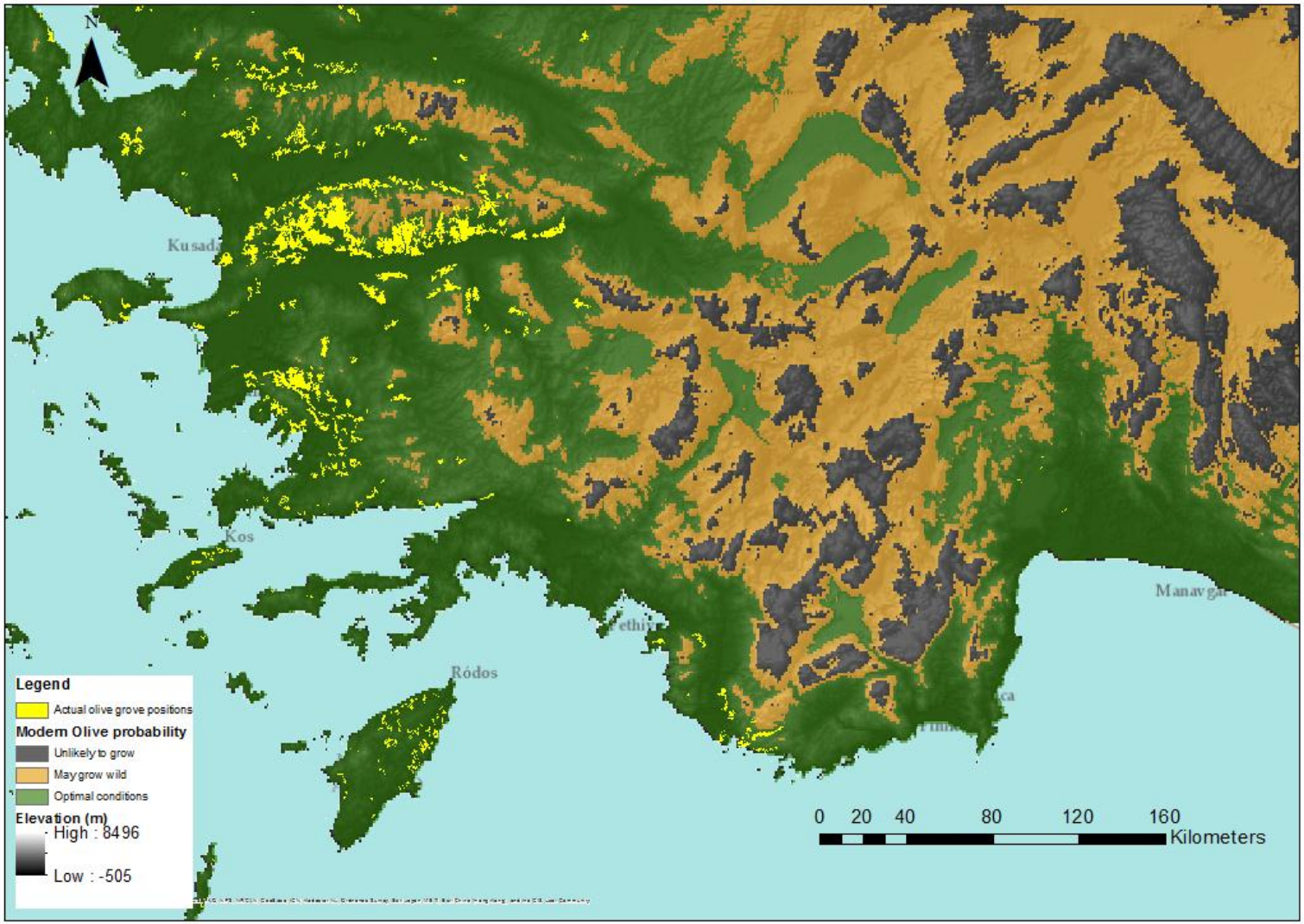


**Figure 7-5 Modern Olea potential, and actual olive grove positions.**

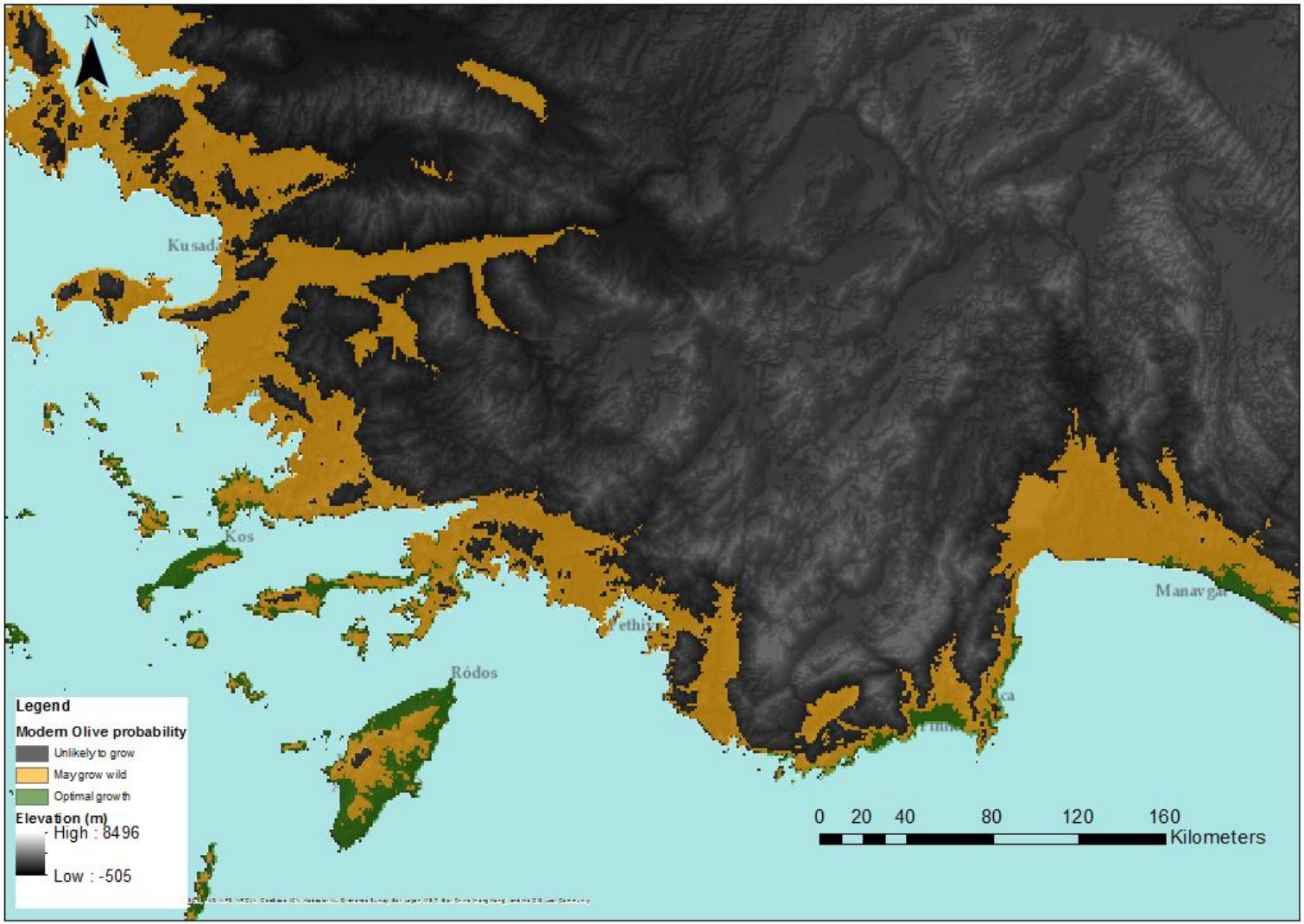


**Figure 7-6 Olea potential under a scenario of -8°C**

## 7.6 RESTRICTION IN PRECIPITATION: IMPLICATIONS FOR STEPPE

As well as arboreal species, the distribution of steppe is important in pollen zones from the glacial period. If a definition of montane steppe is accepted as areas with precipitation between 300 mm to 400 mm, and absolute steppe as areas with precipitation under 300 mm (e.g. Wang 1988), then modelling precipitation allows an estimation of areas of steppe under different precipitation conditions. Using these thresholds, a decrease in precipitation of 200 mm has been shown likely to increase montane and true steppe across southwest Turkey. As shown in Figure 7-7a and Figure 7-7b, steppe is likely to increase from the northeast interior of the country towards the southwest. The area around Karamik is likely to be one of the first areas where pollen analysis has been undertaken that would experience montane, and then true steppic conditions under a scenario of reduced precipitation.

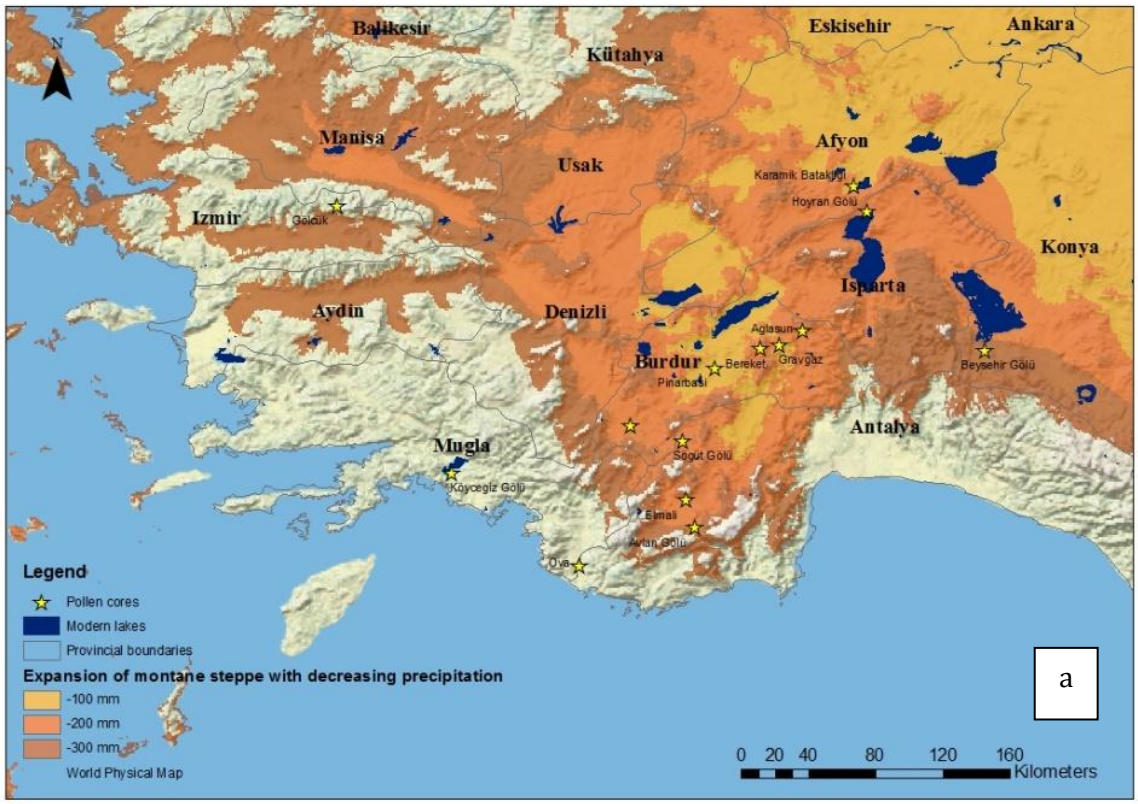


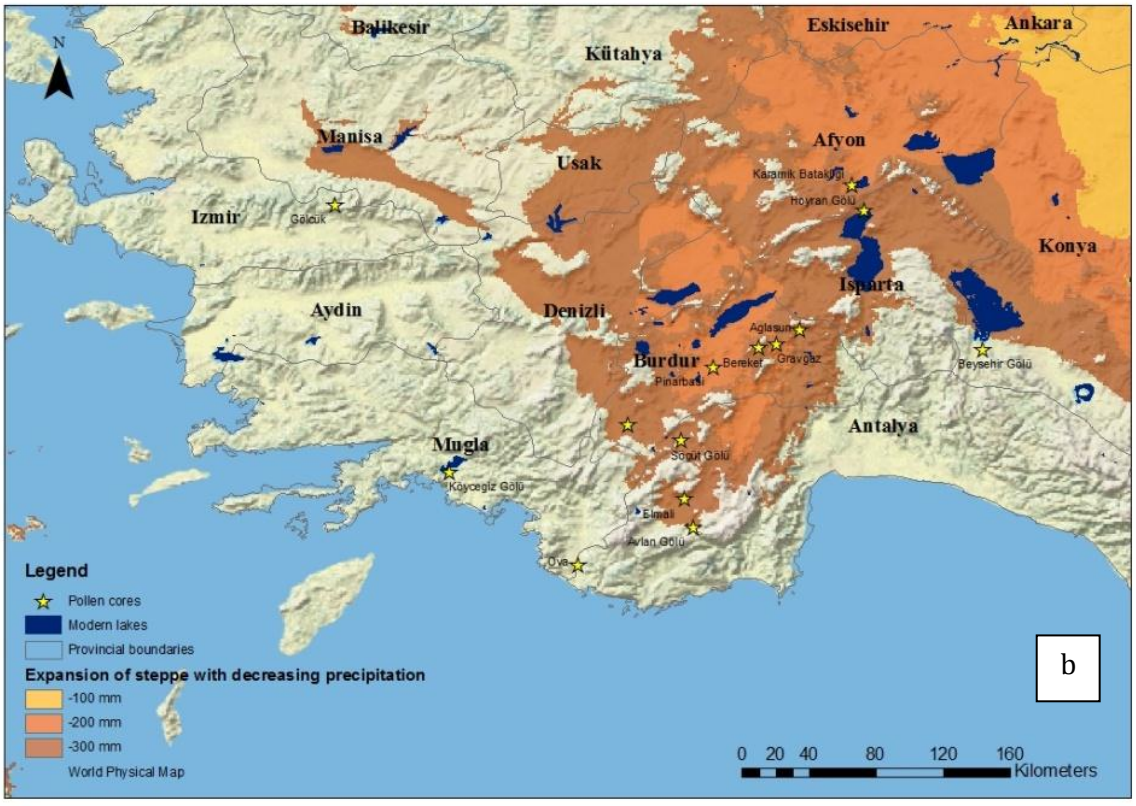


**Figure 7-7 (a) Expansion of montane steppe with decreasing precipitation (b) Expansion of true steppe with decreasing precipitation**

## 7.7 ARIDITY AND HUMIDITY DISTRIBUTION

A further analysis can be undertaken to further explore the potential implications of this balance of low precipitation and temperature across the region of southwest Turkey. Firstly, an aridity index is calculated based on the S8-MR2 model run. This is shown in Figure 7-8a. A second map is produced that estimates the region of southwest Turkey that would have a winter average temperature below freezing (Figure 7-8b).

The combination of these factors produces an intersected model as shown in Figure 7-8c, which suggests that aridity and humidity in the Eu-Mediterranean zone of southwest Turkey may have manifested themselves in different ways depending on altitude. In mountainous areas such as Mt Sandıras, humidity is likely to be coupled with below average freezing temperatures in winter, meaning that any precipitation that fell may be more likely to fall as snow, and may have potentially allowed a build-up in mountainous areas. It may be possible therefore, that this mechanism is consistent with glacial advance as reported by Sarikaya et al. (2008). At the same time, the lower elevation coastal regions around Antalya and Muğla would also have been humid, but (although cold) may not have had a winter with an average temperature below freezing, allowing more frost intolerant species to survive. On the west coast a more semi-arid and mild climate may have been more likely, with little precipitation, but average temperatures above freezing during winter.

In the interior low temperatures are likely to have hampered evaporation, providing a mechanism for lake levels to remain high. However precipitation would also be low, hampering available water for vegetation growth, leading to steppic formations. In contrast, local high elevation areas may have attracted orographic rainfall and snowfall when moisture was available, providing melt-water and runoff into rivers and lakes, and areas where cold tolerant species could grow.

Utilising climate and vegetation modelling, and comparing model output to pollen and palaeoclimatological data, this study therefore provides a model for steppic vegetation and aridity alongside high lake levels, glacial expansion and glacial refugia. In light of this modelling, it would be particularly interesting to test these modelled refugia areas using standard palaeoecological techniques once suitable coring sites can be found, although it is acknowledged that this hypothesis would also need to be tested at a large number of potential palaeoecological sites; something that would be difficult for this region.

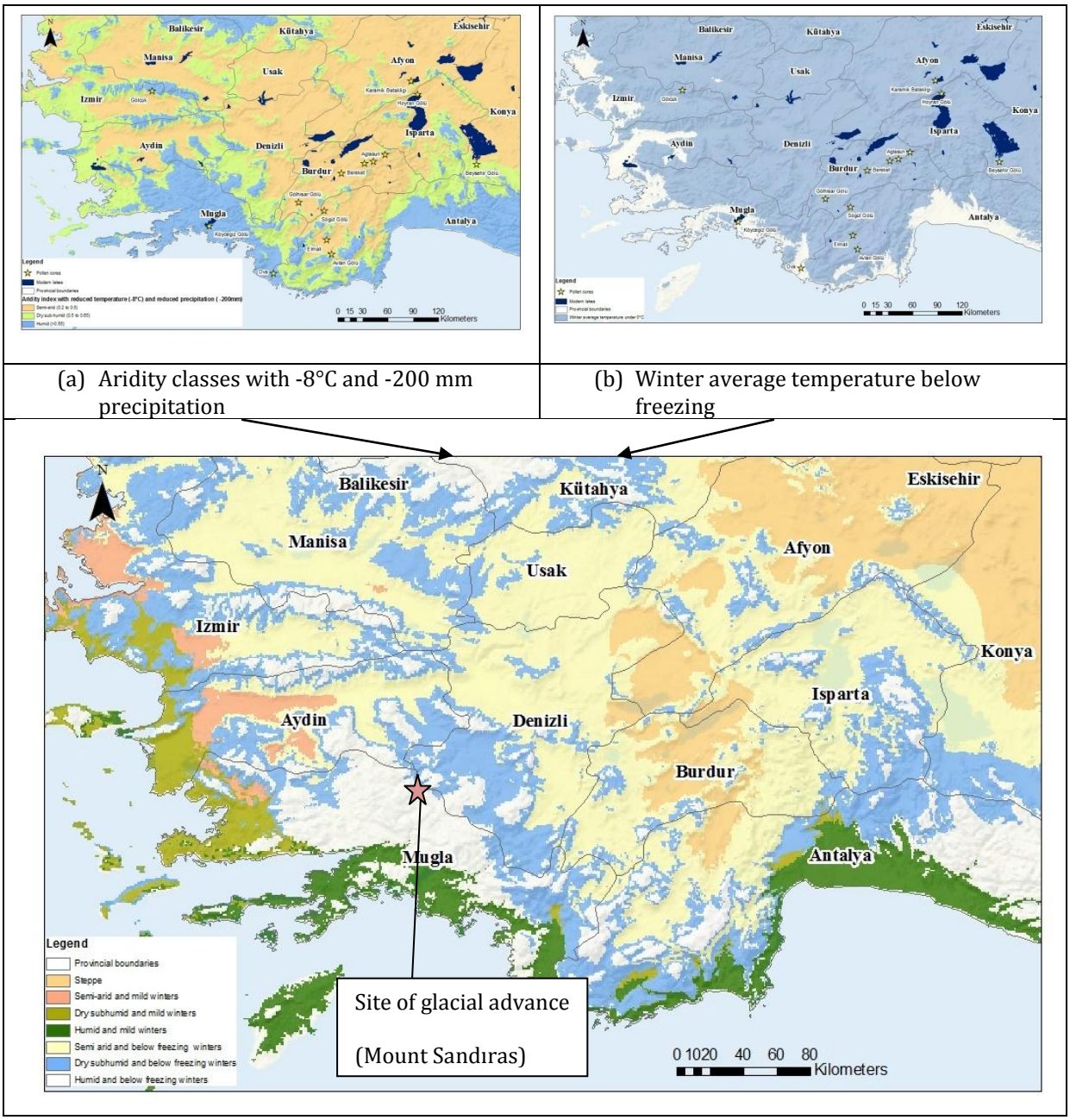


**Figure 7-8 (a) Aridity index classes under a regime of -8°C and -200 mm. (b) Areas where average winter temperature are likely to be below freezing with a -8°C drop in temperatures. (c) A combination of these two pieces of information. This suggests areas where a combination of humidity and cold winters could lead to snow build up, as well as potential refugia areas where mild winters and humid conditions are more likely. Also shown is the location of Mount Sandıras, where maximum glacial advance is found at ~20.4 ± 1.3 $^{10}$Be ka yr BP.**

## 7.8 POTENTIAL VEGETATION DISTRIBUTION; A REGIONAL PERSPECTIVE

**In addition to the overview of model outputs mapped in Chapter 6, this section will examine in more more detail the best fitting vegetation model output for the Last Glacial Maximum period. It enhances the enhances the model output by also mapping potential areas of persistent snow and ice cover, that may that may have implications for vegetation growth not modelled in the original output.**

Figure 7-9 identifies some of the main mountainous areas in the southwest that were modelled to consist of coniferous areas, and for ease of reference, Figure 7-10 provides an overview of relative species percentages (displayed first in chapter 5). This map will be elaborated on below by examining specific areas of interest, at a species level.

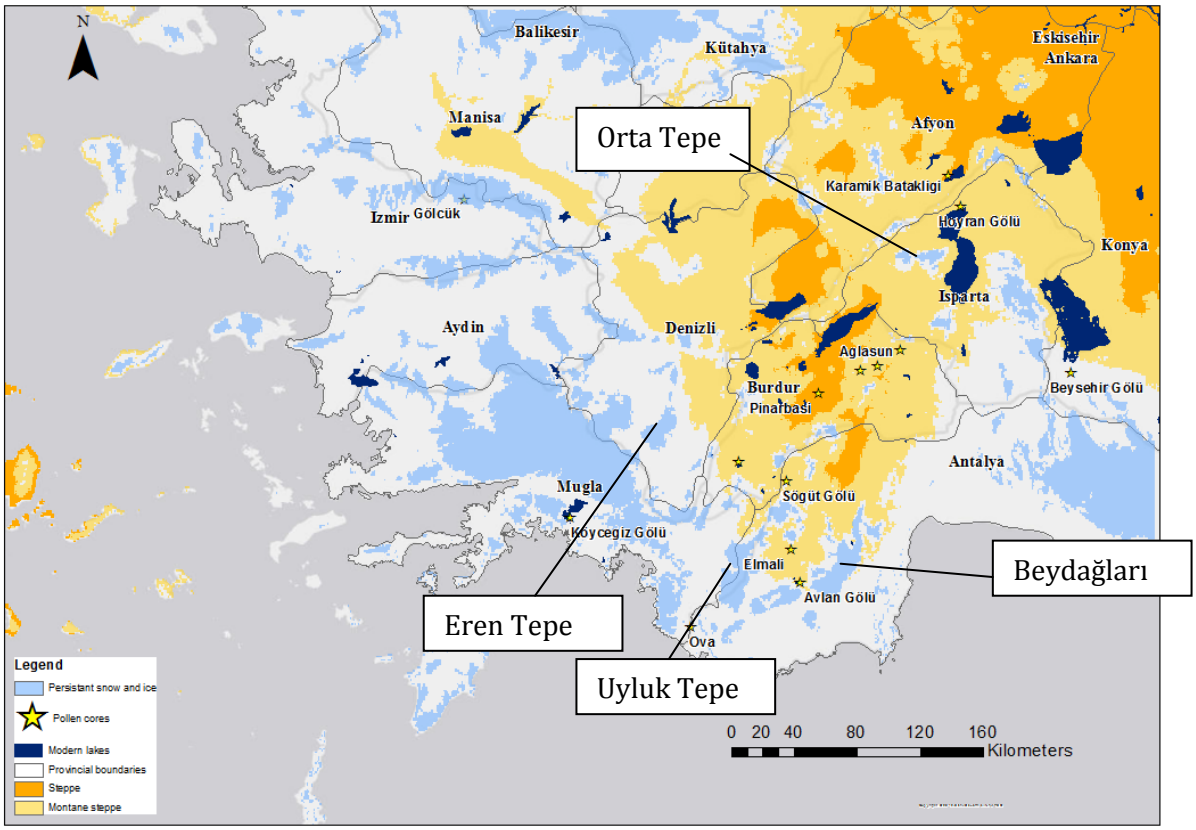


**Figure 7-9 Summary map identifying some of the mountainous regions where coniferous species are modelled to cluster under conditions of -8°C and -200 mm precipitation**

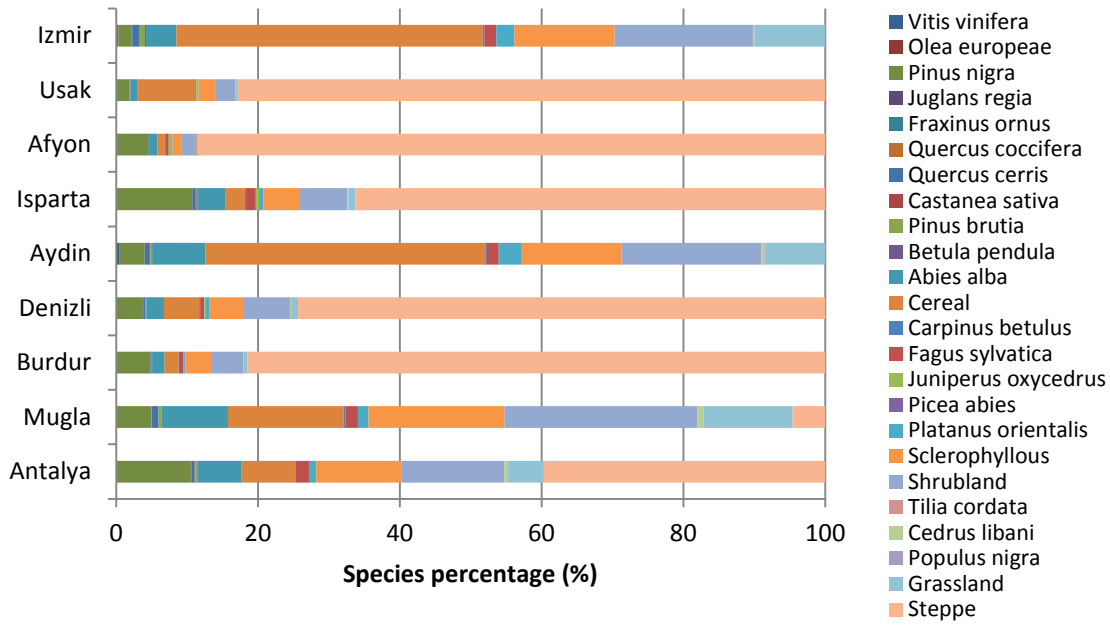


**Figure 7-10 Relative species percentages across southwest Turkey under conditions of -8°C and -200 mm precipitation**

The results of model run S8-MR2 suggest that the interior areas of southwest Turkey in the vicinity of Karamik (Figure 7-11) would have been more arid than today, and would comprise mostly of steppic species. Some high elevation peaks such as Orta Tepe would be likely to have persistent ice and snow. This matches well with direct interpretation of the pollen data undertaken by van Zeist et al. (1975). Model output also suggests that much of Isparta, around Ağlasun (Figure 7-12) and some parts of Antalya such as around Elmali (Figure 7-13) would comprise of steppe with patchy trees, mainly *Abies*, *Pinus nigra* and some *Juniperus*. In addition to this, higher elevation areas such as the Beydağları area of Antalya, Uyluk Tepe on the border between Muğla and Antalya, Eren Tepe in Denizli and Orta Dağ on the Denizli / Afyon border would be particularly at risk of persistent snow and ice cover. Any species growing here would need to be cold tolerant coniferous species such as *Pinus, Abies and Cedrus.* Finally, Figure 7-14 shows a map of the area of Manavgat, demonstrating that cold intolerant species such as Olea and Quercus coccifera are shown to be restricted to a strip along the coast.

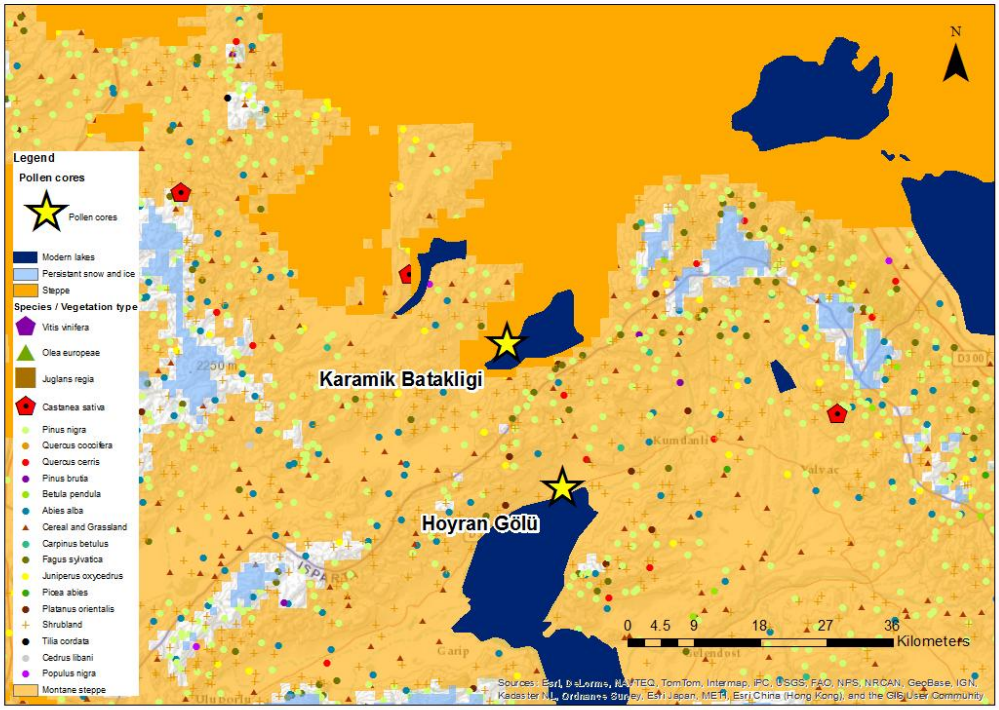


**Figure 7-11 Model output over Isparta and Afyon showing steppic conditions.**

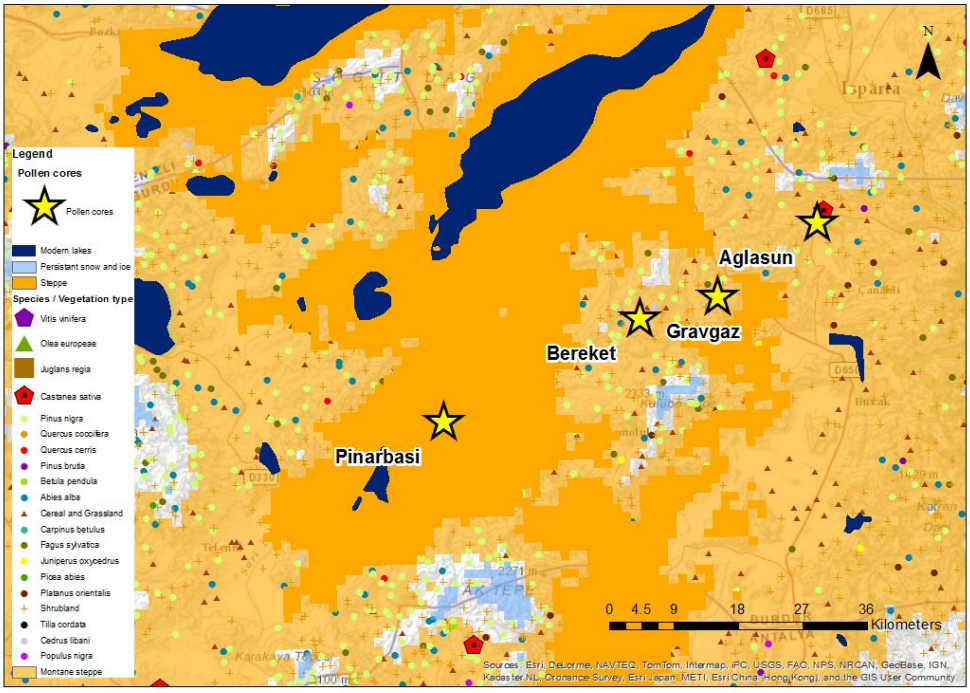


**Figure 7-12 Model output over Burdur and Denizli showing the predominance of steppe across this area.**

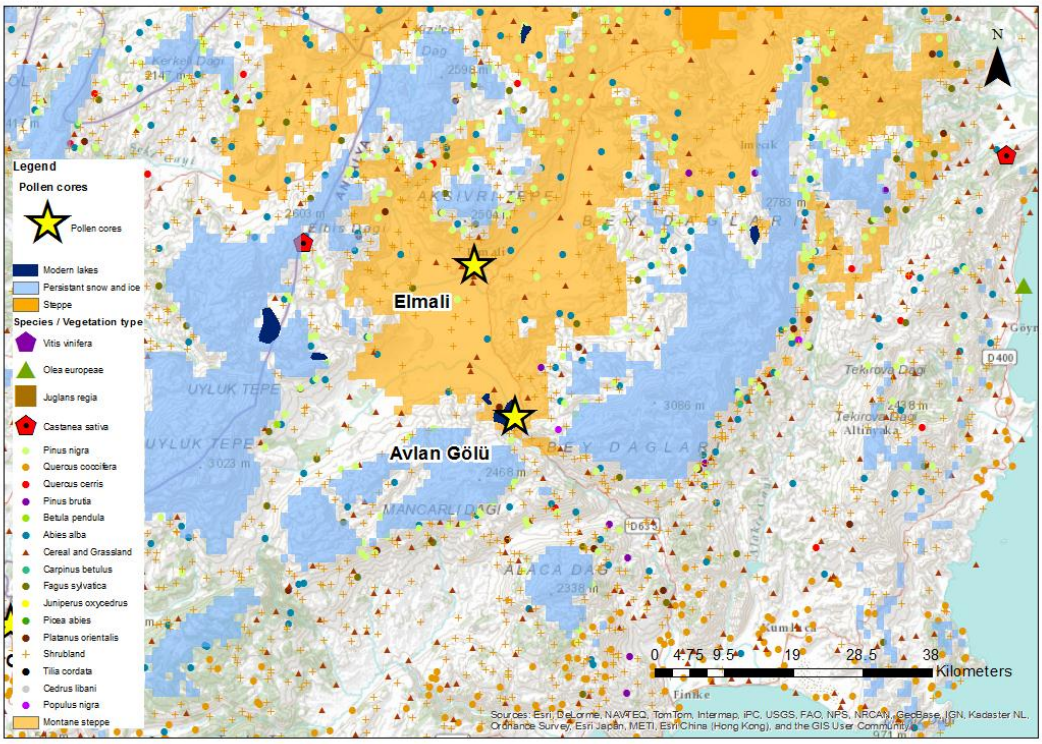


**Figure 7-13 Model output over Beydağları and Uyluk Tepe showing probable snow and ice cover at these high elevation (~3000 m) sites.**

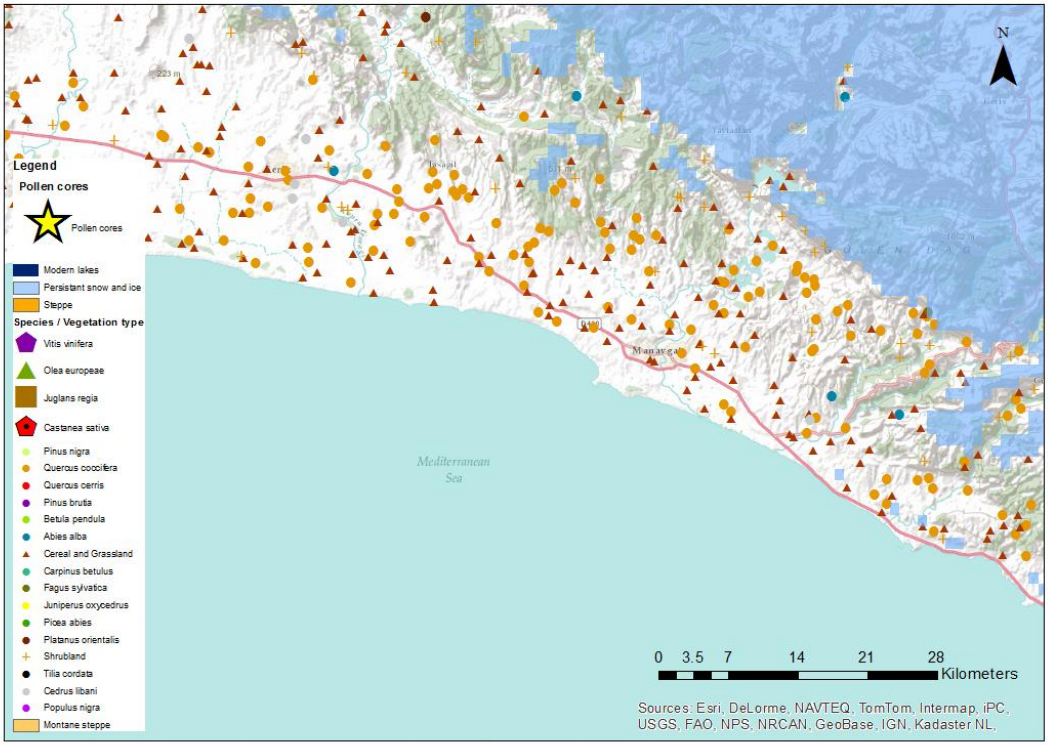


**Figure 7-14 Model output over Manavgat in Antalya showing high *Quercus coccifera* probability**

## 7.9 ELEVATION LIMITS UNDER REDUCED TEMPERATURE AND PRECIPITATION

As well as geographical distribution, the relative elevation spread of key species can be analysed under this climate scenario. Figure 7-17 shows the potential elevation spread of key species under modern climatic conditions. This can be compared to Figure 7-16 that shows the same species under S8-MR2. This plot shows that under such a reduction in precipitation and temperature, Mediterranean evergreen species such as *Quercus coccifera* and Olea europaea would be likely to be restricted to ~600 or 700 m in elevation. Steppe is to be found between 400 and 1500 m, and higher elevation deciduous and coniferous species such as *Pinus nigra* and *Abies alba* are modelled to be found up to 1700 m.

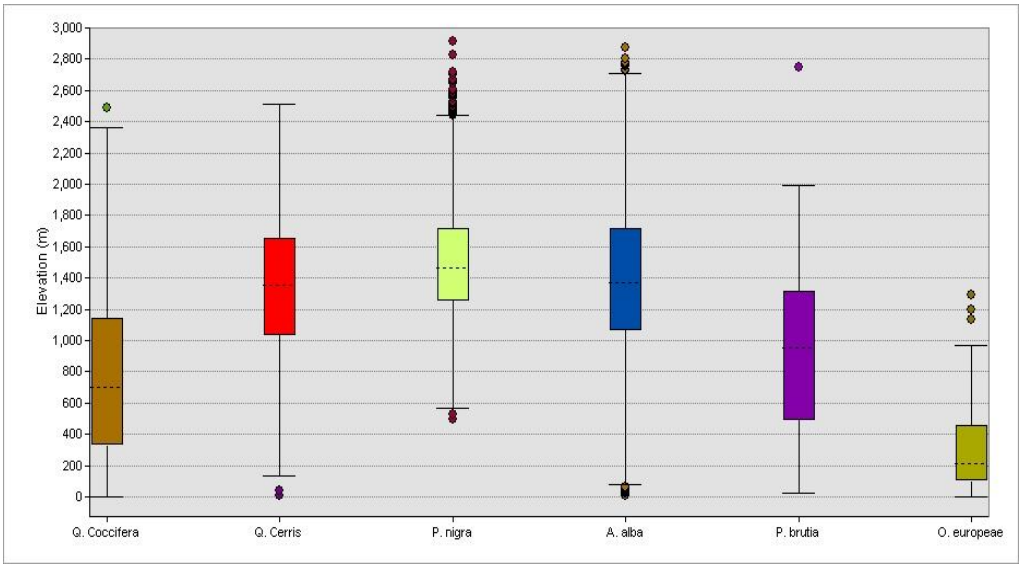


**Figure 7-15 Boxplot showing the elevation spread of a selection of species under modern conditions, showing the 25th, 50th (dashed median line) and 75th quartile. The step value is 1.5 beyond which are outliers.**

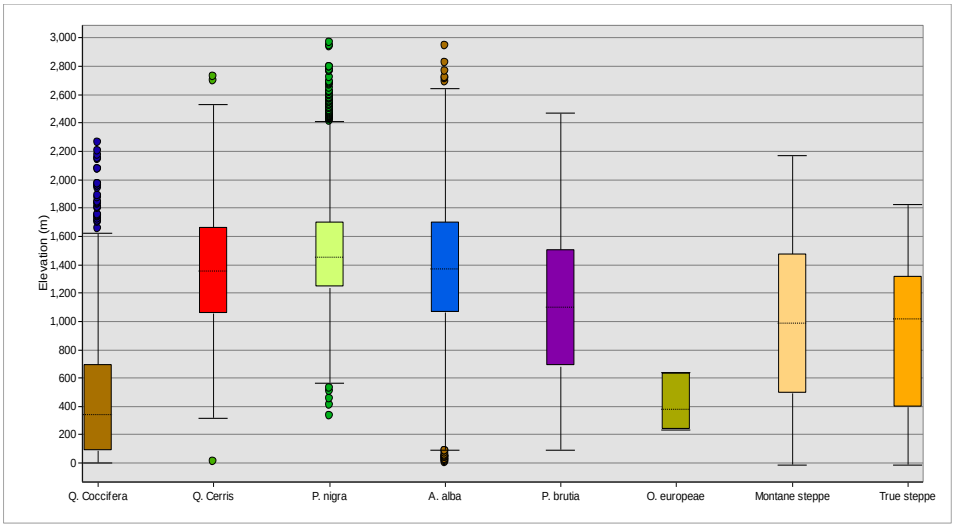


**Figure 7-16 Boxplot showing the elevation spread of a selection of species modelled under a low precipitation and temperature scenario, showing the 25th, 50th (dashed median line) and 75th quartile. The step value is 1.5 beyond which are outliers.**

A further graph was produced that investigated the elevation limits of species if it is assumed that trees would not grow in areas of potentially persistent snow and ice. The results of this are shown in Figure 7-17. This acted to further restrict arboreal species from high elevations above around 1500 m. The elevation limits of all three scenarios are tabulated in Table 7-4.

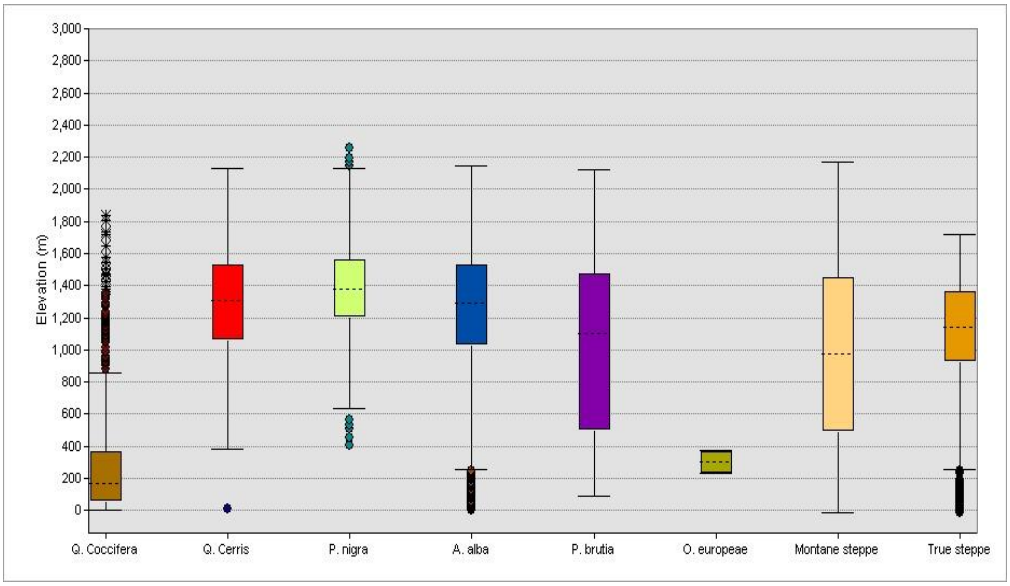


**Figure 7-17 Boxplot showing the elevation spread of a selection of species modelled under a low precipitation and temperature scenario, where it is assumed that areas likely to be under snow and ice will not allow trees to grow. Showing the 25th, 50th (dashed median line) and 75th quartile. The step value is 1.5 beyond which are outliers.**

**Table 7-4 Elevation limits of species under modern climatic conditions, and under model run S8-MR2.**

| | | Q. coccifera | Q. cerris | P. nigra | A. alba | P. brutia | O. europeae | Montane steppe | True steppe |
|---|---|---|---|---|---|---|---|---|---|
| Modern | Max | 2490 | 2511 | 2911 | 2877 | 2751 | 1288 | 0 | 0 |
| Cold temp and low precipitation | | 2258 | 2725 | 2965 | 2940 | 2470 | 636 | 2169 | 1821 |
| Persistent snow and ice | | 1837 | 2131 | 2259 | 2144 | 2125 | 373 | 2169 | 1717 |
| Modern | Average | 771 | 1341 | 1503 | 1373 | 950 | 317 | 0 | 0 |
| Cold temp and low precipitation | | 469 | 1375 | 1491 | 1368 | 1087 | 470 | 987 | 915 |
| Persistent snow and ice | | 294 | 1259 | 1389 | 1237 | 1028 | 304 | 973 | 1086 |
| Modern | 1st Quartile | 325 | 1034 | 1249 | 1061 | 497 | 102 | 0 | 0 |
| Cold temp and low precipitation | | 86 | 1050 | 1235 | 1060 | 678 | 234 | 490 | 394 |
| Persistent snow and ice | | 47 | 1055 | 1196 | 1026 | 521 | 269 | 488 | 921 |
| Modern | Median | 698 | 1354 | 1463 | 1369 | 955 | 210 | 0 | 0 |
| Cold temp and low precipitation | | 342 | 1354 | 1449 | 1368 | 1102 | 553 | 986 | 1012 |
| Persistent snow and ice | | 165 | 1307 | 1378 | 1295 | 1102 | 304 | 973 | 1144 |
| Modern | 3rd Quartile | 1147 | 1658 | 1726 | 1720 | 1321 | 460 | 0 | 0 |
| Cold temp and low precipitation | | 701 | 1664 | 1705 | 1707 | 1509 | 636 | 1477 | 1323 |
| Persistent snow and ice | | 374 | 1537 | 1571 | 1539 | 1477 | 338 | 1456 | 1367 |

## 7.10 DISCUSSION

The occurrence of higher than present lake levels in *Artemisia*-dominated steppe around the Last Glacial Maximum (24-19 Cal ka yr BP) is a feature of palaeoenvironmental records from Spain, Iran, Greece and Turkey (Prentice, Guiot et al. 1992), however the reasons for this apparent contradiction have led to a longstanding debate between palynologists, palaeoclimatologists and climate modellers.

A number of modelling studies agree that temperatures are likely to have between 5-10°C lower during the LGM, potentially due to strong westerly advection from the cold North Atlantic (Kutzbach and Guetter 1986; Harrison, Prentice et al. 1992; Robinson, Black et al. 2006).

Evidence from the palaeoclimatology and GCMs (Kutzbach and Guetter 1986; Harrison, Prentice et al. 1992; Bar-Matthews and Ayalon 1997; McGarry, Bar-Matthews et al. 2004; Hayes, Kucera et al. 2005; Robinson, Black et al. 2006; Jones, Roberts et al. 2007), and further evidence from the palynological community (Niklewski and Van Zeist 1970; van Zeist, Woldring et al. 1975; Arslanov, Dolukhanov et al. 2007) suggests that cold and arid conditions were prevalent during the LGM.

However, as discussed by Prentice, some evidence for a cool and humid climate exist (Broccoli and Manabe 1987). Glacial deposit mapping in Turkey suggests glacial advance during this period (Sarıkaya, Zreda et al. 2008), and lake level evidence from Konya basin and Lake Van suggests generally high lake levels throughout the LGM (Bartov, Stein et al. 2002; Bartov, Goldstein et al. 2003.) Based on PFT and non-quantitative biomization methods (AP/NAP ratios), a new modelling study by Şenkul and Doğan also suggests that climatic conditions were cool and humid in the southwest of Turkey during the LGM as opposed to cool and arid (Şenkul and Doğan 2012). However, the results of this study should be interpreted under the caveat that the effects of vegetation distance away from the pollen site, long distance travel and pollen

productivity are not taken into account in AP/NAP ratios. Further the PFT approach does not take into account the potential variability in precipitation and temperature across the region.

Prentice, Guiot et al. (1992) suggest that the ice-age climate of the Mediterranean region was characterised by cold winters, intense winter precipitation and summer drought, based on experiments that related the sensitivity of lake levels and vegetation to different components of the water balance (runoff versus evapotranspiration). However, again the model does not account for spatial variability across the region for this result.

The novel aspect of this thesis is that it does highlight the potential spatial variability of precipitation and temperature balance, which results in some interesting conclusions. The vegetation modelling method used supports previous estimates of temperature reduction of ~8°C. Based on comparison with pollen from Karamik core, and incorporating estimates of pollen travel, this study suggests that winter precipitation, at least around Karamik, was potentially 200 mm less than the modern average. It further suggests however, that hillslope areas were particular focal points for coniferous forest, and that refugia areas may have been present near the coast. This point warrants further discussion.

As part of a wide ranging palynological study by Van Zeist and Bottema (1991), the statement was made that only the northern coast of Anatolia was covered with forests during the LGM, while the majority of the Mediterranean coastal regions were covered with steppe forests. However, the results of this study, along with another recent modelling effort (Şenkul and Doğan 2012) suggests that this may need reappraisal. Results from vegetation modelling within this thesis have suggested that refugia areas for Mediterranean species such as *Quercus coccifera, Pinus brutia, Olea europaea* and *Vitis vinifera* may have been possible at certain key locations on the Antalya and Muğla coast of southwest Turkey, and further refugia were found for more cold-tolerant species in the mountainous hillslopes of the Oro-Mediterranean region. This therefore adds discussion to the work of Brewer et al. (2002), Krebs et al. (2004) and Taberlet and Cheddadi (2002), by promoting the south of Turkey as a potential refugia area. The

importance of this approach is that it has retrodicted potential areas of refugia in areas where pollen evidence is not available.

### 7.10.1 **Discussion against historical and archaeological evidence**

To conclude this section of modelling, the outcomes of the study will be discussed in relation to archaeological data. By incorporating this aspect of the picture at this stage of the thesis, it is hoped that the utility of the model in providing context for archaeological and historical studies will be highlighted.

Although evidence of human activity is present in the Middle East from at least the Pleistocene onwards (Zohary 1973; Vermoere 2002), our knowledge during the Epipalaeolithic and Palaeolithic is very incomplete. Persistent archaeological sites are rare, and our knowledge of the range of plants used by prehistoric populations is fragmentary due to selective preservation. In particular the distinction between cultivated and wild plants is difficult to establish (Martinoli 2009). Nonetheless, it is known that plant collection and plant usage in some areas of the Levant was considered to be quite mature, even at 23 Cal ka yr BP, including use of emmer wheat and barley, almonds, pistachio, wild olives and wild grape, and refined composite tools have been found such as reaping knives used for wild plant harvesting (Nadel and Hershkovitz 1991; Weiss, Wetterstrom et al. 2004; Martinoli 2009),

Archaeological surveys and excavations throughout the 20$^{th}$ century have identified over 200 Palaeolithic sites throughout Turkey, however, little is known about Epipalaeolithic communities within the Lake District of southwest Turkey. Surface finds do testify to the existence of human activity (Schoop 2005), but only from around 18 Cal ka yr BP (Martinoli 2009). The main evidence of occupation is found at the rock-cut cave of Beldibi, Belbasi, Öküzini and Karain, and some fascinating analyses of those cave deposits and surface finds that do exist

hint at the potential complexity of these early communities (Albrecht 1988; Yalçinkaya, Otte et al. 2002; Martinoli 2009). This includes 'nutshell' and fruit remnants from *Prunus, Amygdalus, Pistacia, Quercus, Crataegus, Celtis, Pyrus, Rosa and Vitis (Martinoli 2009).*

Although the earliest evidence so far in southwest Turkey is later than the first research question of this thesis, the interaction of climate and vegetation during this early period is an important developmental step in creating the conditions for later Epipalaeolithic communities of the area to exploit. In addition, it must be remembered that absence of archaeological evidence from earlier than 18 Cal ka yr BP is not necessarily evidence for absence, and analysis of the vegetation and environment may provide further insights into possible areas of exploitation by these early communities.

With this in mind, Figure 7-18 displays the location of Palaeolithic sites currently known about across southwest Turkey. It is particularly of interest that the number of Upper Palaeolithic sites is limited, and is focused predominantly around river valley and cave sites at low elevations in the Eu-Mediterranean zone. Kuhn (2002) suggests that this is not entirely an artefact of geology or biases in past investigations, as cave sites above 500 m elevation across wider western Europe are seldom occupied during this period, and that this is likely to be due to the cold and dry interval of the late Pleistocene. In addition, the central Anatolian plateau, being as it is generally over 1000 m in altitude is theorised to have only supported very low populations. This model of settlement fits well with the output to this modelling study. Superimposing Palaeolithic sites onto the main aridity classes shows that sites are not located in steppe or high elevation areas, and are more likely in areas with above freezing average winter temperature. They are also more likely to be found in areas near to woodland resources.

One of the most detailed studies of Palaeolithic archaeology has been the excavation and analysis at Karain cave in Antalya (Albrecht 1988). Interpretations of micromammalia, molluscs and pollen evidence have allowed a high level overview of climate to be discerned that can be compared to model output. The evidence suggests a favourable climate (defined as one that is

temperate with precipitation equally distributed throughout the year) during the 'early' Upper Palaeolithic (~40 000 $^{14}$C yr BP), and a 'worsening' of climate during the middle Upper Palaeolithic. The results of this modelling study support this by providing evidence for low temperatures and precipitation around this period. By the 'late' Upper Palaeolithic (~14 000 $^{14}$C yr BP, around the time of the Bølling-Allerød interstadial) conditions (particularly precipitation) were seen to improve (Albrecht 1988; Uerpmann, Albrecht et al. 1992).

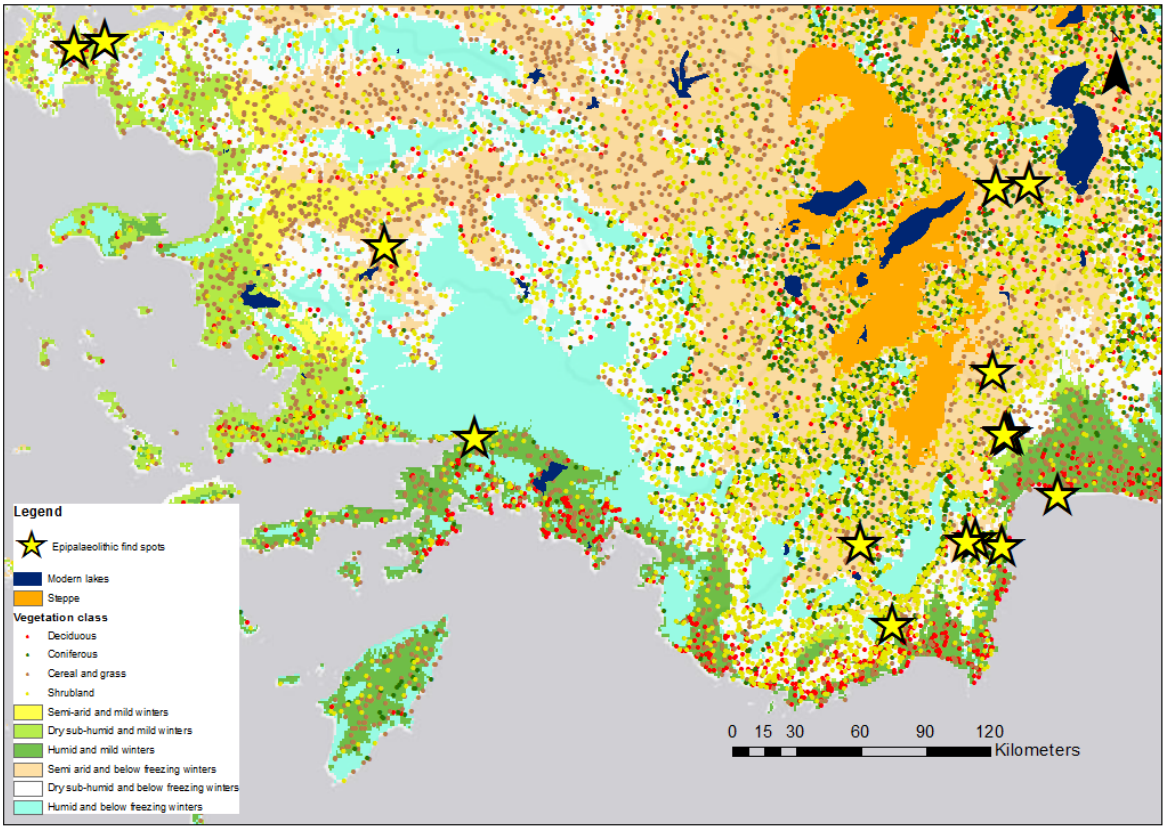


**Figure 7-18 Palaeolithic site locations from the Tay GIS database overlaid with climate zones and main vegetation zones, under a scenario of -8°C average temperature and -200 mm precipitation. The figure shows that those Palaeolithic sites currently discovered are located relatively close to the coast, generally in humid or dry sub-humid areas, particularly in Antalya, and at low altitude.**

The potential variation in vegetation and landscape between the plains and the mountainous southwest may have also had implications for trade, travel and relations with other

Epipalaeolithic communities. It is known that Epipalaeolithic communities in the plains were in contact with communities further south as evidenced by obsidian travel into the Near East (Cauvin and Chataigner 1998), but it may be the case that items with a more organic origin were also traded based on coveted items from environments different from their own (Goring-Morris, Hovers et al. 2009). It would therefore be of further interest to undertake analysis to examine if differences in the material finds of the Palaeolithic sites in southwest Turkey bore any correlation to the potential regional differences in climate shown in Figure 7-8, in terms of the fauna hunted, or the method of hunting.

## 7.11 Summary of findings for Research Question 1.

In summary, model output data for the LGM period in southwest Turkey has therefore demonstrated that a climatic scenario reconstructed from a range of climate proxy data can explain that an increase in humidity due to low temperature and precipitation could have led to an increase in lake levels and glacial activity, and could occur concurrently with the widespread distribution of steppic species in southwest Turkey. The alternative hypothesis of this research question is therefore accepted. Furthermore, the model has identified potential refugia areas for cold and arid intolerant species.

Under a significant reduction in precipitation and temperature (i.e. between -4 to -8°C average temperature and between -100 to -300 mm winter precipitation), it is likely that humidity and aridity across southwest Turkey would have been significantly different than current conditions. Under a geographically consistent drop in temperature and precipitation, the interior of southwest Turkey was modelled to experience a semi-arid environment, whilst more southerly regions such as Muğla and Antalya experienced greater humidity.

Vegetation modelling raised the possibility of refugial areas in these high humidity areas, and on mountain hillslopes, where cold and drought-intolerant species may have been restricted to. Typically 'Mediterranean' species such as *Olea europaea* and *Quercus coccifera*, whilst unlikely to flourish in many areas of the southwest, did show potential distribution along the low elevation coastal areas of Antalya and Muğla.

In addition to changes in aridity and humidity, it is also probable that under a large reduction in temperature of ~6-8°C, average winter temperatures across most of southwest Turkey did not to move above freezing, having significant implications for hydrological cycles.

# 8 RESEARCH QUESTION 2: VEGETATION MODELLING FRAMEWORK RESULTS AND DISCUSSION

## 8.1 RESEARCH QUESTION

Does the model framework provide further evidence to support or reject a lag in tree expansion at the beginning of the Holocene (~11 to 8 Cal ka yr BP), and if so, is there evidence for a climatic reason for this?

## 8.2 RESEARCH QUESTION 2 HYPOTHESES

Based on previous literature, and reconstructed climate evidence, the modelling process for research question 2 starts out with 2 hypotheses, which may be supported or rejected by the model output.

**Table 8-1Model hypotheses for Research Question 2**

| |
|---|
| **H1: Pollen zones from southwest Turkey suggest a lag in tree expansion at the beginning of the Holocene**<br><br>**H0: Pollen zones from southwest Turkey do not suggest a lag in tree expansion at the beginning of the Holocene** |
| If H1 is true, then: |
| **H2: Model output supports the suggestion of a climatic reason for a lag in tree expansion at the beginning of the Holocene**<br><br>**H0: Model output does not support the suggestion of a climatic reason for a lag in tree expansion at the beginning of the Holocene** |

## 8.3 CHRONOLOGICAL MODELLING

Climate records suggest the beginning of climate amelioration at ~11 Cal ka yr BP, continuing until around 8 Cal ka yr BP. Chronological modelling has shown that 4 sites have pollen zones likely to cover this early Holocene period; Pınarbaşı, Karamik, Sögüt and Gölhisar.

By using Bayesian statistics it was possible to estimate the likelihood that particular pollen zones began or ended before or after 11 Cal ka yr BP. Figure 8-1 displays the highest probability density (hpd) plots for the beginning and end of relevant pollen zone, and highlighted with a blue dashed line is the point at which climate amelioration potentially started. Table 8-2 displays the probable age range of the zones.

Examining each zone in turn and starting with Pınarbaşı, zone 1 reflects a steppic open landscape. Although the chronological uncertainty for this zone is high, it is statistically likely to have been deposited predominantly before climate amelioration. A date for the transition to Pınarbaşı zone 2 is relatively uncertain as 62% of the hpd falls after the threshold of 11 000 Cal yr BP. Here, chronological uncertainty precludes clear evidence for either immediate reaction to climate amelioration, or evidence for a lag.

Karamik zone 4 and Sögüt zone 3 are likely to cover the period up until at least 10 Cal ka yr BP and in the case of Karamik up to 8 Cal ka yr BP. These zones may therefore be expected to show increases in tree pollen if pollen responded immediately to amelioration. However, this is not the case. Although Karamik does undergo an increase in *Poaceae*, significant increases in tree pollen are not seen. Assuming climate amelioration did occur at ~11 Cal ka yr BP; this therefore provides evidence for a significant lag between amelioration and tree expansion at the high elevation site of Sögüt, and the interior site of Karamik. Similarly, the change from an open landscape at Gölhisar from pollen zone 1 to tree expansion during zone 2a, very likely occurs after 10 Cal ka yr BP.

In summary, of the testable pollen cores, no support has been found for an immediate reaction of vegetation to climate amelioration at 11 Cal ka yr BP. Moderate evidence supports the case that a lag of around 1000 to 3000 years occurred between climate amelioration and tree expansion based on the sites of Karamik, Sögüt and Gölhisar. The support for a lag at Gölhisar in particular is interesting as this has a relatively robust chronology. By exploring the chronology of pollen zones in this way, the analysis has provided a more measured approach to the investigation of potential lags. Although the methodology is useful, it is however recommended that it is reassessed once more pollen cores with greater chronological control are found, as the quality of evidence is not yet considered strong enough to provide a definitive regional answer.

By comparing analytical pollen from these zones to simulated pollen under different climate conditions, the next section will examine the potential magnitude of climate change that may have led to the changes in vegetation seen at the beginning of the Holocene.

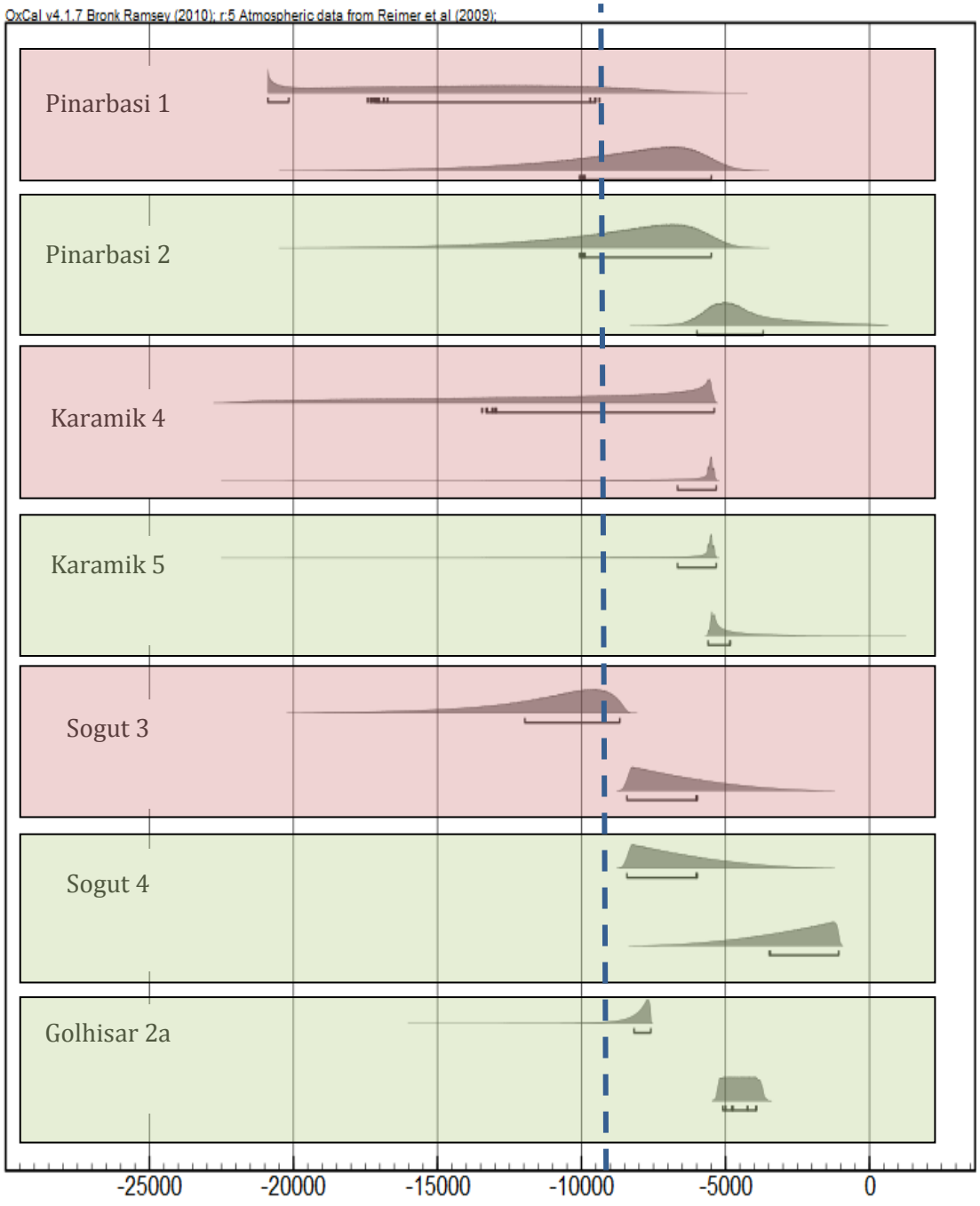


**Figure 8-1 Pollen zones likely to cover the early Holocene period, and associated highest probability density plots. The top distribution is the beginning of the zone and the bottom distribution is the end of the zone. The blue dashed line represents the estimated beginning of climate amelioration. Pollen zones marked in red represent an open landscape. Pollen zones in green represent a significant increase in tree pollen. Brackets are the 68.2% highest probability density range. Chronological modelling suggests a significant lag between climate amelioration and pollen zones reflecting an increase in tree pollen.**

**Table 8-2 Most probable pollen zones to cover the period of aridity between 12 000 and 8000 Cal yr BP**

| Site | Zone | Beginning (Cal yr BP 68.2%) | Ending (Cal yr BP 68.2%) | Pollen assemblage |
|---|---|---|---|---|
| Early Holocene | | | | |
| Pınarbaşı | 1 | 22837 to 11444 | 11955 to 7434 | Open landscape Devoid of tree pollen |
| Karamik | 4 | 15406 to 7340 | 8614 to 7270 | NAP, Increase in Gramineae |
| Sögüt | 3 | 13916 to 10619 | 10371 to 7925 | NAP, but increase in Quercus |
| Tree expansion | | | | |
| Pınarbaşı | 2 | 11955 to 7434 | 7945 to 5604 | Increase in Pinus |
| Sögüt | 4 | 10371 to 7925 | 5427 to 3017 | Increase in Quercus cerris and Juniperus |
| Gölhisar | 2a | 10125 to 9542 | 7042 to 5874 | High Pinus |
| Karamik | 5 | 8614 to 7270 | 7552 to 6779 | Increase in Pinus and Quercus |

## 8.4 VEGETATION MODEL OUTPUT UNDER A VARIETY OF CLIMATE CONDITIONS: DISSIMILARITY WITH ANALYTICAL POLLEN EVIDENCE

This section discusses the results of similarity measures between simulated pollen output and actual pollen data for the Early Holocene period (12 000 to 8000 Cal yr BP). Bayesian modelling suggests that Pınarbaşı zones 1 and 2, Karamik zones 4 and 5, Sögüt zones 3 and 4, and Gölhisar zone 2a cover this period. Half of the zones reflect a generally open landscape, and half of them reflect a significant increase in tree pollen (predominantly *Quercus* and *Pinus*). Although at Pınarbaşı it is difficult to determine whether a lag occurred, chronological modelling does suggest a 1000 year lag at Sögüt, and Gölhisar and a 3000 year lag at Karamik.

Simulated pollen from 27 different climate scenarios was compared to all of these pollen zones, the output from which is displayed in two radar diagrams. Figure 8-2 examines model-data links with pollen zones that reflect open landscapes, and Figure 8-3 represents model-data links with pollen zones that contain tree expansion signatures.

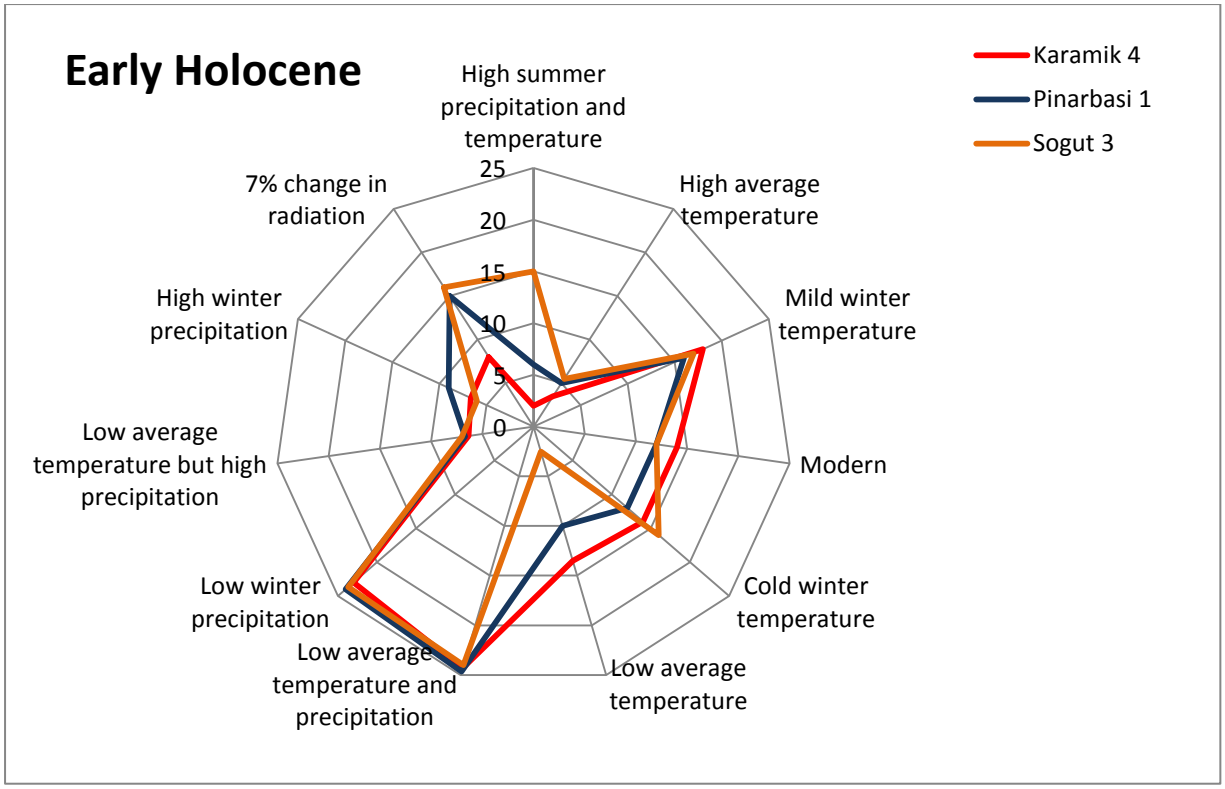


**Figure 8-2 Radar diagram showing degree of similarity between simulated pollen under different climatic scenarios and analytical pollen data for the early Holocene. The most similar climate scenarios are found with low average temperature and precipitation.**

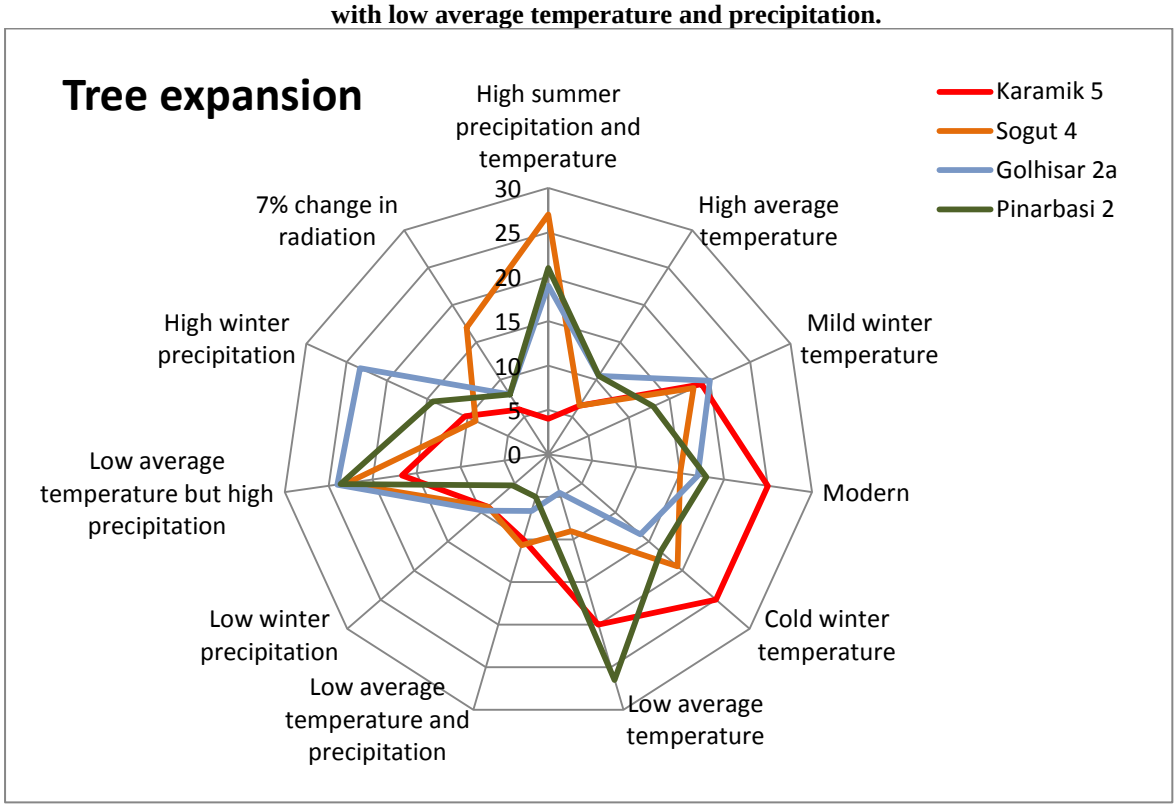


**Figure 8-3 Radar diagram showing degree of similarity between simulated pollen under different climatic scenarios and analytical pollen data after tree expansion. Some spatial variation is found between**

**Karamik and other pollen cores. In comparison with previous zones, the most similar climate scenarios are now found with increased precipitation, and in some cases, warmer temperatures.**

The first point to note in Figure 8-2 is that disparate pollen zones from different sites in southwest Turkey show a relatively similar profile in the early Holocene when analytical pollen is compared to model output. This suggests that pollen cores have a relatively similar species makeup at this point, and that this is likely to be due to a spatially consistent climate scenario. Similar to the LGM period, the most similar pollen simulations are under a scenario of low temperature and low precipitation

Now considering Figure 8-3, a large change in model-data similarity has occurred at all pollen sites. The best agreement between simulated and analytical pollen is now met by climate scenarios with high precipitation. Gölhisar and Pınarbaşı have similar profiles reflecting low average temperature and high winter precipitation. At the high elevation site of Sögüt although high agreement is reached with this scenario, better agreement is reached under a scenario of high summer precipitation and temperature. The interior site of Karamik is the only site that does not show high similarity to scenarios of high precipitation, although it does show an increase in precipitation from Karamik zone 4. The best scenario here is now shown under modern climatic conditions.

These results can be examined in more detail by looking at individual model runs. In Figure 8-4 the highest average rank for all sites considered is model run S8-MR2 (-8°C, -200 mm). However under Figure 8-5 a dramatic change in rank has occurred, to the extent that the highest average rank is now under a scenario of +300 mm precipitation (S6-MR3), an increase of 500 mm.

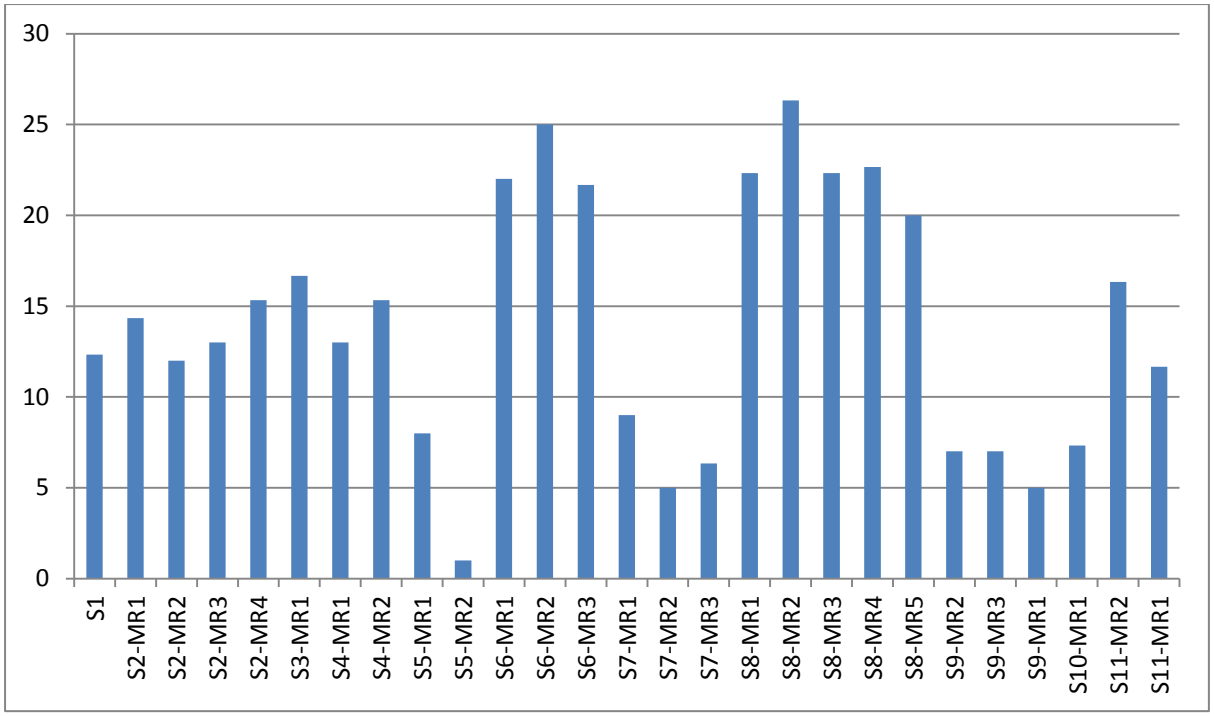


**Figure 8-4 Model-data similarity for pollen zones representing an open landscape during the Early Holocene. Graph shows average model ranks for a selection of model runs. The highest rank is found under a model run with -200 mm winter precipitation, and low average temperatures (-8°C).**

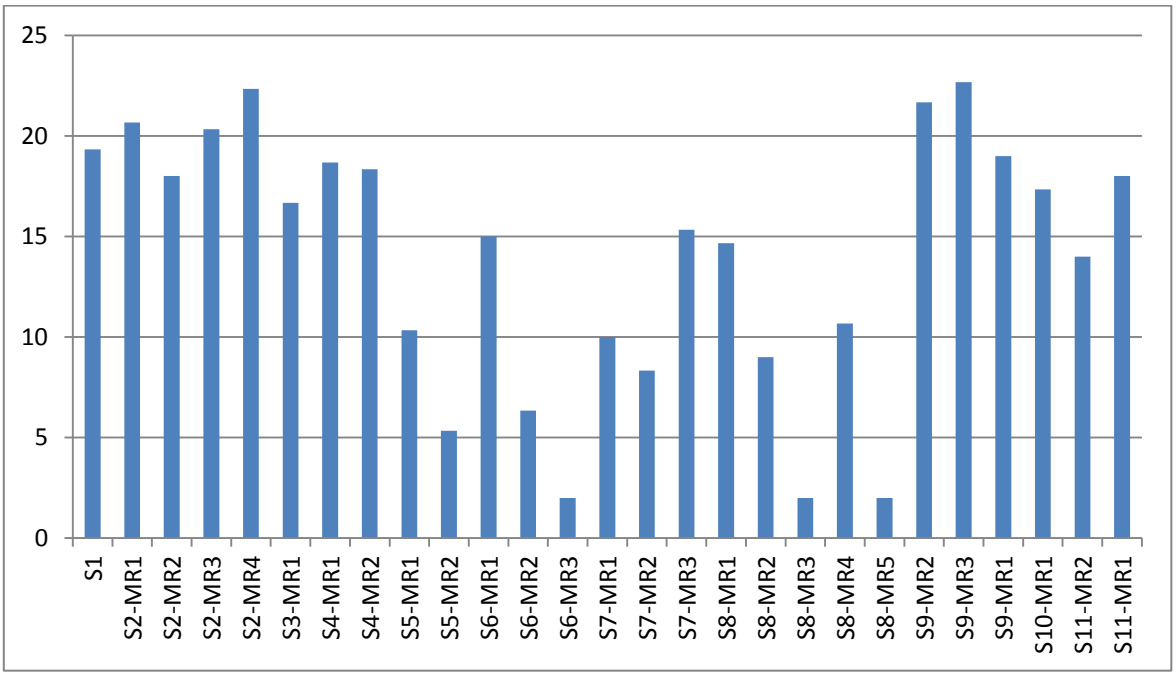


**Figure 8-5 Model-data similarity for pollen zones representing tree expansion during the Early Holocene. Graph shows average model ranks for a selection of model runs. The highest rank is found under a model run with +300 mm winter precipitation, and low average temperatures (-8°C).**

Table 8-3 shows the raw dissimilarity measures between climate scenarios and each pollen zone reflecting steppic species. All pollen zones here reflect a consistent scenario of low precipitation and low temperature. However now considering Table 8-4, as tree expansion occurs, the most similar climate scenario differs across the region.

**Table 8-3 Dissimilarity measures between model output and data for pollen zones reflecting steppic species at the beginning of the Holocene**

| | Dissimilarity | | | Rank | | | |
|---|---|---|---|---|---|---|---|
| **Scenario** | **PZ-1** | **KZ-4** | **SgZ-3** | **PZ-1** | **KZ-4** | **SgZ-1** | **Average Rank** |
| **S1** | 1.40 | 0.90 | 0.65 | 11 | 14 | 12 | 12 |
| **S2-MR1** | 1.39 | 0.89 | 0.64 | 13 | 16 | 14 | 14 |
| **S2-MR2** | 1.40 | 0.90 | 0.65 | 10 | 13 | 13 | 12 |
| **S2-MR3** | 1.40 | 0.90 | 0.54 | 9 | 12 | 18 | 13 |
| **S2-MR4** | 1.40 | 0.90 | 0.54 | 12 | 15 | 19 | 15 |
| **S3-MR1** | 1.31 | 0.88 | 0.56 | 15 | 18 | 17 | 17 |
| **S4-MR1** | 0.96 | 0.93 | 0.90 | 26 | 10 | 3 | 13 |
| **S4-MR2** | 0.96 | 0.89 | 0.92 | 27 | 17 | 2 | 15 |
| **S5-MR1** | 1.41 | 1.05 | 0.74 | 8 | 6 | 10 | 8 |
| **S5-MR2** | 1.60 | 1.31 | 1.03 | 1 | 1 | 1 | 1 |
| **S6-MR1** | 1.02 | 0.69 | 0.48 | 23 | 23 | 20 | 22 |
| **S6-MR2** | 1.01 | 0.66 | 0.40 | 24 | 25 | 26 | 25 |
| **S6-MR3** | 1.05 | 0.80 | 0.49 | 19 | 21 | 25 | 22 |
| **S7-MR1** | 1.05 | 1.12 | 0.86 | 18 | 5 | 4 | 9 |
| **S7-MR2** | 1.53 | 1.23 | 0.84 | 2 | 4 | 9 | 5 |
| **S7-MR3** | 1.50 | 0.92 | 0.82 | 3 | 11 | 5 | 6 |
| **S8-MR1** | 1.02 | 0.69 | 0.47 | 22 | 24 | 21 | 22 |
| **S8-MR2** | 1.01 | 0.64 | 0.35 | 25 | 27 | 27 | 26 |
| **S8-MR3** | 1.04 | 0.79 | 0.48 | 21 | 22 | 24 | 22 |
| **S8-MR4** | 1.04 | 0.66 | 0.42 | 20 | 26 | 22 | 23 |
| **S8-MR5** | 1.06 | 0.81 | 0.53 | 17 | 20 | 23 | 20 |
| **S9-MR2** | 1.44 | 1.01 | 0.74 | 6 | 9 | 6 | 7 |
| **S9-MR3** | 1.44 | 1.01 | 0.74 | 7 | 7 | 7 | 7 |
| **S9-MR1** | 1.45 | 1.28 | 0.74 | 4 | 3 | 8 | 5 |
| **S10-MR1** | 1.44 | 1.29 | 0.63 | 5 | 2 | 15 | 7 |
| **S11-MR2** | 1.32 | 1.01 | 0.58 | 14 | 19 | 16 | 16 |
| **S11-MR1** | 1.27 | 0.86 | 0.66 | 16 | 8 | 11 | 12 |

**Table 8-4 Dissimilarity measures between model output and data for pollen zones reflecting tree expansion at the beginning of the Holocene**

| | Dissimilarity | | | | Rank | | | | |
|---|---|---|---|---|---|---|---|---|---|
| **Scenario** | **PZ-2** | **KZ-5** | **SgZ-4** | **G-2a** | **PZ-2** | **KZ-5** | **SgZ-4** | **G-2a** | **Average Rank** |
| **S1** | 1.21 | 0.78 | 0.85 | 0.57 | 18 | 25 | 15 | 17 | 19 |
| **S2-MR1** | 1.20 | 0.78 | 0.85 | 0.57 | 19 | 27 | 16 | 16 | 21 |
| **S2-MR2** | 1.22 | 0.78 | 0.85 | 0.58 | 16 | 24 | 14 | 12 | 18 |
| **S2-MR3** | 1.22 | 0.78 | 0.76 | 0.57 | 15 | 23 | 23 | 14 | 20 |
| **S2-MR4** | 1.21 | 0.78 | 0.76 | 0.57 | 17 | 26 | 24 | 13 | 22 |
| **S3-MR1** | 1.28 | 0.90 | 0.81 | 0.50 | 13 | 19 | 18 | 20 | 17 |
| **S4-MR1** | 0.83 | 0.92 | 0.89 | 0.91 | 27 | 18 | 11 | 5 | 19 |
| **S4-MR2** | 0.89 | 0.86 | 0.92 | 0.90 | 26 | 22 | 7 | 7 | 18 |
| **S5-MR1** | 1.26 | 1.24 | 0.91 | 0.73 | 14 | 8 | 9 | 10 | 10 |
| **S5-MR2** | 1.60 | 1.36 | 1.09 | 0.69 | 7 | 5 | 4 | 11 | 5 |
| **S6-MR1** | 1.55 | 1.01 | 0.79 | 0.56 | 10 | 16 | 19 | 18 | 15 |
| **S6-MR2** | 1.65 | 1.20 | 0.99 | 0.88 | 4 | 10 | 5 | 9 | 6 |
| **S6-MR3** | 1.78 | 1.42 | 1.19 | 1.25 | 2 | 1 | 3 | 2 | 2 |
| **S7-MR1** | 1.32 | 1.16 | 0.92 | 0.48 | 11 | 11 | 8 | 21 | 10 |
| **S7-MR2** | 1.31 | 1.32 | 0.96 | 0.47 | 12 | 7 | 6 | 22 | 8 |
| **S7-MR3** | 1.14 | 1.12 | 0.86 | 0.36 | 20 | 13 | 13 | 27 | 15 |
| **S8-MR1** | 1.55 | 1.01 | 0.78 | 0.57 | 9 | 15 | 20 | 15 | 15 |
| **S8-MR2** | 1.65 | 1.15 | 0.90 | 0.98 | 5 | 12 | 10 | 4 | 9 |
| **S8-MR3** | 1.78 | 1.40 | 1.19 | 1.25 | 1 | 3 | 2 | 1 | 2 |
| **S8-MR4** | 1.60 | 1.12 | 0.87 | 0.91 | 6 | 14 | 12 | 6 | 11 |
| **S8-MR5** | 1.78 | 1.41 | 1.26 | 1.18 | 3 | 2 | 1 | 3 | 2 |
| **S9-MR2** | 1.00 | 0.89 | 0.77 | 0.46 | 24 | 20 | 21 | 23 | 22 |
| **S9-MR3** | 0.99 | 0.89 | 0.76 | 0.45 | 25 | 21 | 22 | 24 | 23 |
| **S9-MR1** | 1.03 | 1.22 | 0.74 | 0.43 | 22 | 9 | 26 | 25 | 19 |
| **S10-MR1** | 1.13 | 1.38 | 0.71 | 0.53 | 21 | 4 | 27 | 19 | 17 |
| **S11-MR2** | 1.55 | 0.92 | 0.85 | 0.41 | 8 | 17 | 17 | 26 | 14 |
| **S11-MR1** | 1.00 | 1.34 | 0.74 | 0.88 | 23 | 6 | 25 | 8 | 18 |

Karamik pollen zone 5 best reflects a scenario with an increase in precipitation of ~ 200 mm since the previous zone. This results in a modern climate, but perhaps with colder winters than the modern average, with moderate agreement at 0.78. The high elevation site of Sögüt best reflects a scenario with summer precipitation of ~50 mm more than the modern average, and summer temperature of around 2°C above the modern average. This is again only a moderate fit however at 0.71. The intramontane site of Gölhisar shows best agreement between model and pollen data under conditions of +300 mm precipitation, with good agreement at 0.36.

Although the pollen record at Ova Gölü (one of two coastal sites) begins too late to play a significant part in the discussion of the lag in tree pollen at the beginning of the Holocene, it is also worth discussing as part of this section. The first pollen zone here is modelled to have been deposited between around 8801 – 6962 Cal yr BP and 7416 - 5930 Cal yr BP (68.2%), or around 6852 - 5013 BC to 5467 – 4947 BC. It is important because it provides the first evidence of the vegetation assemblage of these coastal regions in southwest Turkey since the LGM. The zone contains a mixture of deciduous and evergreen *Quercus, Juniperus, Alnus, Ulmus, Olea* and *Vitis*. This is remarkable as it reflects the type of species expected to have been present in this area supposing it was a refugia area during the last Ice Age.

Furthermore, when this assemblage was compared to multiple simulated pollen assemblages (Figure 8-6), the type of climate scenarios most likely to produce the assemblage were found to be scenarios with high winter precipitation, high average temperature and high summer precipitation and temperature. Figure 8-7 shows the model run with the best fit is S5-MR1, which is a scenario with an average temperature of 2°C above the modern average, with the second best fitting model run reflecting +300 mm precipitation.

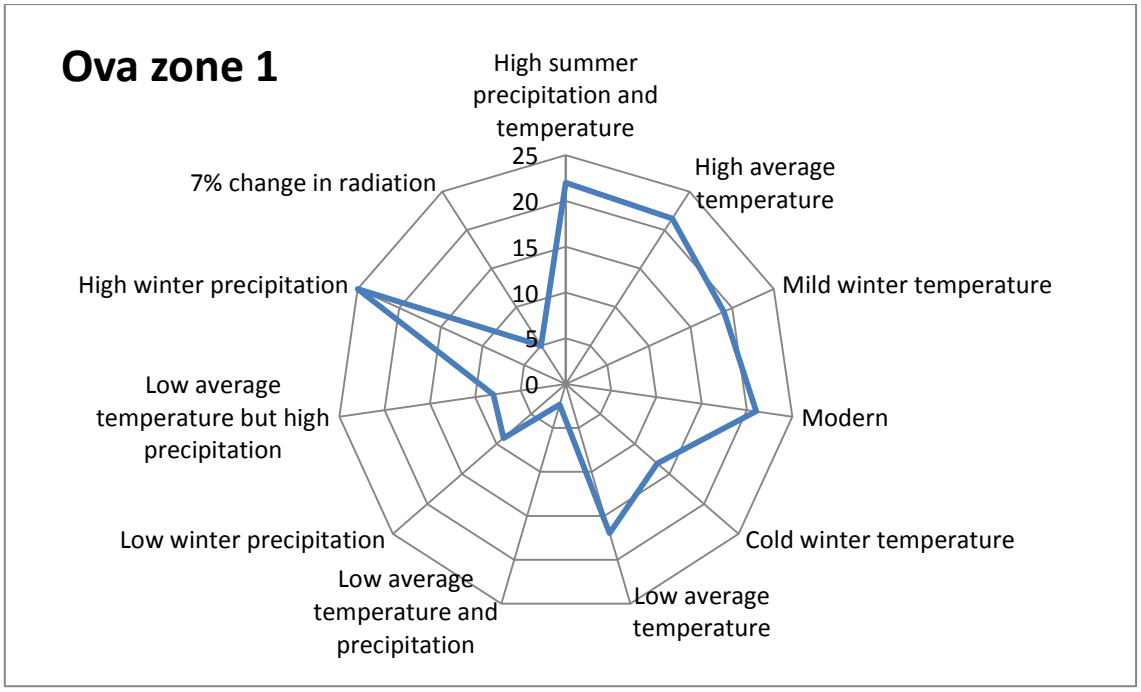


**Figure 8-6 Radar diagram showing degree of similarity between simulated pollen under different climatic scenarios and analytical pollen data for Ova pollen zone 1. This pollen zone shows similarity to scenarios of high precipitation and summer temperature**

The modelling exercise therefore firstly suggests a link between tree expansion at the beginning of the Holocene and increased precipitation and temperature throughout southwest Turkey. However, how vegetation reacts to this ameliorating climate is seen to differ across the region. At the intramontane sites of Gölhisar (increase of 500 mm) Pınarbaşı (increase of 300 mm), and the interior site of Karamik (increase of 200 mm), it is seen to be winter precipitation that is most likely to link to an increase in *Quercus* and *Pinus.* At the high elevation site of Sögüt and the coastal site of Ova modelling suggests that it is instead a rise in summer temperature, as well as precipitation that has led to an increase in trees.

It is important to remember that this modelling exercise only considers a selection of scenarios, and that the model relies on a number of modern analogue assumptions, so it would be premature to conclude that this magnitude of precipitation change is accurate without further analysis and modelling efforts. However, the process does suggest that a large increase in winter precipitation and temperature could have resulted in the first tree expansion evidenced

at the beginning of the Holocene, but that summer precipitation and temperature also increased to allow tree expansion at high elevation sites.

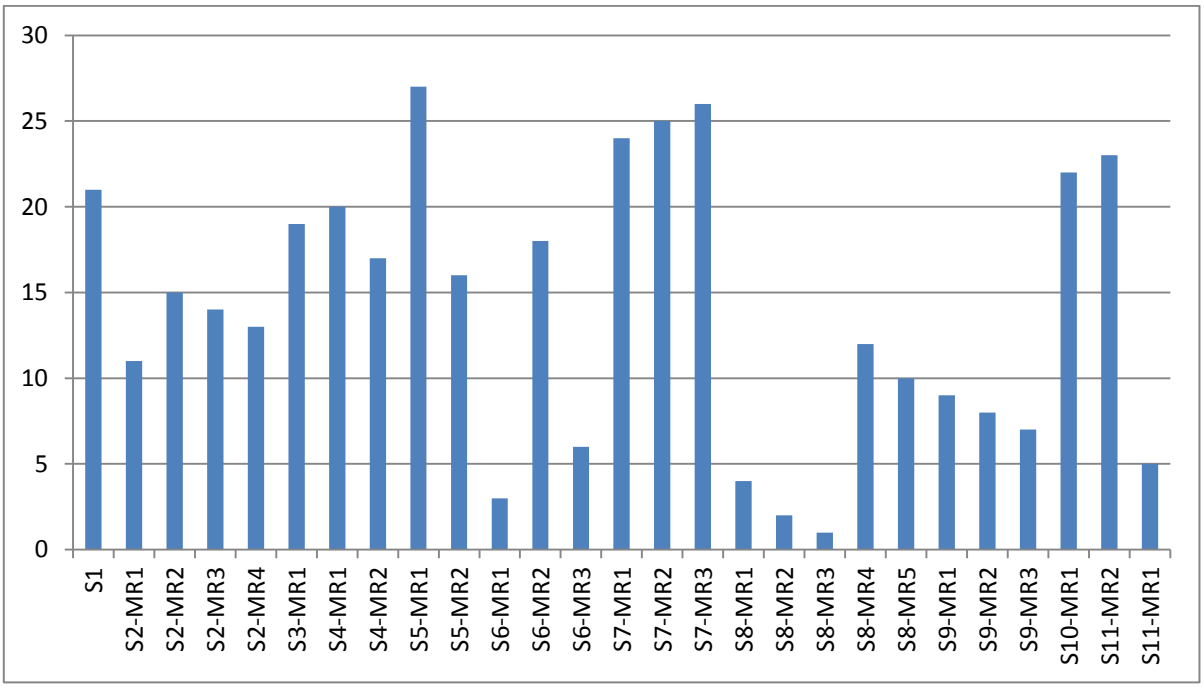


**Figure 8-7 Model-data similarity for Ova pollen zone 1 during the Early Holocene. Graph shows average model ranks for a selection of model runs.**

## 8.5 POTENTIAL VEGETATION DISTRIBUTION; A LOCAL PERSPECTIVE

As there is a division between the best fitting climate models for different pollen cores, a single model output across the region is not possible. Instead the discussion shall focus on specific areas.

Starting with the most interior site of Karamik, for the pollen zone just prior to tree expansion (zone 4) the best fitting vegetation model output is shown in Figure 8-8. This scenario represents predominantly steppic conditions, with scattered stands of *Pinus, Abies, Juniperus* and *Picea*. Species are restricted by both cool temperatures and precipitation.

Comparing this to the next pollen zone (zone 5 starting between ~9587 and 7719 Cal yr BP) where close to modern climate conditions are retrodicted, Figure 8-9 now shows a decrease in steppic species and *Juniperus*, and an increase in shrubland and grassland in the valleys, and *Pinus, Abies* and *Quercus* pollen at higher elevations. There is also a small amount of potential for *Castanea* and *Vitis* growth. Although no records are available from Hoyran for this time, if similar conditions occurred around this basin, one could expect a mixture of shrubland, grassland, *Abies* and *Quercus* around this area.

As will be discussed in the model evaluation section (Chapter 10) despite relatively good model fit, there is a notable underestimation in the model of the amount of Poaceae. The amount of Poaceae is an interesting component of both zones 4 and 5, and may correlate with similar increases in grassland at Eski Acigöl and Lake Van concurrent with early climate amelioration.

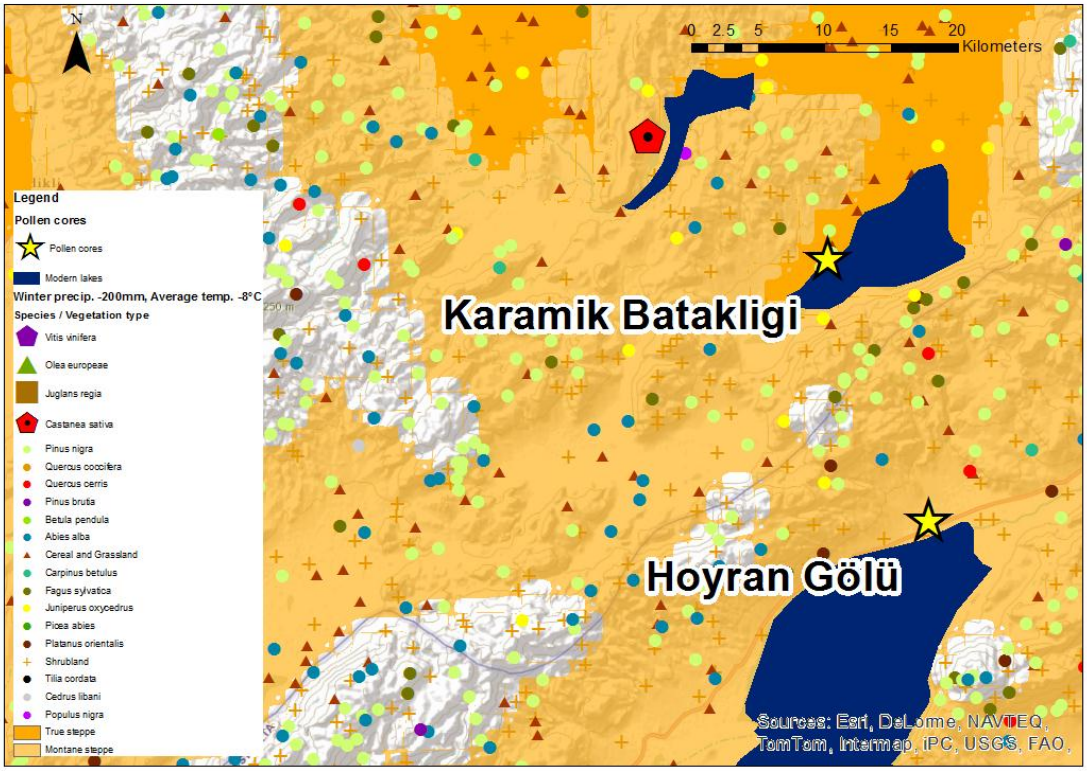


**Figure 8-8 Model output around Karamik matching pollen from zone 4.**

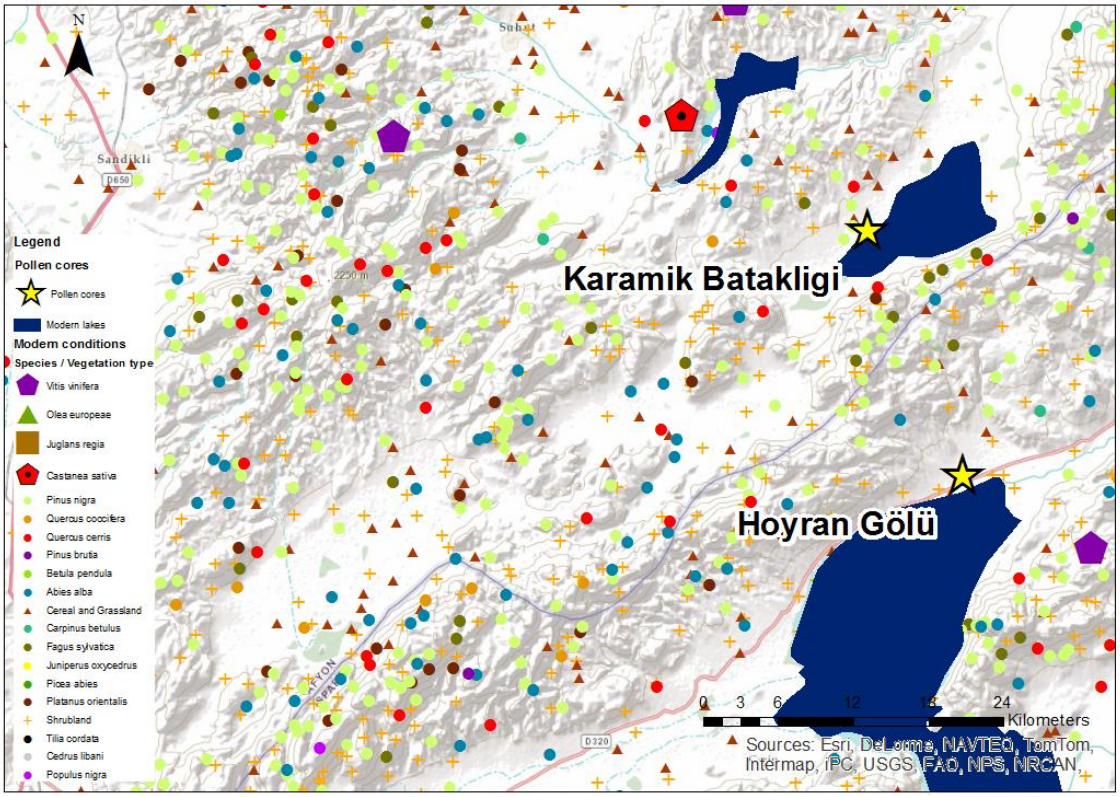


**Figure 8-9 Model output around Karamik matching pollen from zone 5.**

Moving south, the pollen cores of Ağlasun, Gravgaz and Bereket do not have records covering this period, and so the next pollen core to discuss is Pınarbaşı. This is a site at 1034 m elevation. Pollen zone 1 is devoid of tree pollen during the early Holocene period and consists mainly of NAP, predominantly *Artemisia* steppe. This is represented well in Figure 8-10 as Pınarbaşı is found in a particularly arid depression. It is likely that under a scenario of low temperature and precipitation the areas would have been predominantly steppe and montane steppe, with some small areas providing areas for *Pinus* and *Cedrus* to survive. If this climate scenario also applied to Ağlasun, Gravgaz and Bereket, these areas can also be expected to reflect montane steppe during this period.

In the next pollen zone, there is a rapid expansion of *Pinus*, until it forms ~95% of the pollen proportion. In comparison to Karamik, the best fitting model is S9-MR1, which has higher than

modern winter precipitation (+100 mm), but still reflects low temperatures (-8°C). This suggests slightly more precipitation was available in this area than in the interior. The result is an increase in *Pinus nigra, Abies, Quercus cerris,* grassland and shrubland around the coring site.

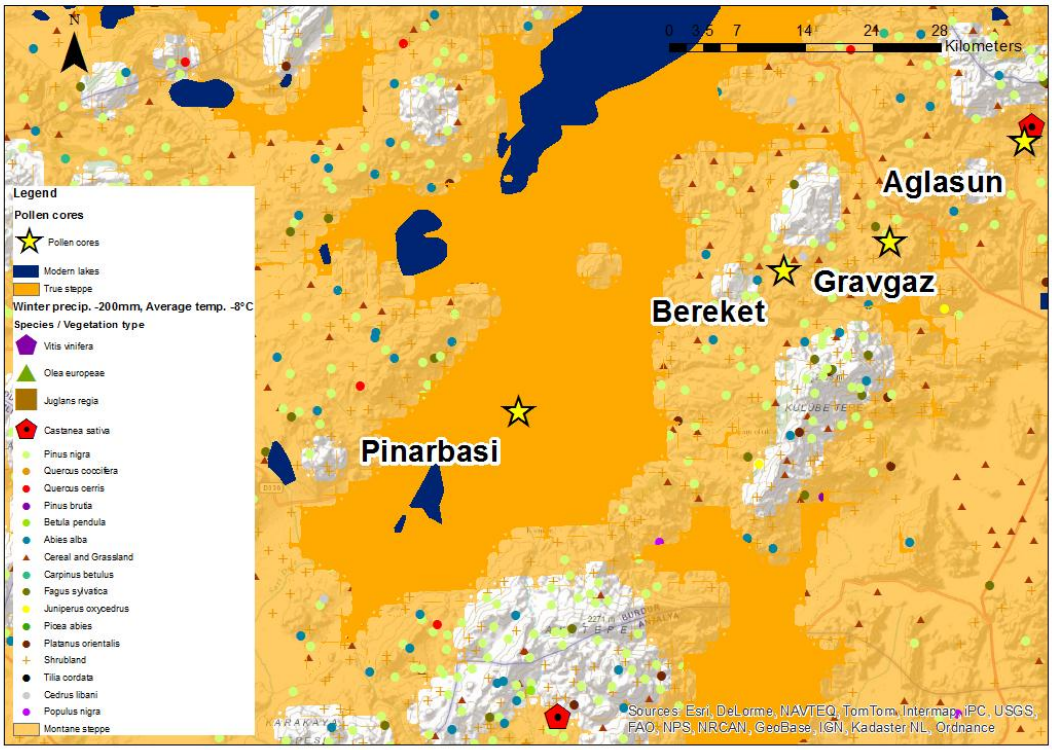


**Figure 8-10 Local vegetation model output around Pınarbaşı under S8-MRs**

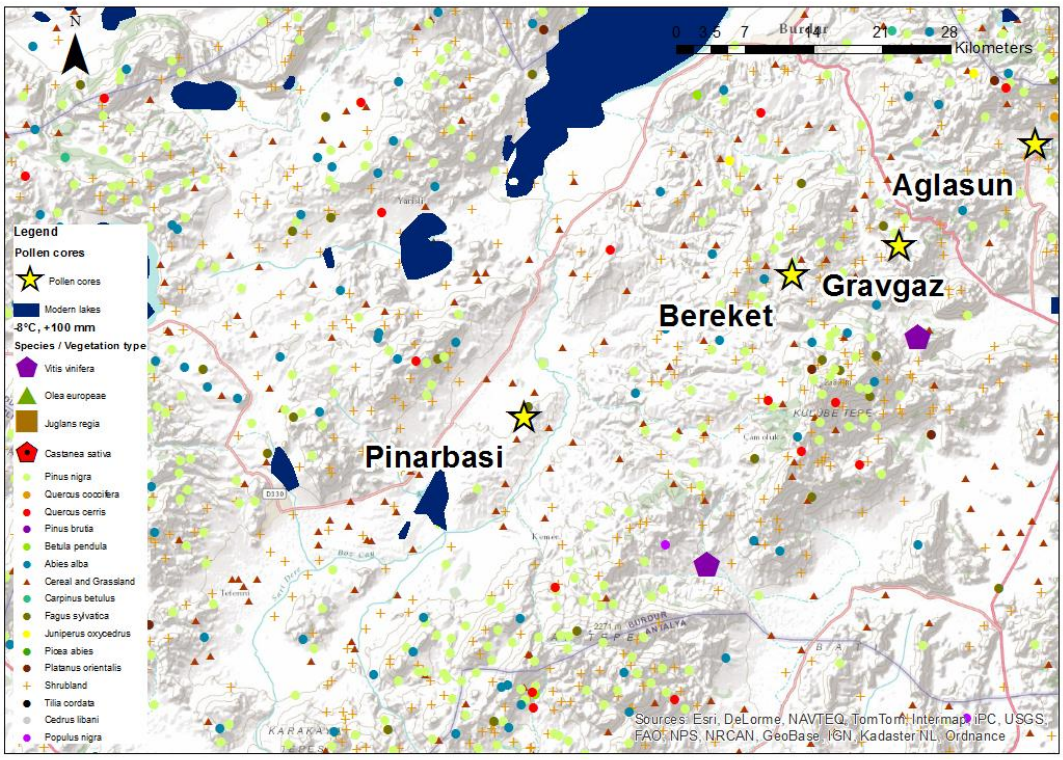


**Figure 8-11 Local vegetation model output around Pınarbaşı under S9-MR1**

Moving further south again, and at slightly lower elevation, the intramontane site of Gölhisar (~900m asl) reflects moderate *Pinus* levels, high NAP, a small amount of *Quercus cerris* and *coccifera* input and very low pollen influx in zone 1. This zone is best correlated with a scenario of cold temperatures (-8°C) but +200 mm precipitation (S9-MR2). As pollen influx in this zone is very low, the evergreen *Quercus* pollen may have appeared through long-distance travel. The modelling results support this as *Quercus coccifera* is not retrodicted to occur within the area of interest (Figure 8-12)

During the next Gölhisar zone (2a), the best correlation between simulated pollen and analytical pollen was reached with a scenario of modern temperatures, and +300 mm winter precipitation (S7-MR3). Under this magnitude of increased winter precipitation, the model predicts an increase in deciduous species, particularly *Quercus coccifera*, but also *Betula, Carpinus, Olea* and *Vitis,* and a small increase in *Pinus nigra, Abies* and grassland. It also predicts a decrease in

steppic indicators, *Fraxinus* and *Juniperus*. Figure 8-13 shows vegetation model output for this scenario, showing widespread *Quercus coccifera*, and a mixture of *Abies, Carpinus, Quercus cerris* and *Juniperus* at higher elevations. It is tentatively suggested that this site may show the potential expansion limit of *Quercus coccifera* at around 8 Cal ka yr BP.

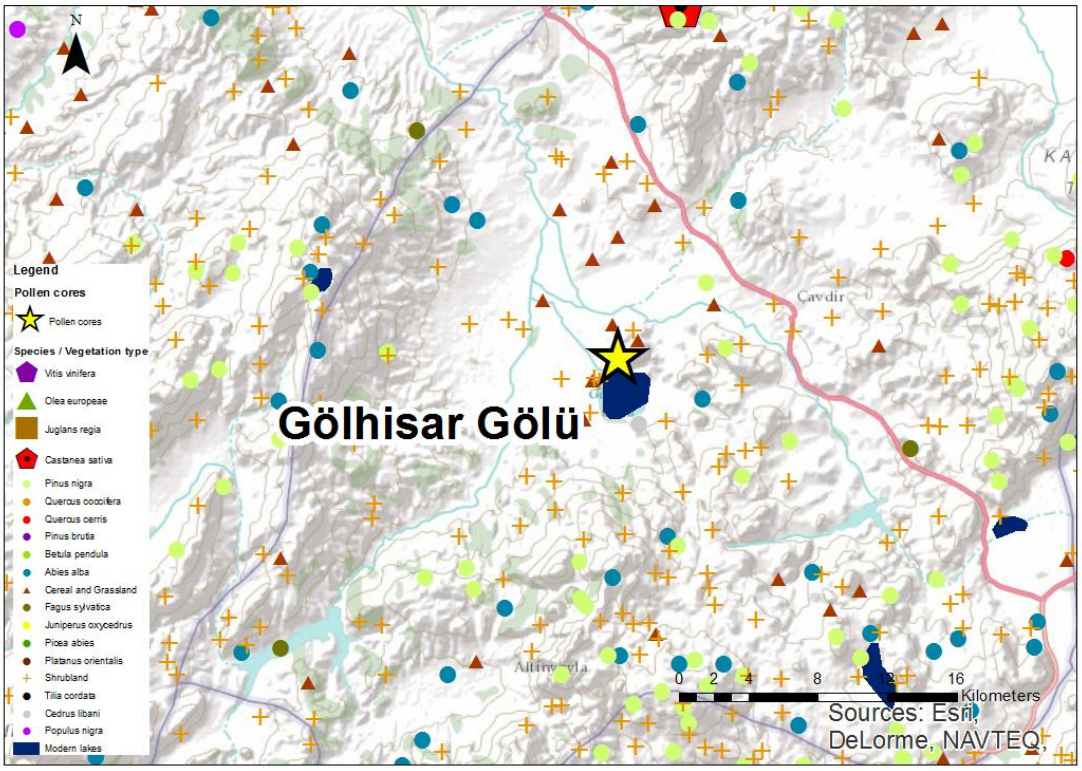


Figure 8-12 Local vegetation model output around Gölhisar under a model run S9-MR2

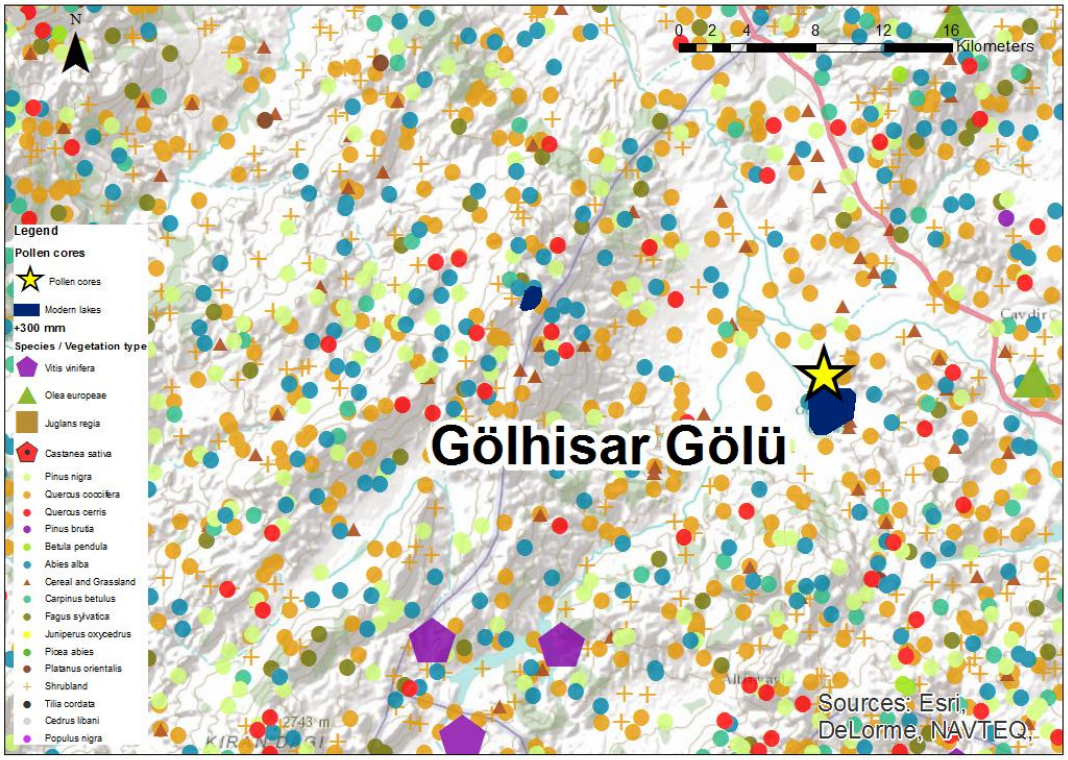


**Figure 8-13 Local vegetation model output around Gölhisar under model run S7-MR3**

The high elevation site of Sögüt (~1400 m) is the next site that has pollen records for this period. Figure 8-14 displays the model output that best matches analytical pollen from zone 3, which represents the period up to at least 10000 Cal yr BP, but potentially up to 8000 Cal yr BP. This zones does not show a tree expansion phase, and as is shown in the figure, the area is composed predominantly of montane steppe, with some clusters of *Pinus* and *Cedrus*, a small amount of *Quercus cerris*, and patches of *Fagus* and *Platanus*.

In comparison to this, Figure 8-15 shows the best fitting situation from the next pollen zone (zone 4). During the tree expansion phase at Sögüt, the best matching scenario is found under increased summer precipitation and also +2°C summer temperature. As at Gölhisar, This is met with an increase in *Quercus coccifera*, however not to the same extent as the site further to the west and at lower elevation. An increase in *Quercus cerris, Betula* and *Carpinus* is also seen. The decrease in steppe has allowed an increase in grassland and Cerealia.

A montane site to the west of SW Turkey, pollen at Gölcük (1049 m) reflects high *Quercus* in the oldest pollen zone; however this is dated to around 9696±1604 Cal yr BP and a lag cannot be supported or denied.

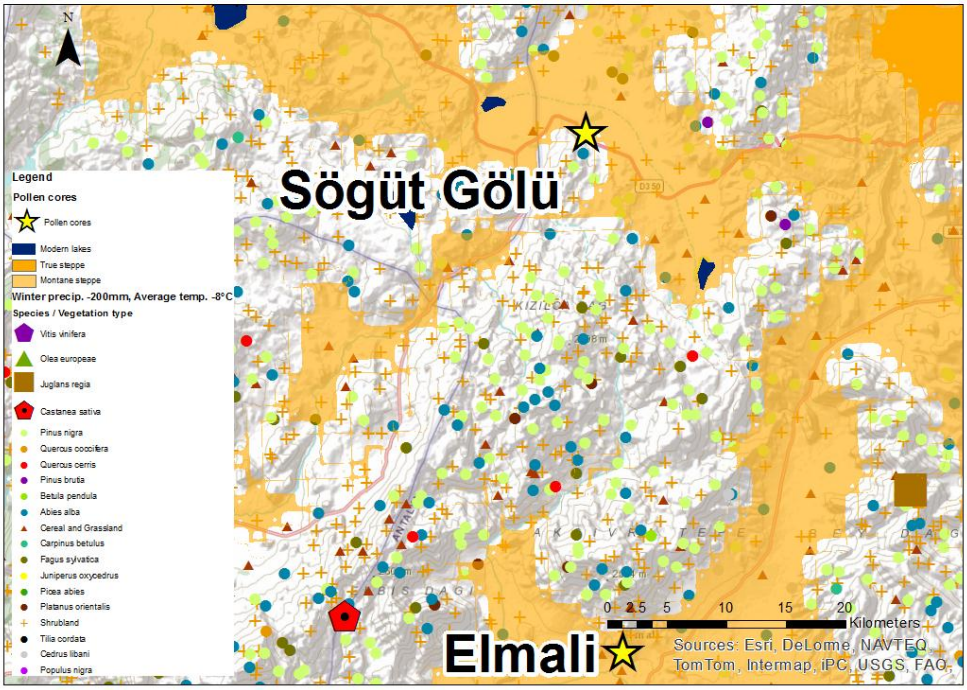


**Figure 8-14 Vegetation model output around Sögüt Gölü before tree expansion, under model run S8-MR2**

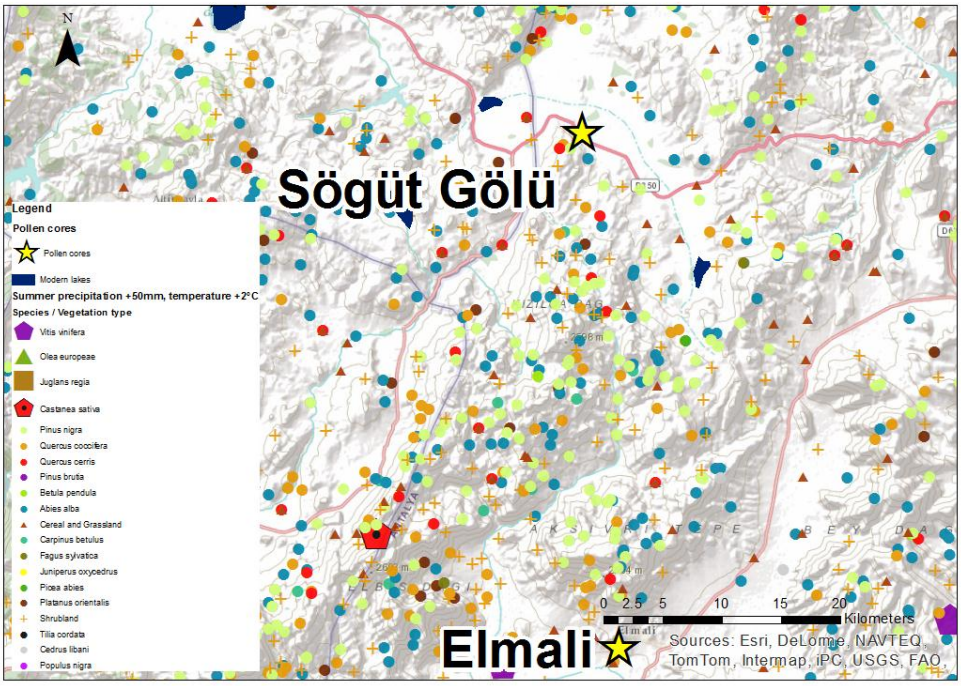


**Figure 8-15 Vegetation model output around Sögüt Gölü under model run S10-MR1**

Finally, the earliest pollen zone from the coastal site of Ova reflects a pollen assemblage with a high proportion of *Quercus coccifera*. The best matching scenario is found under an average temperature increase of 2°C, and the best fitting vegetation scenario is shown in Figure 8-16.

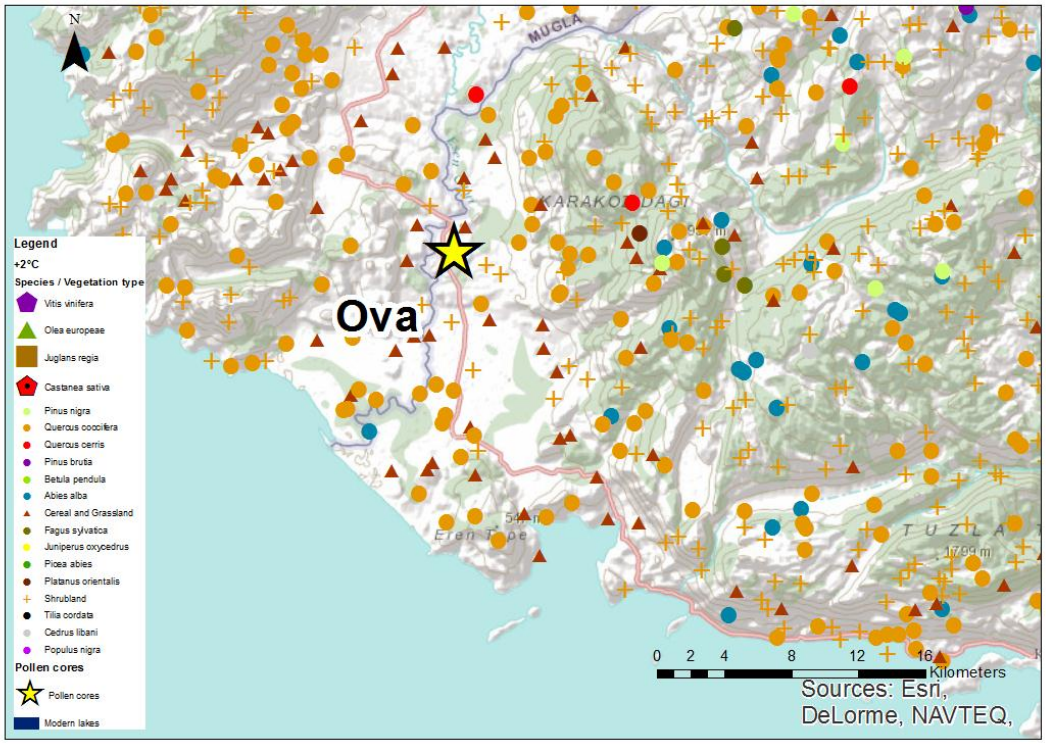


**Figure 8-16 Vegetation model output around the site of Ova Gölü under S5-MR1**

## 8.6 DISCUSSION

As discussed by Brewer et al. (2002) the change between glacial and interglacial period was not smooth or uni-directional. A rapid increase in temperature was witnessed at the beginning of the Holocene, with temperatures increasing rapidly to values above the present day, while increased humidity transfer from the Atlantic Ocean over the European continent resulted in higher precipitation. It is these combined climatic conditions that provided favourable conditions for the colonisation of temperate forest species (Brewer, Cheddadi et al. 2002).

Whereas soil development and species competition is proposed as a mechanism for short scale migrational factors, climatic changes are thought to be the cause of millennial scale changes in vegetation (Whitlock and Bartlein 1997). The results from this modelling study support this theory, as expansion of *Quercus* and *Pinus* woodland is found to be correlated to the increase of precipitation and temperature across southwest Turkey.

The pattern of expansion evidenced in Turkey at the beginning of the Holocene is part of a much larger expansion of *Quercus* across Europe beginning in the Late Glacial period, over a number of millennia. Expansion from primary refugia sites is seen across Italy, the western Iberian coast and the Alps by the middle of the late-glacial interstadial (Nicol-Pichard 1987). However there is little observed increase in Greek and Turkish sites during this period, considered to be due to lack of available precipitation (Bottema 1979; Brewer, Cheddadi et al. 2002). A secondary refugia set across Europe is postulated during the interglacial transition period of the Younger Dryas, when vegetation was again restricted by unfavourable climatic conditions.

From the beginning of the Holocene, a shift in climate to warmer conditions, with increased summer insolation and increasing moisture availability is witnessed (Huntley and Prentice 1993). The spread of oak in this second phase is considered by Brewer et al. (2002) to have been aided by these secondary refugia areas from the Younger Dryas period. A rapid spread is

then seen between ~10 Cal ka yr BP and 8 Cal ka yr BP across France, Ireland and England. However the Alps are considered to be a major barrier to its spread northwards.

Evidence from this study also suggests that *Quercus* spread through southwest Turkey between 10 and 8 Cal ka yr BP. Comparing this evidence with evidence from the Zagros-Anti-Taurus Mountains, *Quercus* spread is delayed until the middle Holocene at around 6300 Cal yr BP (Roberts, Reed et al. 2001; Wick, Lemcke et al. 2003; Djamali, Akhani et al. 2010).

Five main reasons for migrational lag have been defined in previous literature; climatic change, migrational lag, delay in population increase, human disturbance and fire disturbance (Tinner and Lotter 2006). When investigating human and fire disturbance indicators in the spread of *Fagus* and *Abies*, Tinner and Lotter (2006) found no evidence for either human agency or fire being a major contributor to the spread of these two species during the early Holocene. Instead, a cool and wet climate following the 8.2 Cal ka yr BP event was deemed the most likely explanation.

Evidence from southwest Asia suggests that forest migration lag occurred in interior areas due to a climate drier than present during the early part of the Holocene (Roberts and Wright 1993), and Van Zeist et al. (1975) also posits that tree increase in the southwest of Turkey at the beginning of the Holocene is controlled by increased moisture availability, which this study supports.

The results from this study also support those found by Finsinger et al. (2006) who discuss that the distribution of *Quercus* and *Pinus* in the southern Alps during the **Allerød** period is linked to the presence of increased moisture and low temperatures.

In terms of summer climate, it has been hypothesised that changes in insolation at the beginning of the Holocene had an impact on atmospheric circulation, potentially leading to an intensification of Indian summer monsoonal rainfall and an increase in humidity in the northern borderlands of the eastern Mediterranean, i.e. Greece and Turkey (Rossignol-Strick 1987;

Rohling and Hilgen 1991). This in turn may have led to an increase in summer depressions across the Eastern Mediterranean.

Model output from this thesis has found correlation between pollen assemblages and two distinct climatic scenarios. The first is the increase of Quercus from the coast inland, correlated with an increase in average temperature and winter precipitation values. The second is an increase in mixed woodland into higher elevations, correlated to an increase in summer precipitation and temperature. This modelling outcome on its own does not provide sufficient evidence to support the theory of Rossignol-Strick, however it is interesting that the types of species expected to benefit from a rise in summer precipitation and temperature are found to increase at the beginning of the Holocene.

Following bioclimatic mapping of the individual climate envelopes of species, and supplementing this with previous research, *a priori* species information can be employed to discuss these results further. Considering the spread of *Quercus coccifera* at the beginning of the Holocene, this species requires ~140 mm precipitation in the winter, and a similar figure can be said for *Pinus brutia*. Slightly less is required for *Quercus cerris*, ~110 mm of winter precipitation – and it is known that this autumn and winter precipitation is particularly important for the growth of this species. Therefore we would expect *Quercus coccifera* and *Pinus brutia* to be located nearer the coast where slightly higher winter precipitation is found. *Quercus cerris* may be found in more interior regions, but only if autumn and winter precipitation allow.

For *Pinus nigra*, adequate spring and summer precipitation is required. An increase in *Pinus* pollen after a lag in the early Holocene therefore tends to suggest an increase in summer precipitation and temperature as well as winter precipitation, supporting the theory of Djamali et al. (2010)

Comparing these envelopes to grassland requirements, only 94 mm precipitation over winter is required for grassland to thrive. It is therefore not surprising that in the interior areas where

*Pinus* and *Quercus* could not thrive, grassland took over when precipitation only increased slightly, such as at Eski Acıgöl and Karamik.

### 8.6.1 Discussion against archaeological evidence

The early Holocene corresponds to the Aceramic and Ceramic Neolithic period in archaeological classification. These periods witnessed profound economic, social and technological changes which began the transformation of human communities from hunter-gatherers into settled Neolithic village farmers (Turner, Roberts et al. 2010). Anatolia in particular is a crucial flashpoint for Neolithic development due to its geographical position, complex geology and unique topography. Notable sites during this period are Aşıklı Höyük, Çatal Höyük, Can Hasan and Güvercinkayası. There are many important theories surrounding the spread of Neolithic communities that cannot be given justice within this discussion section, but the interested reader is directed to Asouti and Fairbairn (2010) Fairbairn and Weiss (2009) and Duru (1999).

In the early Holocene, it is considered that steppic areas such as the Central Plains of Konya provided an ideal hunter gatherer landscape. The Neolithic hunter-gatherer communities in this area were intricately linked with the presence of large herds of gregarious animals, notably aurochs, mouflon and the wild horse(Schoop 2005). At the same time, evidence from Hacılar between 8500-6500 BC reveals the earliest plant domesticates such as *Triticum monococcum*, *Hordeum spontaneum*, *Triticum dicoccum* and *Lens culinaris*. Barley in particular seems to be the most important crop in Hacılar based on macrobotanical research (Helbaek 1970). Schoop posits that this verdant plains environment provided the perfect conditions for communal societies to develop (Schoop 2005). Archaeological remains have suggested that the Neolithic settlements of the Central Anatolian plains are generally large, cell like structures of buildings clustered in blocks (Schoop 2005). They are generally long term settlements, being renovated and rebuilt multiple times, but on the same plan, and occupation of these settlements is

generally between ~7000 and 5000 BC. They are generally social structures with communal travel over roof structures and through passage ways, but privately owned rooms.

Importantly, this period correlates with modelling results suggesting an increase in precipitation across southwest Turkey. An increase in Gramineae is first evidenced at the interior plains site of Karamik at the beginning of the Holocene, followed by an increase in *Pinus* and *Quercus*.

Typical settlements in the southwest 'Lake District' are found to be considerably smaller than the Central Anatolian Plains, with the earliest evidence only appearing from ~6400 BC, after the establishment of trees across the southwest.

Settlements tend to be laid out linearly and are situated in the basins and the open shorelines of the lakes, suggesting access to water, and open, valley landscapes were preferable. Despite a long stratigraphical record there is little evidence for regular rebuilding on the same plan, as was the case in the Central Plains. Buildings tend to be free-standing one room houses with lots of space. In contrast to the roof entrance model of the plains, the entrance here is at ground level (Schoop 2005). The theory posited by Schoop is that the dense woodland, complex topography and relative isolation of the southwest led to more individualistic societies, that had adapted to hunting in topographically difficult, wooded areas. Forests near the coastal regions and into the Oro-Mediterranean zone were likely to have been particularly dense based on modelling studies. This is interesting when compared to the distribution of Neolithic sites from the Tay GIS as shown in Figure **8-17**, and expanded in Table 8-5 (With a key in Table 8-6). Firstly, there is a relative lack of sites located in the coastal and Eu-mediterranean zone. It is interesting to question whether this could be due to the density of woodland precluding traditional hunter-gathering practices, or early cultivation of cereals in this area? (Of course it could instead amount to a preservation bias issue.) A further point to note considering category 4 in Table 8-5 is that there are a significant amount of Neolithic sites (particularly clustered in present day Burdur province) that are located in areas that were modelled previously as steppe

for the Epipalaeolithic period - although clearly, the potential for preservation bias must be kept in mind. Was this area particularly chosen because it provided a relatively open landscape still, allowing traditional hunting practices alongside small scale cultivation or grazing?

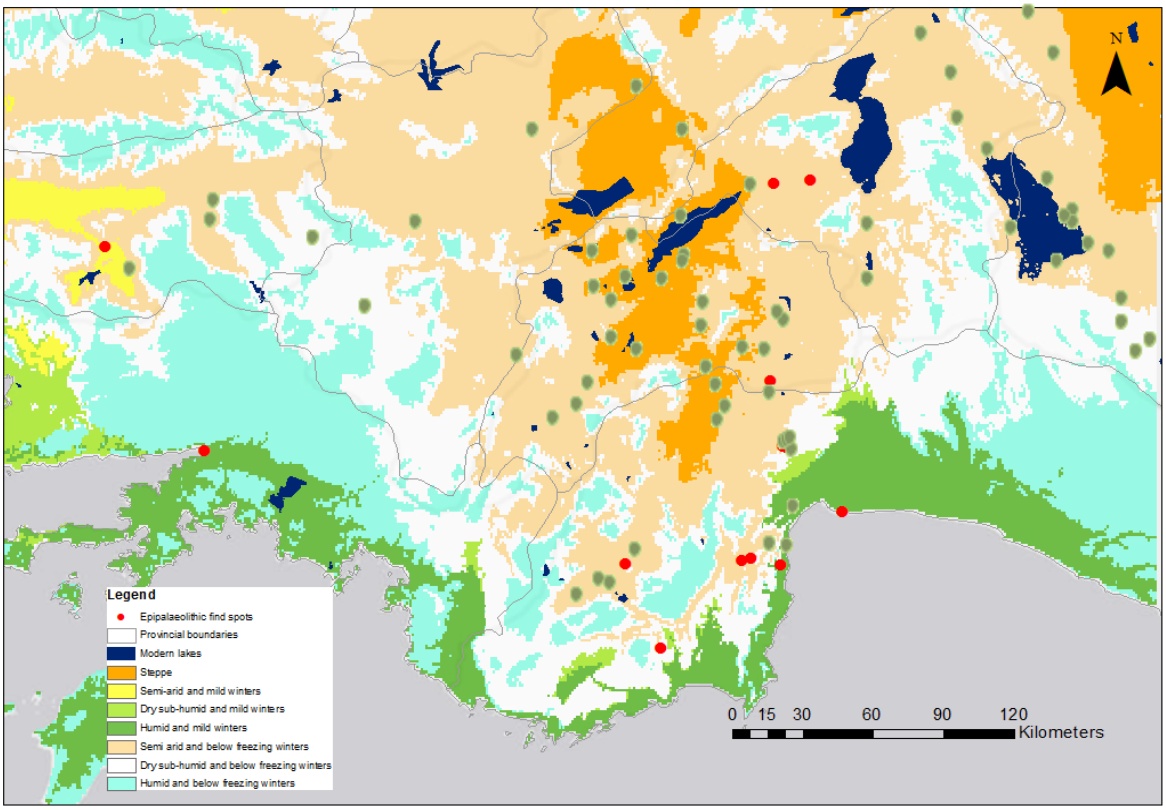


Figure 8-17 Epipalaeolithic and Neolithic archaeological find density (green points) showing area that was modelled as steppe during the Late Glacial period.

**Table 8-5 A cross reference of Neolithic find sites with modeled climate classes during the Late Glacial period**

| | Climate (key in Table 8-6) | | | | |
|---|---|---|---|---|---|
| **Province** | **1** | **2** | **3** | **4** | **5** |
| **Aydin** | Cine Tepecik | | Aphrodisias - Pekmez | | |
| | Kavaklikahve | | | | |
| | Hamidiye | | | | |
| **Denizli** | Karakurt | | Baharlar | Candir Hoyuk | |
| | Surmeli Hoyuk | | Camur Hoyuk | | |
| **Burdur** | Cavdir | | | Kagilcik Magarasi | |
| | Karamusa | | | Yenice | |
| | Seydiler | | | Duden | |
| | Baskuyu 1 | | | Sazak | |
| | Kanlitepe | | | Derekoy 1 | |
| | Golde | | | Hacilar | |
| | Aziziye | | | Kuracay | |
| | Karaaliler | | | Cigirtkankaya | |
| | Hoyucek | | | Ilyas 1 | |
| | Incirdere | | | Kecili | |
| **Antalya** | Akcay 1 | Beldibi / Kumbucagi | Gokhoyuk | Efeoglu | |
| | Hacimusalar / Beyler | Domuzburnu / Gurma | | Yagca Tas Hoyuk | |
| | Tekke | | | Kizlar Hoyuk 4 | |
| | Gokpinar | | | Eskikoy Yeri | |
| | Belbasi | | | | |
| | Carkini | | | | |
| | Karain Magarasi | | | | |
| | Bademadaci | | | | |
| **Isparta** | Kovada Golu | | | Incirlitepe | |
| | Tepeli | | | | |
| | Yenikoy Hoyuk | | | | |
| | Yakaemir | | | | |
| | Kuyucak | | | | |
| | Teknepinar | | | | |
| | Topraktol | | | | |
| **Konya** | Alan Hoyuk | | Seydisehir Hoyuk | | |
| | Erbaba | | Suberde / Gorukluk Tepe | | |
| | Yilan Hoyuk | | Kanal Hoyuk | | |
| | Beysehir Hoyuk C | | | | |
| | Cukurkent | | | | |
| | Cem Cem | | | | |
| | Bektemur Hoyuk | | | | |
| | Hanvakfi Eski | | | | |
| | Yorukmezari | | | | |
| | Golyolu | | | | |
| **Afyon** | | | | Ak Hoyuk | |

**Table 8-6 Climate key**

| Code | Climate |
|---|---|
| **1** | Semi-arid and below freezing winters |
| **2** | Humid and mild winters |
| **3** | Dry sub-humid and below freezing winters |
| **4** | Steppe |
| **5** | Humid and below freezing |

That local sources of wood were also important to Neolithic communities is attested to at Çatal Höyük, where it has been demonstrated that wood in the early phase of Neolithic settlement was collected from local wetlands, and over time, more intensive harvesting from local foothills became apparent (Fairborn 2005; Fairbairn and Weiss 2009; Longford, Drinnan et al. 2009; Asouti and Fairbairn 2010). What part the expansion of woodland, and the types of species available in different areas played in the use of wood by early settlers is an interesting question, and the extent to which woodland was seen as an attractive landcover, versus a difficult terrain to hunt and farm within. Evidence of forest fire activity also increases at the beginning of the Holocene (Wick, Lemcke et al. 2003) although it is difficult to discern whether this is evidence of human clearance or natural forest fires, and pollen data for deforestation during this time period for Beyşehir suggest that at ~7000 Cal yr BP, an increase in *Centaurea solstitialis* may be associated with the deforestation of *Quercus* (Bottema and Woldring 1984)

Schoop (2005) identifies Anatolia as the critical interface between east and west Neolithization, whilst noting that it was only around 8000 BC (mid PPBN) that a production economy was established in Central Anatolia, significantly later than that of the Fertile Crescent further east. Schoop suggests that this is because of the geographical isolation of the Central Plains from other regions due to the high mountain chains and dense forest surrounding the region. However, this is caveated with the knowledge that trade links were established both east and west during this period so is not wholly convincing. It is instead posited from this study that the

beginning of production coincides with the timing of increased winter precipitation across the region resulting in the expansion of cereals. The fact that these species are all self-pollinators means that they cannot be easily traced in pollen records. However, the increase in Poaceae and Cerealia during the early Holocene has been identified in the pollen record of Karamik. Model results suggest that the climate became favourable enough for these species to become more prevalent at around 8000 BC, potentially allowing local communities to grow crops and graze animals with more stability.

It is also interesting to note that the period covered by the first zone of the coastal pollen core of Ova is likely to cover the same period as the sophisticated human occupation discovered by archaeologists throughout the southwest Turkish lake district, at sites such as Hacılar, Kuruçay, Höyücek, Bademagacı and Karain cave. Utilising Bayesian techniques, these occupation phases have been mapped by Thissen (2010); an example from Hacılar is shown in Figure 8-18.

Even though most known Neolithic sites were not found in the coastal regions, through pottery typology, Thissen infers that Neolithic communities had trade links and travelled widely around southwest Turkey. If this inference is accepted, it is likely that Neolithic settlers may have come into contact with a mixture of Eu-Mediterranean species such as *Olea* and *Vitis* on an ad-hoc basis. Evidence for *Olea* and *Vitis* pollen is also found throughout most of the Köyceğiz pollen core, the bottom of which is modelled to start between 7318 Cal yr BP to 5453 Cal yr BP, again during either the Ceramic Neolithic or the Chalcolithic. Furthermore, there is the possibility that pollen zone 2a at Ağlasun, which reflects *Juglans*, *Olea* and *Platanus* may start between 6568 and 5793 Cal yr BP.

Evidence at Can Hasan suggests that *Juglans regia, Prunus* and *Crataegus* may show evidence of early cultivation (Woldring and Cappers 2001) but even if this is not accepted, it does represent the exploitation of naturally occurring fruit trees by Neolithic communities (Zohary and Hopf 1993).

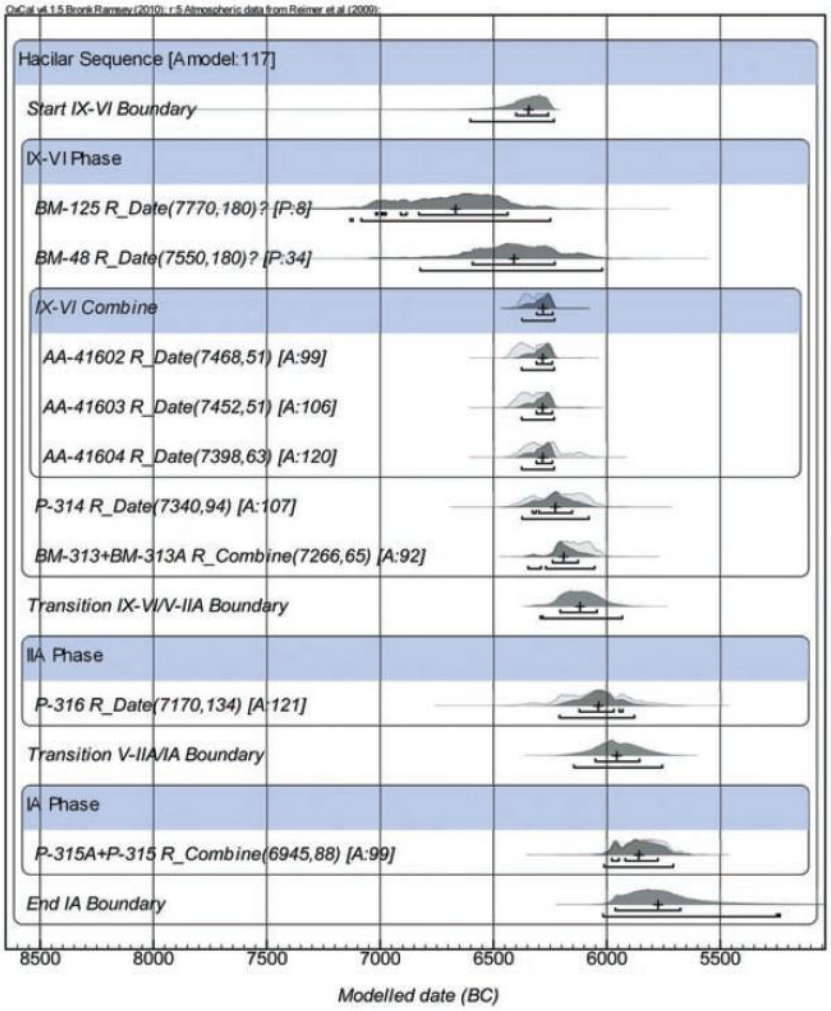


**Figure 8-18 Bayesian modelling of $^{14}C$ dates showing the stages of occupation at Hacılar during the Neolithic (From Thissen 2010).**

## 8.7 SUMMARY OF FINDINGS FOR RESEARCH QUESTION 2.

At the beginning of the Holocene NAP and particularly *Artemisia* in pollen core evidence is high. Some evidence exists at Karamik for an increase in Gramineae and Cerealia, matching evidence from Eski Acigöl and Lake Van. When tree pollen percentages do increase, there is a split between predominantly *Pinus* at Karamik and Pınarbaşı, and deciduous *Quercus* at Sögüt, Gölhisar and Gölcük. The difference between the marginal plains area of Karamik, where grassland is important in the early Holocene, the Oro-Mediterranean site of Pınarbaşı, where *Pinus, Cedrus* and *Abies* is found in more abundance, and the *Quercus coccifera* and *Pinus brutia* found at Ova, Gölhisar and Sögüt is notable.

When this patterning of vegetation was examined chronologically, modelling analysis does suggest a lag in tree expansion was evident in southwest Turkey at the beginning of the Holocene. This therefore accepts the alternative hypothesis of the Research Question (H1). Furthermore, modelling supports the suggestion of a climatic reason for this expansion, therefore supporting alternative hypothesis H2.

Chronological modelling using Bayesian analysis has allowed the investigation of the age of onset of significant tree expansion, which suggests that the expansion of trees during the early Holocene may not have been synchronous across the region, adding new evidence to the debate.

# 9 RESEARCH QUESTION 3: VEGETATION MODELLING FRAMEWORK RESULTS AND DISCUSSION

## 9.1 RESEARCH QUESTION

To what extent can the model framework inform whether phases of cultivation during the Beyşehir Occupation Phase (3.8 to 1.4 Cal ka yr BP) were influenced by climate and mediated by human agency?

## 9.2 RESEARCH QUESTION HYPOTHESES

Four hypotheses were established for this research question, the first of which posited that the beginning of the Beyşehir Occupation Phase was synchronous across southwest Turkey. The second hypothesis posited that evidence exists for the continuation of cultivation throughout the Mid-Bronze Age. The third hypothesized that climate change is implicated in the expansion of the Beysehir Occupation Phase, and the fourth posits that the end of the phase is synchronized across southwest Turkey. These hypotheses will be supported or rejected by the model output.

**Figure 9-1 Hypotheses for Research Question 3**

| |
|---|
| H1: The beginning of the BO phase is synchronous across southwest Turkey<br><br>H0: The beginning of the BO phase is not synchronous across southwest Turkey |
| H2: Chronological modelling suggests the continuation of cultivation throughout the Mid-Bronze Age<br><br>H0: Chronological modelling does not suggest the continuation of cultivation throughout the Mid-Bronze Age |

| |
|---|
| H3: Climate change is implicated in the expansion of the BO phase during the Hellenistic to Late Roman period<br><br>H0: Climate change is not implicated in the expansion of the BO phase during the Hellenistic and Late Roman period |
| H4: The end of the BO phase is synchronized across southwest Turkey<br><br>H0: The end of the BO phase is not synchronized across southwest Turkey |

## 9.3 CHRONOLOGICAL MODELLING

### 9.3.1 Evidence for a proto Beyşehir Occupation Phase?

The Beyşehir Occupation Phase has generally been estimated to encompass the period from 3500 / 3200 $^{14}$C BP to 1500 $^{14}$C BP based on pollen records from Beyşehir Gölü (Bottema, Woldring et al. 1986; Eastwood, Roberts et al. 1998; Vermoere, Bottema et al. 2002; England, Eastwood et al. 2008).

As more cores have been analyzed however, and occupation phases identified in further pollen sequences, a more complex chronological picture is emerging which requires deeper investigation. Figure 9-2 shows the un-calibrated radiocarbon ages from cores in the region, suggesting that the occupation phase may begin as late as ~2270 $^{14}$C BP in some cores, and last until ~1200 $^{14}$C BP. The end of the phase has been best constrained at Gölhisar to the 7$^{th}$ century AD (Eastwood, Roberts et al. 1999), however the end of the phase at other sites such as Bereket and Sögüt was interpreted to be earlier. Importantly, the mixture of un-calibrated and calibrated radiocarbon ages previously made it challenging to understand the spatial and temporal nature of the phase, and also challenging to compare palaeoecological data with archaeological data. One of previous debates surrounding the Beyşehir Occupation Phase was therefore the extent of its regional synchronicity.

| Place | Radiocarbon age ($^{14}$C yrs BP) | Depth (cm) |
|---|---|---|
| Beyşehir Golu I[1] | *c.* 3500 BP – *c.* 1550 BP | 300–120 |
| Köyceğiz Gölu[1] | *c.* 3200 BP – *c.* 2900 BP | 410–370 |
| Söğüt Gölu[1] | *c.* 3000 BP – ?1900 BP | 210–110 |
| Pınarbaşı[2] | *c.* 3000 BP – *c.* 1200 BP | 150–90 |
| Gölhisar Gölu (GHA/B.92)[3] | *c.* 3000 BP – *c.* 1300 BP | 260–90 |
| Gravgaz 1996[4] | *c.* 2280 BP – *c.* 1270 BP | 521–261 |
| Gravgaz 1999[5] | *c.* 2270 BP – *c.* 1480 BP | 453–182 |

**Figure 9-2 Comparison of duration and depth of the Beyşehir Occupation Phase in some pollen cores from SW Turkey. After Vermoere, Bottema et al. (2002). Data from: [1]van Zeist et al. (1975); [2]Bottema and Woldring (1984); [3]Eastwood (1997); [4, 5]Vermoere et al. (2000);**

Despite a number of coring and analysis efforts, a complete comparison of the temporal onset of arboriculture across regional records had not previously been quantitatively attempted due to a limited number of chronologically well constrained sediment cores. The use of Bayesian statistical analysis undertaken as part of this thesis goes some way towards the reassessment of this data, to better understand the potential spatial and temporal patterning of arboriculture across the region and to provide a new lens through which to formulate key hypotheses and questions about the period.

In order to assess the definition of the Beyşehir Occupation Phase, each core was analysed to identify the first pollen zone in which an indication of potential arboriculture is found. This is identified as those zones that show a significant proportion of pollen (i.e. over 1%) from a species that is usually associated with arboriculture, such as *Olea*, *Vitis*, *Juglans* or *Castanea*. The posterior age estimate of these pollen zones that reflect a potential arboriculture signal were plotted as shown in Figure 9-3. By plotting these zones on one chart, it is possible to understand where and when species commonly used as cultivation indicators are first found in pollen

records of southwest Turkey. The envelope of 1400 Cal BC to 600 Cal AD was then overlaid in the figure (in green) to represent the 'traditional' temporal extent of the Beyşehir Occupation Phase. This allowed an examination of both how well the synchronized pollen zones fit into the traditional temporal extent, and how cultivation may have expanded through time.

The modelling includes more recent evidence from Ağlasun alongside evidence from other pollen sites, and shows that the onset of significant proportions of fruit tree pollen is actually much dispersed through time, and does not only find its first expression at the traditional start of the Beyşehir Occupation phase for most sites. Furthermore, there is a potential division between those sites that show very early fruit tree indicators such as the sites of Ova, Köyceğiz and Ağlasun, and the rest of the sites which show cultivation during the traditional Beysehir Occupation Phase.

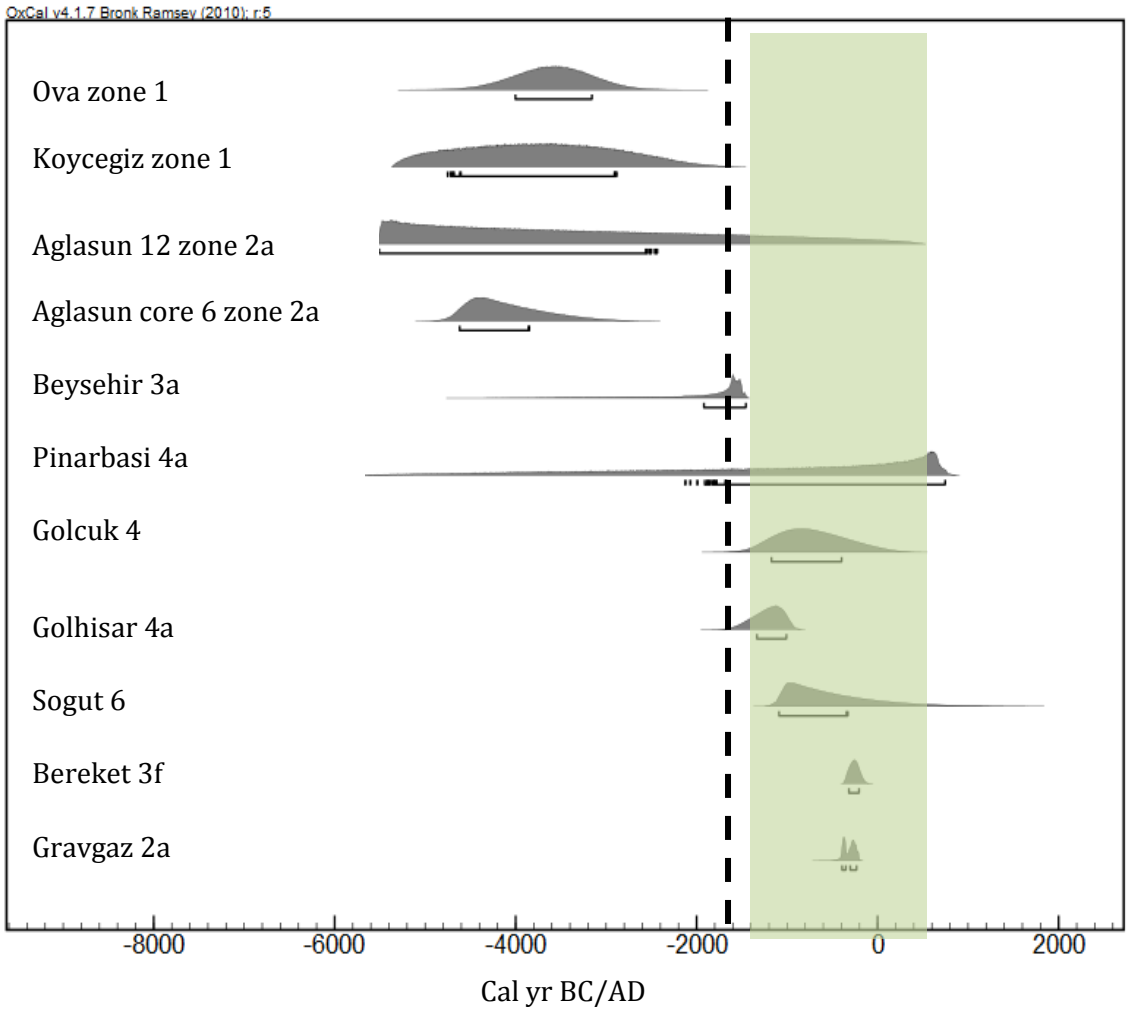


**Figure 9-3 This figure shows posterior age estimates for the beginning of pollen zones that first contain a significant percentage of pollen from species that are commonly cultivated. The original temporal extent of the Beyşehir Occupation Phase is shown in green, and the position of the Santorini tephra is the black dashed line. Brackets show the 68.2% highest probability density range.**

Figure 9-4 displays the potential order of onset spatially, along with associated chronological uncertainty. This allows a moderate trend to be found; that of the expansion of fruit tree indicators appearing at the coast during the Chalcolithic and Bronze Age, then expanding into inter-montane valley sites during the Iron Age, gradually pushing into higher elevation (Sögüt, number 8), Bereket, Gravgaz and the interior site of Hoyran (number 11) during the . Cultivation indicators are not found at site 12 (Karamik), one of the most interior sites.

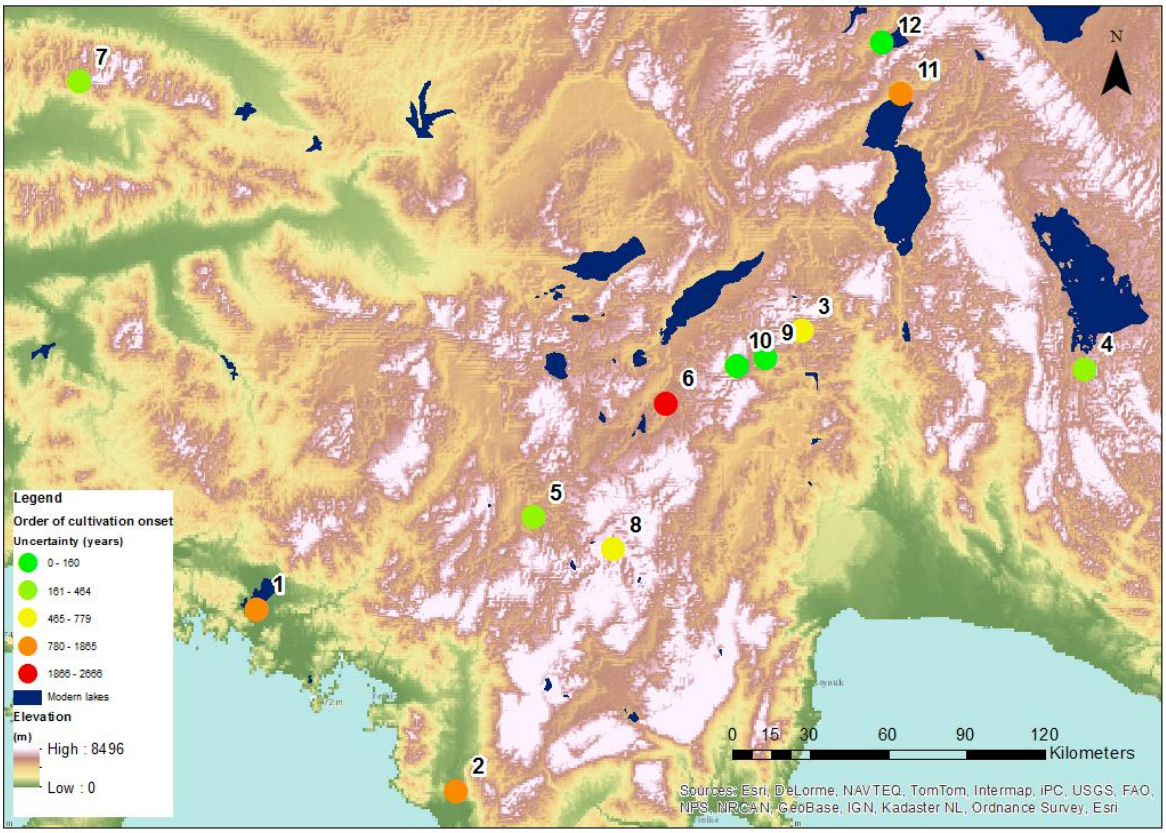


**Figure 9-4 Map of southwest Turkey showing the order that potential arboriculture indicators appearing in pollen core records.**

In terms of the species, significant amounts of *Olea*, but also *Pistacia*, *Platanus* and Poaceae / Gramineae (along with small amounts of *Plantago*, *Sanguisorba* and *Cerealia*) is found at the three early sites of Ova, Köyceğiz and Ağlasun. Modelling suggested that core 12 zone 2a at Ağlasun was likely to start being deposited between ~7450 and 4375 Cal yr BP (68.2% hpd), and core 6 zone 2b was likely to start being deposited between 5250 and 4471 Cal yr BP (68.2% hpd), which places this change during the late Chalcolithic to early Bronze Age.

Significantly, these species are classified by Bottema and Woldring (1984) as natural distributions, and the potential use of them by Chalcolithic communities is not alluded to. Putting aside the limited proportion of fruit tree pollen, if the species assemblage is judged under the later Beyşehir Occupation Phase criteria, we see that fruit tree pollen, along with

Cerealia and disturbance indicators make up the traditional trio of cultivation indicators. It is only the small proportion of these species that is different from the later phase.

From an archaeological perspective, it is the case that important societal developments are evident during the Chalcolithic, the most obvious being the development of charcoal-dependent industries leading to clearances of trees (Smith 1996). The Chalcolithic period sees a change in settlement pattern compared to the earlier Neolithic, with villages confined by perimeter walls, potentially reflecting a change in social structures, economies and settlement hierarchies, moving towards a chiefdom system (Vanhaverbeke and Waelkens 2003).

Combining this with evidence for the development of irrigation agriculture at Hacılar (Helbaek 1970) and an increasing population, is it then plausible to suggest that the presence of these species may actually point to low level arboriculture, or the development of new farming techniques? The correlation of three pollen sites reflecting fruit tree pollen through Bayesian modelling perhaps adds weight to the statement by Vermoere that it is during this period that farmers and herdsmen started to exploit valleys and mountain slopes in such an exhaustive way that it is recorded palynologically (Vermoere 2002). Whilst not of the same magnitude as the later Beyşehir Occupation Phase, is this the reflection of a proto-occupation phase? Settlement patterns of the Early Bronze Age are mainly small open villages, and seasonal camp sites inhabited by pastoral groups, many of which show continuation with earlier Chalcolithic structures (Vanhaverbeke and Waelkens 2003). In comparison, the main feature of the end of the Early Bronze Age (around 2000 to 1600 BC) is a sudden decline in the number of sites, with some evidence of violent destruction and conflagration (Vanhaverbeke and Waelkens 2003). During the Middle to Late Bronze Age, the Luwian culture dominated Western Anatolia, however archaeological evidence for settlements during this period is rare, and the overarching impression is one of a grave decline in material culture (Vanhaverbeke and Waelkens 2003). Settlement patterns are considered to be in the main centered around small agricultural communities (Vanhaverbeke 1999), although the potential importance of Assyrian mercantile

settlements in other areas of Turkey is also discussed by Vanhaverbeke and Waelkens (2003). This background sets the scene for investigation of the second hypothesis in this section, that of the potential continuation of cultivation during the Mid-Bronze Age, despite cultural upheaval.

### 9.3.2 A re-assessment of palaeoecological records throughout the Mid-Bronze Age.

Previous discourse has highlighted the apparent contradiction between pollen records suggesting continuity of cultivation throughout the Mid Bronze Age, and the absence of archaeological records. Two theories were suggested to explain this contradiction, either superposition had occurred and MBA settlements had turned into Iron Age settlements, or the resolution / chronological accuracy of the pollen cores was such that a hiatus in cultivation could not be distinguished. Following Bayesian modelling and synchronization of pollen cores, it is now possible to reassess this contradiction.

The key period of absence from archaeological records is between ~2000 / 1900 BC, and 1600 BC.

**Table 9-1 Pollen zones correlated with the 2nd millennium BC, and evidence for cultivation**

| Site | Zone | Conditions | Zone Begins (68.2%) | Rule out hiatus in cultivation during 2nd millennium BC? |
|---|---|---|---|---|
| Ova | Hiatus | Assemblage with *Olea* pollen turns into Hiatus | Between 5400 BC and 4900 BC | No |
| Köyceğiz | 3c | *Vitis* and *Olea* pollen turns into Pinus forest with negligible human impact | Between 2387 BC and 1446 BC | No |
| Sögüt | 5 | Increase in *Pinus*. No cultivation indication. | Between 3478 BC to 1068 BC | No |
| Gölhisar | 3 | *Pinus*, and peak in *Artemisia* following tephra layer | Between 2611 BC and 1647 BC | No |
| Pınarbaşı | 3b | *Cedrus*, Open vegetation. Only Cerealia at end of zone | Between 3350 BC to 607 AD | No |
| Beyşehir | 3a | Decrease in *Pinus* and *Cedrus*. Increase in *Fraxinus ornus*, *Juglans* and *Castanea*. Increase in *Plantago*. Increase in deciduous *Quercus* and *Juniperus*. High *Salix* | Between 1921 BC to 1457 BC | Yes |
| Ağlasun 6 | 2c | Coniferous forest | Between 2614 BC to 1864 BC | No |
| Ağlasun 12 | 2a | Cultivation indicators | Between 5511 BC to 2426 BC | Yes |

| | | | | |
|---|---|---|---|---|
| Hoyran | 1 | High *Pinus*, *Cedrus* and *Artemisia* | Between 3809 BC to 2478 BC | No |
| Gölcük | 5a | Poor pollen preservation, *Pinus*, *Quercus coccifera* and *Artemisia* | Between 6422 BC to 1429 BC | No |
| Karamik | 6 | Coniferous forest | | No |

Comparing each pollen core in turn, although Ova is one of the first sites to show *Olea* and *Vitis* pollen, the phase at this core is lost at around 5400 and 4900 BC (i.e. during the Chalcolithic period) due to a hiatus. The pollen record is not recovered until after the Bronze Age. A hiatus can occur for many reasons, either through a period of aridity, a series of hot summers, or changes in hydrological geology leading to a temporary drying up of the Ova basin. It is not necessarily the case that *Olea* and *Vitis* stopped growing in the basin at this time, but no records survive to show this one way or the other.

At Köyceğiz, cultivation indicators for the period between 2000 and 1600 BC are also not significant, as a decline in *Olea* and *Vitis* is seen, concurrently with an increase in *Pinus*. This increase in *Pinus* is also found at Sögüt and Gölhisar, and predominantly coniferous species are also found at Pınarbaşı, Ağlasun, Gölcük and Karamik with varying levels of chronological certainty. Evidence for cultivation is found at Beyşehir and Ağlasun, however both of these zones have high chronological uncertainty. Thus, there is no convincing evidence for a continuation of cultivation throughout the Mid-Bronze Age.

The Late Bronze Age period begins at around 1600 BC, and correlates to the eruption of Santorini, which is evidenced in pollen cores across the region. Following this marker, an increase in cultivation is again seen across the region. In fact, following Bayesian modelling, the chronological boundary for the beginning of cultivation at Beyşehir (between 1890 and 1457 BC) does not preclude it from also being deposited after the Santorini tephra layer.

The main settlement sites in the Late Bronze Age are the sites of Troy and Beycesultan. Although evidence for settlements is again rare, the importance of Indo-European based cultures, and in particular the importance of the Luwian state of Arzawa is attested to in Hittite

sources. The origins of this Luwian culture, and the influence of the later Hittite and Hurrian cultures are also discussed in relation to southwest Turkey in Vanhaverbeke and Waelkens (Vanhaverbeke and Waelkens 2003).

### 9.3.3 The Anatolian Dark Ages

Following the fall of the Hittite Empire, scholars are divided as to whether the region of southwest Turkey falls into an 'Anatolian Dark Age' at the beginning of the Iron Age (~1200 BC). Archaeological evidence is scarce, however questions remain as to whether the chronological framework that identifies the phase is valid (James, Thorpe et al. 1991; Vanhaverbeke and Waelkens 2003).

Again, comparing this phase with pollen evidence, it is interesting that Beyşehir shows a reduction in cultivation indicators at around 1000 BC, and does not recover even after the Anatolian Dark Ages. There is also a pause in cultivation indicators at Köyceğiz at this time, and a further hiatus is found at Ova. Furthermore, although it is possible that cultivation was present at Gölcük and Gölhisar, it is more likely that they began cultivation in the later Iron Age. Thus, following chronological modelling, no convincing evidence can be found in this analysis for significant cultivation during the Anatolian Dark Ages.

### 9.3.4 The beginning of the Beysehir Occupation Phase, and the expansion of cultivation during the Iron Age, Hellenistic and Roman period

The Iron Age represents the beginning of an expansion of agricultural signatures in a number of pollen cores across southwest Turkey. It reflects the arrival of the Phrygian culture into Anatolia at around the 9$^{th}$ century BC, who extended their influence perhaps as far south as Elmalı, and as

far west as Sardis and Lydia. A second important cultural shift is seen with the introduction of the Lydian culture between ~685 to 547/6 BC.

Bayesian modelling is used here to examine potential patterns in the expansion of this agricultural signature across southwest Turkey. Figure 9-6 displays the point at which pollen cores across the southwest that first show an increase in agricultural pollen during this period, representing the Bayesian Occupation Phase. Table 9-2 shows the 68.2% highest probability density range for the beginning of each pollen zone associated with this increase, along with a median value. Chronological analysis shows that Pınarbaşı, Gölcük, Gölhisar and Sögüt all begin to show cultivation indicators around the 7th Century BC, that of the traditional beginning of the phase. This is also around the time that Köyceğiz re-establishes cultivation indicators.

Calibrating this sequence with calendrical dates also allows us to correlate this period with the Lydian period. This is particularly of note, as the kingdom boasts a dynastic sequence, and can be gathered from the Greek tradition, first of all from Herodotos (Vanhaverbeke and Waelkens 2003) The Lydian rule extended its rule westward from the Greek city states. The link with Greece was strong, and the reign of Kroisos, son of Alyattes is closely linked with Greek history. One wonders whether the expansion of *Olea* and *Vitis* cultivation during this period was in part a further facet of the imposition of hegemony over western Anatolia. An increase in organisation, communication, commercial and military routes and stable conditions as discussed by Vanhaverbeke and Waelkens (2003) suggests that the Lydians were active in changing the landscape of Anatolia during this period.

Following the defeat of the Lydian king Kroisos by the Persian leader Kyros, Asia Minor became part of the Persian (Achaemenid) empire. This period is considered to be a period of relative peace as discussed by Vanhaverbeke and Waelkens (2003), until the expansion of the troops of Alexander the Great through Asia Minor at 334-333 BC marked the end of the Achaemenid rule of Asia Minor, and the beginning of the Hellenistic period in southwest Turkey (Vanhaverbeke and Waelkens 2003).

Further cultivation indicators are found at the sites of Bereket and Gravgaz, which have a median start date of around 300 BC. Tentatively, this seems to suggest cultivation expansion during the Hellenistic period, however it is important to note that core records were not available for any time prior to the 7th century BC and so it is unknown whether cultivation occurred before this period.

As well as the archaeological and historical narrative, a further interesting feature of this cultivation phase can now be established following chronological modelling. Figure 9-4 displays the potential order of onset spatially, along with associated chronological uncertainty. This allows a moderate trend to be found; that of expansion of cultivation indicators from the coast, following inter-montane valleys, gradually pushing into higher elevation (Sögüt, number 8) and interior (Hoyran, number 11) sites. Cultivation indicators are not found at site 12 (Karamik), one of the most interior sites.

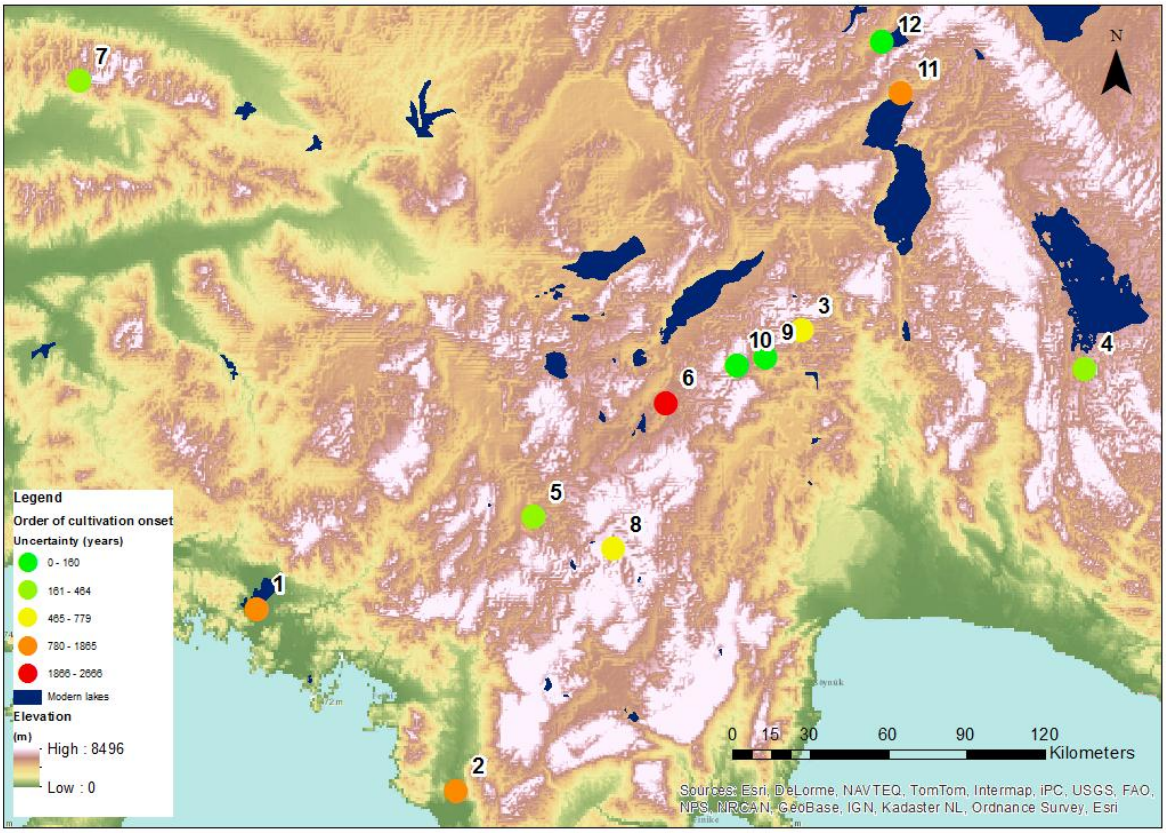


**Figure 9-5 Map of southwest Turkey showing the order that potential arboriculture indicators appearing in pollen core records.**

Furthermore, the median age of onset of cultivation of all pollen zones since the beginning of the Iron Age was plotted against the elevation of each site. As shown in Figure 9-7 a relatively strong relationship was found between site elevation, and the median date of onset of cultivation ($R^2$=0.76). This is particularly interesting when compared with evidence for the end of the Beyşehir Occupation Phase, which will be discussed in the next section.

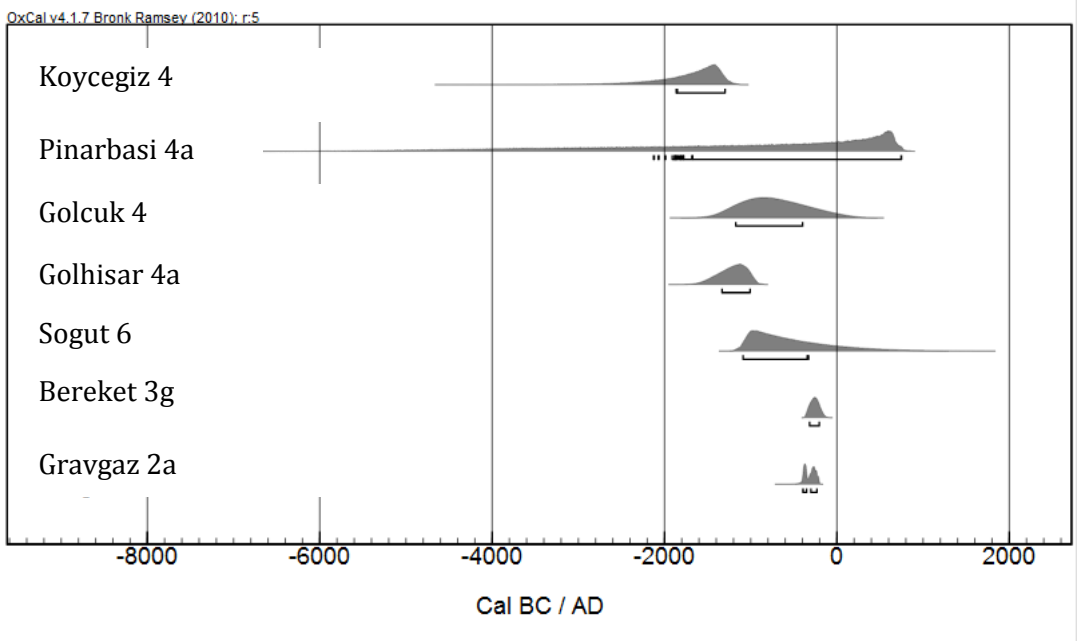


**Figure 9-6 Highest probability density plots of pollen zone boundaries marking the beginning of the Beyşehir Occupation Phase**

**Table 9-2 68.2% highest probability density range for the beginning of pollen zones marking the beginning of the Beyşehir Occupation Phase**

| | Prior (BC / AD) | | | | |
|---|---|---|---|---|---|
| **Name** | **from** | **to** | **%** | **m** | **Elevation** |
| Köyceğiz 3c/4 | -1862 | -1296.5 | 68.2 | -1615.5 | 2 |
| Gölcük 3/4 | -1173 | -397.5 | 68.2 | -751 | 558 |
| Golhisar3/4a | -1333 | -1007.5 | 68.2 | -1195.5 | 930 |
| Pınarbaşı 3b/4a | -2127 | 747 | 68.1 | -789 | 1042 |
| Bereket 3f/3g | -359.5 | -252.5 | 68.2 | -296 | 1420 |
| Gravgaz 1c/2a | -392.5 | -232.5 | 68.2 | -303.5 | 1700 |
| Sögüt 5/6 | -1088 | -328 | 68.2 | -640 | 1400 |

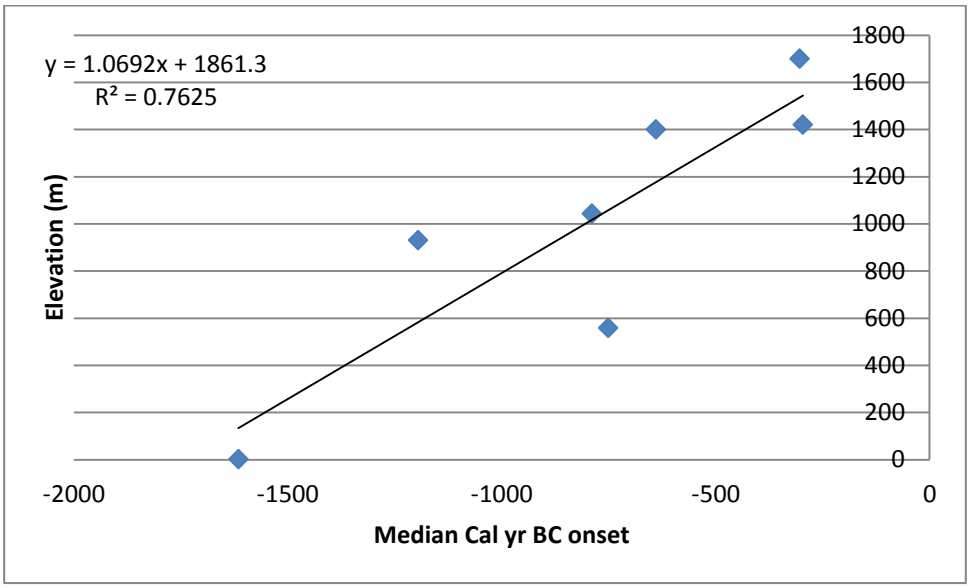


**Figure 9-7 Relationship between the median probability of onset of the Beyşehir Occupation Phase and elevation, showing a moderately strong correlation.**

### 9.3.5 **The end of the Beyşehir Occupation Phase**

By plotting the age of pollen zones which show a large reduction in cultivable species or arboriculture indicators (as shown in Figure 9-8) it can be shown that the contraction of these species across the southwest of Turkey does not occur simultaneously.

The high elevation site of Bereket is one of the first sites to show a decrease in cultivation indicators by ~AD 200. Following this, three sites decrease in cultivation indicators in relatively quick succession; the high elevation sites of Gravgaz (~AD 600) and Sögüt (~AD 615), and then the intramontane basin site of Gölhisar (~700 AD). Hoyran retains a small level of cultivated species pollen until around AD 900.

There are then three sites that still show cultivation indicators after the traditional end of the Beyşehir Occupation Phase. Pınarbaşı may show cultivation indicators until ~AD 1692, although it has very high chronological uncertainty. The westernmost site of Gölcük, and the coastal site of Köyceğiz also show low levels of cultivation through at the end of the Beyşehir Occupation Phase, and indeed, continue to show intermittent arboriculture pollen until the present.

In addition, a relatively strong relationship is found between the median age of decline of Beyşehir Occupation Phase indicators, and elevation ($R^2$=0.79). This is a very interesting result, as it suggests that the development and decline of the phase were to a certain extent influenced by elevation. Does this in turn suggest that the Beyşehir Occupation Phase was influenced by climate which would allow cultivation to be pushed to higher elevations? Or could it still be the case that the end of the phase was instead dictated by the Arab incursions, that indirectly made higher elevation sites more risky / impossible to cultivate, resulting in a slow abandonment of higher elevation sites?

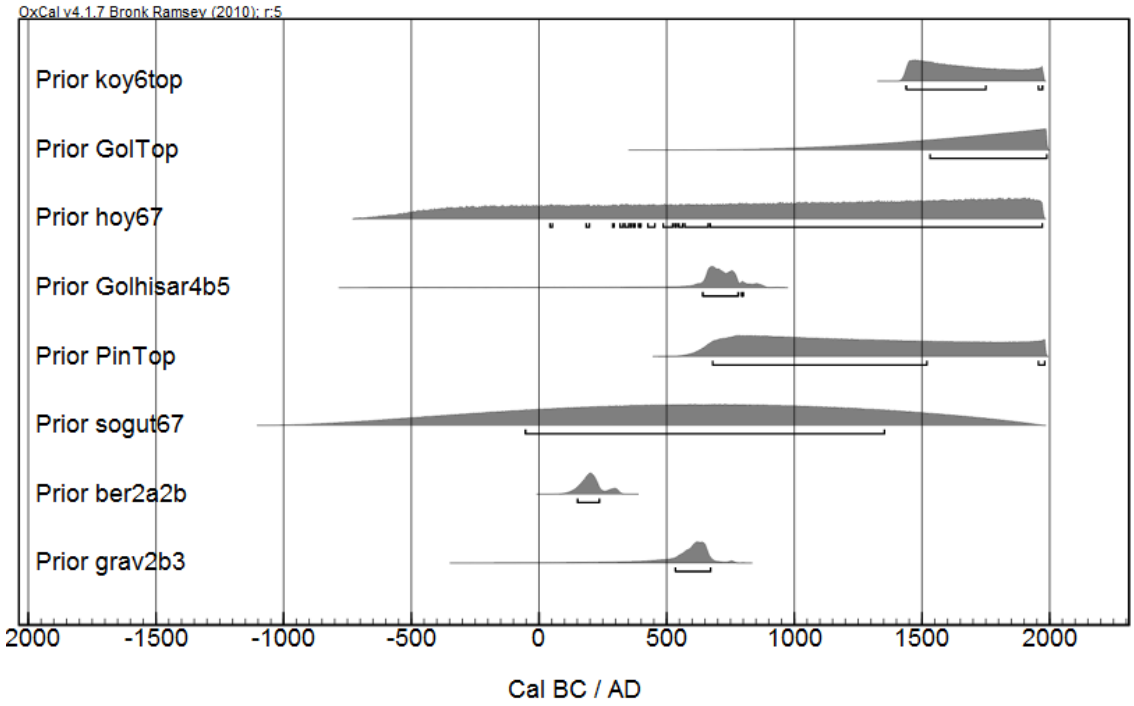


**Figure 9-8 Highest probability density plots of pollen zones showing a large decrease in cultivation indicators.**

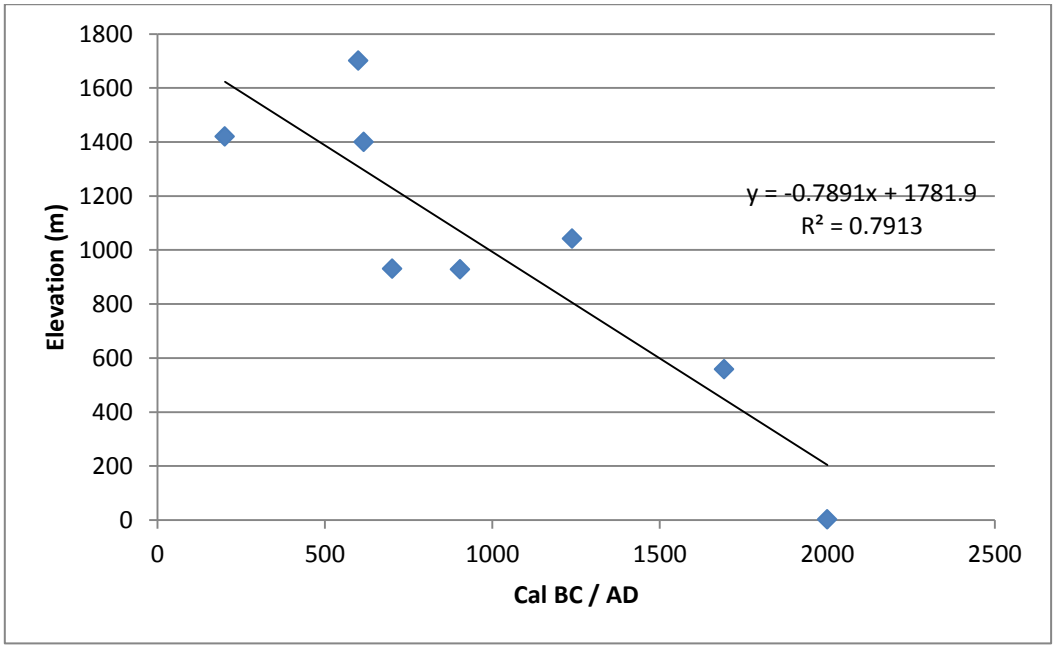


**Figure 9-9 Median probability of pollen zones representing the end of the Beyşehir Occupation Phase, showing a strong relationship with elevation.**

## 9.4 MULTIPLE SPECIES PROBABILITY UNDER A VARIETY OF CLIMATE CONDITIONS: DISSIMILARITY WITH ANALYTICAL POLLEN EVIDENCE

One way of providing further evidence to the debate is by comparing pollen cores from during and after the Beyşehir Occupation Phase with simulated pollen under an array of different climate scenarios. If pollen reflects a scenario of higher precipitation and / or temperature, then this may provide further evidence for a climatic reason for cultivation at increased elevations.

This section therefore discusses the results of vegetation model output with multiple species, under a variety of climate scenarios. Figure 9-10 shows the result of this analysis for key pollen zones considered to reflect the Beyşehir Occupation Phase. High values represent scenarios that are most similar to analytical pollen data.

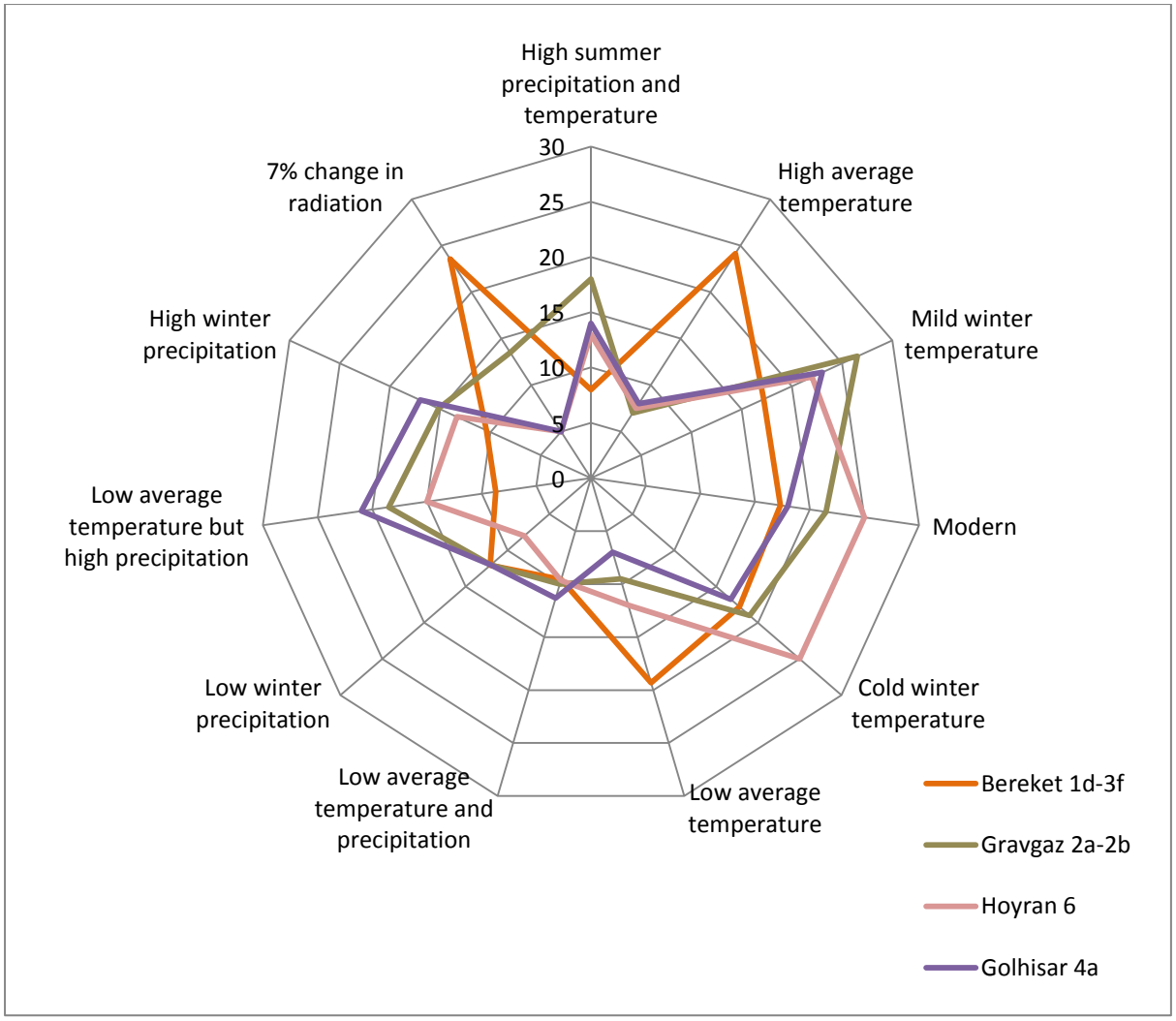


**Figure 9-10 Comparison of simulated pollen with analytical pollen, Beyşehir Occupation Phase. The vertical scale represents relative rank. The higher the rank, the more similar the simulated pollen is to actual pollen values.**

The results of this analysis show that although there is not a consistent response from all pollen zone-model comparisons, there is a general trend. The lower elevation sites of Gölhisar, Hoyran and Bereket shows good correlation with scenarios under high average temperature, and increased seasonality potentially caused by changes in radiation. Gravgaz shows correlation with mild winter temperature and Hoyran is most similar to scenarios with a climate similar to today.

This can be broken down into individual model runs as shown in Figure 9-11 and Figure 9-12. Gravgaz shows best agreement with a scenario of +2°C average temperature, and the second

best fit is a scenario with +200 mm winter precipitation. The best fit scenario for Bereket is with high summer temperatures (+2°C) and high summer precipitation (+50 mm). This is also the best fitting model for Gölhisar 4a, and for Sögüt zone 6. This analysis therefore begins to provide some support for the possibility that climatic changes aided the Beyşehir Occupation Phase and potentially allowed cultivation at higher elevation sites.

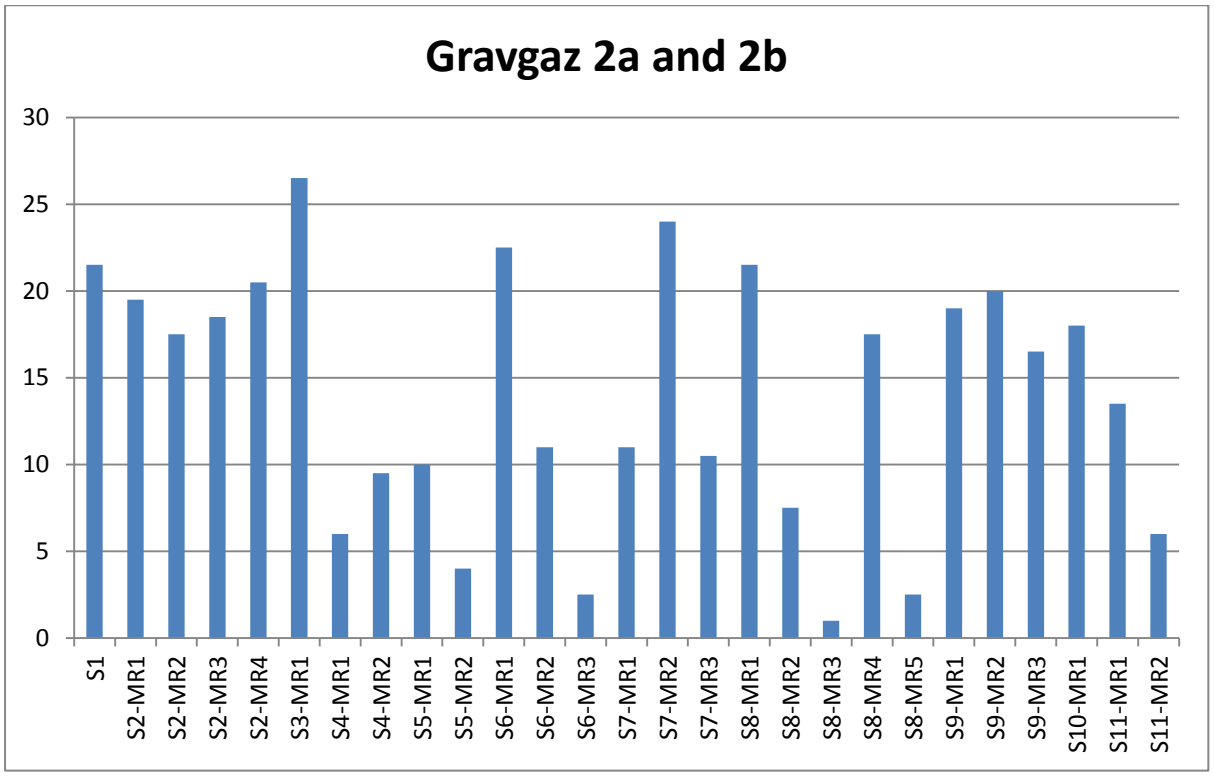


**Figure 9-11 Model run ranks when compared with Gravgaz zones 2a and 2b.**

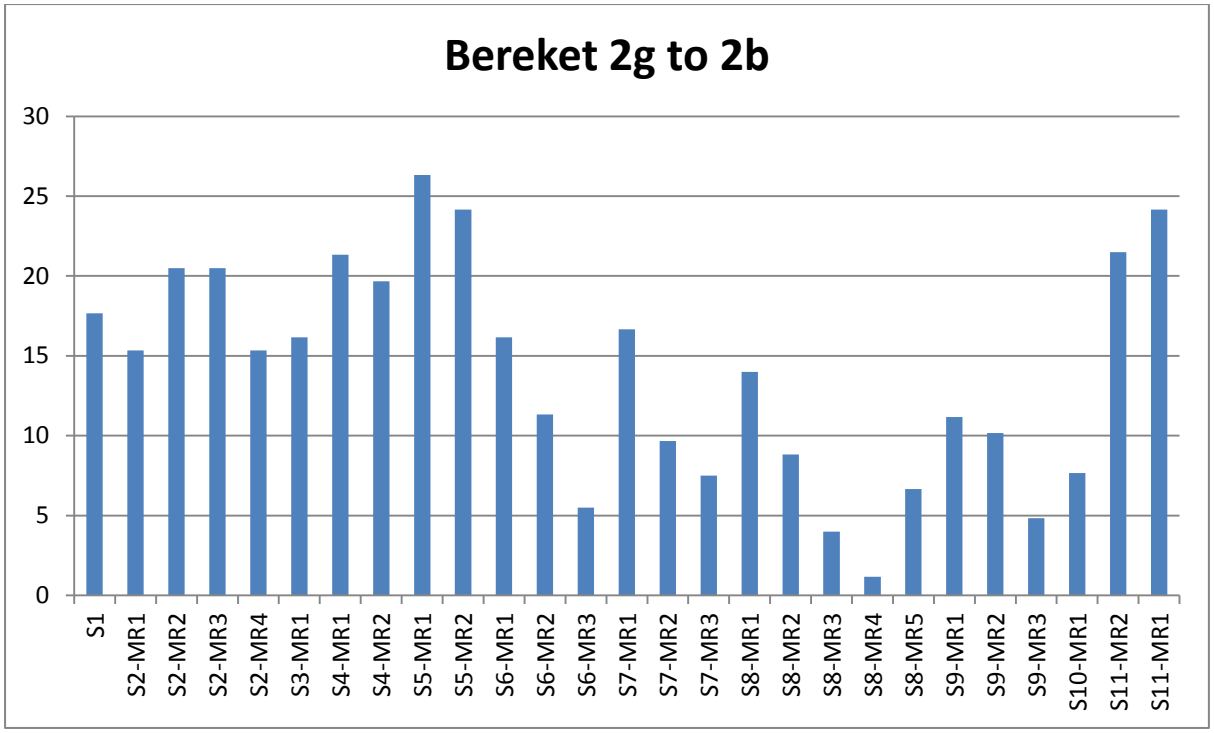


**Figure 9-12 Model run ranks when compared with Bereket zones 2g to 2b**

A further test was undertaken to compare these model runs with pollen cores from after the Beyşehir Occupation Phase. Figure 9-13 shows the difference in correlation between Bereket 2a and 2b, where 2b is deposited during the Beyşehir Occupation Phase and 2a is not. It shows a change in best fitting climate scenario between the two zones, suggesting a reduction in high average temperatures towards a scenario with lower average temperatures.

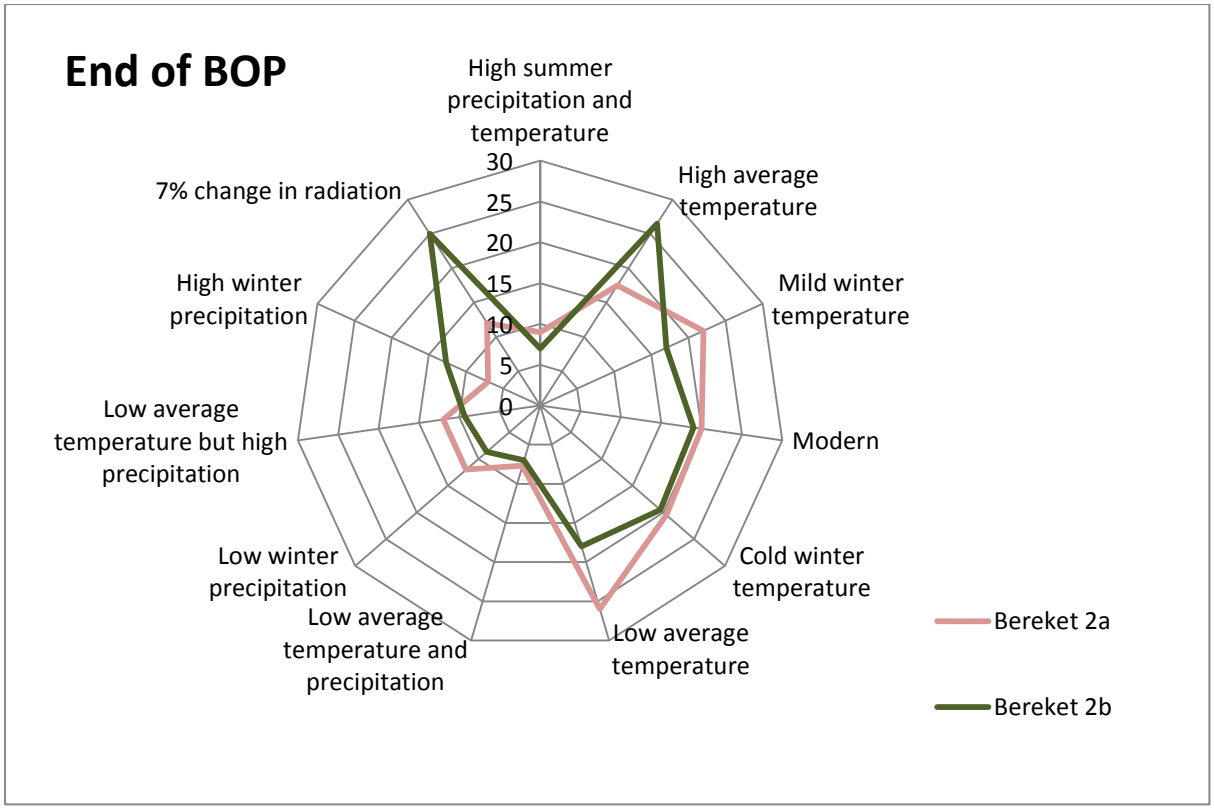


**Figure 9-13 Comparison of model output for Bereket zone 2b (During the Beyşehir Occupation Phase) and Bereket 2a (Post Beyşehir Occupation Phase) showing a change in correlation with climate scenarios.**

Many sites show evidence for cooler temperatures and high winter precipitation following the Beyşehir Occupation Phase. Gölhisar still shows the best agreement with high summer precipitation and temperature although it has higher dissimilarity than before. Sögüt shows an increase in winter precipitation of +300 mm above the modern average, and Gravgaz shows high winter precipitation +200 mm.

Many reasons for the end of the Beysehir Occupation phase have been discussed in previous literature. It is plausible that historical events such as the 3rd century crisis, Sassanian raids, Gothic raids, plague and climate change may all have played their role in the decline of material culture and cultivation from 300 AD onwards (Mitchell 1995; Vermoere, Smets et al. 2000; Vanhaverbeke and Waelkens 2003; Izdebski 2011). The end of the phase is associated with a marked increase in arboreal pollen values and a decrease or disappearance of cultivated trees and secondary anthropogenic indicators, and evidence for extensive conflagration is also found

(Kaniewski, Paulissen et al. 2007). Establishing an end date for the Beyşehir Occupation Phase is considered crucial by Izdebski (2011) for reconstructing Late Antique agricultural history, however this study suggests that it is not the end date per se, but the variability in the date of contraction alongside geographical distribution, that provides insight into Late Antique agricultural history.

Cultivation decrease across southwest Turkey is mirrored by significant decreases in settlement habitation at around AD 600 (Vanhaverbeke, Vionis et al. 2009) suggesting the end of intensive cultivation and the estate economy. Cities are still considered important, however a decline in urban amenities is evidenced, to the extent that Late Antiquity should be considered a village economy (Vanhaverbeke and Waelkens 2003).

However, the events of the period between AD 300 and AD 600 did seem to impact the rural economy as well. It is known that the cultivation phase at Bereket already ends by around AD 350 to 400, evidenced by a decrease in olive pollen. At Gravgaz, a complex picture of cultivation contraction can be seen. A decrease in olive and cereal cultivation is seen here at the end of the 3rd century AD. Following this they return but at lower abundance, and show a slow decline in favour of deciduous woodland, meadows and pine forest by AD 640 (Vermoere, Smets et al. 2000; Bakker, Paulissen et al. 2012b).

Izdebski (2011) posits that one of the key factors that must have facilitated the unparalleled development of late antique agriculture were climate fluctuations; in particular that the period was unusually humid. Modelling evidence has found support for this theory, and modelling also suggests a decrease in optimal climate conditions at the end of the phase. The changing profile of pollen assemblage (from *Olea* and *Vitis* to Cerealia, *Pinus* and grazing indicators) is coherent with a cooling and moistening of the climate, and the relationship with elevation is particularly interesting. But this should only represent the beginning of new discussions alongside archaeological and historical evidence to bring further clarity to the phase.

## 9.5 SIGNIFICANT CLIMATE-SPECIES RELATIONSHIPS

### 9.5.1 Olive cultivation

These findings can be discussed further in relation to the important question of *Olea* cultivation throughout the Beyşehir Occupation phase.

A significant sub-debate in recent historical, archaeological and palaeoecological studies of the southwest is that of the extent and elevation of olive cultivation. A major question was crystallised by Mitchell when he posits whether 'the extent of olive cultivation was determined by environmental or cultural factors'(Mitchell 2005 p.84). To what extent this shift of typical 'Mediterranean' cultivation inland was due to increasingly favourable climatic conditions inland, increased cultural density or changing cultural priorities is yet to be fully understood.

Significant amounts of archaeological evidence are being encountered across Turkey suggesting widespread olive oil and wine production throughout Antiquity. The main evidence comes in the form of grape or olive presses, press weights, crushing vats and amphora for the storage and distribution of wine and oil. In Rough Cilicia olive oil production workshops are found on roads up to settlements on the coast, and there is evidence for Hellenistic era fortified towers being adapted in the later Roman period to olive oil production (Aydinoğlu 2008a). In Antioch dense settlements rooted in the olive oil industry have been found dating back to the 2nd to 5th centuries AD (De Giorgi 2008). In the southwest, evidence for cereal, wine and olive production during Antiquity is found in Karia under the Lelegian culture, in the territory of Hierapolis, and near Sagalassos in Burdur (De Giorgi 2008).

Aydinoğlu states that during Antiquity a 'pastoral and agricultural economy paved the way for a structure of production, road networks and organisations' (2008a p.3). This makes the bold statement that where conditions were favourable for cultivation, workshops, people, and even road networks followed. Aydinoğlu is quick to point out that the relationship between production and cultivation was not purely based on the climate, but that the distribution of

these workshops mainly around the coast and intermontane valley sides were also weighted by the ease of transportation of resources to build and support the settlements that developed. At Antioch, De Giorgi states that there was a

'Unique combination of favourable environmental resources, availability of capital and ultimately institutional schemes that contributed to the emergence of a thriving olive oil industry.'

(De Giorgi 2008 p.98)

Mitchell also suggests that the determining factors for olive cultivation are likely to be stable political and economic conditions, and some financial latitude enabling long-term investment into olive trees that take 15 years before their first fruiting, and variable harvests (Mitchell 2005)

Figure 9-14 shows probable Roman road positions across southwest Turkey, olive workshop locations, and the percentage component of olive in pollen cores across the southwest. Cores with high olive pollen are correlated to road positions, but this is equally likely to be because cores are taken in depressions, and roads are also likely to be constructed at lower elevations, as opposed to roads being built where cultivation potential is high.

Furthermore, it is interesting that high *Olea* pollen percentages do not match with known olive workshop locations. Although there is a potential that this may well be a preservation bias, or a bias of surveying extent, it could instead suggest that olive is not processed near where it is grown, or that high pollen percentages at high elevations are not due to cultivated olive being in the locality. This again poses a few of questions - was pollen at this elevation from long distance travel, was it instead from wild / escaped *Olea* trees that are not processed, or were there even two levels of olive economy being undertaken, with official, high quality olive production for export at lower elevations, and more marginal local olive cultivation undertaken at high elevations?

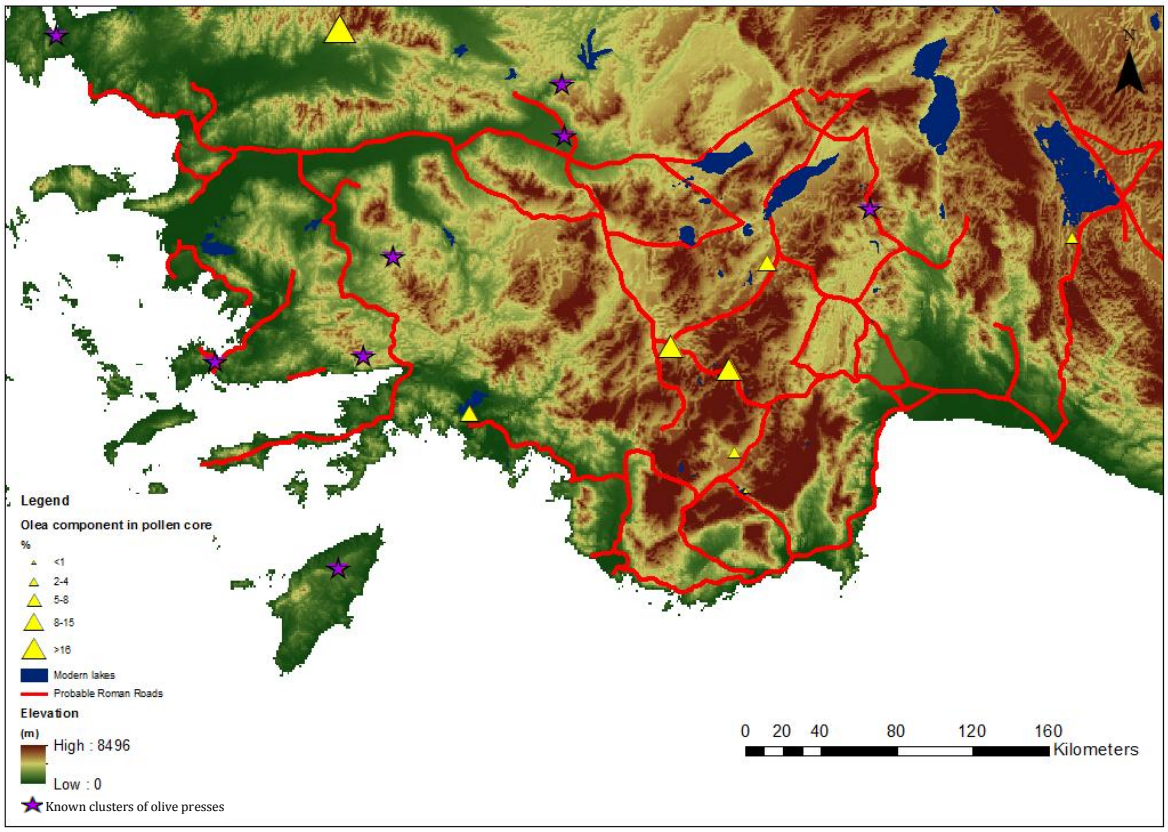


**Figure 9-14 Position of probable road positions (AWMC 2011) during the Hellenistic and Roman period cross referenced against known olive oil workshops (Aydinoğlu 2008b) and pollen core locations showing the percentage component Olea pollen during the Beyşehir Occupation Phase (Using data from Eastwood, Leng et al. 2007)**

Modelling output has raised the possibility of increased precipitation and temperature playing a role in cultivation at these high elevation sites. In order to test whether high levels of *Olea* pollen at these high elevation sites are possible, a GIS modelling test will be undertaken.

Figure 9-15 shows the modern probability of *Olea* from the rare events regression modelling, which is based on modern stand locations. Overlaid on this is known locations of clusters of olive presses, and relative *Olea* pollen in pollen core sites. This figure is interesting for two main reasons. Firstly the contrast between areas of modern *Olea* potential at low elevations, and the high percentage of Olea pollen at high elevations during the Beyşehir Occupation Phase is

pronounced. Secondly, olive workshop sites are generally found at lower elevations in relatively 'safe' areas.

To examine this in more detail, it is known that winter absolute temperature is one of the major restrictions to Olea growth. The potential for restrictive winter temperatures under modern conditions was mapped against olive press positions and *Olea* pollen as shown in Figure 9-16.

This figure emphasises that areas where high percentage *Olea* pollen is found during the Beyşehir Occupation Phase correlate to areas that today carry a risk of severe damage to Olive trees due to cold winter temperatures. Although most known workshop locations are within relatively 'safe' areas, there is one olive press area to the northeast of Pınarbaşı that is in a high risk zone.

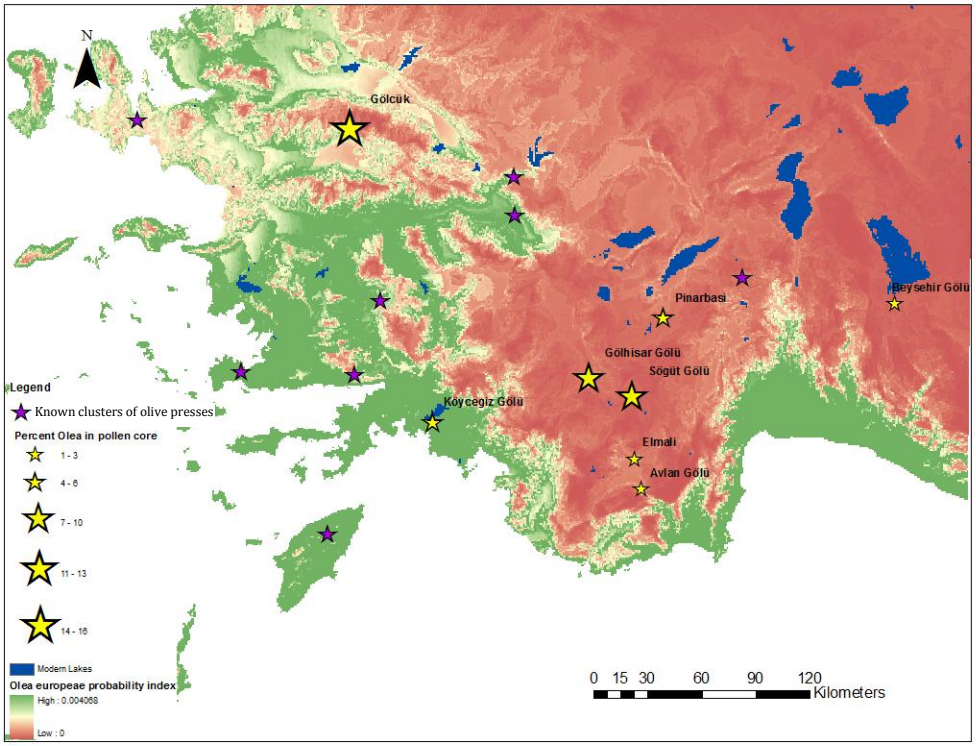


**Figure 9-15 Modern *Olea* potential cross referenced with known olive workshop positions and the percentage *Olea* component found in pollen cores.**

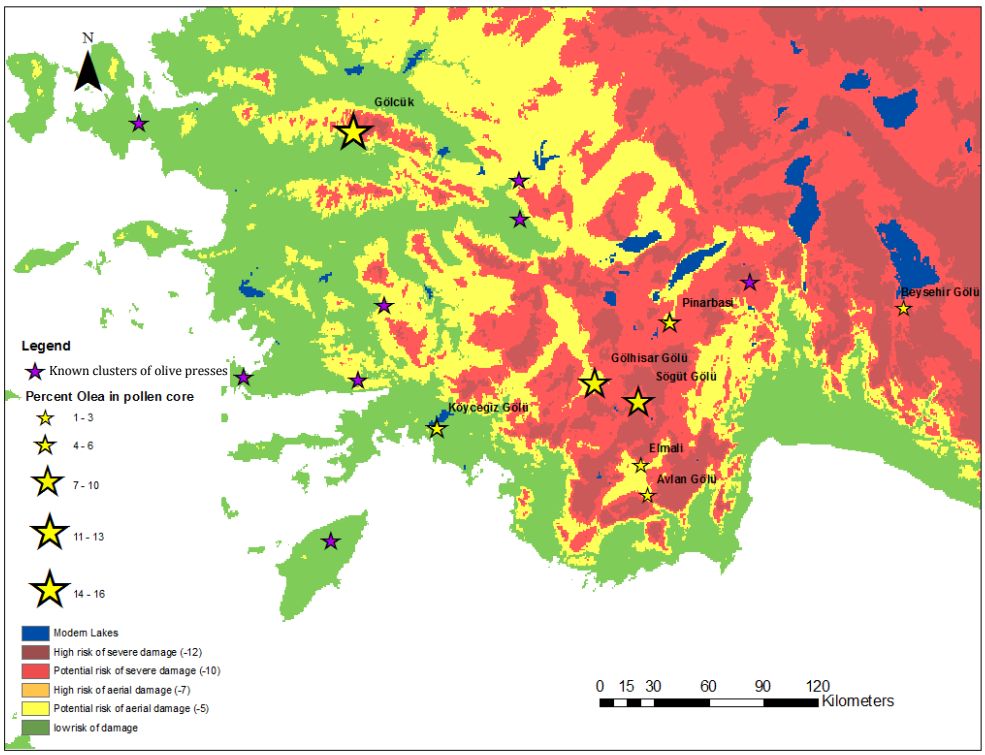


**Figure 9-16 Modern *Olea* winter temperature risk cross referenced with known olive workshop positions and the percentage *Olea* component found in pollen cores.**

Comparison of simulated pollen against analytical pollen data has suggested that an increase in average temperature of ~2°C may have occurred during the Hellenistic and Roman period. It is interesting to model the potential impact of this on olive potential across the region. Figure 9-17 demonstrates that under such a circumstance the high risk areas for olive contract largely across much of the high elevation areas of southwest Turkey. Comparing this variable to high pollen percentages and press locations again, it is now the case that all locations with high *Olea* percentages are in areas with at most, a potential risk of aerial damage over a period of ~30 years.

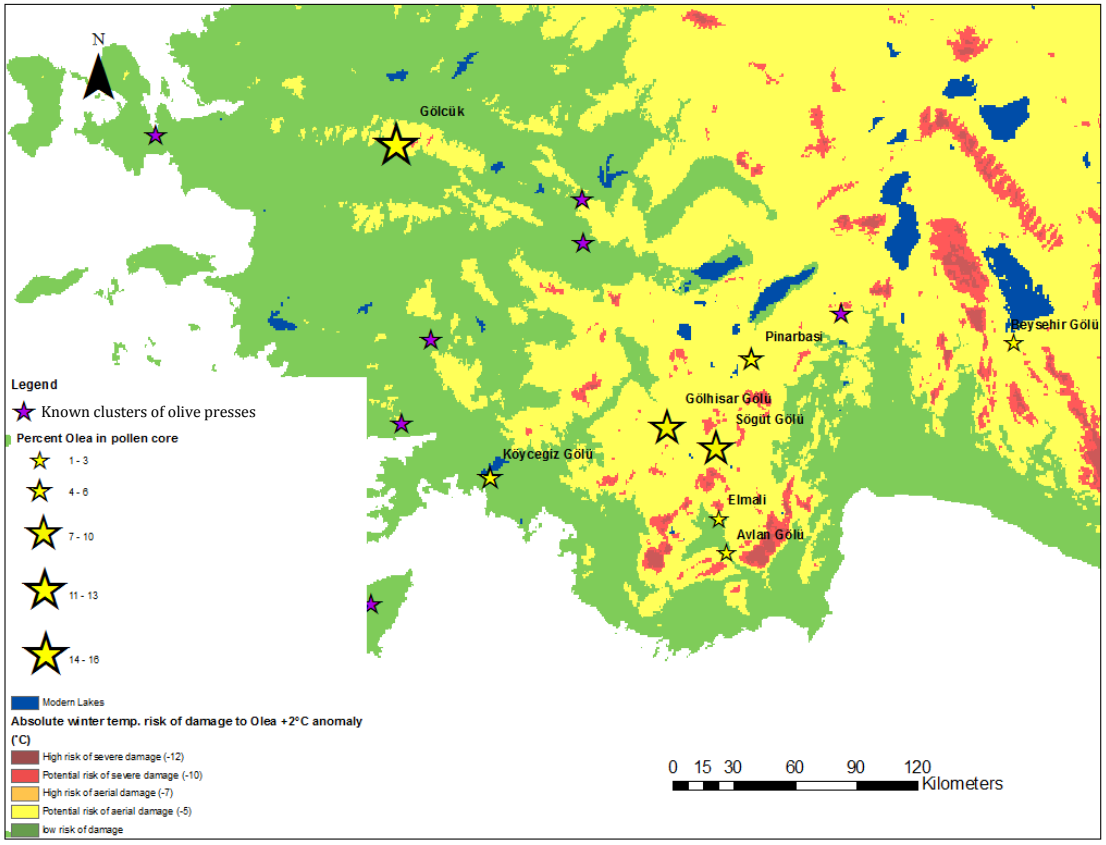


**Figure 9-17 *Olea* potential under a scenario of +2°C cross referenced with known positions of olive press clusters and the percentage *Olea* component found in pollen cores.**

The implications of this can even be modelled at the landscape scale. Figure 9-18 shows the location of press weights across the territory of Hierapolis in yellow or blue dots. Here we have a set of presses that have been classified into positively identified olive press locations (yellow dots), or press weights that may have been used for olive, grape or walnut crushing (blue dots). It is possible to see that those positively identified as olive press weights tend to be located on the hillside or bottom of the valley, whereas unclassified press weights tend to be found at higher elevations at the top of the plateau.

Overlaid onto this is a classification of potential damage to olive plants based on modern climatic records .This shows that under modern conditions, a number of the press weights are found in areas that carry the risk of potential aerial damage to trees over a 30 year period. However no press weights are found in areas of very high risk. If a scenario of +2°C is now

modelled as in Figure 9-19, it is found that those press weights classified as forming olive workshops are now found within areas with a low risk of damage.

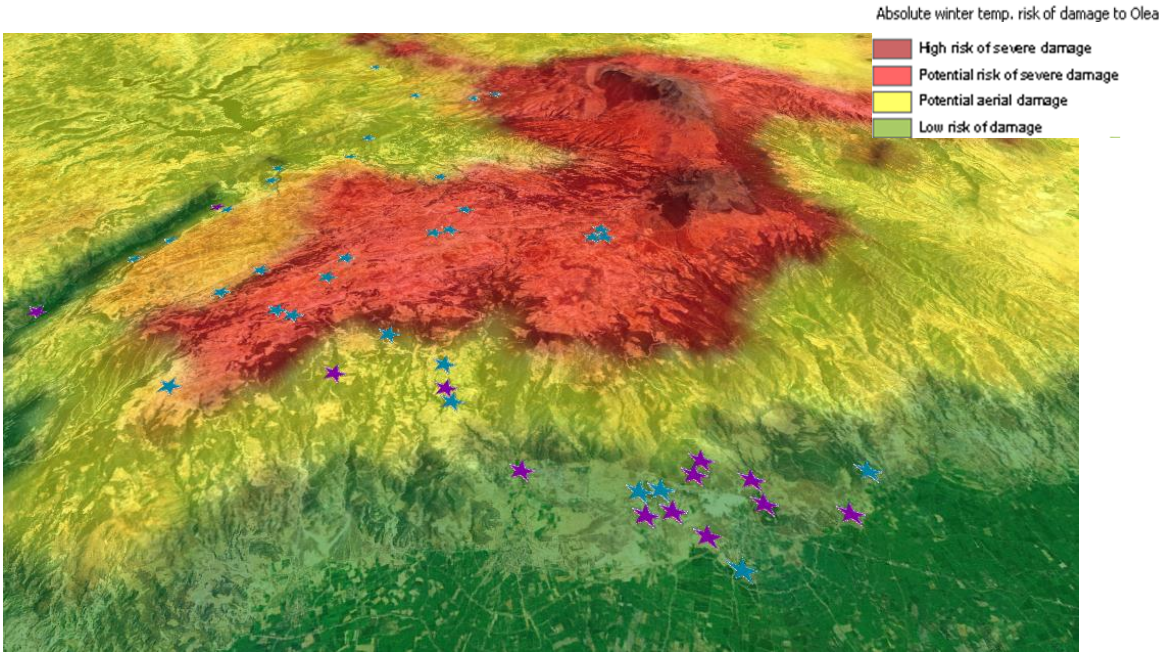


**Figure 9-18 Press weight locations across the territory of Hierapolis, with a modern climatic scenario. Purple stars are identified olive presses. Blue stars may be olive or grape presses**

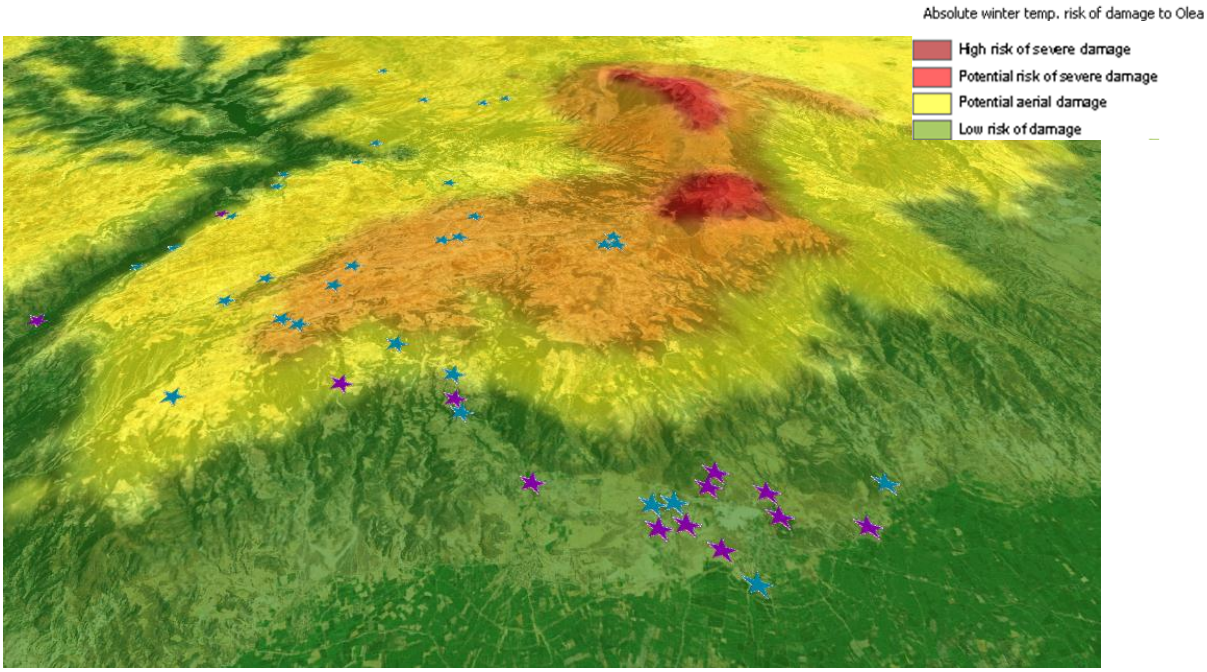


**Figure 9-19 Press weights locations across the territory of Hierapolis, with a scenario of +2°C temperature. Purple stars are identified olive presses. Blue stars may be olive or grape presses**

A similar analysis can be undertaken in the territory of Sagalassos, where again press weights have been found. They have not been positively identified as olive or grape presses, and it was a particularly interesting debate whether they may have been used for olives at this high elevation (~1400 m). Considering Figure 9-20, it is shown that all of these press weights are found in areas with a potential risk of severe damage to plants.

With a scenario of +2°C (Figure 9-21), it can be demonstrated that all of these press weights would now be found in areas of potential aerial damage. Based only on winter absolute temperature, it would seem that although there would be a small amount of risk growing olive trees at this altitude, and farmers in the modern period do not tend to grow in these risky areas. However, it would not be likely to kill the trees, only damage their aerial foliage.

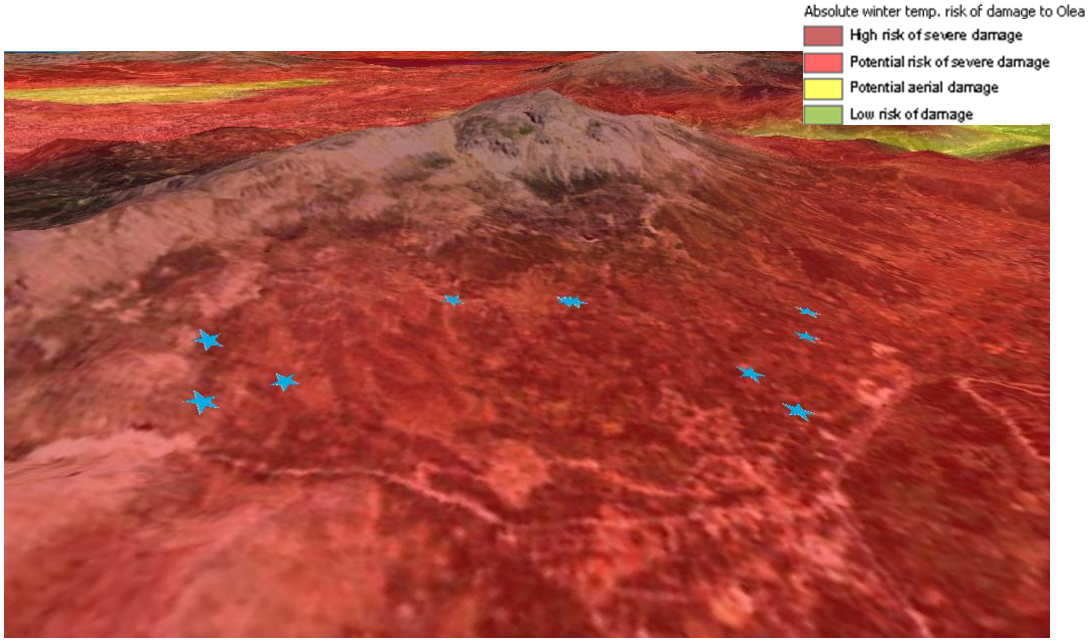


**Figure 9-20 Press weight locations across the territory of Sagalassos, with a modern climatic scenario**

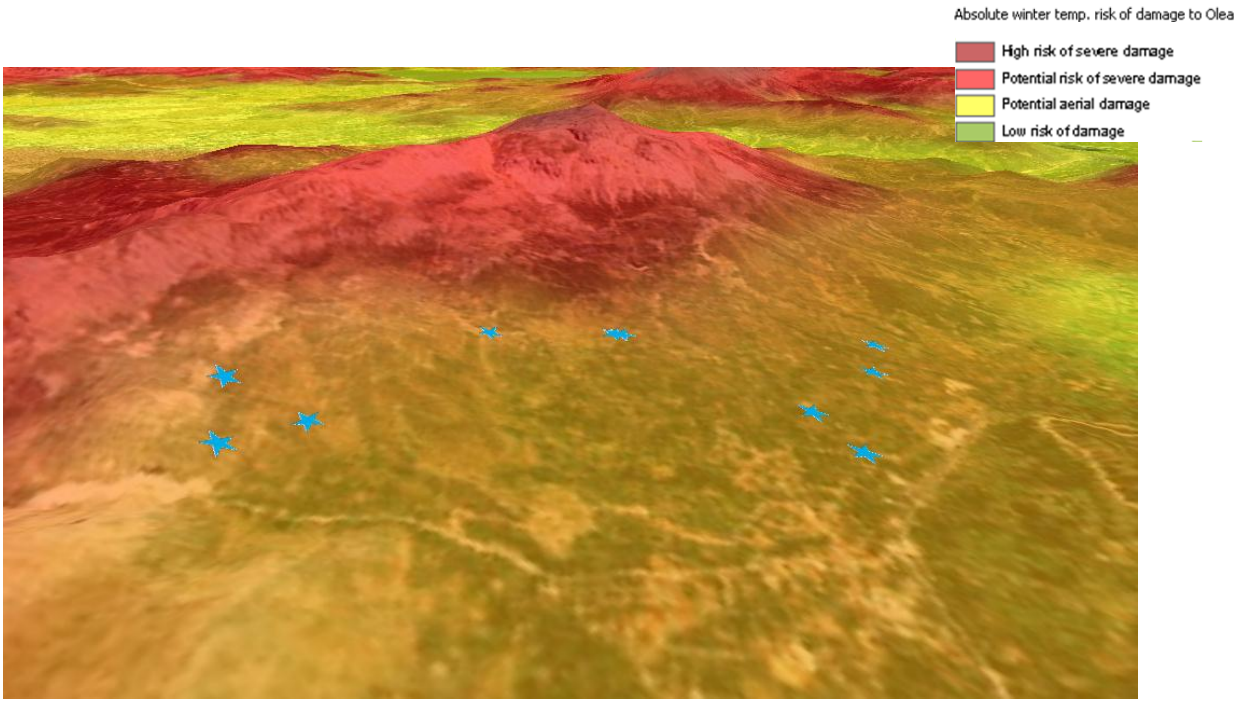


**Figure 9-21 Press weight locations across the territory of Sagalassos, with a modern climatic scenario**

The average elevation for olive growth is ~300 m for cultivation, and up to 700 m for wild olive under modern conditions, with a potential maximum elevation of ~2000 m. The average elevation under +2°C would be ~400 m for cultivation, and up to ~814 m for wild olive, and in favourable areas up to a maximum of 2300 m.

## 9.6 SUMMARY OF RESEARCH QUESTION 3

Chronological modelling of pollen zones across southwest Turkey has allowed the tentative rejection of the hypothesis that the beginning of the Beyşehir Occupation phase is synchronous across southwest Turkey. Modelling has shown a potential expansion into higher elevations over the Hellenistic and Roman period.

Chronological modelling of pollen zones has also allowed the tentative rejection of the hypothesis that cultivation continued through the Mid-Bronze Age. Following synchronisation of pollen cores and the modelling of uncertainty, there is not strong evidence to suggest widespread cultivation through the Mid-Bronze Age.

Hypothesis 3 stated that climate change is implicated in the expansion of the Beyşehir Occupation phase during the Hellenistic to Late Roman period. Modelling does suggest that increased temperature and possibly also precipitation permitted arboriculture species such as *Olea* and *Vitis* to be grown at high elevations during the Beyşehir Occupation Phase.

Finally, chronological modelling suggested that the end of the Beyşehir Occupation Phase was not synchronous across southwest Turkey. In a reversal of the beginning of the phase, it seems that cultivation stopped at high elevation sites first, and contraction of agriculture continued downhill. Only two sites were found to continue arboriculture after the Beyşehir Occupation Phase ended; at the coastal site of Köyceğiz and the western site of Gölcük.

# 10 EVALUATIVE DISCUSSION AND CONCLUSIONS

## 10.1 SUCCESS OF THESIS AGAINST OVERALL RESEARCH AIM

This thesis began by stating that vegetation is a critical component of Mediterranean palaeolandscape studies, but that data quality and quantity, a lack of understanding of Mediterranean vegetation processes, and complex environments may preclude important palaeolandscape debates from being answered adequately. It was also stated that in order to better understand multifaceted debates, the assimilation of data from different fields of study has an instrumental part to play alongside robust, detailed, single discipline studies.

It was posited that a hybrid modelling framework could help to overcome some of previously encountered issues by incorporating a suite of bioclimatic, spatial, chronological and palynological modelling elements. This thesis therefore aimed to develop a vegetation modelling framework set in the Mediterranean environment of southwest Turkey, to engage with 3 key research questions, targeting disputed areas of Mediterranean palaeoenvironmental history.

A modelling framework was subsequently built, that extended and adapted previously researched model components to fit the particular requirements of the environment and the research questions. The modelling methodology began by identifying plant and tree bioclimatic ranges. This followed the tradition of researchers such as Laurent (2004) and Prentice (Prentice, Cramer et al. 1992). To investigate relative probability across the landscape, Logistic Regression is employed, which has previously been used to examine the probability of dichotomous presence / absence of species (Augustin, Cummins et al. 2001; Fangliang, Zhou et al. 2003; Flantua, van Boxel et al. 2007). By doing so, this section of the model displayed different vegetation assemblages across the landscape in an organic, continuous manner based

on a number of environmental variables, which was motivated by the ideas of polyclimax succession.

The Natural Potential approach of Spikins (2000), Caseldine (2007) and Fyfe (2006) inspired the next section of modelling whereby retrodictive vegetation modelling is discussed alongside palynological data. It also uses previously established translation tools (HUMPOL), to convert from vegetation to pollen (Bunting and Middleton 2005; Bunting, Twiddle et al. 2007), acknowledging pollen productivity and dispersal principles to compare model output with pollen evidence. Bayesian modelling provided the basis for synchronising analytical pollen data, and modelling chronological uncertainty, previously employed successfully in relation to archaeological investigations (Buck, Kenworthy et al. 1991).

The successful incorporation of these techniques within a modelling framework is the first novel component of this thesis. The second component is that in order to be comparable with historical and archaeological data, the model was developed using high resolution climate data and single species vegetation distribution using Europe-wide datasets. Furthermore, a third novel outcome is that the model suite has been successfully applied to a relatively under-researched area, that of Mediterranean southwest Turkey.

The role of GIS in the development of the modelling methodology has also been significant. The ability to link statistical modelling with the visualization of model outputs, and the capability to map relative probability and uncertainty provides an invaluable tool to present ideas and relationships. The ongoing development of GIS technology and tools continue to provide the opportunity for greater integration of sophisticated modelling efforts with novel visualization techniques.

As well as the novel methodology of the thesis, the modelling framework has also been employed to provide some very interesting results with regards to 3 research questions. As with any model, the results should always be interpreted within the context of the scope and limitations of the model, and the assumptions that have inevitably been used to provide a

tractable solution. Therefore, before summarizing key conclusions and findings of the model in relation to the aim and research questions, the next section will provide a reflective evaluative discussion of the model framework, exploring model limitations, assumptions and potential improvements.

## 10.2 EVALUATIVE DISCUSSION

### 10.2.1 Model performance

Where possible, the model components have had accuracy and precision checks undertaken. Starting with defining the accuracy and precision of the underlying source data, the degree of agreement (User and Producer accuracy) between actual species distribution and model species distribution was calculated for the whole of Europe. All species achieved above 75% accuracy, above the recommended cutoff for a well-fitting model. A further check was undertaken to assess the degree of accuracy between model prediction and species distribution in Turkey, which achieved an $R^2$ value of 0.85.

#### 10.2.1.1 Bootstrap test

The sensitivity of regression equation parameters was also checked (although for concision is not detailed here), using a Bootstrap analysis. The regression was bootstrapped using 1000 samples, and in order to undertake replication, a Mersenne Twister with a seed point of 200000. A classification cutoff of 0.5 was used, with 20 maximum iterations. Simple sampling was used. A model run was tested by changing regression parameters to the 95% upper and lower bounds of the bootstrap, and then re-calculating pollen simulations. This analysis showed that the end correlation between pollen simulation and climate was insensitive to the changing of the regression parameters to these extremes, suggesting a robust analysis. The accuracy of pollen simulation was assessed against modern pollen data, which again gave good agreement.

#### 10.2.1.2 Model fit

As part of model analysis, it was also useful to understand where relative underestimation and overestimation of simulated pollen occurred compared to analytical pollen data at the species level. To assess this, each of the best fitting model runs was compared with analytical pollen as shown in Figure 10-1.

This analysis showed that Poaceae, *Cedrus* and *Artemisia* were the three species that were most under or over-estimated in the analysis. Considering that *Cedrus* is generally underestimated in

pollen data, for simulated Cedrus pollen to be lower than actual pollen analytical data suggests a significant underestimation in the model. This is considered to be due to a lack of adequate climatic range data based on its current distribution. Natural *Cedrus* forests have been depleted markedly (e.g. Khuri, Shmoury et al. 2000), and so accurate bioclimatic range data are lacking. *Cedrus* is found to be a key species in pollen records and may hold the key for better understanding the climate in interior regions of Turkey. It is suggested therefore, that further laboratory tests at a cellular level would be advantageous to understand temperature tolerances, and further natural distribution research to understand its potential macro bioclimatic range across Europe. *Cedrus* is known to succeed in full sunlight, and is tolerant of low rainfall, cold winters and heavy snowfall, but does not do well under severe frosts. All of these traits do correlate to the type of climatic scenarios encountered during the model scenarios encountered so far, and support its success during both the last glacial period and the early Holocene.

With respect to Poaceae, it is underestimated both during the Last Glacial Maximum and during the early Holocene. It is possible that this underestimation could again be due to the fact that natural grasslands have also reduced over time leading to a lack of adequate bioclimatic range data for this family. Another reason may be that pollen productivity may be different in this region than the parameter used from northern Europe. Furthermore, some species of the Poaceae family are aquatic grasses, that would not be marked on the modern grassland distribution again leading to an underestimation.

Finally, *Artemisia* is likely to have been overestimated due to the assignment of steppic areas as being predominantly composed of *Artemisia*. Again, PPE data for *Artemisia* are required from Mediterranean regions to confirm it covers similar habitats as northern Europe.

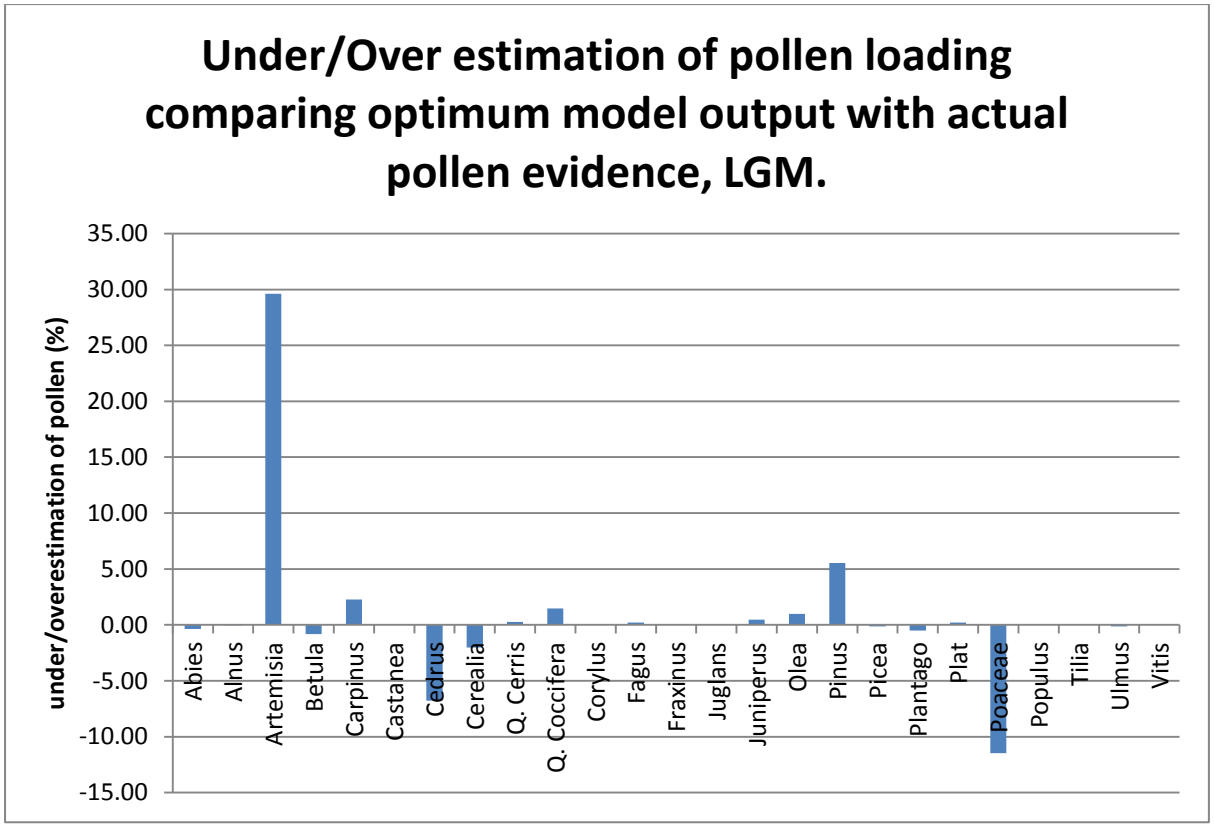


**Figure 10-1 Difference between model output and empirical pollen evidence for Karamik zone 1, with -8°C average temperature and -200 mm winter precipitation**

In summary, an array of checks was undertaken where possible to provide confidence in the model results, and identify where improvement could be made. It is acknowledged that further sensitivity tests should be carried out, and more data collected before the outcomes of the modelling framework are proven to be robust.

There are also areas of the model that are difficult to test for precision and accuracy, which is always the case with a vegetation model that is based on modern relationships, but used to compare to past vegetation data. As stated throughout the thesis, it is important to recognize that the principle of Uniformitarianism applies.

#### 10.2.1.3 Climate scenarios

In terms of the link between vegetation and climate, as the analysis is a correlative analysis, the potential for equifinality should be acknowledged. It should also be considered that only a

selection of potential climate scenarios were tested in the model, and that the analysis therefore reflects the most similar scenario of those tested, not the most similar climate scenario of all possibilities.

#### 10.2.1.4 Species set

Although a relatively large suite of species were considered as part of the analysis, a number of species could not be examined because no adequate modern species distribution information was available from which to create bioclimatic variables. This predominantly applied to many of the steppic assemblage, and some tree species of lesser importance in the pollen record. But it also included potentially informative species such as *Pistacia* and *Carya*, and important groups of species such as steppe. As discussed above, a further subset of modelled species did not match well with species from pollen records. However these limitations are also useful in that they identify particular species against which to target future work.

## 10.3 IMPROVEMENTS TO THE MODEL AND FUTURE WORK

If more time were available, there are a number of potential improvements to the model, and follow on work that could provide further insight.

#### 10.3.1.1 Pollen productivity values

In order to convert from vegetation to pollen, pollen productivity values are generally based on previous work in a northern European setting. It is possible that pollen productivity values for species may be different within a Mediterranean setting. For the purposes of demonstrating the framework previous pollen productivity values were used, however a future area of work should be the establishment of Mediterranean pollen productivity estimates, in order to refine the results from this analysis.

#### 10.3.1.2 Model structure

Instead of the relative measures used in this thesis, it would be useful to devise a threshold to assess 'good', 'moderate' or 'poor' similarity between simulated pollen and analytical pollen.

#### 10.3.1.3 Automation

The model developed in the thesis was for the main part reliant on manual entry of regression equations, manual conversion of data formats and manual collation of statistics. Since the inception of the thesis the GIS software has developed, allowing more semi-automatic models to be produced, with interactive scripting allowing a great deal of time saving. The initial re-write of the model would require a not insignificant amount of time to develop, but then the process of running the model would be much quicker and a larger number of model runs could be developed.

Furthermore, the integration of the 'R' statistical program with ArcGIS may now allow further time-saving in terms of statistical analysis from model output. A further very useful addition could be the integration of the HUMPOL model suite with ArcGIS, to allow the whole process to be undertaken as one modelling exercise.

#### 10.3.1.4 In depth analysis against archaeological and historical data

Although it was deemed important not to ignore the archaeological and historical context of the research questions, it was recognized that an in-depth archaeological and historical analysis could not be carried out as part of this thesis. However, it would be very interesting to discuss the potential implications of this research with the archaeological community, and to test some of the hypotheses that are suggested by the work.

#### 10.3.1.5 Examining other periods in the history and prehistory of southwest Turkey

Due to time constraints the model only looked at three research questions within the thesis. However the potential for examination of other research questions within southwest Turkey is high; for instance looking at the impact of the Younger Dryas on vegetation, whether mid-

Holocene aridity cycles affected vegetation distribution and the extent to which vegetation is linked to climate after the Byzantine era etc.

There is also scope to use the model framework in other areas of the Mediterranean. It would be interesting, for instance, to run the analysis again in Eastern Turkey where further palaeoecological data is available, or further afield in Greece, or Israel, where data allowed.

## 10.4 CONCLUSIONS

This thesis has successfully developed and implemented a bioclimatic vegetation model tailored to the Mediterranean southwest Turkey.

Novel research was achieved in this thesis due to a number of adaptations in data input, methodology and visualization. High resolution data input allowed model output to be 1km in resolution, adequate for engagement with key palaeoenvironmental and cultural debates at the landscape to regional scale. By modelling individual species, it was possible to compare model output with empirical pollen data through the translation tool of the HUMPOL model suite. Furthermore, the chronology of southwest Turkish pollen cores was modelled, allowing investigation of the synchronicity of the cores, and the probability of event timing.

As well as a novel methodology, it is applied to southwest Turkey, which had not previously been subject to many detailed palaeoecological modelling efforts. In doing so it has been able to analyse the development and exploration of Mediterranean vegetation assemblage, and the links between vegetation dynamics, and climate through time.

The sections below summarise the key findings from model output in relation to the three research questions of the thesis.

### 10.4.1 Conclusions from Research Question 1

The first research question that was asked of the model framework was whether it could be employed to provide a coherent narrative to explain evidence of high lake stands concurrent with steppic vegetation signatures during the Late Glacial period (~23 to 19 Cal ka yr BP).

Bayesian modelling of pollen cores demonstrated that although chronological uncertainty is on average higher for early pollen zones, Karamik core zones 1 and 2 were likely to cover the Last Glacial Maximum period.

The successful comparison of pollen simulation with analytical pollen data suggested that reduced precipitation (-200 mm) and average temperatures (-8°) were likely during the Last Glacial period. Whilst the link between steppic assemblages and restricted temperature and precipitation is not a new theory, what is novel is that through identification of this climate scenario, GIS modelling provided an appreciation of how reduced temperature and precipitation may have changed aridity and humidity across the region. This is a key breakthrough as it demonstrates the potential concurrency of glacial expansion in the mountainous areas in the south, a low evaporation rate preserving high lake levels across the region, but also low absolute precipitation available for plant growth leading to steppic formations.

A third important conclusion is that the model identified potential refugia areas for cold intolerant species such as *Olea* near to the southerly coastal areas of Antalya and Mugla, and potential refugia areas on mountain slopes in the Oro-Mediterranean region for *Pinus, Cedrus* and *Abies* due to summer orographic rainfall. This finding is likely to be of interest in further debates surrounding the development and definition of the typical 'Mediterranean' environment, as it suggests that typically Mediterranean species, and a climate resembling a modern Mediterranean climate may have been present in very specific locations near the coast and on the offshore islands.

The findings from this research are also likely to be of interest to archaeologists, with whom it would be very fruitful to discuss the potential implications of such variation in vegetation and climate on the early societies of the Epipalaeolithic. The findings could be discussed alongside the variation in finds across the region, or they could be used to assess potential areas of further archaeological interest.

### 10.4.2 **Conclusions from Research Question 2**

The second research question asked whether the model framework could provide further evidence to support or reject a lag in tree expansion at the beginning of the Holocene (~11 to 8 Cal ka yr BP).

Bayesian modelling has allowed a reassessment of the expansion of woodland throughout southwest Turkey during the early Holocene. The analysis does indeed support evidence for a lag of between 1000 to 3000 years between the assumed point of amelioration at 11 Cal ka yr BP, and a significant increase in arboreal pollen represented in pollen diagrams across southwest Turkey.

Modelling output supports the multitude of studies that found evidence for increased precipitation during the early Holocene, and this modelling study links the increase in precipitation to the expansion of trees inland. Further to this, comparing pollen simulations to analytical pollen suggests that a large increase in winter precipitation may be responsible for the increase in arboreal pollen in lower elevation sites, whereas an increase in summer precipitation is also a potential factor from higher elevation sites such as Sögüt. Whether this increase was due to wider shifts in large scale atmospheric features such as the NAO would be interesting to assess in future research.

The findings also have implications for the establishment of a Mediterranean climate and vegetation across the region, as an increase in typically Mediterranean species such as *Quercus coccifera* and *Olea europaea* is correlated to this increase in winter precipitation. An expansion from the coastal regions for typically Mediterranean species is suggested, which fits with the previous findings of refugia areas at the coast.

Alongside analysis of vegetation-climate interactions, the potential utility of the vegetation modelling framework in providing additional context for the analysis of Neolithic societal development should also not be underestimated. Previous interpretations of Neolithic archaeology have shown the variety of societal adaptations that can occur due to differences in terrain, vegetation and climate (Schoop 2005), and that developmental shifts are theorised to occur more often in marginal and dynamic environments. Even if over a long timescale of thousands of years, the magnitude of vegetation and climate change across the region must have had significant implications for the early societies utilising the landscape, and this would be very interesting to explore further.

### 10.4.3 **Conclusions from Research Question 3**

The third research question that was asked of the model framework was whether it could be employed to understand the timing, magnitude and reasons for the Beyşehir Occupation Phase.

The synchronisation of pollen zone chronologies firstly provided support for the theory that the Beyşehir Occupation Phase was not synchronous across the southwest of Turkey. It is furthermore proposed that three main phases of cultivation may be discerned.

The analysis began by looking at early potential indications of cultivation across the region. Pollen assemblages recorded at Ova zone 2, Köyceğiz zone 3b , Ağlasun core 6 zone 2b and Ağlasun core 12 zone 2a are interpreted as showing small increases in cultivation indicators during the early Bronze Age. An increase is seen in arboriculture species such as *Olea, Juglans, Pistacia*, Cerealia and *Platanus*, and also secondary anthropogenic indicators such as *Sanguisorba*, *Artemisia* and *Plantago.* It was considered important to identify these zones as part of discussion on cultivation as these may represent early interactions with natural species that go on to become cultivated species, or early experiments with agriculture.

A second phase was examined that looked at potential cultivation indicators through the Mid-Bronze Age. Following Bayesian modelling, it was discovered that there was little evidence for cultivation indicators during this period, apart from the site of Beyşehir. This is interesting as it supports the archaeological settlement record, however it does conflict with Hittite sources that suggest important settlements did exist during the period. If a contraction did indeed occur, then what the potential reasons for this are, the magnitude of contraction, and the potential importance of Beyşehir as a site that does show cultivation are all important questions.

The third phase examined the expansion of the Occupation Phase, which was delineated by the Santorini tephra layer, and was evidenced by cultivation indicators at Gölhisar, Pınarbaşı, Gölcük, Sögüt, Gravgaz and Bereket. A moderate relationship between time of onset and elevation was found for this phase. Cultivation at high elevations was found to occur later than cultivation at lower elevations. The end of the Beyşehir Occupation Phase during the Roman, Late Roman and Byzantine periods shows a strong relationship with elevation. The high elevation sites of Gravgaz and Bereket stopped arboriculture before mid-elevation sites, which generally stopped cultivation before low elevation sites.

Following comparison of simulated pollen with analytical pollen for the Beyşehir Occupation Phase, a link was found between the cultivation phase and an increase in temperature. This was examined in relation to the key cultivated species of *Olea*. It was demonstrated that such an increase in temperature would potentially allow the expansion of *Olea* into high elevation sites with only a small risk of aerial damage to the leaves during the winter period.

Furthermore, the end of the phase was linked with a cooling of the climate, and potentially an increase in precipitation. Combining this evidence with the Bayesian analysis suggesting an increase in high elevation cultivation during the phase, and a contraction to lower elevations at the end, it seems likely that a favourable climate had a significant role to play in the expansion of cultivation during the Hellenistic and Roman periods. However it is also important to

acknowledge the multitude of other factors that lead to the remarkable phase, including substantial trade links, a favourable economic climate, political will, individual and societal ingenuity, resource availability and more. The role of political instability, plague, the devastating earthquake at Sagalassos and the Arab incursions of the 7th Century are all likely to have contributed to the decline in cultivation and contraction in society during this period. For this reason, it is hoped that this analysis does not negate or overrule, but complements previous research that adds further valid and interesting perspectives to the debate.

# BIBLIOGRAPHY


Albert, P. S. and L. M. McShane (1995). "A Generalized Estimating Equations Approach for Spatially Correlated Binary Data: Applications to the Analysis of Neuroimaging Data." Biometrics **51**(627-638).

Albrecht, G. (1988). "Preliminary results of the excavation in the Karain B cave near Antalya / Turkey: The upper Palaeolithic assemblages and the upper pleistocene climatic development." Paléorient **14**(2): 211-222.

Altaweel, M. (2008). "Investigating agricultural sustainability and strategies in northern Mesopotamia: results produced using a socio-ecological modeling approach." Journal of Archaeological Science **35**(4): 821-835.

Andersen, S. (1970). "The relative pollen productivity and pollen representation of north European trees, and correction factors for tree pollen spectra." Danmarks Geologiske Undersøgelse (Afhanlinger), II. Rœkke, **96**: 1-96.

Arslanov, K. A., P. M. Dolukhanov, et al. (2007). "Climate, Black Sea levels and human settlements in Caucasus Littoral 50,000-9000 BP." Quaternary International **167-167**: 121-127.

Arthur, W. B. (1994). "Inductive reasoning and bounded rationality." The American Economic Review **84**(2).

Asouti, E. and A. Fairbairn (2010). Farmers, gatherers or horticulturalists? Reconstructing landscapes of practice in the Early Neolithic. Landscapes in Transition. B. L. Finlayson and G. Warren. Oxford, Oxbow books**:** 161-172.

Athanassopoulos, E. and L. Wandsnider (2004). Mediterranean archaeological landscapes: current issues. Philadelphia, University of Pennsylvania Museum of Archaeology and Anthropology.

Augustin, N. H., R. P. Cummins, et al. (2001). "Exploring spatial vegetation dynamics using logistic regression and a multinomial logit model." Journal of Applied Ecology **38**: 991-1006.

Augustin, N. H., M. A. Mugglestone, et al. (1996). "An Autologistic Model for the Spatial Distribution of Wildlife." Journal of Applied Ecology **33**(2): 339-347.

AWMC. (2011). "Pleiades." Retrieved November, 2011, from http://pleiades.stoa.org/.

Aydinoğlu, Ü. (2008a). Olive Oil Production in Rough Cilicia: Production Installations - Settlement Pattern - Dating. Olive oil and wine production in Anatolia during Antiquity. Ü. Aydinoğlu and A. K. Şenol. İstanbul, Research Center of Cilician Archaeology.

Aydinoğlu, Ü. (2008b). Olive oil and wine production in Anatolia during Antiquity. İstanbul, Research Center of Cilician Archaeology.

Baird, D. (2004). Settlement expansion on the Konya Plain, Anatolia: 5th-7th centuries AD. The Late Antique Countryside, Late Antique Archaeology. L. Bowden, L. Lavan and C. Machado. **2:** 219-246.

Baker, R. G., J. Van Nest, et al. (1989). "Dissimilarity coefficients for fossil pollen spectra from Iowa and western Illinois during the last 30,000 years." Palynology **13**(13): 63-77.

Bakker, J., E. Paulissen, et al. (2012b). "Climate, people, fire and vegetation: new insights into vegetation dynamics in the Eastern Mediterranean since the 1st century AD." Climate of the Past Discussion **8**: 3379-3444.
Bar-Matthews, M. and A. Ayalon (1997). "Late Quaternary palaeoclimate in the Eastern Mediterranean region from stable isotope analysis of speleothems at Soreq Cave, Israel." Quaternary Research **47**: 155-168.
Bar-Matthews, M., A. Ayalon, et al. (2003). "Sea-land oxygen isotopic relationships from planktonic foraminifera and speleothems in the Eastern Mediterranean region and their implication for palaeorainfall during interglacial intervals." Geochimica et Cosmochimica Acta **67**: 3181-3199.
Bar-Matthews, M., A. Ayalon, et al. (2000). "Timing and hydrological conditions of Sapropel events in the Eastern Mediterranean, as evident from speleothems, Soreq Cave, Israel." Chemical Geology **169**: 145-156.
Bar-Matthews, M., A. Ayalon, et al. (1999). "The Eastern Mediterranean palaeoclimate as a reflection of regional events: Soreq cave, Israel." Earth and Planatery Science Letters **166**: 85-95.
Bartov, Y., S. L. Goldstein, et al. (2003). "Catastrophic arid episodes in the eastern Mediterranean linked with the North Atlantic Heinrich events." Geology **31**: 439-442.
Bartov, Y., M. Stein, et al. (2002). "Lake levels and sequence stratigraphy of Lake Lisan, the late Pleistocene precursor to the Dead Sea." Quaternary Research **57**: 9-21.
Bennett, K. D. (1994). "Confidence intervals for age estimates and deposition times in late-Quaternary sediment sequences." The Holocene **4**: 337-348.
Bennett, K. D. (1999). "Data-handling methods for Quaternary microfossils." Past and present climate, environment and societal change, from http://chrono.qub.ac.uk/datah/depthage.html.
Besag, J. (1972). "Nearest-Neighbour Systems and the Auto-logistic Model for Binary Data." Journal of the Royal Statistical Society **Series B**(36): 192-236.
Betancourt, P. P. (1987). "Dating the Aegean Late Bronze Age with Radiocarbon." Archaeometry **29**(1): 45-49.
Blaauw, M. (2010). "Methods and code for 'classical' age-modelling of radiocarbon sequences." Quaternary Geochronology **3**: 1-7.
Botkin, D. B., J. F. Janak, et al. (1972). "Some ecological consequences of a computer model of forest growth." Journal of Ecology **60**: 849-872.
Bottema, S. (1979). "Pollen analytical investigations in Thessaly (Greece)." Palaeohistoria **XXI**: 20-40.
Bottema, S. and H. Woldring (1984). "Late Quaternary vegetation and climate of southwestern Turkey Part II." Palaeohistoria **26**: 123-149.
Bottema, S., H. Woldring, et al. (1986). Palynological investigations on the relation between prehistoric man and vegetation in Turkey: Beysehir occupation phase. OPTIMA, Proceedings of the fifth meeting, Istanbul University.
Bottema, S., H. Woldring, et al. (1993). "Late Quaternary vegetation history and climate in northern Turkey." Palaeohistoria **35/36**: 13-72.
Box, E. I., D. W. Crumpacker, et al. (1993). "A Climatic Model for Location of Plant Species in Florida, USA." Journal of Biogeography **20**(629-644).
Box, E. O. (1981). Macroclimate and plant forms: an introduction to predictive modelling in phytogeography. The Hague, Junk.
Braak, C. J. F. T. (1987). "The analysis of vegetation-environment relationships by canonical correspondence analysis." Plant Ecology **69**(1-3): 69-77.

Bradshaw, R. H. W. (1980). "Modern pollen representation factors in southeast England." Journal of Ecology **69**: 49-70.
Brewer, S., R. Cheddadi, et al. (2002). "The spread of deciduous Quercus throughout Europe since the last glacial period." Forest ecology and management **156**(1): 27-48.
Broccoli, A. J. and S. Manabe (1987). "The influence of continental ice, atmospheric CO2 and land albedo on the climate of the last glacial maximum." Climate Dynamics **1**: 87-99.
Bronk Ramsey, C. (2001). "Development of the radiocarbon calibration program OxCal." Radiocarbon **43**(2A): 355-363.
Bronk Ramsey, C. (2008a). "Deposition models for chronological records." Quaternay Science Reviews **27**(1-2): 42-60.
Bronk Ramsey, C. (2008b). "Bayesian analysis of radiocarbon dates." Radiocarbon **51**(1): 337-360.
Broström, A., A. B. Neilson, et al. (2008). "Pollen productivity estimates of key European plant taxa for quantitative reconstruction of past vegetation: a review." Vegetation History and Archaeobotany **17**: 461-478.
Broughton, T. R. S. (1938). Roman Asia minor. An Economic Survey of Ancient Rome T. Frank. New Jersey, Paterson. **IV**.
Buck, C. E., W. Cavanagh, et al. (1996). Bayesian Approach to Interpreting Archaeological Data, John Wiley and Sons.
Buck, C. E., J. B. Kenworthy, et al. (1991). "Combining archaeological and radiocarbon information - a Bayesian approach to calibration." Antiquity **65**(808-821).
Bugmann, H. (1994). On the ecology of mountainous forests in a changing climate: A simulation study. PhD. Thesis no. 10638. Zurich, Switzerland, Swiss Federal Institute of Technology.
Bugmann, H. K. M., X. Yan, et al. (1996). "A comparison of forest gap models: model structure and behaviour." Climatic Change **34**(2): 289-313.
Bunting, M. J. and D. Middleton (2005). "Modelling pollen dispersal and deposition using HUMPOL software, including simulating windroses and irregular lakes." Review of Palaeobotany and Palynology **134**(3-4): 185-196.
Bunting, M. J., C. L. Twiddle, et al. (2007). "Using models of pollen dispersal and deposition in hilly landscapes: Some possible approaches." Palaeogeography, Palaeoclimatology, Palaeoecology **259**(1): 77-91.
Calamassi, R., E. Paoletti, et al. (2001). "Frost hardening and resistance in three Aleppo pine (Pinus halepensis Mill.) provences." Israel Journal of Plant Sciences **49**(3).
Calcote, R. (1995). "Pollen source area and pollen productivity: evidence from forest hollows. ." Journal of Ecology **83**: 591-602.
Carmel, Y., R. Kadmon, et al. (2001). "Spatiotemporal predictive models of Mediterranean Vegetation Dynamics." Ecological Applications **11**(1): 268-280.
Caseldine, C., R. Fyfe, et al. (2007). "Simulating the nature of vegetation communities at the opening of the Neolithic on Achill Island, Co. Mayo, Ireland - the potential role of models of pollen dispersal and deposition." Review of Palaeobotany and Palynology **144**: 135-144.
Cauvin, M. C. and C. Chataigner (1998). Distribution de l'obsidienne dans les sites archéologiques du Proche et Moyen Orient. L'obsidienne au Proche et Moyen Orient. Du volcan à l'outil A. Gourgaud, B. Gratuze, N. Arnaudet al. Oxford**:** 325-350.

Christensen, N. L. (1988). Succession and natural disturbance: paradigms, problems and preservations of natural ecosystems. Ecosystem management for parks and wilderness. J. Agee and D. Johnson. Washington, University of Washington Press.
Coulton, J. J. (1988). Balboura Survey. Annual report of the British Institute of Archaeology at Ankara. **40:** 13-15.
Coulton, J. J. (1988). "'Balboura Survey'." Annual report of the British Institute of Archaeology at Ankara **40**: 13-15.
Cox, P. (2001). Description of the "TRIFFID" Dynamic Global Vegetation Model. Hadley Centre technical note 24. London, Hadley Centre.
Cramer, W., A. Bondeau, et al. (2001). "Global responses of terrestrial ecosystem structure and function to CO2 and climate change: results from six dynamic global vegetation models." Global Change Biology **7**: 357-373.
D'Agostini, G. (2003). "Bayesian inference in processing experimental data: principles and basic applications." Reports on Progress in Physics **66**: 1386-1419.
Dansereau, P. (1957). Biogeography: An Ecological Perspective. . New York, Ronald Press.
Davis, M. B. (1963). "On the theory of pollen analysis." American Journal of Science **261**: 897-912.
De Giorgi, A. U. (2008). Olive oil production in the Antiochene from the Early Empire into Late Antiquity. Olive oil and wine production in Anatolia during Antiquity. Ü. Aydinoğlu and A. K. Şenol. İstanbul, Cilician Institute of Archaeology**:** 97-107.
Dean, J. S., G. J. Gumerman, et al. (2000). Understanding Anasazi culture change through agent-based modeling. Dynamics in human and primate societies: agent-based modeling of social and spatial processes. T. A. Kohler and G. J. Gumerman. Oxford, Oxford University Press.
Di Pasquale, G., P. Di Martino, et al. (2004). Forest History in the Mediterranean Region. Recent dynamics of the Mediterranean vegetation and landscape. S. Mazzoleni, G. Di Pasquale, M. Mulligan, P. Di Martino and F. Rego, John Wiley & Sons**:** 13-20.
Diaz, R., Ø. Johnsen, et al. (2009). "Variation in spring and autumn freezing resistance among and within spanish wild populations of Castanea sativa." Annals of Forest Science **66**(708): 12.
Djamali, M., H. Akhani, et al. (2010). "Indian Summer Monsoon variations could have affected the early-Holocene woodland expansion in the Near East." The Holocene **20**(5): 813-820.
Duru, R. (1999). The Neolithic of the Lake District. Neolithic Turkey. The cradle of civilization. M. Ozdogan and N. Basgelen. Istanbul.
Eastwood, W. J., R. Fyfe, et al. (2011). "Quantitative vegetation modelling in southwest Turkey." Heritage Turkey. British Institute of Ankara Research Reports **1**(2011).
Eastwood, W. J., M. J. Leng, et al. (2007). "Holocene climate change in the eastern Mediterranean region: a comparison of stable isotope and pollen data from Lake Gölhisar, southwest Turkey." Journal of Quaternary Science **22**(4): 327-341.
Eastwood, W. J., N. Roberts, et al. (1998). "Palaeoecological and archaeological evidence for human occupance in southwest Turkey: the Beysehir Occupation Phase." Anatolian Studies **48**: 69-86.
Eastwood, W. J., N. Roberts, et al. (1999). "Holocene environmental change in southwest Turkey: a palaeoecological record of lake and catchment-related changes." Quaternary Science Reviews **18**(4-5): 671-695.

Eastwood, W. J., J. Tibby, et al. (2002). "The environmental impact of the MInoan eruption of Santorini (Thera): statistical analysis of palaeoecological data from Golhisar, southwest Turkey." The Holocene **12**: 431-444.
Eklöf, M., A. Broström, et al. (2004). "OPENLAND3: a computer program to estimate plant abundance around pollen sampling sites from vegetation maps: a necessary step for calculation of pollen productivity estimates." Review of Palaeobotany and Palynology **132**(1-2): 67-77.
England, A., W. J. Eastwood, et al. (2008). "Historical landscape change in Cappadocia (central Turkey): a palaeoecological investigation of annually laminated sediments from Nar lake." The Holocene **18**(8): 1229-1245.
Erdtman, G. (1969). Handbook of Palynology - An introduction to the Study of Pollen Grains and Spores. Copenhagen, Munksgaard.
Fagerlind, F. (1952). "The real signification of pollen diagrams." Botanista Nortiser **105**: 185-224.
Fairbairn, A. and E. Weiss (2009). From foragers to farmers. Oxford, Oxbow.
Fairborn, A. (2005). "A History of Agricultural Production at Neolithic Çatalhöyük East, Turkey." World Archaeology **37**(2): 197-210.
Fangliang, H. E., J. Zhou, et al. (2003). "Autologistic regression model for the distribution of vegetation." Journal of Agricultural, Biological and Environmental Statistics **8**(2): 205-222.
Filipova, M., E. V. Kvavadze, et al. (2010). "Estimating absolute pollen productivity for some European Tertiary-relict taxa." Vegetation history and Archaeobotany **4**: 351-364.
Finsinger, W., W. Tinner, et al. (2006). "The expansion of hazel (Corylus avellana L.) in the southern Alps: a key for understanding its early Holocene history in Europe?" Quaternary Science Reviews **25**(5-6).
Flantua, S. G. A., J. H. van Boxel, et al. (2007). Application of GIS and logistic regression to fossil pollen data in modelling present and past spatial distribution of the Colombian savanna. GISRUK 2007, NUIM, Co. Kildare.
Fleitmann, D., H. Cheng, et al. (2009). "Timing and climatic impact of Greenland interstadials recorded in stalagmites from northern Turkey." Geophysical Research Letters **36**: 5.
Fontugne, M. R., M. Arnold, et al. (1994). Palaeoenvironment, sapropel chronology and River Nile discharge during the last 20,000 years as indicated by deep sea sediment records in the Eastern Mediterranean. Late Quaternary Chronology and Palaeoclimates of the Eastern Mediterranean. O. Bar-Yosef and R. S. Kra**:** 75-88.
Forbes, H. A. and H. A. Koster (1976). "Fire, axe and plow: Human influence on local plant communities in the southern Argolid." Regional variation in modern Greece and Cyprus: Toward a perspective on the ethnography of Greece **268**: 109-126.
Fosberg, F. R. (1967). A classification of vegetation for general purposes. Guide to the Checklist for I.B.P. Areas. G. F. Peterken. Oxford, Blackwell Scientific Publications**:** 73-120.
Foster, J. J., E. Barkus, et al. (2006). Understanding and Using Advanced Statistics. London, SAGE Publications.
Franklin, J. (1995). "Predictive vegetation mapping: geographic modelling of biospatial patterns in relation to environmental gradients." Progress in Physical Geography **19**(4): 474-499.
Friend, A. D., H. H. Shugart, et al. (1993). "A physiology-based model of forest dynamics." Ecology letters **74**: 797-797.

Fyfe, R. (2006). "GIS and the application of a model of pollen deposition and dispersal: a new approach to testing landscape hypotheses using the POLLANDCAL models." Journal of Archaeological Science **33**: 483-493.
Fyllas, N. M., O. L. Phillips, et al. (2007). "Development and parameterization of a forest gap dynamics simulator for the North-Eastern Mediterranean region (GREFOS)." Ecological modelling **204**: 439-456.
Gilks, W., S. Richardson, et al. (1996). Markov Chain Monte Carlo in Practice, Chapman and Hall.
Goodchild, M. F., S. Guoqing, et al. (1992). "Development and test of an error model for categorical data." International Journal of Geographic Information Systems **6**(87-104).
Goring-Morris, A. N., E. Hovers, et al. (2009). The dynamics of Pleistocene and Early Holocene settlement patterns and human adaptations in the Levant: an overview. Transitions in Prehistory: Essays in Honor of Ofer Bare-Yosef. J. Shea and D. Lieberman. Oxford, Oxbow Books**:** 185-252.
Grove, A. T. and O. Rackham (2003). The Nature of Mediterranean Europe. New Haven and London, Yale University Press.
Haldon, J. (2006). Social Transformation in the 6th-9th C. East. Social and Political Life in Late Antiquity. W. Bowden, A. Gutteridge and C. Machado. Leidon, Brill**:** 603-647.
Harrison, S. P., I. C. Prentice, et al. (1992). "influence of insolation and glaciation on atmospheric circulation in the north-atlantic sector - implications of general-circulation model experiments for the late Quaternay climatology of Europe." Quaternary Science Reviews **11**: 283-299.
Hayes, A., M. Kucera, et al. (2005). "Glacial Mediterranean sea surface temperatures based on planktonic foraminiferal assemblages." Quaternary Science Reviews **24**: 999-1016.
He, F., J. Zhou, et al. (2003). "Autologistic Regression Model for the Distribution of Vegetation." Journal of Agricultural, Biological and Environmental Statistics **8**(2): 205-222.
Heiri, O. and F. L. André (2010). "How does taxonomic resolution affect chironomid-based temperature reconstruction." Journal of Palaeolimnology **44**: 589-601.
Helbaek, H. (1970). The plant husbandry of Haçilar. Excavations at Haçilar. J. Mellart. Edinburgh, Edinburgh University Press**:** 189-244.
Holdridge, L. R. (1947). "Determination of world formations from simple climatic data." Science **105**(367-368).
Hormes, A., F. Preusser, et al. (2003). "Radiocarbon and luminescence dating of overbank deposits in outwash sediments of the Last Glacial Maximum in North Westland, New Zealand." New Zealand Journal of Geology and Geophysics **46**: 95-106.
Hunter, M. D. (1992). "Playing chutes and ladders: Heterogeneity and the relative roles of bottom up and top down forces in natural communities." Ecology letters **73**(3).
Huntley, B. and I. C. Prentice (1993). Holocene vegetation and climates of Europe. Global Climates Since the Last Glacial Maximum. H. E. J. Wright, J. E. Kutzbach, T. I. Webbet al. Minnesota, University of Minnesota Press**:** 136-168.
Imai, K., G. King, et al. (2007). Relogit: Rare events logistic regression for dichotomous dependent variables. Zelig: Everyone's Statistical Software. K. Imai, G. King and O. Lau.

Issar, A. (1998). Climate change and history during the Holocene in the Eastern Mediterranean region. Water, environment and society in times of climatic change: contributions. A. Issar and N. Brown, Kluwer**:** 113-128.
Issar, S. A. and D. Yakir (1997). "The Roman Period's Colder Climate." Biblical Archaeologist **60**(2).
Izdebski, A. (2011). "Why did agriculture flourish in the late antique East? The role of climate fluctuations in the development and contraction of agriculture in Asia Minor and the Middle East from the 4th till the 7th c. AD." Millenium **8**: 291-312.
Jacobson, G. L. and R. H. W. Bradshaw (1980). "The selection of Sites for Palaeovegetational Studies." Quaternary Research **16**: 80-96.
James, I., N. Thorpe, et al. (1991). Centuries of Darkness. A challenge to the Conventional Chronology of Old World Archaeology. London.
Jones, M. D., C. N. Roberts, et al. (2007). "Quantifying climatic change through the last glacial-interglacial transition based on lake isotope palaeohydrology from central Turkey." Quaternary Research **67**: 463-473.
Kaniewski, D., V. De Laet, et al. (2007). "Long-term effects of human impact on mountainous ecosystems, western Taurus Mountains, Turkey." Journal of Biogeography **34**(11): 1975-1997.
Kaniewski, D., E. Paulissen, et al. (2007). "A high resolution Late Holocene landscape ecological history inferred from an intramontane basin in the Western Taurus Mountains, Turkey." Quaternary Science Reviews **26**: 2201-2218.
Keane, R. E., C. J. Cary, et al. (2004). "A classification of landscape fire succession models: spatial simulations of fire and vegetation dynamics. ." Ecological modelling **179**: 3-27.
Khuri, S., M. R. Shmoury, et al. (2000). "Conservation of the Cedrus libani populations in Lebanon: history, current status and experimental application of somatic embryogenesis." Biodiversity and Conservation **9**(9): 1261-1273.
King, G. and L. Zeng (2001). "Explaining Rare Events in International Relations." International Organisation **55**: 693-715.
Köppen, W. (1936). Das Geographisches System der Kilmate. Handbuch der Klimatologie. W. Köppen and R. Geiger. Berlin, Gebrüder Borntraeger.
Krebs, P., M. Conedera, et al. (2004). "Quaternary refugia of the sweet chestnut (Castanea sativa Mill.) an extended palynological approach." Vegetation History and Archaeobotany **13**.
Küchler, A. W. (1967). Vegetation Mapping. Ronald Press. New York.
Kuhn, S. (2002). "Palaeolithic archaeology in Turkey." Evolutionary Anthropology **11**: 198-210.
Kutzbach, J. E. and P. J. Guetter (1986). "the influence of changing orbital parameters and surface boundary conditions with climate simulation conditions for the past 18000 years." Journal of Atmospheric Science **43**: 1726-1759.
Lamb, H. H. (1977). Climate: Present, Past and Future. Climatic History and the Future. H. H. Lamb. London, Methuen. **2:** 835.
Landmann, G., A. Reimer, et al. (1996). "Climatically induced lake level changes at Lake Van, Turkey, during the Pleistocene/Holocene transition." Global Biogeochemical Cycles **10**: 797-808.
Laurent, J. M., A. Bar-Hen, et al. (2004). "Refining vegetation simulation models: From plant functional types to bioclimatic affinity groups of plants." Journal of Vegetation Science **15**(6): 739.

Longford, C., A. Drinnan, et al. (2009). Archaeobotany of Sos Hoyuk, northeast Turkey. New directions in archaeological science. B. Marwick. Canberra, ANU E press.
Magie, D. (1950). Roman Rule in Asia Minor to the end of the Third Century after Christ. Princeton, Princeton University Press.
Magny, M., C. Miramont, et al. (2002). "Assessment of the impact of climate and anthropogenic factors on Holocene Mediterranean vegetation in Europe on the basis of palaeohydrological records." Palaeogeography, Palaeoclimatology, Palaeoecology **186**(1-2): 47-59.
Maher, L. J. J. (2000) "Modpol.exe: a tool for searching for modern analogs of Pleistocene pollen data." Inqua sub-commission on data handling methods **Newsletter 20**.
Martinoli, D. C. (2009). Plant food economy and environment during the epipalaeolithic in southwest Anatolia: an investigation of the botanical macroremains from Öküzini and Karain B. Faculty of Science. Basel, University of Basel. **PhD**.
McGarry, S., M. Bar-Matthews, et al. (2004). "Constraints on hydrological and paleotemperature variations in the Eastern Mediterranean region in the last 140 ka given by the dD values of speleothem fluid inclusions." Quaternary Science Reviews **23**: 919-934.
Médail, F. and K. Diadema (2009). "Glacial refugia influence plant diversity patterns in the Mediterranean Basin." Journal of Biogeography **36**(7): 1333-1345.
Mellaart, J. (1958). "Excavations at Hacilar." Anatolian Studies **8**: 127-156.
Mellaart, J. (1962). "Çatal Hüyük excavations 1961." Archälogischer Anzeiger: 1-11.
Mellaart, J. (1962). "Excavations at Çatal Hüyük, first preliminary report." Anatolian Studies **12**: 41-65.
Migowski, C., M. Stein, et al. (2006). "Holocene climate cariability and cultural evolution in the Near East from the Dead Sea sedimentary record." Quaternary Research **66**: 421-431.
Millington, J., J. Wainwright, et al. (2009). "Modelling Mediterranean landscape succession-disturbance dynamics: A landscape fire-succession model." Environmental Modelling and Software: 1196-1208.
Mitchell, S. (1995). Land, Men and Gods in Asia Minor. The Celts in Anatolia and the impact of Roman rule, Clarendon Press.
Mitchell, S. (2005). Olive cultivation in the Economy of Asia Minor. Patterns in the economy of Asia Minor. S. Mitchell and C. Katsari. Swansea**:** 82-113.
Mooney, D. and R. Swift (1999). A Course in Mathematical Modeling, The Mathematical Association of America.
Nadel, D. and I. Hershkovitz (1991). "New subsistence data and human remains from the earliest Levantine Epipalaeolithic." Current Anthropology **32**(223-239).
Naveh, Z. (1982). "Mediterranean landscape evolution and degradation as multivariate biofunctions: Theoretical and practical implications." Landscape Plannin **9**(2): 125-146.
Neilsen, A. B. (2005). "Quantifying the relationship between pollen sedimentation in lakes and land cover using historical maps." Geological Survey of Denmark and Greenland Bulletin **7**: 49-52.
Nicol-Pichard, S. (1987). "Analyse pollinique d'une séquence tardi et postglaciare à Tourves (Var, France)." Ecologie Mediterranea **13**: 29-42.
Niklewski, J. and W. Van Zeist (1970). "A Late Quaternary pollen diagram for NW Syria." Acta Botanica Neerlandica **9**(737-54).

Orland, I. J., M. Bar-Matthews, et al. (2009). "Climate deterioration in the eastern Mediterranean as revealed by ion microprobe analysis of a speleothem that gre from 2.2 to 0.9 ka in Soreq Cave, Israel." Quaternary Research **71**: 27-35.
Oswald, W. W., L. B. Brubaker, et al. (2003). "Pollen-vegetation calibration for tundra communities in the Arctic Foothills, northern Alaska." Journal of Ecology **91**: 1022-1033.
Overpeck, J. T., T. I. Webb, et al. (1985). "Quantitative interpretation of fossil pollen spectra: Dissimilarity coefficients and the method of modern analogs." Quaternary Research **23**(1): 87-108.
Oxcal. (2010). "Analysis Details." Retrieved October, 2010, from http://c14.arch.ox.ac.uk/oxcalhelp/hlp_analysis_detail.html.
Parsons, R. W. and I. C. Prentice (1981). "Statistical approaches to R-values and pollen-vegetation relationship." Review of Palaeobotany and Palynology **32**: 127-152.
Peng, C. (2000). "From static biogeographical model to Dynamic Global Vegetation Model: A global perspective on modelling vegetation dynamics." Ecological modelling **25**: 33-54.
Peng, C., J. Guiot, et al. (2011). "Integrating models with data in ecology and palaeoecology: advances towards a model-data fusion approach." Ecology letters **14**: 522-536.
Piotrowska, N., M. Blaauw, et al. (2010). "Constructing deposition chronologies for peat deposits using radiocarbon dating." Mires and Peat **7**: 1-14.
Prell, W. L. (1985). The stability of low-latitude sea-surface temperatures: An evaluation of the CLIMAP reconstruction with emphasis on the positive SST anomalies. Washington DC, Department of Energy**:** 60.
Prentice, C., W. Cramer, et al. (1992). "A global biome model based on plant physiology and dominance, soil properties and climate." Journal of Biogeography **1992**(19): 117-134.
Prentice, I. C. (1980). "Multidimensional scaling as a research tool in Quaternary palynology: A review of theory and methods." Review of Palaeobotany and Palynology **31**: 71-104.
Prentice, I. C. (1985). "Pollen representation, source area, and basin size: toward a unified theory of pollen analysis." Quaternary Research **23**: 76-86.
Prentice, I. C. (1988). Records of vegetation in time and space: the principles of pollen analysis. Vegetation history. H. Leith. The Netherlands, Kluwer Academic Publishers. **7**.
Prentice, I. C., J. Guiot, et al. (1992). "Mediterranean vegetation, lake levels and palaeoclimate at the Last Glacial Maximum." Nature **360**: 658-660.
Prentice, I. C. and R. W. Parsons (1983). "Maximum liklihood linear calibration of pollen spectra in terms of forest composition." Biometrics **39**: 1051-1057.
Rackham, O. (1992). Mixtures, mosaics and clones: the distribution of trees within European woods and forests. The ecology of mixed-species stands of trees. M. G. R. Cannell, D. C. Malcolm and P. A. Robertson. London, Blackwell**:** 1-20.
Raunkiaer, C. (1934). The life forms of plants and statistical plant geography. Oxford, Clarendon Press.
Reimer, P. J., M. G. L. Baillie, et al. (2009). "IntCal09 and Marine09 radiocarbon age calibration curves, 0–50,000 years cal BP." Radiocarbon **51**(4): 1111-1150.
Roberts, C. N. (1983). "Age, palaeoenvrionments and climatic significance of Late Pleistocene Konya Lake, Turkey." Quaternary Research **19**: 154-171.

Roberts, C. N., W. J. Eastwood, et al. (1997). The age and causes of Mid-Late Holocene environmental change in southwest Turkey. Third Millennium BC Climate Change and Old World Collapse, . Nüzhet Dalfes, G. Kukla and H. Weiss. Berlin Heidelberg, Spreinger-Verlag**:** 411-429.
Roberts, C. N., J. M. Reed, et al. (2001). "The tempo of Holocene climate change in the eastern Mediterranean region: new high-resolution crater-lake sediment data from central Turkey." The Holocene **11**(6): 721-736.
Roberts, C. N. and H. E. J. Wright (1993). Vegetational, lake-level and climatic history of the Near East and Southwest Asia. Global climates since the last glacial maximum. H. E. J. Wright, J. E. Kutzbach, T. I. Webbet al. Minneapolis, University of Minnesota Press**:** 194-220.
Roberts, L. (1987). "Documents d'Asie Mineure." The Classical Review **40**(1).
Roberts, N. (1990). Human-induced landscape change in south and southwest Turkey during the later Holocene. Man's role in the shaping of the Eastern Mediterranean landscape. S. Bottema, G. Entjes-Nieborg and W. v. Zeist. Rotterdam**:** 53-67.
Roberts, N., D. Brayshaw, et al. (2011). "The mid-Holocene climatic transition in the Mediterranean: Causes and consequences." The Holocene **21**: 3-13.
Roberts, N., M. D. Jones, et al. (2008). "Stable isotope records of Late Quaternary climate and hydrology from Mediterranean lakes: the ISOMED synthesis." Quaternary Science Reviews **27**(25-26): 2426-2441.
Roberts, N. and H. E. Wright (1993). Vegetational, lake level, and climatic history of the Near East and Southwest Asia. Global climates since the last glacial maximum. J. H E Wright, J. E. Kurtzbach, T. W. IIIet al. Minneapolis, University of Minnesota Press. (COHAMP volume)**:** 53-67.
Robinson, S. A., S. Black, et al. (2006). "A review of palaeoclimates and palaeoenvironments in the Levant and Easter Mediterranean from 25,000 to 5000 years BP: setting the environmental background for the evolution of human civilisation." Quaternary Science Reviews **25**: 1517-1541.
Rohling, E. J. and F. J. Hilgen (1991). "The eastern Mediterranean climate at times of sapropel formation: a review." Geologie en Mijnbouw **70**: 253-264.
Rossignol-Strick, M. (1987). "Rainy periods and bottom water stagnation initiating brine accumulation and metal concentrations: 1. the Late Quaternary." Palaeoceanography **2**: 333-360.
Rossignol-Strick, M. (1999). "The Holocene climatic optimum and pollen records of sapropel 1 in the Eastern Medierranean, 9000-6000 BP." Quaternary Science Reviews **18**: 515-530.
Sachs, H. M., T. Webb III, et al. (1977). "Palaeoecological transfer functions." Annual Review of Earth Planetary Science **5**: 159-178.
Sarıkaya, M. A., M. Zreda, et al. (2008). "Cold and wet Last Glacial Maximum on Mount Sandıras, SW Turkey, inferred from cosmogenic dating and glacier modelling." Quaternary Science Reviews **27**: 269-780.
Schoop, U. D. (2005). The Late Escape of the Neolithic from the Central Anatolian Plain. How did farming reach Europe. C. Lichter. **BYZAS 2:** 41-58.
Şenkul, Ç. and U. Doğan (2012). "Vegetation and climate of Anatolia and adjacent regions during the Last Glacial period." Quaternary International **3**: 1-13.
Shugart, H. H., M. Y. Antonovsky, et al. (1986). Climatic change and forest ecosystems. The greenhouse effect, climatic change and ecosystems. B. R. Bolin, J. Döös, J. Jäger and R. A. Warrick. Chichester, Wiley**:** 475-521.

Smith, B., I. C. Prentice, et al. (2001). "Representation of vegetation dynamics in the modelling of terrestrial ecosystems: comparing two contrasting approaches within European climate space." Global Ecology and Biogeography **10**(6): 621-637.
Smith, B., I. C. Prentice, et al. (2001). "Representation of vegetation dynamics in the modelling of terrestrial ecosystems: comparing two contrasting approaches within European climate space." Global Ecology and Biogeography **10**: 621-638.
Smith, C. D. (1996). Where was the 'wilderness' in Roman times? Human landscapes in Classical antiquity. London, Routledge**:** 154-179.
Spikins, P. (2000). "GIS Models of Past Vegetation: An example from Northern England, 10,000-5000BP." Journal of Archaeological Science **27**: 219-234.
Stevens, L. R., H. E. J. Wright, et al. (2001). "Changes in seasonality of climate during the Lateglacial and Holocene at Lake Zeribar, Iran." The Holocene **11**: 747-756.
Sugita, S. (1993). "A model of Pollen Source Area for an Entire Lake Surface." Quaternary Research **39**: 239-244.
Sugita, S. (1994). "Pollen representation of vegetation in Quaternary sediments: theory and method in patchy vegetation." Journal of Ecology **82**(811-897).
Sugita, S. (1997). Reconstruction of fire disturbance and forest succession from fossil pollen in lake sediments: potential and limitations. Sediment records of biomass burning and global change. J. S. Clark, H. Cashier, J. G. Goldmmer and B. J. Stocks. Berlin, Springer-Verlag**:** 387-412.
Sugita, S. (2007a). "Theory of quantitative reconstruction of vegetation I: pollen from large sites REVEALS regional vegetation compostion." The Holocene **17**(2): 229-241.
Sugita, S. (2007b). "Theory of quantitative reconstruction of vegetation II: All you need is LOVE." The Holocene **17**(2): 243-257.
Sugita, S., S. T. Andersen, et al. (1998). Quantification of land surfaces cleared of forests during the Holocene. Palaeoklimaforschung / Palaeoclimate Research. M. J. Gaillard, B. E. Berglund, N. Frenzel and U. Huckried. Stuttgart, Gustac Fisher Verlag. **27:** 125-131.
Sugita, S., M. J. Gaillard, et al. (1999). Landscape openness and pollen records: a simulation approach. **9:** 409-421.
Sugita, S. and A. E. Scott (2007). POLLEN METHODS AND STUDIES | POLLSCAPE Model. Encyclopedia of Quaternary Science. Oxford, Elsevier**:** 2561-2570.
Sutton, O. G. (1953). Micrometeorology: a study of physical processes in the lowest layers of the Earth's atmosphere. New York, McGraw-Hill Book Company Inc.
Sykes, M. T., I. C. Prentice, et al. (1996). "A bioclimatic model for the potential distribution of northern European tree species under present and future climates." Journal of Biogeography **23**: 203-233.
Sykes, M. T., I. C. Prentice, et al. (2001). "An introduction to the European Terrestrial Ecosystem Modelling Activity." Global Ecology and Biogeography **10**: 581-593.
Taberlet, P. and R. Cheddadi (2002). "Quaternary refugia and persistence of biodiversity." Science **297**: 2009-2010.
Tauber, H. (1965). "Differential pollen dispersion and the interpretation of pollen diagrams." Danmarks Geologiske Undersøgelse (Afhanlinger), Rœkke II **89**: 1-69.
Thirgood, J. V. (1981). Man and the Mediterranean: a history of resource depletion. London, Academic Press.
Thissen, L. (2010). "The Neolithic-Chalcolithic sequence in the SW Anatolian Lakes Region." Documenta Praehistorica **XXXVII**: 633-636.

Tinner, W. and A. F. Lotter (2006). "Holocene expansions of Fagus silvaticva and Abies alba in Central Europe: where are we after eight decades of debate?" Quaternary Science Reviews **25**: 526-549.
Tomaselli, R. (1977). "The Degradation of the Mediterranean Maquis." Ambio **6**(6).
Toner, M. and P. Keddy (1997). "River hydrology and riparian wetlands: a predictive model for ecological assembly." Ecological Applications **7**: 236-246.
Turner, R., N. Roberts, et al. (2010). "Fire, climate and the origins of agriculture: Micro-charcoal records of biomass burning during the Last Glacial-Interglacial transition in Southwest Asia." Journal of Quaternary Science **25**: 371-386.
Uerpmann, H. P., G. Albrecht, et al. (1992). "Late Pleistocene and Early Holocene finds from Öküzini: A contribution to the settlement history of the Bay of Antalya, Turkey." Paléorient **18**(2): 123-141.
van West, C. R. (1994). Modelling prehistoric climatic variability and agricultural production in southwestern Colorado: a GIS approach. Reports of Investigations. Pullman, Washington State University Department of Anthropology.
van Zeist, W. and S. Bottema (1977). "Palynological investigations in western Iran." Palaeohistoria **19**: 1995.
van Zeist, W. and S. Bottema (1982). Vegetational history of the Eastern Mediterranean and Near East during the last 20,000 years. Palaeoclimates, Palaeoenvironments and Human Communities in Eastern Mediterranean Region in later Prehistory. Oxford, British Archaeological Report, International Series. **133:** 277-321.
van Zeist, W. and S. Bottema (1991). Late Quaternary vegetation of the Near East. Beihefte zum Tubinger Atlas des vorderen orients, naturwissenschaften A. Reihe. Weisbaden, Dr Ludwig Reichert Verlag. **18:** 156.
van Zeist, W., H. Woldring, et al. (1975). "Late Quaternary vegetation and climate of southwestern Turkey." Palaeohistoria **17**: 55-143.
van Zeist, W. and H. E. J. Wright (1963). "Preliminary pollen studies at Lake Zeribar, Zagros Mountains, southwestern Iran." Science **140**: 65-67.
Vanhaverbeke, H. (1999). The evolution of the settlement pattern on the territory of Sagalassos (Pisidia, SW Turkey). Palaeo-ecology and palaeo-economy from the prehistoric until recent times. (Unpublished PhD thesis), K. U. Leuven.
Vanhaverbeke, H., A. K. Vionis, et al. (2009). What happened after the 7th century AD? A different perspective on Post-Roman rural Anatolia. Archaeology of the Countryside in Medieval Anatolia. Leuven, Nederlands Instituut voor het Nabije Oosten**:** 177-190.
Vanhaverbeke, H. and M. Waelkens (2003). The Chora of Sagalassos. The evolution of the settlement pattern from prehistoric until recent times. Belgium, Brepolis.
Vermoere, M. (2002). Holocene vegetation history in the territory of Sagalassos (southwest Turkey) A palynological approach, K.U. Leuven. **PhD**.
Vermoere, M., S. Bottema, et al. (2002). Palynological evidence for late-Holocene human occupation recorded in two wetlands in SW Turkey. **12:** 569-584.
Vermoere, M., E. Smets, et al. (2000). "Late Holocene Environmental Change and the Record of Human Impact at Gravgaz near Sagalassos, Southwest Turkey." Journal of Archaeological Science **27**(7): 571-595.
Vogiatzakis, I. N. and G. H. Griffiths (2006). "A GIS-based empirical model for vegetation prediction in Lefka Ori, Crete." Plant Ecology **184**(2): 311-323.
von Post, L. (1916). "Om skogstädpollen i sydsvenska torfmosselagerföljder." Geologiska Föreningen i Stockholm Forhandlingar **38**: 384-390.

Waelkens, M. (1999). "Man and Environment in the territory of Sagalassos, a classical city in southwest Turkey." Quaternary Science Reviews **18**(4-5): 697-709.
Waelkens, M. (2000). Sagalassos and Pisidia during the Late Bronze Age. Report on the survey and excavation campaigns of 1996 and 1997. Acta Archaeological Lovaniensia Monographiae. M. Waelkens and L. Loots. Leuven, Leuven University Press. **11/B:** 473-485.
Waelkens, M., E. Paulissen, et al. (1997). The 1994 and 1995 surveys on the territory of Sagalassos. Sagalassos IV. Report on the Fifth Excavation Campaign of 1994 (Acta Archaeological Lovaniensia). M. Waelkens. Leuven. **9:** 11-102.
Wang, J. T. (1988). "The steppes and deserts of the Xizang Plateau (Tibet)." Vegetatio **75**: 135-142.
Weiss, B. (1982). "The decline of Late Bronze Age civilisation as a possible response to climatic change." Climatic change **4**(2): 173-198.
Weiss, E., W. Wetterstrom, et al. (2004). "The broad spectrum revisited: evidence from plant remains." Proceedings of the National Academy of Sciences of the United States of America **101**(9551-9555).
Wheatley, D. and M. Gillings (2002). Spatial technology and archaeology: the archaeological applications of GIS. New York, Taylor and Francis.
Whitlock, C. and P. J. Bartlein (1997). "Vegetation and climate change in northwest America during the past 125 kyr." Nature **388**: 57-61.
Wick, L., G. Lemcke, et al. (2003). "Evidence of Lateglacial and Holocene climatic change and human impact in eastern Anatolia: high-resolution polen, charcoal, isotopic and geochemical records from the laminated sediments of Lake Van, Turkey." The Holocene **13**(5): 665-675.
Willemsen, D. (2011). "Wind Roses - South Turkey." from http://www.sailingissues.com/windroses-turkey.html.
Woodward, F. I. (1987). Climate and plant distribution. Cambridge, Cambridge University Press.
Wu, H. and F. W. Huffer (1997). "Modelling the Distribution of Plant Species using the Autologistic Regression Model." Environmental and Ecological Statistics **4**: 49-64.
Yakar, T. (2006). Dating the sequence of the final destruction / abandonment of the LBA settlements: Towards a better understanding of events that led to the collapse of the Hittite Kingdom. Structure and Dating in Hittite Archaeology. D. P. Mielke, U. D. Schoop and J. Seeher. Instanbul, Deutsches Archäeologisches Institut Istanbul.
Yalçinkaya, I., M. Otte, et al. (2002). La grotte d'Öküzini: évolution du paléolithique final du sud-ouest de l'Anatolie Liege.
Zavala, M. A., J. M. Espelta, et al. (2000). "Constraints and trade-offs in Mediterrnaean plant communities: the case of mixed holm oak-Aleppo pine forests." Botanical Reivew **66**: 119-149.
Zavala, M. A. and E. Zea (2004). "Mechanisms maintaining biodiversity in Mediterranean pine-oak forests: insights from a spatial simulation model." Plant Ecology **171**: 197-207.
Zohary, D. and M. Hopf (1993). Domestication of plants in the Old World: the origin and spread of cultivated plants in west Asia, Europe and the Nile valley. Oxford, Clarendon Press.
Zohary, M. (1973). Geobotanical Foundations of the Middle East. Stuttgart-Amsterdam.

# A GIS approach to palaeovegetation modelling in the Mediterranean: the case study of southwest Turkey

**By**

**Anneley McMillan**

## Informational Appendices

This section contains information appendices to provide background to the palaeoecology and palaeoclimatology of the Mediterranean, and the study are of southwest Turkey. It presents background information to the data used to build the vegetation model, along with justification for its inclusion. It also contains tabular data, graphs, charts and maps from model runs that provide further detail to the main thesis body.

**Table of contents**

1 Appendix defining the Mediterranean ..... 5

2 Appendix Palaeoclimatological and palaeoecological information from the wider Mediterranean ..... 7

3 Appendix The environment of southwest Turkey ..... 18

4 Appendix Palaeoclimatological and Palaeoecological data from southwest Turkey ..... 22

5 Appendix The Beyşehir Occupation Phase ..... 35

6 Appendix Review of model data sources ..... 40

7 Appendix Sampling ..... 58

8 Appendix Test statistics comparing variables of species distribution with the European control dataset ..... 63

9 Appendix Rare Events Logistic Regression output ..... 72

10 Appendix Background to model runs ..... 79

11 Appendix Radiocarbon Calibration and Bayesian analysis ..... 99

**Table of figures**

Figure 4-1 Pollen coring locations across southwest Turkey ..... 26

Figure 6-1 The distribution of *Vitis* throughout Europe (EEA 2000) ..... 41

Figure 6-2 The distribution of *Quercus cerris* throughout Europe (after Köble and Seufert 2001) ..... 42

Figure 6-3 The distribution of *Pinus brutia* throughout Turkey (OGM 1997) ..... 42

Figure 6-4 Worldclim monthly precipitation data (February), 1950-2000 ..... 53

Figure 6-5 The relationship between average winter temperatures and absolute minimum temperatures through Turkey ..... 54

Figure 6-6 Modelled absolute winter minimum temperature mapped across southwest Turkey ..... 54

Figure 7-1 Example of species random stratified sample ..... 61

Figure 8-1 relative correlation of winter precipitation regression co-efficient with species distribution ..... 78

Figure 9-1 (a) Absolute winter minimum temperatures based on 30 year reference period (b) Absolute winter minimum temperatures based on -6°C below modern average ..... 81

Figure 9-2 (a) modern average annual temperature, with key areas of low and high temperature highlighted (b) Probable extent of below freezing average winter temperatures under different winter temperature anomalies. Note that the colours do not represent different temperatures, only whether the area is likely to be freezing of below under each model run (i.e. under a model run with average temperatures -2°C lower than modern conditions, for instance) ..... 84

Figure 9-3 CORINE land cover, overlaid with annual temperature isotherms. This shows that bare ground is correlated to areas of low temperature. ..... 85

Figure 9-4(a) Modern winter precipitation (b) Winter precipitation -200 mm ..... 87

Figure 9-5 CORINE land cover with winter precipitation isohyets superimposed, showing correlation between high winter precipitation and forest distribution. ..... 88

Figure 9-6 (a) Aridity index under modern conditions (b) Aridity classifications, where semi-arid is between 0.2 and 0.5, dry sub-humid is between 0.5 and 0.65 and humid is over 0.65. .... 90

Figure 9-7 CORINE land cover, overlaid with the isohume of humidity ..... 91

Figure 9-8 (a) Aridity classification under -8°C temperature (b) Difference in aridity between modern values and -8°C with -100 mm, showing increase in humidity across most of the region. ..... 92

Figure 9-9 (a) Difference in aridity between modern values and a scenario with -8°C and -200 mm winter precipitation, showing areas in Muğla and Antalya where humidity has increased, and areas in the interior where aridity has increased (b) Difference in aridity between modern values and -8°C with -300 mm, showing increase in aridity across most of the region. ..... 94

Figure 9-10 The difference between modern aridity and potential aridity due to change in radiation at the beginning of the Holocene..... 95

Figure 9-11 (a) Summer precipitation +50 mm (b) The difference between modern aridity and aridity due to increased summer precipitation and temperature. ..... 97

Figure 9-12 CORINE land cover, overlaid with summer precipitation isohyets. ..... 98

# 1 APPENDIX: DEFINING THE MEDITERRANEAN

This thesis develops vegetation modelling within the particular context of a Mediterranean environment. In order to achieve this, it is firstly instructive to understand and characterise the Mediterranean. However, defining this environment in itself is not a straightforward task, as the concept of the Mediterranean has been traditionally done in a variety of ways. The *Mediterraneus* is the c. 1400 Latin term for "midland", and *Mediterraneum mare* equates to the sea between the land (OED 2011). The Romans called the Mediterranean Sea the Mare Nostrum (our Sea), or occasionally Mare Internum (Sallust, Jug. 17), and at the height of the Empire owned much of the land around it. The Greek term *Mesogeios* (Μεσόγειος), is comprised of two terms; μέσο meaning "middle" and γη meaning "land or earth"(Liddell and Scott 1940). The Mediterranean Sea and Mediterranean countries surrounding the sea have traditionally been intricately linked with each other, and can at one level be defined topographically as existing since the Mediterranean Sea was formed, some 5.33 million years ago during the Zanclean flood (Garcia-Castellanos, Estrada et al. 2009). The Mediterranean Basin today stretches over c. 3800 km west-east and 1000 km north-south, between 30°N and 45°N (Blondel and Aronson 2004) and covers portions of Europe, Asia and Africa. Due to the size of the region, a distinct split has traditionally been defined between the Western Mediterranean (west of the Sicily-Cap Bon line) and the Eastern Mediterranean (Grove and Rackham 2003).

However, in addition to this definition, the term 'Mediterranean' has also been used in a more fuzzy sense to define a particular climate regime or vegetation assemblage that is traditionally thought of as being typified in the Mediterranean environment. This is where definitions start to become fuzzy as an area has sometimes been defined as 'Mediterranean' by its vegetation (a 'bioindicator' approach), and usually considers species such as *Olea europeae*, *Quercus ilex* and *Citrus* to be typically Mediterranean (Grove and Rackham 2003; Blondel and Aronson 2004). Indeed, Pliny the Elder (AD 23-79) used the area of olive cultivation to define the limits of the Mediterranean.

Another way of defining the Mediterranean region is by using a bioclimatic view, stating that the Mediterranean is the area that has a transitional regime, between cold temperate and dry tropical climates (Blondel and Aronson 2004). Variations in climatic regime are apparent spatially across the Mediterranean, but also temporally, both through long scale climate change, and shorter scale extreme events. If the Mediterranean is instead defined climatologically, and it is known that the climate of the Mediterranean has shifted dramatically through time, this suggests a different view of the consistency of the Mediterranean through time. Pertinently, Blondel and Aronson assert that:

> 'The Mediterranean climate we know today only began to appear during the late Pliocene, about 3.2 Myr BP, as part of a global cooling trend (Suc 1984) and became firmly established throughout the region about 2.8 Myr BP.' (Blondel and Aronson 2004 p. 21)

Although they state that the area of the Mediterranean has been interspersed by glacial and interglacial cycles since, the above assertion raises an interesting question as to whether it is really the case that since the Pliocene, the 'default' climate in the Mediterranean region has been

a Mediterranean one, and that glacial and interglacial cycles that do not fit this definition are temporary aberrations. Particularly since little is known about seasonal climate cycles throughout this period, it begs the question what magnitude and longevity of climatic shifts are allowable to still define the region as climatically 'Mediterranean'?

Blondel and Aronson (2004) define the modern Mediterranean climate as one with an alternating hot-dry and cold-wet season, where summer is the driest season, during which there is a prolonged period of drought, requiring ecophysiological adaptations. Due to this, spring and autumn seasons are deemed essential for plant growth, carrying with it the risk of early and late frosts which can damage plants that are active during these times. A key question here is whether strict definitions of a particular precipitation or temperature regime would therefore exclude mountainous areas as having a Mediterranean climate as they have their own microclimates dictated by their orographic nature (Blondel and Aronson 2004).

It is because of this inherent complexity and dynamism, that the Mediterranean is sometimes defined by a culmination of factors such as described by Gaussen (1954), or *The Corrupting Sea* (Horden and Purcell 2000). In this case the Mediterranean is differentiated from its neighbours by the vague notion of the 'sheer intensity and complexity of the ingredients of the paradigm' (Horden and Purcell 2000 p.37). The particular qualities of the Mediterranean here are as seen from an anthropological perspective, and are described as (1) a particular set of risks due to climatic and political uncertainty, (2) a distinctive production regime aimed at coping with this risk (3) extreme topographical fragmentation and (4) the distinctive regime of communications due to a landlocked sea, complex coastlines and islands.

If 'The Mediterranean' is called in relation to climatological, ecological, or socio-political concepts, its boundaries would shift through time, therefore creating a propensity to 'pulse', to expand and contract with environmental and cultural conditions, as suggested in (Braudel 1996). It is therefore considered key to make a distinction between *the* Mediterranean, defined as those countries surrounding the Mediterranean Sea, with other areas that might experience a fluctuating Mediterranean climate or Mediterranean vegetation assemblage.

Within this first definition, Turkey is undoubtedly a country within the Mediterranean. Furthermore, there are also areas within Turkey, particularly the southwest, which fall today under the more transient definitions of Mediterranean climate, and Mediterranean flora. The parallel and interlinked definitions of the 'typical' Mediterranean, particularly in terms of evidence for and against its continuity and longevity are considered important issues in this thesis. In essence, the vegetation modelling approach needs to replicate modern Mediterranean vegetation well, but also need to have the capability to investigate how other forms of environment can coalesce, as climate, culture and vegetation shifts further away from its current regime.

# 2 APPENDIX: PALAEOCLIMATOLOGICAL AND PALAEOECOLOGICAL INFORMATION FROM THE WIDER MEDITERRANEAN

## 2.1 PALAEOENVIRONMENTAL DATA

A wealth of different lines of palaeoenvironmental evidence are available to inform on past vegetation and climate phases. Fossil pollen assemblages are the primary source of information on past vegetation composition and pattern (Jackson and Lyford 1999). Core sediments and sections taken from sites of interest have the potential to provide a continuous record of pollen assemblages over time, and interpretation of these records can inform researchers of changes in the wider environment. Gaining past vegetation composition and distribution from such data is complex however, as interpretation depends on many factors such as preservation bias, pollen productivity, fall speed and deposition environment (Davis 1963; Sugita 1993; Sugita 1994; Calcote 1995; Bunting, Twiddle et al. 2007; Broström, Neilson et al. 2008). Past vegetation composition can also be studied by examining macrofossils, or through palaeobotanical evidence found either in situ, or as part of archaeological excavations (e.g. Martinoli 2009). It is important to note that plant and tree remains that are not in situ also provide challenges in interpretation in terms of dating and the source of the material. Pollen and macrofossil evidence have also been used as climate proxies (Guiot and Pons 1986; Barboni, Harrison et al. 2004; Peyron, Goring et al. 2011). However difficulties are encountered here due to the reaction of vegetation to factors other than climate, such as disease, human interference, animal browsing, etc. (Kaniewski, De Laet et al. 2007a; Bradshaw 2008; Caseldine, Fyfe et al. 2008).

Within the context of this thesis, reconstructed climate evidence will be taken from those proxies that are considered to be 'independent', i.e. those that do not rely on pollen evidence for their interpretation. Independent climatic reconstructions can be made by analysing various different proxies; such as lake deposits (Bartov, Stein et al. 2002), speleothems (McGarry, Bar-Matthews et al. 2004), groundwater, animal bone, diatoms, foraminifera (Hayes, Kucera et al. 2005) or snail shells (Goodfriend 1999). Depending on the material, different climatic conversions, retrodictions and transfer functions can be applied.

Stable isotope analysis can be undertaken on a number of materials such as wood, soil, organics and sediments, to investigate the ratio of various isotopes, such as carbon (13C/12C), oxygen ($O^{18}/O^{16}$), nitrogen ($^{15}N/^{14}N$) and hydrogen (D/H) (Goodfriend 1999). Stratigraphical interpretation of sediments can reveal information on the temporal frequency and spatial characteristics of hydrological cycles impacted by climatic shifts (Bartov, Stein et al. 2002). The identification and classification of Foraminifera can be used to investigate basin characteristics, including water depth and mixing regimes (Hayes, Kucera et al. 2005). Dating methods such as radiocarbon, Uranium-Thorium or Thermoluminescence dating allow climate proxies to be anchored and compared with other data through time.

Although lake isotope values depend on a multitude of factors such as temperature, seasonality and air mass source, the predominant control is water balance, with more negative $\delta^{18}O$ values indicating periods of greater moisture availability (Roberts, Jones et al. 2008; Roberts, Eastwood et al. 2011b).

Aside from individual proxy evidence, climate models which assimilate modern data with palaeoclimate evidence to create general climatic rules are also used to retrodict climatic situations (Robinson, Black et al. 2006). It is important to note that all of these 'independent' climate proxies, just like palynological evidence, can be affected by factors aside from climate, and their interpretation always contains some uncertainty. Different proxies have different levels of uncertainty due to the differential constraint and knowledge of these other variables. A summary of some of the main advantages and disadvantages of climate proxies are displayed in

Table 2-1. As well as uncertainty in climate interpretation, temporal uncertainty also differs depending on the quality of dating substance and type of dating approach applied. This will be discussed in more detail later in this chapter.

**Table 2-1 Advantages of different palaeoclimate proxies (after Goodfriend 1999)**

| Method | Input data | Advantages | Disadvantages |
|---|---|---|---|
| Oxygen isotope analysis | Groundwater, lake deposits, | Variables that affect analysis relatively well known | Depends on knowledge of metabolic effects, inflows and outflows into lakes, evaporation rates, fractionation, |
| Speleothem oxygen isotope analysis | 18O, 13C and 87Sr / 86SR | Variables that affect analysis relatively well known | Depends on knowledge of latitude, altitude, air temperature, groundwater processes. Assumes carbonate has been precipitation in isotopic equilibrium with cave drip water. |
| Carbon isotope analysis | Soil organic matter, teeth, bone, Snail shells, | Variables that affect analysis relatively well known | Depends on knowledge of metabolic pathway of carbon fixation, knowledge of plant species |
| Fluvial sediments | Terraces, fans, Aeolian sediments | Can highlight hydrological regime | Lack of dateable materials |
| GCM | Assimilates modern climate data or other proxy data | Can be used to test hypotheses, indicate mechanisms | Low spatial resolution |
| Deep sea cores (Sea surface temperature, sea-surface salinity, continental run-off) | Foraminifera, | Continuous | Low temporal resolution |
| Cosmogenic nuclide analysis | Glacial sediments | Provides direct evidence of glacier extent | Can be reworked by subsequent processes |

## 2.2 PALAEOCLIMATOLOGY OF THE MEDITERRANEAN SINCE THE LAST GLACIAL MAXIMUM

This section will summarise some of the main lines of evidence previously used to define climatic change in the Mediterranean since the Last Glacial Maximum (LGM). It is not a definitive review, but highlights the main events in order to act as a basis for comparison with pollen evidence. It will be marked, where relevant, by key palaeoclimate phases in the northern hemisphere (such as Heinrich events), and will highlight key contrasts with pollen evidence where they exist. The review incorporates the summary by Robinson et al. (2006), and chronology generally follows the conversion by Robinson et al. (2006) into consistent Cal yr BP dates.

### 2.2.1 The Last Glacial Maximum

The Last Glacial Maximum is defined as occurring between ~25-19 Cal ka yr BP, and is defined by a low stand in sea levels, and by a solar insolation minimum, based on changes to orbital mechanics (Walker 1995; Walker, Bjorck et al. 1999; Sarnthein, Gersonde et al. 2003). Evidence for climate conditions in the Mediterranean during this period come from a number of different approaches and are broadly in agreement in terms of a cooler environment. Foraminifera proxy data from the Levantine Basin indicates cool Sea Surface Temperatures (Hayes, Kucera et al. 2005), and stable isotope analysis indicates low average temperatures in Israel (McGarry, Bar-Matthews et al. 2004). Stable isotope analysis also suggests climatic aridity in Turkey (Roberts, Jones et al. 2008).

There is not yet agreement on the variation and magnitude of cooling, due to the variety of study areas, proxy evidence used and methodologies followed, but a number of studies have published preliminary estimates. For instance, evidence from Peqiin, Soreq and Efrayim cave in Israel (McGarry, Bar-Matthews et al. 2004) suggests a low average temperature of ~7 to 14 °C, as opposed to ~20 °C today. Affek et al. (2008) estimates a reduction of ~6 to 7 °C based on clumped isotope thermometry. Sea Surface Temperature (SST) reconstructions retrodict that SST across the Eastern Mediterranean were likely to have been -2°C cooler using foraminifera, and -5 to 6°C cooler using the alkenone method (Emeis, Schulz et al. 1998; Emeis, Struck et al. 2000; Emeis, Schulz et al. 2003). Little is known about the seasonality of this reduction in temperatures, although Robinson et al. (2006) undertook GCM modelling using the UK Met Office (UKMO) GCM, based on CLIMAP SST and the Peltier ice sheet reconstructions. This showed that in general, cooler winters would be prevalent, leading to potentially less evaporation.

Long term lake level and sea level records have also provided evidence for Late Glacial and early Holocene climate interpretation across the Mediterranean (Stein 2001; Bartov, Stein et al. 2002; Robinson, Black et al. 2006). Using this data, it is surmised that catastrophic events in the northern hemisphere have the capacity to create drought conditions in the Mediterranean (Bartov, Stein et al. 2002; Bartov, Goldstein et al. 2003). This is evidenced by the temporary lowering of lake levels recorded at Lake Lisan (Jordan) at around 24 Cal ka yr BP, which is correlated with Heinrich event 2 (Bartov, Stein et al. 2002; Bartov, Goldstein et al. 2003). Following this event, lake levels rose and generally stayed high for the remainder of the Late Glacial period.

The end of the last ice age commences at around 19 Cal ka yr BP. On a broad scale, the increase in insolation from changes in orbital cycles is considered to have played a significant part in the

retreat of northern hemispheric ice and the termination of the last ice age, although it cannot be considered as the only factor (Clark, McCabe et al. 2004; Denton, Anderson et al. 2010).

### 2.2.2 The Late Glacial period, including the Bølling-Allerød interstadial and the Younger Dryas

Between ~18 to 14 Cal ka yr BP cool SST are still evident in the Red Sea (Arz, Pätzold et al. 2003a), however signs of warmer average temperatures start to appear in land-based records (Emeis, Schulz et al. 1998; Emeis, Struck et al. 2000; Emeis, Schulz et al. 2003). High lake levels continued at Lake Lisan until a rapid decrease and low lake stand between 17 and 16 Cal ka yr BP, correlated with Heinrich event 1 (Bartov, Stein et al. 2002; Landmann, Abu Qudaira et al. 2002; Bartov, Goldstein et al. 2003). A reduction in precipitation and evaporation during these Heinrich events are thought to be correlated to the collapse of the North Atlantic deep water circulation, causing reduced evaporation and less precipitation (Bartov, Goldstein et al. 2003). This matches well with the GCM retrodiction by Robinson (2006).

Between 15 Cal ka yr BP and 12.7 Cal ka yr BP is the period known as the Bølling-Allerød interstadial. Orbital variations resulted in ~7 to 8% more insolation in summer and 7 to 8% less insolation (than current values) in winter in the Northern hemisphere at its peak (Kutzbach and Webb 1993). By 14.5 Cal ka yr BP a 4.5 °C increase in Red Sea SST is seen (Arz, Pätzold et al. 2003a). Warming was also recorded in Tyrrhenian and Adriatic cores (Ariztegui, Asioli et al. 2000) A high stand is also seen in the Dead Sea (Neev and Emery 1967; Landmann, Abu Qudaira et al. 2002) suggesting warm and humid conditions.

By 13 Cal ka yr BP lake sediment records at Wadi Faynan in Israel have started to reflect a dry climatic phase (McLaren, Gilbertson et al. 2004), and a Halite layer in Dead Sea sedimentology has been interpreted as reflecting very low water levels (Neev and Emery 1967; Yechieli, Magaritz et al. 1993). Evidence from lake shrinkage from north and west Africa also points to arid phases between 13 to 11 Cal ka yr BP (Kutzbach and Street-Perrott 1985). Gastropod evidence from Israel also suggests a drier climate than present, through to 12.5 Cal ka yr BP. This dry phase has been correlated with the Younger Dryas cold phase in the northern hemisphere. Despite indications of arid conditions and increasing temperatures, the coastal plain of Israel is considered to have undergone wetter conditions prior to 12.5 Cal ka yr BP, with increasing aridity since (Gvirtzman and Wieder 2001).

### 2.2.3 The Early Holocene

A large amount of evidence exists for a significant increase in precipitation, and warm temperatures between 11 Cal ka yr BP and 7.4 Cal ka yr BP. This is from isotopic analysis (Bar-Matthews, Ayalon et al. 1999; Goodfriend 1999; Bar-Matthews, Ayalon et al. 2000; Bar-Matthews, Ayalon et al. 2003), gastropod characterisation, soil characterisation, foraminifera (Rossignol-Strick 1999), flood sediments and climate modelling (Kutzbach and Guetter 1986). The magnitude of change is estimated at up to 300 mm greater than modern averages.

Within this generally humid climatic optimum, a cold, arid episode has been recorded in the northern hemisphere, named the 8.2 ka yr event. This event has been associated with an interruption North Atlantic ocean dynamics, and widespread cooling (Brooks 2006)

After this period, oxygen isotope evidence from Qunf cave in southern Oman suggests a slow decrease in precipitation associated with a change in the monsoon regime. This may suggest a more negative North Atlantic Oscillation (NAO) and / or southward movement of the ITCZ, in response to a decline summer insolation at 30°N (Fleitmann, Burns et al. 2003).

### 2.2.4 The Mid Holocene

A body of evidence suggests that after 5900 Cal yr BP precipitation decreased in the northern hemisphere, which appears to have been associated with a general global cooling and a retreat southwards of the northern hemisphere monsoon systems (Brooks 2006). Similarly to the 8.2 Cal ka yr BP event, this episode has also been linked to changes in the North Atlantic. There is a strong hypothesis that cold events in the North Atlantic are synchronous with cool, arid episodes in the low to mid-latitudes (Kreutz, Mayewski et al. 1997; de Menocal, Oritz et al. 2000; Fleitmann, Burns et al. 2003). This episode seems to be correlated to the period of desiccation, which resulted in the creation of the global desert belt. (Brooks 2006).

By 5.1 Cal ka yr BP, isotope values from Soreq cave show a period of increased aridity, perhaps reflecting a reduction of 400mm precipitation from modern values (Bar-Matthews, Ayalon et al. 1999; Affek, Bar-Matthews et al. 2008). Grove and Rackham emphasise the slow aridisation of the climate throughout this period (Grove and Rackham 2003).

### 2.2.5 The Late Holocene

From 2.5 Cal ka yr BP onwards, increasing aridity, lower precipitation and increasing average temperature is estimated from isotopic records in Soreq, Peqiin and Efrayim caves (Bartov, Stein et al. 2002; Bartov, Goldstein et al. 2003; Barton, Sarjoughan et al. 2006).

However, short term anomalies to this general trend are apparent. In particular, evidence from around the Mediterranean during the Hellenistic and Roman periods suggest a warmer and wetter phase than present day conditions, particularly between ~1950 and 1600 Cal yr BP, or 200 BC to AD 400 (e.g. Lamb 1977). Speleothem records at Soreq cave provides evidence for a rise in humidity at ~1950 Cal yr BP (Orland, Bar-Matthews et al. 2009) and the Dead Sea shows an increase in levels around this time (Migowski, Stein et al. 2006). In addition, wood from a Roman siege ramp (from the Fortress of Masada above the Dead Sea) has also been analysed for its isotopic content, which indicates humid conditions at ~ 1950 Cal yr BP (Issar and Yakir 1997).

Investigation of dinoflagellate cysts from the south-eastern Gulf of Taranto, Italy (Chen, Zonneveld et al. 2011), suggests that SST and air temperature may have been warmer in the Mediterranean during the Roman Period, particularly at around 1900 Cal yr BP or ~60 BC to AD 90. After 90 AD these high and stable temperatures are seen to decrease. Evidence for higher temperatures has also been found in the Alps between ~400 BC and 0 AD, based on stalactite records (Frisia, Borsato et al. 2005) and reduced glacial extent (Holzhauser, Magny et al. 2005; Giraudi 2009). Periods of cyclicity of around 7-8 and 11 years are also found in environmental records from Taranto (Chen, Zonneveld et al. 2011), where changes in river discharge suggests links between increased precipitation and increased temperature.

However, the picture is more complicated than a coherent rise in humidity and temperature. Evidence is available to suggest lower SST and air temperature in the Bermuda Rise region, for instance, between 2000 BC and 200 AD (Keigwin 1996), meaning that temperature change may

have been variable and regional, and other areas of the Mediterranean such as Lake Pamvotis in Greece provide evidence for a more arid phase at around 1950 Cal yr BP (Frogley et al. 2001).

As climatology reaches closer to the present day, some proxies become too coarse to provide adequate differentiation of climate over the century or decadal view that human cultural phases are measured by. In the Classical period, historical climatological evidence is sometimes also incorporated alongside other climate proxies, to enhance the range of climate perspectives available.

During the Roman period, there are a few indications that two rainy seasons were present (spring and autumn) at least in some areas of the Mediterranean Basin such as Palestine and Sicily in the late centuries BC and early centuries AD, where today the main rain is in autumn (Grove and Rackham p.142). This is based only on textual evidence, and should be treated with caution, however Theophrastus remarks that the plains of Latium near Rome produced beech of exceptional size. This statement has been used by Grove and Rackham (2003) to suggest that summers would have to have been less arid.

In Italy, Grove and Rackham (2003) also use evidence from Pliny to suggest colder winters in the first century AD than today around the Citta de Castello basin, as Pliny documents that winter temperature 'rejects and expels myrtle, olives and other things which flourish in favourable weather'. A similar story is found in Theophrastus, as he refers to increasingly severe winters around the 4th century AD in the Cretain plains. Nonetheless, in Spain, historical accounts suggest that in the second century BC, Mount Aphrodite was 'planted round with olives', where they are marginal today (Grove and Rackham 2003).

The climate of North Africa at the time of the Roman Empire is considered by some to have been wetter than present, inferred from fauna, water resources, water control systems and evidence of grain export (though this could say more about the changing nature of agricultural exports than climate change per se) (Grove and Rackham 2003). In their summary of climate change during Antiquity, Grove and Rackham generally conclude that there is evidence that the Mediterranean Basin seems to have been a little cooler, and less arid than the present day, with larger areas having

**Table 2-2 A selection of independent climate evidence relating to the Mediterranean since the Last Glacial Maximum**

| Date (Cal yr BP) | Author | Geographical area | Study site | Methodology | Climatology |
|---|---|---|---|---|---|
| 25-19 | Robinson et al. 2006 | Levant | Change in Levant climatology | UKMO GCM based on CLIMAP SST and Peltier ice sheet reconstructions | LGM predictions: Cooler winters, less evaporation, dry summers as present. |
| 25-19 | McGarry et al. 2004 | Israel | Soreq, Peqiin and Efrayim Caves | D/O18 | Low average temperature (7-14°C) |
| 24 | Bartov et al. 2002, 2003, | Jordan | Lake Lisan | Sedimentology and stratigraphy | Lake level lowering |
| 23.8 | N/A | Northern Hemisphere | | | Heinrich event 2 |
| 25-19 | Hayes et al. 2005 | Eastern Mediterranean | Levantine basin | Foraminifera from deep sea cores | SST 2°C colder than present, particularly colder summer temperatures |
| 25-19 | Emeis et al. (1998, 2000, 2003) | Eastern Mediterranean | Levantine basin | Alkenone method | SST 5-6°C cooler than present. |
| 14-18 | N/A | Northern Hemisphere | N/A | N/A | Heinrich event 1 |
| 18-14 | Arz et al. 2003 | Northern Red Sea | Northern Red Sea | Alkenone method | Cool SST |
| 18-9.5 | Emeis et al. (1998, 2000, 2003) | Eastern Mediterranean | Levantine basin | alkenone method | Warmer temperatures |
| 16-17 | Landmann et al. 2002 | Jordan | Lake Lisan, Damya formations | Geochemical, mineralogical, sedimentalogical study (gypsum / argonite ratio) | low stand synchronous with Heinrich event 1 |
| 16.5 | Arz et al. 2003 | Northern Red Sea | Northern Red Sea | Alkenone method | Very cool SST |

| Date (Cal yr BP) | Author | Geographical area | Study site | Methodology | Climatology |
|---|---|---|---|---|---|
| 16-17 | Bartov et al. 2003, | Jordan | Lake Lisan | Sedimentology and stratigraphy | low stand synchronous with Heinrich event 1 |
| 15 | Bartov et al. 2002, | Jordan | Lake Lisan | Sedimentology and stratigraphy | Lake level peak in Jordan |
| 15-12.7 | N/A | Northern Hemisphere | N/A | N/A | Bolling-Allerod interstadial |
| 14.5 | Arz et al. 2003 | Northern Red Sea | Northern Red Sea | Alkenone method | 4.5°C increase in SST. |
| 14.5-12.8 | Ariztegui et al. 2000 | Tyrrhenian Sea | Tyrrhenian Sea | Sedimentology, stratigraphy, foraminifera | Warming of Tyrrhenian and Adriatic sea |
| 13.7 | MacLaren et al. 2004 | Levant | Wadi Faynan | Sedimentology and stratigraphy | dry climatic phase |
| 13 | Neev and Emery 1995, Landmann 2002 | Jordan | Dead sea | | High stand during Bolling-Allerod |
| 13-11 | N/A | Northern Hemisphere | | | Younger Dryas |
| 13-11 | Neeve and Emery 1967, Yechieli et al. 1993 | Jordan | Dead sea | Sedimentology and stratigraphy | Halite layer in Dead Sea Basin<br><br>Low lake levels corrrelated with younger dryas? |
| 12.9-12.5 | Magaritz and Heller (1980) | Israel | | Gastropods, Carbon isotope, Oxygen isotope | Climate more dry than present (Younger dryas) |
| 13-11 | Kutzbach and Street-Perrott 1985 | West Africa | | Lake sedimentology | Arid phase |
| >12.5 | Gvirtzman and Wieder 2001 | Israel | Coastal plain of Israel | soil characteristion, TL dating, Radiocarbon | Wet conditions |

| Date (Cal yr BP) | Author | Geographical area | Study site | Methodology | Climatology |
|---|---|---|---|---|---|
| 11-7.8 | Goodfriend (1999) | Israel | Negev desert | Carbon isotope | Increased precipitation (+300mm) |
| 11 to 7 | Bar-Matthews (1999, 2000, 2003) | Israel | Soreq Cave, Israel | Oxygen isotope, Carbon isotope, Strontium isotope | Increased precipitation |
| 10.95 | Goodfriend (1991, 1999) | Israel | | Gastropod characterisation | more frequent storms |
| 10-8 | McGarry et al. 2004 | Israel | Soreq, Peqiin and Efrayim Caves | Deuterium isotope, Oxygen isotope | warm average temps 14-17°C |
| 10.7-8.8 | Rossignol-Strick 1999 | | | Foraminifera from deep sea cores | Warmer temperatures |
| 10.7-7.5 | Gvirtzman and Wieder 2001 | Israel | Coastal plain | Soil characteristion, TL dating, Radiocarbon | Wet phase from soil evidence <800mm annual precip |
| 8.5 | Frumkin et al. 1991, 1994 | Levant | | Flood sediments in salt caves | high stand |
| 8-7.5 | Bar-Matthews (1999, 2000, 2003) | Israel | Soreq Cave, Israel | Oxygen isotope, Carbon isotope, Strontium isotope | Annual precip ~600mm |
| 8.5-7 | Bar-Matthews (1999, 2000, 2003) | Israel | Soreq Cave, Israel | Oxygen isotope, Carbon isotope, Strontium isotope | Deluge |
| 7.4 | Goodfriend (1999) | Israel | Negev desert | Carbon isotope | Increased precipitation (+300mm) |
| 5.1 | Bar-Matthews (1999, 2000, 2003) | Israel | Soreq Cave, Israel | Oxygen isotope, Carbon isotope, Strontium isotope | Increased aridity (-400mm) |
| 5 | Hazan et al. 2005 | Jordan | Lake Tiberias, Jordan | Sedimentology and stratigraphy | High stand |
| 4.7 | Bar-Matthews (1999, 2000, 2003) | Israel | Soreq Cave, Israel | Oxygen isotope, Carbon isotope, Strontium isotope | Increased precipitation and temperature |
| <2.5 | Bar-Matthews (1999, 2000, 2003) | Israel | Soreq Cave, Israel | Oxygen isotope, Carbon isotope, Strontium isotope | Increased aridity, low rainfall |
| 0.8-1.2 | McGarry et al. 2004 | Israel | Soreq, Peqiin and Efrayim Caves | Deuterium isotope, Oxygen isotope | high average temperature (~20.22°C) |

## 2.3 PALAEOVEGETATION OF THE MEDITERRANEAN REGION SINCE THE LAST GLACIAL MAXIMUM

The landscape of the Mediterranean during the Late Glacial period is considered to have been significantly different from modern vegetation both in terms of species assemblage and distribution. Evidence from the eastern Mediterranean, in particular Lake Zeribar, in the lake Zagros mountains, first started to cement the observation of predominantly steppic communities of plants (van Zeist and Wright 1963). Typical species found were herbs such as *Artemisia,* chenopods and Umbellifers up until around 12.5 Cal ka yr BP. Evidence from Mirabad in Iran also shows the steppic nature of the vegetation during the late glacial period, proving that oak was not just restricted to valley areas, but was effectively eliminated from whole regions due to aridity (van Zeist and Wright 1963; van Zeist and Bottema 1977; Roberts and Wright 1993). Pollen signatures from the Dead Sea-Jordan rift valley shows a similar steppic assemblage (Niklewski and Van Zeist 1970). However, in Greece, oak increased sharply at ~17 Cal ka yr BP in the low elevation site of Tenaghi Philippon, and concurrent increases in elm, linden, hazel and pistachio suggest a distinct change in climate (Roberts and Wright 1993). In southern France and the Pyrenees steppic vegetation during the last glacial maximum was interpreted from pollen records, but from ~14 Cal Ka yr BP, previously steppic areas started to be colonized by relatively arctic species such as birch and willow and then oak and elm (Guiot and Pons 1986),

By ~10 Cal ka BP oak, and pistachio are more prevalent at Lake Zeribar, grasses and tree pollen increase (van Zeist and Wright 1963). This is also the case at Mirabad, with oak woodland established by ~10 Cal ka BP and some Mediterranean species present. Greece reflects deciduous forest by ~10 Cal ka yr BP, and Sapropel evidence from the eastern Mediterranean sea also shows frequent deciduous tree pollen between ~10 and 7 Cal ka yr BP (Rossignol-Strick 1999). This has been interpreted as evidence for increasing precipitation and warmer temperatures. Pollen evidence from Lake Accesa in central Italy suggests unusually wet winters, dry summers, and enhanced seasonality during this early Holocene period (Peyron, Goring et al. 2011)

In addition to the records of widespread steppe and savannah in the Late Glacial period, certain key areas in the Mediterranean such as the area surrounding the Black Sea (Fleitmann, Cheng et al. 2009), and northern Greece (Roberts and Wright 1993) are considered potential areas for refugia (Brewer, Cheddadi et al. 2002). These pockets of refugia are thought to have suitable climates to host endemic species and mixed forest species such as *Quercus, Pinus, Fagus, Abies, Corylus, Ulmus, Tilia and Fraxinus* (Bottema 1980; Moody, Rackham et al. 1996) in times of wider unfavourable climate. The synchronisation of $\delta^{13}C$ and $\delta^{18}O$ records from Sofular Cave and the western Black Sea respectively suggest a fast re-vegetation of C3 plants at 17.7 Cal ka yr BP and 12.5 Cal ka yr BP in this area. This is in contrast to the lag seen between climatic changes and the achievement of vegetation equilibrium evidenced by the delay of oak expansion in the interior areas of the Taurus mountain ridge in the early Holocene (van Zeist and Bottema, 1991. Wick et al, 2003).

In general, vegetation across the Mediterranean is therefore interpreted to be steppic in nature during the Last Glacial Maximum, aside from restricted but important refugia areas (Kelly and

Huntley 1991; Reille, Gamisans et al. 1997; Wick, Lemcke et al. 2003). Throughout the early Holocene, an increase in deciduous oaks and pine is recorded (Grove and Rackham 2003).

Moving into the Mid-Holocene, palynological evidence from Italy and Greece is used as a basis for climate modelling, and shows a distinct wet period at 8.2 Cal ka yr BP (Peyron, Goring et al. 2011). This matches well with independent climate records suggests warming temperatures (Arz, Pätzold et al. 2003a), and a relatively wet phase between 8.8 Cal ka yr BP and 7.8 Cal ka yr BP (Bar-Matthews, Ayalon et al. 1999; Goodfriend 1999; Bar-Matthews, Ayalon et al. 2000; Bar-Matthews, Ayalon et al. 2003). Peyron et al. (2011) also note a shift to more drought tolerant species between 7.8 Cal ka yr BP and 5 Cal ka yr BP and interpret reduced seasonal contrast during this time. By ~6.8 Cal ka yr BP a decrease in woodland is seen in the eastern Mediterranean (van Zeist and Bottema 1977). After 5 cal ka yr BP, there is more evidence for the aridization of the climate, based on pollen records. For instance, between ~4.4 Cal ka yr BP and ~2.5 cal ka yr BP (2500 to 500 BC) the palynological signature of Hula Basin in northern Israel went from wet and humid to warm and arid (Horowitz 1971; van Zeist and Bottema 1982)

# 3 APPENDIX: THE ENVIRONMENT OF SOUTHWEST TURKEY

In order to devise a model to suit the environment of southwest Turkey, both past and present, it was first instructive to understand the geography of the study area in terms of its geology and pedology, and to assess its modern climate and vegetation. This provided background to be contrasted with the climatology and vegetation interpreted from palynological and independent climate evidence, which aided the definition of model variables, species and scenarios the vegetation model will need to encompass.

### 3.1.1 Geology and pedology

Due to its geological history, the topography, sedimentology and geology of southwest Turkey is complex. The terrain is rugged, with high mountain ranges, steep valleys and intramontane basins, which hold many of the useful palaeoenvironmental lake sediments (Eastwood, Roberts et al. 1999). The average elevation across the whole of Turkey is 1132 m, and plains of 0 – 250 m only cover one tenth of the country (Aksoy, Panagos et al. 2010) demonstrating its vertiginous nature. It is thought that as a consistent landmass, Anatolia was formed in the Cretaceous period, due to a convergence of microcontinents that broke off from Gondwanaland, effectively eliminating the Neotethyan oceans (Garfunkel 2004). As these oceans closed, a mixture of continental crust, ocean basin, and island arc sediment were deformed and pushed up to form part of these mountain ranges. This crustal movement has formed large central massifs such as the Menderes Massif. Tectonic activity in the Miocene and Eocene is evidenced by a system of *nappes*, or overthrusting faults, where the strike of individual mountain ranges is roughly perpendicular to the axis of the mountain range as a whole (Garfunkel 2004).

Many of the sediments found in southwest Turkey are relatively old. Palaeozoic sediments are found in the Tauride block; Late Precambrian rocks and late Ordovician glacial deposits in particular are exposed in the Menderes Massif, all pointing to a Gondwanaland as the original source of these deposits (Garfunkel 2004).

The most abundant soil type in Turkey is the Leptosol, due to the tectonically induced steep slopes, mass transportation of soils and the continuous alteration of the landscape (Erol 1981). In the west, these tend to be lithic leptosols associated with chromic luvisols, commonly known as Red Mediterranean Soils or Terra Rossa, which is in an advanced state of weathering, and has been leached of carbonates. These tend to form over limestone bedrock on steep hillsides (Aksoy, Panagos et al. 2010). Rendzic leptosols, haplic cambisols and luvic kastanozems are also common. The quaternary colluvial material deposited at the foot of grabens is more likely to consist of Mollic Leptosol, otherwise known as the Red or Red-Brown Mediterranean soil (Aksoy, Panagos et al. 2010). In drier parts of the country Calcisols are found, which tend to form on ancient lake basins and mudflow deposits (Dinc, Senol et al. 2005; Aksoy, Panagos et al. 2010). In slightly more temperate habitats, they are replaced by Cambisols. Along river valleys and lake basins Fluvisols are present, as are Arenosols, along large current or ancient river courses, and along coastal sand dunes. Vertisols, Acrisols, Regosols and Andosols also exist in small areas. A further elaboration on the multifaceted geology and pedology of Turkey is out of the scope of this thesis, although the interested reader is directed to Garfunkel (2004), Ustaömer and Robertson (Bender, Hamilton et al. 1997), Taymaz et al. (2007).

### 3.1.2 **Climate**

The climate of Turkey is predominantly characterised by seasonal alternations of frontal depressions (with polar air masses and subtropical high pressure areas), and subsiding maritime tropical and continental tropical air masses (Türkeş 1996). Principal weather systems originate from the Atlantic Ocean, passing over Europe or the Mediterranean Sea (Bakker, Paulissen et al. 2012b).

Turkey is considered to be positioned in a climate transition zone, meaning that the Eastern Mediterranean is sensitive to precipitation, temperature, and the origin of storm tracks (Bar-Matthews, Ayalon et al. 1999; Bakker, Paulissen et al. 2012b). These seasonal attributes are altered by changes in the position of the westerly jet stream, the extension of the subtropical low-pressure belt and changes to the Siberian high-pressure system (Türkeş 1996). Relative changes in these factors determine the boundary between humid Mediterranean and continental climate. (Roberts and Wright 1993; Wick, Lemcke et al. 2003). Climate variability in the wider region is modulated by the North Atlantic Oscillation (NAO), fluctuations in which can create stronger or weaker easterly surface winds and wintertime storms, resulting in cooler and drier or warmer and wetter winters (Bakker, Kaniewski et al. 2012a). The importance of the link between North Atlantic climatic changes and the NAO in past climatic changes in southwest Turkey may be significant. Interacting with these, the topographical setting due to its geological history has a large impact on both macro and microclimatology.

The climate of Turkey has been classified in a number of ways to reflect these macroclimate and macrotopography considerations. Perhaps the most well-known of classifications is the Köppen classification (1936), and the Thornthwaite classification (Thornthwaite 1948). The Köppen-Geiger classification (e.g. Peel, Finlayson et al. 2007) divides Turkey firstly into the coastal areas of the Mediterranean Sea and the Black Sea, which have a 'Csa' climate. This is a warm temperate Mediterranean climate, the main characteristics of which are warm and dry summers, and winters that are generally wet, with moderate temperature. The temperature of the warmest month is on average above 22°C (1936). Secondly the mountainous regions of Anatolia are classified as having a 'Dsa' Climate. This is a snowy climate with a dry summer and the warmest month above 22°C and the coldest month below -3°C (1936). The climate of the Central Anatolian Plateau can be classified as a 'BSk' Climate, a cold, dry climate with a dry summer and annual average temperatures under 18°C (1936).

Van Zeist et al. (1975) using climate data from Davis (1965), describes the southwestern region of Turkey as having a typical Mediterranean climate. Türkeş (1996) categorises the rainfall in the southwest as Mediterranean (MED) and Mediterranean to Central Anatolia Transition (MEDT) towards the interior of the region. Around 67% of precipitation occurs during winter and spring, when the eastern Mediterranean is influenced by frontal mid-latitude and Mediterranean depressions. Precipitation is generally greater on the south coast than on the west (~1000 mm versus 700 mm), and humidity is relatively high. This is compared to the mountainous interior, where precipitation decreases, but a greater proportion of it falls in summer. Snow is usual on these peaks during winter. In the Central-Anatolian Plateau precipitation is very low, but mainly falls during the autumn and winter. Humidity is also low.

Temperatures near the coast are mild, and winters rarely fall below freezing. In the mountains, summer temperatures are similar to the coast, however winter temperatures are much colder.

The Central-Anatolian plateau also experiences cold winters, however, here summer temperatures are also lower.

### 3.1.3 Current vegetation

Van-Zeist, Woldring et al. (1975) utilise the 'Geobotanical Foundation of the Middle East' by Zohary (1973) along with other sources, to construct general maps of vegetation belts across the southwest of Turkey. Under this classification, the vegetation of southwest Turkey shows demonstrable differences in vegetation assemblages under the different climatic and topographic features discussed above.

Four main zones of vegetation are defined by Zohary; the Eu-Mediterranean zone in the mild coastal regions, the Oro-Mediterranean zone in the mountainous hillslopes, the Alpine zone on areas of high plateau, and the Xero-Euxinian zone in the dry interior. Although these vegetation belts are generalised, it is important to remember that a large amount of variation is found within different combinations of climate, geology and soil type. To gain a better understanding of these zones, the following discussion summarises the writings of Van Zeist et al. (1975).

The Eu-Mediterranean belt consists mainly of evergreen species, and is found in the coastal regions of southwestern Turkey at elevations from sea level to 800m. The can further be divided into zones of Ceratonio-Pistacion lentisci (i.e. *Pistacio lentiscus, Olea europeae oleaster, Quercus calliprinos, Juniperus phoenicica*) up to ~300m, and Quercion calliprini (i.e. *Quercus calliprinos, pistacia palaestina, Phyllyrea media, arbutus andrachne)* anywhere within the zone. If there are favourable conditions such as a ready source of water (for instance, in the Menderes valley) the Eu-Mediterranean zone can penetrate further inland, but usually is not found above 600-700 m (Van Zeist et al. 1975). Alongside water courses are found species such as *Salix* spec., *Ulmus campestris,* Populus spec., *Vitex agnus-casts and Alnus glutinosa.* Van-Zeist et al. (1975) emphasise that *Pinus brutia* forests are important for the composition of the Eu-Mediterranean zone, and frequently undergrowth of any of the above species occur within these forests. This is an important point when undertaking palaeoecological mapping and pollen dispersal modelling, as forests cannot simply be modelled as pure homogenous stands.

The Oro-Mediterranean belt is found within the range of ~800-2000 m (only as low as 800 m on the southern and western slopes of the Taurus). Again, this can be split out into two zones, between ~800-1200 m deciduous and coniferous forests are found, containing *Pinus brutia* (often concurrent with *Quercus calliprinos*), and at higher or colder elevations *Pinus nigra* (often concurrent with *Quercus cerris*). *Quercus* prefer deeper soils, whereas *Pinus* are more resilient on steep slopes with poorer soil. From ~1200m upwards to the upper timber-line at ~2000 m coniferous forests predominate (van Zeist, Woldring et al. 1975), constituting of species such as *Pinus nigra, Cedrus libani, Abies cilicica and Juniperus excelsa.* Undergrowth shrubs are still found within forests, however pure stands are also observed.

The Alpine zone contains mainly dry top lawns above the tree lines, and is defined by species such as *Astragalus angustifolius, Astragalus microcephalus, Acantholimon echinus and Onobrychis* (Schwarz 1936). These are spiny cushion-shaped species. Other species include Labiatae, Scrophulariaceae, Boraginaceae and Graminineae.

The Xero-Euxinian vegetation belt is found north and east of the Oro-Mediterranean belt. It currently contains a much more continental climate as it moves towards the Central Anatolian

Plateau. It is classified by Van Zeist, Woldring et al. (1975) as forest-steppe, which is defined as largely steppe, with sparse tree cover (this is opposed to steppe-forest, which indicates an open forest). The steppe vegetation is dominated by *Artemisia fragans*. Other species include *Astragalus spp., Centaurea spp., Eryngium spp. Salvia cryptantha* etc. As in the Oro-Mediterranean zone, the predominant forest species are *Quercus cerris, Quercus pubescens, and Juniperus excelsa* with *Pinus nigra* taking the highest elevations. Van Zeist, Woldring et al. (1975) state that these are often reduced to brushwood due to cutting and grazing, and that little original oak forest-steppe is left. Consequently the area is more open than the Oro-Mediterranean landscape. However, the exact separation between Oro-Mediterranean and Xero-Euxinian, and indeed forest and steppe is fuzzy, and is often compounded by anthropogenic effects.

As well as these altitudinal classes of vegetation, four general types of Mediterranean communities can be identified and are discussed by Vermoere (2002a). The Matorral is generally dominated by Quercus coccifera, with patches of Olea europeae and Pistacia. The difference between Matorral and Maquis is ill-defined. Maquis tends to contains Quercus coccifera as a main component, but usually in shrub form as opposed to tree form, and can be associated with species such as *Fraxinus ornus, Juniperus, Pistacia, Myrtus, Acer monspessulanum, Fontanesia phillиraeoides*. Garrigue is generally more associated with aromatic low shrubs such as cistus, phlomis, salvia and sideritis, whilst Phrygana consists of low, thorny and xerophytic formations of shrubs. A key debate discussed by Quezel (1981) is whether Mediterranean schlerophllous formations represent climax vegetation. Later research by Pons and Quezel (Pons and Quezel 1985) suggest that this may be the case in the semi-arid regions of the Mediterranean, but in sub-humid and humid areas may be more complex.

# 4 APPENDIX PALAEOCLIMATOLOGICAL AND PALAEOECOLOGICAL DATA FROM SOUTHWEST TURKEY

Evidence to investigate the climate of southwest Turkey is firstly available from geochemical analysis of glacial deposits in the Kaçkar mountains in eastern Turkey, and Mount Sandıras in western Turkey (Akçar, Yavuz et al. 2007; Sarıkaya, Zreda et al. 2008). Further evidence is available in the form of lake level reconstructions and isotopic analysis from across the country. At Eski Acıgöl in central Turkey, Jones et al. (2007) use isotope records to quantify climatic change throughout the last glacial to interglacial period. Climate proxy data from Konya Palaeo-lake in central Turkey is also available (Roberts 1983), and at Lake Van in eastern Turkey, oxygen isotope records, Mg/Ca ratios and pollen from the laminated autochthonous carbonate sediments have allowed a climatological interpretation for the last 13 000 years to be attempted (Schoell 1978; Landmann, Reimer et al. 1996; Wick, Lemcke et al. 2003). More recent climatic evidence is available from Lake Nar (England, Eastwood et al. 2008).

### 4.1.1 Evidence for climatic change during the Last Glacial Maximum and Late Glacial period

Using Cosmogenic nuclide ($^{10}$Be) dating, the possibility of glacial advance between 26 ± 1.2 $^{10}$Be ka BP to 18.3 ± 0.9 $^{10}$Be ka BP has been demonstrated by Akçar et al. (2007) in the Kaçkar mountains in eastern Turkey, matching relatively well with evidence of low temperatures from other independent climate data. In the absence of further evidence this period is provisionally considered the peak of the LGM in the Eastern Black Sea Mountains (Akçar, Yavuz et al. 2007). In Western Turkey, a local glacial maximum occurred at ~20.4 ± 1.3 $^{10}$Be ka yr BP (Sarıkaya, Zreda et al. 2008). This glacial maximum coincides with evidence of high lake level stands from the Konya basin (Roberts 1983). Records from Lake Van provide evidence of regional relative humidity through lake levels fluctuations. The lake input depends on precipitation, and as it is a terminal lake, and closed system, the output is primarily controlled by fractionation processes connected to evaporation. This strongly depends on relative humidity and to a lesser extent, temperature (Wick, Lemcke et al. 2003). Lake Van also shows high lake levels at this point (Landmann, Reimer et al. 1996), suggesting either high precipitation or low evaporation.

A 1-dimensional ice flow model was utilised by Sarıkaya et al. (2008). This estimated that temperatures during the LGM may have been ~8.5 to 11.5°C lower that modern values. This is a larger decrease in temperature than other proxies have found in the Mediterranean (cf Emeis, Schulz et al. 1998; Emeis, Struck et al. 2000; Emeis, Schulz et al. 2003; McGarry, Bar-Matthews et al. 2004). The model also demonstrated that almost double the precipitation of modern values would be required to sustain these glaciers. As Konya Palaeo-lake is considered to be dominated by runoff and direct precipitation (Roberts 1983) Jones et al. (2007) also suggest that high lake levels between ~25 Cal ka BP to ~19 Cal ka yr BP could equate to high precipitation. Nonetheless, the competing theory of low precipitation but low evaporation cannot be discounted either. This has been a major debate, as previously discussed by Kuzucuoğlu and Roberts (1998) using high lake level evidence in the east of Turkey, and Fontugne et al. (1999) using evidence from the Konya Plain. Under the assumption of low evaporation rates, an accumulation of snow would occur during the winter, and lowered

summer insolation would occur during the summer, leading to a limited build-up of moraines (Akçar, Yavuz et al. 2007). The relative shifts in $\delta^{18}O_{recorded}$ between Lake Van and Eski Acıgöl also suggests that there may have been a steeper moisture gradient between the coastal and interior regions than the present day.

The retreat of the Kavron Palaeoglacier at around 18.3±1 0.9 $^{10}$Be ka yr BP correlates with low lake levels across Turkey and the reactivation of Aeolian dune systems (Kuzucuoğlu and Roberts 1998; Fontugne, Kuzucuoğlu et al. 1999). Jones et al. (2007) interpret this as a cold and dry period, though there are some indicators that there are the beginnings of warmer temperatures across the wider Mediterranean (Emeis, Schulz et al. 1998; Emeis, Struck et al. 2000; Emeis, Schulz et al. 2003).

Ice free valleys are estimated in Eastern Turkey by 15.5 ± 0.7 $^{10}$Be ka yr BP (Akçar, Yavuz et al. 2007), with some advances in western Turkey at 16.2 ± 0.5 $^{10}$Be ka yr BP, potentially correlated with Heinrich event 1 (Sarıkaya, Zreda et al. 2008), and Eastern Turkey between 13 ± 0.8 $^{10}$Be ka yr BP and 11.5 ± 0.8 $^{10}$Be ka yr BP, which are potentially correlated with the Younger Dryas phase (Akçar, Yavuz et al. 2007). A rather constant humidity close to current conditions is estimated at Lake Van (Wick, Lemcke et al. 2003)

### 4.1.2 Evidence for climate change during the Early Holocene period

Authigenic stable isotopic and mineralogy data from Lake Van suggest that even as early as ~12.4 Cal ka yr BP there was a rapid change to more humid climatic conditions than the preceding late glacial period, and lake levels are high (Wick, Lemcke et al. 2003). Between 11 and 9 Cal ka yr BP humidity continues to increase at Lake Van. Geochemical and isotopic indicators from cores taken at Eski Acigöl dry crater lake also reflects deep water conditions and low salinities during this period (Roberts, Reed et al. 2001). As part of the ISOMED synthesis (Roberts, Jones et al. 2008) normalisation of isotopic records across a series of Eastern Mediterranean lakes was carried out, allowing multi-centennial trends to be analysed. This analysis showed that more negative values were found before 7900 $^{14}$C BP, suggesting high moisture availability. In particular analysis of lake shorelines and lake cores from the Dead Sea provided evidence for high water levels between 10 Cal ka yr BP and 8 Cal ka yr BP, and a fall in levels at around 7.7 Cal ka yr (Migowski, Stein et al. 2006).

The impact of the 8.2 Cal ka yr BP event is not discussed explicitly during this thesis, however recent research suggests there may be a link between climatic changes occurring at 8.2 Cal ka yr BP and the increase in fortifications and large scale conflagrations in Pisidia. For more details see Clare (2008)

### 4.1.3 Evidence for climate change during the Mid Holocene

In the east Mediterranean, the overall climatic trend from independent palaeoclimate evidence fits with evidence of cooling and rainfall reduction from more widespread northern hemisphere records. An overall trend from more negative to more positive isotope values suggesting increased aridity was found between ~8500 to 5000 Cal yr BP from cave carbonate records (Frumpkin, Ford et al. 2000; Verheyden, Nadar et al. 2008). A similar picture has been found from lake palaeohydrological records (Roberts, Jones et al. 2008) (Snyder, Wasylik et al. 2001). Geochemical and isotopic evidence from cores taken at Eski Acigöl suggest that between ~6000

and 5100 Cal yr BP there was a significant decrease in lake levels, destroying stratification and ending laminae formation (Roberts, Reed et al. 2001).

A positive trend in fire activity is identified by Vannière et al. (2011) in central Turkey from ~6 Cal ka yr BP to 3.5 Cal ka yr BP. Vannière et al. suggest that increased fire activity during this period could be linked more to changes in land use and human impact.

After 5500 Cal yr BP, changing insolation allowed the southward migration of the ITCZ. This in turn resulted in the weakening of the Afro- and Asian monsoon system (Vannière, Power et al. 2011), potentially allowing westerlies to gradually deliver more humidity to the southern Mediterranean area (Vannière, Power et al. 2011).

Superimposed on this slow aridisation of the climate are a number of higher frequency climate fluctuations throughout the Mid-Holocene, particularly during the period corresponding to the Bronze Age in archaeological chronology. There is evidence of a cooling of climate in the northern hemisphere between 3000 and 2500 BC or ~ 5000 to 4000 Cal yr BP, which is concurrent with a decline in the level of the Mediterranean Sea, and evidence for increased precipitation and a cold climate in the Near East including around Lake Van (Issar and Zohar 2004).

At 4.2 Cal ka yr BP, a short duration aridity event is considered to be associated with a weakening of the Monsoon circulation system (Bond, Showers et al. 1997), and correlates with minimum lake levels in Northern Africa, extreme aridity in the Sahara and aridity in China during this period based on radiocarbon dates of surface water indicators, palaeosols and lake sediments (Guo, Pertit-Maire et al. 2000). Interpretation of marine isotope records from the Levantine coast, then suggesting a further humid phase between 3500 and 3000 Cal yr BP, which is swiftly followed by climate desiccation (Schilman, Bar-Matthews et al. 2001),

### 4.1.4 Evidence for climate change during the Late Holocene

Further evidence of greater water deficit is found at approximately 1000 BC, potentially correlating with other evidence of late Bronze Age aridity, although this is not precisely dated (Roberts, Reed et al. 2001). After this point, less marked evaporative concentration is recorded, suggesting reduced temperature, increased rainfall or both, through the Iron Age into the Hellenistic period. From lake varve records, Jones et al. (2006) shows that drought frequency was greater prior to ~1400 Cal yr BP in Central Turkey, after which winter precipitation increased and summer evaporation decreased.

The potential reasons for these changes are complex. Local changes in Turkey were considered to be due to variations in winter storm positions, but also potentially changes in the intensity of the Indian Monsoon (Fleitmann, Burns et al. 2003). Dermody et al. (2011) Use an Empirical Orthogonal Function (EOF) analysis to examine a range of climatic proxy data between ~3200 and 1000 Cal yr BP. They find a seesaw in precipitation anomalies between Norway, Spain and Israel on the one hand, and Central Mediterranean and Turkey on the other. Furthermore, they suggest the timing of the shifts is coincident with the 1450 yr cycles in North Atlantic SST (Bond, Showers et al. 1997). Over the Mediterranean, they suggest that the East Atlantic / Western Russia (EA/WR) pattern of precipitation was more dominant than today, and that the mechanism causing changes in precipitation over Europe during the Roman Period was likely to be due to changes in the position and intensity of the jet stream.

Chen et al. linked cycles in precipitation and temperature during this period to solar activity and changes in the North Atlantic Oscillation (NAO), with solar activity potentially modulating the NAO. They, along with other authors suggest that solar activity was likely to have played an important role in Roman climate change (Castagnoli, Bonino et al. 2002; Versteegh, de Leeuw et al. 2007; Taricco, Ghil et al. 2009).

Thus, local changes in humidity and temperature during the Hellenistic and Roman period may have been representative of more widespread changes in atmospheric circulation, ultimately due to changes in solar radiation.

## 4.2 EVIDENCE FOR PALAEOECOLOGICAL CHANGE SINCE THE LAST GLACIAL MAXIMUM

The intramontane valleys of southwest Turkey provide a rich source of fossil pollen evidence to investigate the vegetation assemblage of the region since the Last Glacial Maximum (van Zeist, Woldring et al. 1975; Bottema and Woldring 1984; Bottema, Woldring et al. 1986; Eastwood, Roberts et al. 1998; Vermoere 2002a; Eastwood, Leng et al. 2007; Eastwood, Fyfe et al. 2011). In this study, 16 pollen cores from across southwest Turkey (collected previously as part of research projects reaching back to the 1970s) will be utilised as comparison data for model output. Figure 4-1 introduces the location of these pollen coring locations.

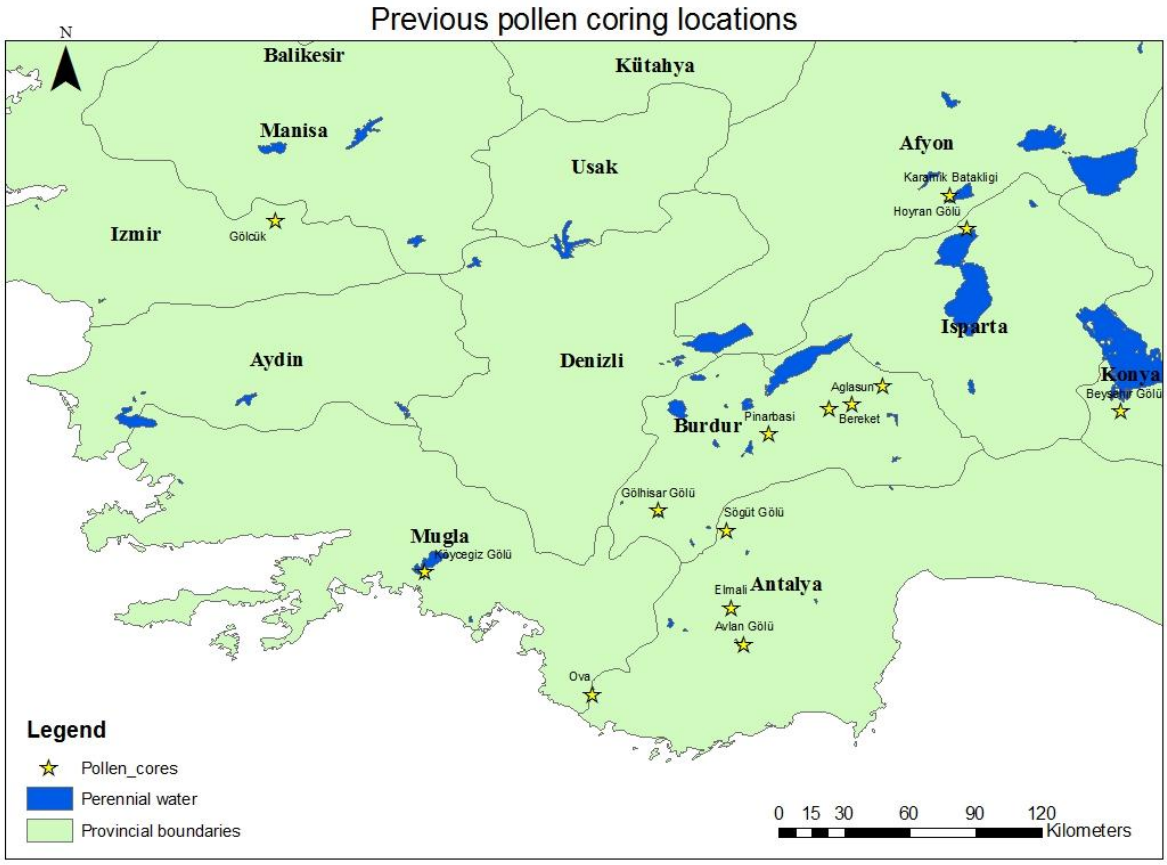


**Figure 4-1 Pollen coring locations across southwest Turkey**

As discussed by Vermoere (2002a), pollen is a useful tool for vegetation reconstruction because pollen grains are resilient and can be well preserved. They are produced widely and occur in great numbers. The pollination of plant species, together with the quantity of plant species determines the composition of the pollen flora deposited on the ground, and the entrapment and preservation of this pollen depends on the deposition environment that the pollen has landed in. Changes that occur to pollen as it is deposited and preserved through time can affect the quantitative relationship between pollen types when recovered from a core (Vermoere 2002a). Low microbial activity is the basic prerequisite for pollen survival, and many soils (particularly sandy soils) are not good preservers of pollen (Vermoere 2002a)

This can be seen in practice, as the geology of the southwest limits the amount of areas where pollen preservation is possible (Bakker, Paulissen et al. 2012b). Most basins have been filled with colluvial and alluvial deposits during the last 3000 years, and many marshes, lakes and wetlands have been drained over the 20th century, leading to poor pollen preservation. Those intramontane lakes that still survive are particular focal points for relatively complete records and have been utilised through previous coring efforts. Along with the deposition environment, the effects of sampling procedures and analysis techniques can also impact on the interpretation of vegetation from pollen sequences.

A further consideration is that the type of pollen available in the pollen cores should be considered. It is important to note that the pollen from entomophilous (insect pollinated) plants is rarely represented in pollen records, unless their pollen is also wind dispersed. In addition, self-pollinating plant species such as Cerealia is also not well represented in pollen records. For this reason it is difficult to trace early agricultural domesticates in the pollen record (Vermoere 2002a). With these provisos in mind, the next section will discuss pollen findings from southwest Turkey.

### 4.2.1 **Beyşehir Gölü**

Beyşehir Gölü is a lake of structural origin, which lies within the vilayets of Konya and Isparta. It is found at an elevation of 1120 m. A Pollen core was retrieved by Van-Zeist, Woldring et al. (1975) to investigate the vegetation composition since the last glaciation. The core was 545 cm long, and 5 zones of vegetation assemblage were identified.

One radiocarbon date was available for the middle of Zone 1, which allows a linear interpolation to be undertaken to estimate the end of the zone at ~5 850 $^{14}$C yr BP, meaning the Zone 1 potentially represented the Late-Glacial, Early Holocene transition. The first zone is characterised by high *Cedrus* and *Pinus* percentages, suggesting coniferous forest cover. Zone 2 was interpolated as ~5 850 – 3 535 $^{14}$C BP (Mid Holocene) and shows an increase in pine, which Van-Zeist, Woldring et al. (1975) attribute to climatic fluctuations.

Zone 3 reflects drastic change in the vegetation of the Beyşehir area (van Zeist, Woldring et al. 1975) and is therefore split into a number of subzones. Firstly there is a dramatic reduction in the level of *Pinus* and *Cedrus,* an increase in *Fraxinus ornus*, *Quercus* and *Betula* and the percentage of herbaceous pollen types such as *Artemisia, Plantago lanceolata* and Gramineae also increase. Cultivated species such as *Juglans, Castanea, Olea, Vitis,* and *Sambucus* appear suggesting widespread deforestation (perhaps for timber) and the onset of cultivation in the area. Near the end of this zone a reversal occurs, with an increasing proportion of pine. Lake taxa composition remain similar, reflecting marshy conditions at the core site, and adding weight to a anthropogenic, not climatic cause for this event.

Subzone 3b contains 1 radiocarbon date, of 3265 $^{14}$C yr BP ±35, however zone boundaries are interpolated (~3 355 – 3205 $^{14}$C BP). This zone intriguingly suggests a temporary reprieve from grazing and an increase in *Pinus.* No other radiocarbon dates are available and other zone boundaries are interpolated. Subzones 3c and 3d (~3 295 to 2 185 BP) show that an increase in intensity of farming and deforestation is again present, with *Abies* and *pinus* decreasing and herbaceous plants increasing. The period from 3 535- 2 185 $^{14}$C BP describes the typical Beyşehir occupation phase signature and is the basis for correlating the signature with other core sites in southwest Turkey.

Zone 3e (~2 185 – 1 550 $^{14}$C BP) reflects the regeneration of the forest, with *Pinus* and *Abies* increasing and herbaceous species decreasing however *Cedrus* failed to recover (van Zeist, Woldring et al. 1975). Zone 4 shows a second period of forest clearance but without an increase in cultivation indicators suggesting wood for timber. Finally Zone 5 represents continuous forest cover dominated by pine.

### 4.2.2 **Karamik Batakliĝi**

In southwest Turkey, Karamik Batakliĝi has the longest period of pollen evidence within southwest Turkey, estimated to cover the Late Glacial period up until close to the present day (van Zeist, Woldring et al. 1975). Karamik Batakliĝi (~ 1000m asl) is a marshy depression within a NE-SW oriented basin in close proximity to the Behsehir / Hoyran *nappe.* A pollen core

was taken within this depression by Van-Zeist, Woldring et al. (1975) which was 600cm in length, capturing the period from ~21 000 BP.

*Artemisia,* Chenopodiacea and Graminineae were predominantly found in Zone 1, equated to ~20 800 -18 600 $^{14}$C BP, along with other Non-Arboreal Pollen and Arboreal Pollen species such as *Quercus, Cedrus, Pinus and Abies* showing that a rich forest-steppe, and steppe-forest vegetation was widespread in the area after the last ice age. In Zone 2, between 18 600 $^{14}$C BP and 14 350 $^{14}$C BP arboreal pollen percentages rose which van Zeist attributes to a moister climate during the early Holocene. In Zone 3 (~ 14 350 – 11 630 $^{14}$C BP) steppe was still evident, with an increase in *Cedrus,* and a decrease in *Quercus* and *Pinus.* Van-Zeist and Woldring interpret this as Cedar encroaching on previously steppe-forest areas due to a warming and moistening of climate.

Within Zone 4 cedar declines but steppic species are proportionally higher, possibly due to the increase in temperature causing drier conditions. This is supported by the appearance of marsh type vegetation in the pollen assemblage, indicative of lower lake levels. It should be noted at this point that pollen from other species which do not seem to fit interpretation of the landscape (such as *Carya*, *Fagus* and *Tilia*) are explained as redeposition, although possible long-distance travel is also considered in some cases. In zone 5 (~8 230 – 5 850 $^{14}$C BP), an increase in forest is seen over area which was previously steppe suggesting a moistening of the climate.

Between zones 5 and 7 there is an alternation in the dominance of *Cedrus* and *Pinus* percentages. Some changes in this ratio are apparently quite swift. The absence of anthropogenic evidence suggests that these fluctuations were climatic in origin (Van-Zeist, Woldring et al. 1975). Zone 6 (~5 850 – 1500 $^{14}$C BP) shows that lake level fluctuations are still apparent due to a change in the percentage of Tubuliflorae and Linguliflorae.

Zone 7 (~1500 $^{14}$C yr BP) shows an increase in herbaceous pollen types; Cerealia and Gramineae indicating along with *Plantago lanceolata* the possibility of grazing in the area. The signature of *Corylus* points to forest clearing, although Van-Zeist, Woldring et al. (1975) are also quick to point out that this could again be a redeposition species. Finally it is important to note that the uppermost deposits in the core still show a high percentage of tree pollen, whereas the area is presently devoid of trees. This may suggest that the core-top is not actually the present day, or it suggests recent deforestation (van Zeist, Woldring et al. 1975).

### 4.2.3 **Gölcük**

Gölcük is a site 15km south of and 900m higher than Sardis (Eastwood, Roberts et al. 1998), and is one of the westernmost pollen cores available. A core of 1200cm was taken by Sullivan (1989) which included four radiocarbon dates. The core bottom is likely to date from the early Holocene with a radiocarbon date in the middle of the first zone of 7400±120 $^{14}$C yr BP. The zone shows high *Quercus* values. There are also low values of *Castanea, Olea* and Cerealia-type. The period of the Beyşehir Occupation Phase according to Sullivan is placed between 960 BC - AD 240. The main cultivated crops were *Olea, Castenea, Vitis* and *Juglans* along with Cereals which may or may not be of human origin. Cultivated species decreased, with an increase in Quercus and Pinus after this phase. However arboriculture (sweet chestnut and walnut) was once again cultivated during the 'Turkish' period (~1100 $^{14}$C BP; Cal AD 975) persisting to sub-recent times (Sullivan 1989), making this an ‘unusual’ site. Evergreen and deciduous oak were therefore co-dominant with pine before and after the BO phase.

### 4.2.4 **Gölhisar Gölü**

In the area around Gölhisar Gölü, Artemisia and Chenopodiaceae covered most of the Near East prior to ~10 500 14C BP, reflecting a late glacial steppic environment as shown in Karamik and Söğüt cores (van Zeist, Woldring et al. 1975). By ~9 500 14C yr BP Pinus forest dominates the arboreal pollen record (at 60%), along with non-arboreal species such as Compositae, Gramineae and Pteridophytes, interpreted by Eastwood, Roberts et al. (1999) as pioneer species. However it is important to note that the overall concentration and influx of all pollen at this time was very low. Therefore pine may not actually be prevalent in close proximity to the lake; its pollen trace may a consequence of long-distance travel. This suggests a fairly open landscape which is undergoing post-glacial succession; a semi-arid climate (Roberts and Wright 1993) with trees in restricted locations ideal for growth such as sheltered areas with good water sources (Eastwood, Roberts et al. 1999).

Between 8600 and 5200 14C BP pollen concentration and accumulation rate fluctuated but showed a general trend of increase, suggesting both a maturing of the vegetation assemblage and a favourable change in climate, comparable with the Karamik core. True pine dominated forest was evident, alongside an increase in evergreen and deciduous oak. Juniper is also present, and is probably under-represented (Eastwood, Roberts et al. 1999). An interesting event commences at around 5200 $^{14}$C yr BP in Golhisar core B, and 5000 $^{14}$C yr BP in Golhisar A. There is a sharp and dramatic increase in Artemisia. This seems to be at the expense of *Pinus*. At this stage no cultivation is found in the core, so this possibly suggests either a time of deforestation, or else removal of forest by some other means (i.e. disease or climate change). The event is seen in other cores, particularly the one at Pinarbasi, where there is a large period of disturbance from even earlier, around 5800 $^{14}$C yr BP.

The Beyşehir Occupation Phase in this area is defined by a drop in the amount of *Pinus* and an increase in cultivation species such as *Olea, Castenea, Fraxinus ornus and Vitis. Pistacia* is also found along with Cerealia-type plants, however these are not strictly anthronogenic influenced plants. The Beyşehir Occupation phase here starts subtly at around 3000 BP (1250 BC) and Eastwood, Roberts et al. (1998) have given the official start date as 3200 BP (1450 BC). The intensity of cultivation increases at around 2600-1300 BP (~800-650 BC) with the introduction of *Juglans* and *Sanguisorba*-type vegetation suggesting a seriously degraded landscape, seemingly at the expense of *Pinus*. This period continued for an extended period, however by 500 AD, *Pinus* had started to regenerate. Eastwood, Roberts et al. (1998) define the end of the BO Phase in this area by 700 AD, with the disappearance of cultivation indicators, and the re-introduction of forest. The addition of a number of radiocarbon dates and a tephra layer supports this as a reasonable declaration.

### 4.2.5 **Gravgaz**

Gravgaz is situated in the Western Taurus mountain range, around 2km to the north of Ağlasun, on a south facing slope at an elevation of 1500-1600 m (Vermoere, Smets et al. 2000). Mesozoic limestone slopes are prevalent. The present day vegetation consists of *Quercus coccifera* up to elevations of 1600 m. To the east are extended forests of *Pinus Brutia* and *Pinus nigra* var. *pallasiana. Abies cilicica* is found on steep slopes. A core sample was taken from a marshy site within the territory of Roman Sagalassos, which represents the late Holocene.

Zone A was characterised by high arboreal pollen, predominantly deciduous *Quercus* and evergreen *Quercus*. Pine, Cedar and Juniper are also present in small amounts. Zone B is composed of low *Pinus* values, however *Quercus* remains important. *Artemisia,* along with small amounts of *Olea europaea, Fraxinus ornus*, and *Plantago lanceolata* suggest low level cultivation.

Zone C shows a return of *Pinus* with steady amounts of other conifers. *Artemisia* levels decrease, and primary anthropogenic indicators increase such as *Fraxinus ornus, Juglans regia,* and *Olea europea.* Zone D shows the continuing recovery of pine. Deciduous *Quercus* trees disappear from the landscape. *Olea europea, Fraxinus ornus* and *Juglans regia* pollen types are absent or poorly represented in this zone. Lithology is peat rich in plant material.

### 4.2.6 **Hoyran Gölü / Eğridir Gölü**

Hoyran Gölü is situated in a north-south oriented basin between the Beyşehir / Hoyran and eastern Lycian *nappes.* Neogene sediments are found to the northwest, north, northeast and east of the lake. Limestone is prevalent as is tertiary volcanic tuff. To the west of the site are the Barla Mountains, which reach elevations of more than 2 500m. A pollen core was taken by Van-Zeist, Woldring et al. (1975) There is some uncertainty whether the bottom of the core represents full glacial conditions (which assuming a constant sedimentation rate and requires a hiatus). If the core is instead postglacial, this is important as van Zeist suggests that changes in vegetation at Hoyran were not climatic in this case, as the same changes were not seen in other cores such as Karamik, suggesting deforestation instead.

This core was not very deep, and as such oldest sampled spectra in this core show high arboreal pollen percentages, probably from between 5 300 to 2 400 $^{14}$C yr BP. *Pinus* and *Cedrus* predominate. Following this an increase in Non-Arboreal Pollen and decrease in arboreal pollen is seen. Steppic vegetation had partly replaced the coniferous forest to the north of Hoyran Gölü. Eventually *Ranunculus* and other steppic species increases. However this is before major opening up of the landscape shown in other areas. Therefore there is a question as to whether the forest is just cleared for timber, or if climatic factors are involved. Van Zeist, Woldring et al. (1975) assume the influence of man is the predominant influence. The last zone which is not dated shows an increase in arboreal pollen, before again diminishing to non-arboreal pollen species. Carya is found in the record, but it is unclear which zone, as it is again assumed to be redeposited, even though it is found in both Beyşehir Gölü (which did not show a ready source of Neogene sediments to the lake) and Karamik.

### 4.2.7 **Köyceğiz Gölü**

Köyceğiz Gölü is sited within the vilayet of Muğla on the Köyceğiz plain. It is surrounded by Mesozoic limestone and ultrabasic rocks, with peat deposits found on the southeastern bank of the lake (Pons and Edelman 1963). Formed in the Holocene times with sea level rise, the lake is oligosaline, and is drained by the Dalyan river into the sea in the winter. During the summer considerable amounts of sea water flow back in. Modern day vegetation in the surrounding area is mainly *Pinus Brutia,* and maquis with *Quercus Calliprinos*. A pollen core was taken by Van-Zeist, Woldring et al. (1975)

The bottom of the pollen core, designated 'Zone 1', correlates to ~ 5 000 $^{14}$C BP, although without a radiocarbon date at this time this is interpolated. *Quercus cerris / infectoria*-type dominated, but it is interesting to note that *Vitis, Olea* and *Artemisia* are other constituents of

the core at this point, suggesting some level of human interaction with the landscape. Above this, zone 2 shows that at some point around 3600 BP *Pinus* pollen percentages became dominant over other arboreal species. Van-Zeist, Woldring et al. (1975) infer a period of more intensive human activity. However the large decrease in *Pinus* found in zone 3 is also suggested as indicative of anthropogenic effect, as large scale deforestation occurred. This is met with an increase in deciduous Quercus, along with species such as *Olea, Vitis, Sanguisorba minor*-type and *Plantago lanceolata*-type. Pteridium is also found which implies bracken taking over cleared areas of forest. During the end of zone 3, human influence was thought to be negligible (van Zeist, Woldring et al. 1975) with *Pinus Brutia* forests dominating around the lake.

Another key point of this pollen diagram is seen in Zone 4, which shows a decrease in *Quercus*, with a large increase in *Artemisia* (*herba-alba*). Zone 5 also shows high Artemisia levels, however pollen from cultivated crops is lacking. It will be shown that this disturbance without agriculture stage is a feature in a number of cores, and could be attributed to either human or climatic impact. Zone 6 shows an increase in *Quercus* and *Pteridium* with low Artemisia suggesting an open landscape, with a small amount of human cultivation present. Finally zone 7 shows an increase in maquis species such as *Pistacia, Myrtus* and *Paliurus.* The core also shows the recent decrease in deciduous oak, attributed to human influence. Crops such as *Vitis* and *Olea* are scarce.

Although human influence is suggested in small amounts throughout much of the core, the most intensive period thought to reflect the Beyşehir Occupation Phase is found between around 3200-2800 $^{14}$C yr BP, as evidenced by cultivated trees, and plants suggesting an over-grazed landscape. As stated earlier this is supported by a radiocarbon date, and also the subsequent discovery of the Santorini tephra layer by Eastwood, Roberts et al. (1998)

### 4.2.8 **Ova Gölü**

Ova Gölü is found on the coast of southwest Turkey, at an elevation of 15-20m. Zone 1 contains *Quercus cerris* and *Quercus calliprinos,* along with *Artemisia, Sanguisorba, Centaurea solstitialis* and Liguliflorae. Zone 2 is thought to represent the period around 4300 $^{14}$C yr BP (~3000 BC) and includes *Olea* and *Juglans* suggesting agriculture in the area.

### 4.2.9 **Söğüt Gölü**

Söğüt Gölü is an intramontane lake found within the vilayet of Burdur and Antalya at an elevation of 1 393m on the eastern Lycian *nappes*. A pollen core was taken by Van-Zeist, Woldring et al. (1975).

The oldest zone is characterized by high herbaceous pollen, with *Artemisia* and Chenopodiaceae playing an important part, suggesting steppic vegetation similar to Karamik and Golhisar. *Pinus* and *Quercus cerris* were the most dominant tree species. An accurate date cannot be given for this zone due to large variations in the sediment accumulation rate at this point. It is placed roughly at the end of the last glacial period when temperatures were cooler than present. Van-

Zeist, Woldring et al. (1975) interpret the high *Artemisia* percentage as also reflecting a dry climate, high winds and a short growing season.

Zone 2 brings increases in *Quercus*, whereas *Pinus, Artemisia* and *Cedrus* decline, possibly suggesting a warmer climate in the early Holocene. In the second part of this zone, *Quercus* then decreases, interpreted as a continuing aridity. Corylus is also found, which does not tolerate dry conditions, and is therefore is suggested as redeposition (van Zeist, Woldring et al. 1975).

Zone 3 first shows a decrease in *Quercus* at around ~8 700 $^{14}$C yr BP and reflects an open landscape with few trees. Van-Zeist, Woldring et al. (1975) equate this to a climate unsuitable for tree growth, which is in contrast to other cores at around this time. Arboreal Pollen does recover in this zone, along with *Pinus* making over 50% of the pollen assemblage. *Juniperus* appears, and an amelioration of the climate is interpreted, particularly due to an increase in precipitation (van Zeist, Woldring et al. 1975). Then, near the end of this zone, arboreal pollen again decreases and *Artemisia* increases dramatically. suggesting increased aridity.

Zone 4 shows a decrease in *Artemisia* with an increase in tree cover, suggesting a general increase in humidity and the distribution of forest determined by altitude and exposure. The large proportion of deciduous oak suggests that the climate was drier than at present. The end of this zone is estimated at ~3 655 $^{14}$C yr BP. Zone 5 shows an increase in *Pinus*, which Van-Zeist, Woldring et al. (1975) equate to anthropogenic influence as well as an increase in humidity. Zone 6 shows a near continuous decrease in arboreal pollen from *Pinus, Quercus* and *Juniperus.* This is interpreted as the Beyşehir Occupation phase for this area and can be dated with relative confidence to around 3000 $^{14}$C yr BP. Interestingly, *Cedrus* percentage did not diminish, suggesting that deforestation did not occur in the area occupied by cedar. However *Olea europa, Fraxinus ornus, Juglans regia* and *Vitis vinifera* are proportionally high, reflecting cultivation in the area, *Artemisia,* Cerealia-type (e.g. *Humulus* or *Cannabis*) and particularly *Plantago Lanceolata*-type reaffirm this. The signature of *Olea* in particular is interesting as it would be found at ~1400 m, higher than its altitudinal limit today, signifying a milder climate. At the end of this zone, another dramatic shift occurs, and the forest is reintroduced slowly from around 2100 $^{14}$C yr BP, but this time is predominantly *Pinus,* as *Quercus* and *Juniperus* do not recover. This can be compared to the Beyşehir occupation phase found at Beyşehir and Gölhisar Gölü. The end of the BO phase here is estimated at ~1900 $^{14}$C yr BP with the disappearance of cultivated trees, however without a nearby radiocarbon date this is reliant on linear interpolation. Zone 7 is characterised by high *Pinus* percentages, along with a small amount of *Cedrus* pointing to predominant *Pinus* forests throughout the area. This is thought to be the climax vegetation for the area under present day climatic conditions (van Zeist, Woldring et al. 1975). The top of the core was noted not to be contemporary as it did not capture recent deforestation.

### 4.2.1 **Ağlasun**

From Vermoere et al. (2002a) Three pollen diagrams from a transect perpendicular to the Aglasun stream allow a picture of Holocene vegetation evolution from the Neolithic period onwards. Although dominated by deciduous oak woodlands, the vegetation was already diverse in the early Holocene. Coniferous forests and patches of steppe were confined to the high montane belt, and maquis or shrubland occured at lower elevations. The deciduous oak

woodland was cleared at the transition from late Neolithic to early Chalcolithic. From this period onwards, Juglans regia appears in the pollen diagrams, along with secondary anthropogenic indicators. This points to human impact in and near the valley during the Chalcolithic and Bronze Ages periods. The indications of late Holocene Beysehir Occupation are weak. Adter the Byzantine period, deciduous oak woodland was cleared, and light demanding disturbance indicators dominate the pollen diagrams. Patches of wet grasslands disappear, indicating the dessication of the valley (Vermoere 2002a).

### 4.2.2 **Bereket**

The site of Bereket an intramontane basin located at 37°32'42.65 N; 30°17'42.23 E. The Bereket basin drains today towards Lake Burdur by the Aykırdak Deresi and the Büğdüz Cayı. The basin is surrounded by two mountain ridges: Kokayanık Tepe (1830 m a.s.l.) towards the west and Beşparmak Dağları (2280 m a.s.l.) towards the north-east.

The below summary is taken from Kaniewski et al. (2007b). The oldest sediments at Bereket, zones 3h to 3g show signs of regional and local fires. Kaniewski et al. suggest that human disturbances probably started well before the beginning of the core due to the abundant charcoal remains apparent in Ber 3h.

Between ~ cal 280 BC and AD 400 (zones 3f to 2a) the Beysehir Occupation Phase is present at Bereket. The beginning of this phase is met with crop cultivation during Hellenistic times, Castanea sativa, Fraxinus ornus, Juglans regia and Vitis. Olea only occurs as trace values. The continuous development of frticulture did not occur before cal ~250 BC (Ber-3d). Kaniewski suggest this exemplifies the discontinuous start of rural practices and tree cultivation in high elevation sites (i.e. above 1400 m). The period also contains two abandonment phases (Ber-3c and Ber 3a). a number of fire episodes are present, followed by a strong increase of pine forest succeeded by steppe-forest.

Between ~40 BC – AD ~400 (Ber-2i to Ber 2a) is a particularly intensive period of cultivation with the highest human pressure ever recorded in the basin. This period sees the exploitation of Olea europeae and Pistacia atlantica. Other Hellenistic indicators are also present such as Castanea sativa, Fraxinus ornus and Juglans regia, Corylus and Vitis. This is followed by a period of arboriculture decline (Ber-2a), characterised by a lack of charcoal and an increase in Quercus coccifera. Olea disappeared by cal. AD ~300 whilst crop cultivation and other arboriculture species disappeared abou AD 450.

The end of the BO phase (somewhere between AD 350 and 450) is characterised by a catastrophic event with massive fires, partial or total destruction of the cultivated species and strong decreases in steppe forest. This is met with a dramatic increase in pinus, and an increasing number of shallow water species, followed by stagnant open water.

Following an abandonment phase of ~ 200 years (until around AD 650), Ber 1c shows the introduction of a new but limited cultivation phase evidenced by an increase in Poaceae cerealia tp, Castanea sativa and Juglans regia. Secondary Anthropogenic Indicators are also present.

Since 1950, an expansion of pine forest is seen, and an increase of exposed shore plants reflects the artificial drainage of the Bereket marshes (Ber-1b and Ber-1a).

# 5 APPENDIX: THE BEYŞEHIR OCCUPATION PHASE

Research question 3 is interested in defining a particular period of human impact known as the Beyşehir Occupation Phase, named after the place where this anthropogenically influenced period was first discovered. The phase was discovered through palynological investigations from coring activities.

A concise definition of what makes the phase unique is hard to find. Eastwood et al. (1998). suggest that the phase is the first period that shows 'Unambiguous' evidence of human impact. Although patchy evidence for cereal cultivation, animal husbandry and even arboriculture is available since the early Holocene, it is likely to be the intensive combination of cereal crops, grazing indicators and arboriculture indicators in one place that marks the period out as unique.

Although the period of arboriculture was certainly realised by van Zeist, Woldring et al. (1975) the cementing of the term 'Beyşehir Occupation Phase' was achieved by Bottema et al. (1986). Since then, a number of reassessments of the phase have occurred (Bottema and Woldring 1990; Eastwood, Roberts et al. 1998; Vermoere, Bottema et al. 2002b) The phase is most clearly visible in SW Turkey, but defining the full spatial extent of the phase is difficult as there are only a few sites in central Turkey (such as Nar Gölü) that have yielded palaeoecological records. However, a similar phase has been recorded in sporadic sites in NW Turkey and northwestern Greece (England, Eastwood et al. 2008).

Furthermore, the timing of the Beyşehir Occupation Phase is not yet consistently agreed. Working from van Zeist et al. (1975), Vermoere (2002a) defines the BO phase for Beyşehir as commencing at ~3500 $^{14}$C BP (~1800 Cal BC), whereas Eastwood et al. (1998) suggest the beginning to be around 3200 $^{14}$C BP (1450 Cal BC), continuing at some sites until around 1500 $^{14}$C BP (Cal. AD 600).

Pollen evidence is interpreted as showing evidence for forest clearance, crop cultivation and arboriculture. The beginning and the end of the phase is defined mainly by an increase in species such as grape (*Vitis vinifera*), walnut (*Juglans regia*), olive (*Olea europeae*) and manna ash (*Fraxinus ornus*), but also the plane tree (*Platanus europaeus*). Secondary Anthropogenic Indicators (SAI) such as *Plantago lanceolata* and *Sanguisorba minor* are also found as part of this phase and are taken as indications of disturbed land, or grazing (van Zeist, Woldring et al. 1975). The end of the phase appears to be marked by the regrowth of woodland with P*inus* being the dominant species. Previous to the BO phase mixed woodland was more prevalent, with *Quercus*, *Cedrus* and *Juniperus*.

One feature of the Beyşehir Occupation phase is that pollen evidence from Beyşehir, Pınarbaşı, Sögüt and Gölhisar suggest a period of deforestation occurred across the region. Radiocarbon dates this to around 3200 $^{14}$C BP (1450 Cal BC). A decrease in arboreal pollen need not always suggest deforestation (Vermoere 2002a), however Van Zeist et al. (1975) suggest that as lake taxa remain similar, this decrease in arboreal pollen represents interference by man as opposed to climatic change. Charcoal evidence from Bereket (a high resolution and robustly dated record) also adds weight to this discussion and provides evidence of multiple phases of burning, interpreted as forest clearance to support agricultural activities throughout the Hellenistic and

Roman periods (Kaniewski, Paulissen et al. 2007b). The beginning of the phase at Bereket also shows two phases of abandonment at the beginning, which highlights the discontinuity of cultivation in these high elevation sites.

Cultivation assemblages are seen to differ throughout the region. For instance, olive and walnut are found to be important at Gölhisar, Sögüt, Gölcük and Gravgaz. A large spread of cultivation is present at Pınarbaşı with olive, walnut, manna, sweet chestnut, pistachio and cereals. Manna ash is important at Sögüt, Beyşehir, Gravgaz, Elmali and Pınarbaşı. At Gölcük, vines and sweet chestnut are most important. The phase is also weakly expressed at Köyceğiz, however there is no trace in pollen diagrams at Ova and Karamik, and it is only barely discernible at Hoyran.

A number of features of the phase can be distinguished. At Gölhisar, an intensification of cultivation increases at around 2600-1300 BP (~800-650 BC) with a pollen assemblage suggesting a seriously degraded landscape. An intensive period of cultivation is also found at Gölcük, which according to Sullivan is placed between 960 BC - AD 240.

As well as cereal and arboriculture indicators, evidence for grazing is present at many sites. For instance, although arboriculture is not found at Karamik, Zone 7 shows an increase in herbaceous pollen types; Cerealia and Gramineae indicating along with *Plantago lanceolata* which are interpreted as grazing indicators.

Many of the pollen sites lie close to archaeological sites. Gölhisar Gölü lies within the ancient territory of Kibyra, a Classical city which is contemporary with and adjacent to Balboura and part of the Kibyra Tetropolis (Kibyratis). Gölcük lies 15 km south of the ancient city of Sardis. Gravgaz is 25km southwest of Sagalassos, and Köyceğiz is ~5km east of Kaunos.

Although first identified through pollen records, supporting evidence for the phase is found in archaeological records. An archaeological survey by Coulton (Ashmolean Museum, Oxford) of Balboura, one of the tetrad of Classical cities including Kibyra, Bubon and Oenoanda, uncovered sites from the prehistoric period to the Byzantine era (Coulton 1988), however, as discussed by Eastwood, the most dense period of human occupation is found to be between the Hellenistic and Late Roman period. Archaeological evidence from Sagalassos suggests an increase in hilltop sites between 300 - 450 AD (Harrison, mountain and plain) and a similar retraction at AD 600. It is not only the mountainous southwest that experiences this expansion. As discussed in Baird (2004) and Niewöhner (2006) the Central Anatolian Plain also sees significant settlement expansion during this period. Furthermore, Turkey is not unique in its evidence for a prosperous rural economy and impressive extant ruins from late antiquity (between ~4$^{th}$ and 6$^{th}$ centuries AD). Ruins also exist on the Syrian Limestone Massif. A common theme is found with rapid settlement expansion after around 200 BC, and retraction and near abandonment at around AD 600 to 700.

However, palynological and archaeological records are not always in good agreement (Roberts 1990; Eastwood, Roberts et al. 1998). For instance, the Balboura survey did not find any conclusive evidence of Middle or Late Bronze Age settlement (Coulton 1988), whereas pollen records suggest that this is a period of deforestation. Furthermore, the second millennium BC is not well represented in the archaeological record, but pollen records suggest that this is a cultivation phase.

Eastwood et al. (1998) suggest that this dichotomy between deforestation indicators and lack of archaeological evidence may be due to the chronological resolution and imprecision in radiocarbon dates. Another explanation may be that of cultural superposition, however. It is fortunate that this period covers the proto-historical period, and historical accounts from Hittite sources does seem to suggest that there were important settlements located in the southwest during this period (Waelkens 2000). This is important as it may suggest that the influence of Luwians on classical culture could have been considerable (Vermoere 2002a).

The end of the BO phase is associated with a marked increase in arboreal pollen values and a decrease or disappearance of cultivated trees and secondary anthropogenic indicators. Establishing end date for the Beyşehir Occupation Phase is considered crucial by Izdebski (2011) for reconstructing late antique agricultural history. However, pollen evidence suggests that cultivation does not stop abruptly, but decreases with certain species (i.e. Olea) stopping before others (such as Cerealia and Juglans).

The cultivation phase at Bereket ends by around 350 to 400 AD, evidenced by a decrease in olive pollen. This also correlates with evidence of extensive burning, followed by a large increase in Pinus pollen (Kaniewski, Paulissen et al. 2007b). Whether a concurrent increase in shallow water species is due to aridification or a large injection of erosive material following denudation is to be questioned. Herbaceous steppe predominates following the cultivation stage.

At Gravgaz, a complex picture of cultivation retraction can be seen. Cereal pollen and arboriculture are generally present between the 3rd and 7th centuries AD, however a decrease in cereal and olive cultivation is seen at the end of the 3rd century AD. Following this they return but at lower abundance, and show a slow decline in favour of deciduous woodland, meadows and pine forest by 640 AD (Vermoere, Smets et al. 2000; Bakker, Paulissen et al. 2012b).

Interestingly, the cultivation decrease is mirrored by significant decreases in settlement habitation, similarly at around 600 AD (vanhaverbeke – late antiquity) suggesting the end of intensive cultivation and the estate economy. However, the extent of retraction is not known for certain, and various issues surrounding the representation of pollen in pollen records, preservation bias, and a lack of comprehensive archaeological surveys across the region still leave significant uncertainty.

For instance, a continuation of wheat is seen at Gravgaz, and in other areas some form of cultivation continues, for instance pollen records from Canaklı suggest a continuation of pastoral indicators after the 7th century. This leads to the suggestion that perhaps pastoral activities were more resilient considering the environmental conditions of the late 1st millennium AD.

By 500 AD, *Pinus* had started to regenerate at Gölhisar. Eastwood, Roberts et al. (1998) define the end of the BO Phase in this area by 700 AD, with the disappearance of cultivation indicators, and the re-introduction of forest. The addition of a number of radiocarbon dates and a tephra layer supports this as a reasonable declaration. Beyşehir also shows evidence for the regeneration of Pinus and Abies following a decline in arboriculture indicators.

The uppermost deposits in the Karamik core still show a high percentage of tree pollen, whereas the area is presently devoid of trees. This may suggest that the core-top is not actually the present day, or it suggests recent deforestation (van Zeist, Woldring et al. 1975).

At Gölcük, arboriculture (sweet chestnut and walnut) was once again cultivated during the 'Turkish' period (~1100 $^{14}$C BP; Cal AD 975) persisting to sub-recent times (Sullivan 1989) making this an 'unusual' site. Evergreen and deciduous oak were co-dominant with pine before and after the BO phase.

#### 5.1.1.1 Factors influencing the phase

A number of factors influencing the Beyşehir Occupation Phase have been posited. Tephra evidence is present in a number of cores from the eruption of Santorini. At Gölhisar (Eastwood, Tibby et al. 2002) it is dated to ~3300 $^{14}$C BP ( ~1640 Cal BC). It is also found at Gölcük Gölü (Sullivan 1988; Sullivan 1990), and Köyceğiz (Sullivan 1990). The presence of the Santorini Tephra Layer (STL) has been suggested as a possible instigator of direct (climate change) or indirect influence on the phase, for instance socio-economic breakdown leading to population movements (Eastwood, Roberts et al. 1998). In particular, the BO phase at Köyceğiz, Gölhisar, Sögüt and Pınarbaşı may be synchronised with this event. However, the phase is also visible at Beyşehir and Ağlasun prior to this boundary, and so Roberts et al. (Roberts, Eastwood et al. 1997) argue that the eruption was probably not directly implicated in the commencement of the phase.

One of the main puzzles discussed by many scholars such as Izdebski (2011), Mitchell (2005), Vanhaverbeke and Waelkens (2003) etc. is that agricultural expansion is not restricted to fertile valleys with good transport links, but also to high elevations, central plains, and modern day deserts. In particular Izdebski (2011) articulates that whereas many historians assumed a narrative of economic hardship and conflict, evidence from the wider rural economy may tell a different story, outside of the socio-political framework of economic history.

Izdebski (2011) posits that one of the key factors that must have facilitated the unparalleled development of late antique agriculture were climate fluctuations; in particular that the period was unusually humid. Evidence is predominantly found from pollen studies (Bottema and Woldring 1984; Bottema, Woldring et al. 1993), which are not independent sources of evidence for this thesis. One potential reason for the increase in *Platanus* during the BO phase is that it was planted for shade, as it is today in Anatolian villages (Eastwood, Roberts et al. 1998). Another facet of the increase in cultivation intensity may have been due to the particular social and technological developments of the Hellenistic and Roman society.

High levels of Olea pollen were found at relatively high elevation sites, such as Sögüt (elevation 1400 m). This finding lead to some researchers to suggest that this evidence of Olea cultivation expansion may instead be a matter of pollen representation, for instance, Bottema et al. (1993) suggest that the Olea pollen recorded at high elevation sites is actually a result of long-distance travel from olive groves nearer the coast. It is known that Olea pollen grains are relatively small and light, and can travel great distances. However, as stated by Eastwood et al. (1998) other sites such as Avlan and Elmalı are closer to the coast but do not show this large Olea signature. Furthermore, sites that show high amounts of Olea pollen are separated from coastal olive groves by high mountain ranges (Roberts 1990). Modern surface samples have shown that Olea has an average pollen value of 0.8% for Oro-Mediterranean pine-forest vegetation, in

comparison to ~4.6 or 5.2% in the Eu-Mediterranean pine forest zone where olives naturally grow today (van Zeist, Woldring et al. 1975; Roberts 1990; van Zeist and Bottema 1991; Roberts, Eastwood et al. 1997). On balance, evidence suggests that the increase in Olea pollen does indeed represent a local increase in cultivation.

Further evidence is available from archaeological survey evidence from both the Balboura and Sagalassos territories. A number of large stone weights with perforated loops have been found, and are interpreted as parts of olive presses (Coulton 1988; Waelkens, Paulissen et al. 1997; Waelkens 1999). If these weights were associate with olive pressing then it is assumed that climate conditions must have been more favourable during the BO phase for the cultivation of olives (Roberts 1990). However, if the press weights cannot be positively identified as Olive presses, then evidence of cultivation resides purely with pollen analysis.

If this is the case, what kind of climate scenario might be required to support this intensity of cultivation? Roberts (1990) has calculated that winter and spring temperatures must have been ~2-3° warmer than today, assuming a 500 m upward shift in the limit of olive cultivation and considering local lapse rates of ~0.6 ° per 100 m (Eastwood, Roberts et al. 1998).

After around 2400 $^{14}$C BP, an increase in Non-Arboreal Pollen and decrease in arboreal pollen is seen at Hoyran Gölü, and steppic vegetation had partly replaced the coniferous forest to the north of the site. Eventually *Ranunculus* and other steppic species increases. There is a question as to whether the forest is just cleared for timber, or if climatic factors are involved. Van Zeist, Woldring et al. (1975) assume the influence of man is the predominant influence.

The phase poses some intriguing questions. These can be defined around four main issues. Firstly, what were the conditions that lead to the beginning of the phase, and how did it develop? Secondly, What level of cultivation occurred during the Mid-Bronze Age and the Anatolian dark age? Thirdly, what is the magnitude of agricultural expansion of during the Hellenistic to Late Roman period, and what were the reasons behind it? Finally, what are the reasons for the swift decline and abandonment of previously cultivated areas?

# 6 APPENDIX: REVIEW OF MODEL DATA SOURCES

## 6.1 HIGH RESOLUTION VEGETATION DISTRIBUTION DATA AVAILABILITY

Although many sources of vegetation data distribution exist, within horticultural manuals and digital atlases, for instance, the Atlas Florae Europa (Lahti and Lampinen 1999), or EUFORGEN (2009) many of these sources do not offer the kind of detail and resolution required by this study to adequately investigate the links between vegetation species, climatic and edaphic factors at anything other than the regional scale. It proved difficult to find data that was high resolution, accurate and consistent throughout Europe. Indeed, as discussed in Chapter 3, many recent studies are still using data at the 0.5° resolution, which is considered rather coarse for useful conclusions at the local or even landscape scale. Data from EUFORGEN (2009) was fairly consistent and high resolution, but it was considered that there was a fairly inconsistent methodology used throughout Europe, and little information was available as to how this was achieved.

After a comprehensive search, three sources of vegetation species distribution data were available that were deemed to have the required attributes, although all datasets still had limitations. The first dataset is from the CORINE land cover 2000 product (CEC 1994; EEA 2000). This is a satellite imagery based land cover interpretation, and maps forest, agriculture and urban classes at 250 m resolution, which is considerably higher than most other products. The geometric accuracy of the satellite images on which the data is derived is within 25 m, and the geometric accuracy of the digitised data is better than 100 m (JRC 2005). The accuracy of the thematic classification is estimated at around 85% (JRC 2005). Three layers pertaining to relevant species distribution (olive groves, grape vines and sclerophyllous plants) were downloaded for assessment. As a proviso, it should be noted that vegetation patches less than 25 m were not included in the original product due to the restrictions of the satellite imagery it was derived from (JRC 2005), and is a small limitation on the data. The other main limitation of this data is that apart from grape and olive, species are lumped into groups, which may preclude the potential correlation of vegetation with climate and edaphic factors. However, CORINE data is one of the highest resolution and most accurate products available.

The second source of data was from Köble and Seufert (2001) from the JRC which is based on classification of CORINE 2000 landcover data into species specific maps using ICP Forest data to plot forest density (UN-ECE 1998). The Tree Species Distribution for Europe data is a dataset of 137 raster maps, 115 of which give the percentage of a single tree species across Europe with a resolution of 1 km by 1 km. Another map shows the areas where no species classification was possible. Therefore, areas that are within the classification area are thought to provide an adequate representation of species presence and absence. The main point to note is that this represents species within forests, not on farmland or other open land. It is therefore likely to show species distribution within the climatic envelopes that it can exist in a forest environment, and where it can thrive despite other species. The field data that helped to create the dataset was based on 16 by 16 km sample plots of forest condition across Europe, which across 30 countries amounted to 5513 plots. The percentages for each species were then interpolated between sites.

The third source of data was a 1997 forestry map (OGM 1997) from the Turkish Directorate (Orman Genel Müdürlüğü), a sub-division of the Ministry of the Environment and Forestry (Çevre ve Orman Bakanlığı). The data differentiated key forest species such as P*inus brutia, Pinus nigra, Cedrus* and Q*uercus*. As this is taken from in-field data, it is considered relatively accurate. The data is presented at 1:100 000 scale, and was converted to 1 km resolution raster layers. The main limitation of this data is that it was not available for the whole of Turkey.

Figure 6-1 shows an example of the CORINE 2000 land cover shapefile for vineyard distribution throughout Europe. It should be noted that no data is available for Africa, and is only shown for reference. Figure 6-2 shows a sample of Quercus cerris distribution data from The Tree Species Distribution for Europe, and Figure 6-3 shows an example of Turkish forestry data.


**Figure 6-1 The distribution of *Vitis* throughout Europe (EEA 2000)**

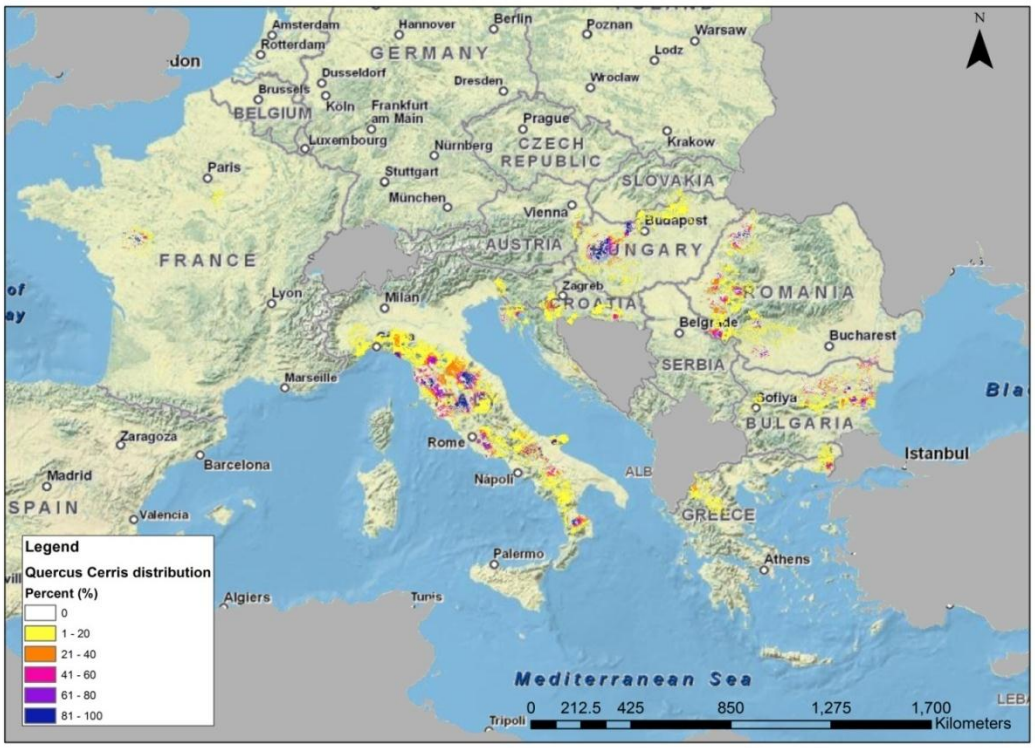


**Figure 6-2 The distribution of *Quercus cerris* throughout Europe (after Köble and Seufert 2001)**

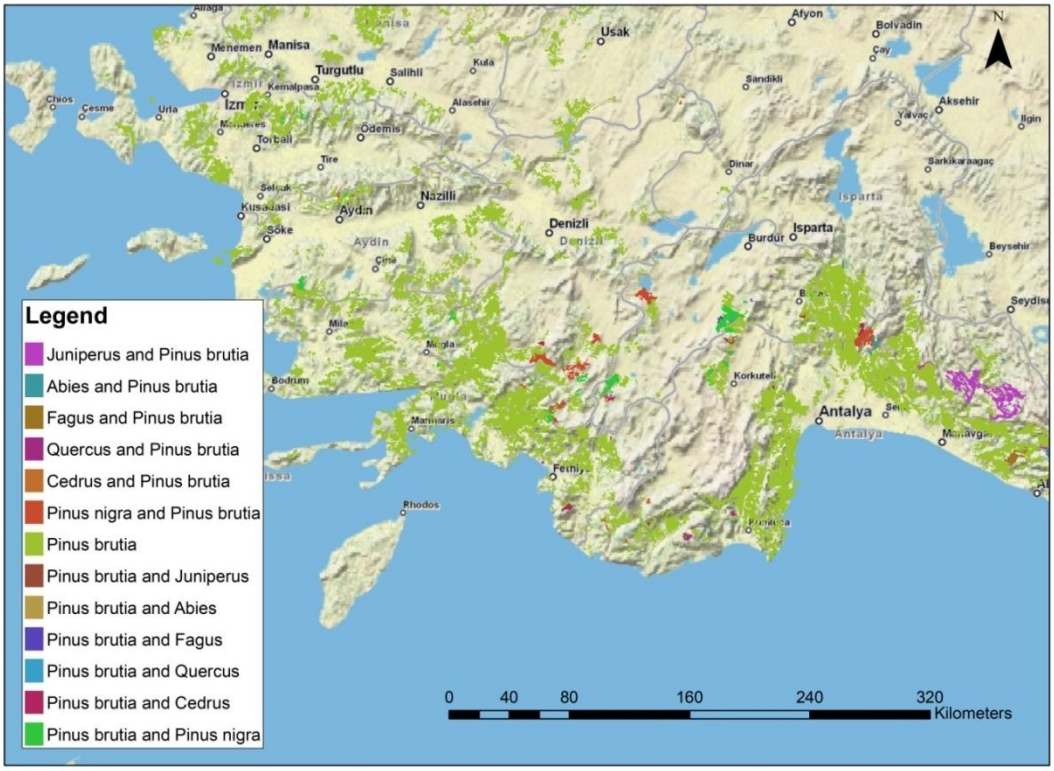


**Figure 6-3 The distribution of *Pinus brutia* throughout Turkey (OGM 1997)**

#### 6.1.1.1 Revised species choice based on data availability

Not all of the key pollen species are available in the JRC, CORINE and Turkish Directorate dataset. The identification of key species to model and the extent of coverage will therefore also be restricted by vegetation data availability. Table 6-1 summarises the main issues that were considered when choosing the final species, and Table 6-2 shows the final species choice.

**Table 6-1 Main considerations for model species choice**

| Identified issues | Solution | Assumption |
|---|---|---|
| **1. Definition of species:**<br><br>Some pollen is not able to be identified at the species level e.g. *Pinus* | Definition of key species to model is in this case based on *a priori* knowledge. E.g. decision to model *Pinus nigra* and *Pinus brutia* | Assumes *a priori* knowledge is adequate. |
| **2. Species substitution**<br><br>e.g. information on *Cedrus libani* is not available | Where specific species in the pollen record is not available, substitute for similar. E.g. *Cedrus libani* for *Cedrus deodara* | Assumes species distributions are similar. |
| **3. Lack of species**<br><br>e.g. no *Artemisia* distribution | Where a species is not available but is still a key indicator, its distribution is modelled based on *a priori* knowledge e.g. *Artemisia* is modelled as the main constituent of a 'steppe' class which is dictated by precipitation. | Assumes *a priori* knowledge is adequate. |
| **4. Data extent**<br><br>Some species distributions are not available for Turkey, only the rest of Europe e.g. *Alnus* | Use data from the rest of Europe to characterise species | Assumes data from the rest of Europe adequately maps the climatic and edaphic range of the species. |
| **5. Merging datasets**<br><br>Where data is available for Turkey separately from the rest of Europe data is merged | Datasets will be merged to gain full data representation | Assumes data resolution and type is the same. Requires pre-processing. |
| **6. Representation of species distribution**<br><br>Species distribution from data may not fully represent the climatic or edaphic envelope in real life | Gain most up to date, high quality data products. Use field based data where possible. | Assumes species distribution data represents a statistically significant sample of the species' population. |

**Table 6-2 Cross referencing important pollen record species with JRC data availability**

| Species important in pollen record | JRC species | Final species choice |
|---|---|---|
| *Pinus, pinaceae* | *Pinus brutia, Pinus halepensis, Pinus nigra, Pinus pinaster, Pinus sylvestris* | *Pinus brutia, Pinus nigra* |
| *Alnus* | *Alnus cordata, Alnus glutinosa* | *Alnus cordata* |
| *Quercus cerris*-tp | *Quercus cerris* | *Quercus cerris* |
| *Quercus coccifera*-tp | *Quercus coccifera* | *Quercus coccifera* |
| *Betula* | *Betula pendula, Betula pubescens* | *Betula pendula* |
| *Cedrus libani, Cedrus* | *Cedrus atlantica, Cedrus Deodara* | *Cedrus deodara* |
| *Abies Cilicica* | *Abies alba, Abies cephalonica* | *Abies alba* |
| *Juniperus* | *Juniperus oxycedrus, Juniperus communis, Junipers phoenecia* | *Juniperus oxycedrus* |
| *Carpinus betulus* | *Carpinus betulus* | *Carpinus betulus* |
| *Corylus* | *Corylus avellana* | *Corylus avellana* |
| *Fagus* | *Fagus sylvetica, Fagus orientalis, Fagus moes* | *Fagus sylvatica* |
| *Platanus orientalis* | *Platanus orientalis* | *Platanus orientalis* |
| *Populus* | *Populus nigra, populous alba* | *Populus nigra* |
| *Tilia* | *Tilia cordata, Tilia platanus* | *Tilia cordata* |
| *Ulmus*-tp | *Ulmus glabra, Ulmus laev, Ulmus minor* | *Ulmus glabra* |
| *Olea*-tp, *Oleaceae* indeterminate, *Olea europeae* | *Olea europeae*, agriculture olive | *Olea europeae* |
| *Juglans, Juglans regia* | *Juglans regia, Juglans nigra* | *Juglans regia* |
| *Cerealia*-tp | Dry agriculture | Dry agriculture |
| *Fraxinus ornus* | *Fraxinus ornus* | *Fraxinus ornus* |
| *Vitis vinifera* | *Vitis vinifera*, agriculture vine | *Vitis vinifera* |
| *Castanea sativa* | *Castanea sativa* | *Castanea sativa* |
| *Poaceae*[a] */ Gramineae* | Grassland | Grassland |
| *Artemisia* | Not available | Modelled as steppe class defined by precipitation range (>300mm) |
| *Plantago lanceolata* | Not available | Assumed constituent of grassland |
| *Centaurea solstitialis* | Not available | Assumed constituent of grassland |

### 6.1.1.2 Identification of key vegetation parameters based on *A priori* species knowledge

This section summarises a review of *a priori* knowledge of the key species that will be modelled in this thesis. The data was used to identify key parameters that affect vegetation growth in order to begin to couple environmental parameters with vegetation parameters. Table 3 summarises this literature search.

**Table 3 *a priori* species information for key species modelled in this thesis**

| Species | Main characteristics | References |
|---|---|---|
| **Pinus brutia:**<br>Evergreen<br>Fast-growing<br><45m | Prefers hot, dry summers and mild rainy winters[1]<br>Prefers average temperature of 12-20°C[2]<br>Optimum germination temperature 20°C[3]<br>Winter hardiness for *halepensis* around -12°C[4]<br>Requires 400-2000 mm annual precipitation[5]<br>Drought resistant once established but regeneration and obstacle[6]<br>Photoinhibition avoiding[7]<br>Light demanding[1,5]<br>Found on cracked limestone, colluvial, marl and flysch deposits[8]<br>Does not tolerate poorly drained soils[1]<br>Very well fire adapted[1,5] | [1] Qezel (2000)<br>[2] Gezer (1986) Boydak (2004)<br>[3] Tilki and Dirik (2007)<br>[4] Calamassi et al. (2001)<br>[5] Boydak (2004)<br>[6] Boydak et al. (2003b)<br>[7] Martínez-Ferri, Manrique et al. (2004)<br>[8] Atalay, Sezer et al. (1998) |
| **Quercus cerris:**<br>Deciduous<br>Fast growing<br><35m | Limited at northern extent of range by winter temperature and southern range by available moisture / drought[9,10]<br>Spring precipitation important for growth[11,12,13]<br>June temperatures and autumn precipitation important for growth[12,13]<br>Requires at least 500 mm annual precipitation[14]<br>Drought sensitive, tolerance not avoidance strategy[11, 15]<br>Susceptible to disease in drought weakened state[16]<br>Winter temperature tolerance down to ~-23°C[17]<br>Prefers deep, fertile loam soils[18] | [9] Thompson, Anderson et al. (2000)<br>[10]Brewer, Cheddadi et al. (2002)<br>[11]Nardini et al. (1999)<br>[12]Romagnoli and Copipietro (1996)<br>[13]Corona et al. (1995)<br>[14]Rossignol-Strick (1995)<br>[15]Lo Gullo et al. (1995)<br>[16]Vannini et al. (1996)<br>[17]PFAF (2009a)<br>[18]Chittendon (1956) |
| **Quercus coccifera:**<br>Evergreen<br>Slow growing<br><4m | Dependent on summer precipitation[19]<br>Negatively correlated with cold winter temperatures[19,20]<br>Relatively drought tolerant, however regeration is an obstacle[21]<br>Requires at least 300 mm annual precipitation[22]<br>Winter temperature tolerance between -23°C and -27°C in evergreen oak[23,24]<br>Resistant to browsing, felling and burning[25]<br>Prefers deep fertile loam although can grow on thinner soils[26] | [19]Tessier et al. (1994)<br>[20]Patón, García-Herrera et al. (2009)<br>[21]Villar-Salvador (1997)<br>[22]Jurgenson et al. (2009)<br>[23]PFAF (PFAF 2009b)<br>[24]Morin et al. (2007)<br>[25] Rodà (Rodà 1999)<br>[26] Bean (Bean 1987) |
| **Pinus nigra:**<br>Evergreen<br>Fast growing<br><30m | Drought tolerant once established, however drought can cause growth restriction[18]<br>Spring and summer precipitation important for growth[19]<br>Cool years encourage growth[29]<br>Winter temperature tolerance generally below -30°C [30]<br>Rapid regeneration after grazing, but not after wildfire [31]<br>Succeeds on most soil types, but does poorly on poorly drained soils [18,26] | [27] Gassner et al. (1942)<br>[28] Akkemik and Aras (2005)<br>[29] Sevgi and Akkemik (2007)<br>[30] Sutinen et al. (1992)<br>[31] Escudero et al. (1997)<br>[31] Espelta et al.(2003) |
| **Betula pendula:**<br>Deciduous<br>Fast growing<br><20m | Winter temperature tolerance down to -45°C [32]<br>Increased duration of chilling days reaults in reduced time to bud burst [33]<br>Is not considered a particularly drought tolerant tree. Has a drought avoidance strategy[34]<br>Pioneer species[35]<br>Tolerates most soil types, but prefers well drained acidic soil in sunny position[18] | [32] PFAF (2009c)<br>[33] Myking and Heide (1995)<br>[34] Wendler and Millard (1995)<br>[35] Atkinson (Atkinson 1992) |

| Species | Main characteristics | References |
|---|---|---|
| **Fagus sylvatica:**<br>Deciduous<br>Fast growing<br><30m | Chilling and long photoperiods important for budburst[36,37]<br>Drought sensitive[38]<br>Flood tolerant[39]<br>Dependent on adequate rainfall[40]<br>Very shade tolerant[40]<br>Subject to early frost damage[40]<br>Can become dominant species[40]<br>Tolerates most soils but prefers a light alkaline soil[18] | [36] Heide (1993)<br>[37] Kramer (1994)<br>[38] Ellenburg (1992)<br>[39] Ranney and Bir (1994)<br>[40] Huxley et al. (1992) |
| **Cedrus libani:**<br>Evergreen<br>Slow growing<br><30m | Grows well in acidic and calcareous soils, requiring good drainage[41,42]<br>Often found in soil formed along cracks in limestone bedrock[42]<br>Drought tolerant<br>Can tolerate summers without precipitation[42]<br>Significant timber source[42]<br>Light demanding; fire is an effective method for regeneration of Cedrus [42]<br>Current distribution considered to be highly degraded due to timber and grazing[42] | [41] Kantarcı (Kantarcı 1990)<br>[42] Boydak (Boydak 2003a)<br>[43] Bariteau and Ferandes (1990)<br>[44] Ducrey (Ducrey 1993) |
| **Abies alba:**<br>Evergreen<br>Fast growing<br><45m | Very shade tolerant tree [26,45]<br>Spring and summer precipitation important for growth [45]<br>Drought sensitive [45]<br>Winter minimum temperature tolerance down to -34°C [46]<br>Cold winter restricts growth [45]<br>Cold winter in previous year can affect next year's growth [47]<br>Hardy when dormant, but early spring frosts can cause damage [48]<br>Tolerates most soils, however prefers moist soils, and grows well in heavy clay soils that are slightly acidic.[49] | [45] Rolland et al. (1999)<br>[46] PFAF (PFAF 2009d)<br>[47] Becker (Becker 1989)<br>[48] Mitchell (1972)<br>[49] Rushforth (Rushforth 1991) |
| **Juniperus oxycedrus:**<br>Evergreen<br>Fast growing<br><15m | Winter minimum temperatures tolerance down to around -17°C[49]<br>Precipitation requirement for Juniperus phoenecia ~150 mm[50]<br>Precipitation requirement for Juniperus excelsa between 500 – 1000 mm[51]<br>Considered drought tolerant[51]<br>Succeeds on most soils[18]<br>Current distribution considered to be highly degraded due to grazing[51] | [50] Ghrabi (Ghrabi 2011)<br>[51] Ozkan et al. (Ozkan, Gulsoy et al. 2010) |
| **Alnus glutinosa:**<br>Deciduous<br>Fast growing<br><25m | Precipitation requirement of at least 400mm[52]<br>Moderately drought tolerant[52]<br>Winter minimum temperature tolerance down to around -40°C[53]<br>Prefers heavy soils in a damp location[18,26] | [52] Duke (1983)<br>[53] PFAF (PFAF 2009f) |

| Species | Main characteristics | References |
|---|---|---|
| **Picea abies:**<br>Evergreen<br>Fast-growing<br><30m | Winter minimum temperature tolerance down to around -35°C[54]<br>Young shoots frost tender[18] | [54] PFAF (PFAF 2009g) |
| **Tilia cordata:**<br>Deciduous<br>Fast growing<br><30m | Winter minimum temperature tolerance down to around -40°C[55]<br>Requires warm summers in order to produce viable seeds[56]<br>Close relationship between precipitation and flowering[56]<br>Prefers moist loam in alkaline or neutral soils[18] | [55] PFAF (PFAF 2009j)<br>[56] Spano et al. (1999) |
| **Carpinus betulus** | No information available | |
| **Populus nigra** | No information available | |
| **Ulmus glabra** | No information available | |
| **Olea europeae:**<br>Evergreen<br>Slow growing<br><15m | Vulnerable to low winter temperatures. Widely damaged by temperatures under -10°C to -12°C[57,58]<br>~12.5°C required for budburst[58]<br>Fairly large amount of days heat accumulation (119.5°C), and GDD (210°C) required to produce fruit[59]<br>High temperature (>40°C) can prevent germination[60]<br>Drought tolerant species, can survive without summer precipitation[61,62]<br>Requirement of ~700 to 800 mm annual precipitation estimated [63]<br>Tolerant of poor soil conditions, and has a preference for calcareous soils [18]<br>Can require 6-15 years growth to start fruiting[40] | [57] Bartolozzi and Fontanazza (1999)<br>[58] Larcher (1970)<br>[59] Galàn et al. (2001)<br>[60] Koubouris et al. (2009)<br>[61] Saei et al. (Saei, Zamani et al. 2006)<br>[62] Rousseau et al. (2008)<br>[63] Tognetti et al. (Tognetti, d'Andria et al. 2006) |
| **Castanea sativa:**<br>Deciduous<br>Slow growing<br><20m | Requires 15 years growth to start fruiting[64]<br>Responds positively to warm spring and summer air temperatures, but negatively to autumn heat[64]<br>Responds positively to early spring preciptation, but negatively to early summer and autumn precipitation[65]<br>Winter chilling required to break dormancy, increased chilling units reduces budburst threshold potentially meaning earlier budburst[67]<br>Does not grow well on limestone soils, prefers siliceous rock types[64,68]<br>Require good drainage[64,68]<br>Winter minimum temperature tolerance down to around -28°C[55] | [64] Fauve-Chamoux. (2011)<br>[65] Mirchev et al. (2009)<br>[66] Fernández-López et al. (2011)<br>[67] Chuine and Cour (1999)<br>[68] Gobet et al. (Gobet, Tinner et al. 2000)<br>[69] PFAF (PFAF 2009k) |

| Species | Main characteristics | References |
|---|---|---|
| **Juglans regia:**<br>Deciduous<br>Moderate growing<br><20m | Winter minimum temperature tolerance down to around -27°C[52]<br>Average temperature of 10-15°C and average winter temperatures above 2.5°C considered optimum.[70]<br>Below winter temperature of -4.4°C germination did not occur[70]<br>Spring temperature of >14°C is required for germination[71]<br>Precipitation over 310 mm required[52]<br>Can require 6-15 years growth to start fruiting[40]<br>Requires a deep, well drained loam soil and a sunny position[26] | [70] Loacker (Loacker, Kofler et al. 2007)<br>[71] Luza and Polito (Luza and Polito 1985) |
| **Vitis vinifera:**<br>Deciduous<br>Fast growing<br><15m | Temporary chilling injury below -10°C[72]<br>Winter minimum temperature tolerance down to around -20°C[26]<br>Budbreak requires average temperature over 8.7°C[72]<br>High spring temperatures (between 17-20°C)required for optimal flowering. Above this temperature fruit set is poor.[72]<br>Precipitation above 400mm required[73]<br>Prefers a deep rich moist but well drained soil[40]<br>Prefers calcareous soils[40] | [72] Jackson (Jackson 2008)<br>[73] Oliviera (Oliveira 1998) |
| **Fraxinus ornus:**<br>Deciduous<br>Fast growing<br><9m | Variable fruit production between years [74]<br>Once mature, hardy to -28°C [74]<br>Optimal precipitation is in the range 500-650mm[74]<br>A successful resprouter, resistant to grazing, wildfire and cutting[74]<br>Prefers a rich deep loam soil which is well drained.[40,74]<br>Is outcompeted by oak on non-disturbed land, but outcompetes oak on disturbed land[74] | [74] Fraxigen (Fraxigen 2005) |
| **Corylus avellana:** | No information available | |
| **Centaura solstitialis:**<br>Annual<br><1m | Drought tolerant, but quickly exploits wet years[75,76]<br>Found in areas with precipitation >250mm[76]<br>Tolerates dry, low fertility and alkaline soils[18]<br>Thorny and competitive, able to create inpenetrable stands[75]<br>Found on grasslands with deep well drained soils, cultivated soils, open woodlands, orchards, vinyards, roadsides and abandoned areas[76] | [75] DiTomasco (DiTomasco 2001)<br>[76] Wilson et al. (Wilson, Jette et al. 2003) |
| **Artemisia vulgaris:**<br>Perennial<br><1m | Vegetative growth occurs from early spring to late autumn[77]<br>Grows in dense stands[77]<br>Spreads quickly via extensive rhizone system[78]<br>Found on grasslands, cultivated soils, open woodlands, orchards, vinyards, roadsides and abandoned areas[77]<br>Contains allolochemicals which aid its spread[78] | [77] Barney and DiTommaso (2003)<br>[78] Barney, Hay et al. (Barney, Hay et al. 2005) |
| **Plantago lanceolata:**<br>Perennial<br><50cm | Succeeds in any moderately fertile soil that is not waterlogged[40,79]<br>Drought tolerant[79]<br>Considered signature species for cultivation having been found in old hayfields, pastures, lawns, farmyards, waste places and along roadsides[80] | [79] Moore (Moore 2011)<br>[80] Cavers et al. (Cavers, Bassett et al. 1980) |

The review found a multitude of environmental and biological parameters that differentiate species. These can be broken down into a number of areas. Firstly, environmental forcing factors, such as the effect of photoinhibition on photosynthetic apparatus, the effect of fire on plant structures, and the effect of precipitation, cold, frost and drought have important implications for plant processes. However, anthropogenically influenced forcing factors, such as the effect of clearcutting and grazing are also shown to be important. These factors have been shown to affect different species in different ways, with plants tending to show physiological differences, and behavioural strategies, depending on their provenance and the likelihood of such factors having been a common occurrance in their evolution. This results in different reactions to forcing factors such as drought, with some species being classed as drought avoiding, and others being classed as drought tolerating.

Where species have not adapted to these forcing factors adequately, species environmental ranges and thresholds can be identified. These thresholds have been shown not to be static, and depend on the provenance of the subspecies, as well as the life history of the particular plant. In a broad sense, however, certain parameters have been identified both in this brief description of prior knowledge, and in previous vegetation models, which can differentiate species by these environmental restrictions. Some of these pertinent parameters from an ecological and environmental perspective based on the information contained in Appendix 7 are shown in Table 6-4.

**Table 6-4 Common forcing factors, ecological parameters and environmental parameters.**

| Forcing factor | Ecological parameter | Environmental parameter |
|---|---|---|
| Cold winter temperatures | Winter minimum threshold, Cold tolerance, acclimation requirements | Absolute winter minimum temperature, Speed of temperature decrease, amount of chilling days, temperature seasonality |
| Spring frost | Frost tolerance, Deacclimation requirements, | Speed of temperature increase, date of first frost |
| Drought | Drought strategy, minimum precipitation requirement, seasonal precipitation requirement | Annual preciptiation, Seasonal precipitation, Aridity / humidity, Average temperature, minimum and maximum temperature, radiation intensity, temperature seasonality, precipitation seasonality |
| Photoinhibition | Tolerance of photoinhibition | Insolation / radiation intensity and duration, |
| Fire | Fire tolerance, Fire strategy | No. of fires, intensity of fires, peak temperature of fire |
| Natural Competition | Allelopathy, allometry, growth speed, | Light, Shade, land cover, |
| Anthropogenic influence | Grazing tolerance, Clearcutting tolerance, Coppicing tolerance, Timber quality, Forage quality | Amount and type of grazing, amount of deforestation. Topography, growing degree days |
| Edaphic | Soil type requirements, pH requirements, Drainage requirements, | Soil type, geology, pH, Drainage, |

### 6.1.2 **High resolution climate data**

The research questions introduced in Chapter 1 all have climatic aspects. These are summarised in Table 6-5. Furthermore, the potential bioclimatic indicators that would link vegetation to climate, and therefore link vegetation to the research questions, are also detailed, based on the information contained within Appendix 1, giving a theoretical basis for bioclimatic modelling.

**Table 6-5 Research question, potential climatic conditions, and potential bioclimatic indictors**

| Research quesion | Potential climatic conditions | Potential bioclimatic parameters |
|---|---|---|
| 1. Last Glacial Maximum conditions | Low Temperature<br>Low precipitation<br>Low evaporation<br>Unknown humidity / aridity balance, | Absolute minimum winter temperature.<br>Average seasonal temperatures<br>Amount of chilling days<br>Speed of seasonal cooling / warming<br>Seasonal precipitation<br>Potential Evaporation<br>Humidity / Aridity index<br>Topography, edaphic |
| 2. Early Holocene conditions | Warming average temperatures,<br>Increasing precipitation,<br>Potentially cold winters, increasing insolation in summer, reduced in winter. | Absolute minimum winter temperature<br>Average seasonal temperature<br>Amount of chilling days<br>Speed of seasonal cooling / warming<br>Amount of Growing Degree Days<br>Insolation / radiation<br>Seasonal precipitation<br>Topography, edaphic |
| 3. Late Holocene conditions: Beysehir Occuption Phase | Climate similar to modern.<br>Potentially more precipitation and temperature, some potential for periods with cold winters. | Absolute minimum winter temperature<br>Maximum temperature<br>Average seasonal temperature<br>Amount of chilling days<br>Speed of seasonal cooling / warming<br>Amount of Growing Degree Days<br>Insolation / radiation<br>Seasonal precipitation<br>Aridity / humidity<br>Topography, edaphic |

It was acknowledged that other vegetation affecting parameters such as fire, grazing and deforestation are extremely important in certain periods. However, the inclusion of these parameters into the model was deemed to create too much complexity and be too intractable. It is instead recommended that these factors are considered as further layers of analysis after the bioclimatic vegetation model created in this thesis. The most straightforward variables known to affect vegetation range are precipitation and temperature. Further to this, humidity, aridity, chilling and growing degree days, speed of acclimation / deacclimation, evaporation and insolation measures are noted as potentially important factors. The remainder of this section therefore assesses the amount of Geospatial data available to define these bioclimatic ranges under modern and palaeoclimatic conditions.

#### 6.1.2.1 Temperature and Precipitation

A relatively large range of geospatial precipitation and temperature products are now available, however data is incredibly variable in quality and transparency, as well as spatial and temporal resolution. Traditional methods of precipitation and temperature mapping use meteorological station data, with some kind of spatial averaging or interpolation between stations. However, interpolated products from meteorological station data alone can only offer moderate resolution. Recent products generally map parameters at resolutions of 0.5°, possibly 0.25° (GPCC 2009) and do not capture the potentially high variability of precipitation between stations. If comparing with 1 km resolution species distribution data, large uncertainties and loss of precision is likely.

Over recent years, the development of sophisticated, high resolution visual and radar sensors (such as GOES 11 and 12, DMSP SSM/I, NOAA AMSU, TRMM and AMSR-E) has allowed High Resolution Precipitation Products (HRPP) from satellite are becoming a consistent, reliable source of data. Recent methodologies include the Climate Prediction Center Morphing Method (CMORPH), the Precipitation Estimation from Remotely Sensed Information using Artificial Neural Networks (PERSIANN), TRMM Multi-satellite Precipitation Analysis (TMPA), and the National Research Laboratory (NRL) blended precipitation dataset (NRL-blended), which can all produce products at 0.25° resolution (Sohn, H. et al. 2010). However, two main disadvantages are considered with these datasets. The first is in terms of data accuracy. Providing that adequate meteorological gauge data is available within the study area, Shen et al. (2010) still considers ground-based observations as the most accurate reflection of precipitation received at the ground, although that is not to say that meteorological stations do not have their own biases and inaccuracies. The second consideration is much harder to counter however, as for the methodology intended, the temporal extent of the data is important, and is undoubtedly much greater in meteorological gauge data than satellite measurements. Good quality satellite based climate product archives are often not yet more than 10 years old, however, the World Meteorological Organisation suggest that at least 30 years worth of data should be considered to gain a robust output from statistical analyses.

Only one climatic product addressed both the temporal and spatial requirements of the methodology, as well as having both precipitation and temperature climate layers. The WorldClim climate layers are calculated based on 50 years of data from 1950-2000, exceeding the WMOs requirements. The precipitation product is based on an interpolation of average monthly climate data from weather stations on a 30 arc-second resolution (2005). The climate database was compiled from a number of organisations, including the Global Historical Climatology Network (GHCN), the FAO and the WMO. These were interpolated using a spline interpolator, with SRTM elevation data, latitude and longitude as independent variables. This led to a 1km resolution precipitation product, and a 1km mean, min and max temperature product. For more information on the general methodology, consult Hijmans et al. (2005). For more information on the interpolation method, consult Hutchinson (1995).

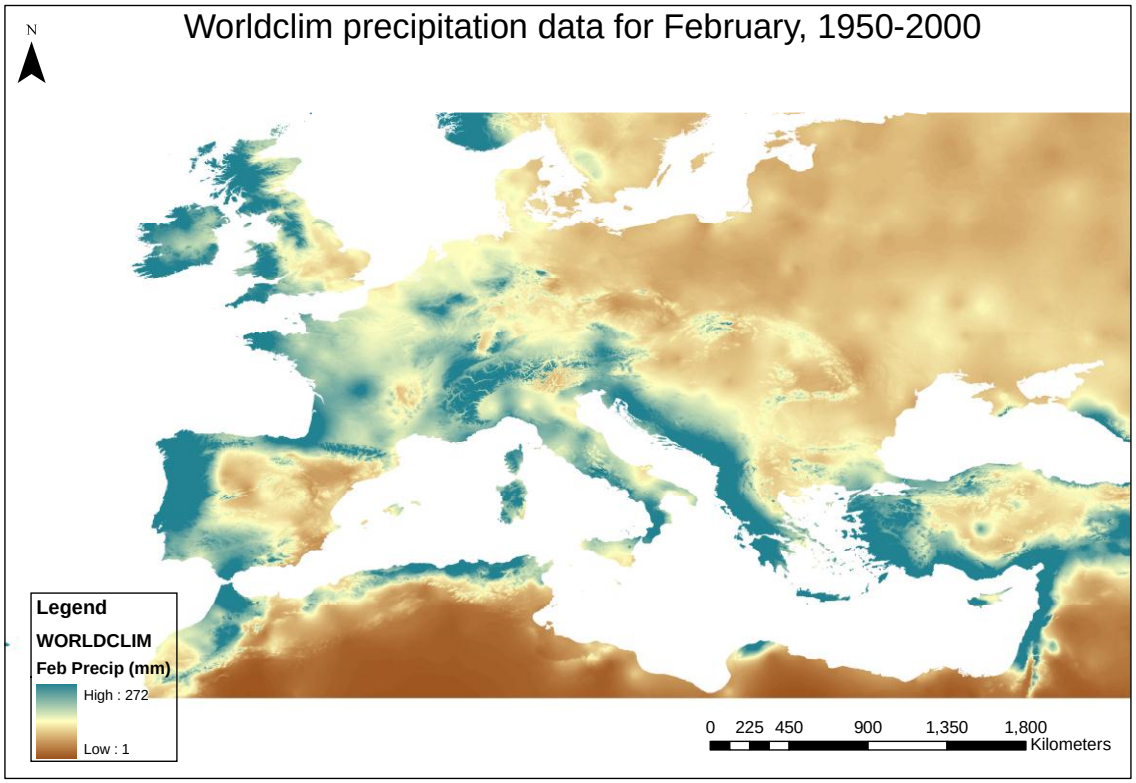


**Figure 6-4 Worldclim monthly precipitation data (February), 1950-2000**

As well as monthly precipitation and temperature data, bioclimatic variables were also available from WorldClim. This further provided Annual Mean Temperature, Annual precipitation, Maximum temperature of the Warmest Month, Minimum Temperature of the Coldest Month, Temperature Seasonality and Precipitation Seasonality. An 'Area of Steppe' variable was also defined by thresholding the annual precipitation product at <400 mm and <300 mm, and which has been identified in previous literature as the estimated boundary for the transition into montane-steppe, and true-steppe respectively (Wang 1988)

### 6.1.2.2 Absolute winter minimum temperature

Winter Minimum Temperature has been identified as a potentially important parameter to engage with research questions in this thesis. The product was not available through WorldClim data, and in fact, no high resolution products were available for the whole of Europe. However, absolute winter minimum temperature was available for 7 meteorological stations in Turkey (Van, Siva, Rize, Kastamonou, Istanbul, Isparta and Finike), from GHCN data (NCDC 2010). In order to gain an estimate of winter minimum temperature, these points were regressed against the average winter temperature dataset as shown in Figure 6-5, which gave a relatively linear response with $R^2$=0.84, a t value of 5.09 and a p value of 0.0038. The standard deviation is +/- 2.91°C and the standard error is +/- 2.72°C.

There are a number of points to note. Firstly, that there is some variation in the relationship, reflected in the standard deviation and standard error. This will have to be taken into account if potential winter minimum temperature and its impact on vegetation is modelled. The second point to note is that there are not many areas in southwest Turkey that have an absolute winter

minimum temperature under -10 °C based on the 30-year reference period. This means that the lower temperature range is less well constrained. The relationship was mapped across the whole of Turkey as shown in Figure 6-6 these low winter temperature areas are seen to be restricted to areas of high elevation.

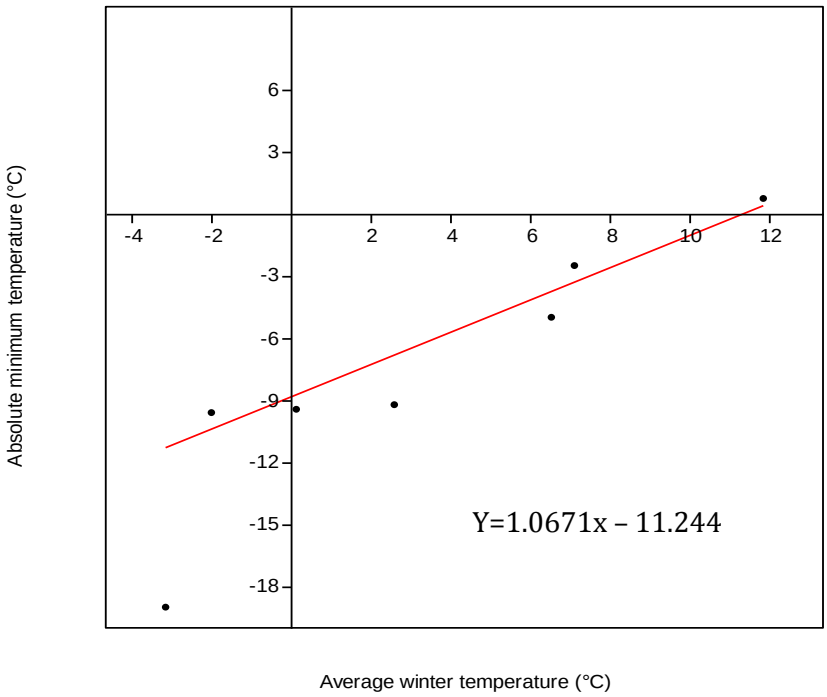


**Figure 6-5** The relationship between average winter temperatures and absolute minimum temperatures through Turkey

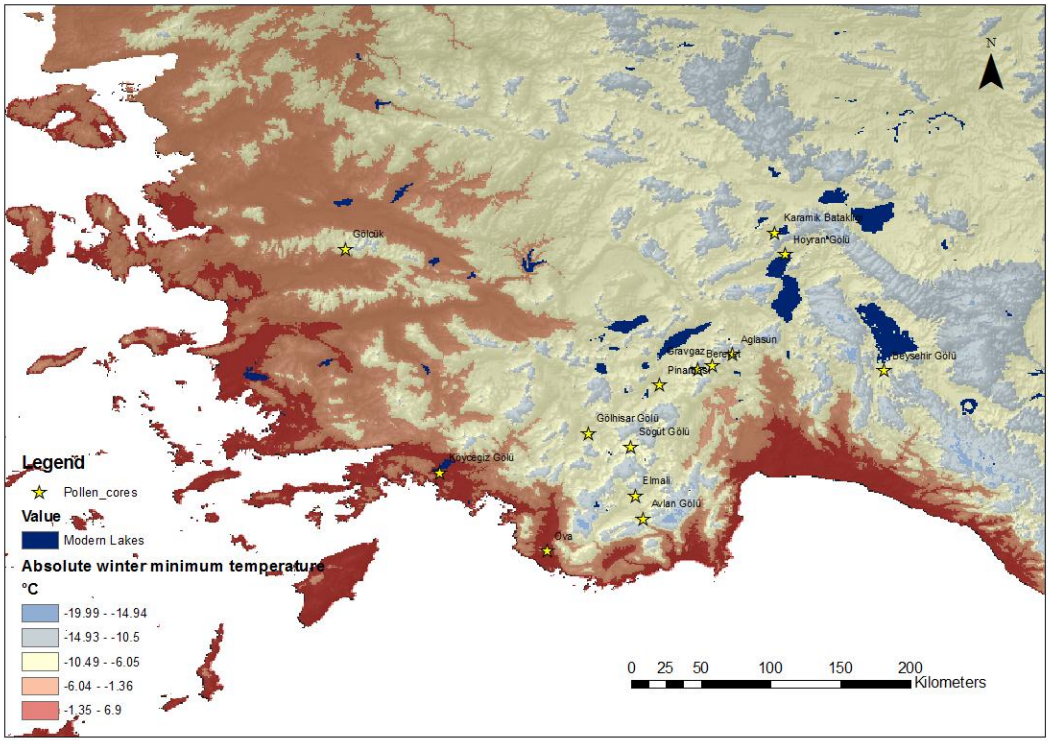


**Figure 6-6 Modelled absolute winter minimum temperature mapped across southwest Turkey**

### 6.1.2.3 Vegetation winter temperature limits

Species limits for winter temperature were based on previous literature sources outlined in Appendix 1. By thresholding the temperature map produced above by estimated species tolerance, it is possible to identify the relative reaction of species to scenarios of decreased winter temperature

Table 6-6 Species Absolute Winter Temperature Limits

| Species | Minimum absolute winter temperature (°C) | Species | Minimum absolute winter temperature (°C) |
|---|---|---|---|
| *Olea europeae* | -10 | *Ulmus glabra* | -28 |
| *Pinus brutia* | -12 | *Pinus nigra* | -30 |
| *Platanus* | -17 | *Cedrus libani* | -30 |
| *Juniperus oxycedrus* | -18 | *Corylus avellana* | -34 |
| *Vitis vinifera* | -20 | *Abies alba* | -34 |
| *Quercus coccifera* | -27 | *Hordeum vulgare* | -34 |
| *Quercus cerris* | -23 | *Picea* | -35 |
| *Plantago lanceolata* | -23 | *Secale cereale* | -40 |
| *Juglans regia* | -27 | *Artemisia vulgaris* | -40 |
| *Carpinus betulus* | -28 | *Tilia cordata* | -40 |
| *Fraxinus ornus* | -28 | *Betula pendula* | -45 |
| *Castanea sativa* | -28 | *Populus nigra* | -45 |
| *Fagus sylvatica* | -28 | | |

### 6.1.2.4 Evaporation, aridity and humidity

Further derived climate products utilising Worldclim data were available from the Consultative Group on International Agricultural Research (Zomer, Trabucco et al. 2007; Zomer, Trabucco et al. 2008; CGIAR 2010). Aridity and humidity were identified as a key model parameter to engage with the research questions of the thesis. The CGIAR provide a 1 km resolution Aridity Index (AI) dataset. This is calculated as shown in Equation 1.

$$AI = MAP/MAE$$

**Equation 1 Aridity Index**

Where MAP is Mean Annual Precipitation and MAE is the Mean Annual Potential EvapoTranspiration.

Mean Annual Precipitation is gained directly from WorldClim, whereas Potential Evapotranspiration (PET), which is a measure of the ability of the atmosphere to remove water through evapo-transpiration processes, is calculated as shown in Equation 2 (CGIAR 2007). This method follows the Hargreaves model (Hargreaves, Hargreaves et al. 1985)

$$PET = 0.0023 * RA * (Tmean + 17.8) * TD^{0.5} (mm / month)$$

**Equation 2 Potential Evapotranspiration**

Where RA is radiation at the top of the atmosphere, expressed in mm/month as equivalent of evaporation. Tmean is mean monthly temperature (°C), TD is daily temperature range, calculated as the difference between average monthly maximum and minimum temperature. TD is an effective proxy to describe the effect of cloud cover on the quantity of extra-terrestrial radiation reaching the land surface (CGIAR 2007). RA is available as a monthly product from CGIAR. Average, minimum and maximum monthly temperature inputs use the WorldClim datasets. The availability of all the components for the Aridity Index will potentially be useful to the model, as it will allow the alteration of aridity through changes in precipitation, temperature, or incoming radiation.

#### 6.1.2.5 Growing Degree Days, Chilling Days and Speed of Acclimation / Deacclimation

It was decided that Growing Degree Days, Chilling Days and Speed of Acclimation / Deacclimation would not be included in the analysis. This was done for three reasons. Firstly, no high resolution GDD or Chilling day products were available. To create these products and acclimation / deacclimation statistics would require large amounts of daily climatological data across Europe and a methodology similar to the Worldclim methodology. This was deemed out of the scope of the project. Secondly, no consistent *a priori* information was available on species Growing Degree thresholds, Chilling Days and species acclimation / deacclimation processes. Thirdly, palaeoclimatological information on these parameters is sparse at best, and so the inclusion of these parameters was deemed over-parameteristion for something that is poorly constrained.

### 6.1.3 High resolution topographic and edaphic data

Soil type, geology and topography have been found to be an important influence on vegetation growth (Tansley 1920; Gleason 1926). As such, this data will be included in the multivariate model. For consistency, the edaphic and topographic data will be required to match the vegetation distribution data of 1 $km^2$. SRTM topographic data is the closest consistent data source which will be used for this.

Unfortunately, bedrock type was not available in GIS form for the whole of Europe (Specifically Turkey was not available), and so soil type data was utilized instead. It is acknowledged that this is a potential limitation of the model, as soil types may have changed over the course of the Holocene, however, broad soil types are found to relate to the underlying geology in southwest Turkey, and it was considered better than not including any edaphic or geological information in the model. It is also possible that as and when digital geology data is available, it can be incorporated into the model instead.

Soil data was available from the Harmonised World Soil Database (HWSD) v 1.1 (FAO/IIASA/ISRIC/ISSCAS/JRC 2009). The data is in 30 arc second raster format, with over 16000 different soil mapping units that combines existing regional and national updates of soil information worldwide (including SOTER, the European Soil Bureau Network, Soil map of China and the World Inventory of Soil Emissions). The reliability of the data over Europe is assessed as being the highest of all of the entries in the database. Although many soil parameters are available in the database (i.e. organic carbon, pH, water storage capacity, soil depth etc.), five

pertinent attributes were examined, in order to attain relatively parsimonious further analysis. These were the major soil mapping unit (SMU), water storage capacity, texture, percent organic carbon, and pH.

# 7 APPENDIX: SAMPLING

In order to compare statistically whether a species is found in a particular climate envelope, or a particular soil type, it is useful to compare the environmental distribution of where a species is found, to where it is not found, and see if the two are statistically different. However, the difficulty lies in defining the two cases. The JRC data mapped species proportion within forest areas across Europe. These proportions were changed into simpler presence and absence of each species. If species presence is recorded, we can be fairly confident of this. But species absence may refer to actual absence, absence of sampling, or absence of recording. Actual absence is likely in most cases. Absence of sampling is broadly covered in this dataset by the 'not classified' areas in the map, and water bodies, which can be easily masked from analysis. However, absence of recording is more difficult. In this case it may refer to trees that exist outside of forests – a fairly large number, but are instead classified under the catch all classes of agricultural land or urban areas. Furthermore, it is important to note that the distribution of some species considered markers for cultivation (such as *Castanea Sativa* and *Juglans regia*) considered their distribution only in forests and were not singled out in agricultural areas, whereas other such as *Olea europeae* and *Vitis vinifera* were mapped throughout their range. Forest is generally restricted or absent in valleys due to climatic, edaphic or agricultural reasons, most likely a mixture of all of these factors in combination.

The first assumption then, is that samples will be a representative distribution of the species, but it will not be composed of the whole population. The second assumption is that species populate areas where climatic and edaphic attributes are favourable, and the third that the broad scale distribution of species adequately represents their climatic envelopes.

It was decided to take samples throughout Europe to examine the difference in environmental conditions between sample sets of individual species, and biomes (sclerophyllous, shrub areas and grassland), remembering that (a) samples should represent a significant distribution of the species, but it will not be composed of the whole population, and (b) that differences in environmental envelopes may not only be climate related, but also cultural or edaphic and so simple bivariate correlations cannot be considered definitive.

### 7.1.1 Sampling methodology

1. JRC species distribution data was imported into ArcGIS software package. For each species, the proportion data was reclassified into species presence and absence rasters.

2. Secondly, sampling was undertaken within these rasters using the Spatial Ecology Hawth's Analysis Tools plugin (www.spatialecology.com). Within this toolset is a 'generate random points' tool which was used to generate random points within both classes.

3. Species presence data was fairly small in area compared to species absence (i.e. presence data was 'rare' compared to absence data). Therefore, in order to gain a representative selection, sampling on the dependent variable is undertaken, otherwise known as a case-controlled methodology. This requires taking a larger sample of the

rare event than is proportionally realistic (King and Zeng 2001). To this end, an endogenous stratified sample of species presence and absence was undertaken across Europe.

4. The amount of sample points required was then calculated. The whole area of Europe under investigation was ~8,155,642 km$^2$. For an unknown population of species presence, only a small subset of samples is required for statistical robustness. An appropriate sample size was calculated using two methods, one for an unknown population (Equation 3), and one assuming the population is known, in which case a finite population correction is used (Equation 4).

$$n = \frac{z^2 p(1-p)}{c^2}$$

**Equation 3**

$$n_2 = \frac{n}{1 + \frac{n-1}{N}}$$

**Equation 4**
After Israel (1992)

Where *n* is the sample size, *N* is the population size, Z is the critical value of the chosen confidence interval, also known as the alpha level (1.96 for a 95% confidence level), *c* is the confidence interval, expressed as a decimal (set to 0.01) and *p* is the probability of incorrectly failing to reject the null hypothesis that there is no difference in the average values, otherwise known as the beta value. This was set to 50% (0.5).

For statistics to be calculated with 95% accuracy at a 1% margin of error requires a minimum sample size (*n*) of 9604 for an unknown population (at 1km$^2$ resolution, equal to 9604 pixels). The area of known species presence for key species was entered into Equation 4, which led to various values between 8000-9000 samples. To cover both situations, a sample of 10 000 randomised points were created throughout the olive distribution area. A further dataset of 10 000 randomised points was extracted from the rest of Europe (including non forested areas, but excluding no-data areas and water bodies) to act as a control dataset. An example of the random point dataset created is shown in Figure 7-1.

5. Once the points were extracted, Worldclim monthly temperature (averages) and precipitation data were downloaded for tiles 15-17. Data was converted from binary files to ESRI ASCII files for use within ArcGIS using DIVA-GIS import and export facility. Once imported into ArcGIS they were converted into a continuous mosaic for further analysis.

6. Bioclimatic data (precipitation and temperature seasonality, average minimum and maximum temperature) were downloaded and calibrated.

7. SRTM topographic data was downloaded for the area, and slope and aspect were calculated.

8. Harmonised Soil Database data was converted to raster data. Soil type, Available water content, drainage, organic carbon and pH data were extracted.

9. CGIAR aridity and insolation data were downloaded. Aridity data was calibrated, and taken forward for modelling.

10. All data was transformed to a common projected co-ordinate system, Lambert Equal Area Conformal Conic.

11. The points were then intersected with WorldClim precipitation and temperature data, Bioclimatic data, SRTM topography and soil data, adding attributes to each point, which could be further analysed statistically. As there were some differences in pixel alignment between different data sources, some points ended up with no-data values for some layers, due to being placed on the edge of land on one layer, and being classified as 'sea' in another. These points were excluded from the analysis, leaving just under 10 000 pixels for each species, but still more than the 9604 to remain robust. The amount of presence and absence points available after clipping points that fell just outside of the environmental data is shown in Table 7-1

12. The final geospatial database attached to each species shapefile contained the parameters in Table 7-2.

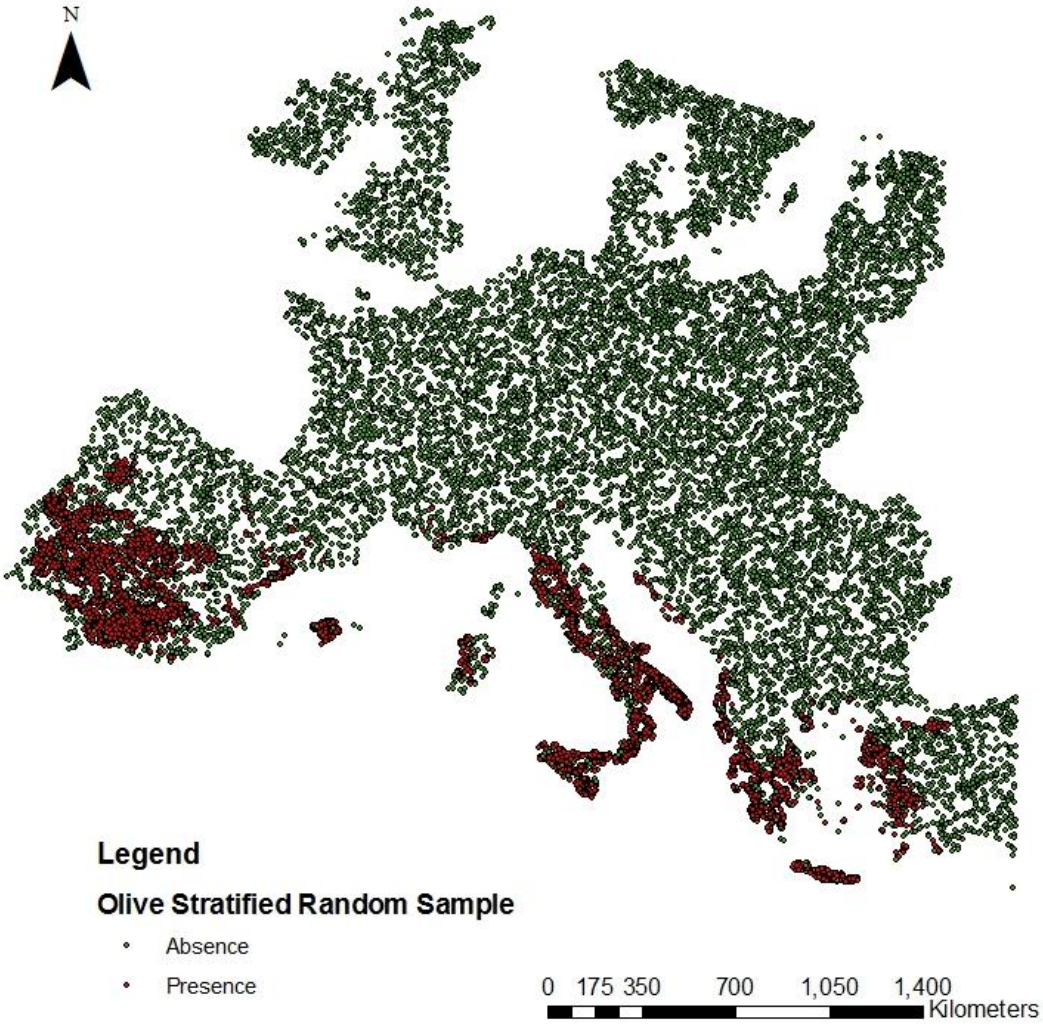


**Figure 7-1 Example of species random stratified sample**

**Table 7-1 Sample count for species presence and absence**

| Species | Species present sample | Species negative control |
|---|---|---|
| *Quercus cerris* | 12462 | 13594 |
| *Quercus coccifera* | 13706 | 11946 |
| *Pinus brutia* | 13288 | 13512 |
| *Pinus nigra* | 14918 | 11077 |
| *Betula pendula* | 10271 | 13312 |
| *Olea europeae* | 13514 | 14537 |
| *Cedrus libani* | 11356 | 14547 |
| *Castanea sativa* | 13045 | 13989 |
| *Fraxinus ornus* | 13295 | 13737 |
| *Juglans regia* | 13135 | 13977 |
| *Vitis vinifera* | 13560 | 16409 |
| *Carpinus betulus* | 14993 | 12109 |
| *Platanus orientalis* | 13302 | 13682 |
| *Fagus sylvatica* | 14973 | 11861 |
| *Picea abies* | 9700 | 13729 |
| *Alnus cordata* | 13401 | 13724 |
| *Abies alba* | 13380 | 13539 |
| *Ulmus glabra* | 13598 | 13488 |
| *Corylus avellana* | 13256 | 13853 |
| Dry agriculture | 14602 | 11138 |
| Sclerophyllous | 14426 | 12090 |
| Shrubland | 14250 | 13742 |
| Grassland | 13980 | 14652 |

**Table 7-2 Final species parameters**

| Variable name | Description | Data type |
|---|---|---|
| Dependent variable | | |
| PRES_AB | Species presence or absence | Binary |
| Climatic variables | | |
| TAV_AU | Average autumn temperature | Interval scale (°C ) |
| TAV_SP | Average spring temperature | Interval scale (°C ) |
| TAV_SU | Average summer temperature | Interval scale (°C ) |
| TAV_WI | Average winter temperature | Interval scale (°C ) |
| TMIN | Average minimum of the coldest month | Interval scale (°C ) |
| TMAX | Average maximum temperature of the warmest month | Interval scale (°C ) |
| PREC_WI | Sum winter precipitation | Interval scale (mm) |
| PREC_SP | Sum spring precipitation | Interval scale (mm) |
| PREC_SU | Sum summer precipitation | Interval scale (mm) |
| PREC_AU | Sum autumn precipitation | Interval scale (mm) |
| AI_CAL | Aridity index value | Interval scale (0-1) |
| Edaphic variables | | |
| SU_Code | Soil mapping unit | Nominal |
| Texture | Soil texture (fine, med, coarse) | Ordinal (0-3) |
| Drainage | Drainage class | Ordinal (0-5) |
| pH | pH class | Ratio scale |
| OC | Organic carbon soil content | Interval scale |
| AWC | Soil water content | Interval scale |
| Topographic variables | | |
| SRTM | SRTM elevation | Interval scale (metres) |
| SLOPE | Slope angle | Interval scale (degrees) |
| Aspect | Aspect | Ordinal |

# 8 APPENDIX TEST STATISTICS COMPARING VARIABLES OF SPECIES DISTRIBUTION WITH THE EUROPEAN CONTROL DATASET

## 8.1 PRECHECK: VARIABLE SKEWNESS AND KURTOSIS

Using a value of 0.2 (Wuensch 2011) as a threshold for great skewness, most variables are found to be significantly skewed. Both presence and absence variables were run through a Kolmogorov-Smirnoff test, which resulted in all null hypotheses (that the distribution was normal) being rejected at the 95% confidence level. In order to check whether this was likely for the whole population as well as the sample, the standard error of skewness (SES) and kurtosis (SEK) was calculated (Equation 5 and Equation 6 respectively). The sample skewness divided by the SES gains the test statistic. For a two tailed test at the 0.05 significance level, all variables are over the critical value of 2 (or -2), which shows that it is very likely that the unknown population is skewed. This is also the case with both presence and absence distributions. The sample skewness divided by the SEK to gain the second test statistic. Variables are again over the critical value of 2 (or -2) suggesting that the unknown population is also likely to show strong kurtosis. This has important implications for further analysis, as certain tests, such as ANalysis Of VAriance, for instance, cannot be undertaken on non-normally distributed data.

**Equation 5 Standard error of Skewness**

$$SES = \sqrt{\frac{(6n)(n-1)}{(n-2)(n+1)(n+3)}}$$

$$Z_{g1} = \frac{g_1}{SES}$$

**Equation 6 Standard error of Kurtosis**

$$SEK = 2(SES)\sqrt{\frac{n^2-1}{(n-3)(n+5)}}$$

$$Z_{g2} = \frac{g_2}{SEK}$$

after Cramer (1997)

## 8.2 STATISTICAL TESTS TO COMPARE DISTRIBUTIONS

In order to choose the correct statistical tests to compare distributions, the characteristics of the data were tabulated as shown in Table 4.

Table 11, then each statistical test was considered to see if the assumptions of the test were met, as shown in Table 4.

**Table 11 Summary of data characteristics**

| Parameter | Characteristic |
|---|---|
| Distribution | Non-normally distributed |
| Scale | Generally equal interval scale apart from pH |
| Sample dependence | Independent, randomly drawn |
| Data type | Mixture of nominal, ordinal and continuous |
| Parametric or non-parametric | Non-parametric |

Three statistical tests were appropriate to compare the presence and absence of species. The Comparison of Medians test firstly compared only the medians of the distributions. Then the Mann-Witney two sample rank-sum test compared the distributions by examining the central tendency. Thirdly, the Moses Extreme Reaction test was able to compare the range of present and absent samples by examining the change in the tails of the distribution.

Each variable from each species dataset was compared with its equivalent control point file based on values from the rest of Europe. All statistics were calculated on raw data, as opposed to log transformed values. The SPSS 'independent samples' nonparametric test was used to calculate these statistics.

**Table 4 Statistical test summary to assess applicability**

| Test | Tests | Assumptions | Assumptions met? |
|---|---|---|---|
| **ANOVA** | Compares variance | (1) Independent samples<br>(2) Continuous<br>(3) Normal distribution<br>(4) Two or more samples<br>(5) Homoscedasticity | No (not normally distributed) |
| **Kolmogorov-Smirnoff** | Compares shape of distribution (observed cumulative differences) | (1) Independent samples<br>(2) 1 sample | Yes to test skewness significance for one sample, not to compare across groups |
| **Mann Whitney** | Compares distributions using ranks (change in median / central tendency) | (1) Independent samples<br>(2) Ordinal or continuous<br>(3) Normal or non-normal<br>(4) Two samples | Yes – apart from nominal variables |
| **Kruskal Wallis** | Compares variance using ranks | (1) Independent samples<br>(2) Ordinal or continuous<br>(3) Normal or non-normal<br>(4) More than two samples<br>(5) unordered samples | No (only two samples) |
| **Jonckheere-Terpstra for k samples** | Compares distributions using ordered differences | (1) Independent samples<br>(2) Nominal, ordinal or continuous<br>(3) more than two samples<br>(4) ordered samples | No, (only two samples) |
| **Wald Wolfowitz for 2 samples** | Tests whether a series of numbers is random | (1) independent samples<br>(2) sample is recorded in order of occurrence<br>(3) observations are categorized into two distinct types | No (not recorded in order of occurrence) |
| **Moses Extreme Reaction test (MTER)** | Compares ranges across groups (change in tails) | (1) Independent samples<br>(2) two samples<br>(3) ordinal or continuous | Yes |
| **Comparison of medians** | Compares medians | (1) Independent samples<br>(2) Two or more samples | Yes |
| **Cramer's phi** | Intercorrelation | (1) Independent samples<br>(2) Nominal or higher | Yes |

## 8.3 COMPARISON OF MEDIANS

The null hypothesis for the comparison of medians test is that data in the two distributions are independent samples with significantly similar medians. The test used the pooled sample median, and comparisons were done in a pairwise manner (as opposed to stepwise step-down).

**Null hypothesis H0**. The median value of variable x within species y areas is not significantly different to the rest of Europe.

**Alternative hypothesis H1**. The median value of variable x in species y areas is significantly different to the rest of Europe.

## 8.4 COMPARISON OF DISTRIBUTIONS

The null hypothesis for the Mann-Whitney test is that data in the two distributions are independent samples from significantly similar continuous distributions with equal medians. The alternative is that they do not have significantly similar continuous distributions with equal medians. The sampling distribution for large samples is approximately normal with mean and standard deviations calculated as in Equation 7 and Equation 8. The $z$ statistic measures the significance of the result, and in the case of a large sample such as this, is compared to normal significance levels. $U$ is the Wilcoxon - Mann-Whitney test result, calculated as in Equation 10.

**Null hypothesis $H_0$.** The distribution of variable x within species y areas is not significantly different to the rest of Europe.

**Alternative hypothesis $H_1$** . The distribution of variable x in species y areas is significantly different to the rest of Europe.

$$\mu_U = \frac{n_1 n_2}{2}$$

**Equation 7**

$$\sigma_U = \sqrt{\frac{n_1 n_2 (n_1 + n_2 + 1)}{12}}$$

**Equation 8**

$$z = \frac{U - \mu_U}{\sigma_U}$$

**Equation 9**

$$U = n_1 n_2 + \frac{n_1(n_1 + 1)}{2} - \sum_{i=n_1+1}^{n_2} R_i$$

**Equation 10**

after Statistics Solutions (2009)

where $n_1$ is the sample size for olive distribution, $n_2$ is the sample size for Europe precipitation distribution, $U$ is the Mann-Kendall statistics, z is the z score and $R_i$ is the rank of the sample

size. For more information on the calculation of the Mann-Whitney statistic, consult Gibbons (1985) and Hollander and Wolfe (1999).

The significance level is chosen as 0.05. Comparing this to the *p* value, all seasons are below this critical value, and the null hypothesis can therefore be rejected at the 5% significance level, stating that seasonal precipitation distribution is significantly different to the rest of Europe.

## 8.5 COMPARISON OF RANGE (MTER)

The null hypothesis for MTER is that the range of the two distributions is significantly similar. The alternative hypothesis is that the range of the two distributions is not significantly similar. Outliers were computed from sample data as opposed to a specified number of outliers.

**Null hypothesis $H_0$.** The range of variable x within species y areas is not significantly different to the rest of Europe.

**Alternative hypothesis $H_1$** . The range of variable x in species y areas is significantly different to the rest of Europe.

## 8.6 COMPARISON OF CATEGORICAL DATA (CRAMER'S PHI)

The null hypothesis for Cramer's phi is that there is no association between the two categorical variables. The alternative hypothesis is that there is a degree of association between two categorical variables (ClinTools 2005).

$$\phi_c \sqrt{\frac{\chi^2}{N\,(k\,-\,1)}}$$

Where N = Total number of subjects and K = the smaller of the number of rows or columns.

**Null hypothesis $H_0$.** No association between two categorical variables

**Alternative hypothesis $H_1$** . Association between two categorical variables.

**Table 13 List of variables entered into each statistical test**

| Medians | MW (Distribution) | MTER (Ranges) | Cramer's phi |
|---|---|---|---|
| Summer precipitation | Summer precipitation | Summer precipitation | pH |
| Autumn precipitation | Autumn precipitation | Autumn precipitation | Aspect |
| Winter precipitation | Winter precipitation | Winter precipitation | Soil type |
| Spring precipitation | Spring precipitation | Spring precipitation | Soil drainage class |
| Summer average temperature | Summer average temperature | Summer average temperature | Soil texture class |
| Autumn average temperature | Autumn average temperature | Autumn average temperature | |
| Winter average temperature | Winter average temperature | Winter average temperature | |
| Spring average temperature | Spring average temperature | Spring average temperature | |
| Average minimum temperature | Average minimum temperature | Average minimum temperature | |
| Average maximum temperature | Average maximum temperature | Average maximum temperature | |
| Elevation | Elevation | Elevation | |
| Slope angle | Slope angle | Slope angle | |
| Aridity | Aridity | Aridity | |
| Temperature seasonality | Temperature seasonality | Temperature seasonality | |
| Precipitation seasonality | Precipitation seasonality | Precipitation seasonality | |

## 8.7 RESULTS

**Table 14 Results of statistical tests for all species**

| Species | Sig. | Median | Mann Whitney | MTER | Cramer |
|---|---|---|---|---|---|
| Pinus brutia | 0.05 | Reject $H_0$ | Reject $H_0$ | Partially Accept $H_0$ | Accept $H_0$ |
| Quercus cerris | 0.05 | Reject $H_0$ | Reject $H_0$ | Partially Accept $H_0$ | Accept $H_0$ |
| Quercus coccifera | 0.05 | Reject $H_0$ | Reject $H_0$ | Partially Accept $H_0$ | Accept $H_0$ |
| Betula pendula | 0.05 | Reject $H_0$ | Partially accept (p_seas 0.106) | Partially Accept $H_0$ | Accept $H_0$ |
| Castanea sativa | 0.05 | Reject $H_0$ | Reject $H_0$ | Partially Accept $H_0$ | Accept $H_0$ |
| Cedrus libani | 0.05 | Reject $H_0$ | Reject $H_0$ | Reject $H_0$ | Accept $H_0$ |
| Fraxinus ornus | 0.05 | Reject $H_0$ | Partially accept for (or_carb 0.878) | Partially Accept $H_0$ | Accept $H_0$ |
| Juglans regia | 0.05 | Partially accept for (t_seas 0.251) | Reject $H_0$ | Partially Accept $H_0$ | Accept $H_0$ |
| Olea europeae | 0.05 | Reject $H_0$ | Reject $H_0$ | Partially Accept $H_0$ | Accept $H_0$ |
| Pinus nigra | 0.05 | Reject $H_0$ | Reject $H_0$ | Partially Accept $H_0$ | Accept $H_0$ |
| Vitis vinifera | 0.05 | Partially accept (slope 0.267) | Reject $H_0$ | Partially Accept $H_0$ | Accept $H_0$ |
| Juniperus | 0.05 | Partially accept (p_seas) | Partially accept (Prec_sp 0.074) | Partially accept $H_0$ | Accept $H_0$ |
| Alnus | 0.5 | Reject $H_0$ | Accept (pH) $H_0$ | Partially accept $H_0$ | Accept $H_0$ |
| Abies | 0.5 | Reject $H_0$ | Reject $H_0$ | Partially accept $H_0$ | Accept $H_0$ |
| Carpinus betulus | 0.5 | Partially accept (ai_cal, av_aut, prec_win) | Partially accept (pH 0.692) | Partially accept $H_0$ | Accept $H_0$ |
| Corylus avellana | 0.5 | Reject | Reject $H_0$ | Partially accept $H_0$ | Accept $H_0$ |
| Fagus | 0.5 | Partially accept (t_seas) | Partially accept (t_seas) | Partially accept $H_0$ | Accept $H_0$ |
| Platanus | 0.5 | Reject $H_0$ | Partially accept (spring precip) | Partially accept $H_0$ | Accept $H_0$ |

| | | | | | |
|---|---|---|---|---|---|
| Populus | 0.5 | Partially accept (spring precip, autumn precip, av_win) | Partially accept (autumn precip, av_aut) | Partially accept $H_0$ | Accept $H_0$ |
| Ulmus | 0.5 | Reject $H_0$ | Reject $H_0$ | Partially accept $H_0$ | Accept $H_0$ |
| Tilia | 0.5 | Partially accept (ph, av_spr) | Partially accept (ph, organic carbon) | Partially accept $H_0$ | Accept $H_0$ |
| Sclerophyll | 0.5 | Reject $H_0$ | Partially accept (prec_sp) | Partially accept $H_0$ | Accept $H_0$ |
| Shrubland | 0.5 | Partially accept (ai_cal) | Partially accept (av_win, av_aut) | Partially accept $H_0$ | Accept $H_0$ |
| Grassland | 0.5 | Reject $H_0$ | Partially accept (prec_sp) | Partially accept $H_0$ | Accept $H_0$ |

**Table 15 MTER results for each species. Zero = reject $H_0$.**

| MTER | pH | or_car | elevation | slope | spr_prec | aut_prec | win_prec | sum_prec | av_win | av_spr | av_sum | av_aut | aridity | t_seas | p_seas | tmin | tmax |
|---|---|---|---|---|---|---|---|---|---|---|---|---|---|---|---|---|---|
| Brutia | 0 | 1 | 1 | 0 | 1 | 1 | 0 | 0 | 1 | 0 | 0 | 0 | 1 | 1 | 0 | 1 | 0 |
| Cerris | 1 | 1 | 1 | 0 | 0 | 1 | 1 | 1 | 1 | 1 | 1 | 1 | 1 | 1 | 1 | 1 | 1 |
| Coccifera | 1 | 1 | 0 | 0 | 1 | 0 | 0 | 0 | 1 | 0 | 0 | 0 | 1 | 0 | 0 | 1 | 0 |
| Betula | 0 | 0 | 1 | 1 | 0 | 1 | 1 | 1 | 0 | 1 | 0 | 1 | 0 | 0 | 1 | 0 | 1 |
| Castanea | 1 | 1 | 0 | 0 | 0 | 1 | 1 | 0 | 1 | 1 | 1 | 0 | 1 | 1 | 0 | 1 | 1 |
| Cedrus | 0 | 0 | 0 | 0 | 0 | 0 | 0 | 0 | 0 | 0 | 0 | 0 | 0 | 0 | 0 | 0 | 0 |
| Fraxinus | 1 | 1 | 1 | 0 | 0 | 0 | 1 | 0 | 0 | 1 | 0 | 1 | 1 | 1 | 1 | 1 | 1 |
| Juglans | 1 | 0 | 0 | 0 | 1 | 1 | 1 | 1 | 1 | 1 | 1 | 1 | 1 | 0 | 1 | 0 | 1 |
| Olea | 0 | 1 | 1 | 1 | 1 | 1 | 1 | 0 | 0 | 0 | 0 | 0 | 0 | 1 | 0 | 0 | 0 |
| Nigra | 1 | 1 | 0 | 0 | 1 | 1 | 1 | 1 | 1 | 1 | 1 | 1 | 0 | 1 | 1 | 1 | 1 |
| Vitis | 0 | 1 | 1 | 1 | 1 | 1 | 0 | 1 | 0 | 1 | 1 | 1 | 0 | 1 | 1 | 0 | 1 |
| Juniperus | 0 | 1 | 0 | 1 | 1 | 0 | 1 | 1 | 1 | 1 | 1 | 1 | 0 | 1 | 1 | 1 | 0 |
| Alnus | 1 | 1 | 0 | 0 | 0 | 1 | 1 | 1 | 1 | 1 | 1 | 1 | 0 | 0 | 1 | 0 | 1 |
| Abies | 1 | 1 | 0 | 0 | 0 | 0 | 1 | 0 | 1 | 0 | 0 | 0 | 1 | 1 | 1 | 1 | 1 |
| Carpinus betulus | 1 | 1 | 1 | 1 | 1 | 1 | 1 | 1 | 1 | 1 | 1 | 1 | 1 | 1 | 0 | 1 | 1 |
| Corylus avellana | 1 | 1 | 0 | 0 | 1 | 1 | 1 | 1 | 1 | 1 | 1 | 1 | 1 | 1 | 1 | 1 | 1 |
| Fagus | 1 | 1 | 0 | 0 | 0 | 1 | 1 | 0 | 1 | 1 | 1 | 1 | 1 | 1 | 1 | 1 | 1 |
| Platanus | 1 | 0 | 0 | 0 | 1 | 1 | 0 | 1 | 1 | 1 | 0 | 1 | 0 | 1 | 0 | 1 | 0 |
| Populus | 0 | 1 | 1 | 1 | 0 | 0 | 0 | 1 | 1 | 1 | 1 | 1 | 1 | 1 | 1 | 1 | 1 |
| Ulmus | 1 | 1 | 0 | 0 | 0 | 0 | 1 | 0 | 1 | 0 | 0 | 0 | 1 | 1 | 1 | 1 | 1 |
| Tilia | 1 | 1 | 0 | 0 | 0 | 0 | 1 | 1 | 1 | 1 | 1 | 1 | 1 | 1 | 1 | 1 | 1 |
| Sclerophyll | 0 | 1 | 1 | 1 | 1 | 1 | 0 | 0 | 0 | 0 | 0 | 0 | 0 | 1 | 0 | 0 | 0 |
| Shrubland | 0 | 1 | 0 | 0 | 0 | 0 | 0 | 0 | 0 | 0 | 0 | 0 | 0 | 1 | 0 | 0 | 0 |
| Grassland | 0 | 1 | 1 | 1 | 1 | 1 | 0 | 0 | 0 | 0 | 0 | 0 | 0 | 1 | 0 | 0 | 0 |

# 9 APPENDIX: RARE EVENTS LOGISTIC REGRESSION OUTPUT

**Table 9-1 Rare Events Logistic Regression coefficients: Climate, topography and soil characteristics**

| Species no. | 1 | 2 | 3 | 4 | 5 | 6 | 7 | 8 | 9 | 10 | 11 | 12 | 13 | 14 | 15 | 16 | 17 | 18 | 19 | 20 | 21 | 22 | 23 | 24 | 25 | 26 |
|---|---|---|---|---|---|---|---|---|---|---|---|---|---|---|---|---|---|---|---|---|---|---|---|---|---|---|
| **Intercept** | -16.100 | -2.448 | -6.630 | 3.432 | -15.000 | -3.824 | -23.860 | -13.660 | 7.311 | -2.052 | -0.466 | -43.140 | -6.257 | -6.170 | 2.755 | -3.440 | -14.790 | -5.030 | -16.510 | -7.501 | -11.380 | -2.041 | 1.293 | -11.130 | -5.340 | INS |
| **pH** | -0.147 | 0.188 | INS | INS | INS | -0.188 | 0.049 | INS | -0.242 | -0.069 | 0.165 | 0.986 | 0.967 | -0.170 | -0.260 | -0.410 | INS | -0.137 | INS | INS | INS | 0.195 | INS | 0.047 | INS | 0.305 |
| **slope** | 0.148 | 0.113 | 0.123 | 0.129 | 0.720 | 0.068 | 0.119 | 0.181 | 0.047 | 0.164 | -0.015 | -0.037 | 0.048 | 0.067 | 0.055 | 0.051 | 0.125 | 0.101 | 0.024 | 0.062 | 0.129 | 0.089 | 0.156 | 0.032 | 0.147 | -0.241 |
| **SRTM** | -0.001 | 0.004 | 0.001 | 0.000 | 0.000 | 0.002 | 0.002 | 0.001 | -0.001 | 0.001 | -0.002 | 0.005 | 0.002 | 0.000 | 0.000 | INS | 0.001 | 0.001 | 0.002 | 0.006 | 0.000 | 0.004 | 0.002 | 0.002 | INS | -0.001 |
| **AWC** | 0.290 | INS | 0.098 | 0.246 | 0.640 | 0.051 | -0.614 | 0.112 | 0.119 | 0.063 | INS | -0.167 | -0.023 | 0.169 | INS | -0.020 | 0.163 | 0.163 | -0.024 | -0.031 | 0.043 | INS | -0.036 | 0.145 | 0.088 | -0.005 |
| **Drainage** | 0.235 | INS | -0.190 | 0.133 | INS | INS | -0.630 | -0.187 | INS | INS | 0.161 | INS | 0.100 | -0.230 | 0.191 | 0.268 | INS | -0.158 | -0.001 | -0.460 | 0.045 | 0.003 | 0.097 | -0.030 | -0.238 | INS |
| **Texture** | 0.582 | INS | 0.284 | 0.609 | INS | INS | -0.281 | 0.562 | 0.337 | 0.031 | 0.230 | -0.160 | INS | 0.503 | 0.505 | 0.941 | INS | 0.316 | -0.073 | INS | 0.356 | -2.556 | INS | INS | 0.101 | INS |
| **Prec_sum** | -0.055 | 0.009 | INS | VIF | VIF | -0.001 | -0.015 | -0.006 | 0.003 | 0.018 | 0.014 | VIF | 0.019 | 0.018 | 0.017 | -0.110 | INS | 0.032 | -0.004 | 0.024 | 0.028 | VIF | VIF | 0.004 | -0.003 | INS |
| **Prec_win** | VIF | 0.008 | 0.007 | 0.040 | 0.010 | INS | INS | -0.016 | 0.006 | 0.008 | 0.003 | INS | 0.009 | 0.002 | VIF | VIF | VIF | 0.016 | -0.006 | -0.017 | -0.005 | -0.025 | 0.005 | -0.002 | 0.003 | INS |
| **Prec_aut** | -0.013 | 0.021 | 0.020 | 0.013 | 0.010 | 0.029 | 0.025 | 0.031 | 0.022 | 0.007 | 0.017 | 0.019 | 0.009 | 0.010 | 0.016 | 0.063 | INS | INS | 0.003 | 0.054 | -0.014 | 0.008 | 0.018 | 0.007 | VIF | INS |
| **Prec_spr** | INS | 0.008 | 0.010 | -0.024 | 0.010 | VIF | INS | VIF | VIF | VIF | 0.026 | -0.007 | VIF | VIF | -0.010 | -0.010 | 0.041 | VIF | 0.003 | VIF | VIF | 0.036 | 0.008 | VIF | VIF | VIF |
| **Aridity** | 4.761 | -10.120 | -7.520 | -16.860 | -8.900 | -3.843 | -1.790 | -2.349 | -6.219 | -4.554 | -14.180 | VIF | -5.026 | -3.870 | -2.730 | INS | -6.098 | -8.374 | 0.171 | 9.719 | INS | -4.307 | -11.380 | VIF | VIF | INS |
| **T_sum** | VIF | VIF | VIF | VIF | VIF | VIF | VIF | VIF | VIF | VIF | VIF | VIF | VIF | VIF | VIF | VIF | VIF | VIF | VIF | VIF | VIF | VIF | VIF | VIF | VIF | VIF |
| **T_aut** | VIF | VIF | VIF | VIF | VIF | VIF | VIF | VIF | VIF | VIF | VIF | VIF | VIF | VIF | VIF | VIF | VIF | VIF | VIF | VIF | VIF | VIF | VIF | VIF | VIF | VIF |
| **T_win** | VIF | VIF | VIF | VIF | VIF | VIF | VIF | VIF | VIF | VIF | VIF | VIF | VIF | VIF | VIF | VIF | VIF | VIF | VIF | VIF | VIF | VIF | VIF | VIF | VIF | VIF |
| **T_spr** | INS | VIF | VIF | VIF | VIF | VIF | VIF | VIF | VIF | VIF | VIF | VIF | VIF | VIF | VIF | VIF | VIF | VIF | VIF | VIF | VIF | VIF | VIF | VIF | VIF | VIF |
| **T_max** | -0.008 | -0.006 | -0.020 | -0.043 | INS | 0.000 | 0.008 | 0.009 | -0.066 | -0.012 | -0.003 | -0.024 | -0.011 | -0.030 | -0.040 | -0.160 | VIF | VIF | 0.029 | 0.071 | 0.029 | 0.056 | INS | 0.005 | VIF | VIF |
| **T_min** | VIF | 0.001 | VIF | VIF | 0.080 | VIF | VIF | VIF | VIF | VIF | 0.002 | 0.112 | VIF | VIF | VIF | 0.143 | VIF | VIF | VIF | VIF | VIF | VIF | VIF | VIF | VIF | VIF |
| **T_seas** | 0.002 | 0.002 | 0.001 | 0.001 | 0.000 | 0.000 | 0.002 | 0.001 | 0.001 | -0.051 | 0.000 | 0.004 | 0.000 | 0.001 | 0.001 | 0.006 | 0.001 | 0.000 | 0.001 | -0.003 | 0.000 | -0.003 | -0.001 | 0.000 | INS | INS |
| **P_seas** | -0.028 | -0.072 | -0.030 | -0.824 | 0.000 | -0.070 | -0.098 | -0.036 | -0.049 | 0.000 | INS | 0.034 | -0.011 | -0.090 | -0.050 | -0.190 | 0.002 | -0.092 | -0.047 | -0.272 | -0.070 | -0.104 |  | 0.028 | 0.009 | INS |
| **Or_car** | INS | INS | -0.560 | -1.077 | -15.000 | -0.068 | -0.662 | -0.054 | INS | -0.007 | INS | INS | INS | -0.090 | INS | INS | INS | -0.035 | INS | INS | INS | 0.067 | -0.135 | INS | INS | -0.030 |

**Table 9-2 Rare Events Logistic Regression coefficients: Soil type**

| Species no. | 1 | 2 | 3 | 4 | 5 | 6 | 7 | 8 | 9 | 10 | 11 | 12 | 13 | 14 | 15 | 16 | 17 | 18 | 19 | 20 | 21 | 22 | 23 | 24 | 25 | 26 |
|---|---|---|---|---|---|---|---|---|---|---|---|---|---|---|---|---|---|---|---|---|---|---|---|---|---|---|
| Calcisol | 1.226 | INS | INS | INS | INS | INS | INS | INS | INS | INS | INS | INS | INS | INS | INS | INS | INS | INS | INS | INS | INS | INS | INS | INS | INS | INS |
| Fluvisol | 0.432 | INS | INS | 0.107 | INS | 0.191 | INS | INS | INS | INS | INS | INS | INS | INS | INS | INS | INS | INS | INS | INS | INS | INS | INS | INS | INS | INS |
| Vertisol | 0.904 | INS | INS | INS | INS | INS | INS | 0.953 | -1.552 | INS | INS | INS | INS | INS | INS | INS | INS | INS | INS | INS | INS | INS | INS | INS | INS | 0.7 |
| Podzol | INS | 0.725 | INS | INS | 0.702 | 0.155 | INS | INS | 0.443 | INS | INS | INS | INS | 0.424 | INS | INS | INS | INS | INS | INS | INS | INS | INS | INS | 0.195 | INS |
| Luvisol | INS | INS | 0.84 | INS | INS | 0.171 | 2.363 | 0.947 | INS | 0.696 | INS | 1.404 | 0.576 | INS | INS | INS | 0.814 | 0.832 | INS | INS | 0.847 | INS | INS | INS | 0.01 | INS |
| Regosol | INS | INS | 1.144 | INS | INS | INS | INS | 0.993 | 1.321 | 1.163 | INS | INS | INS | INS | INS | 1.159 | INS | 0.985 | 0.185 | INS | 1.534 | 0.705 | INS | INS | 1.041 | INS |
| Cambisol | INS | INS | 0.767 | INS | 0.386 | 0.338 | 2.339 | 0.96 | 0.4802 | 0.949 | INS | INS | 0.76 | 0.473 | 0.452 | INS | INS | 0.748 | 0.113 | 1.367 | 0.665 | INS | INS | INS | INS | 0.512 |
| Alfisol | INS | INS | 1.493 | INS | INS | INS | INS | INS | INS | INS | INS | INS | INS | 2.044 | INS | INS | INS | INS | INS | INS | INS | INS | INS | INS | INS | INS |
| Gleysol | INS | INS | INS | 1.484 | INS | INS | INS | INS | INS | INS | INS | INS | INS | INS | INS | INS | INS | INS | INS |  | INS | INS | INS | 0.829 | 0.489 | INS |
| Leptosol | INS | INS | INS | 0.955 | INS | -0.059 | INS | INS | 0.6925 | 0.412 | INS | INS | 0.678 | INS | 0.529 | INS | INS | INS | INS | 1.071 | INS | INS | 1.362 | INS | INS | INS |
| Phaeozem | INS | INS | INS | INS | INS | INS | 3.68 | 1.071 | INS | INS | INS | INS | INS | INS | INS | INS | INS | INS | INS | INS | INS | INS | INS | INS | 0.919 | 0.93 |
| Chernozem | INS | INS | INS | INS | INS | INS | INS | 1.047 | INS | INS | INS | INS | INS | INS | INS | INS | INS | INS | 0.388 | INS | INS | INS | INS | INS | 0.697 | 1.243 |
| Andisol | INS | INS | INS | INS | INS | INS | INS | INS | 1.721 | 1.128 | INS | INS | INS | INS | 0.613 | INS | 1.705 | INS | INS | INS | INS | INS | INS | INS | INS | INS |
| Anthrosol | INS | INS | INS | INS | INS | INS | INS | INS | 1.759 | INS | INS | INS | INS | 2.41 | INS | INS | INS | 2.548 | INS | INS | 1.48 | INS | INS | INS | INS | INS |
| Arenosol | INS | INS | INS | INS | INS | 0.849 | INS | INS | 0.3719 | INS | INS | INS | INS | INS | INS | INS | INS | 0.65 | INS | INS | 0.92 | INS | INS | INS | INS | INS |
| Podluvisol | INS | INS | INS | INS | INS | 0.744 | INS | INS | 0.743 | INS | INS | INS | INS | INS | INS | INS | INS | INS | INS | INS | INS | INS | INS | INS | INS | INS |
| Pluvisol | INS | INS | INS | INS | INS | INS | INS | INS | INS | 0.828 | INS | INS | INS | INS | INS | INS | INS | INS | INS | INS | INS | INS | INS | INS | INS | INS |
| Greyzem | INS | INS | INS | INS | INS | INS | INS | INS | INS | INS | 1.212 | INS | INS | INS | INS | INS | INS | 2.124 | INS | INS | 2.283 | INS | INS | INS | 1.082 | INS |
| Acrisol | INS | INS | INS | INS | INS | INS | INS | INS | INS | INS | INS | INS | INS | INS | INS | INS | INS | INS | INS | INS | INS | 1.073 | INS | INS | -1.545 | 1.793 |
| Planosol | INS | INS | INS | INS | INS | INS | INS | INS | INS | INS | INS | INS | INS | INS | INS | INS | INS | INS | INS | INS | INS | 1.555 | INS | INS | INS | INS |
| Histosol | INS | INS | INS | INS | INS | INS | INS | INS | INS | INS | INS | INS | INS | INS | INS | INS | INS | INS | INS | INS | INS | INS | INS | 0.864 | 0.457 | INS |
| Kastenozem | INS | INS | INS | INS | INS | INS | INS | INS | INS | INS | INS | INS | INS | INS | INS | INS | INS | INS | INS | INS | INS | INS | INS | INS | -1.973 | INS |
| Solonchak | INS | INS | INS | INS | INS | INS | INS | INS | INS | INS | INS | INS | INS | INS | INS | INS | INS | INS | INS | INS | INS | INS | INS | INS | 1.019 | INS |
| Solonetz | INS | INS | INS | INS | INS | INS | INS | INS | INS | INS | INS | INS | INS | INS | INS | INS | INS | INS | INS | INS | INS | INS | INS | INS | 1.54 | INS |

**Table 9-3 Rare Events Logistic Regression coefficients: Aspect**

| Species no. | 1 | 2 | 3 | 4 | 5 | 6 | 7 | 8 | 9 | 10 | 11 | 12 | 13 | 14 | 15 | 16 | 17 | 18 | 19 | 20 | 21 | 22 | 23 | 24 | 25 | 26 |
|---|---|---|---|---|---|---|---|---|---|---|---|---|---|---|---|---|---|---|---|---|---|---|---|---|---|---|
| East | 0.267 | INS | INS | INS | INS | INS | 618 | INS | INS | 0.218 | INS | INS | INS | INS | INS | 0.334 | INS | INS | 0.125 | INS | 0.19 | INS | INS | INS | INS | INS |
| Northeast | INS | INS | INS | INS | 0.104 | INS | 0.575 | INS | INS | 0.213 | INS | INS | INS | INS | INS | INS | INS | INS | INS | 0.389 | 0.131 | INS | INS | INS | INS | INS |
| Northwest | INS | INS | INS | INS | INS | INS | 0.575 | INS | INS | INS | INS | INS | INS | INS | INS | INS | INS | INS | INS | 0.321 | INS | INS | INS | INS | INS | -0.107 |
| North | INS | INS | INS | INS | INS | INS | 0.643 | INS | INS | 0.175 | INS | INS | INS | INS | INS | INS | INS | INS | INS | 0.484 | INS | INS | INS | INS | INS | 0.151 |
| West | INS | INS | INS | INS | INS | INS | 0.615 | INS | INS | INS | INS | INS | INS | INS | INS | INS | INS | INS | INS | 0.316 | INS | INS | 0.238 | INS | INS | INS |
| Southwest | INS | INS | INS | INS | INS | INS | INS | INS | INS | INS | INS | 0.808 | INS | INS | INS | INS | INS | INS | INS | 0.29 | INS | 0.159 | INS | INS | INS | 0.093 |
| Southeast | INS | INS | INS | INS | INS | INS | INS | INS | INS | INS | INS | 0.467 | INS | INS | INS | 0.478 | INS | INS | INS | INS | INS | INS | INS | INS | INS | INS |
| South | INS | INS | INS | INS | INS | INS | INS | INS | INS | INS | INS | INS | INS | INS | INS | 0.392 | INS | INS | INS | INS | INS | INS | INS | INS | INS | 0.097 |

**Table 9-4 Species key**

| | | | |
|---|---|---|---|
| 1 | *Pinus brutia* | 9 | *Betula pendula* |
| 2 | *Pinus nigra* | 10 | *Fagus sylvatica* |
| 3 | *Quercus cerris* | 11 | *Vitis vinifera* |
| 4 | *Quercus coccifera* | 12 | *Cedrus libani* |
| 5 | *Olea europeae* | 13 | *Abies alba* |
| 6 | *Castanea sativa* | 14 | *Ulmus glabra* |
| 7 | *Juglans regia* | 15 | *Picea abies* |
| 8 | *Fraxinus ornus* | 16 | *Alnus cordata* |
| 9 | *Betula pendula* | 17 | *Platanus orientalis* |
| 10 | *Fagus sylvatica* | 18 | *Carpinus betulus* |
| 11 | *Vitis vinifera* | 19 | *Populus nigra* |
| 12 | *Cedrus deodara* | 20 | *Corylus avellana* |
| 13 | *Abies alba* | 21 | *Tilia cordata* |
| 14 | *Ulmus glabra* | 22 | *Juniperus oxycedrus* |

| | | | |
|---|---|---|---|
| 15 | *Picea abies* | 23 | Sclerophylous |
| 16 | *Alnus cordata* | 24 | Shrubland |
| 17 | *Platanus orientalis* | 25 | Grassland |
| 18 | *Carpinus betulus* | 26 | Dry agriculture |

**Table 5 Classification accuracy of the Rare Events Regression analysis**

| | True negative | False negative | Negative % correct | True positive | False positive | Positive % correct | Overall accuracy |
|---|---|---|---|---|---|---|---|
| ***Pinus brutia*** | 11265 | 2247 | 83.4 | 12448 | 840 | 93.7 | 88.5 |
| ***Pinus nigra*** | 8191 | 2886 | 73.9 | 13014 | 1904 | 87.2 | 81.6 |
| ***Quercus cerris*** | 10152 | 3576 | 74 | 9561 | 2939 | 76.5 | 75.2 |
| ***Quercus coccifera*** | 10405 | 1541 | 87.1 | 13244 | 462 | 96.6 | 92.2 |
| ***Olea europeae*** | 12111 | 1242 | 83.3 | 12272 | 2426 | 90.8 | 86.9 |
| ***Castanea sativa*** | 15435 | 3354 | 82.1 | 7810 | 3327 | 70.1 | 77.7 |
| ***Juglans regia*** | 10824 | 3153 | 77.4 | 11792 | 1343 | 89.8 | 83.4 |
| ***Fraxinus ornus*** | 10897 | 2840 | 79.3 | 10631 | 2664 | 80 | 79.6 |

| | | | | | | | |
|---|---|---|---|---|---|---|---|
| ***Betula pendula*** | 10860 | 2452 | 81.6 | 5547 | 2724 | 67.1 | 76 |
| ***Fagus sylvatica*** | 2890 | 8971 | 75.6 | 12318 | 2655 | 82.3 | 79.3 |
| ***Vitis vinifera*** | 11879 | 4530 | 72.4 | 10540 | 3020 | 77.7 | 74.8 |
| ***Cedrus deodara*** | 11193 | 3354 | 76.9 | 10547 | 809 | 92.9 | 83.9 |
| ***Abies alba*** | 10748 | 2791 | 79.4 | 10880 | 2500 | 81.3 | 80.3 |
| ***Ulmus glabra*** | 10205 | 3283 | 75.7 | 11146 | 2452 | 82 | 78.8 |
| ***Picea abies*** | 11404 | 2325 | 83.1 | 5026 | 2650 | 65.5 | 76.8 |
| ***Alnus cordata*** | 12139 | 1585 | 88.5 | 13290 | 111 | 99.2 | 93.7 |
| ***Platanus orientalis*** | 10566 | 3116 | 77.2 | 11101 | 2201 | 83.5 | 80.3 |
| ***Carpinus betulus*** | 8375 | 3734 | 69.2 | 13019 | 1974 | 86.8 | 78.9 |
| ***Populus nigra*** | 7272 | 3737 | 77.1 | 11168 | 2731 | 80.4 | 74 |
| ***Corylus avellana*** | 11434 | 2419 | 82.5 | 12876 | 380 | 97.1 | 89.7 |
| ***Tilia cordata*** | 8636 | 3509 | 71.1 | 13443 | 1557 | 89.6 | 81.3 |
| ***Juniperus oxycedrus*** | 11215 | 2533 | 81.6 | 13117 | 226 | 98.3 | 89.8 |
| **Sclerophylous** | 9833 | 3357 | 81.3 | 13796 | 630 | 95.6 | 89.1 |
| **Shrubland** | 9585 | 2545 | 79 | 3181 | 6766 | 68 | 74 |
| **Grassland** | 8469 | 3567 | 70.4 | 11205 | 3441 | 76.5 | 73.7 |
| **Dry agriculture** | 5636 | 5502 | 50.6 | 2119 | 12483 | 85.5 | 70.4 |

The modelling of these co-efficients allows the relative correlation of each variable across the range of species examined, as demonstrated in Figure 9-1.

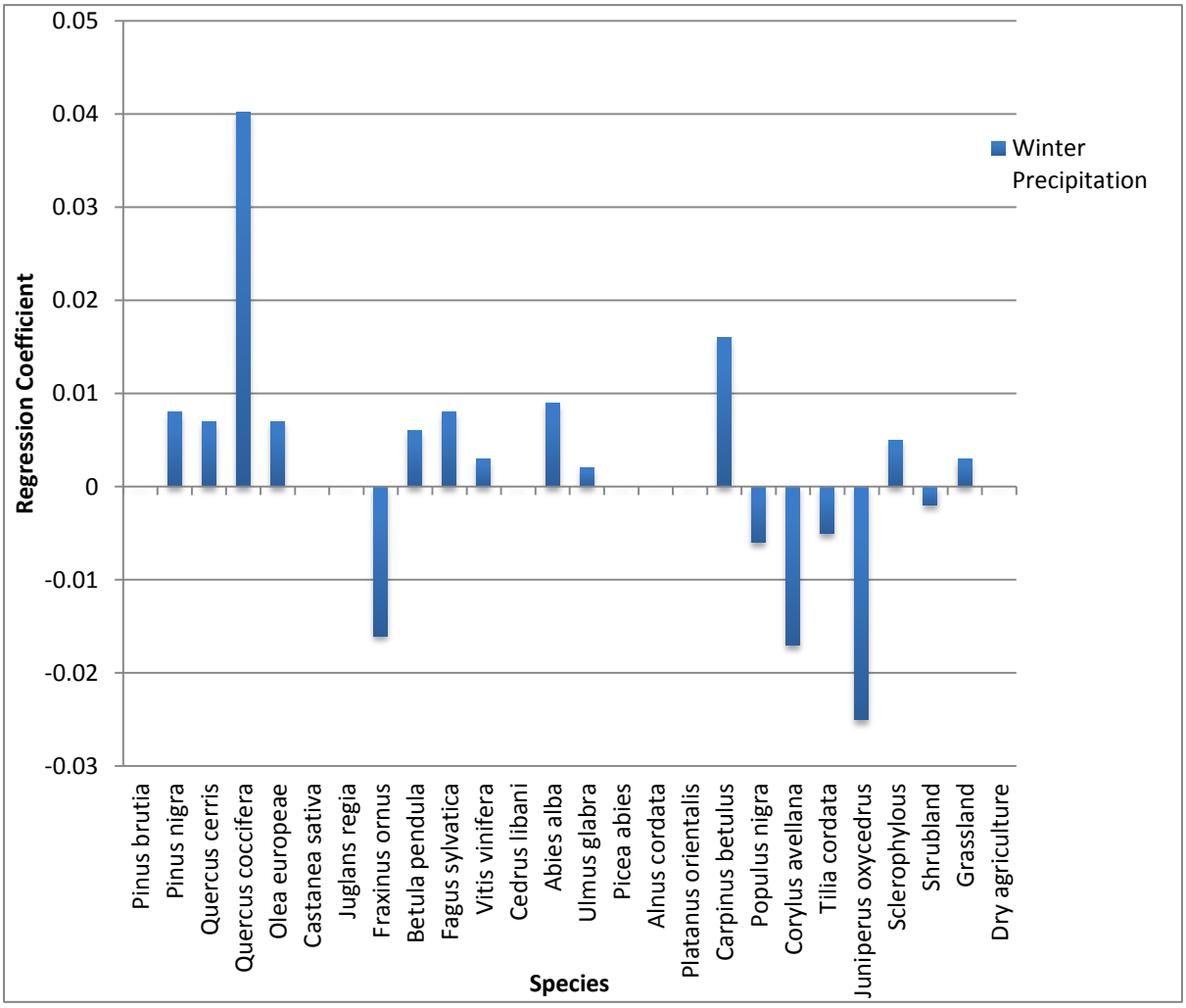


**Figure 9-1 relative correlation of winter precipitation regression co-efficient with species distribution**

# 10 APPENDIX: BACKGROUND TO MODEL RUNS

### 10.1.1 **Modern conditions (S1)**

The model developed in Chapter 4 is based on modern conditions. Comparing modern vegetation potential to vegetation assemblages of the past allows a baseline level of understanding to investigate the magnitude of species assemblage change over time. Modern species probability has been shown to relate to temperature, precipitation, aridity and edaphic variables. It would be interesting to discover whether any of the pollen assemblages considered as part of the research questions have similar species potential to modern conditions, or whether they show poor agreement, suggesting a dramatically different set of circumstances.

The following subsections discuss how vegetation may depart from modern species assemblage under specific changes in climate.

### 10.1.2 **Absolute Winter Minimum temperature (S2, S3)**

Absolute winter minimum temperature[1] was found to be a significant factor in the distribution of key species across Europe. Figure 10-1a displays an estimate of the absolute winter minimum temperatures likely to occur across the study area based on a probability of at least a 1 in 30 year event. Considering these records, in recent times, it is unlikely that winter minimum temperatures below -20°C ±2.91°C would commonly encountered in southwest Turkey, even in mountainous areas. However some of the higher elevation areas of Antalya and Burdur, and the interior regions of Isparta and Konya are likely to experience at least 1 event in 30 years where winter temperatures fall below -12°C. This has implications for arboriculture as it may kill groves of *Olea europeae*. In addition to this *Pinus brutia* is likely to be damaged by such a severe event. This variability begins to explain the current distribution of species in southwest Turkey, with *Olea* and *Pinus brutia* generally restricted to areas at lower elevations.

Variability in absolute winter temperature may prove to be a key factor for species distribution in more than one of the research questions of the thesis. Firstly, reconstructed climate evidence suggests that winter temperatures may have been a great deal colder during the Last Glacial Maximum. This may have acted to restrict the distribution of *Olea, Pinus brutia* and perhaps *Quercus* to relatively warmer locations in the region. Secondly, warmer average temperatures during the Roman period have been suggested as a contributory factor to the proliferation of Olive pollen at high altitude sites during the Beyşehir Occupation Phase.

It is therefore anticipated that analytical pollen from these periods may reflect a species assemblage under colder or warmer winter temperature conditions respectively. If this is the case then it helps to support a link between climate and vegetation. If there is not a similarity, then either another climate scenario may more likely, the vegetation is being impacted by something not accounted for in the model, or the relationship between climate factors and vegetation is not well modeled. These options will be discussed in the remaining chapters for each research question.

[1] Derived from the temperature of the coldest day of the year as measured at a weather station, averaged over 30 years.

To investigate the potential impact of this on vegetation potential, modelling runs were undertaken with winter minimum temperatures reduced by iterations of 2°C, down to -8°C below the present day average, to cover estimates of temperature decrease during Glacial and Late Glacial periods (e.g. Emeis, Schulz et al. 1998; Emeis, Struck et al. 2000; Emeis, Schulz et al. 2003).

Under the largest reduction in winter minimum temperature (Scenario S2-MR3), the vast majority of southwest Turkey would routinely have winter absolute minimum temperatures below -12°C±2.91°C, as shown in Figure 10-1b. As discussed above, this would prove to be important for certain modelled species, as it would restrict those that are recorded as being intolerant of low winter temperatures such as *Olea europeae* and *Pinus brutia*, and perhaps *Platanus*, *Juniperus* and *Vitis* from thriving or migrating into the region. The implications of this will be discussed in the results chapter.

In addition to this, winter temperatures below -20°C become more common throughout the mountainous areas of Isparta, Antalya and Konya, which may restrict even moderately tolerant winter species such as *Quercus*. However, even under these conditions, if only the direct effect of winter temperature is considered, it is likely that relatively hardy species such as *Carpinus*, *Fraxinus*, *Cedrus*, *Abies*, *Betula* and *Pinus nigra* would not be significantly restricted by this scenario.

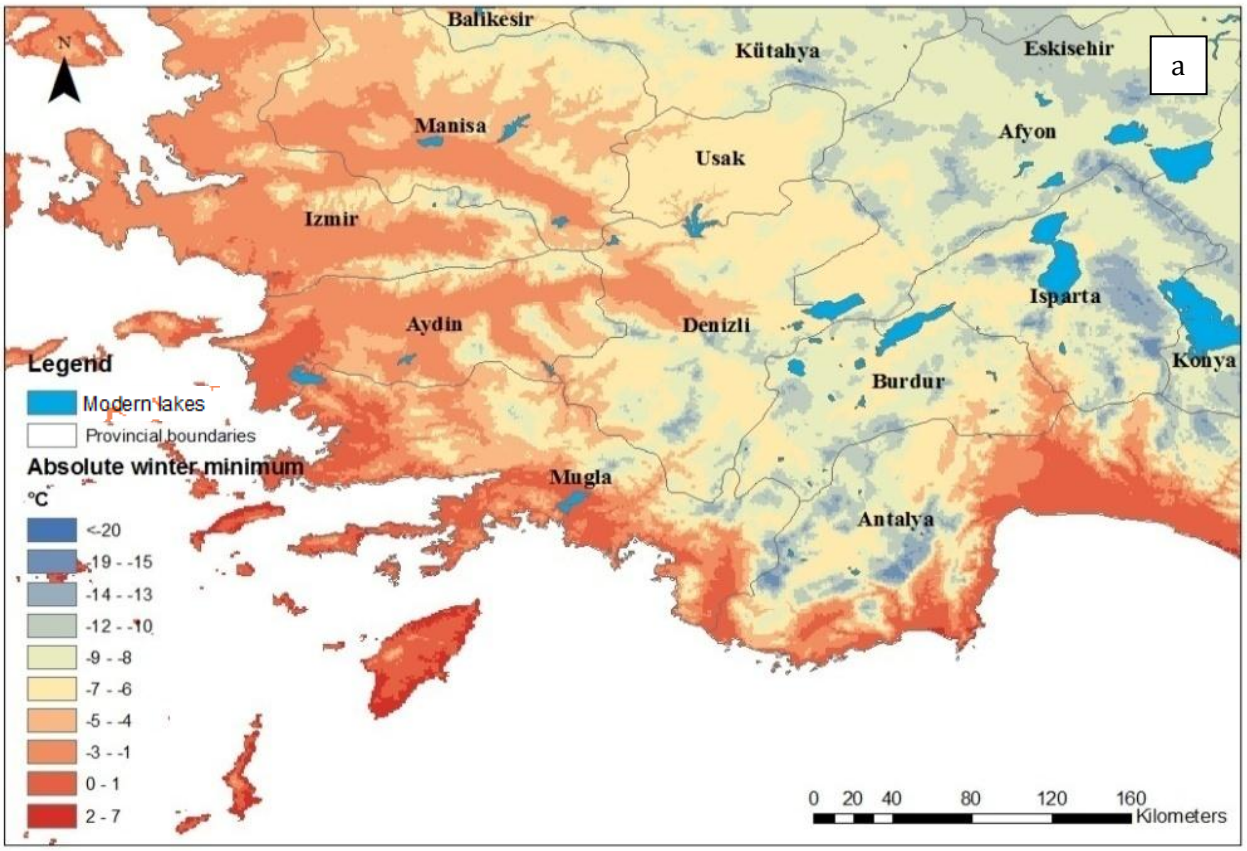


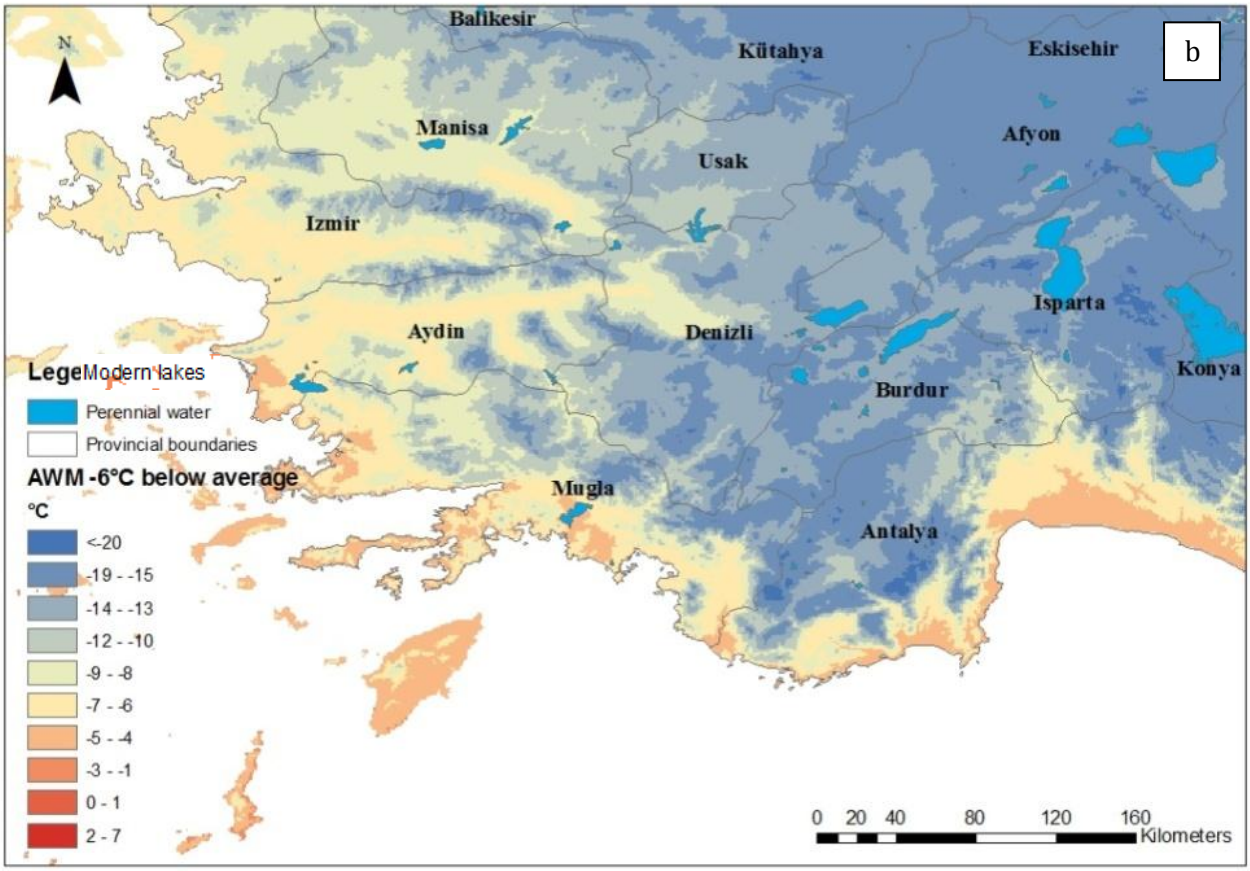


**Figure 10-1 (a) Absolute winter minimum temperatures based on 30 year reference period (b) Absolute winter minimum temperatures based on -6°C below modern average**

### 10.1.3 **Average minimum and maximum temperature (S4, S5)**

As well as absolute winter temperature, the average minimum[2] and maximum[3] temperature has been found to be a significant factor in the distribution of key species across Europe.

Figure 10-2a displays an overview of annual average temperatures likely to occur across the study area. The mountainous regions across southwest Turkey are shown to have the lowest average temperature, such as Uyluk Tepe, Bey Dağları, Namaxga Tepesı and Orta Tepe. The annual average temperature is around 5°C, with summer temperatures reaching 13°C, and winter temperature dropping to an average of -5°C at these high elevations between around 2500 - 3000 m. In the interior regions of Denizli, Burdur, Afyon and Isparta, an overall average temperature of around 10°C is experienced, with summer temperatures averaging around 20°C and winter temperatures dropping to around freezing.

Some of the warmest average temperatures are found in the western valleys of the Büyük and Küçük Menderes (large and small meander rivers), the low elevation plain of Antalya around Aksu Çayı (which is today fairly urbanised) and Muğla around the Dalaman Çayı. An overall average temperature of around 18 °C is achieved, with summer temperatures averaging around 27 °C, and in winter these areas can still retain an average temperature of around 11 °C at elevations below 100 metres. When travelling from high elevation sites such as Avlan to the low elevation plain of Antalya there can therefore be changes in temperature in the region of +16 °C across 40 km.

The distribution of temperature across southwest Turkey has implications for vegetation distribution. One of the most striking correlations in Figure 10-3 is the distribution of open vegetation / bare ground areas with high elevation areas that endure average annual temperatures under around 9°C. This treeline is calculated to be at around 1800 m. Forested areas are generally found between 9°C and 15°C. Arable areas are found between 15°C and 18°C near to the coast, and between 9°C and 15°C in the interior. Of course the positioning of arable land is also correlated with relatively flat land with good soils, which are generally at lower elevations and consequently warmer temperatures.

Previous research has estimated that average temperatures have fallen to levels significantly lower than the modern average on several occasions throughout the Late Glacial and Holocene. During the last ice age average temperatures in the region may have been reduced by <8°C (Sarıkaya, Zreda et al. 2008), and cooler temperatures are also evidence during the climatic fluctuations in the mid-Holocene.

Figure 10-2b shows how average winter temperatures potentially drop below freezing over large areas of southwest Turkey under this situation. With an estimated -6 to -8°C large areas of the southwest could have experienced prolonged freezing conditions and snow cover (dependent on the amount of precipitation available) further reducing the capacity of vegetation to flourish in the interior of the country.

[2] Derived from the average of one month's daily minimum temperature readings from a weather station, averaged over 30 years.
[3] Derived from the average of one month's daily maximum temperature readings from a weather station, averaged over 30 years.

There is also evidence for positive temperature anomalies throughout the Holocene; during the early Holocene 'climate optimum', during mid-Holocene climate fluctuations, and potentially during the Roman 'warm period' (Chen, Zonneveld et al. 2011).

Considering these findings, it is anticipated that analytical pollen from the last glacial period, and the mid Holocene may show similarities to model output under reduced temperature, and analytical pollen from the mid-Holocene and Roman period may show similarities to model output under increased temperature. To investigate, modelling runs pertaining to an average maximum and average minimum temperature anomaly of +4°C , +2°C, 0°C -4°C and -8°C were run, the magnitude of which was decided from previous literature.

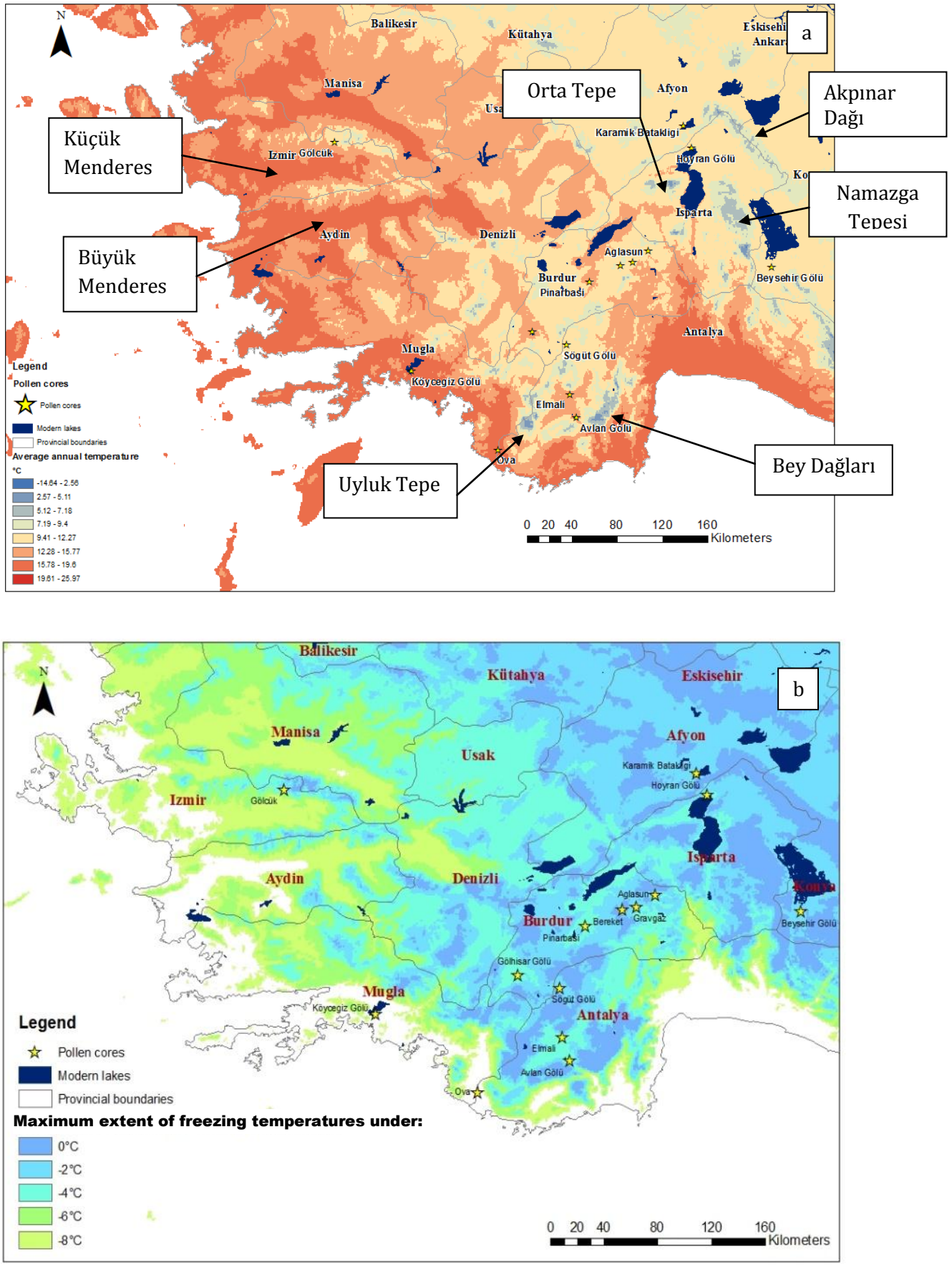





**Figure 10-2 (a) modern average annual temperature, with key areas of low and high temperature highlighted (b) Probable extent of below freezing average winter temperatures under different winter temperature anomalies. Note that the colours do not represent different temperatures, only whether the area is likely to be freezing of below under each model run (i.e. under a model run with average temperatures -2°C lower than modern**

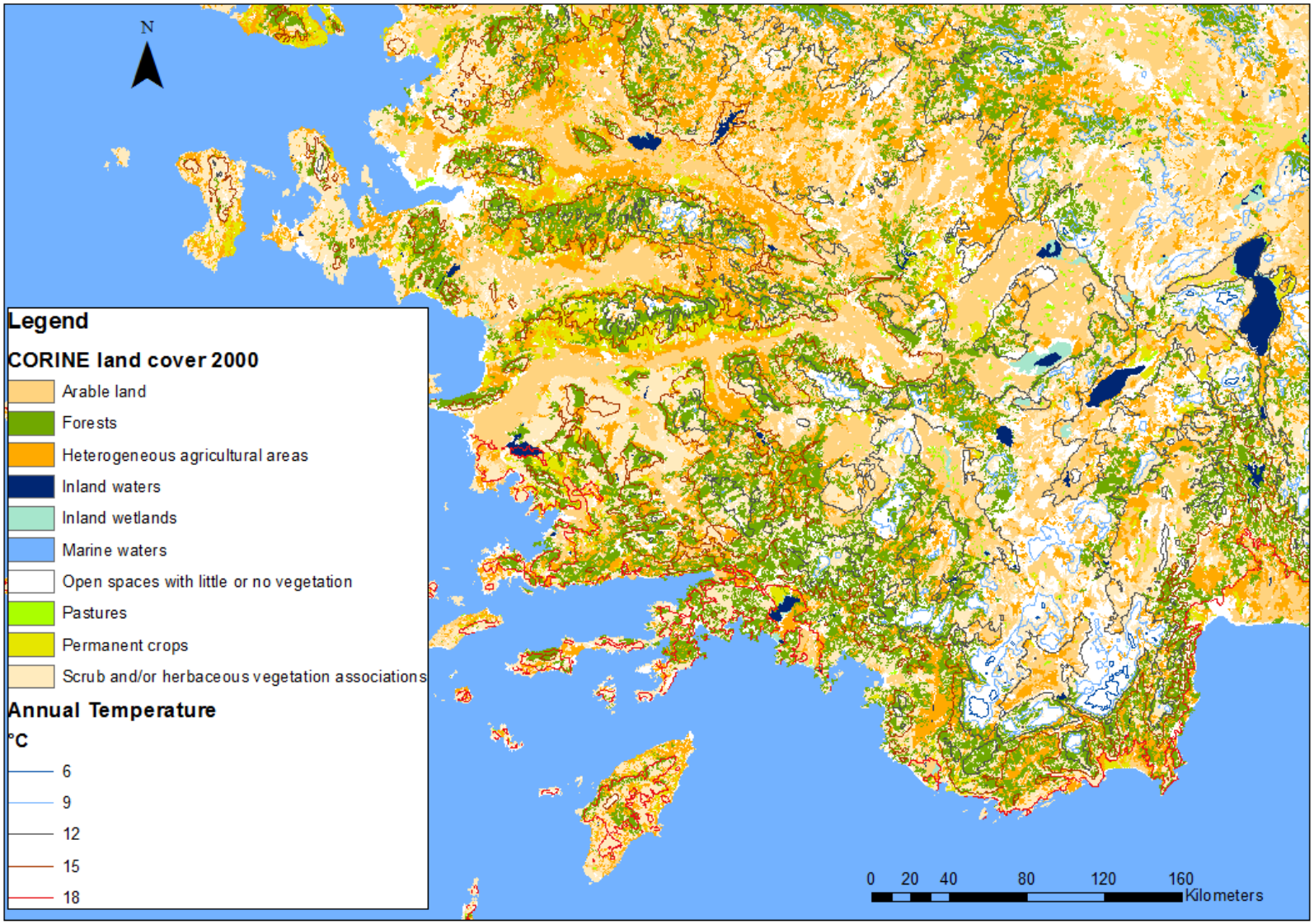


**Figure 10-3 CORINE land cover, overlaid with annual temperature isotherms. This shows that bare ground is correlated to areas of low temperature.**

### 10.1.4 **Varying winter precipitation (S6, S7)**

Seasonal precipitation was found to be a significant factor in the distribution of key modelled species across Europe. Most annual precipitation under the modern Mediterranean climate is delivered in the autumn and winter. Figure 10-4a displays the gradient of modern long term average winter precipitation across southwest Turkey, which is seen to decrease towards the interior of the region. Parts of Muğla and Antalya are shown to have particularly intense winter precipitation.

This gradient in long term precipitation has visible consequences for modern species distribution. As shown in Figure 6.7, modern forest distribution in southwest Turkey is predominantly distributed within the 400 to 600 mm winter precipitation range. The interior of the region is more likely to be composed of arable land, pastures, open spaces with little vegetation, and some small forest areas.

Due to changes in atmospheric circulation, it has been posited that precipitation during the Last Glacial period may have been greatly reduced (Landmann, Reimer et al. 1996; Bartov, Goldstein et al. 2003). Further evidence of reduced precipitation totalling up to 400 mm has been recorded for the Chalcolithic period (~5400 Cal yr BP) and evidence of aridity is also reported for the Bronze Age (Bar-Matthews, Ayalon et al. 1999; Bar-Matthews, Ayalon et al. 2000; Bar-Matthews, Ayalon et al. 2003). There is little evidence to suggest how these anomalies may have been spread across the seasons, however where there is evidence of a large scale negative anomaly, it is obvious that autumn and / or winter precipitation will have been affected, as summer precipitation is low in modern records.

If, during an extreme climatic event, the whole of southwest Turkey was affected by a negative winter precipitation anomaly of around 300 mm, the majority of southwest Turkey is calculated as having less than 100 mm winter precipitation. As shown in Figure 10-4b this only leaves the coastal areas with greater than this amount. This is likely to have significant consequences for tree species, as previous research has shown that many require at least 300 mm annual precipitation to thrive. To investigate these scenarios, model runs were undertaken which decreased winter precipitation by up to 300 mm, in 100 mm intervals.

In comparison, data have also been reported for wetter climatic conditions at the beginning of the Holocene, with an increase of up to 300 mm above current values (Goodfriend 1999). Model runs therefore also looked at positive precipitation anomalies. Under this situation values of over 820 mm would be seen across the coastal province of Muğla and Antalya, whereas precipitation in Ankara would still be ~300 mm.

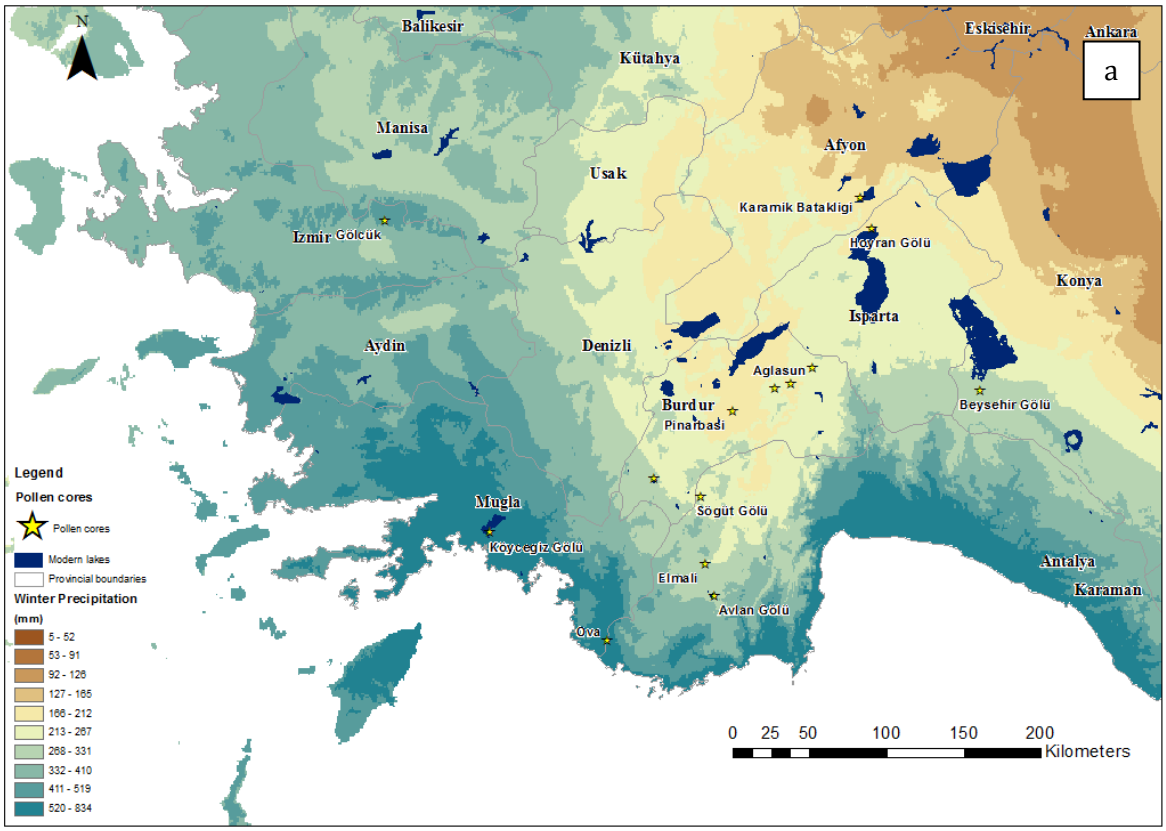


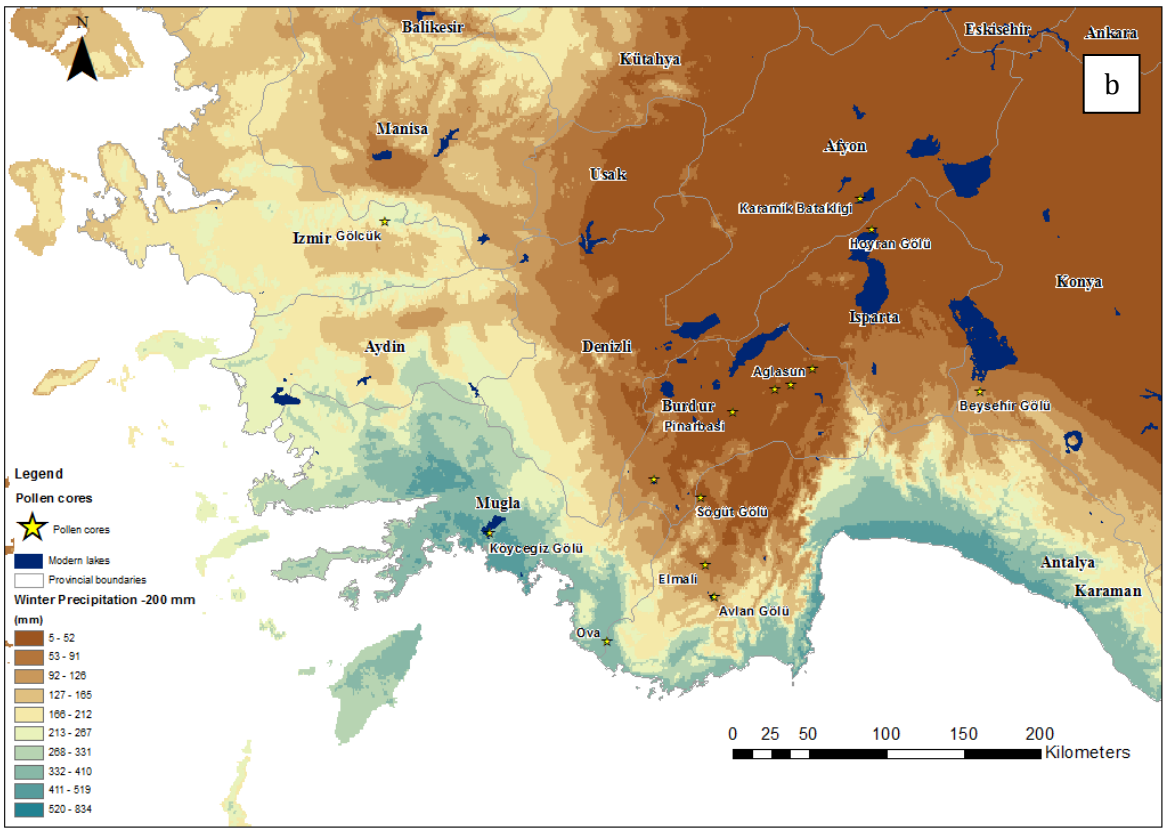


**Figure 10-4(a) Modern winter precipitation (b) Winter precipitation -200 mm**

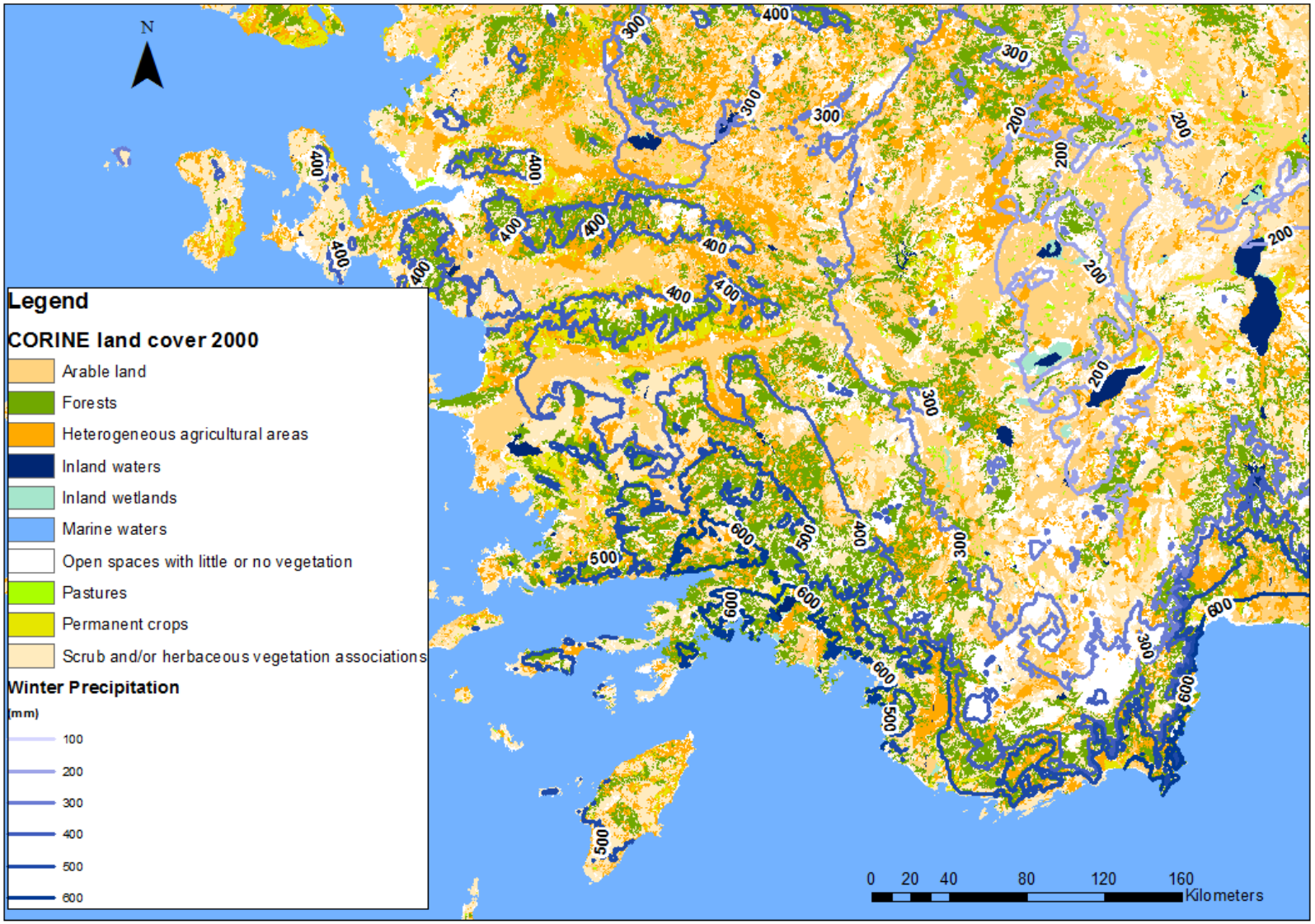


**Figure 10-5 CORINE land cover with winter precipitation isohyets superimposed, showing correlation between high winter precipitation and forest distribution.**

#### 10.1.4.1 Changing aridity / humidity (S8, S9, S10, S11)

As well as changing precipitation and temperature in isolation, the balance of are found to be important to plant growth, dictating potential drought conditions or humid environments.

An Aridity Index can be used to quantify precipitation availability over atmospheric water demand. According to the Hargreaves method, the value of an aridity index is dependent upon precipitation, solar insolation, average temperature, and average minimum and maximum precipitation. The Aridity Index equation allows investigation of how these variables affect overall aridity across a region under different circumstances.

Figure 10-6a shows the CGIAR Global Aridity Index for southwest Turkey based on 30 years worth of data. Higher values of Aridity Index represent more humid conditions. More humid conditions mean more moisture availability for potential vegetation growth. The data show that in modern times, due to the balance of precipitation and temperature that was introduced in previous sections, humidity is greater near the coast, and in mountainous areas. It also shows that further inland, conditions become more arid (Figure 6.3a).

The aridity index can be further classified into areas of humid, dry sub-humid and semi-arid conditions as shown in Figure 10-6b. The coastal regions particularly around Muğla and Antalya are classified as humid, while Denizli, Isparta, Aydin and Izmir are transition zones with areas of humid, dry sub-humid and semi-arid climatic regimes. The provinces of Uşak, Afyon and Konya are relatively arid. Most of the pollen cores taken in Burdur and Isparta provinces are taken in areas that are today semi-arid in nature. Ova, Köyceğiz and Gölcük are pollen cores from more humid areas.

Areas designated as humid incorporate a considerable amount of the forested area within Muğla. However they also incorporate the open poorly vegetated areas of Bey Dağları, and Uyluk Tepe. This shows that humidity can arise from different circumstances; Muğla is humid due to large amounts of precipitation despite warm temperatures, whereas the mountainous regions are humid due to cool temperatures, reducing evaporation despite lower precipitation levels.

The balance between precipitation and temperature are likely to be important for all research questions, but particularly when discussing linkages between hydrological regimes and vegetation distribution in the Late Glacial and Early Holocene periods, and increasing climate aridity in the Mid-Holocene.

For instance, if temperatures decrease, but all other variables stay the same, humidity would be likely to increase, as less water is lost through evaporation and transpiration. This is shown in Figure 10-8a. Under a scenario of -8°C, a decrease in temperature of this magnitude leads to an increase in humid and dry sub-humid areas into the interior of Turkey.

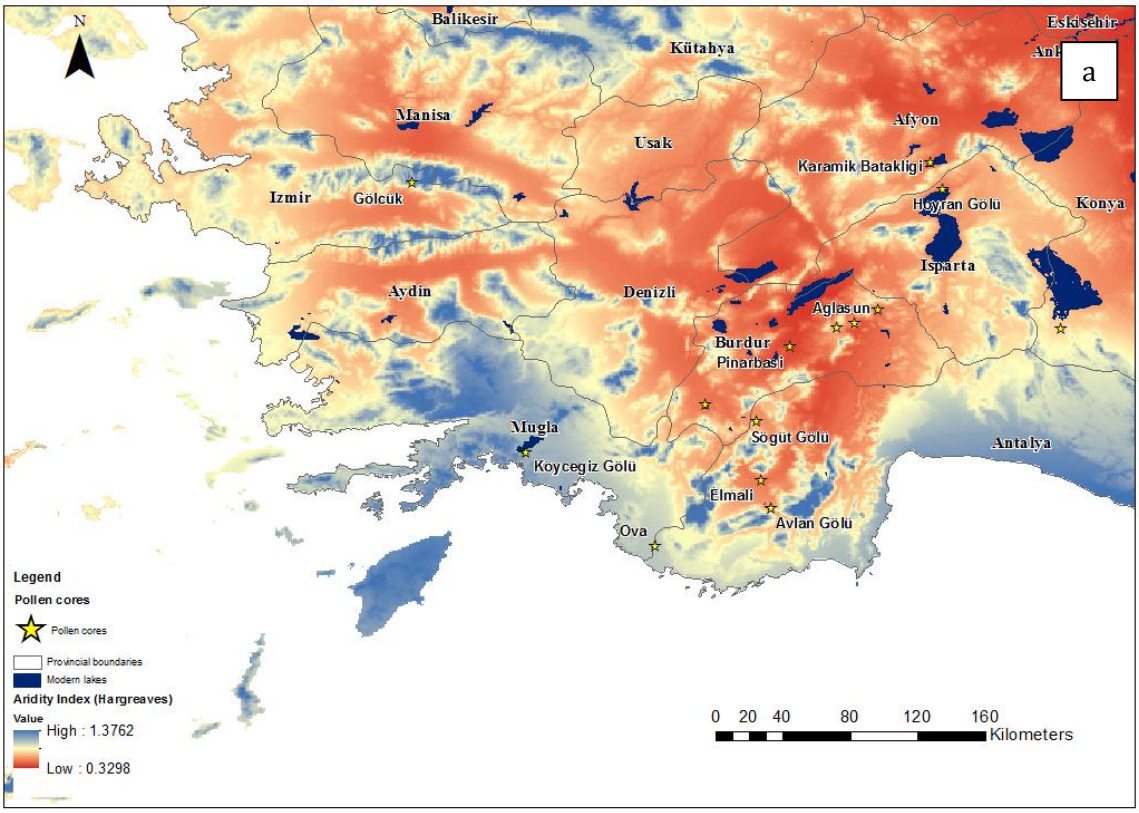


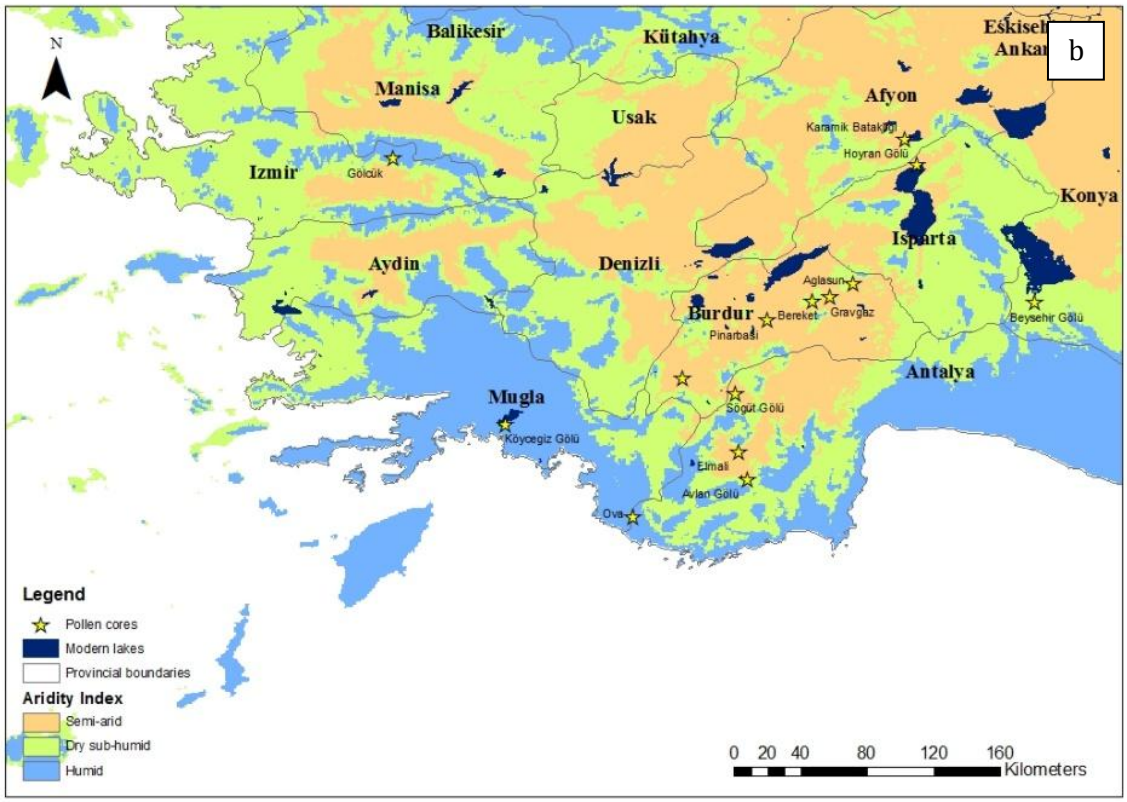


**Figure 10-6 (a) Aridity index under modern conditions (b) Aridity classifications, where semi-arid is between 0.2 and 0.5, dry sub-humid is between 0.5 and 0.65 and humid is over 0.65.**

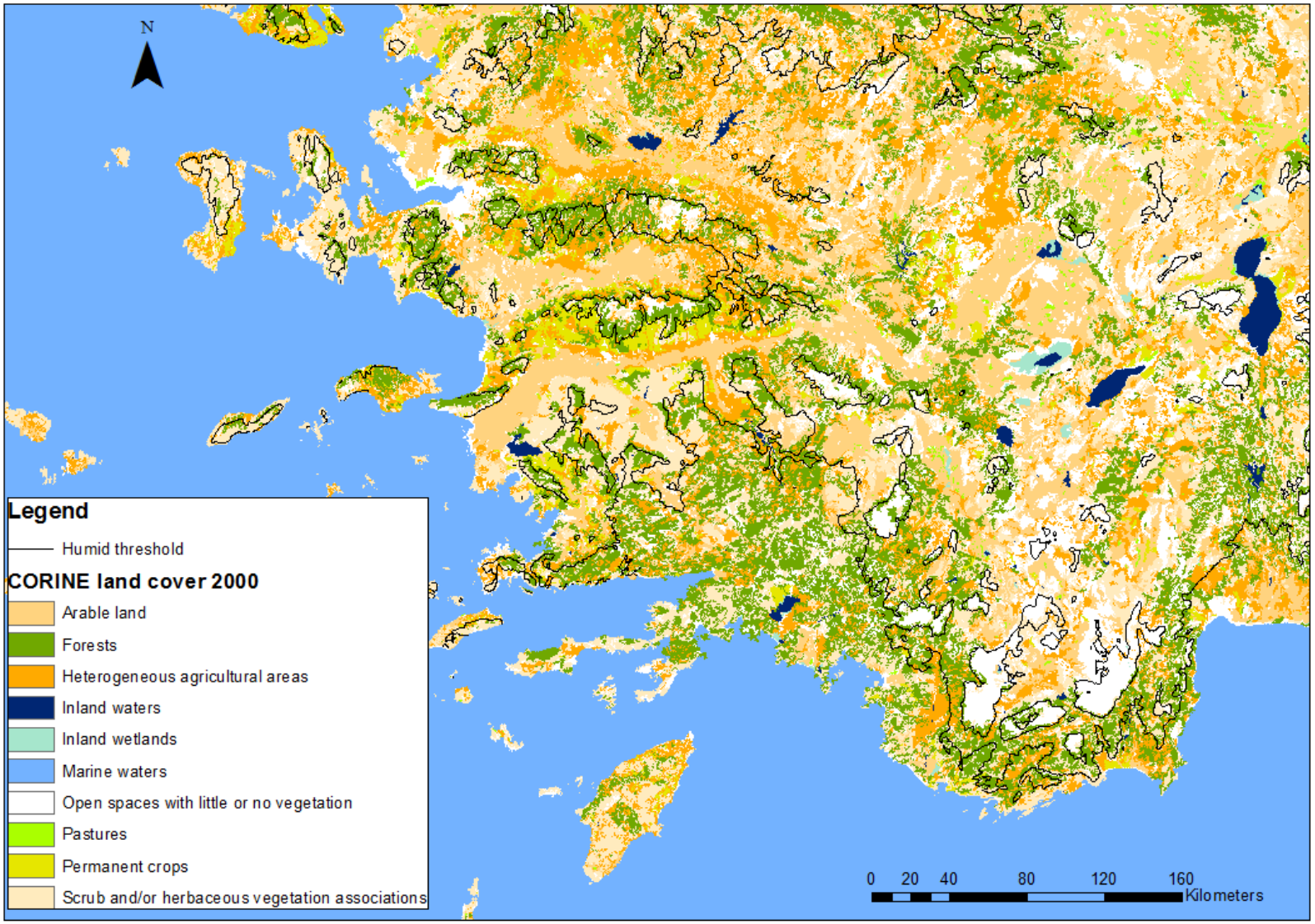


**Figure 10-7 CORINE land cover, overlaid with the isohume of humidity.**

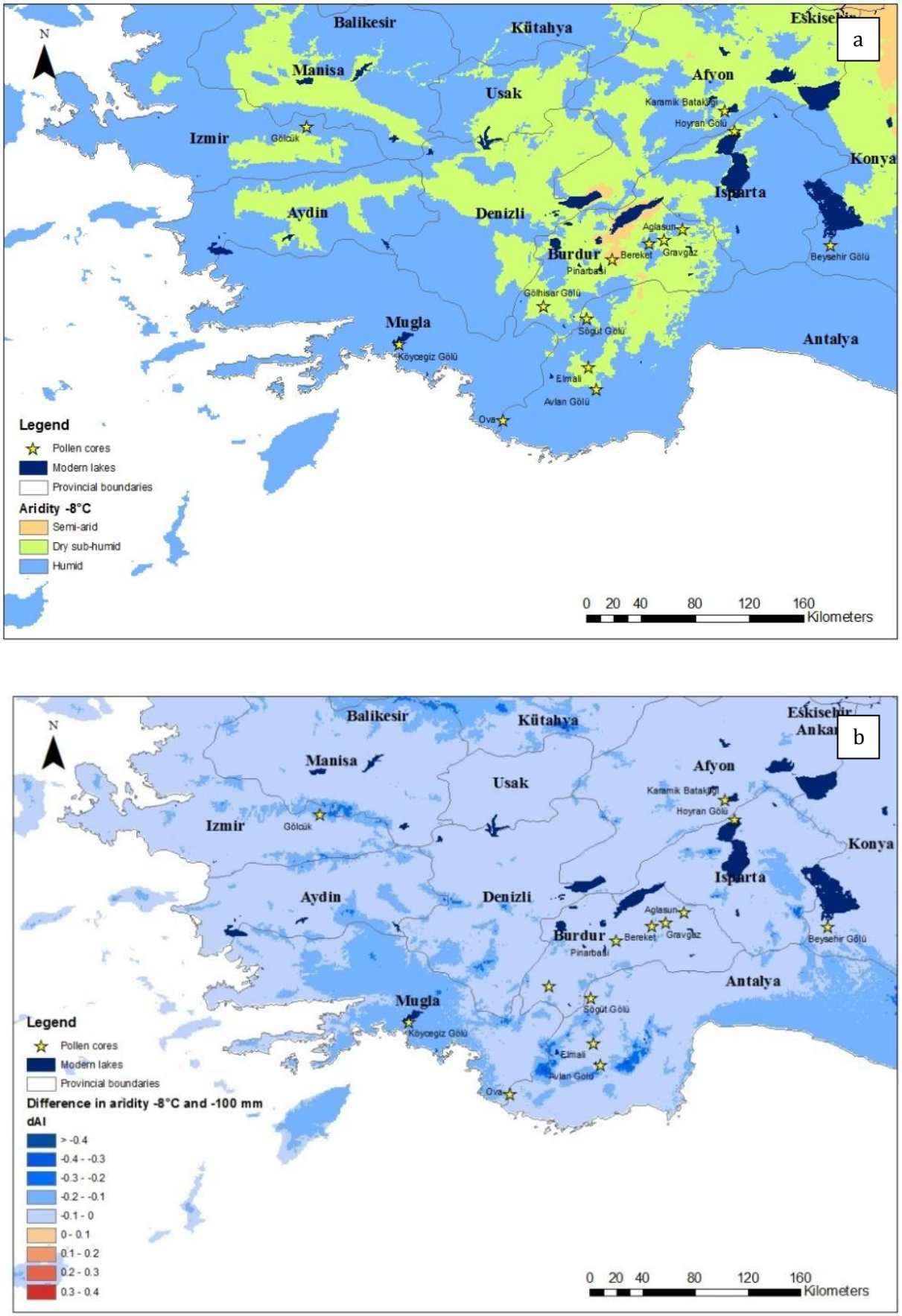


**Figure 10-8 (a) Aridity classification under -8°C temperature (b) Difference in aridity between modern values and -8°C with -100 mm, showing increase in humidity across most of the region.**

Conversely, under reduced precipitation or increased temperature, the southwest is likely to become more arid than modern values, with the coastal areas still having more humidity than the interior. The main difference between aridity due to reduced precipitation or aridity due to increased temperature, is that under increased temperatures coastal areas would become relatively more arid, but under decreased winter precipitation, more aridity would be seen in the interior.

Figure 10-8b demonstrates the potential humidity / aridity across the region if -8°C average temperatures were combined with -100 mm winter precipitation. The diagram shows the difference between the Aridity Index in the modern climate and the Aridity Index with -8°C and -100 mm. A greater increase in humidity is seen in the coastal regions, however the whole region shows an increase in humidity to a certain extent. Further iterations of this scenario have been run, again with low temperatures, but also with further decreasing precipitation. This shows that with -8°C average temperatures, even -200 mm precipitation (Figure 10-9a) can result in higher humidity in the coastal provinces of Muğla and Antalya than today. Conversely, and importantly, the provinces of Konya and Afyon may show a tendency for greater aridity.

Finally, with a decrease of 8°C average temperature, and -300 mm winter precipitation it is likely to be the case that some coastal areas of southwest Turkey could still be classified as humid, although now most areas will become more arid than under modern conditions (Figure 10-9b)

In addition, an Aridity Index can be employed to look at insolation differences. It is known that insolation during the early Holocene increased in summer, and decreased in winter due to variations in orbital parameters (Kutzbach and Guetter 1986). Using the aridity index, the potential direct impact of solar radiation changes in the early Holocene on aridity in southwest Turkey can be calculated, and is shown in Figure 10-10. The figure shows the difference in aridity index between modern values and a scenario with 7% increased summer radiation, and 7% decrease winter radiation. Using this measure, it is calculated that it would have the effect of increasing humidity across the whole region; however a greater increase would be seen in the mountainous areas and at the coast compared to the interior. This can then be correlated with vegetation distribution.

A number of model runs were therefore investigated where more than one variable at once to assess how this affected the balance of aridity or humidity.

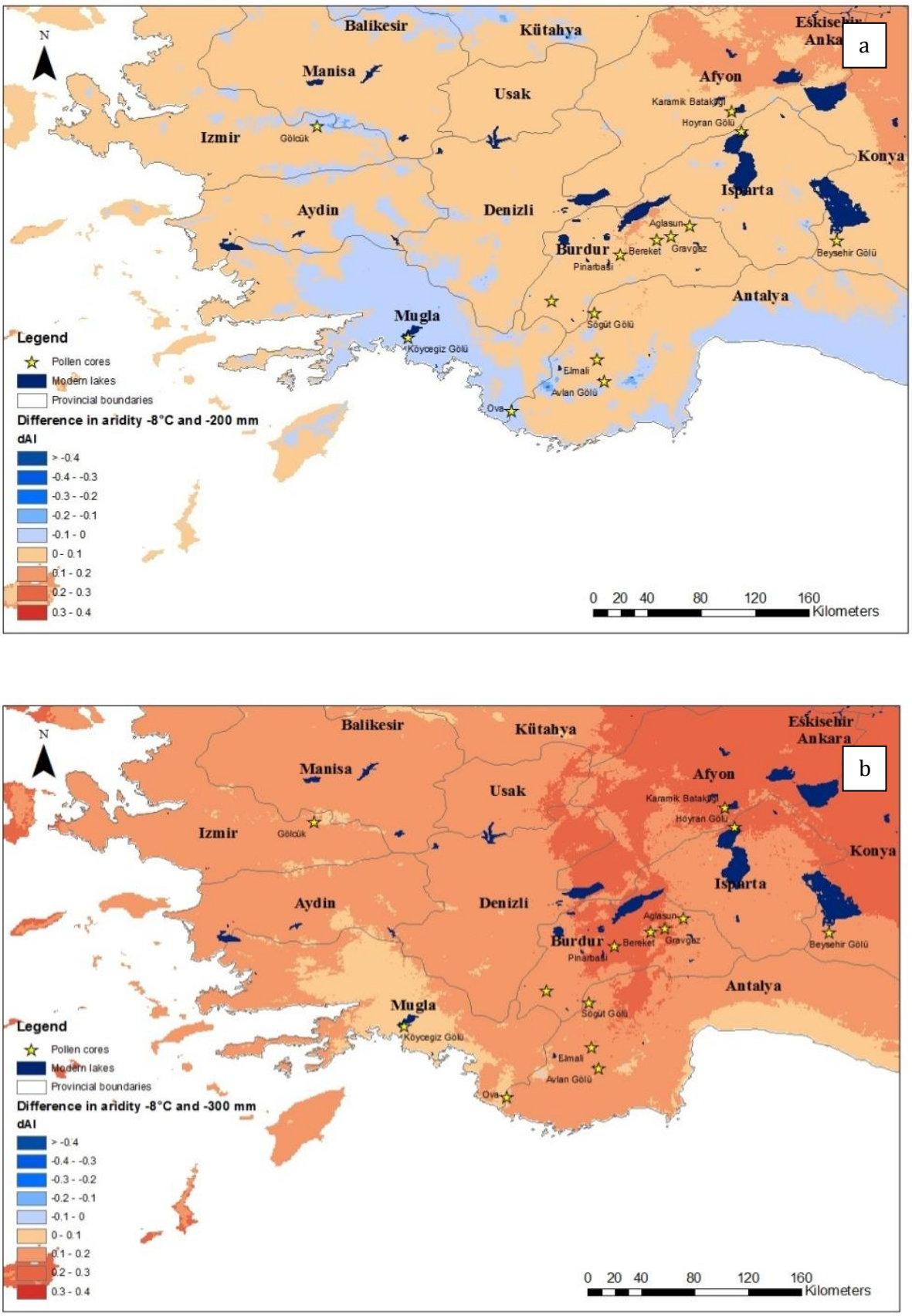





**Figure 10-9 (a) Difference in aridity between modern values and a scenario with -8°C and -200 mm winter precipitation, showing areas in Muğla and Antalya where humidity has increased, and areas in the interior where aridity has increased (b) Difference in aridity between modern values and -8°C with -300 mm, showing increase in aridity across most of the region.**

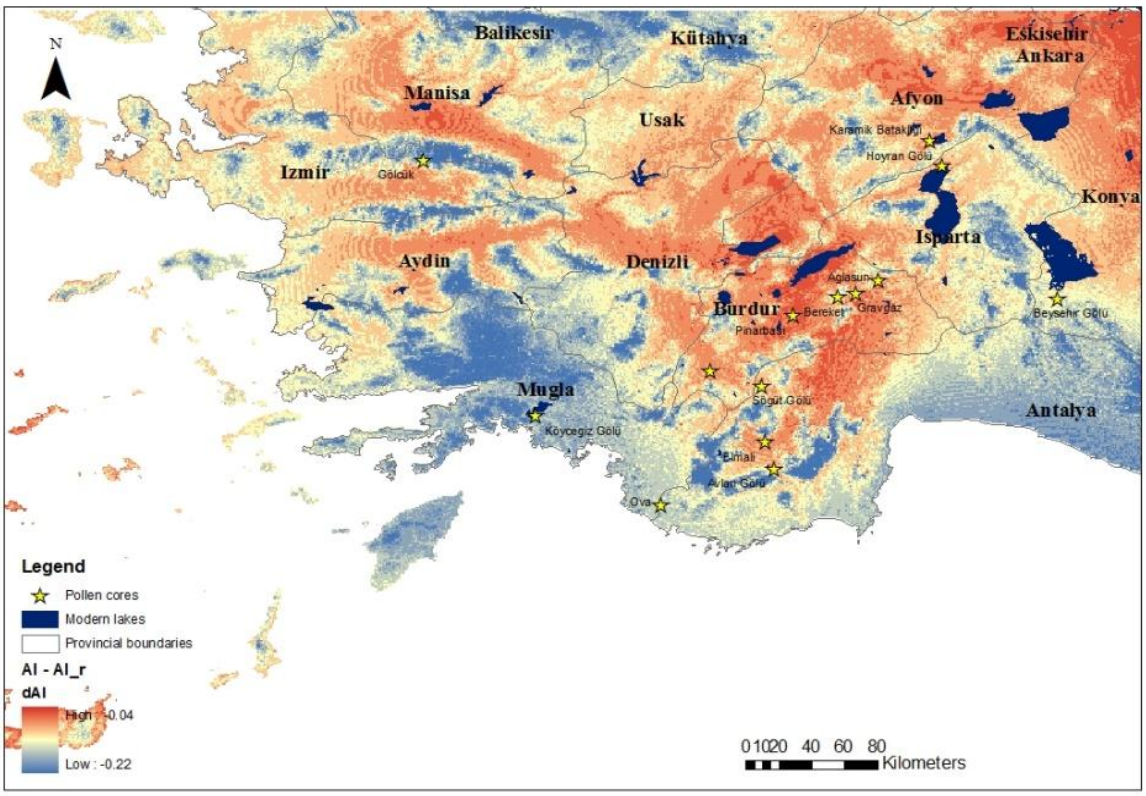


**Figure 10-10 The difference between modern aridity and potential aridity due to change in radiation at the beginning of the Holocene**

#### 10.1.4.2 Varying summer precipitation and temperature (S10)

Summer precipitation was also found to be a significant factor in the distribution of key species across Europe. Figure 10-11a displays the modern long term average summer precipitation. This shows that the western coastal areas of the region, such as the coasts of Aydın, Izmir and Muğla on average have less than 10 mm precipitation in summer. Most of the interior of the region has summer precipitation between 40-70 mm, and high elevation areas such as Afyon can have up to ~130 mm summer precipitation.

Considering Figure 10-12 land cover presently for areas with less than 20 mm summer precipitation is generally arable and heterogeneous agriculture areas, with some patchy forest and bare ground. Conversely, areas where summer precipitation is relatively high such as Bey Dağları and Uyluk Tepe have a relatively bare and open landscape. However, as previously discussed other climatic factors impact on the distribution of vegetation in these areas.

It has been hypothesized that changes in insolation at the beginning of the Holocene had an impact on atmospheric circulation, potentially leading to an intensification of Indian summer monsoonal rainfall and an increase in humidity in the northern borderlands of the eastern Mediterranean, i.e. Greece and Turkey (Rossignol-Strick 1987; Rohling and Hilgen 1991). This in turn may have led to an increase in summer depressions across the Eastern Mediterranean.

Therefore, as well as winter temperature and precipitation changes, summer increases in precipitation and temperature, and their impact on vegetation are also considered. A summer precipitation increase of 50 mm was modelled, which, unlike winter precipitation, mainly impacts the higher interior of the country, as these depressions tend to create orographic rainfall, as shown in Figure 10-11a. Alongside this, an increase in summer temperatures of 2°C was modelled.

When this situation of increase precipitation and temperature was modelled to examine humidity / aridity balance, it was found that the scenario would potentially lead to increased humidity in the interior of southwest Turkey, particularly southern- and eastern-facing slopes, whereas areas near the coast would be more likely to become more arid than under present conditions. Figure 10-11b displays this as the difference between modern aridity / humidity balance, and conditions under increased summer precipitation and temperature.

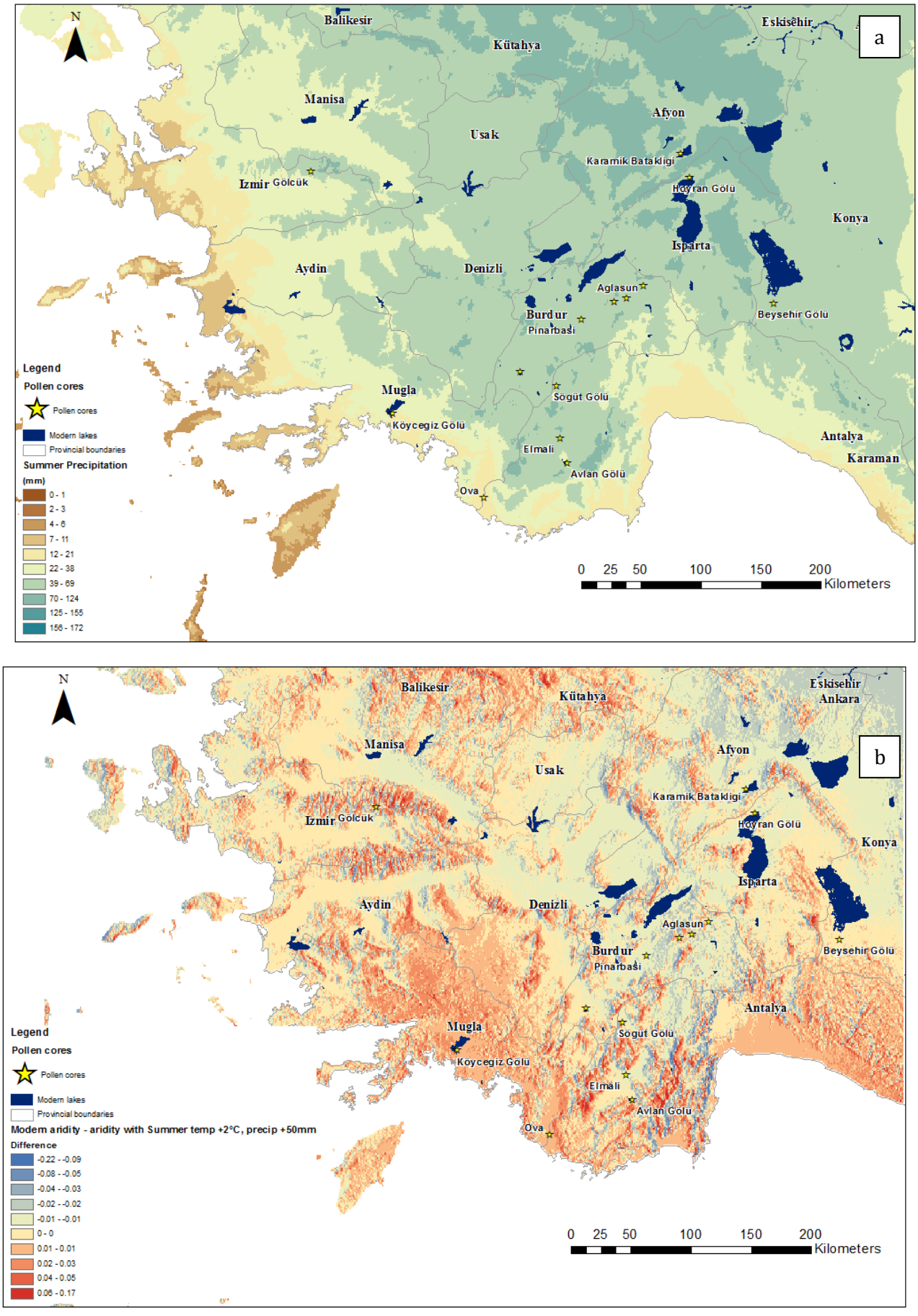


**Figure 10-11 (a) Summer precipitation +50 mm (b) The difference between modern aridity and aridity due to increased summer precipitation and temperature.**

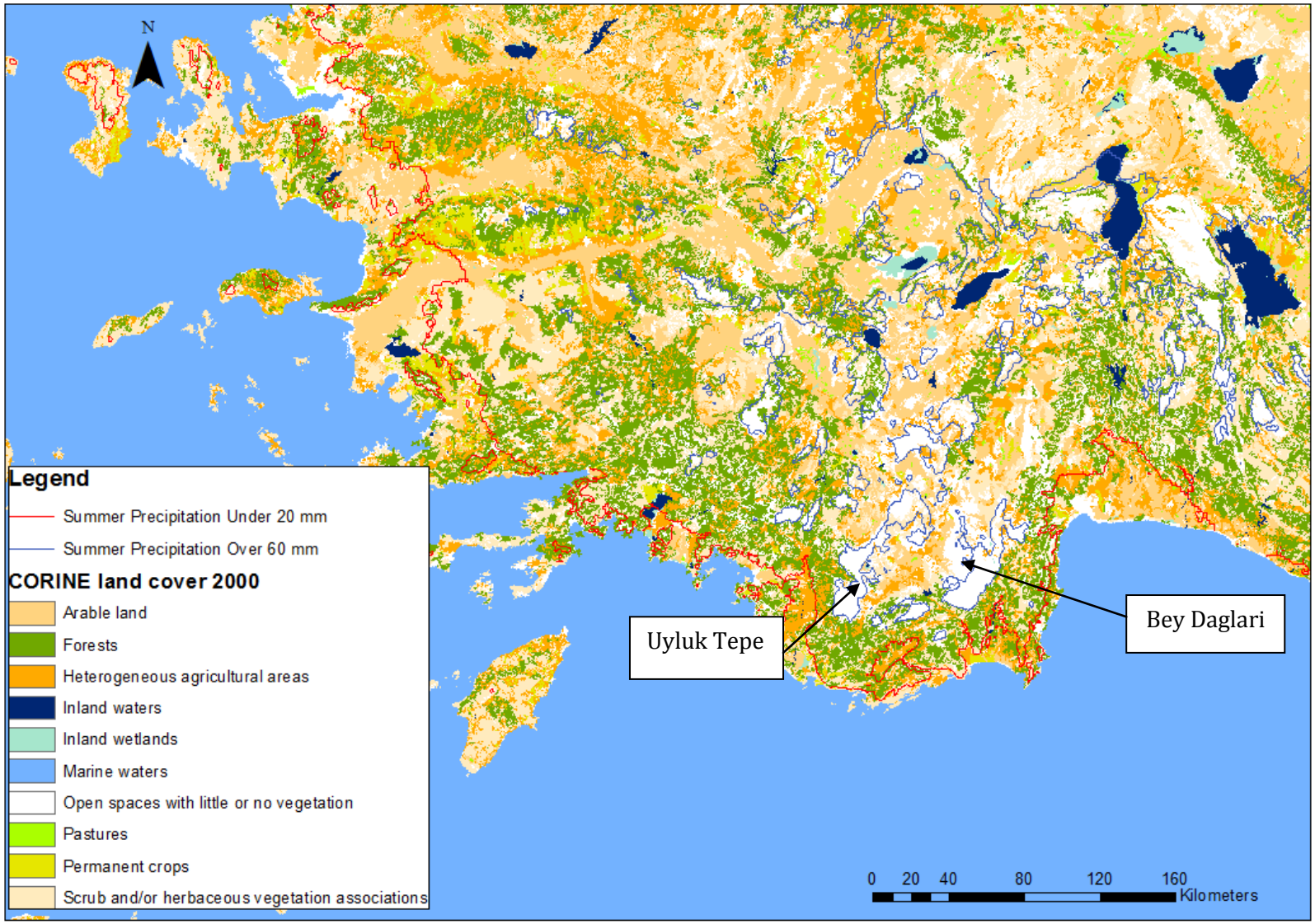


**Figure 10-12 CORINE land cover, overlaid with summer precipitation isohyets.**

# 11 APPENDIX: RADIOCARBON CALIBRATION AND BAYESIAN ANALYSIS

## 11.1 AĞLASUN POLLEN SEQUENCE 6

### 11.1.1 Calibration

| Name | Depth (m) | Uncal. BP | Calibrated (BP) | | | | | |
|---|---|---|---|---|---|---|---|---|
| **Aglasun 6** | | | **68.2% (1σ)** | | **95.4%(2σ)** | | **99.7% (3σ)** | |
| **P_sequence (0.1)** | | | **from** | **to** | **from** | **to** | **from** | **to** |
| R_Date GrN-26341 | 3.14 | 3390 ± 80 | 4777 | 4297 | 4811 | 4183 | 4830 | 4099 |
| R_Date GrN-26342 | 6.5 | 5730 ± 110 | 6651 | 6409 | 6775 | 6302 | 6937 | 6213 |
| R_Date GrN-26343 | 8.13 | 6910 ± 60 | 7820 | 7676 | 7922 | 7622 | 7935 | 7590 |
| R_Date GrN-26344 | 8.83 | 7220 ± 60 | 8155 | 7967 | 8170 | 7950 | 8204 | 7855 |
| R_Date GrN-26345 | 8.89 | 7730 ± 60 | 8579 | 8445 | 8606 | 8405 | 8724 | 8375 |

| Name | Depth (m) | Uncal. BP | Calibrated (BC/AD) | | | | | |
|---|---|---|---|---|---|---|---|---|
| **Aglasun 6** | | | **68.2% (1σ)** | | **95.4%(2σ)** | | **99.7% (3σ)** | |
| P_sequence (0.1) | | | **from** | **to** | **from** | **to** | **from** | **to** |
| R_Date GrN-26341 | 3.14 | 3390 ± 80 | -2828 | -2348 | -2862 | -2234 | -2881 | -2150 |
| R_Date GrN-26342 | 6.5 | 5730 ± 110 | -4702 | -4460 | -4826 | -4353 | -4988 | -4264 |
| R_Date GrN-26343 | 8.13 | 6910 ± 60 | -5871 | -5727 | -5973 | -5673 | -5986 | -5641 |
| R_Date GrN-26344 | 8.83 | 7220 ± 60 | -6206 | -6018 | -6221 | -6001 | -6255 | -5906 |
| R_Date GrN-26345 | 8.89 | 7730 ± 60 | -6630 | -6496 | -6657 | -6456 | -6775 | -6426 |

### 11.1.2 Model runs

| Model | U_seq. | K = 4 (4 cm) | K=1 (1 cm) | K=0.1 (1 mm) | K=0.01 (0.1mm) | Sequence (cal BP) |
|---|---|---|---|---|---|---|
| **A_model** | **26.3** | **38.5** | **67.5** | **98.8** | **96.9** | **98.9** |
| **A_overall** | **32.3** | **44.3** | **69.1** | **98.5** | **96.7** | **98.9** |
| **End of core (top)** | - | - | 2642 to 1622 | 3309 to 1039 | 4350 to 355 | 4798 to 1555 |
| **GrN-26341** | - | - | 4583 to 4100 | 4805 to 4160 | 4815 to 4236 | 4820 to 4241 |
| **GrN-26342** | - | - | 6833 to 6508 | 6790 to 6345 | 6779 to 6306 | 6775 to 6301 |
| **GrN-26343** | - | - | 7933 to 7766 | 7930 to 7670 | 7933 to 7653 | 7922 to 7623 |
| **GrN-26344** | - | - | 8104 to 7946 | 8156 to 7941 | 8168 to 7939 | 8170 to 7950 |
| **GrN-26345** | - | - | 8550 to 8390 | 8595 to 8406 | 8599 to 8405 | 8601 to 8405 |
| **Start of core (bottom)** | - | - | 9459 to 9059 | 9863 to 8785 | 11079 to 8418 | 12247 to 8405 |

### 11.1.1 **Modelled chronology**

| **Name** | **Modelled (BP)** | | | | | | **Modelled (BC/AD)** | | | | | | **Indices** | |
|---|---|---|---|---|---|---|---|---|---|---|---|---|---|---|
| **Aglasun 6** | **68.2% (1σ)** | | **95.4%(2σ)** | | **99.7% (3σ)** | | **68.2% (1σ)** | | **95.4%(2σ)** | | **99.7% (3σ)** | | **Amodel = 96.3** | **Aoverall = 96.3** |
| **P_sequence (0.1)** | **from** | **to** | **from** | **to** | **from** | **to** | **from** | **to** | **from** | **to** | **from** | **to** | **A** | **Convergence** |
| Boundary Top | 4445 | 3436 | 4720 | 2224 | ... | 602 | -2496 | -1487 | -2771 | -275 | ... | 1349 | 100 | 98 |
| A6-2b / A6-2c boundary | 4551 | 3918 | 4790 | 3100 | 4824 | 1677 | -2602 | -1969 | -2841 | -1151 | -2875 | 274 | | 99.9 |
| R_Date GrN-26341 | 4781 | 4299 | 4815 | 4234 | 4833 | 4147 | -2832 | -2350 | -2866 | -2285 | -2884 | -2198 | | 99.9 |
| Spectrum 13 / A6-2b boundary | 5019 | 4449 | 5516 | 4296 | 5965 | 4172 | -3070 | -2500 | -3567 | -2347 | -4016 | -2223 | 99.2 | 99.9 |
| A6-2a / Spectrum 13 boundary | 5970 | 5100 | 6308 | 4746 | 6554 | 4493 | -4021 | -3151 | -4359 | -2797 | -4605 | -2544 | | 99.8 |
| A6-1 / 2a boundary | 6605 | 6047 | 6739 | 5532 | 6890 | 5069 | -4656 | -4098 | -4790 | -3583 | -4941 | -3120 | | 99.9 |
| R_Date GrN-26342 | 6716 | 6436 | 6796 | 6311 | 6976 | 6274 | -4767 | -4487 | -4847 | -4362 | -5027 | -4325 | | 99.8 |
| R_Date GrN-26343 | 7819 | 7676 | 7922 | 7623 | 7935 | 7590 | -5870 | -5727 | -5973 | -5674 | -5986 | -5641 | 97 | 99.9 |
| R_Date GrN-26344 | 8155 | 7967 | 8170 | 7950 | 8204 | 7857 | -6206 | -6018 | -6221 | -6001 | -6255 | -5908 | 100 | 99.9 |
| R_Date GrN-26345 | 8543 | 8430 | 8599 | 8405 | 8700 | 8372 | -6594 | -6481 | -6650 | -6456 | -6751 | -6423 | 99.9 | 99.9 |
| Boundary Bottom | 8960 | 8457 | 9839 | 8411 | 11512 | ... | -7011 | -6508 | -7890 | -6462 | -9563 | ... | 100.5 | 97.8 |

### 11.1.2 **Age-depth plot**

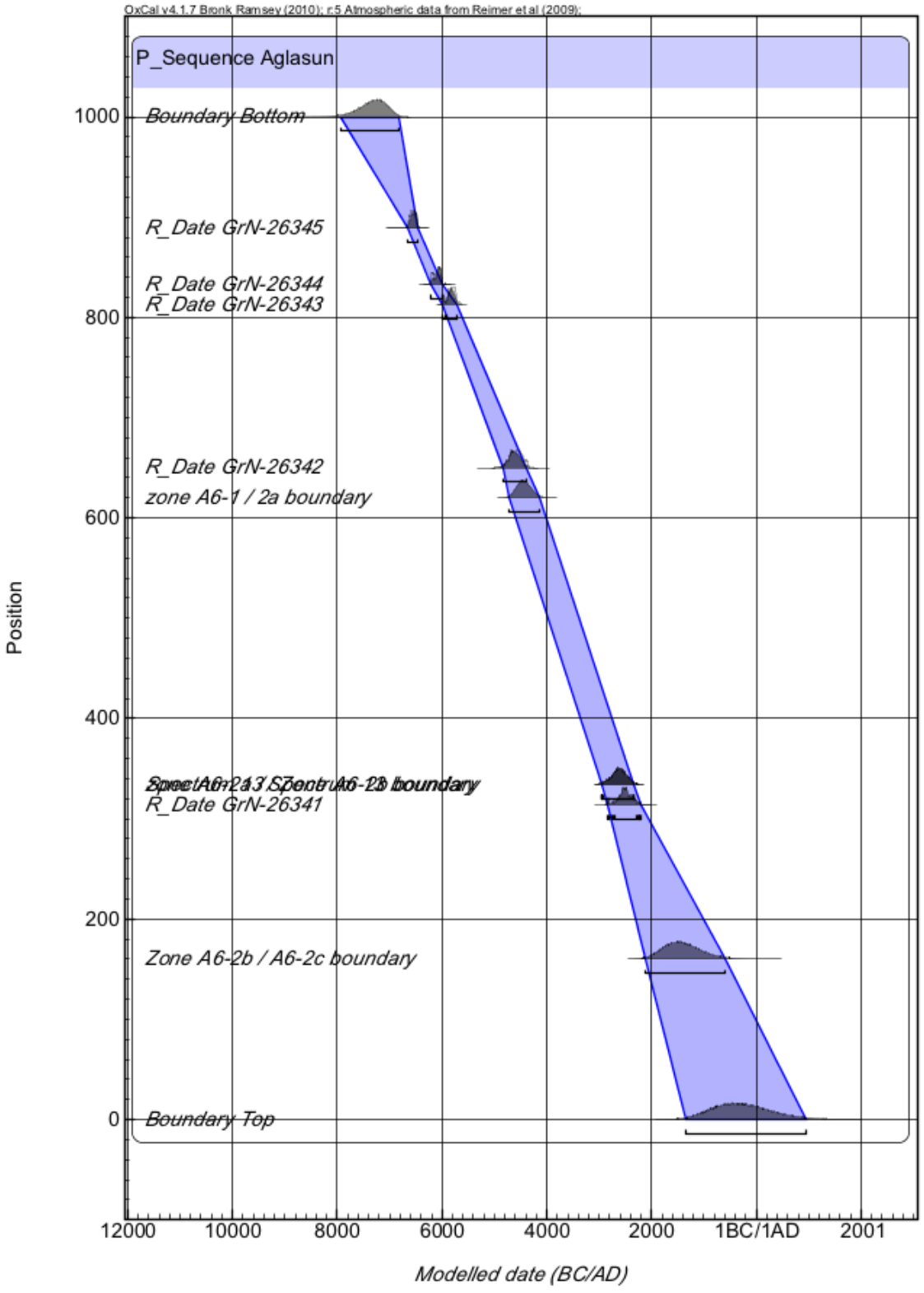

### 11.1.3 Pollen zone chronology and estimated archaeological period

| Zone | Highest Posterior Density beginning (68.2%) | | Estimated archaeological period | Uncertainty (years) |
|---|---|---|---|---|
| | Cal yr BP | Cal BC / AD | | |
| **Zone 1** | 9085 to 8460 | 7136 BC to 6511 BC | Aceramic Neolithic | 625 |
| **Zone 2a** | 6568 to 5793 | 4619 BC to 3844 BC | Chalcolithic | 775 |
| **Spectrum 13** | 6052 to 5021 | 4103 BC to 3072 BC | Chalcolithic | 1031 |
| **Zone 2b** | 5250 to 4471 | 3301 BC to 2522 BC | Chalcolithic - EBA | 779 |
| **Zone 2c** | 4563 to 3813 | 2614 BC to 1864 BC | EBA - MBA | 750 |
| **Top** | 4441 to 3212 | 2492 BC to 1263 BC | EBA - LBA | 1129 |

## 11.2 GOLHISAR

### 11.2.1 Calibration

| Name | Depth (m) | Uncal. | Calibrated (BP) | | | | | |
|---|---|---|---|---|---|---|---|---|
| Golhisar GHA | | | 68.2% (1σ) | | 95.4%(2σ) | | 99.7% (3σ) | |
| Simple Sequence | | | from | to | from | to | from | to |
| R_Date SRR 5184 | 1.63 | 2480±55 | 2710 | 2470 | 2722 | 2363 | 2746 | 2351 |
| R_Date SRR 5185 | 2.45 | 2830±50 | 3000 | 2864 | 3136 | 2792 | 3205 | 2771 |
| R_Date Beta 56673 | 2.71 | 3330±70 | 3638 | 3473 | 3811 | 3397 | 3834 | 3365 |
| R_Date SRR-5180 | 3.37 | 4900±75 | 5726 | 5585 | 5889 | 5471 | 5910 | 5326 |
| R_Date SRR-5181 | 5.39 | 6305±50 | 7270 | 7171 | 7415 | 7029 | 7420 | 7011 |
| R_Date SRR-5182 | 6.14 | 8015±60 | 9007 | 8777 | 9025 | 8648 | 9129 | 8599 |
| R_Date SRR-5183 | 6.95 | 8605±45 | 9602 | 9528 | 9682 | 9502 | 9738 | 9476 |

| Name | Depth (m) | Uncal. | Calibrated (BC/AD) | | | | | |
|---|---|---|---|---|---|---|---|---|
| Golhisar GHA | | | 68.2% (1σ) | | 95.4%(2σ) | | 99.7% (3σ) | |
| Simple Sequence | | | from | to | from | to | from | to |
| R_Date SRR 5184 | 1.63 | 2480±55 | -761 | -521 | -773 | -414 | -797 | -402 |
| R_Date SRR 5185 | 2.45 | 2830±50 | -1051 | -915 | -1187 | -843 | -1256 | -822 |
| R_Date Beta 56673 | 2.71 | 3330±70 | -1689 | -1524 | -1862 | -1448 | -1885 | -1416 |
| R_Date SRR-5180 | 3.37 | 4900±75 | -3777 | -3636 | -3940 | -3522 | -3961 | -3377 |
| R_Date SRR-5181 | 5.39 | 6305±50 | -5321 | -5222 | -5466 | -5080 | -5471 | -5062 |
| R_Date SRR-5182 | 6.14 | 8015±60 | -7058 | -6828 | -7076 | -6699 | -7180 | -6650 |
| R_Date SRR-5183 | 6.95 | 8605±45 | -7653 | -7579 | -7733 | -7553 | -7789 | -7527 |

### 11.2.2 **Model runs**

| **Model** | U_sequence | K = 4 (4 cm) | K=1 (1 cm) | K=0.1 (1mm) | K=0.01 (0.1mm) | Sequence (cal BP) |
|---|---|---|---|---|---|---|
| **A_model** | A_model = | A_model = | A_model= 0.8 | A_model = 77.1 | A_model = 101 | A_model = 100.9 |
| **A_overall** | A_overall = | A_overall = | A_overall = 1 | A_overall = 77.9 | A_overall = 100.9 | A_overall = 100.9 |
| End of core (top) | NA | NA | 548 to -49 | 1328 to -49 | 2660 to 249 | 2716 to 423 |
| SRR-5184 | NA | NA | 2494 to 2345 | 2669 to 2352 | 2739 to 2369 | 2736 to 2368 |
| SRR-5185 | NA | NA | **3334 to 3125** | 3204 to 2870 | 3138 to 2793 | 3079 to 2792 |
| Beta 56673 | NA | NA | 3829 to 3547 | 3721 to 3399 | 3716 to 3390 | 3811 to 3396 |
| SRR-5180 | NA | NA | **5344 to 5073** | 5741 to 5327 | 5887 to 5469 | 5889 to 5471 |
| SRR-5181 | NA | NA | 7425 to 7254 | 7417 to 7162 | 7416 to 7031 | 7415 to 7029 |
| SRR-5182 | NA | NA | **8759 to 8592** | 9000 to 8641 | 9026 to 8648 | 9025 to 8648 |
| SRR-5183 | NA | NA | 9696 to 9525 | 9686 to 9518 | 9675 to 9500 | 9678 to 9500 |
| Start of core (bottom) | NA | NA | 9788 to 9562 | 9889 to 9502 | 10044 to 9482 | 13545 to 9502 |

## 11.2.3 **Modelled chronology**

| **Name** | **Modelled (BP)** | | | | | | **Modelled (BC/AD)** | | | | | | **Indices** | |
|---|---|---|---|---|---|---|---|---|---|---|---|---|---|---|
| **Golhisar GHA** | **68.2% (1σ)** | | **95.4%(2σ)** | | **99.7% (3σ)** | | **68.2% (1σ)** | | **95.4%(2σ)** | | **99.7% (3σ)** | | **Amodel = 96.3** | **Aoverall = 96.3** |
| **Simple Sequence** | **from** | **to** | **from** | **to** | **from** | **to** | **from** | **to** | **from** | **to** | **from** | **to** | **A** | **Convergence** |
| Top Boundary | 2448 | 1378 | 2589 | 351 | 2622 | -45 | 1998 | 1999 | 1998 | 1999 | 1998 | 1999 | | 99.5 |
| zone 4b/5 | 2597 | 1961 | 2702 | 1136 | 2731 | 348 | -499 | 572 | -640 | 1599 | -673 | 1995 | | 99.9 |
| SRR 5184 R_Date(2480,55) | 2617 | 2364 | 2704 | 2359 | 2740 | 2349 | -648 | -12 | -753 | 814 | -782 | 1602 | 98.1 | 100 |
| zone 4a/4b | 2803 | 2538 | 2910 | 2415 | 3015 | 2364 | -668 | -415 | -755 | -410 | -791 | -400 | | 100 |
| SRR 5185 R_Date(2830,50) | 3004 | 2866 | 3137 | 2800 | 3205 | 2777 | -854 | -589 | -961 | -466 | -1066 | -415 | 99.9 | 100 |
| zone 3/4a | 3284 | 2958 | 3490 | 2888 | 3644 | 2814 | -1001 | -765 | -1092 | -610 | -1183 | -488 | | 100 |
| Beta 56673 R_Date(3330,70) | 3680 | 3485 | 3822 | 3406 | 3840 | 3370 | -1055 | -917 | -1188 | -851 | -1256 | -828 | 98.3 | 99.9 |
| zone 2b/3 | 4560 | 3596 | 5249 | 3510 | 5598 | 3442 | -1335 | -1009 | -1541 | -939 | -1695 | -865 | | 99.9 |
| SRR-5180 R_Date(4900,75) | 5728 | 5585 | 5889 | 5472 | 5909 | 5328 | -1622 | -1288 | -1721 | -1086 | -1850 | -976 | 99.8 | 99.9 |
| zone 2a/2b | 7042 | 5874 | 7218 | 5670 | 7323 | 5501 | -1731 | -1536 | -1873 | -1457 | -1891 | -1421 | | 99.9 |
| SRR-5181 R_Date(6305,50) | 7271 | 7172 | 7416 | 7031 | 7421 | 7014 | -2611 | -1647 | -3300 | -1561 | -3649 | -1493 | 99.7 | 100 |
| SRR-5182 R_Date(8015,60) | 9007 | 8778 | 9025 | 8648 | 9130 | 8599 | -3687 | -2729 | -3768 | -2013 | -3901 | -1702 | 99.9 | 99.9 |
| SRR-5183 R_Date(8605,45) | 9598 | 9528 | 9675 | 9500 | 9732 | 9476 | -3779 | -3636 | -3940 | -3523 | -3960 | -3379 | 103.3 | 99.9 |
| zone 1/2a | 10125 | 9542 | 11293 | 9509 | 13372 | 9484 | -5093 | -3925 | -5269 | -3721 | -5374 | -3552 | | 99.9 |
| Bottom Boundary | 10766 | 9628 | 12392 | 9552 | 14964 | ... | -5322 | -5223 | -5467 | -5082 | -5472 | -5065 | | 97.5 |

## 11.2.4 **Age-depth plot**

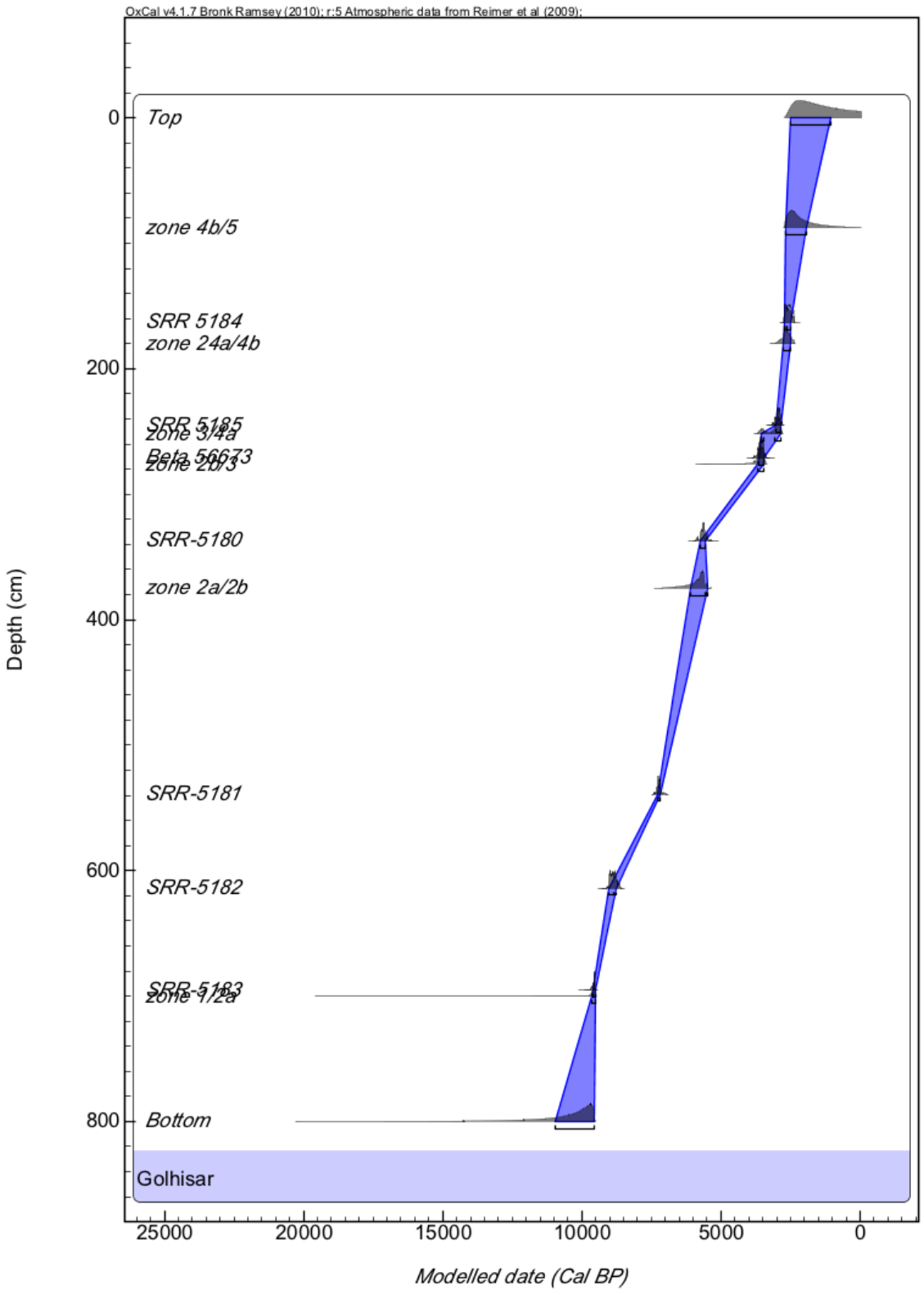

### 11.2.5 **Pollen zone chronology and estimated archaeological period**

| Zone | Highest Posterior Density beginning (68.2%) | | Estimated archaeological period | Uncertainty (years) |
|---|---|---|---|---|
| | Cal yr BP | Cal BC / AD | | |
| **Zone 1** | 10766 to 9628 | 8817 BC to 7679 BC | Epipalaeolithic-Neolithic | 1138 |
| **Zone 2a** | 10125 to 9542 | 8176 BC to 7593 BC | Aceramic Neolithic | 583 |
| **Zone 2b** | 7042 to 5874 | 5093 BC to 3925 BC | Chalcolithic | 1168 |
| **Zone 3** | 4560 to 3596 | 2611 BC to 1647 BC | EBA - MBA | 964 |
| **Zone 4a** | 3284 to 2958 | 1335 BC to 1009 BC | LBA - ADA | 326 |
| **Zone 4b** | 2803 to 2538 | 854 BC to 589 BC | ADA-Lydian | 265 |
| **Zone 5** | 2597 to 1961 | 648 BC to 12 BC | Lydian - Roman | 636 |
| **Top** | 2448 to 1378 | 499 BC to AD 572 | Achaemenid - Late Roman | 1070 |

## 11.3 AĞLASUN 12

### 11.3.1 Calibration

| Name | Depth (m) | Uncal. | Calibrated (BP) | | | | | |
|---|---|---|---|---|---|---|---|---|
| Aglasun 12 | | | 68.2% (1σ) | | 95.4%(2σ) | | 99.7% (3σ) | |
| P_sequence (0.01) | | | from | to | from | to | from | to |
| R_Date OS-33145 | 1.85 | 1580±30 | 1518 | 1417 | 1535 | 1403 | 1561 | 1367 |
| R_Date OS-33146 | 4.75 | 6530±45 | 7489 | 7419 | 7560 | 7327 | 7571 | 7310 |
| R_Date GrN-26691 | 5.57 | 7080±90 | 7998 | 7799 | 8151 | 7689 | 8177 | 7666 |
| R_Date GrN-26692 | 6.39 | 7310±100 | 8280 | 8008 | 8341 | 7960 | 8405 | 7852 |
| R_Date GrA-19428 | 7.57 | 7410±50 | 8312 | 8182 | 8365 | 8058 | 8380 | 8035 |

| Name | Depth (m) | Uncal. | Calibrated (BC/AD) | | | | | |
|---|---|---|---|---|---|---|---|---|
| Aglasun 12 | | | 68.2% (1σ) | | 95.4%(2σ) | | 99.7% (3σ) | |
| R_Date OS-33145 | 1.85 | 1580±30 | 433 | 534 | 415 | 547 | 389 | 584 |
| R_Date OS-33146 | 4.75 | 6530±45 | -5540 | -5470 | -5611 | -5378 | -5622 | -5361 |
| R_Date GrN-26691 | 5.57 | 7080±90 | -6049 | -5850 | -6202 | -5740 | -6228 | -5717 |
| R_Date GrN-26692 | 6.39 | 7310±100 | -6331 | -6059 | -6392 | -6011 | -6456 | -5903 |
| R_Date GrA-19428 | 7.57 | 7410±50 | -6363 | -6233 | -6416 | -6109 | -6431 | -6086 |

### 11.3.2 **Model runs**

| Event | U_sequence | K = 4 (4 cm) | K=1 (1 cm) | K=0.1 (1 mm) | K=0.01 (0.1mm) | Sequence (cal BP) |
|---|---|---|---|---|---|---|
| | A_model = | A_model = | A_model= | A_model = 31.4 | A_model = 54 | A_model = 47.5 |
| | A_overall = | A_overall = | A_overall = | A_overall = 38 | A_overall = 70.5 | A_overall = 60.8 |
| End of core (top) | N/A | N/A | N/A | 471 to -52 | 1396 to -45 | 856 to -52 |
| OS-33145 | N/A | N/A | N/A | 1540 to 1409 | 1536 to 1405 | 1538 to 1406 |
| OS 33146 | N/A | N/A | N/A | 7505 to 7320 | 7562 to 7329 | 7560 to 7327 |
| GrN26691 | N/A | N/A | N/A | **7818 to 7609** | 8010 to 7690 | 8006 to 7694 |
| GrN26692 | N/A | N/A | N/A | 8201 to 7996 | 8316 to 7983 | 8305 to 7988 |
| OS-33147 | N/A | N/A | N/A | 8387 to 8251 | **8379 to 8203** | 8368 to 8198 |
| GRrA19428 | N/A | N/A | N/A | **8400 to 8305** | 8380 to 8208 | 8380 to 8228 |
| Start of core (bottom) | N/A | N/A | N/A | 9360 to 8429 | 10380 to 9628 | 10863 to 8223 |

## 11.3.3 **Modelled chronology**

| **Name** | **Modelled (BP)** | | | | | | **Modelled (BC/AD)** | | | | | | **Indices** | |
|---|---|---|---|---|---|---|---|---|---|---|---|---|---|---|
| **Aglasun 12** | **68.2% (1σ)** | | **95.4%(2σ)** | | **99.7% (3σ)** | | **68.2% (1σ)** | | **95.4%(2σ)** | | **99.7% (3σ)** | | **Amodel = 96.3** | **Aoverall = 96.3** |
| **Simple Sequence** | **from** | **to** | **from** | **to** | **from** | **to** | **from** | **to** | **from** | **to** | **from** | **to** | **A** | **Convergence** |
| Top Boundary | -51 | -52 | -51 | -52 | -51 | -52 | 589 | 1747 | 587 | 1996 | 483 | 2003 | 100 | 100 |
| Zone A12-2d/A12-2e boundary | 1322 | 264 | 1361 | -46 | 1469 | -52 | 547 | 1384 | 495 | 1876 | 461 | 1996 | | 97.3 |
| Zone A12-2c/A12-2d boundary | 1400 | 549 | 1450 | 63 | 1487 | -47 | 470 | 1058 | 435 | 1640 | 421 | 1927 | | 98.1 |
| Zone A12-2b/A12-2c boundary | 1485 | 895 | 1515 | 300 | 1529 | 19 | 434 | 815 | 417 | 1396 | 401 | 1820 | | 99.5 |
| Zone A12-2a/A12-2b boundary | 1516 | 1136 | 1534 | 543 | 1551 | 142 | 424 | 633 | 404 | 1147 | 386 | 1655 | | 99.4 |
| OS-33145 R_Date(1580,30) | 1526 | 1318 | 1546 | 811 | 1564 | 306 | 430 | 525 | 414 | 545 | 387 | 583 | | 99.6 |
| Zone A12-1b/A12-2a boundary | 1521 | 1426 | 1536 | 1405 | 1563 | 1368 | -5512 | -2492 | -5534 | -388 | -5566 | 368 | 99.7 | 99.9 |
| OS-33146 R_Date(6530,45) | 7459 | 4344 | 7485 | 2303 | 7526 | 1591 | -5541 | -5471 | -5613 | -5379 | -5622 | -5363 | | 99.1 |
| GrN-26691 R_Date(7080,90) | 7490 | 7420 | 7562 | 7328 | 7572 | 7312 | -6012 | -5841 | -6057 | -5742 | -6161 | -5668 | 99.6 | 99.9 |
| Zone A12-1a/A12-1b boundary | 7962 | 7789 | 8007 | 7691 | 8110 | 7619 | -6145 | -5935 | -6241 | -5821 | -6328 | -5746 | 97.1 | 99.8 |
| GrN-26692 R_Date(7310,100) | 8097 | 7886 | 8192 | 7776 | 8270 | 7700 | -6236 | -6081 | -6327 | -6022 | -6383 | -5977 | | 98.5 |
| GrA-19428 R_Date(7410,50) | 8185 | 8030 | 8277 | 7972 | 8331 | 7927 | -6371 | -6238 | -6412 | -6217 | -6433 | -6109 | 111.7 | 99.9 |
| Bottom Boundary | 8320 | 8188 | 8361 | 8166 | 8382 | 8055 | -6677 | -6227 | -8416 | ... | -11914 | ... | 103 | 99.8 |

## 11.3.4 **Age-depth plot**

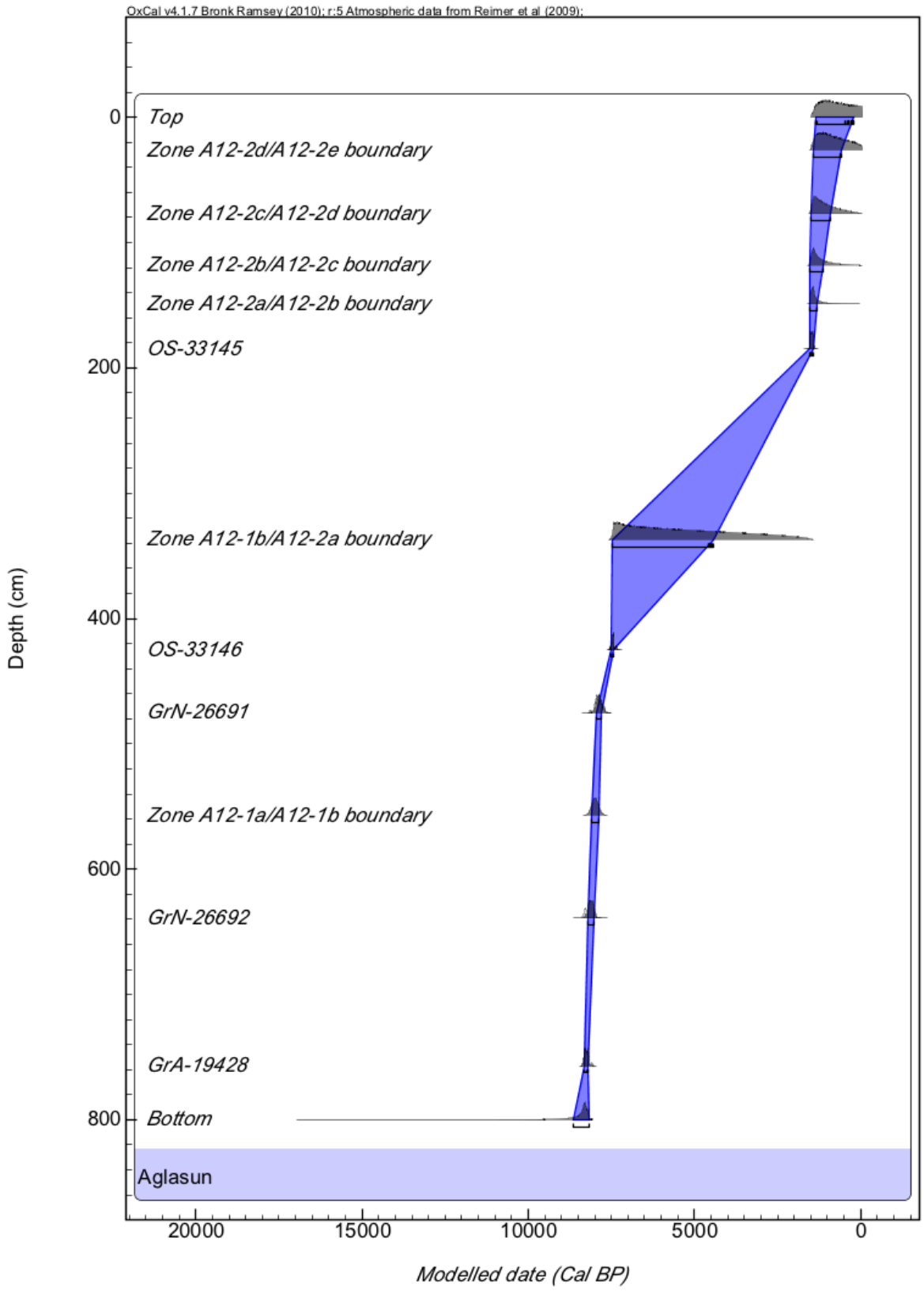

### 11.3.5 **Pollen zone chronology and estimated archaeological period**

| Zone | Highest Posterior Density beginning (68.2%) | |
|---|---|---|
| | Cal yr BP | Cal BC / AD |
| Zone 1a | 8616 to 8177 | 6667 BC to 6228 BC |
| Zone 1b | 8093 to 7881 | 6144 BC to 5932 BC |
| Zone 2a | 7460 to 4375 | 5511 BC to 2426 BC |
| Zone 2b | 1526 to 1320 | AD 425 to AD 630 |
| Zone 2c | 1517 to 1141 | 434 to AD 809 |
| Zone 2d | 1482 to 884 | 468 to AD 1066 |
| Zone 2e | 1410 to 558 | 504 to AD 1393 |
| Top | 1332 to 315 | 618 to AD 1635 |

## 11.4 GRAVGAZ

### 11.4.1 Calibration

| Name | Depth (m) | Uncal. | Calibrated (BP) | | | | | |
|---|---|---|---|---|---|---|---|---|
| Gravgaz | | | 68.2% (1σ) | | 95.4%(2σ) | | 99.7% (3σ) | |
| Simple Sequence | | | from | to | from | to | from | to |
| R_date GrA-19895 | 0.99 | 1010±50 | 971 | 802 | 1052 | 793 | 1065 | 740 |
| R_date OS-25651 | 1.61 | 1410±55 | 1358 | 1285 | 1412 | 1185 | 1518 | 1175 |
| R_Date Beta-142070 | 4.21 | 2220±50 | 2320 | 2156 | 2341 | 2125 | 2353 | 2009 |
| R_Date Beta-142069 | 4.45 | 2270±50 | 2345 | 2180 | 2353 | 2152 | 2468 | 2065 |
| R_Date OS-25652 | 5.79 | 2400±45 | 2650 | 2349 | 2700 | 2341 | 2716 | 2331 |
| R_Date Beta-142073 | 7.54 | 2520±40 | 2730 | 2501 | 2746 | 2466 | 2751 | 2362 |

| Name | Depth (m) | Uncal. | Calibrated (BC/AD) | | | | | |
|---|---|---|---|---|---|---|---|---|
| Gravgaz | | | 68.2% (1σ) | | 95.4%(2σ) | | 99.7% (3σ) | |
| R_date GrA-19895 | 0.99 | 1010±50 | 979 | 1148 | 898 | 1157 | 885 | 1210 |
| R_date OS-25651 | 1.61 | 1410±55 | 592 | 665 | 539 | 765 | 432 | 775 |
| R_Date Beta-142070 | 4.21 | 2220±50 | -371 | -207 | -392 | -176 | -404 | -60 |
| R_Date Beta-142069 | 4.45 | 2270±50 | -396 | -231 | -404 | -203 | -519 | -116 |
| R_Date OS-25652 | 5.79 | 2400±45 | -701 | -400 | -751 | -392 | -767 | -382 |
| R_Date Beta-142073 | 7.54 | 2520±40 | -781 | -552 | -797 | -517 | -802 | -413 |

### 11.4.2 **Model runs**

| Event | U_sequence | K = 4 (4 cm) | K=1 (1 cm) | K=0.1 (0.1mm) | K=0.01 (0.1mm) | Sequence (cal BP) |
|---|---|---|---|---|---|---|
| | A_model = | A_model = | A_model= 0.6 | A_model =89.4 | A_model = 109.8 | A_model = 105.9 |
| | A_overall = | A_overall = | A_overall = 0.6 | A_overall = 88.7 | A_overall = 109.8 | A_overall = 106 |
| End of core (top) | N/A | N/A | N/A | 957 to 487 | 1047 to 220 | 1038 to 93 |
| GrA-19895 | N/A | N/A | N/A | 1171 to 895 | 1057 to 799 | 1055 to 797 |
| OS-25651 | N/A | N/A | N/A | 1386 to 1182 | 1408 to 1184 | 1412 to 1186 |
| Beta-142070 | N/A | N/A | N/A | 2225 to 2066 | 2338 to 2147 | 2330 to 2070 |
| Beta-142069 | N/A | N/A | N/A | 2262 to 2148 | 2348 to 2156 | 2355 to 2176 |
| OS-25652 | N/A | N/A | N/A | 2486 to 2350 | 2608 to 2338 | 2670 to 2339 |
| Beta-142073 | N/A | N/A | N/A | 2752 to 2616 | 2743 to 2490 | 2742 to 2468 |
| Start of core (bottom) | N/A | N/A | N/A | 2849 to 2849 | 2914 to 2459 | 4105 to 2419 |

## 11.4.3 **Modelled chronology**

| **Name** | **Modelled (BP)** | | | | | | **Modelled (BC/AD)** | | | | | | **Indices** | |
|---|---|---|---|---|---|---|---|---|---|---|---|---|---|---|
| **Aglasun 12** | **68.2% (1σ)** | | **95.4%(2σ)** | | **99.7% (3σ)** | | **68.2% (1σ)** | | **95.4%(2σ)** | | **99.7% (3σ)** | | **Amodel = 96.3** | **Aoverall = 96.3** |
| **P_Sequence(0.01)** | **from** | **to** | **from** | **to** | **from** | **to** | **from** | **to** | **from** | **to** | **from** | **to** | **A** | **Convergence** |
| Core taken C_Date(2002) | -51 | -52 | -51 | -52 | -51 | -52 | 2001 | 2002 | 2001 | 2002 | 2001 | 2002 | 100 | 100 |
| Top Boundary | 968 | 633 | 1047 | 216 | 1055 | -52 | 982 | 1317 | 903 | 1735 | 896 | 2003 | | 99.9 |
| GrA-19895 R_Date(1010,50) | 1052 | 838 | 1058 | 799 | 1170 | 762 | 899 | 1113 | 893 | 1152 | 781 | 1189 | 98.8 | 100 |
| OS-25651 R_Date(1410,55) | 1354 | 1284 | 1409 | 1183 | 1516 | 1172 | 596 | 667 | 542 | 767 | 435 | 778 | 100.3 | 99.9 |
| zone 2b/3 | 1416 | 1278 | 1722 | 1182 | 2072 | 1172 | 534 | 672 | 229 | 768 | -123 | 779 | | 99.5 |
| zone 2a/2b | 2302 | 1916 | 2328 | 1579 | 2340 | 1375 | -353 | 34 | -379 | 371 | -391 | 575 | | 99.8 |
| Beta-142070 R_Date(2220,50) | 2323 | 2156 | 2338 | 2146 | 2349 | 2065 | -374 | -207 | -389 | -197 | -400 | -116 | 106.1 | 99.4 |
| Beta-142069 R_Date(2270,50) | 2340 | 2180 | 2348 | 2156 | 2360 | 2135 | -391 | -231 | -399 | -207 | -411 | -186 | 102.4 | 99.1 |
| zone 1c/2a | 2343 | 2183 | 2359 | 2156 | 2458 | 2130 | -394 | -234 | -410 | -207 | -509 | -181 | | 98.8 |
| zone 1b/1c | 2455 | 2350 | 2654 | 2313 | 2680 | 2239 | -506 | -401 | -705 | -364 | -731 | -290 | | 98.9 |
| OS-25652 R_Date(2400,45) | 2452 | 2353 | 2609 | 2338 | 2680 | 2330 | -503 | -404 | -660 | -389 | -731 | -381 | 114.7 | 98.8 |
| zone 1a/1b | 2616 | 2433 | 2710 | 2392 | 2736 | 2358 | -667 | -484 | -761 | -443 | -787 | -409 | | 99.7 |
| Beta-142073 R_Date(2520,40) | 2730 | 2511 | 2743 | 2489 | 2755 | 2398 | -781 | -562 | -794 | -540 | -806 | -449 | 102.8 | 98.2 |
| Bottom Boundary | 2742 | 2513 | 2906 | 2458 | 3635 | ... | -793 | -564 | -957 | -509 | -1686 | ... | | 97.9 |

## 11.4.4 **Age-depth plot**

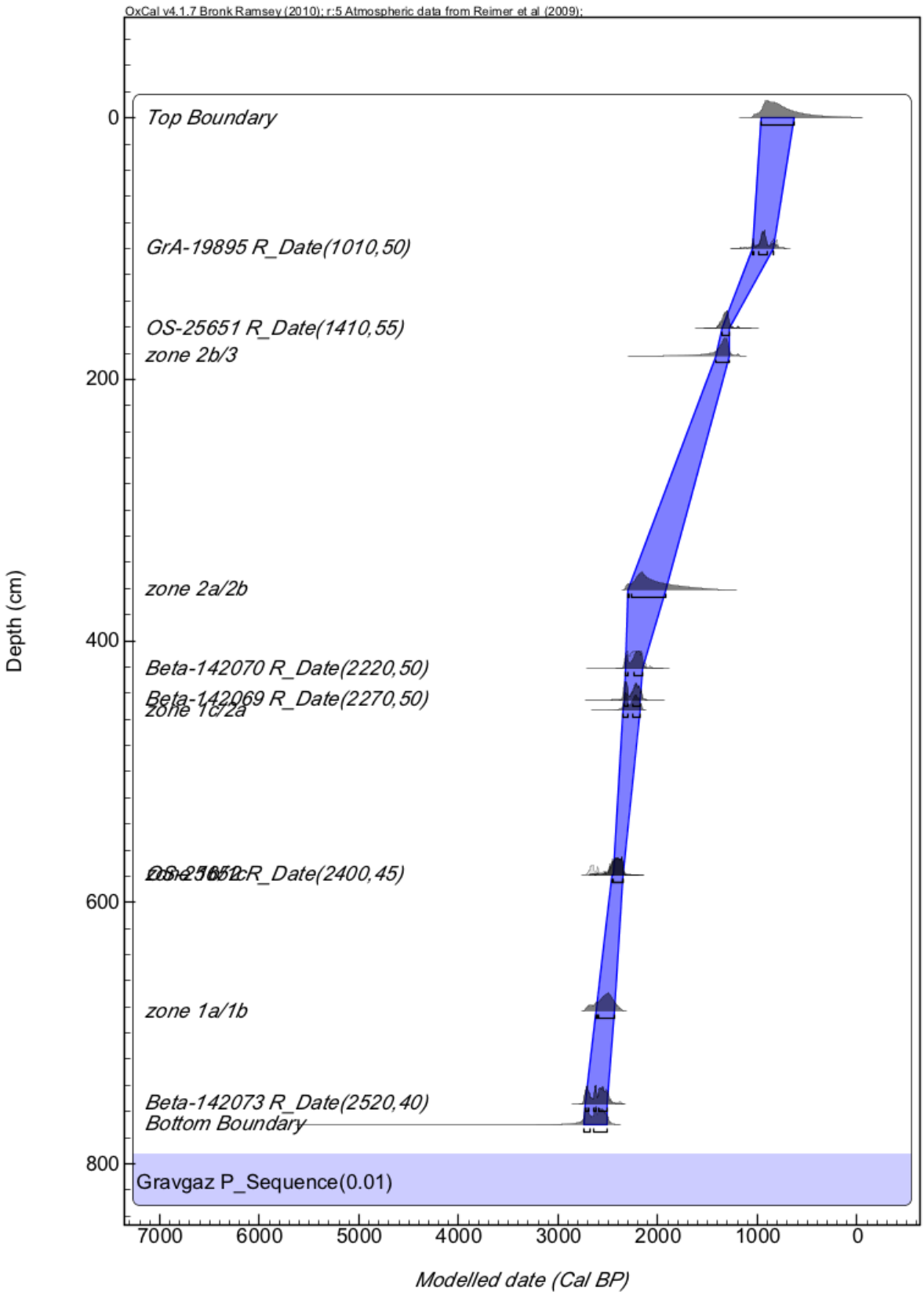

### 11.4.5 **Pollen zone chronology and estimated archaeological period**

| Zone | Highest Posterior Density beginning (68.2%) | |
|---|---|---|
| | Cal yr BP | Cal BC / AD |
| Zone 1a | 2742 to 2513 | 793 BC to 564 |
| Zone 1b | 2616 to 2433 | 667 BC to 484 |
| Zone 1c | 2455 to 2350 | 506 BC to 401 |
| Zone 2a | 2343 to 2183 | 394 BC to 234 |
| Zone 2b | 2302 to 1916 | 353 BC to AD 34 |
| Zone 3 | 1416 to 1278 | AD 534 to AD 672 |
| Top | 968 to 633 | AD 982 to AD 1317 |

## 11.5 BEREKET

### 11.5.1 Calibration

| Name | Depth (m) | Uncal. | Calibrated (BP) | | | | | |
|---|---|---|---|---|---|---|---|---|
| Bereket | | | 68.2% (1σ) | | 95.4%(2σ) | | 99.7% (3σ) | |
| R_Date B-213848 | 0.85 | 107±0.9 | 2326 | 2159 | 2338 | 2151 | 2350 | 2068 |
| R_Date B-213849 | 1.03 | 105±0.4 | 2297 | 2053 | 2306 | 1999 | 2330 | 1987 |
| R_Date B-223548 | 1.57 | 1390±60 | 1984 | 1878 | 1998 | 1825 | 2112 | 1780 |
| R_Date B-210929 | 1.98 | 1580±40 | 1869 | 1739 | 1892 | 1712 | 1948 | 1628 |
| R_Date B-210926 | 2.04 | 1710±40 | 1691 | 1563 | 1709 | 1535 | 1815 | 1421 |
| R_Date B-210927 | 2.86 | 1870±40 | 1519 | 1415 | 1550 | 1381 | 1609 | 1344 |
| R_Date B-193788 | 4.70 | 1970±40 | 1356 | 1268 | 1405 | 1180 | 1518 | 1088 |
| R_Date B-193789 | 6.10 | 2140±40 | 253 | 33 | 255 | 31 | 258 | 30 |
| R_Date B-213851 | 7.83 | 2230±40 | 252 | 34 | 257 | 31 | 259 | 31 |

| Name | Depth (m) | Uncal. | Calibrated (BC/AD) | | | | | |
|---|---|---|---|---|---|---|---|---|
| Bereket | | | 68.2% (1σ) | | 95.4%(2σ) | | 99.7% (3σ) | |
| R_Date B-213848 | 0.85 | 107±0.9 | -377 | -210 | -389 | -202 | -401 | -119 |
| R_Date B-213849 | 1.03 | 105±0.4 | -348 | -104 | -357 | -50 | -381 | -38 |
| R_Date B-223548 | 1.57 | 1390±60 | -35 | 72 | -49 | 125 | -163 | 171 |
| R_Date B-210929 | 1.98 | 1580±40 | 82 | 211 | 59 | 239 | 3 | 323 |
| R_Date B-210926 | 2.04 | 1710±40 | 259 | 388 | 241 | 415 | 136 | 529 |
| R_Date B-210927 | 2.86 | 1870±40 | 431 | 535 | 401 | 569 | 342 | 606 |
| R_Date B-193788 | 4.70 | 1970±40 | 595 | 682 | 545 | 771 | 432 | 862 |
| R_Date B-193789 | 6.10 | 2140±40 | 1698 | 1917 | 1696 | 1919 | 1692 | 1920 |
| R_Date B-213851 | 7.83 | 2230±40 | 1698 | 1917 | 1694 | 1919 | 1691 | 1920 |

## 11.5.2 **Modelled chronology**

| **Name** | **Modelled (BP)** | | | | | | **Modelled (BC/AD)** | | | | | | **Indices** | |
|---|---|---|---|---|---|---|---|---|---|---|---|---|---|---|
| **Bereket** | **68.2% (1σ)** | | **95.4%(2σ)** | | **99.7% (3σ)** | | **68.2% (1σ)** | | **95.4%(2σ)** | | **99.7% (3σ)** | | **Amodel = 96.3** | **Aoverall = 96.3** |
| **P_Sequence(0.01)** | **from** | **to** | **from** | **to** | **from** | **to** | **from** | **to** | **from** | **to** | **from** | **to** | **A** | **Convergence** |
| Bottom | 2525 | 2290 | 2737 | 2212 | 3040 | ... | -576 | -341 | -788 | -263 | -1091 | ... | | 97.2 |
| zone 3g/3h | 2417 | 2250 | 2574 | 2184 | 2830 | 2153 | -468 | -301 | -625 | -235 | -881 | -204 | | 99.8 |
| B-213851 | 2339 | 2234 | 2344 | 2184 | 2351 | 2151 | -390 | -285 | -395 | -235 | -402 | -202 | 95.7 | 99.8 |
| zone 3f/3g | 2310 | 2203 | 2330 | 2146 | 2343 | 2098 | -361 | -254 | -381 | -197 | -394 | -149 | | 99.8 |
| zone 3e/3f | 2267 | 2156 | 2308 | 2107 | 2330 | 2060 | -318 | -207 | -359 | -158 | -381 | -111 | | 99.8 |
| zone 3d/3e | 2225 | 2118 | 2277 | 2071 | 2310 | 2030 | -276 | -169 | -328 | -122 | -361 | -81 | | 99.8 |
| zone 3c/3d | 2181 | 2084 | 2237 | 2037 | 2287 | 2005 | -232 | -135 | -288 | -88 | -338 | -56 | | 99.8 |
| B-193789 | 2150 | 2062 | 2177 | 2007 | 2265 | 1990 | -201 | -113 | -228 | -58 | -316 | -41 | 112 | 99.7 |
| zone 3b/3c | 2115 | 2018 | 2150 | 1969 | 2228 | 1921 | -166 | -69 | -201 | -20 | -279 | 30 | | 99.6 |
| zone 3a/3b | 2071 | 1975 | 2121 | 1931 | 2177 | 1887 | -122 | -26 | -172 | 19 | -228 | 64 | | 99.7 |
| zone 2i/3a | 2027 | 1938 | 2077 | 1900 | 2135 | 1861 | -78 | 12 | -128 | 51 | -186 | 89 | | 99.7 |
| B-193788 | 1991 | 1916 | 2036 | 1873 | 2067 | 1828 | -42 | 34 | -87 | 77 | -118 | 123 | 96.3 | 99.7 |
| zone 2h/2i | 1970 | 1885 | 1999 | 1832 | 2056 | 1782 | -21 | 65 | -50 | 119 | -107 | 168 | | 99.7 |
| zone 2g/2h | 1946 | 1857 | 1984 | 1804 | 2036 | 1747 | 4 | 94 | -35 | 146 | -87 | 203 | | 99.8 |

## 11.5.3 **Modelled chronology (Contd.)**

| Name | Modelled (BP) | | | | | | Modelled (BC/AD) | | | | | | Indices | |
|---|---|---|---|---|---|---|---|---|---|---|---|---|---|---|
| Bereket | 68.2% (1σ) | | 95.4%(2σ) | | 99.7% (3σ) | | 68.2% (1σ) | | 95.4%(2σ) | | 99.7% (3σ) | | Amodel = 96.3 | Aoverall = 96.3 |
| P_Sequence(0.01) | from | to | from | to | from | to | from | to | from | to | from | to | A | Convergence |
| zone 2f/2g | 1922 | 1829 | 1965 | 1776 | 2013 | 1715 | 28 | 122 | -16 | 175 | -64 | 236 | | 99.8 |
| zone 2e/2f | 1900 | 1801 | 1945 | 1746 | 1987 | 1686 | 51 | 150 | 5 | 205 | -38 | 265 | | 99.7 |
| zone 2d/2e | 1874 | 1775 | 1920 | 1716 | 1960 | 1665 | 77 | 175 | 30 | 235 | -11 | 286 | | 99.7 |
| zone 2c/2d | 1849 | 1752 | 1892 | 1685 | 1936 | 1646 | 102 | 199 | 58 | 265 | 15 | 305 | | 99.8 |
| zone 2b/2c | 1824 | 1731 | 1861 | 1657 | 1909 | 1630 | 126 | 219 | 90 | 294 | 42 | 321 | | 99.8 |
| zone 2a/2b | 1799 | 1715 | 1828 | 1636 | 1880 | 1614 | 151 | 236 | 122 | 314 | 70 | 336 | | 99.9 |
| B-210927 | 1759 | 1635 | 1798 | 1620 | 1848 | 1597 | 192 | 316 | 152 | 330 | 103 | 353 | 60.6 | 99.7 |
| B-210926 | 1693 | 1572 | 1708 | 1546 | 1737 | 1521 | 258 | 378 | 243 | 404 | 214 | 430 | 102.4 | 99.8 |
| zone 1d/2a | 1604 | 1473 | 1667 | 1423 | 1705 | 1380 | 347 | 478 | 283 | 527 | 245 | 571 | | 99.9 |
| B-210929 | 1496 | 1407 | 1537 | 1379 | 1568 | 1339 | 455 | 543 | 414 | 572 | 382 | 612 | 100.3 | 99.9 |
| B-223548 | 1357 | 1272 | 1405 | 1182 | 1495 | 1128 | 593 | 678 | 545 | 769 | 455 | 823 | 101.5 | 99.7 |
| zone 1c/1d | 1305 | 795 | 1348 | 426 | 1396 | 239 | 645 | 1155 | 603 | 1524 | 555 | 1712 | | 99.6 |
| zone 1b/1c | 743 | 245 | 1105 | 135 | 1284 | 99 | 1207 | 1706 | 845 | 1816 | 666 | 1851 | | 99.6 |
| B-213849 | 256 | 226 | 259 | 102 | 260 | 33 | 1695 | 1724 | 1691 | 1849 | 1690 | 1918 | 102.4 | 99.9 |
| zone 1a/1b | 252 | 113 | 254 | 33 | 258 | 30 | 1699 | 1837 | 1696 | 1917 | 1693 | 1920 | 96.6 | 99.8 |
| Top | 231 | 26 | 244 | -8 | 250 | -45 | 1720 | 1925 | 1707 | 1959 | 1700 | 1996 | | |

### 11.5.4 **Model runs**

| Event | U_sequence | K = 4 (4 cm) | K=1 (1 cm) | K=0.1 (1 mm) | K=0.01 (0.1mm) | Sequence (cal BP) |
|---|---|---|---|---|---|---|
| | A_model = | A_model = | A_model= | A_model = 6.4 | A_model = 91.3 | A_model = 95.6 |
| | A_overall = | A_overall = | A_overall = | A_overall = 13.5 | A_overall = 90.2 | A_overall = 95.4 |
| End of core (top) | N/A | N/A | N/A | 121 to -57 | 234 to -57 | 226 to -57 |
| B-213848 | N/A | N/A | N/A | 254 to 121 | 255 to 32 | 252 to 31 |
| B-213849 | N/A | N/A | N/A | 259 to 228 | 258 to 34 | 259 to 64 |
| B-223548 | N/A | N/A | N/A | 1376 to 1172 | 1413 to 1180 | 1402 to 1180 |
| B210929 | N/A | N/A | N/A | 1555 to 1406 | 1599 to 1383 | 1545 to 1385 |
| B-210926 | N/A | N/A | N/A | **1610 to 1416** | 1710 to 1448 | 1706 to 1538 |
| B-210927 | N/A | N/A | N/A | **1782 to 1620** | 1876 to 1708 | 1884 to 1714 |
| B-193788 | N/A | N/A | N/A | 2000 to 1867 | 2002 to 1832 | 1999 to 1829 |
| B-193789 | N/A | N/A | N/A | 2301 to 2037 | 2287 to 1995 | 2297 to 1997 |
| B-213851 | N/A | N/A | N/A | 2658 to 2295 | **2341 to 2165** | 2337 to 2155 |
| B-210930 | N/A | N/A | N/A | **2883 to 2343** | 3821 to 2855 | 3825 to 2866 |
| Start of core (bottom) | N/A | N/A | N/A | 2898 to 2343 | 3894 to 2791 | 4844 to 2890 |

## 11.5.5 **Age-depth plot**

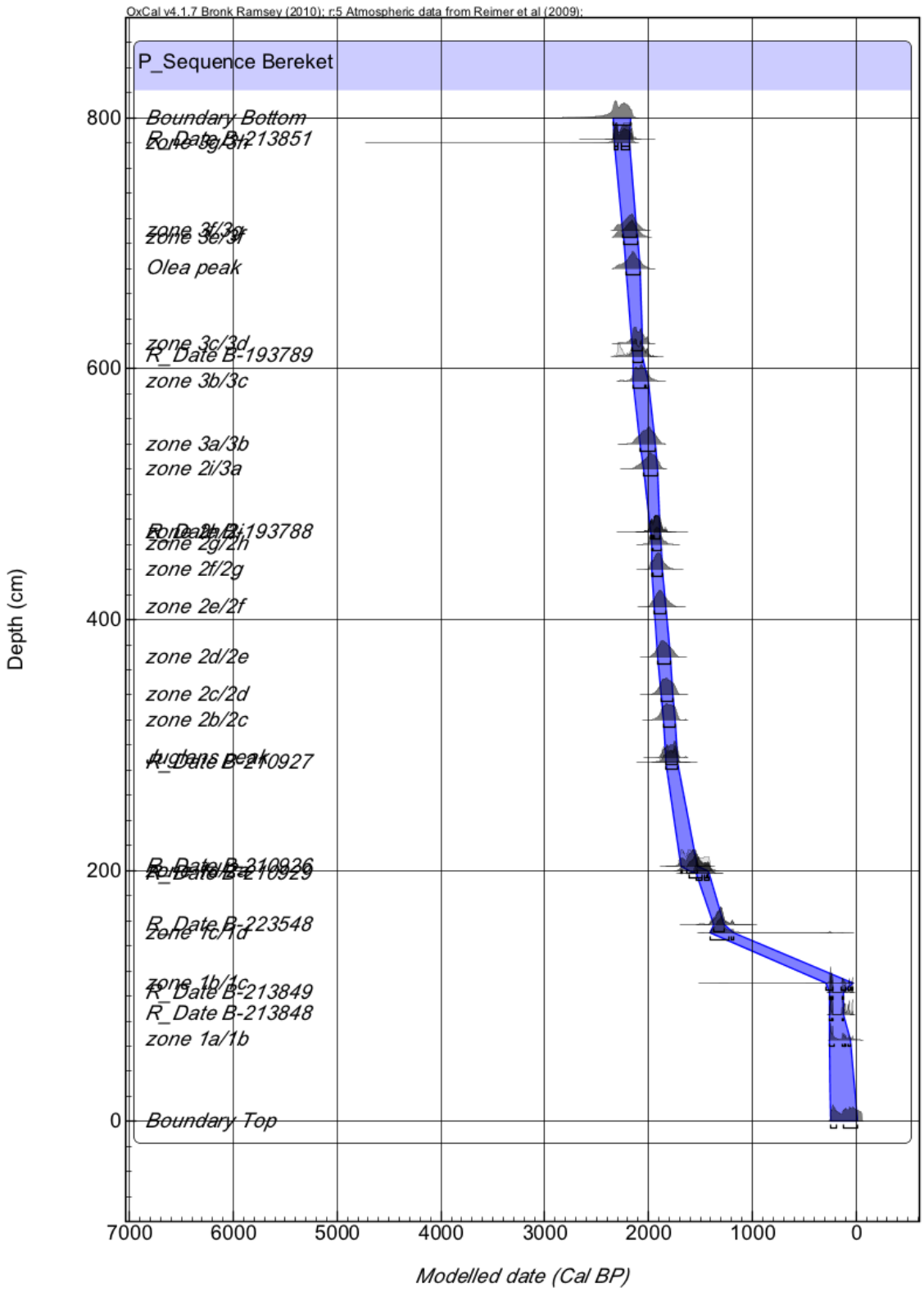

## 11.5.6 **Pollen zone chronology**

| Zone | Highest Posterior Density beginning of zone (68.2%) | |
|---|---|---|
| | Cal yr BP | Cal BC / AD |
| zone 3h | 2525 2290 | 576 BC to 341 |
| zone 3g | 2417 2250 | 468 BC to 301 |
| zone 3f | 2310 2203 | 361 BC to 254 |
| zone 3e | 2267 2156 | 318 BC to 207 |
| zone 3d | 2225 2118 | 276 BC to 169 |
| zone 3c | 2181 2084 | 232 BC to 135 |
| zone 3b | 2115 2018 | 166 BC to 69 |
| zone 3a | 2071 1975 | 122 BC to 26 |
| zone 2i | 2027 1938 | 78 BC to AD 12 |
| zone 2h | 1970 1885 | 21 BC to AD 65 |
| zone 2g | 1946 1857 | AD 4 to AD 94 |
| zone 2f | 1922 1829 | AD 28 to AD 122 |
| zone 2e | 1900 1801 | AD 51 to AD 150 |
| zone 2d | 1874 1775 | AD 77 to AD 175 |
| zone 2c | 1849 1752 | AD 102 to AD 199 |
| zone 2b | 1824 1731 | AD 126 to AD 219 |

## 11.5.7 **Pollen zone chronology (Contd.)**

| Zone | Highest Posterior Density beginning of zone (68.2%) | |
|---|---|---|
| | Cal yr BP | Cal BC / AD |
| zone 2a | 1799 1715 | AD 151 to AD 236 |
| zone 1d | 1604 1473 | AD 347 to AD 478 |
| zone 1c | 1305 795 | AD 645 to AD 1155 |
| zone 1b | 743 245 | AD 1207 to AD 1706 |
| zone 1a | 231 26 | AD 1720 to AD 1925 |
| Top | 102 -57 | AD 1848 to AD 2008 |

## 11.6 BEYSEHIR

### 11.6.1 Calibration

| Name | Depth (m) | Uncal. | Calibrated (BP) | | | | | |
|---|---|---|---|---|---|---|---|---|
| Beysehir | | | 68.2% (1σ) | | 95.4%(2σ) | | 99.7% (3σ) | |
| R_date GrN-6878 | | | 7155 | 6805 | 7167 | 6754 | 7253 | 6678 |
| R_date GrN-6879 | | | 3557 | 3447 | 3572 | 3401 | 3630 | 3380 |

| Name | Depth (m) | Uncal. | Calibrated (BC/AD) | | | | | |
|---|---|---|---|---|---|---|---|---|
| Beysehir | | | 68.2% (1σ) | | 95.4%(2σ) | | 99.7% (3σ) | |
| R_date GrN-6878 | | | -5206 | -4856 | -5218 | -4805 | -5304 | -4729 |
| R_date GrN-6879 | | | -1608 | -1498 | -1623 | -1452 | -1681 | -1431 |

## 11.6.2 **Modelled chronology**

| Name | Modelled (BP) | | | | | | Modelled (BC/AD) | | | | | | Indices | |
|---|---|---|---|---|---|---|---|---|---|---|---|---|---|---|
| Beysehir | 68.2% (1σ) | | 95.4%(2σ) | | 99.7% (3σ) | | 68.2% (1σ) | | 95.4%(2σ) | | 99.7% (3σ) | | Amodel = 99.8 | Aoverall = 99.8 |
| P_Sequence(0.01) | from | to | from | to | from | to | from | to | from | to | from | to | A | Convergence |
| Bottom | 7259 | 6801 | 8865 | ... | 14908 | ... | -5310 | -4852 | -6916 | ... | -12959 | ... | | 95.8 |
| GrN-6878 | 7153 | 6800 | 7165 | 6752 | 7248 | 6688 | -5204 | -4851 | -5216 | -4803 | -5299 | -4739 | 99.9 | 98.9 |
| zone 1/2a | 7155 | 6637 | 7235 | 5233 | 7258 | 4056 | -5206 | -4688 | -5286 | -3284 | -5309 | -2107 | | 95.9 |
| zone 2a/2b | 6899 | 4789 | 6990 | 3740 | 7118 | 3519 | -4950 | -2840 | -5041 | -1791 | -5169 | -1570 | | 97.8 |
| zone 2b/2c | 5791 | 3551 | 6716 | 3504 | 6991 | 3438 | -3842 | -1602 | -4767 | -1555 | -5042 | -1489 | | 97.7 |
| zone 2c/3a | 3839 | 3406 | 5253 | 3383 | 6401 | 3371 | -1890 | -1457 | -3304 | -1434 | -4452 | -1422 | | 95.8 |
| zone 3a/3b | 3565 | 3445 | 4143 | 3376 | 5472 | 3363 | -1616 | -1496 | -2194 | -1427 | -3523 | -1414 | | 98 |
| GrN-6879 | 3557 | 3448 | 3575 | 3401 | 3630 | 3381 | -1608 | -1499 | -1626 | -1452 | -1681 | -1432 | 99.7 | 99.1 |
| zone 3b/3c | 3559 | 3413 | 3629 | 3022 | 3645 | 1964 | -1610 | -1464 | -1680 | -1073 | -1696 | -15 | | 99.3 |
| zone 3c/3d | 3555 | 3039 | 3584 | 2053 | 3628 | 1041 | -1606 | -1090 | -1635 | -104 | -1679 | 909 | | 99.5 |
| zone 3d/3e | 3532 | 2721 | 3562 | 1602 | 3605 | 687 | -1583 | -772 | -1613 | 348 | -1656 | 1264 | | 99.2 |
| zone 3e/4 | 3459 | 2248 | 3532 | 1114 | 3559 | 340 | -1510 | -299 | -1583 | 837 | -1610 | 1610 | | 98.8 |
| zone 4/5 | 3370 | 1869 | 3476 | 713 | 3527 | 162 | -1421 | 82 | -1527 | 1237 | -1578 | 1788 | | 98.6 |
| Top | 3003 | 891 | 3098 | -20 | 3384 | -27 | -1054 | 1059 | -1149 | 1971 | -1435 | 1978 | | 98.7 |

### 11.6.3 **Model runs**

| Event | U_sequence | K = 4 (4 cm) | K=1 (1 cm) | K=0.1 (1 mm) | K=0.01 (0.1mm) | Sequence (cal BP) |
|---|---|---|---|---|---|---|
| | A_model = 94.5 | A_model = 80.3 | A_model= 96.6 | A_model = 99.5 | A_model = 99.7 | A_model = 99.6 |
| | A_overall = 94.6 | A_overall = 81.8 | A_overall = 96.6 | A_overall = 99.5 | A_overall = 99.7 | A_overall = 99.6 |
| End of core (top) | -160 to -884 | 172 to -27 | 402 to -27 | 1417 to -27 | 3096 to -20 | 3542 to -23 |
| GrN-6641 | 3571 to 3400 | 3632 to 3463 | 3612 to 3410 | 3575 to 3403 | 3575 to 3401 | 3574 to 3401 |
| GrN-6451 | 7247 to 6745 | 7031 to 6674 | 7155 to 6745 | 7164 to 6750 | 7165 to 6750 | 7165 to 6750 |
| Start of core (bottom) | 7716 to 7151 | 7481 to 7058 | 7632 to 7056 | 7980 to 6871 | 8972 to 6679 | 14908 to 6799 |

## 11.6.4 **Age-depth plot**

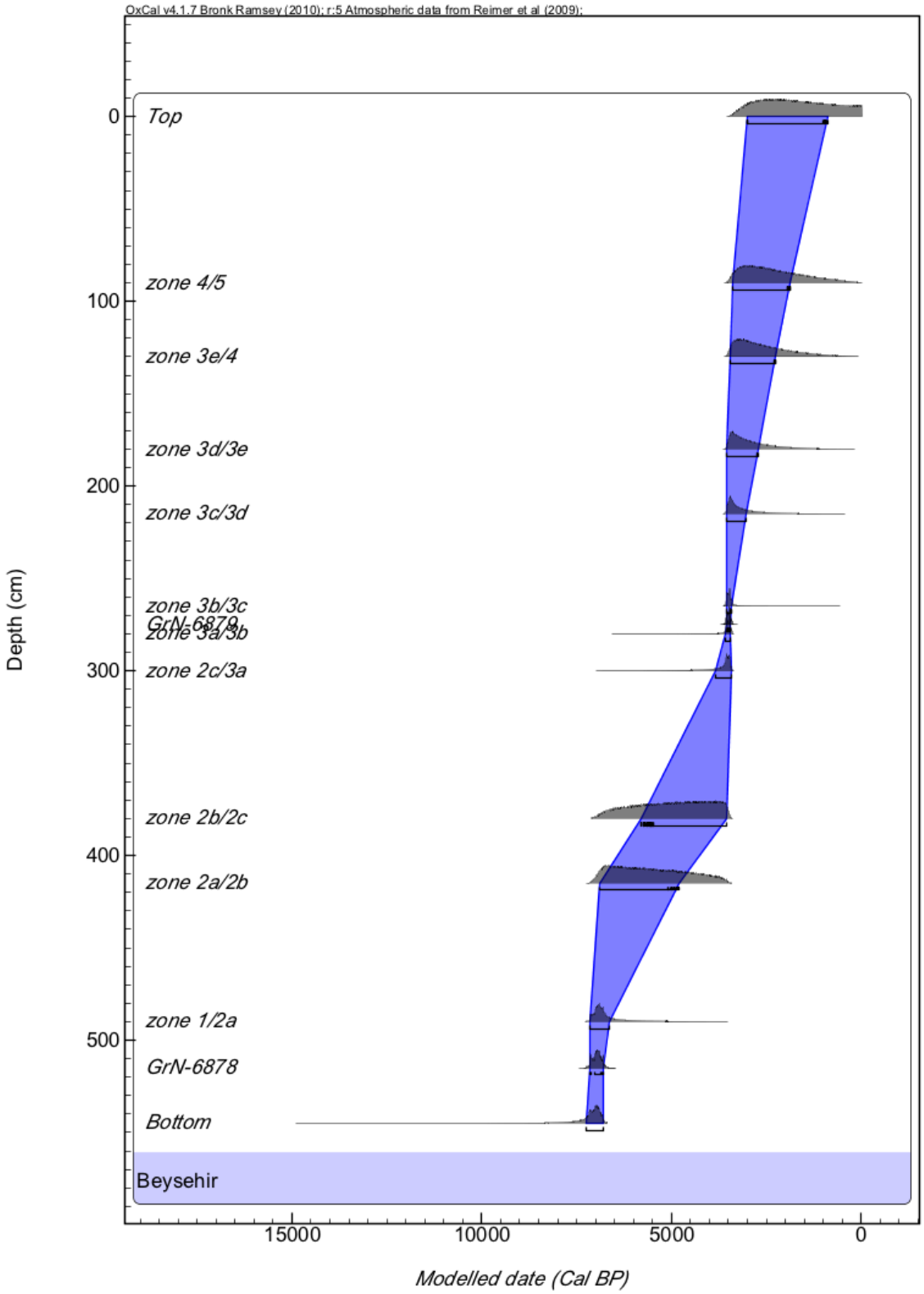

### 11.6.5 **Pollen zone chronology**

| Zone | Highest Posterior Density beginning (68.2%) | |
|---|---|---|
| | Cal yr BP | Cal BC / AD |
| Zone 1 | 7246 to 6799 | 5297 BC to 4850 BC |
| Zone 2a | 7154 to 6610 | 5205 BC to 4661 BC |
| Zone 2b | 6892 to 4913 | 4943 BC to 2964 BC |
| Zone 2c | 5673 to 3574 | 3724 BC to 1625 BC |
| Zone 3a | 3870 to 3406 | 1921 BC to 1457 BC |
| Zone 3b | 3564 to 3446 | 1862 BC 1457 BC |
| Zone 3c | 3559 to 3415 | 1610 BC to 1466 BC |
| Zone 3d | 3555 to 3045 | 1606 BC to 1096 BC |
| Zone 3e | 3533 to 2730 | 1584 BC to 781 BC |
| Zone 4 | 3464 to 2279 | 1515 BC to 330 BC |
| Zone 5 | 3381 to 1915 | 1432 BC to AD 35 |
| Top | 3013 to 951 | 1064 BC to AD 1000 |

## 11.7 HOYRAN

### 11.7.1 Calibration

| Name | Depth (m) | Uncal. | Calibrated (BP) | | | | | |
|---|---|---|---|---|---|---|---|---|
| Hoyran | | | 68.2% (1σ) | | 95.4%(2σ) | | 99.7% (3σ) | |
| R_Date GrN 7324 | 1.75 | 2470±50 | 2705 | 2464 | 2715 | 2362 | 2741 | 2351 |

| Name | Depth (m) | Uncal. | Calibrated (BC/AD) | | | | | |
|---|---|---|---|---|---|---|---|---|
| Hoyran | | | 68.2% (1σ) | | 95.4%(2σ) | | 99.7% (3σ) | |
| R_Date GrN 7324 | 1.75 | 2470±50 | -756 | -515 | -766 | -413 | -792 | -402 |

## 11.7.2 **Modelled chronology**

| Name | Modelled (BP) | | | | | | Modelled (BC/AD) | | | | | | Indices | |
|---|---|---|---|---|---|---|---|---|---|---|---|---|---|---|
| Hoyran | 68.2% (1σ) | | 95.4%(2σ) | | 99.7% (3σ) | | 68.2% (1σ) | | 95.4%(2σ) | | 99.7% (3σ) | | Amodel = 96.3 | Aoverall = 96.3 |
| P_Sequence(0.01) | from | to | from | to | from | to | from | to | from | to | from | to | A | Convergence |
| Bottom | 5758 | 4427 | 5758 | 3028 | 5758 | 2621 | -3809 | -2478 | -3809 | -1079 | -3809 | -672 | | 99.1 |
| zone 1/2 | 3907 | 2665 | 4772 | 2498 | 5310 | 2406 | -1958 | -716 | -2823 | -549 | -3361 | -457 | | 98.3 |
| zone 2/3 | 3552 | 2566 | 4434 | 2429 | 5066 | 2375 | -1603 | -617 | -2485 | -480 | -3117 | -426 | | 99 |
| GrN 7324 | 2705 | 2462 | 2714 | 2362 | 2741 | 2351 | -756 | -513 | -765 | -413 | -792 | -402 | 99.8 | 99.9 |
| zone 3/4 | 2675 | 2123 | 2720 | 1310 | 2741 | 598 | -726 | -174 | -771 | 640 | -792 | 1352 | | 99.7 |
| zone 4/5 | 2532 | 1400 | 2642 | 575 | 2695 | 177 | -583 | 550 | -693 | 1375 | -746 | 1773 | | 98.8 |
| zone 5/6 | 2476 | 1113 | 2587 | 379 | 2668 | 73 | -527 | 838 | -638 | 1572 | -719 | 1877 | | 98.5 |
| zone 6/7 | 1907 | -21 | 2337 | -22 | 2581 | -27 | 43 | 1971 | -388 | 1973 | -632 | 1978 | | 97.7 |
| Top | 1999 | -27 | 2314 | -27 | 2562 | -27 | -50 | 1978 | -365 | 1978 | -613 | 1978 | | 97.2 |

### 11.7.3 **Model runs**

| Event | U_sequence | K = 4 (4 cm) | K=1 (1 cm) | K=0.01 (0.1mm) | K=0.01 (0.1mm) | Sequence (cal BP) |
|---|---|---|---|---|---|---|
| | A_model = 98 | A_model = 99.1 | A_model= 99.4 | A_model = 99.9 | A_model = 100 | A_model = 99.9 |
| | A_overall = 98 | A_overall = 99.1 | A_overall = 99.4 | A_overall = 99.9 | A_overall = 100 | A_overall = 99.9 |
| End of core (top) | 2595 to 1562 | 2665 to -22 | 2656 to -27 | 2673 to -27 | 2701 to -27 | 2698 to -27 |
| GrN-7324 | 2709 to 2356 | 2710 to 2360 | 2711 to 2360 | 2714 to 2362 | 2715 to 2362 | 2715 to 2363 |
| Start of core (bottom) | 3588 to 2554 | 5758 to 2435 | 5758 to 2430 | 5758 to 2430 | 5758 to 2413 | 5758 to 2375 |

## 11.7.4 **Age-depth plot**

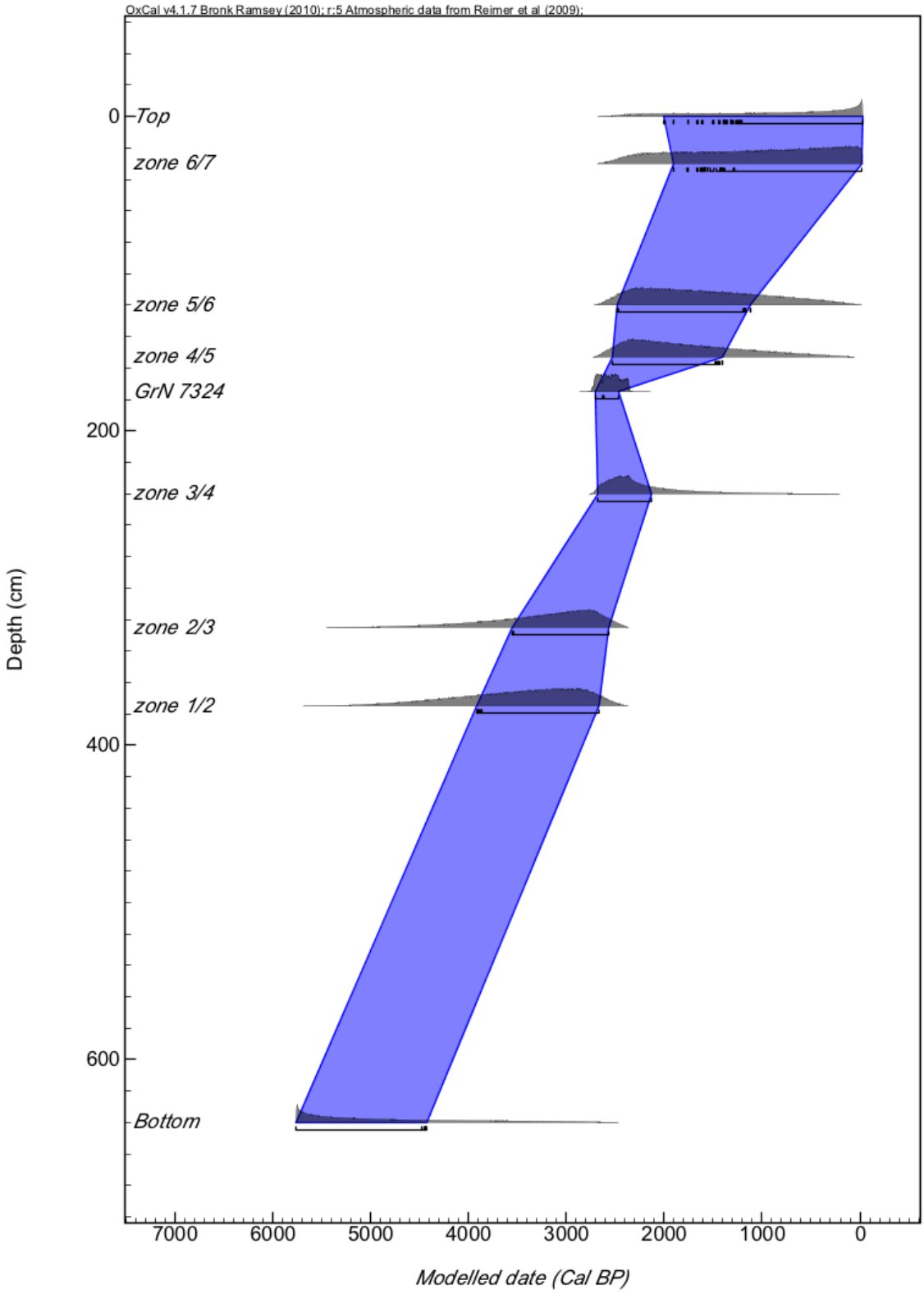

## 11.7.5 **Pollen zone chronology**

| Zone | Highest Posterior Density beginning (68.2%) | |
|---|---|---|
| | Cal yr BP | Cal BC / AD |
| Zone 1 | 5758 to 4427 | 3809 BC to 2478 BC |
| Zone 2 | 3907 to 2665 | 1958 BC to 716 BC |
| Zone 3 | 3552 to 2566 | 1603 BC to 617 BC |
| Zone 4 | 2675 to 2123 | 726 BC to 174 BC |
| Zone 5 | 2532 to 1400 | 583 BC to 550 BC |
| Zone 6 | 2476 to 1113 | 527 BC to AD 838 |
| Zone 7 | 1907 to -21 | AD 43 to AD 1971 |
| Top | 1999 to -27 | AD 50 to AD 1978 |

## 11.8 KOYCEGIZ

### 11.8.1 Calibration

| Name | Depth (m) | Uncal. | Calibrated (BP) | | | | | |
|---|---|---|---|---|---|---|---|---|
| Koycegiz | | | 68.2% (1σ) | | 95.4%(2σ) | | 99.7% (3σ) | |
| R_date GrN-6451 | 3.95 | 3070±55 | 3360 | 3219 | 3399 | 3081 | 3453 | 3023 |
| R_date GrN-6641 | 0.95 | 465±50 | 526 | 503 | 540 | 485 | 555 | 336 |

| Name | Depth (m) | Uncal. | Calibrated (BC/AD) | | | | | |
|---|---|---|---|---|---|---|---|---|
| Koycegiz | | | 68.2% (1σ) | | 95.4%(2σ) | | 99.7% (3σ) | |
| R_date GrN-6451 | 3.95 | 3070±55 | -1411 | -1270 | -1450 | -1132 | -1504 | -1074 |
| R_date GrN-6641 | 0.95 | 465±50 | 1425 | 1448 | 1410 | 1465 | 1396 | 1614 |

## 11.8.2 **Modelled chronology**

| Name | Modelled (BP) | | | | | | Modelled (BC/AD) | | | | | | Indices | |
|---|---|---|---|---|---|---|---|---|---|---|---|---|---|---|
| Hoyran | 68.2% (1σ) | | 95.4%(2σ) | | 99.7% (3σ) | | 68.2% (1σ) | | 95.4%(2σ) | | 99.7% (3σ) | | Amodel = 98.9 | Aoverall = 98.8 |
| P_Sequence(0.01) | from | to | from | to | from | to | from | to | from | to | from | to | A | Convergence |
| Bottom | 7318 | 3674 | 7318 | 3518 | 7318 | 3334 | -5369 | -1725 | -5369 | -1569 | -5369 | -1385 | | 96.8 |
| zone 1/2 | 5843 | 3572 | 7313 | 3421 | 7318 | 3303 | -3894 | -1623 | -5364 | -1472 | -5369 | -1354 | | 97.8 |
| zone 2/3a | 5086 | 3362 | 6583 | 3256 | 7220 | 3199 | -3137 | -1413 | -4634 | -1307 | -5271 | -1250 | | 98.4 |
| zone 3a/3b | 4835 | 3322 | 6351 | 3225 | 7175 | 3159 | -2886 | -1373 | -4402 | -1276 | -5226 | -1210 | | 98.5 |
| zone 3b/3c | 3789 | 3181 | 4993 | 3083 | 6311 | 3008 | -1840 | -1232 | -3044 | -1134 | -4362 | -1059 | | 99.7 |
| zone 3c/4 | 3468 | 3167 | 4327 | 3071 | 5696 | 2994 | -1519 | -1218 | -2378 | -1122 | -3747 | -1045 | | 99.8 |
| GrN-6451 | 3358 | 3219 | 3397 | 3081 | 3451 | 3023 | -1409 | -1270 | -1448 | -1132 | -1502 | -1074 | 99.2 | 99.9 |
| zone 4/5a | 3370 | 3081 | 3443 | 2266 | 3467 | 1279 | -1421 | -1132 | -1494 | -317 | -1518 | 671 | | 99.8 |
| zone 5a/5b | 3253 | 1945 | 3324 | 1035 | 3368 | 629 | -1304 | 5 | -1375 | 915 | -1419 | 1321 | | 99.9 |
| zone 6/7 | 1601 | 510 | 2609 | 502 | 3116 | 485 | 349 | 1440 | -660 | 1449 | -1167 | 1465 | | 99.9 |
| GrN-6641 | 663 | 486 | 1561 | 462 | 2572 | 436 | 1287 | 1464 | 389 | 1488 | -623 | 1514 | | 99.9 |
| Top | 526 | 503 | 540 | 486 | 622 | 455 | 1425 | 1448 | 1410 | 1465 | 1329 | 1495 | 98.9 | 100 |

### 11.8.3 **Model runs**

| Event | U_sequence | K = 4 (4 cm) | K=1 (1 cm) | K=0.1 (1 mm) | K=0.01 (0.1mm) | Sequence (cal BP) |
|---|---|---|---|---|---|---|
| | A_model = | A_model = | A_model= 65.7 | A_model = 98.2 | A_model = 98.7 | A_model = 99 |
| | A_overall = | A_overall = | A_overall = 67.4 | A_overall = 98.1 | A_overall = 98.7 | A_overall = 98.9 |
| End of core (top) | N/A | N/A | 36 to -27 | 217 to -27 | 514 to -21 | 504 to -21 |
| GrN-6641 | N/A | N/A | 629 to 499 | 541 to 491 | 540 to 486 | 540 to 487 |
| GrN-6451 | N/A | N/A | 3374 to 3005 | 3393 to 3079 | 3397 to 3081 | 3397 to 3080 |
| Start of core (bottom) | N/A | N/A | 5647 to 4790 | 7318 to 4324 | 7318 to 3549 | 7318 to 3215 |

## 11.8.4 **Age-depth plot**

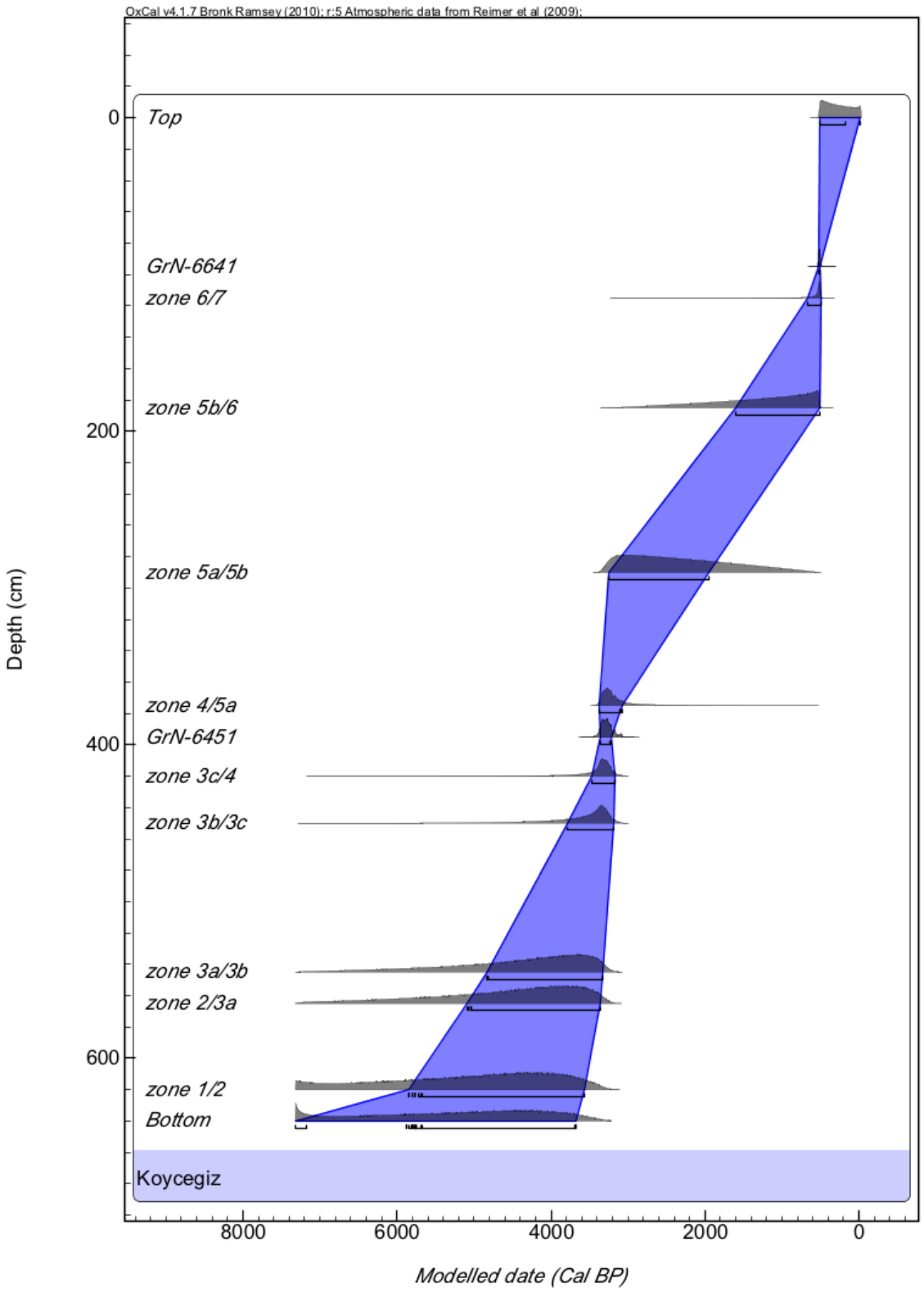

### 11.8.5 **Pollen zone chronology and estimated archaeological period**

| Zone | Highest Posterior Density beginning (68.2%) | |
|---|---|---|
| | Cal yr BP | Cal BC / AD |
| zone 1 | 7318 to 5453 | 5369 BC to 3504 |
| zone 2 | 6702 to 4833 | 4753 BC to 2884 |
| zone 3a | 6081 to 4385 | 4132 BC to 2436 |
| zone 3b | 5470 to 3994 | 3521 BC to 2045 |
| zone 3c | 4336 to 3395 | 2387 BC to 1446 BC |
| zone 4 | 3292 to 2540 | 1343 BC to 591 |
| zone 5a | 2882 1679 | 933 BC to 271 AD |
| zone 5b | 2093 907 | 144 BC to AD 1044 |
| zone 6 | 1209 512 | AD 742 to AD 1439 |
| zone 7 | 512 -21 | AD 1438 to AD 1972 |

## 11.9 SOGUT

### 11.9.1 Calibration

| Name | Depth (m) | Uncal. | Calibrated (BP) | | | | | |
|---|---|---|---|---|---|---|---|---|
| Hoyran | | | 68.2% (1σ) | | 95.4%(2σ) | | 99.7% (3σ) | |
| R_date GrN-6883 | 3.35 | 9180±95 | 10485 | 10242 | 10582 | 10194 | 10733 | 9930 |
| R_date GrN-6452 | 2.15 | 2885±35 | 3070 | 2960 | 3157 | 2887 | 3210 | 2866 |

| Name | Depth (m) | Uncal. | Calibrated (BC/AD) | | | | | |
|---|---|---|---|---|---|---|---|---|
| Hoyran | | | 68.2% (1σ) | | 95.4%(2σ) | | 99.7% (3σ) | |
| R_date GrN-6883 | 3.35 | 9180±95 | -8536 | -8293 | -8633 | -8245 | -8784 | -7981 |
| R_date GrN-6452 | 2.15 | 2885±35 | -1121 | -1011 | -1208 | -938 | -1261 | -917 |

### 11.9.2 **Modelled chronology**

| Name | Modelled (BP) | | | | | | Modelled (BC/AD) | | | | | | Indices | |
|---|---|---|---|---|---|---|---|---|---|---|---|---|---|---|
| Hoyran | 68.2% (1σ) | | 95.4%(2σ) | | 99.7% (3σ) | | 68.2% (1σ) | | 95.4%(2σ) | | 99.7% (3σ) | | Amodel = 96.3 | Aoverall = 96.3 |
| P_Sequence(0.01) | from | to | from | to | from | to | from | to | from | to | from | to | A | Convergence |
| Bottom | 22408 | 11289 | 22408 | 10939 | 22408 | 10557 | -20459 | -9340 | -20459 | -8990 | -20459 | -8608 | | 96.9 |
| zone 1/2 | 17224 | 10638 | 22212 | 10537 | 22394 | 10436 | -15275 | -8689 | -20263 | -8588 | -20445 | -8487 | | 98.7 |
| zone 2/3 | 14159 | 10312 | 19104 | 10243 | 21748 | 10201 | -12210 | -8363 | -17155 | -8294 | -19799 | -8252 | | 99.7 |
| GrN-6883 | 10483 | 10241 | 10580 | 10193 | 10724 | 9929 | -8534 | -8292 | -8631 | -8244 | -8775 | -7980 | 100.4 | 99.7 |
| zone 3/4 | 10576 | 10050 | 10703 | 5981 | 10728 | 3328 | -8627 | -8101 | -8754 | -4032 | -8779 | -1379 | | 97.9 |
| zone 4/5 | 3221 | 2888 | 7238 | 2858 | 10029 | 2853 | -1272 | -939 | -5289 | -909 | -8080 | -904 | | 99.6 |
| GrN-6452 | 3071 | 2961 | 3157 | 2889 | 3209 | 2867 | -1122 | -1012 | -1208 | -940 | -1260 | -918 | 99.5 | 99.8 |
| zone 5/6 | 3103 | 2923 | 3209 | 2418 | 3246 | 1218 | -1154 | -974 | -1260 | -469 | -1297 | 733 | | 99.7 |
| zone 6/7 | 3010 | 1703 | 3069 | 628 | 3136 | 132 | -1061 | 247 | -1120 | 1323 | -1187 | 1818 | | 99.9 |
| Top | 1412 | -27 | 2455 | -27 | 2888 | -27 | 539 | 1978 | -506 | 1978 | -939 | 1978 | | 99.9 |

### 11.9.3 **Model runs**

| Event | U_sequence | K = 4 (4 cm) | K=1 (1 cm) | K=0.01 (0.1mm) | K=0.01 (0.1mm) | Sequence (cal BP) |
|---|---|---|---|---|---|---|
| | A_model = | A_model = | A_model= 13.6 | A_model = 100 | A_model = 97.6 | A_model = |
| | A_overall = | A_overall = | A_overall = 13.9 | A_overall = 99.9 | A_overall = 97.6 | A_overall = |
| End of core (top) | N/A | N/A | 68 to -27 | 2475 to -27 | 616 to -27 | 3026 to -23 |
| GrN-6452 | N/A | N/A | 3331 to 3120 | 3157 to 2890 | 3202 to 2930 | 3156 to 2890 |
| GrN-6883 | N/A | N/A | 10400 to 9690 | 10580 to 10192 | 10573 to 10189 | 10581 to 10192 |
| Start of core (bottom) | N/A | N/A | 17837 to 15233 | 22408 to 10960 | 22408 to 13999 | 22408 to 10244 |

## 11.9.4 **Age-depth plot**

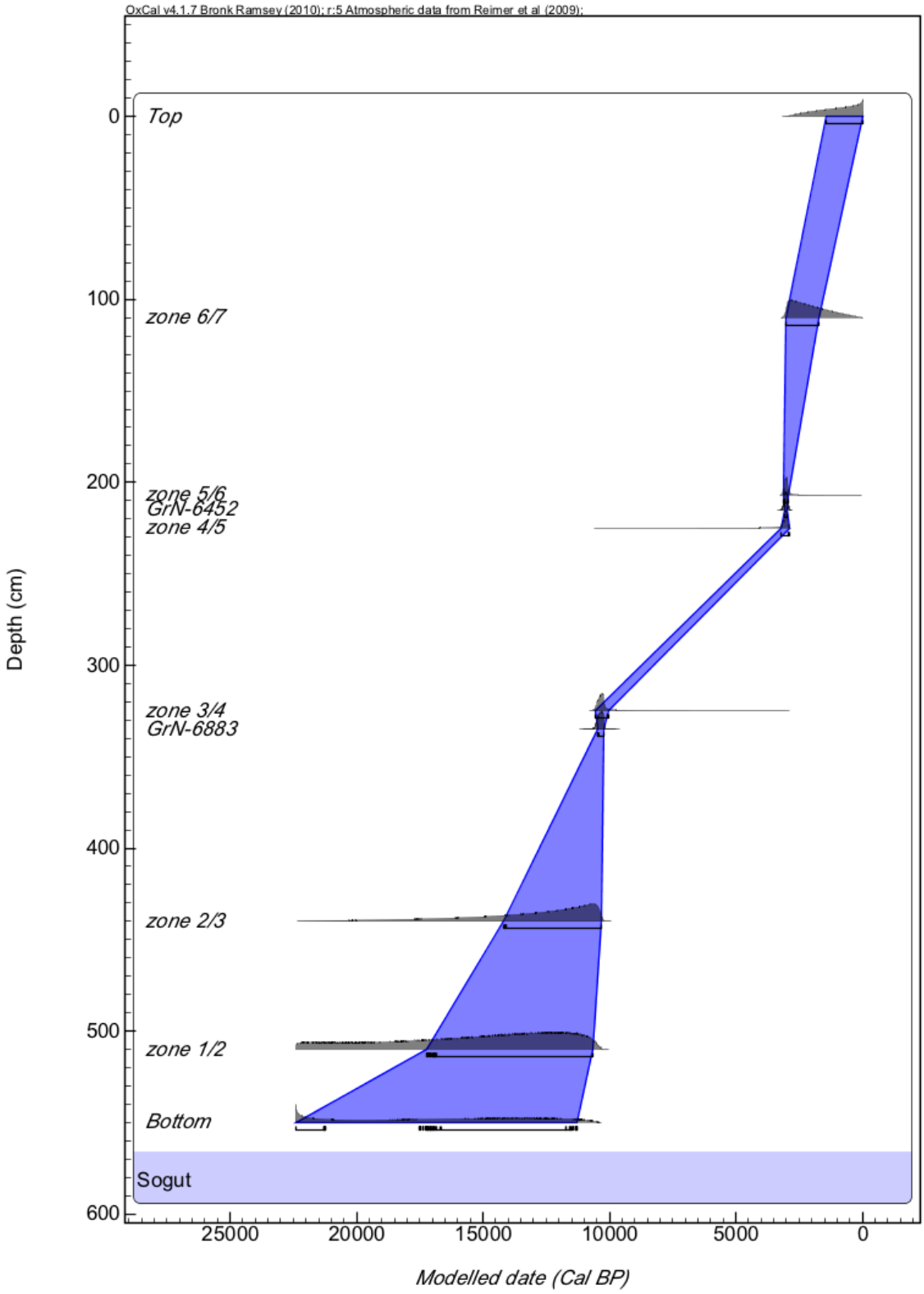

### 11.9.5 **Pollen zone chronology**

| Zone | Highest Posterior Density beginning (68.2%) | |
|---|---|---|
| | Cal yr BP | Cal BC / AD |
| Zone 1 | 22408 to 11908 | 20459 BC to 9959 BC |
| Zone 2 | 15902 to 11196 | 13953 BC to 9247 BC |
| Zone 3 | 13916 to 10619 | 11967 BC to 8670 BC |
| Zone 4 | 10371 to 7925 | 8422 BC to 5976 BC |
| Zone 5 | 5427 to 3017 | 3478 BC to 1068 BC |
| Zone 6 | 3039 to 2279 | 1090 BC to 330 BC |
| Zone 7 | 2004 to 598 | 55 BC to AD 1353 |
| Top | 1038 to -27 | AD 913 to AD 1978 |

## 11.10 OVA

### 11.10.1 Calibration

| Name | Depth (m) | Uncal. | Calibrated (BP) | | | | | |
|---|---|---|---|---|---|---|---|---|
| Ova | | | 68.2% (1σ) | | 95.4%(2σ) | | 99.7% (3σ) | |
| R_date GrN-10483 | 735 | 6550 ±380 | 7734 | 6954 | 8160 | 6564 | 8545 | 6271 |
| R_date GrN-10482 | 172 | 2150 ±100 | 2307 | 2005 | 2346 | 1903 | 2688 | 1811 |

| Name | Depth (m) | Uncal. | Calibrated (BC/AD) | | | | | |
|---|---|---|---|---|---|---|---|---|
| Ova | | | 68.2% (1σ) | | 95.4%(2σ) | | 99.7% (3σ) | |
| R_date GrN-10483 | 735 | 6550 ±380 | -5785 | -5005 | -6211 | -4615 | -6596 | -4322 |
| R_date GrN-10482 | 172 | 2150 ±100 | -358 | -56 | -397 | 48 | -739 | 140 |

### 11.10.2 **Modelled chronology**

| Name | Modelled (BP) | | | | | | Modelled (BC/AD) | | | | | | Indices | |
|---|---|---|---|---|---|---|---|---|---|---|---|---|---|---|
| Hoyran | 68.2% (1σ) | | 95.4%(2σ) | | 99.7% (3σ) | | 68.2% (1σ) | | 95.4%(2σ) | | 99.7% (3σ) | | Amodel = 99 | Aoverall = 99 |
| P_Sequence(0.01) | from | to | from | to | from | to | from | to | from | to | from | to | A | Convergence |
| Bottom | 7820 | 6888 | 8481 | 6405 | 10899 | ... | -5871 | -4939 | -6532 | -4456 | -8950 | ... | | 96.6 |
| GrN-10483 | 7689 | 6889 | 8151 | 6483 | 8449 | 6191 | -5740 | -4940 | -6202 | -4534 | -6500 | -4242 | 97.8 | 98 |
| zone 1/hiatus | 6725 | 4660 | 7327 | 3548 | 7808 | 2750 | -4776 | -2711 | -5378 | -1599 | -5859 | -801 | | 99.7 |
| haitus/zone2 | 5269 | 3137 | 6287 | 2509 | 7084 | 2179 | -3320 | -1188 | -4338 | -560 | -5135 | -230 | | 99.7 |
| zone2/haitus2 | 4033 | 2344 | 5338 | 2117 | 6417 | 1965 | -2084 | -395 | -3389 | -168 | -4468 | -16 | | 99.7 |
| haitus2/zone3 | 2329 | 2044 | 2685 | 1872 | 3963 | 1724 | -380 | -95 | -736 | 79 | -2014 | 226 | | 98.9 |
| GrN-10482 | 2313 | 2044 | 2349 | 1902 | 2696 | 1815 | -364 | -95 | -400 | 48 | -747 | 135 | 100.4 | 99.5 |
| Top | 1995 | 704 | 2079 | 7 | 2261 | -37 | -46 | 1246 | -130 | 1943 | -312 | 1988 | | 99.9 |

### 11.10.3 **Model runs**

| Event | U_sequence | K = 4 (4 cm) | K=1 (1 cm) | K=0.1 (0.1mm) | K=0.01 (0.1mm) | Sequence (cal BP) |
|---|---|---|---|---|---|---|
| | A_model = | A_model = 97 | A_model= 99.2 | A_model =99.3 | A_model = 98.8 | A_model = 99.6 |
| | A_overall = | A_overall = 97 | A_overall = 99.2 | A_overall = 99.3 | A_overall = 98.8 | A_overall = 99.6 |
| End of core (top) | 964 to 134 | 961 to 83 | 1001 to 52 | 1278 to -32 | 2091 to 19 | 2105 to -31 |
| GrN-10482 | 2346 to 1903 | 2345 to 1903 | 2346 to 1925 | 2349 to 1925 | 2349 to 1903 | 2349 to 1903 |
| GrN-10483 | 8182 to 6492 | 8304 to 6498 | 8180 to 6517 | 8162 to 6494 | 8039 to 6448 | 8104 to 6491 |
| Start of core (bottom) | 8340 to 6607 | 8458 to 6618 | 8355 to 6639 | 8334 to 6590 | 8501 to 6399 | 19837 to 6775 |

### 11.10.4 **Age-depth plot**

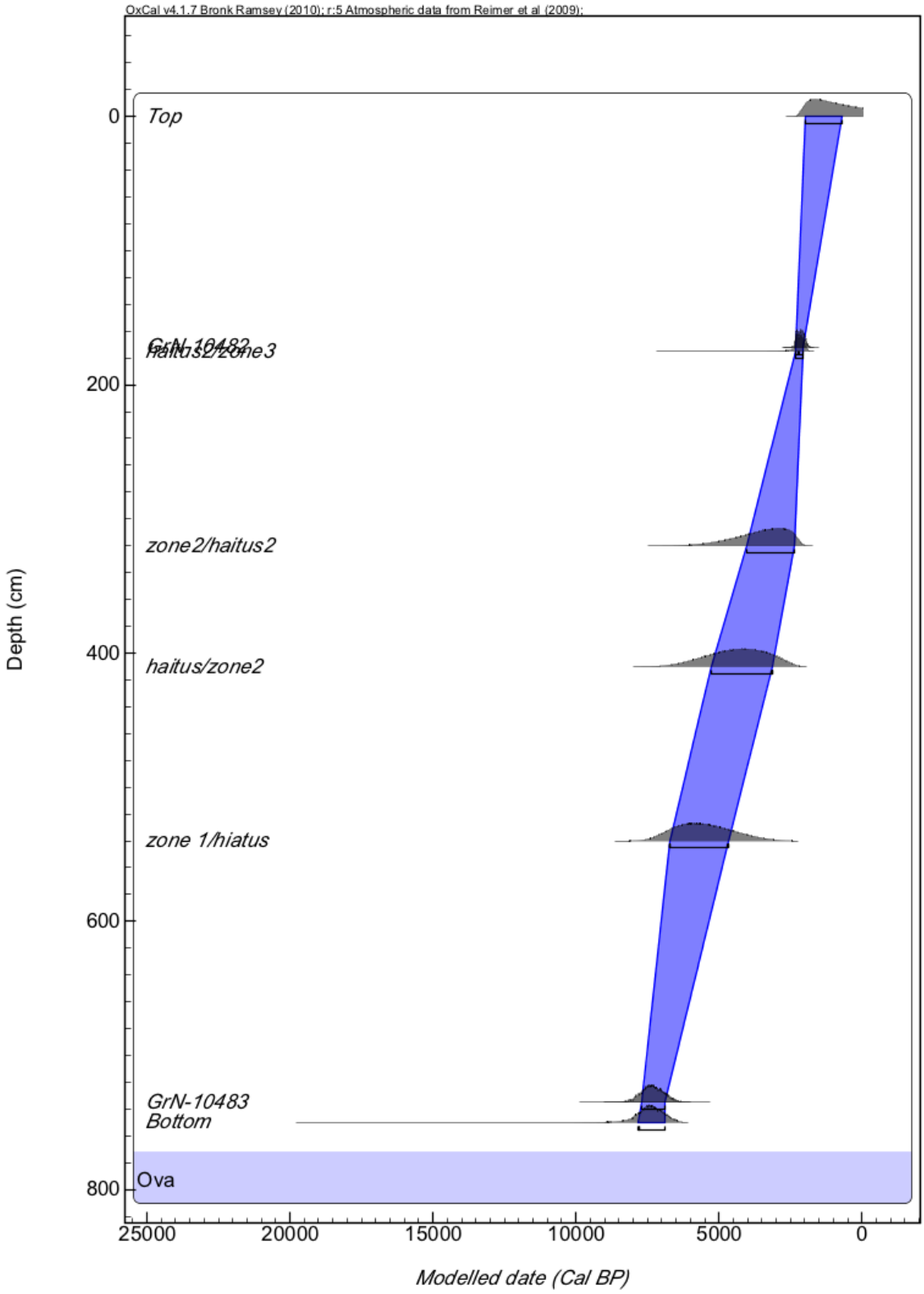

### 11.10.5 **Pollen zone chronology and estimated archaeological period**

| Zone | Highest Posterior Density beginning of zone (68.2%) | |
|---|---|---|
| | Cal yr BP | Cal BC / AD |
| zone 1 | 8801 to 6962 | 6852 5013 |
| hiatus | 7416 to 5930 | 5467 4947 |
| zone 2 | 6751 to 4759 | 4802 2810 |
| haitus 2 | 4562 to 2658 | 2613 709 |
| zone 3 | 3307 to 2119 | 1358 170 |
| Top | 2231 to 1210 | 282 741 AD |

## 11.11 PINARBASI

### 11.11.1 Calibration

| Name | Depth (m) | Uncal. | Calibrated (BP) | | | | | |
|---|---|---|---|---|---|---|---|---|
| Pinarbasi | | | 68.2% (1σ) | | 95.4%(2σ) | | 99.7% (3σ) | |
| GrN-10480 | 295 | 6550 ±660 | 8011 | 6750 | 8855 | 6184 | 9555 | 5603 |
| GrN-10479 | 95 | 1370 ±70 | 1350 | 1185 | 1410 | 1095 | 1518 | 1061 |

| Name | Depth (m) | Uncal. | Calibrated (BC/AD) | | | | | |
|---|---|---|---|---|---|---|---|---|
| Pinarbasi | | | 68.2% (1σ) | | 95.4%(2σ) | | 99.7% (3σ) | |
| GrN-10480 | 295 | 6550 ±660 | -6062 | -4801 | -6906 | -4235 | -7606 | -3654 |
| GrN-10479 | 95 | 1370 ±70 | 601 | 766 | 540 | 855 | 432 | 889 |

### 11.11.2 **Modelled chronology**

| Name | Modelled (BP) | | | | | | Modelled (BC/AD) | | | | | | Indices | |
|---|---|---|---|---|---|---|---|---|---|---|---|---|---|---|
| Hoyran | 68.2% (1σ) | | 95.4%(2σ) | | 99.7% (3σ) | | 68.2% (1σ) | | 95.4%(2σ) | | 99.7% (3σ) | | Amodel = 100.2 | Aoverall = 100.2 |
| P_Sequence(0.01) | from | to | from | to | from | to | from | to | from | to | from | to | A | Convergence |
| Bottom | 22837 | 11209 | 22837 | 9813 | 22837 | 8004 | -20888 | -9260 | -20888 | -7864 | -20888 | -6055 | | 97.7 |
| zone 1/2 | 11939 | 7436 | 16247 | 6688 | 19768 | 6155 | -9990 | -5487 | -14298 | -4739 | -17819 | -4206 | | 98.6 |
| GrN-10480 | 7925 | 6669 | 8580 | 6005 | 9349 | 5600 | -5976 | -4720 | -6631 | -4056 | -7400 | -3651 | 100.1 | 98.8 |
| zone 2/3a | 7936 | 5607 | 8461 | 2843 | 9032 | 1468 | -5987 | -3658 | -6512 | -894 | -7083 | 482 | | 98.3 |
| zone 3a/3b | 5924 | 1331 | 7160 | 1273 | 8207 | 1159 | -3975 | 620 | -5211 | 677 | -6258 | 791 | | 97.1 |
| zone 3b/4a | 4242 | 1199 | 6525 | 1178 | 7708 | 1086 | -2293 | 752 | -4576 | 772 | -5759 | 864 | | 98.2 |
| GrN-10479 | 1352 | 1186 | 1413 | 1098 | 1518 | 1063 | 599 | 765 | 538 | 853 | 432 | 887 | 100.2 | 99.6 |
| zone 4a/4b | 1354 | 1178 | 1511 | 797 | 1525 | 218 | 597 | 772 | 440 | 1153 | 426 | 1732 | | 95.4 |
| Top | 1271 | -31 | 1279 | -31 | 1371 | -37 | 680 | 1981 | 672 | 1981 | 580 | 1988 | | 98.5 |

### 11.11.3 **Model runs**

| Event | U_sequence<br>A_model = 0<br>A_overall = 0 | K = 4 (4 cm)<br>A_model = 0<br>A_overall = 0 | K=1 (1 cm)<br>A_model= 12.9<br>A_overall = 17.3 | K=0.1 (1 mm)<br>A_model = 97.6<br>A_overall = 97.6 | K=0.01 (0.1mm)<br>A_model = 100.4<br>A_overall = 100.4 | Sequence (cal BP)<br>A_model = 100.2<br>A_overall = 100.2 |
|---|---|---|---|---|---|---|
| End of core (top) | - | - | 141 to -37 | 528 to -37 | 1277 to -31 | 1242 to -31 |
| GrN-10480 | - | - | **1531 to 1266** | 1509 to 1171 | 1413 to 1099 | 1413 to 1098 |
| GrN-10479 | - | - | **6530 to 4832** | 8317 to 5927 | 8559 to 6018 | 8603 to 6000 |
| Start of core (bottom) | - | - | 15992 to 11055 | 22837 to 12678 | 22837 to 9805 | 22837 to 6587 |

### 11.11.4 **Age-depth plot**

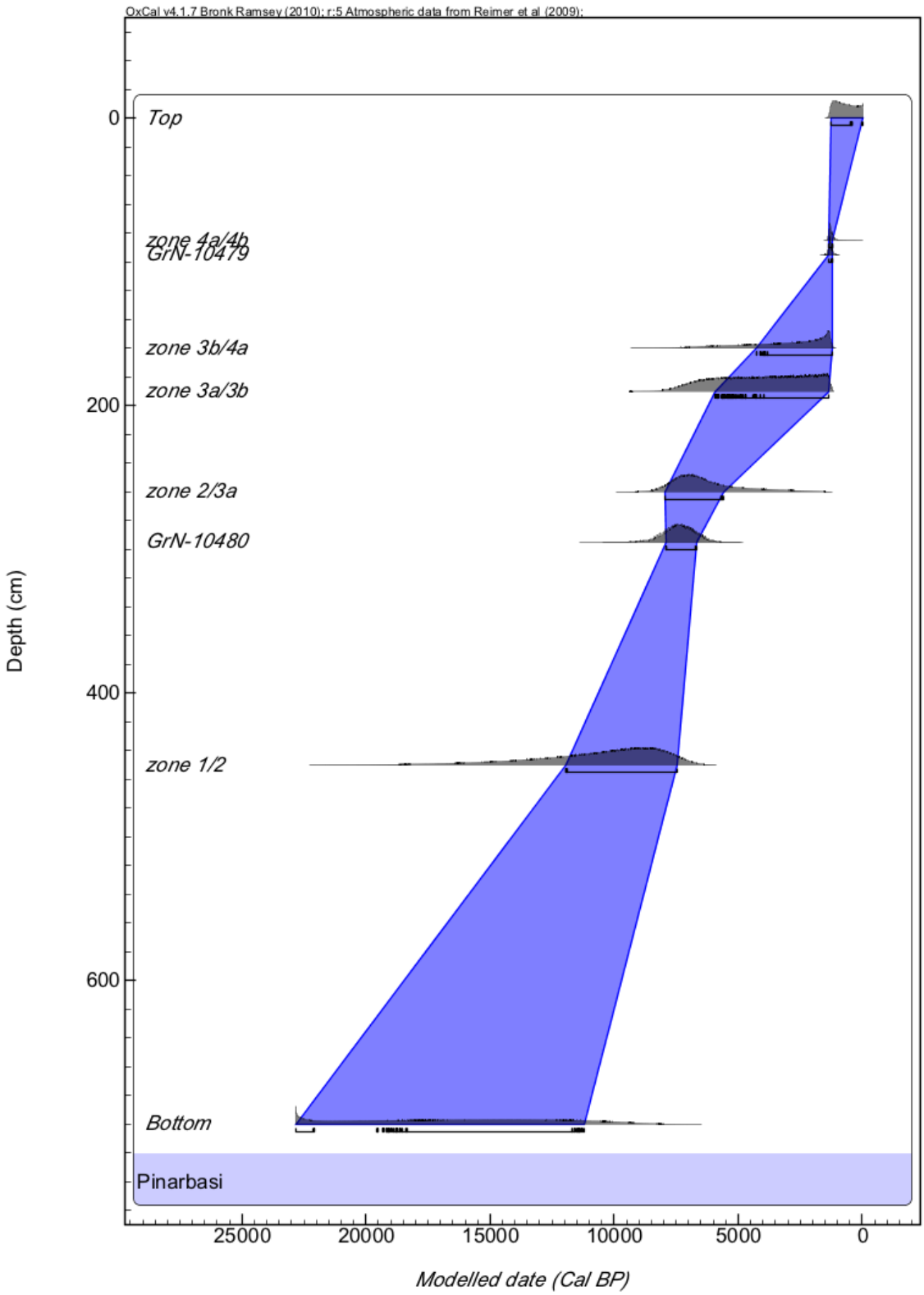

### 11.11.5 **Pollen zone chronology**

| Zone | Highest Posterior Density beginning (68.2%) | |
|---|---|---|
| | Cal yr BP | Cal BC / AD |
| zone 1 | 22837 to 11444 | 20888 BC to 9495 BC |
| zone 2 | 11955 to 7434 | 10006 BC to 5485 BC |
| zone 3a | 7945 to 5604 | 5996 BC to 3655 BC |
| zone 3b | 5299 to 1343 | 3350 BC to 607 AD |
| zone 4a | 3861 to 1195 | 1912 BC to 755 AD |
| zone 4b | 1354 to 1177 | AD 597 to AD 773 |
| Top | 1268 to -31 | AD 683 to AD 1981 |

## 11.12 GOLCUK

### 11.12.1 Calibration

| Name | Depth (m) | Uncal. | Calibrated (BP) | | | | | |
|---|---|---|---|---|---|---|---|---|
| **Pinarbasi** | | | **68.2% (1σ)** | | **95.4%(2σ)** | | **99.7% (3σ)** | |
| R_date GC-1 | 10.02 | 7400±120 | 8359 | 8056 | 8412 | 7981 | 8552 | 7869 |
| R_date GC-2 | 8.99 | 3110±160 | 3549 | 3078 | 3690 | 2882 | 3885 | 2760 |
| R_date GC-3 | 8.55 | 2970±270 | 3445 | 2796 | 3834 | 2471 | 4236 | 2157 |
| R_date GC-4 | 4.65 | 1640±70 | 1612 | 1417 | 1707 | 1387 | 1815 | 1332 |

| Name | Depth (m) | Uncal. | Calibrated (BC/AD) | | | | | |
|---|---|---|---|---|---|---|---|---|
| **Pinarbasi** | | | **68.2% (1σ)** | | **95.4%(2σ)** | | **99.7% (3σ)** | |
| R_date GC-1 | 10.02 | 7400±120 | -6410 | -6107 | -6463 | -6032 | -6603 | -5920 |
| R_date GC-2 | 8.99 | 3110±160 | -1600 | -1129 | -1741 | -933 | -1936 | -811 |
| R_date GC-3 | 8.55 | 2970±270 | -1496 | -847 | -1885 | -522 | -2287 | -208 |
| R_date GC-4 | 4.65 | 1640±70 | 338 | 534 | 244 | 564 | 135 | 619 |

### 11.12.2 Model runs

| Event | U_sequence<br>A_model = 0<br>A_overall = 0 | K = 4 (4 cm)<br>A_model = 0<br>A_overall = 0 | K=1 (1 cm)<br>A_model=<br>A_overall = | K=0.1 (1 mm)<br>A_model = 27.9<br>A_overall = 20.9 | K=0.01 (0.1mm)<br>A_model = 110.6<br>A_overall = 108.9 | Sequence (cal BP)<br>A_model = 104.2<br>A_overall = 103.4 |
|---|---|---|---|---|---|---|
| End of core (top) | N/A | N/A | N/A | 140 to -42 | 898 to -42 | 1562 to -35 |
| GC-4 | N/A | N/A | N/A | 1812 to 1440 | 1711 to 1391 | 1710 to 1388 |
| GC-3 | N/A | N/A | N/A | **4073 to 3250** | 3608 to 2776 | 3466 to 2379 |
| GC-2 | N/A | N/A | N/A | **4409 to 3536** | 3697 to 2976 | 3716 to 2965 |
| GC-1 | N/A | N/A | N/A | 8330 to 7863 | 8400 to 7977 | 8405 to 7979 |
| Start of core (bottom) | N/A | N/A | N/A | 10587 to 8911 | 13440 to 8099 | 18082 to 8002 |

### 11.12.3 **Modelled chronology**

| Name | Modelled (BP) | | | | | | Modelled (BC/AD) | | | | | | Indices | |
|---|---|---|---|---|---|---|---|---|---|---|---|---|---|---|
| Hoyran | 68.2% (1σ) | | 95.4%(2σ) | | 99.7% (3σ) | | 68.2% (1σ) | | 95.4%(2σ) | | 99.7% (3σ) | | Amodel = 110.5 | Aoverall = 108.8 |
| P_Sequence(0.01) | from | to | from | to | from | to | from | to | from | to | from | to | A | Convergence |
| Bottom | 10563 | 8339 | 13366 | 8114 | 18082 | 8027 | -8614 | -6390 | -11417 | -6165 | -16133 | -6078 | | 96.2 |
| GC-1 | 8332 | 8045 | 8399 | 7979 | 8542 | 7868 | -6383 | -6096 | -6450 | -6030 | -6593 | -5919 | 98.8 | 99.6 |
| zone 5a/5b | 8367 | 3314 | 8371 | 3275 | 8422 | 3079 | -6418 | -1365 | -6422 | -1326 | -6473 | -1130 | | 97.2 |
| GC-2 | 3560 | 3172 | 3699 | 2983 | 3889 | 2846 | -1611 | -1223 | -1750 | -1034 | -1940 | -897 | 105.1 | 99 |
| zone 4/5a | 3447 | 3049 | 3629 | 2795 | 3820 | 2526 | -1498 | -1100 | -1680 | -846 | -1871 | -577 | | 97.4 |
| GC-3 | 3438 | 3000 | 3580 | 2768 | 3764 | 2456 | -1489 | -1051 | -1631 | -819 | -1815 | -507 | 117.4 | 97.3 |
| zone 3b/4 | 3170 | 2395 | 3388 | 1946 | 3571 | 1656 | -1221 | -446 | -1439 | 5 | -1622 | 295 | | 99.5 |
| zone 3a/3b | 2162 | 1542 | 2671 | 1438 | 3109 | 1385 | -213 | 408 | -722 | 513 | -1160 | 565 | | 99.4 |
| zone 2c/3a | 1753 | 1438 | 2223 | 1380 | 2729 | 1323 | 198 | 513 | -274 | 570 | -780 | 628 | | 99.4 |
| GC-4 | 1687 | 1422 | 1711 | 1392 | 1817 | 1339 | 263 | 528 | 240 | 559 | 133 | 612 | 99.1 | 99.6 |
| zone 2b/2c | 1620 | 1336 | 1712 | 1024 | 1815 | 657 | 330 | 614 | 238 | 926 | 135 | 1293 | | 99.6 |
| zone 2a/2b | 1592 | 1208 | 1689 | 834 | 1788 | 476 | 358 | 742 | 262 | 1117 | 163 | 1474 | | 99.5 |
| zone 1/2a | 1473 | 918 | 1594 | 525 | 1688 | 237 | 478 | 1032 | 356 | 1426 | 262 | 1713 | | 99.2 |
| Top | 425 | -38 | 891 | -42 | 1235 | -42 | 1525 | 1989 | 1060 | 1993 | 715 | 1993 | | 99.7 |

### 11.12.4 **Age-Depth model**

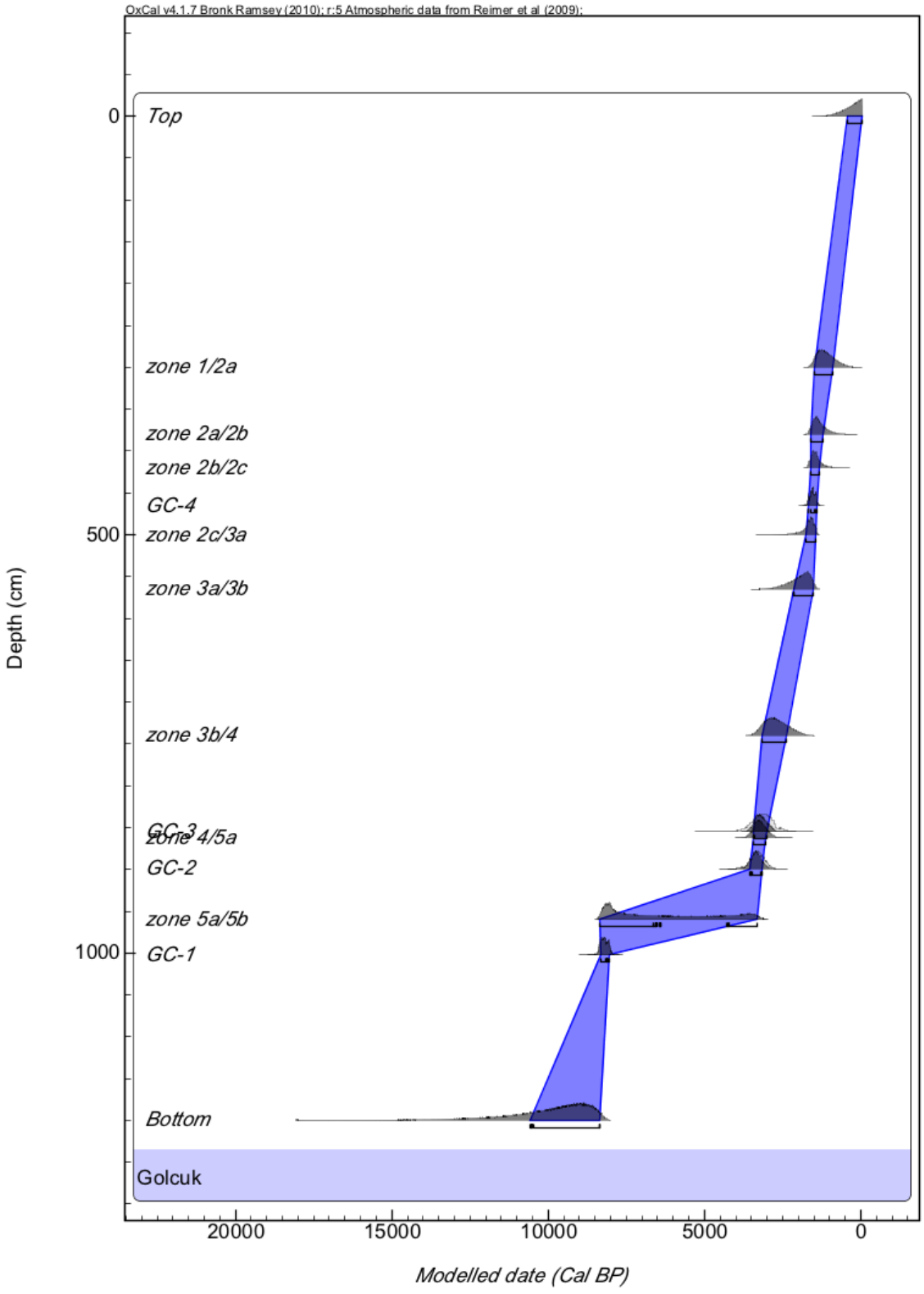

### 11.12.5 **Pollen zone chronology**

| Zone | Highest Posterior Density beginning (68.2%) | |
|---|---|---|
| | Cal yr BP | Cal BC / AD |
| zone 5b | 10514 to 8355 | 8565 BC to 6406 BC |
| zone 5a | 8371 to 3378 | 6422 BC to 1429 BC |
| zone 4 | 3446 to 3051 | 1497 BC to 1102 BC |
| zone 3b | 3124 to 2348 | 1175 BC to 399 BC |
| zone 3a | 2134 to 1539 | 185 BC to AD 411 |
| zone 2c | 1748 to 1437 | AD 203 to AD 514 |
| zone 2b | 1621 to 1338 | AD 330 to AD 613 |
| zone 2a | 1591 to 1206 | AD 360 to AD 744 |
| zone 1 | 1465 to 914 | AD 486 to AD 1036 |
| Top | 419 to -38 | AD 1531 to AD 1989 |

**Bibliography**


Affek, H. P., M. Bar-Matthews, et al. (2008). "Glacial / interglacial temperature variations in Soreq cave speleothems as recorded by 'clumped isotope' thermometry." Geochimica et Cosmochimica Acta **72**: 5351-5360.

Akçar, N., V. Yavuz, et al. (2007). "Palaeoglacial records from Kavron Valley, NE Turkey: field and cosmogenic exposure dating evidence." Quaternary International **164-165**: 170-183.

Akkemik, Ü. and A. Aras (2005). "Reconstruction (1689-1994 AD) of April-August preciptiation in the souther part of central Turkey." International Journal of Climatology

**25**(4): 537-548.

Aksoy, E., P. Panagos, et al. (2010). Integration of the Soil Database of Turkey into European Soil Database 1:1.000.000. JRC Scientific and Technical Reports. Ispra, JRC.

Ariztegui, D., A. Asioli, et al. (2000). "Palaeoclimate and the formation of sapropel S1: inferences from Late Quaternary lacustrine and marine sequences in the central Mediterranean region." Palaeogeography, Palaeoclimatology, Palaeoecology **158**: 215-240.

Arz, H. W., J. Pätzold, et al. (2003a). "Influence of Northern Hemisphere climate and global sea level rise on the restricted Red Sea marine environments during termination I." Palaeoceanography **18**.

Atalay, I., I. Sezer, et al. (1998). "Kızılçam (Pinus brutia Ten.) ormanlarının ekolojik özellikleri ve tohum nakli açısından bölgelere ayrılması." Orman Ağaçları ve Tohumları **6**.

Atkinson, M. D. (1992). "Betula pendula Roth (B. verrucosa Ehrh.) and B. pubescens Ehrh." Journal of Ecology **80**(837-870): 837-870.

Baird, D. (2004). Settlement expansion on the Konya Plain, Anatolia: 5th-7th centuries AD. The Late Antique Countryside, Late Antique Archaeology. L. Bowden, L. Lavan and C. Machado. **2:** 219-246.

Bakker, J., D. Kaniewski, et al. (2012a). "Numerically-derived evidence for late Holocene climate change and its impact on human presence in the south-west Taurus Mountains, Turkey." Holocene **22**: 425-438.

Bakker, J., E. Paulissen, et al. (2012b). "Climate, people, fire and vegetation: new insights into vegetation dynamics in the Eastern Mediterranean since the 1st century AD." Climate of the Past Discussion **8**: 3379-3444.

Bar-Matthews, M., A. Ayalon, et al. (2003). "Sea-land oxygen isotopic relationships from planktonic foraminifera and speleothems in the Eastern Mediterranean region and their implication for palaeorainfall during interglacial intervals." Geochimica et Cosmochimica Acta **67**: 3181-3199.

Bar-Matthews, M., A. Ayalon, et al. (2000). "Timing and hydrological conditions of Sapropel events in the Eastern Mediterranean, as evident from speleothems, Soreq Cave, Israel." Chemical Geology **169**: 145-156.

Bar-Matthews, M., A. Ayalon, et al. (1999). "The Eastern Mediterranean palaeoclimate as a reflection of regional events: Soreq cave, Israel." Earth and Planatery Science Letters **166**: 85-95.

Barboni, D., S. P. Harrison, et al. (2004). "Relationships between plant traits and climate in the Mediterranean region: a pollen data analysis." Journal of Vegetation Science **15**: 635-646.

Bariteau, M. and P. Ferandes (1990). L'Amelioration des Cedrus en France. Proceedings of the international Cedar Symposium, Antalya, Ormancılık Araş. Enst. Muhtelif Yayınlar (Ankara).
Barney, J. N. and A. DiTommaso (2003). "The biology of Canadian weeds. 118. Artemisia vulgaris L." Canadian journal of plant science **83**: 205-215.
Barney, J. N., A. G. Hay, et al. (2005). "Isolation and characterization of allelopathic volatiles from mugwort (Artemisia vulgaris)." Journal of Chemical Ecology **31**(2): 247-265.
Bartolozzi, F. and G. Fontanazza (1999). "Assessment of frost tolerance in olive (Olea europaea L.)." Scientia horticulturae **81**(3): 309-319.
Barton, C. M., H. Sarjoughan, et al. (2006). Modelling Long-Term Landscape Dynamics and the Emergence of Intensification (Draft). Society for American Archaeology 70th Annual Meeting.
Bartov, Y., S. L. Goldstein, et al. (2003). "Catastrophic arid episodes in the eastern Mediterranean linked with the North Atlantic Heinrich events." Geology **31**: 439-442.
Bartov, Y., M. Stein, et al. (2002). "Lake levels and sequence stratigraphy of Lake Lisan, the late Pleistocene precursor to the Dead Sea." Quaternary Research **57**: 9-21.
Bean, W. (1987). Trees and Shrubs Hardy in the British Isles. London, John Murray.
Becker, M. (1989). "The role of climate on present and past vitality of Silver Fir forests in the Vosges mountains of northeastern France." Canadian journal of forestry resources **19**: 1110-1117.
Bender, B., S. Hamilton, et al. (1997). "Leskernick: stone worlds; alternative narratives; nested landscapes." Proceedings of the Prehistoric Society **63**: 147-178.
Blondel, J. and J. Aronson (2004). Biology and wildlife of the Mediterranean region. New York, Oxford University Press.
Bond, G., W. Showers, et al. (1997). "A pervasive millenial-scale cycle in North Atlantic Holocene and glacial cycles." Science **278**: 1257-1266.
Bottema, S. (1980). "Palynological investigations on Crete." Review of Palaeobotany and Palynology **24**: 257-289.
Bottema, S. and H. Woldring (1984). "Late Quaternary vegetation and climate of southwestern Turkey Part II." Palaeohistoria **26**: 123-149.
Bottema, S. and H. Woldring (1990). Anthropogenic indicators in the pollen record of the Eastern Mediterranean. Man's role in the shaping of the Eastern Mediterranean landcape. S. Bottema, G. Entjes-Nieborg and W. Van Zeist. Rotterdam**:** 231-264.
Bottema, S., H. Woldring, et al. (1986). Palynological investigations on the relation between prehistoric man and vegetation in Turkey: Beysehir occupation phase. OPTIMA, Proceedings of the fifth meeting, Istanbul University.
Bottema, S., H. Woldring, et al. (1993). "Late Quaternary vegetation history and climate in northern Turkey." Palaeohistoria **35/36**: 13-72.
Boydak, M. (2003a). "Regeneration of Lebanon cedar (Cedrus libani A. Rich.) on karstic lands in Turkey." Forest Ecology and Management **178**(231-243).
Boydak, M. (2004). "Silvicultural characteristics and natural regeneration of Pinus brutia Ten. - a review." Plant Ecology **171**: 153-163.
Boydak, M., H. Dirik, et al. (2003b). "Effect of water stress on germination of six provenances of Pinus Brutia seeds from different bioclimatic zones of Turkey." Turkish Journal of Agriculture and Forestry **27**: 91-97.
Bradshaw, R. H. W. (2008). "Detecting human impact in the pollen record using data-model comparison." Vegetation History and Archaeobotany **17**: 597-603.
Braudel, F. (1996). The Mediterranean and the Mediterranean World in the Age of Philip II. Berkeley and Los Angeles, University of California Press.

Brewer, S., R. Cheddadi, et al. (2002). "The spread of deciduous Quercus throughout Europe since the last glacial period." Forest ecology and management **156**(1): 27-48.
Brooks, N. (2006). "Cultural responses to aridity in the Middle Holocene and increased social complexity." Quaternary International **151**: 29-49.
Broström, A., A. B. Neilson, et al. (2008). "Pollen productivity estimates of key European plant taxa for quantitative reconstruction of past vegetation: a review." Vegetation History and Archaeobotany **17**: 461-478.
Bunting, M. J., C. L. Twiddle, et al. (2007). "Using models of pollen dispersal and deposition in hilly landscapes: Some possible approaches." Palaeogeography, Palaeoclimatology, Palaeoecology **259**(1): 77-91.
Calamassi, R., E. Paoletti, et al. (2001). "Frost hardening and resistance in three Aleppo pine (Pinus halepensis Mill.) provenances." Israel Journal of Plant Sciences **3**(49): 179-186.
Calcote, R. (1995). "Pollen source area and pollen productivity: evidence from forest hollows. ." Journal of Ecology **83**: 591-602.
Caseldine, C., R. Fyfe, et al. (2008). "Pollen modelling, palaeoecology and archaeology: virtualisation and/or visualisation of the past?" Vegetation History and Archaeobotany **17**: 543-549.
Castagnoli, G. C., G. Bonino, et al. (2002). Solar radiation variability in the last 1400 years recorded in the carbon isotope ratio of a Mediterranean sea core. Solar Variability and Solar Physics Missions, Advances in Space Research. C. Frohlich, J. M. Pap, L. Dame and E. Marsch. Oxford, Pergamom-Elsevier Science Ltd. **:** 1989-1994.
Cavers, P. B., I. J. Bassett, et al. (1980). "The biology of Canadian weeds. 47. Plantago lanceolata L." Canadian journal of plant science **60**: 1269-1282.
CEC (1994). CORINE land cover. Technical Guide. Luxembourg.
CGIAR (2007). Global Geospatial Potential EvapoTranspiration & Aridity Index. Methodology and Dataset Description.
CGIAR. (2010). "Global aridity and PET database." from http://www.cgiar-csi.org/data/item/51-global-aridity-and-pet-database.
Chen, L., K. A. F. Zonneveld, et al. (2011). "Short term climate variability during "Roman Classical Period" in the eastern Mediterranean." Quaternary Science Reviews **30**(27-28): 3880-3891.
Chittendon, F. (1956). RHS Dictionary of Plants plus Supplement. Oxford, Oxford University Press.
Chuine, I. and P. Cour (1999). "Climatic determinants of budburst seasonality in four temperate-zone tree species." New Phytology **143**: 339-349.
Clare, L., E. J. Rohling, et al. (2008). "Warfare in Late Neolithic / Early Chalcolithic Pisidia, southwestern Turkey. Climate induced social unrest in the late 7th millenium calBC." Documenta Praehistorica **15**: 65-92.
Clark, P. U., A. M. McCabe, et al. (2004). "Rapid rise of sea level 19,000 years ago and its global implications." Science **304**(5674): 1141-1144.
ClinTools. (2005). "Cramer's phi." from http://www.clintools.com/products/org/WebHelp/odds_ratio_generator_help/phi_cramer_s_phi.htm.
Corona, P., M. Romagnoli, et al. (1995). "Stem annual increments as ecobiological indicators in Turkey oak (Quercus cerris L.)." Trees - Structure and Function **10**(1): 13-19.
Coulton, J. J. (1988). "'Balboura Survey'." Annual report of the British Institute of Archaeology at Ankara **40**: 13-15.
Davis, M. B. (1963). "On the theory of pollen analysis." American Journal of Science **261**: 897-912.

de Menocal, P. B., J. Oritz, et al. (2000). "Coherent high- and low-latitude climate variability during the Holocene Warm Period." Science **288**: 2198-2202.
Denton, G. H., R. F. Anderson, et al. (2010). "The Last Glacial Termination." Science **328**(5986): 1652-1656.
Dermody, B. J., H. J. de Boer, et al. (2011). "Revisiting the humid Roman hypothesis: novel analyses depict oscillating patterns." Climate of the Past Discussion **7**: 2355-2389.
Dinc, U., S. Senol, et al. (2005). Soil survey and soil database of Turkey, Soil resources of Europe. JRC-IES European Soil Bureau Research Report, JRC-IES**:** 371-375.
DiTomasco, J. (2001). Element stewardship abstract for Centaurea solstitialis. Virginia, The Nature Conservancy.
Ducrey, M. (1993). Adaptation du Cedre de 1' Alas (Cedrus atlantica Monetti) au climat méditerranéen: aspect écophysiologiques de sa réaction à la secheresse. le Cédre de 1' Atlas. O. M' Hırıt, A. Samik and M. Malagnoux, Ann. Rech. For. Maroc. **27:** 140-153.
Duke, J. (1983). "Handbook of energy crops." Retrieved March, 2010, from http://www.hort.purdue.edu/newcrop/duke_energy/dukeindex.html.
Eastwood, W. J., R. Fyfe, et al. (2011). "Quantitative vegetation modelling in southwest Turkey." Heritage Turkey. British Institute of Ankara Research Reports **1**(2011).
Eastwood, W. J., M. J. Leng, et al. (2007). "Holocene climate change in the eastern Mediterranean region: a comparison of stable isotope and pollen data from Lake Gölhisar, southwest Turkey." Journal of Quaternary Science **22**(4): 327-341.
Eastwood, W. J., N. Roberts, et al. (1998). "Palaeoecological and archaeological evidence for human occupance in southwest Turkey: the Beysehir Occupation Phase." Anatolian Studies **48**: 69-86.
Eastwood, W. J., N. Roberts, et al. (1999). "Holocene environmental change in southwest Turkey: a palaeoecological record of lake and catchment-related changes." Quaternary Science Reviews **18**(4-5): 671-695.
Eastwood, W. J., J. Tibby, et al. (2002). "The environmental impact of the MInoan eruption of Santorini (Thera): statistical analysis of palaeoecological data from Golhisar, southwest Turkey." The Holocene **12**: 431-444.
EEA (2000). CORINE land cover technical guide - Addendum 2000, European Environment Agency**:** 105.
Ellenberg, H. (1992). Vegetation Mitteleuropas mit den Alpen. Stuttgart, Germany, Eugen Ulmer Verlag.
Emeis, K. C., H. M. Schulz, et al. (2003). "Eastern Mediterranean surface water temperatures and d18O composition during depotision of sapropels in the late Quaternary." Palaeoceanography **18**.
Emeis, K. C., H. M. Schulz, et al. (1998). "Stable isotope and temperature records of sapropels from ODP Sites 964 and 967: constraining the physical environment of sapropel formation in the Eastern Mediterranean Sea." Proceedings of the Ocean Drilling Program. Scientific Results **160**: 309-331.
Emeis, K. C., U. Struck, et al. (2000). "Temperature and salinity of Mediterranean Sea surface waters over the last 16,000 years: constraints on the physical environment of S1 sapropel formation based on stable oxygen isotopes and alkenone unsaturation ratios." Palaeogeography, Palaeoclimatology, Palaeoecology **158**: 259-280.
England, A., W. J. Eastwood, et al. (2008). "Historical landscape change in Cappadocia (central Turkey): a palaeoecological investigation of annually laminated sediments from Nar lake." The Holocene **18**(8): 1229-1245.
Erol, O. (1981). "Neotectonic and Geomorphological Evolution of Turkey." Zeitschrift für Geomorphologie Annals of Geomorphology, N. F.Supp. Bd. **40**: 193-211.

Escudero, A., S. Barrero, et al. (1997). "Effects of high temperatures and ash on seed germination of two Iberian pines (Pinus nigra ssp salzmannii, P sylvestris var iberica)." Annuals of Forest Science **54**: 553-562.
Espelta, J. M., J. Retana, et al. (2003). "An economic and ecological multi-criteria evaluation of reforestation methods to recover burned Pinus nigra forests in NE Spain." Forest Ecology and Management **180**(1-3): 185-198.
EUFORGEN. (2009). "European Forest Genetic Resources Programme Distribution Maps." Retrieved January, 2010, from http://www.euforgen.org/distribution_maps.html.
FAO/IIASA/ISRIC/ISSCAS/JRC (2009). Harmonized World Soil Database (version 1.1), FAO.
Fauve-Chamoux, A. (2011). The Cambridge World History of Food.
Fernández-López, J., P. Alcàzar, et al. (2011). Castanea sativa. Technical guidelines for genetic conservation and use, EUFORGEN.
Fleitmann, D., J. Burns, et al. (2003). "Holocene forcing of the Indian Monsoon recorded in a stalagmite from southern Oman." Science **300**: 1737-1739.
Fleitmann, D., H. Cheng, et al. (2009). "Timing and climatic impact of Greenland interstadials recorded in stalagmites from northern Turkey." Geophysical Research Letters **36**: 5.
Fontugne, M., C. Kuzucuoğlu, et al. (1999). from Pleniglacial to holocene; a 14C chronostratigraphy of environmental changes in the Konya Plain, Turkey. The Late Quaternary in the Eastern Mediterrnaean Region. C. N. Roberts, C. Kuzucuoğlu and K. M. **18:** 573-591.
Fraxigen (2005). Ash species in Europe: biological characteristics and practical guidelines for sustainable use. Oxford, Oxford Forestry Institute, University of Oxford.
Frisia, S., A. Borsato, et al. (2005). "Climatic variability in the SE Alps of Italy over the past 17 000 years reconstructed from a stalagmite record." Boreas **34**(4): 445-455.
Frumpkin, A., D. C. Ford, et al. (2000). "Palaeoclimate and vegetation of the last glacial cycles in Jerusalem from a speleothem record." BGlobal Biogeochemidal Cycles **14**(3): 863-870.
Galàn, C., H. Garcia-Mozo, et al. (2001). "The role of temperature in the onset of the Olea europaea L. pollen season in southwestern Spain." International Journal of Biometeorology **45**(1): 8-12.
Garcia-Castellanos, F. Estrada, et al. (2009). "Catastrophic flood of the Mediterranean after the Messinian salinity crisis." Nature **462**: 778-781.
Garfunkel, Z. (2004). "Origin of the Eastern Mediterranean basin: a reevaluation." Tectonophysics **391**: 11-34.
Gassner, G. and F. Christiansen-Weniger (1942). "Dendroklimatologische Untersuchungen ¨uber die Jahresringentwicklung der Kiefern in Anatolien." Nova Acta Leopoldina **12**: 1-134.
Gaussen, H. (1954). Théorie et classification des climats et microclimats. 8th Congress of International Botany, Paris.
Gezer, A. (1986). "The Sylviculture of Pinus brutia in Turkey." **1**(86): 55-66.
Ghrabi, Z. (2011). "Juniperus phoenicia L." A guide to medicinal plants in North Africa, from http://www.uicnmed.org/nabp/database/HTM/PDF/p38.pdf.
Giraudi, C. (2009). "Late Holocene glacial and periglacial evolution of the upper Orco Valley, northwestern Italian Alps." Quaternary Research **71**(1): 1-8.
Gleason, H. A. (1926). "The individualistic concept of the plant succession." Bulletin of the Torrey Botanical Club **53**: 7-26.

Gobet, E., W. Tinner, et al. (2000). "Influence of human impact and bedrock differences on the vegetation history of the Insubrian southern Alps." Vegetation history and Archaeobotany **9**: 175-187.
Goodfriend, G. A. (1999). "Terrestrial stable isotope records of Late Quaternary palaeoclimates in the eastern Mediterranean region." Quaternary Science Reviews **18**: 501-513.
GPCC. (2009). "Global Precipitation Analysis Products." 2009, from http://www.cgd.ucar.edu/cas/catalog/surface/precip/gpcc.html.
Grove, A. T. and O. Rackham (2003). The Nature of Mediterranean Europe. New Haven and London, Yale University Press.
Guiot, J. and A. Pons (1986). Une méthode de reconstruction quantitative du climat à partir de chroniques pollenanalytiques: le climat de la France depuis 15000 ans. Académie des Science, Comptes Rendus, Paris.
Guo, Z., N. Pertit-Maire, et al. (2000). "Holocene non-orbital climatic events in present-day arid areas of northern Africa and China." Global and Planetary Change **26**: 97-103.
Gvirtzman, G. and M. Wieder (2001). "Climate of the last 53,000 years in the Eastern Mediterranean, based on soil-sequence stratigraphy in the coastal plain of Israel." Quaternary Science Reviews **20**: 1827-1849.
Hargreaves, G. L., G. H. Hargreaves, et al. (1985). "Irrigation water requirements for Senegal River Basin." Journal of Irrigation and Drainage Engineering **111**(3): 265-275.
Hayes, A., M. Kucera, et al. (2005). "Glacial Mediterranean sea surface temperatures based on planktonic foraminiferal assemblages." Quaternary Science Reviews **24**: 999-1016.
Heide, O. M. (1993). "Dormancy release in beech buds (Fagus sylvatica) requires both chilling and long days." Physiologia Plantarum **89**(1): 187-191.
Hijmans, R. J., S. E. Cameron, et al. (2005). "Very high resolution interpolated climate surfaces for global land areas." International Journal of Climatology **25**(15): 1965-1978.
Holzhauser, H., M. Magny, et al. (2005). "Glacier and lake-level variations in west-central Europe over the last 3500 years." Holocene **15**(6): 789-801.
Horden, P. and N. Purcell (2000). The Corrupting Sea. Oxford, Blackwell.
Horowitz, A. (1971). "Climatic and vegetation developments in northeastern Israel during Upper Pleistocene-Holocene times." Pollen et Spores **13**(255-7).
Hutchinson, M. F. (1995). "Interpolating mean rainfall using thin plat smoothing splines." International Journal of Geographical Information Systems **9**: 385-403.
Huxley, A., M. Griffiths, et al. (1992). The New RHS Dictionary of Gardening, Macmillan Reference.
Israel, G. D. (1992). Determining Sample Size. I. f. F. a. A. Sciences, University of Florida.
Issar, A. and M. Zohar (2004). Climate Change - Environment and Civilization in the Middle East. Berlin, Heidelberg, New York, Springer.
Issar, S. A. and D. Yakir (1997). "The Roman Period's Colder Climate." Biblical Archaeologist **60**(2).
Izdebski, A. (2011). "Why did agriculture flourish in the late antique East? The role of climate fluctuations in the development and contraction of agriculture in Asia Minor and the Middle East from the 4th till the 7th c. AD." Millenium **8**: 291-312.
Jackson, R. (2008). Wine science: principles and applications. Burlington, London, San Diego, Academic Press.
Jackson, S. and M. Lyford (1999). "Pollen dispersal models in Quaternary plant ecology: Assumptions, parameters, and prescriptions." The Botanical Review **65**(1): 39-75.

Jones, M. D., C. N. Roberts, et al. (2007). "Quantifying climatic change through the last glacial-interglacial transition based on lake isotope palaeohydrology from central Turkey." Quaternary Research **67**: 463-473.
JRC (2005). IMAGE2000 and CLC2000 Products and Methods. Ispra, European commission Joint Research Centre.
Jurgensen, M. F., D. S. Page-Dumroese, et al. (2009). Wood stakes as an index of soil organic matter decomposition in a climatic gradient along the Spanish Mediterranean Coast. EGU General Assembly 2009, Vienna, Austria.
Kaniewski, D., V. De Laet, et al. (2007a). "Long-term effects of human impact on mountainous ecosystems, western Taurus Mountains, Turkey." Journal of Biogeography **34**(11): 1975-1997.
Kaniewski, D., E. Paulissen, et al. (2007b). "A high resolution Late Holocene landscape ecological history inferred from an intramontane basin in the Western Taurus Mountains, Turkey." Quaternary Science Reviews **26**: 2201-2218.
Kantarcı, M. D. (1990). Türkiye'de sedir ormanlarının yayılış alanlarında ekolojik ilişkiler (Ecological relationships in the natural distribution of cedar forests in Turkey). Proceedings of the International Cedar Symposium, Antalya, Ormancılık Araş. Ens. Muhtelif Yayınlar (Ankara).
Keigwin, L. D. (1996). "The little ice age and medieval warm period in the Sargasso sea." Science **274**(5292): 1504-1508.
Kelly, M. G. and B. Huntley (1991). "An 11 000-year record of vegetation and environment from Lago di Martignano, Latium, Italy." Journal of Quaternary Science **6**(3): 2009-2224.
Köble, R. and G. Seufert (2001). Novel maps for forest tree species in Europe. "A changing atmosphere", 8th European symposium on the Physico-Chemical Behaviour of Atmosperic Pollutants, Torino, JRC Ispra, Institute for Environment and Sustainability.
Köppen, W. (1936). Das Geographisches System der Kilmate. Handbuch der Klimatologie. W. Köppen and R. Geiger. Berlin, Gebrüder Borntraeger.
Koubouris, G. C., I. T. Metzidakis, et al. (2009). "Impact of temperature on olive (Olea europaea L.) pollen performance in relation to relative humidity and genotype." Environmental and Experimental Botany **67**(1): 209-214.
Kramer, K. (1994). "Selecting a model to predict the onset of growth in Fagus sylvatica." Journal of Applied Ecology **31**(1): 172-181.
Kreutz, K. J., P. A. Mayewski, et al. (1997). "Bipolar changes in atmospheric circulation during the Little Ice Age." Science: 1294-1296.
Kutzbach, J. E. and P. J. Guetter (1986). "the influence of changing orbital parameters and surface boundary conditions with climate simulation conditions for the past 18000 years." Journal of Atmospheric Science **43**: 1726-1759.
Kutzbach, J. E. and E. A. Street-Perrott (1985). "Milancovitch forcing of fluctuations in the level of tropical lakes from 18 to 0 kyr bp." Nature **317**: 130-134.
Kutzbach, J. E. and T. Webb, III (1993). Conceptual Basis for Understanding Late-Quaternary Climates. Global Climates since the Last Glacial Maximum. H. E. Wright, J. E. Kutzback, T. Webb, IIIet al. MInneapolis, University of Minnesota Press.
Kuzucuoğlu, C. and N. Roberts (1998). "Evolution de l'Environment en Anatolie, de 2000 à 6000 BP." Palaeorient **23**(2): 7-24.
Lahti, T. and R. Lampinen (1999). "From dot maps to bitmaps: Atlas Florae Europaeae goes digital." Acta Botanica Fennica **162**: 5-9.
Lamb, H. H. (1977). Climate: Present, Past and Future. Climatic History and the Future. H. H. Lamb. London, Methuen. **2:** 835.

Landmann, G., G. Abu Qudaira, et al. (2002). "Geochemistry of the Lisan and Damya Formations in Jordan, and implications for palaeoclimate." Quaternary International **89**: 45-57.
Landmann, G., A. Reimer, et al. (1996). "Climatically induced lake level changes at Lake Van, Turkey, during the Pleistocene/Holocene transition." Global Biogeochemical Cycles **10**: 797-808.
Larcher, W. (1970). "Kalteresistenz und uberwinterungsvermogen mediterraner Holzpflanzer." Oecologia Plantarum **5**: 267-286.
Liddell, H. G. and R. Scott (1940). A Greek-English Lexicon. Oxford, Clarendon Press.
Lo Gullo, M. A., S. Salleo, et al. (1995). "Relations between vulnerability to xylem embolism and xylem conduit dimensions in young trees of Quercus cerris." Plant, Cell and Environment(18): 661-669.
Loacker, K., W. Kofler, et al. (2007). "Spread of walnut (Juglans regia L.) in an Alpine valley is correlated with climate warming." Flora - morphology, distribution, functional ecology of plants **202**(1): 70-78.
Luza, J. G. and V. S. Polito (1985). "In vitro germination and storage of English walnut pollen." Scientia horticulturae **27**: 303-316.
Martínez-Ferri, E., E. Manrique, et al. (2004). "Winter photoinhibition in the field involves different processes in four co-occurring Mediterranean tree species." Tree Physiology **24**: 981-990.
Martinoli, D. C. (2009). Plant food economy and environment during the epipalaeolithic in southwest Anatolia: an investigation of the botanical macroremains from Öküzini and Karain B. Faculty of Science. Basel, University of Basel. **PhD**.
McGarry, S., M. Bar-Matthews, et al. (2004). "Constraints on hydrological and paleotemperature variations in the Eastern Mediterranean region in the last 140 ka given by the dD values of speleothem fluid inclusions." Quaternary Science Reviews **23**: 919-934.
McLaren, S. J., D. D. Gilbertson, et al. (2004). "Quaternary palaeogeomophologic evolution of the Wadi Faynan area, southern Jordan." Palaeogeography, Palaeoclimatology, Palaeoecology **205**: 131-154.
Migowski, C., M. Stein, et al. (2006). "Holocene climate cariability and cultural evolution in the Near East from the Dead Sea sedimentary record." Quaternary Research **66**: 421-431.
Mirchev, S., M. Lyubenova, et al. (2009). "Dendrochronological investigation on Castanea Sativa Mill. in Belasitza Mountain and western Balkans (Berkovitza Mountain)." Biotechnology and biotechnological equipment(EQ 23/SE): 377-380.
Mitchell, A. F. (1972). Conifers in the British Isles. A descriptive handbook. London, HMSO.
Mitchell, S. (2005). Olive cultivation in the Economy of Asia Minor. Patterns in the economy of Asia Minor. S. Mitchell and C. Katsari. Swansea**:** 82-113.
Moody, J., O. Rackham, et al. (1996). "Environmental archaeology of prehistoric NW Crete." Journal of Field Archaeology **23**: 273-297.
Moore, G. (2011). Plantain (Plantago lanceolata), Government of Western Australia Department of Agriculture and Food.
Morin, X., T. Améglio, et al. (2007). "Variation in cold hardiness and carbohydrate concentration from dormancy induction to bud burst amoung provenances of three European oak species." Tree Physiology **27**: 817-825.
Myking, T. and O. M. Heide (1995). "Dormancy release and chilling requirement of buds of latitudinal ecotypes of Betula pendula and B. pubescencs." Tree Physiology **15**(11): 697-704.

Nardini, A., M. A. Lo Gullo, et al. (1999). "Competitive strategies for water availability in two Mediterranean Quercus species." Plant, Cell and Environment **22**: 109-116.
NCDC. (2010). "GHCN." 2. from http://www.ncdc.noaa.gov/ghcnm/.
Neev, D. and K. O. Emery (1967). "The Dead Sea." Geological Survey of Israel Bulletin **41**: 1-147.
Niewöhner, P. (2006). "Aizanoi and Anatolia. Town and countryside in Late Antiquity." Millenium **3**: 239-253.
Niklewski, J. and W. Van Zeist (1970). "A Late Quaternary pollen diagram for NW Syria." Acta Botanica Neerlandica **9**(737-54).
OED (2011). Oxford English Dictionary. Oxford English Dictionary, Oxford University Press.
OGM (1997). Forestry map of Turkey, Orman Genel Müdürlüğü, Çevre ve Orman Bakanlığı.
Oliveira, M. (1998). "Calculation of budbreak and flowering base temperatures for Vitis vinifera cv. Touriga Francesca in the Douro region of Portugal." American journal of enology and viticulture **49**(1): 74-78.
Orland, I. J., M. Bar-Matthews, et al. (2009). "Climate deterioration in the eastern Mediterranean as revealed by ion microprobe analysis of a speleothem that gre from 2.2 to 0.9 ka in Soreq Cave, Israel." Quaternary Research **71**: 27-35.
Ozkan, K., S. Gulsoy, et al. (2010). "Site properties for crimean juniper (Juniperus excelsa) in semi-natural forests of south western Anatolia, Turkey." Journal of Environmental Biology **31**: 97-100.
Patón, D., R. García-Herrera, et al. (2009). "Influence of cliamte on radial growth of Holm Oak (Quercus ilex subsp. ballota desf) from SW Spain." Geochronometria **34**: 49-56.
Peel, M. C., B. L. Finlayson, et al. (2007). "Updated world map of the Koppen-Geiger climate classification." Hydrological Earth Systems Science **11**: 1633-1644.
Peyron, O., S. Goring, et al. (2011). "Holocene seasonality changes in the central Mediterranean region reconstructed from the pollen sequences of Lake Accesa (Italy) and Tenaghi Philippon (Greece)." The Holocene **21**(1): 131-146.
PFAF. (2009a). "Quercus cerris - L." Retrieved November, 2009, from http://www.pfaf.org/user/Plant.aspx?LatinName=Quercus+cerris.
PFAF. (2009b). "Quercus coccifera - L." Retrieved November, 2009, from http://www.pfaf.org/user/Plant.aspx?LatinName=Quercus+coccifera.
PFAF. (2009c). "Betula pendula." Retrieved November, 2009, from http://www.pfaf.org/user/Plant.aspx?LatinName=Betula+pendula.
PFAF. (2009d). "Abies alba." Retrieved November, 2009, from http://www.pfaf.org/user/Plant.aspx?LatinName=Abies+alba.
PFAF. (2009f). "Alnus glutinosa." Retrieved November, 2009, from http://www.pfaf.org/user/plant.aspx?latinname=Alnus+glutinosa.
PFAF. (2009g). "Picea abies." Retrieved November, 2009, from http://www.pfaf.org/user/Plant.aspx?LatinName=Picea+abies.
PFAF. (2009j). "Tilia Cordata." Retrieved 15/10/2010, from http://www.pfaf.org/user/Plant.aspx?LatinName=Tilia+cordata.
PFAF (2009k). "Castanea sativa."
Pons, A. and P. Quezel (1985). The history of the flora and vegetation and past and present human disturbance in the Mediterranean region. Plant conservation in the Mediterranean area. **7:** 25-43.
Pons, L. J. and C. H. Edelman (1963). A soil survey of Köyceğiz-Dalaman area (Turkey). Ankara.

Quezel, P. (1981). Floristic composition and phytosociological structure of sclerophyllous matorral around the Mediterranean. Ecosystems of the world 2. Mediterranean type shrublands. F. di Castri. Amsterdam, Elsevier.
Quezel, P. (2000). Taxonomy and biogeography of Mediterranean pines (Pinus halepensis and Pinus brutia). Ecology, Biogrography and Management of Pinus halepensis and P. brutia Forest Ecosystems in the Mediterranean Basin. Leiden, Backhuys**:** 1-12.
Ranney, T. G. and R. E. Bir (1994). "Comparative flood tolerance of birch rootstock." Journal of the American society for horticultural science **119**(1): 43-48.
Reille, M., J. Gamisans, et al. (1997). "The late-glacial at Lac de Creno (Corsica, France): a key site in the western Mediterranean basin." New Phytology **135**: 547-559.
Roberts, C. N. (1983). "Age, palaeoenvrionments and climatic significance of Late Pleistocene Konya Lake, Turkey." Quaternary Research **19**: 154-171.
Roberts, C. N., W. J. Eastwood, et al. (1997). The age and causes of Mid-Late Holocene environmental change in southwest Turkey. Third Millennium BC Climate Change and Old World Collapse, . Nüzhet Dalfes, G. Kukla and H. Weiss. Berlin Heidelberg, Spreinger-Verlag**:** 411-429.
Roberts, C. N., J. M. Reed, et al. (2001). "The tempo of Holocene climate change in the eastern Mediterranean region: new high-resolution crater-lake sediment data from central Turkey." The Holocene **11**(6): 721-736.
Roberts, C. N. and H. E. J. Wright (1993). Vegetational, lake-level and climatic history of the Near East and Southwest Asia. Global climates since the last glacial maximum. H. E. J. Wright, J. E. Kutzbach, T. I. Webbet al. Minneapolis, University of Minnesota Press**:** 194-220.
Roberts, N. (1990). Human-induced landscape change in south and southwest Turkey during the later Holocene. Man's role in the shaping of the Eastern Mediterranean landscape. S. Bottema, G. Entjes-Nieborg and W. Van Zeist. Rotterham**:** 53-67.
Roberts, N., W. J. Eastwood, et al. (2011b). "Climatic, vegetation and cultural change in the eastern Medierranean during the mid-Holocene environmental transition." The Holocene **21**: 147-162.
Roberts, N., M. D. Jones, et al. (2008). "Stable isotope records of Late Quaternary climate and hydrology from Mediterranean lakes: the ISOMED synthesis." Quaternary Science Reviews **27**(25-26): 2426-2441.
Roberts, N. and H. E. Wright (1993). Vegetational, lake level, and climatic history of the Near East and Southwest Asia. Global climates since the last glacial maximum. J. H E Wright, J. E. Kurtzbach, T. W. IIIet al. Minneapolis, University of Minnesota Press. (COHAMP volume)**:** 53-67.
Robinson, S. A., S. Black, et al. (2006). "A review of palaeoclimates and palaeoenvironments in the Levant and Easter Mediterranean from 25,000 to 5000 years BP: setting the environmental background for the evolution of human civilisation." Quaternary Science Reviews **25**: 1517-1541.
Rodà, F. (1999). Ecology of Mediterranean evergreen oak forests, Springer.
Rohling, E. J. and F. J. Hilgen (1991). "The eastern Mediterranean climate at times of sapropel formation: a review." Geologie en Mijnbouw **70**: 253-264.
Rolland, C., R. Michalet, et al. (1999). "Ecological requirements of Abies alba in the French Alps derived from dendro-ecological analysis." Journal of Vegetation Science **10**: 297-306.
Romagnoli, M. and G. Codipietro (1996). "Pointer years and growth in Turkey oak (Quercus cerris L) in Latium (central Italy). A dendroclimatic approach." Annals of Forest Science(53): 671-684.

Rossignol-Strick, M. (1987). "Rainy periods and bottom water stagnation initiating brine accumulation and metal concentrations: 1. the Late Quaternary." Palaeoceanography **2**: 333-360.
Rossignol-Strick, M. (1995). "Sea-land correlation of pollen records in the Eastern Mediterranean for the glacial-interglacial transition: biostratigraphy versus radiometric time-scale." Quaternary Science Reviews **14**: 893-915.
Rossignol-Strick, M. (1999). "The Holocene climatic optimum and pollen records of sapropel 1 in the Eastern Medierranean, 9000-6000 BP." Quaternary Science Reviews **18**: 515-530.
Rousseaux, C., J. P. Benedetti, et al. (2008). "Leaf-level responses of olive trees (Olea europaea) to the suspension of irrigation during the winter in an arid region of Argentina." Scientia horticulturae **115**(2): 135-141.
Rushforth, K. (1991). Conifers, Batsford Ltd.
Saei, A., Z. Zamani, et al. (2006). "Influence of drought stress periods on olive (Olea eruopaea L. cv. Lard) leaves stomata." International journal of agriculture and biology **8**(4): 430-433.
Sarıkaya, M. A., M. Zreda, et al. (2008). "Cold and wet Last Glacial Maximum on Mount Sandıras, SW Turkey, inferred from cosmogenic dating and glacier modelling." Quaternary Science Reviews **27**: 269-780.
Sarnthein, M., R. Gersonde, et al. (2003). "Overview of Glacial Atlantic Ocean Mapping (GLAMAP 2000)." Palaeoceanography **18**(1030): 6.
Schilman, B., M. Bar-Matthews, et al. (2001). "Global climate instability reflected by eastern Mediterranean marine records during the late Holocene." Palaeogeography, Palaeoclimatology, Palaeoecology **176**: 157-176.
Schoell (1978). Oxygen isotope analysis on authigenic carbonates from Lake Van sediments and their possible bearing on the climate of the past 10,000 years. The Geology of Lake Van, Kurtman. E. T. Degens. Ankara, The Mineral Research and Exploration Institute of Turkey.
Schwarz, O. (1936). "Die Vegetationsverhältnisse Westantoliens." Botanische Jahrbücher **67**: 297-436.
Sevgi, O. and Ü. Akkemik (2007). "A dendrochronological study on Pinus nigra Arn. at different altitudes of northern slopes of Kazdaglari, Turkey." Journal of Environmental Biology **28**(1): 73-75.
Shen, Y. A., Y. W. Xiong, et al. (2010). "Performance of high-resolution satellite preciptiation products over China." Journal of Geophysical Research **115**.
Snyder, J. A., K. Wasylik, et al. (2001). "Diatom-based conductivity reconstruction and palaeoclimatic interpretation of a 40-ka record from Lake Zeribar, Iran." The Holocene **11**: 737-745.
Sohn, B. J., H.-J. H., et al. (2010). "Validation of Satellite-Based High Resolution Rainfall Products over the Korean Peninsula Using Data from a Dense Rain Gauge Network." Journal of Applied Meteorology and Climate **49**(4): 701.
Spano, D., C. Cesaraccio, et al. (1999). "Phenological stages of natural species and their use as climate indicators." International Journal of Biometeorology **42**: 124-133.
Stein, M. (2001). "The sedimentary and geochemical record of Neogene-Quaternary water bodies in the Dead Sea Basin - Inferences for the regional palaeoclimatic history." Journal of Paleolimnology **26**: 271-282.
Suc, J. P. (1984). "Origin and evolution fo the Mediterranean vegetation and climate in Europe." Nature **307**: 409-432.
Sugita, S. (1993). "A model of Pollen Source Area for an Entire Lake Surface." Quaternary Research **39**: 239-244.

Sugita, S. (1994). "Pollen representation of vegetation in Quaternary sediments: theory and method in patchy vegetation." Journal of Ecology **82**(811-897).
Sullivan, D. G. (1988). "The discovery of Santorini Minoan tephra in western Turkey." Nature **333**: 552-554.
Sullivan, D. G. (1989). Human induced vegetation change in western Turkey: Pollen evidence from central Lydia. Unpublished PhD thesis. Berkley, University of California.
Sullivan, D. G. (1990). Minoan tephra in lake sediments in Western Turkey, dating the eruption and assessing the atmospheric dispersal of the ash. Thera and the Aegean World III. D. A. Hardy and C. Renfrew. London. **Volume 3 - Chronology:** 114-119.
Sutinen, M. L., J. P. Palta, et al. (1992). "Seasonal differences in freezing stress resistance of needles of Pinus nigra and Pinus resinosa: evaluation of the electrolyte leakage method." Tree Physiology **11**: 241-254.
Tansley, A. G. (1920). "The classification of vegetation and the concept of development." Journal of Ecology **8**: 118-149.
Taricco, C., M. Ghil, et al. (2009). "Two millennia of climate variability in the central Mediterranean." Climate of the Past **5**(2): 171-181.
Taymaz, T., J. Jackson, et al. (2007). "Active tectonics of the north and central Aegean Sea." Geophysical Journal International **106**(2): 433-490.
Tessier, L., P. Nola, et al. (1994). "Deciduous Quercus in the Mediterranean region: tree-ring / climate relationships." New Phytologist **126**: 355-367.
Thompson, R. S., K. H. Anderson, et al. (2000). Atlas of relations between climatic parameters and distributions of important trees and shrubs in North America, Hardwoods. US Geological Survey Professional Paper**:** 423.
Thornthwaite, C. W. (1948). "An approach toward a rational classification of climate." Geographical review **38**(1): 55-94.
Tilki, F. and H. Dirik (2007). "Seed germination of three provenances of Pinus Brutia (Ten.) as influenced by stratification, temperature and water stress." Journal of Environmental Biology **1**(28): 133-136.
Tognetti, R., R. d'Andria, et al. (2006). "The effect of deficit irrigation on crop yield and vegetative development of Olea europaea L. (cvs. Frantoio and Leccino)." European journal of agronomy **25**: 356-364.
Türkeş, M. (1996). "Meteorologial Drought in Turkey: A Historical Perspective, 1930-93." Drought Netowrk News (1994-2001).
UN-ECE (1998). Manual on methods and criteria for harmonized sampling, assessment, monitoring and analysis of the effects of air pollution on forests, International Co-operative Programme on Assessment and Monitoring of Air Pollution Effects on Forests. .
van Zeist, W. and S. Bottema (1977). "Palynological investigations in western Iran." Palaeohistoria **19**: 1995.
van Zeist, W. and S. Bottema (1982). Vegetational history of the Eastern Mediterranean and Near East during the last 20,000 years. Palaeoclimates, Palaeoenvironments and Human Communities in Eastern Mediterranean Region in later Prehistory. Oxford, British Archaeological Report, International Series. **133:** 277-321.
van Zeist, W. and S. Bottema (1991). Late Quaternary vegetation of the Near East. Beihefte zum Tubinger Atlas des vorderen orients, naturwissenschaften A. Reihe. Weisbaden, Dr Ludwig Reichert Verlag. **18:** 156.
van Zeist, W., H. Woldring, et al. (1975). "Late Quaternary vegetation and climate of southwestern Turkey." Palaeohistoria **17**: 55-143.

van Zeist, W. and H. E. J. Wright (1963). "Preliminary pollen studies at Lake Zeribar, Zagros Mountains, southwestern Iran." Science **140**: 65-67.
Vanhaverbeke, H. and M. Waelkens (2003). The Chora of Sagalassos. The evolution of the settlement pattern from prehistoric until recent times. Belgium, Brepolis.
Vannière, B., M. J. Power, et al. (2011). "Circum-Mediterranean fire activity and climate changes during the mid-Holocene environmental transition (8500-2500 cal. BP)." The Holocene **21**(1): 53-73.
Vannini, A., R. Valentini, et al. (1996). "Impact of drought and Hypoxylon mediterraneum on oak decline in the Mediterranean region." Annals of Forest Science **53**(2-3): 753-760.
Verheyden, S., F. H. Nadar, et al. (2008). "Palaeoclimate reconstruction in the Levant region from the geochemistry of a Holocene stalagmite from the Jeita cave, Lebanon." Quaternary Research **70**: 368-381.
Vermoere, M. (2002a). Holocene vegetation history in the territory of Sagalassos (southwest Turkey) A palynological approach, K.U. Leuven. **PhD**.
Vermoere, M., S. Bottema, et al. (2002b). Palynological evidence for late-Holocene human occupation recorded in two wetlands in SW Turkey. **12:** 569-584.
Vermoere, M., E. Smets, et al. (2000). "Late Holocene Environmental Change and the Record of Human Impact at Gravgaz near Sagalassos, Southwest Turkey." Journal of Archaeological Science **27**(7): 571-595.
Versteegh, G. J. M., J. W. de Leeuw, et al. (2007). "Temperature and productivity influences on U-37(K') and their possible relation to solar forcing of the Mediterranean winter." Geochemistry, Geophysics, Geosystems **8**: 14.
Villar-Salvador, P., P. Castro-Díez, et al. (1997). "Stem zylem features in three Quercus (Fagaceae) species along a climatic gradient in NE Spain." Trees **12**: 90-96.
Waelkens, M. (1999). "Man and Environment in the territory of Sagalassos, a classical city in southwest Turkey." Quaternary Science Reviews **18**(4-5): 697-709.
Waelkens, M. (2000). Sagalassos and Pisidia during the Late Bronze Age. Report on the survey and excavation campaigns of 1996 and 1997. Acta Archaeological Lovaniensia Monographiae. M. Waelkens and L. Loots. Leuven, Leuven University Press. **11/B:** 473-485.
Waelkens, M., E. Paulissen, et al. (1997). The 1994 and 1995 surveys on the territory of Sagalassos. Sagalassos IV. Report on the Fifth Excavation Campaign of 1994 (Acta Archaeological Lovaniensia). M. Waelkens. Leuven. **9:** 11-102.
Walker, M. J. C. (1995). "Climatic changes in Europe during the last glacial / interglacial transition." Quaternary International **28**: 63-76.
Walker, M. J. C., S. Bjorck, et al. (1999). "Isotopic 'events' in the GRIP ice core: a stratotype for the Late Pleistocene. ." Quaternary Science Reviews **18**: 1143-1150.
Wang, J. T. (1988). "The steppes and deserts of the Xizang Plateau (Tibet)." Vegetatio **75**: 135-142.
Wick, L., G. Lemcke, et al. (2003). "Evidence of Lateglacial and Holocene climatic change and human impact in eastern Anatolia: high-resolution polen, charcoal, isotopic and geochemical records from the laminated sediments of Lake Van, Turkey." The Holocene **13**(5): 665-675.
Wilson, L. M., C. Jette, et al. (2003). Biology and biological control of yellow starthistle.
Wuensch, K. L. (2011). "Skewness, Kurtosis and the Normal Curve." from http://core.ecu.edu/psyc/wuenschk/docs30/Skew-Kurt.docx.
Yechieli, Y., M. Magaritz, et al. (1993). "Late Quaternary geological history of the Dead Sea area, Israel." Quaternary Research **39**: 59-67.
Zohary, M. (1973). Geobotanical Foundations of the Middle East. Stuttgart-Amsterdam.

Zomer, R. J., A. Trabucco, et al. (2008). "Climate change mitigation: A spatial analysis of global land suitability for clean development mechanism afforestation and reforestation." Agriculture, Ecosystems and Environment **126**: 67-80.
Zomer, R. J., A. Trabucco, et al. (2007). Carbon, Land and Water: A global analysis of the hydrologic dimensions of climate change mitigation through afforestation / reforestation.